

NUREG/CR-5395  
EPRI/NP-6480  
BAW-2078  
Vol. 10

---

# Multiloop Integral System Test (MIST): Final Report

## RELAP5/MOD2 MIST Analysis Comparisons

---

Prepared by J. A. Klingenfus, M. V. Parece/B&W

Prepared for  
U.S. Nuclear Regulatory  
Commission  
and  
Electric Power Research Institute  
and  
Babcock & Wilcox Owners Group

9002120143 891231  
PDR NUREG  
CR-5395 R PDR

## AVAILABILITY NOTICE

### Availability of Reference Materials Cited in NRC Publications

Most documents cited in NRC publications will be available from one of the following sources:

1. The NRC Public Document Room, 2120 L Street, NW, Lower Level, Washington, DC 20555
2. The Superintendent of Documents, U.S. Government Printing Office, P.O. Box 37082, Washington, DC 20013-7082
3. The National Technical Information Service, Springfield, VA 22161

Although the listing that follows represents the majority of documents cited in NRC publications, it is not intended to be exhaustive.

Referenced documents available for inspection and copying for a fee from the NRC Public Document Room include NRC correspondence and internal NRC memoranda; NRC Office of Inspection and Enforcement bulletins, circulars, information notices, inspection and investigation notices; Licensee Event Reports; vendor reports and correspondence; Commission papers; and applicant and licensee documents and correspondence.

The following documents in the NUREG series are available for purchase from the GPO Sales Program: formal NRC staff and contractor reports, NRC-sponsored conference proceedings, and NRC booklets and brochures. Also available are Regulatory Guides, NRC regulations in the *Code of Federal Regulations*, and *Nuclear Regulatory Commission Issuances*.

Documents available from the National Technical Information Service include NUREG series reports and technical reports prepared by other federal agencies and reports prepared by the Atomic Energy Commission, forerunner agency to the Nuclear Regulatory Commission.

Documents available from public and special technical libraries include all open literature items, such as books, journal and periodical articles, and transactions. *Federal Register* notices, federal and state legislation, and congressional reports can usually be obtained from these libraries.

Documents such as theses, dissertations, foreign reports and translations, and non-NRC conference proceedings are available for purchase from the organization sponsoring the publication cited.

Single copies of NRC draft reports are available free, to the extent of supply, upon written request to the Office of Information Resources Management, Distribution Section, U.S. Nuclear Regulatory Commission, Washington, DC 20555.

Copies of industry codes and standards used in a substantive manner in the NRC regulatory process are maintained at the NRC Library, 7920 Norfolk Avenue, Bethesda, Maryland, and are available there for reference use by the public. Codes and standards are usually copyrighted and may be purchased from the originating organization or, if they are American National Standards, from the American National Standards Institute, 1430 Broadway, New York, NY 10018.

## DISCLAIMER NOTICE

This report was prepared as an account of work sponsored by an agency of the United States Government. Neither the United States Government nor any agency thereof, or any of their employees, makes any warranty, expressed or implied, or assumes any legal liability of responsibility for any third party's use, or the results of such use, of any information, apparatus, product or process disclosed in this report, or represents that its use by such third party would not infringe privately owned rights.

NUREG/CR-5395  
EPRI/NP-6480  
BAW-2078  
Vol. 10

Multiloop Integral System Test (MIST): Final Report  
RELAP5/MOD2 MIST Analysis Comparisons

Date Published: December 1989

Principal Authors

J. A. Klingenfus  
M. V. Parece

Major Contributors

J. R. Gloudemans  
M. B. McGuirk  
P. L. Ploch  
M. A. Rinckel  
J. C. Seals

Prepared by

Babcock & Wilcox  
Nuclear Power Division  
3315 Old Forest Road  
Lynchburg, VA 24506-0935

Babcock & Wilcox  
Research and Development Division  
Alliance Research Center  
1562 Beeson Street  
Alliance, OH 44601

Prepared for

Division of Systems Research  
Office of Nuclear Regulatory Research  
U. S. Nuclear Regulatory Commission  
Washington, DC 20555  
NRC FINs B8909, D1734

Electric Power Research Institute  
P. O. Box 10412  
Palo Alto, CA 94303

Babcock & Wilcox Owners Group  
P. O. Box 10935  
Lynchburg, VA 24506-0935

## ABSTRACT

The multiloop integral system test (MIST) facility is part of a multiphase program started in 1983 to address small-break loss-of-coolant accidents (SBLOCAs) specific to Babcock & Wilcox (B&W) designed plants. MIST is sponsored by the U.S. Nuclear Regulatory Commission, the B&W Owners Group, the Electric Power Research Institute, and B&W. The unique features of the B&W design, specifically the hot leg U-bends and steam generators, prevented the use of existing integral system data or existing integral system facilities to address the thermal-hydraulic SBLOCA questions. MIST and two other supporting facilities were specifically designed and constructed for this program, and an existing facility -- the once-through integral system (OTIS) -- was also used. Data from MIST and the other facilities will be used to benchmark the adequacy of system codes, such as RELAP5/MOD2 and TRAC-PF1, for predicting abnormal plant transients. The MIST program included funding for seven individual RELAP pre- and post-test predictions. The comparisons against data and final conclusions are the subject of this volume of the MIST Final Report.

## CONTENTS

	Page
1. INTRODUCTION . . . . .	1-1
2. PRETEST PREDICTIONS . . . . .	2-1
2.1. MIST Test 3109AA Pretest Prediction . . . . .	2-2
2.1.1. MIST Test 3109AA Steady-State Conditions . . . . .	2-2
2.1.2. MIST Test 3109AA Transient Comparisons . . . . .	2-3
2.1.3. MIST Test 3109AA Pretest Conclusions . . . . .	2-6
2.2. MIST Test 3406AA Pretest Prediction . . . . .	2-40
2.2.1. MIST Test 3406AA Steady-State Conditions . . . . .	2-40
2.2.2. MIST Test 3406AA Transient Comparisons . . . . .	2-41
2.2.3. MIST Test 3406AA Pretest Conclusions . . . . .	2-44
3. POST-TEST PREDICTIONS . . . . .	3-1
3.1. MIST Test 320503 Post-Test Prediction . . . . .	3-3
3.1.1. MIST Test 320503 Base Case Modifications . . . . .	3-5
3.1.2. MIST Test 320503 Transient Comparisons . . . . .	3-5
3.1.3. MIST Test 320503 Post-Test Conclusions . . . . .	3-8
3.2. MIST Test 320302 Post-Test Prediction . . . . .	3-44
3.2.1. MIST Test 320302 Base Case Modifications . . . . .	3-44
3.2.2. MIST Test 320302 Transient Comparisons . . . . .	3-44
3.2.3. MIST Test 320302 Post-Test Conclusions . . . . .	3-47
3.3. MIST Test 340213 Post-Test Prediction . . . . .	3-81
3.3.1. MIST Test 340213 Base Case Modifications . . . . .	3-81
3.3.2. MIST Test 340213 Transient Comparisons . . . . .	3-82
3.3.3. MIST Test 340213 Post-Test Prediction . . . . .	3-85
3.4. MIST Test 3502CC Post-Test Prediction . . . . .	3-121
3.4.1. MIST Test 3502CC Base Case Modifications . . . . .	3-121
3.4.2. MIST Test 3502CC Transient Comparisons . . . . .	3-122
3.4.3. MIST Test 3502CC Post-Test Conclusions . . . . .	3-126
3.5. MIST Test 3801AA Post-Test Prediction . . . . .	3-155
3.5.1. MIST Test 3801AA Base Case Modifications . . . . .	3-155
3.5.2. MIST Test 3801AA Transient Comparisons . . . . .	3-155
3.5.3. MIST Test 3801AA Post-Test Conclusions . . . . .	3-160
4. CONCLUSIONS . . . . .	4-1
5. REFERENCES . . . . .	5-1

## List of Tables

Table	Page
1.1. Scale for Characterizing the Degree of Agreement Between the Test Data and the Code Predictions . . . . .	1-4
1.2. Key MIST Elevations . . . . .	1-5
2.1.1. MIST Test 3109AA Calculated and Measured Initial Steady-State Conditions . . . . .	2-3
2.2.1. MIST Test 3406AA Calculated and Measured Initial Steady-State Conditions . . . . .	2-40
2.2.2. MIST Test 3406AA Sequence of Events Comparisons . . . . .	2-43
3.1. Phenomena and Observations Considered During Test Selection for Code Benchmarking . . . . .	3-4
3.2. MIST Tests and Sponsors for RELAP5/MOD2 Benchmarks . . . . .	3-5
3.1.1. MIST Test 320503 Calculated and Measured Initial Steady-State Conditions . . . . .	3-7
3.1.2. MIST Test 320503 Sequence of Events Comparisons . . . . .	3-8
3.2.1. MIST Test 320302 Calculated and Measured Initial Steady-State Conditions . . . . .	3-46
3.2.2. MIST Test 320302 Sequence of Events Comparisons . . . . .	3-46
3.3.1. MIST Test 340213 Calculated and Measured Initial Steady-State Conditions . . . . .	3-84
3.3.2. MIST Test 340213 Sequence of Events Comparisons . . . . .	3-84
3.4.1. MIST Test 3502CC Calculated and Measured Initial Steady-State Conditions . . . . .	3-125
3.4.2. MIST Test 3502CC Sequence of Events Comparisons . . . . .	3-126
3.5.1. MIST Test 3801AA Calculated and Measured Initial Steady-State Conditions . . . . .	3-158
3.5.2. MIST Test 3801AA Sequence of Events Comparisons . . . . .	3-159

## List of Figures

Figure	
1.1	RELAP5/MOD2 MIST Loop A Noding Diagram . . . . . 1-6
1.2	RELAP5/MOD2 MIST Loop B Noding Diagram . . . . . 1-7
2.1.1	System Pressures . . . . . 2-8
2.1.2	Reactor Vessel Pressure . . . . . 2-9
2.1.3	Steam Generator A Secondary Pressure . . . . . 2-10
2.1.4	Steam Generator B Secondary Pressure . . . . . 2-11
2.1.5	Steam Generator A Primary and Stub Level . . . . . 2-12
2.1.6	Steam Generator B Primary and Stub Level . . . . . 2-13
2.1.7	Hot Leg A Riser Level . . . . . 2-14
2.1.8	Hot Leg B Riser Level . . . . . 2-15
2.1.9	Steam Generator Secondary Collapsed Liquid Levels . . . . . 2-16
2.1.10	Core Region Collapsed Liquid Levels . . . . . 2-17
2.1.11	Core Region Collapsed Liquid Levels . . . . . 2-18
2.1.12	Pressurizer Collapsed Liquid Level (PZLV20) . . . . . 2-19
2.1.13	Primary System Boundary Flow Rates . . . . . 2-20

Figures (Cont'd)

Figure		Page
2.1.14	Steam Generator A Flow Rate (Ssfor20) . . . . .	2-21
2.1.15	Steam Generator B Flow Rate (Ssfor21) . . . . .	2-22
2.1.16	Steam Generator A Flow Rates (Sssor20) . . . . .	2-23
2.1.17	Steam Generator B Flow Rates (Sssor21) . . . . .	2-24
2.1.18	HPI Total Flow Rates . . . . .	2-25
2.1.19	Loop A1 Cold Leg (Venturi) Flow Rate (C1VN20) . . . . .	2-26
2.1.20	Loop A2 Cold Leg (Venturi) Flow Rate (C2VN20) . . . . .	2-27
2.1.21	Loop B1 Cold Leg (Venturi) Flow Rate (C1VN20) . . . . .	2-28
2.1.22	Loop B2 Cold Leg (Venturi) Flow Rate (C4VN20) . . . . .	2-29
2.1.23	Primary System Venturi Flow Rates . . . . .	2-30
2.1.24	Core Exit Reactor Vessel Fluid Temperature (RVTC11) . . . . .	2-31
2.1.25	Core Inlet Reactor Vessel Fluid Temperature (DCRT01) . . . . .	2-32
2.1.26	Loops A/B SG Exit Primary Fluid Temperatures (RTDs) . . . . .	2-33
2.1.27	Cold Leg Nozzle Fluid Temperatures, Top/Bottom of Rake (21.3 ft, CnTC11/14s) . . . . .	2-34
2.1.28	Cold Leg Nozzle Fluid Temperatures, Top/Bottom of Rake (21.3 ft, Cc1tca2) . . . . .	2-35
2.1.29	Cold Leg Nozzle Fluid Temperatures, Top/Bottom of Rake (21.3 ft, Cc1tcb1) . . . . .	2-36
2.1.30	Cold Leg Nozzle Fluid Temperatures, Top/Bottom of Rake (21.3 ft, Cc1tcv2) . . . . .	2-37
2.1.31	Single-Phase Discharge Temperatures (VITC01s) . . . . .	2-38
2.1.32	Steam Generator Secondary Saturation and Control Temperatures . . . . .	2-39
2.2.1	System Pressures . . . . .	2-45
2.2.2	Reactor Vessel Pressure . . . . .	2-46
2.2.3	Steam Generator A Secondary Pressure . . . . .	2-47
2.2.4	Steam Generator B Secondary Pressure . . . . .	2-48
2.2.5	Steam Generator A Primary and Stub Level . . . . .	2-49
2.2.6	Steam Generator B Primary and Stub Level . . . . .	2-50
2.2.7	Hot Leg A Riser Level . . . . .	2-51
2.2.8	Hot Leg B Riser Level . . . . .	2-52
2.2.9	Steam Generator Secondary Collapsed Liquid Levels . . . . .	2-53
2.2.10	Core Region Collapsed Liquid Levels . . . . .	2-54
2.2.11	Core Region Collapsed Liquid Levels . . . . .	2-55
2.2.12	Pressurizer Collapsed Liquid Level (PZLV20) . . . . .	2-56
2.2.13	Leak Flow Rates . . . . .	2-57
2.2.14	Steam Generator A Flow Rate (Ssfor20) . . . . .	2-58
2.2.15	Steam Generator B Flow Rate (Ssfor21) . . . . .	2-59
2.2.16	Steam Generator A Flow Rates (Cssor20) . . . . .	2-60
2.2.17	Core Flood Tank Pressure . . . . .	2-61
2.2.18	HPI Total Flow Rates . . . . .	2-62
2.2.19	Loop A1 Cold Leg (Venturi) Flow Rate (C1VN20) . . . . .	2-63
2.2.20	Loop A2 Cold Leg (Venturi) Flow Rate (C2VN20) . . . . .	2-64
2.2.21	Loop B1 Cold Leg (Venturi) Flow Rate (C1VN20) . . . . .	2-65
2.2.22	Loop B2 Cold Leg (Venturi) Flow Rate (C4VN20) . . . . .	2-66
2.2.23	Primary System Venturi Flow Rates . . . . .	2-67
2.2.24	Core Exit Reactor Vessel Fluid Temperature (RVTC11) . . . . .	2-68
2.2.25	Core Inlet Reactor Vessel Fluid Temperature (DCRT01) . . . . .	2-69

Figures (Cont'd)

Figure	Page	
2.2.26	Loops A/B SG Exit Primary Fluid Temperatures (RTDs) . . . . .	2-70
2.2.27	Cold Leg Nozzle Fluid Temperatures, Top/Bottom of Rake (21.3 ft, CnTC11/14s) . . . . .	2-71
2.2.28	Cold Leg Nozzle Fluid Temperatures, Top/Bottom of Rake (21.3 ft, Cc1tca2) . . . . .	2-72
2.2.29	Cold Leg Nozzle Fluid Temperatures, Top/Bottom of Rake (21.3 ft, Cc1tcb1) . . . . .	2-73
2.2.30	Cold Leg Nozzle Fluid Temperatures, Top/Bottom of Rake (21.3 ft, Cc1tcb2) . . . . .	2-74
3.1.1	System Pressures . . . . .	3-9
3.1.2	Reactor Vessel Pressure . . . . .	3-10
3.1.3	Steam Generator A Secondary Pressure . . . . .	3-11
3.1.4	Steam Generator B Secondary Pressure . . . . .	3-12
3.1.5	Steam Generator A Primary and Stub Level . . . . .	3-13
3.1.6	Steam Generator B Primary and Stub Level . . . . .	3-14
3.1.7	Hot Leg A Riser Level . . . . .	3-15
3.1.8	Hot Leg B Riser Level . . . . .	3-16
3.1.9	Steam Generator Secondary Collapsed Liquid Levels . . . . .	3-17
3.1.10	Core Region Collapsed Liquid Levels . . . . .	3-18
3.1.11	Core Region Collapsed Liquid Levels . . . . .	3-19
3.1.12	Pressurizer Collapsed Liquid Level (PZLV20) . . . . .	3-20
3.1.13	Leak Flow Rates . . . . .	3-21
3.1.14	Steam Generator A Flow Rate (Ssfor20) . . . . .	3-22
3.1.15	Steam Generator B Flow Rate (Ssfor21) . . . . .	3-23
3.1.16	Steam Generator A Flow Rates (Ccssor20) . . . . .	3-24
3.1.17	Steam Generator B Flow Rates (Sssor21) . . . . .	3-25
3.1.18	HPI Total Flow Rates . . . . .	3-26
3.1.19	Loop A1 Cold Leg (Venturi) Flow Rate (C1VN20) . . . . .	3-27
3.1.20	Loop A2 Cold Leg (Venturi) Flow Rate (C2VN20) . . . . .	3-28
3.1.21	Loop B1 Cold Leg (Venturi) Flow Rate (C1VN20) . . . . .	3-29
3.1.22	Loop B2 Cold Leg (Venturi) Flow Rate (C4VN20) . . . . .	3-30
3.1.23	Reactor Core Exit Subcooling Margin . . . . .	3-31
3.1.24	Core Exit Reactor Vessel Fluid Temperature (RVTC11) . . . . .	3-32
3.1.25	Core Inlet Reactor Vessel Fluid Temperature (DCRT01) . . . . .	3-33
3.1.26	Loops A/B SG Exit Primary Fluid Temperatures (RTDs) . . . . .	3-34
3.1.27	Cold leg Nozzle Fluid Temperatures, Top/Bottom of Rake (21.3 ft, CnTC11/14s) . . . . .	3-35
3.1.28	Cold Leg Nozzle Fluid Temperatures, Top/Bottom of Rake (21.3 ft, Cc1tca2) . . . . .	3-36
3.1.29	Cold Leg Nozzle Fluid Temperatures, Top/Bottom of Rake (21.3 ft, Cc1tcb1) . . . . .	3-37
3.1.30	Cold Leg Nozzle Fluid Temperatures, Top/Bottom of Rake (21.3 ft, Cc1tcb2) . . . . .	3-38
3.1.31	CLPD Leak Fluid Temperature (TC01s) . . . . .	3-39
3.1.32	Steam Generator Secondary Saturation and Control Temperature . . . . .	3-40
3.1.33	Loops A/B SG Primary Inlet Fluid Temperatures (RTDs) . . . . .	3-41
3.1.34	Cold Leg A Discharge Collapsed Liquid Levels (CnLV23s) . . . . .	3-42
3.1.35	Cold Leg B Discharge Collapsed Liquid Levels (CnLV23s) . . . . .	3-43



Figures (Cont'd)

Figure	Page
3.2.1	System Pressures . . . . . 3-48
3.2.2	Primary Pressure . . . . . 3-49
3.2.3	Steam Generator A Secondary Pressure . . . . . 3-50
3.2.4	Steam Generator B Secondary Pressure . . . . . 3-51
3.2.5	Steam Generator A Primary and Stub Level . . . . . 3-52
3.2.6	Steam Generator B Primary and Stub Level . . . . . 3-53
3.2.7	Hot Leg A Riser Level . . . . . 3-54
3.2.8	Hot Leg B Riser Level . . . . . 3-55
3.2.9	Steam Generator Secondary Collapsed Liquid Levels . . . . . 3-56
3.2.10	Core Region Collapsed Liquid Levels . . . . . 3-57
3.2.11	Core Region Collapsed Liquid Levels . . . . . 3-58
3.2.12	Pressurizer Collapsed Liquid Level (PZLV20) . . . . . 3-59
3.2.13	Leak Flow Rates . . . . . 3-60
3.2.14	Steam Generator A Flow Rate (Ssfor20) . . . . . 3-61
3.2.15	Steam Generator B Flow Rate (Ssfor21) . . . . . 3-62
3.2.16	Steam Generator A Flow Rates (Cссор20) . . . . . 3-63
3.2.17	Steam Generator B Flow Rates (Sссор21) . . . . . 3-64
3.2.18	HPI Total Flow Rates . . . . . 3-65
3.2.19	Loop A1 Cold Leg (Venturi) Flow Rate (C1VN20) . . . . . 3-66
3.2.20	Loop A2 Cold Leg (Venturi) Flow Rate (C2VN20) . . . . . 3-67
3.2.21	Loop B1 Cold Leg (Venturi) Flow Rate (C1VN20) . . . . . 3-68
3.2.22	Loop B2 Cold Leg (Venturi) Flow Rate (C4VN20) . . . . . 3-69
3.2.23	Core Exit Reactor Vessel Fluid Temperature (RVTC11) . . . . . 3-70
3.2.24	Core Inlet Reactor Vessel Fluid Temperature (DCRT01) . . . . . 3-71
3.2.25	Loops A/B SG Exit Primary Fluid Temperatures (RTDs) . . . . . 3-72
3.2.26	Cold Leg Nozzle Fluid Temperatures, Top/Bottom of Rake (21.3 ft, CnTC11/14s) . . . . . 3-73
3.2.27	Cold Leg Nozzle Fluid Temperatures, Top/Bottom of Rake (21.3 ft, Cc1tca2) . . . . . 3-74
3.2.28	Cold Leg Nozzle Fluid Temperatures, Top/Bottom of Rake (21.3 ft, Cc1tcb1) . . . . . 3-75
3.2.29	Cold Leg Nozzle Fluid Temperatures, Top/Bottom of Rake (21.3 ft, Cc1tcb2) . . . . . 3-76
3.2.30	Single-Phase Discharge Temperatures (VITCO1s) . . . . . 3-77
3.2.31	Steam Generator Secondary Saturation and Control Temperatures . . . . . 3-78
3.2.32	Cold Leg A Discharge Collapsed Liquid Levels (CnLV23s) . . . . . 3-79
3.2.33	Cold Leg B Discharge Collapsed Liquid Levels (CnLV23s) . . . . . 3-80
3.3.1	System Pressures . . . . . 3-86
3.3.2	Primary Pressure . . . . . 3-87
3.3.3	Steam Generator A Secondary Pressure . . . . . 3-88
3.3.4	Steam Generator B Secondary Pressure . . . . . 3-89
3.3.5	Steam Generator A Primary and Stub Level . . . . . 3-90
3.3.6	Steam Generator B Primary and Stub Level . . . . . 3-91
3.3.7	Hot Leg A Riser Level . . . . . 3-92
3.3.8	Hot Leg B Riser Level . . . . . 3-92
3.3.9	Steam Generator Secondary Collapsed Liquid Levels . . . . . 3-94
3.3.10	Core Region Collapsed Liquid Levels . . . . . 3-95
3.3.11	Core Region Collapsed Liquid Levels . . . . . 3-96

Figures (Cont'd)

Figure		Page
3.3.12	Pressurizer Collapsed Liquid Level (PZLV20)	3-97
3.3.13	Primary System SGTR Leak Flow Rates	3-98
3.3.14	Steam Generator A Flow Rate (Ssfor20)	3-99
3.3.15	Steam Generator B Flow Rate (Ssfor21)	3-100
3.3.16	Steam Generator A Flow Rates (Cssor20)	3-101
3.3.17	Steam Generator B Flow Rates (Sssor21)	3-102
3.3.18	HPI Total Flow Rates	3-103
3.3.19	Loop A1 Cold Leg (Venturi) Flow Rate (C1VN20)	3-104
3.3.20	Loop A2 Cold Leg (Venturi) Flow Rate (C2VN20)	3-105
3.3.21	Loop B1 Cold Leg (Venturi) Flow Rate (C1VN20)	3-106
3.3.22	Loop B2 Cold Leg (Venturi) Flow Rate (C4VN20)	3-107
3.3.23	Primary System Venturi Flow Rates	3-108
3.3.24	Core Exit Reactor Vessel Fluid Temperature (RVTC11)	3-109
3.3.25	Core Inlet Reactor Vessel Fluid Temperature (DCRT01)	3-110
3.3.26	Loops A/B SG Exit Primary Fluid Temperatures (RTDs)	3-111
3.3.27	Cold Leg Nozzle Fluid Temperatures, Top/Bottom of Rake (21.3 ft, CnTC11/14s)	3-112
3.3.28	Cold Leg Nozzle Fluid Temperatures, Top/Bottom of Rake (21.3 ft, Ccltca2)	3-113
3.3.29	Cold Leg Nozzle Fluid Temperatures, Top/Bottom of Rake (21.3 ft, Ccltcb1)	3-114
3.3.30	Cold Leg Nozzle Fluid Temperatures, Top/Bottom of Rake (21.3 ft, Ccltcb2)	3-115
3.3.31	Loops A/B SG Primary Inlet Fluid Temperatures (RTDs)	3-116
3.3.32	Steam Generator Secondary Saturation and Control Temperatures	3-117
3.3.33	Downcomer A Fluid Temperatures Below RVVVs, Elevation 23.8 ft (DCTCs)	3-118
3.3.34	Downcomer B Fluid Temperatures Below RVVVs, Elevation 23.8 ft (DCTCs)	3-119
3.3.35	Reactor Vessel Upper Head Fluid Temperatures (RVTC23)	3-120
3.4.1	System Pressures	3-128
3.4.2	Steam Generator A Primary and Stub Level	3-129
3.4.3	Steam Generator B Primary and Stub Level	3-130
3.4.4	Hot Leg A Riser Level	3-131
3.4.5	Hot Leg B Riser Level	3-132
3.4.6	Steam Generator Secondary Collapsed Liquid Levels	3-133
3.4.7	Core Region Collapsed Liquid Levels	3-134
3.4.8	Core Region Collapsed Liquid Levels	3-135
3.4.9	Pressurizer Collapsed Liquid Level (PZLV20)	3-136
3.4.10	Cold Leg A Discharge Collapsed Liquid Level (CnLV23s)	3-137
3.4.11	Cold Leg B Discharge Collapsed Liquid Level (CnLV23s)	3-138
3.4.12	Cold Leg A Suction Collapsed Liquid Levels (CnLV22s)	3-139
3.4.13	Cold Leg B Suction Collapsed Liquid Levels (CnLV22s)	3-140
3.4.14	Steam Generator A Flow Rate (Ssfor20)	3-141
3.4.15	Steam Generator B Flow Rate (Ssfor21)	3-142
3.4.16	Steam Generator A Flow Rates (Cssor20)	3-143
3.4.17	Steam Generator B Flow Rates (Sssor21)	3-144
3.4.18	Noncondensable Gas Volumes	3-145

Figures (Cont'd)

Figure		Page
3.4.19	Loop A1 Cold Leg (Venturi) Flow Rate (C1VN20) . . . . .	3-146
3.4.20	Loop A2 Cold Leg (Venturi) Flow Rate (C2VN20) . . . . .	3-147
3.4.21	Loop B1 Cold Leg (Venturi) Flow Rate (C1VN20) . . . . .	3-148
3.4.22	Loop B2 Cold Leg (Venturi) Flow Rate (C4VN20) . . . . .	3-149
3.4.23	Primary System Venturi Flow Rates . . . . .	3-150
3.4.24	Core Exit Reactor Vessel Fluid Temperature (RVTC11) . . . . .	3-151
3.4.25	Core Inlet Reactor Vessel Fluid Temperature (DCRT01) . . . . .	3-152
3.4.26	Loops A/B SG Exit Primary Fluid Temperatures (RTDs) . . . . .	3-153
3.4.27	Steam Generator Secondary Saturation and Control Temperatures . . . . .	3-154
3.5.1	System Pressure . . . . .	3-161
3.5.2	Reactor Vessel Pressure . . . . .	3-162
3.5.3	Steam Generator A Secondary Pressure . . . . .	3-163
3.5.4	Steam Generator B Secondary Pressure . . . . .	3-164
3.5.5	Steam Generator A Primary and Stub Level . . . . .	3-165
3.5.6	Steam Generator B Primary and Stub Level . . . . .	3-166
3.5.7	Hot Leg A Riser Level . . . . .	3-167
3.5.8	Hot Leg B Riser Level . . . . .	3-168
3.5.9	Steam Generator Secondary Collapsed Liquid Levels . . . . .	3-169
3.5.10	Core Region Collapsed Liquid Levels . . . . .	3-170
3.5.11	Core Region Collapsed Liquid Levels . . . . .	3-171
3.5.12	Pressurizer Collapsed Liquid Level (PZLV20) . . . . .	3-172
3.5.13	Primary System Boundary Flow Rates . . . . .	3-173
3.5.14	Primary System Boundary Flow Rates . . . . .	3-174
3.5.15	Steam Generator A Flow Rate (Ssfor20) . . . . .	3-175
3.5.16	Steam Generator B Flow Rate (Ssfor21) . . . . .	3-176
3.5.17	Steam Generator A Flow Rates (Cssor20) . . . . .	3-177
3.5.18	Steam Generator B Flow Rates (Sssor21) . . . . .	3-178
3.5.19	Cold Leg A1 Flow . . . . .	3-179
3.5.20	Cold Leg A2 Flow . . . . .	3-180
3.5.21	Cold Leg B1 Flow . . . . .	3-181
3.5.22	Cold Leg B2 Flow . . . . .	3-182
3.5.23	Primary System Venturi Flow Rates . . . . .	3-183
3.5.24	Void Fraction . . . . .	3-184
3.5.25	Void Fraction . . . . .	3-185
3.5.26	Void Fraction . . . . .	3-186
3.5.27	Void Fraction . . . . .	3-187
3.5.28	Integrated PORV Flow . . . . .	3-188
3.5.29	Total System Mass . . . . .	3-189
3.5.30	Core Exit Reactor Vessel Fluid Temperature (RVTC11) . . . . .	3-190
3.5.31	Core Inlet Reactor Vessel Fluid Temperature (DCRT01) . . . . .	3-191
3.5.32	Loops A/B SG Exit Primary Fluid Temperatures (RTDs) . . . . .	3-192
3.5.33	Loops A/B SG Primary Inlet Fluid Temperatures (RTDs) . . . . .	3-193



## EXECUTIVE SUMMARY

The multiloop integral system test (MIST) facility was a scaled 2-by-4 (2 hot legs and 4 cold legs) physical model of a Babcock & Wilcox (B&W), 177 fuel assembly lower-d-loop, nuclear steam supply system (NSSS). MIST was designed to operate at typical plant pressures and temperatures. Experimental data obtained from this facility during post-small-break loss-of-coolant accident (SBLOCA) testing are used for computer code benchmarking and verification.

The MIST facility consisted of two 19-tube, once-through steam generators (UTSG), a reactor vessel, a pressurizer, two hot legs, four cold legs with scaled reactor coolant pumps, a closed secondary system, simulated reactor vessel vent valves, and a core flood tank. Boundary conditions were supplied by auxiliary feedwater injection, high pressure injection (HPI), a pressurizer power-operated relief valve, hot leg and reactor vessel high point vents, and various critical flow orifice locations for scaled leak simulations. Guard heaters were used in conjunction with passive insulation to reduce system model heat losses. A general layout of the MIST facility is illustrated in Figure 1.

Three separate code analysis tasks were undertaken for the MIST program using several versions of the RELAP5 code series. The first task was a MIST design verification analysis with the B&W version 3.0 of RELAP5/MOD1.<sup>1</sup> Three pretest predictions were performed with the B&W version 4.0 of RELAP5/MOD2<sup>2</sup> as the second task. The final task included five post-test predictions with subsequent versions 7.0 and 8.0 of RELAP5/MOD2.<sup>2</sup>

The design verification analysis was performed to substantiate the preliminary facility design and augment the desired transient initial conditions. The results of these calculations coupled with results from a similar TRAC-PF1 code analysis are documented in the Multi-Loop Integral System Test Design Verification Analysis Report.<sup>3</sup> The analysis efforts resulted in various changes in the specified steady-state control parameters.

Three pretest predictions were performed with RELAP. The analysis results for tests 310000 (nominal 10 cm<sup>2</sup> cold leg pump discharge (CLPD)), 320201 (50 cm<sup>2</sup> CLPD with evaluation model HPI), and 34302 (10 tube low steam generator tube rupture (SGTR)) were contained in the MIST RELAP5/MOD2 Pretest Prediction report.<sup>4</sup> At the time that report was released, the tests had not been performed. Therefore, reference 4 contains only the RELAP results without data comparisons. The comparison against the data is contained within this document for the nominal and SGTR cases. The 50 cm<sup>2</sup> case was calculated with an equivalent evaluation model HPI while the test was performed with full HPI, rendering any direct comparison meaningless.

Five post-test code calculations were performed under the MIST contract. Tests 320302 (10 cm<sup>2</sup> cold leg pump suction (CLPS)), 320503 (10 cm<sup>2</sup> CLPD with leak isolation), 340213 (1 tube high SGTR), 350200 (noncondensable gas threshold), and 3801AA (core uncover with pumps running) were executed and the results are compared against the test data within this document. The input model used for these calculations was described in the RELAP5/MOD2 MIST Post-Test Model Description report<sup>5</sup> sponsored by the B&W Owners Group.

The conclusions derived from the analysis efforts indicated that the MIST facility provided expected plant typical SBLOCA thermal-hydraulic behavior suitable for benchmarking and code evaluation. The code calculated results produced reasonable agreement to the data for all tests. The major system trends and behavior were predicted by RELAP5/MOD2 and the base input model. Generally, interactions between the governing thermal-hydraulic phenomena were calculated to occur in fashions similar to the actual facility behavior lending credibility to the predictive powers of the code and input modeling techniques. Use of similar modeling techniques on the full size NSSSs with RELAP5/MOD2 should produce results which can generally be trusted and utilized over a fairly wide range of SBLOCA and plant operational transients.

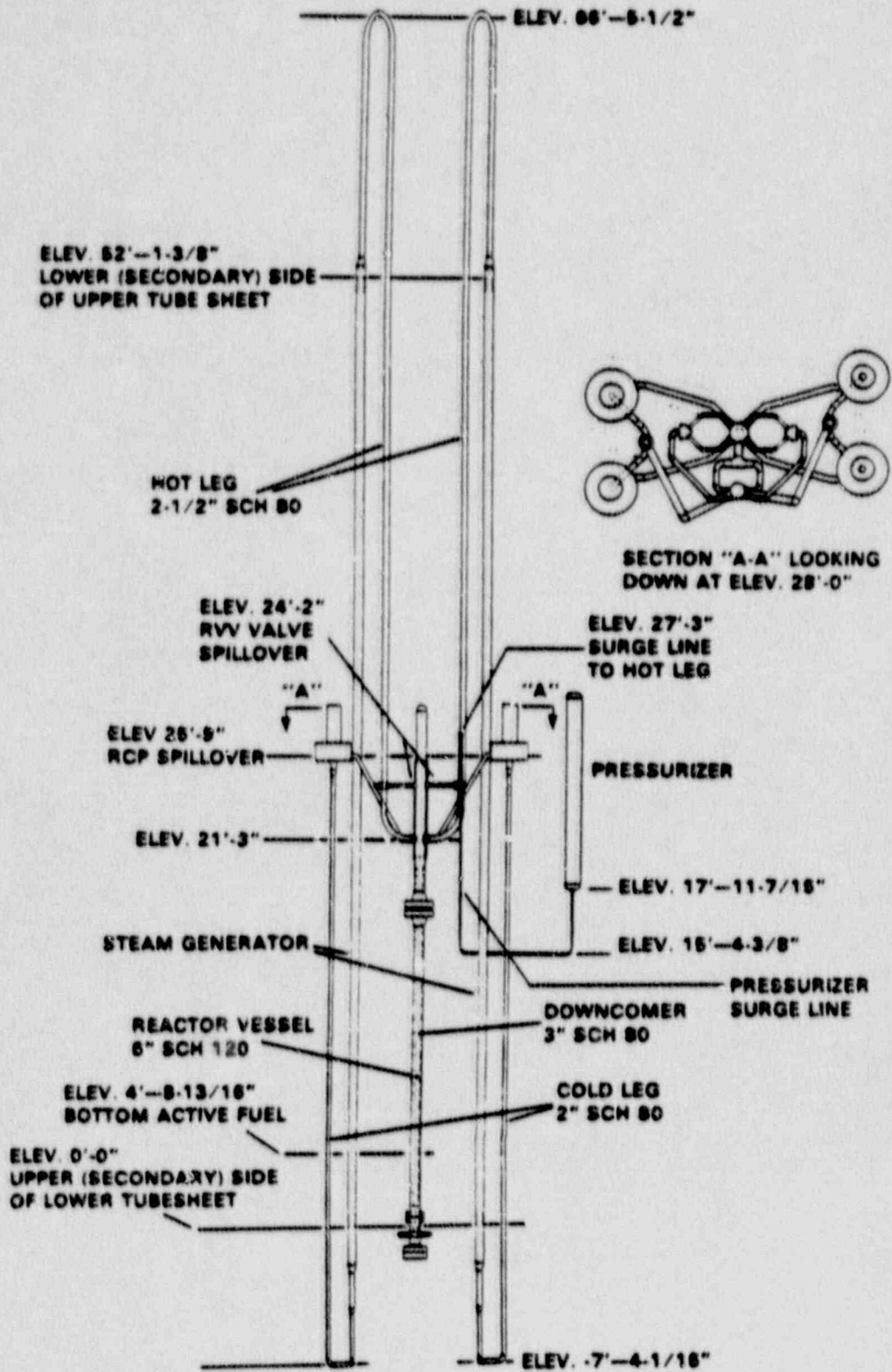


Figure 1. MIST reactor coolant system arrangement





## 1. INTRODUCTION

The multiloop integral system test (MIST) facility was a 2-by-4, full pressure and temperature simulation of the Babcock and Wilcox (B&W) lowered-loop nuclear steam supply system (NSSS). MIST was sponsored by the U.S. Nuclear Regulatory Commission, the B&W Owners Group, the Electric Power Research Institute, and B&W. The facility was scaled and designed to provide additional test data for understanding and verifying the transient thermal-hydraulic phenomena which occurs in B&W nuclear plants. The major emphasis in MIST is to acquire the integral system experimental data during SBLOCA events for use in code benchmarking. Reasonable prediction of the governing MIST (and plant) behavior is required for ensuring the ability of the code formulation and input model to adequately calculate overall thermal-hydraulic system performance during these events. Consistent modeling techniques for both the full size NSSS and the MIST facility will then provide the mechanism to extrapolate the code calculations to the plant predictions.

Three separate code analysis tasks were undertaken as part of the MIST program. The intent of these tasks was to assess not only the code and input model, but also the facility operation and initial conditions. The first task required constructing a MIST facility model from preliminary design information and predicting the steady-state and transient portions of the nominal scaled 10 cm<sup>2</sup> CLPD break transient. The REDBL5 code<sup>1</sup> (B&W version of RELAP5/MOD1) was used for this effort which was termed the design verification analysis. A similar but separate TAC-PF1 calculation was performed by the Los Alamos National Laboratory (LANL) to help verify the facility design and operation. The goal of these initial calculations was to provide aid in determining the initial and boundary conditions necessary for observing certain governing phenomena. The results of these analyses are not contained within this document. They were released under a separate cover: Multi-Loop Integral System Test Design Verification Report<sup>3</sup>. As a result of these

analyses the specified initial conditions were modified such that the initial conditions specified hot leg subcooling instead of primary pressure along with core power, pressurizer level, steam generator secondary level, and steam generator secondary pressure. Several other facility hardware and/or control changes were subsequently made such that the design verification analysis was incompatible as a one-to-one comparison against a performed test.

The second analysis task was to convert the input model to RELAP5/MOD2 format and perform three pretest predictions. The tests chosen were two SBLOCAs and a SGTR. They were chosen not only to evaluate the code and input model predictive capabilities, but also to provide insight into facility operation and control. The calculated code results from this effort were described in the RELAP5/MOD2 MIST Pretest Predictions report<sup>4</sup>. Comparisons against the actual test data and discussions of the results is contained in this report for two of the three predictions. A different boundary condition was used for the third test thus invalidating that comparison.

The final analysis effort consisted of performing five post-test calculations with an updated input model. The pretest prediction model was upgraded with observed information on such items as loop pressure drops, auxiliary feed-water (AFW) wetting and heat transfer, uncompensated heat losses, final component volumes, and additional diagnostic control variable edits. The B&W Owners Group sponsored these model updates which are documented within the RELAP5/MOD2 MIST Post-Test Model Description report<sup>5</sup>. The post-test prediction cases included two natural circulation SBLOCA events, a SGTR, a noncondensable gas (NCG) threshold test, and a pumps running SBLOCA which included partial core uncovering.

In addition to the five post-test predictions performed as part of the MIST program, the B&W Owners Group sponsored RELAP5/MOD2 post-test predictions of two OTIS tests<sup>7,8</sup> and six MIST tests.<sup>9-14</sup> Those calculations are not discussed in this report. However, they are mentioned here because they provide additional cases of RELAP5/MOD2 code assessment with respect to IST data. For further information, the reader is directed to those reports.

LANL generated a scale by which the agreement between the code prediction and the test results could be characterized. This scale, shown in Table 1.1.,

was an attempt to standardize a grading system which would at least define overall comparison results. In this system both the code and input model are considered as contributors to the final result. Deficiencies may therefore be related to either the code or the input model. Although this system cannot completely remove the subjectivity of the predictive powers of codes, it at least defines the categories of acceptance and presents a consistent scale for communication of the results.

Since the input models were described within reports released during the MIST program, they will not be described in detail here. The input deck included models for the following components: reactor vessel, two hot legs, four cold legs, pressurizer, two multi-channel once-through steam generators (OTSGs), four reactor coolant pumps, external annular reactor vessel downcomer, reactor vessel vent valves (RVVVs), core flood tank, high pressure injection (HPI) and various primary leak sites. The leak sites included the power operated relief valve (PORV), cold leg pump discharge (CLPD) B1 leak, cold leg pump suction (CLPS) B1 leak, and hot leg high point vents. The complete model, shown in Figures 1.1. and 1.2., consisted of approximately 155 control volumes, 175 junctions, 145 heat structures with 540 mesh points, 260 control variables, and 50 logical or variable trips. The modeling techniques and nodal densities used in developing this input deck are comparable to those used for modeling full size B&W NSSS.

Several notes and definitions may be useful in providing a better understanding of the transient comparison data. A rather general set of comparison plots was defined both for the pre- and post-test predictions. In some tests certain of the test or prediction plots may have been unavailable for one reason or another. This was especially true with various test flow rate plots such as cold leg, downcomer, or boundary system flows. (For example, the pretest predictions did not include cold leg collapsed levels.) At times certain plots may have been meaningless, that is, collapsed levels which were always full or variables which were constant or zero. In other cases, the plots may have been unusable because of out of range or multi-phase data. When instances such as these arose, the affected plots were often deleted from the base set. Also, very few temperature plots were included, especial-

ly if the thermocouple was in a region which changed phases. The reason was primarily due to the two individual phasic temperatures which RELAP computed. The component level plots were calculated as collapsed levels both for RELAP and the test. These levels were in terms of elevations with a datum of zero at the steam generator lower tube sheet upper face (SGLTSUF). A list of the key system elevations with respect to this datum is given in Table 1.2. This list will be exceedingly helpful in understanding the transient scenarios.

Table 1.1. Scale for Characterizing the Degree of Agreement  
Between the Test Data and the Code Predictions

Level of Agreement	Characteristics of This Agreement
EXCELLENT	No code/model deficiencies noted for this application. The major and minor system trends were each predicted correctly and the calculations were usually within the data uncertainty band. Similar applications with this code and consistent input models can be used with confidence.
REASONABLE	Minor code/model deficiencies noted for this application. The major system trends were predicted correctly although various parameters were frequently outside test data uncertainty band. The minor system trend variations did not significantly effect the overall results. Correct conclusions can be reached for similar applications with this code and consistent input models.
MINIMAL	Significant code/model deficiencies noted for this application. Some major system trends were predicted incorrectly. The results were often far outside data uncertainty bands. Use of the code for similar applications may produce correct conclusions if used carefully.
INSUFFICIENT	Major code/model deficiencies noted for this application. Major system trends were not predicted. Calculated trends opposite or entirely different from data. The code should not be used for these applications without extensive code or model changes and verification.

Table 1.2. Key MIST Elevations

<u>Component or Location</u>	<u>Elevation (ft) wrt SGLTSUF</u>
Bottom of active steam generator tubes	0.00
Nominal initial secondary level	5.00
Secondary 95% operating-range collapsed level	31.60
AFW injection location	50.87
Top of active tube region	52.11
Cold leg pump suction low point	-7.42
Reactor coolant pump spill-over	25.75
Hot leg and cold leg nozzle centerline	21.25
Active core inlet	4.74
Active core outlet	16.74
RVVV spill-over	24.21
Top of reactor vessel	29.38
Pressurizer surge line connection to hot leg	27.25
Pressurizer surge line low point	15.36
Bottom of pressurizer	17.95
Top of pressurizer	30.19
Hot leg U-bend spill-over	66.46

Figure 1.1 RELAP5/MOD2 MIST Loop A Noding Diagram

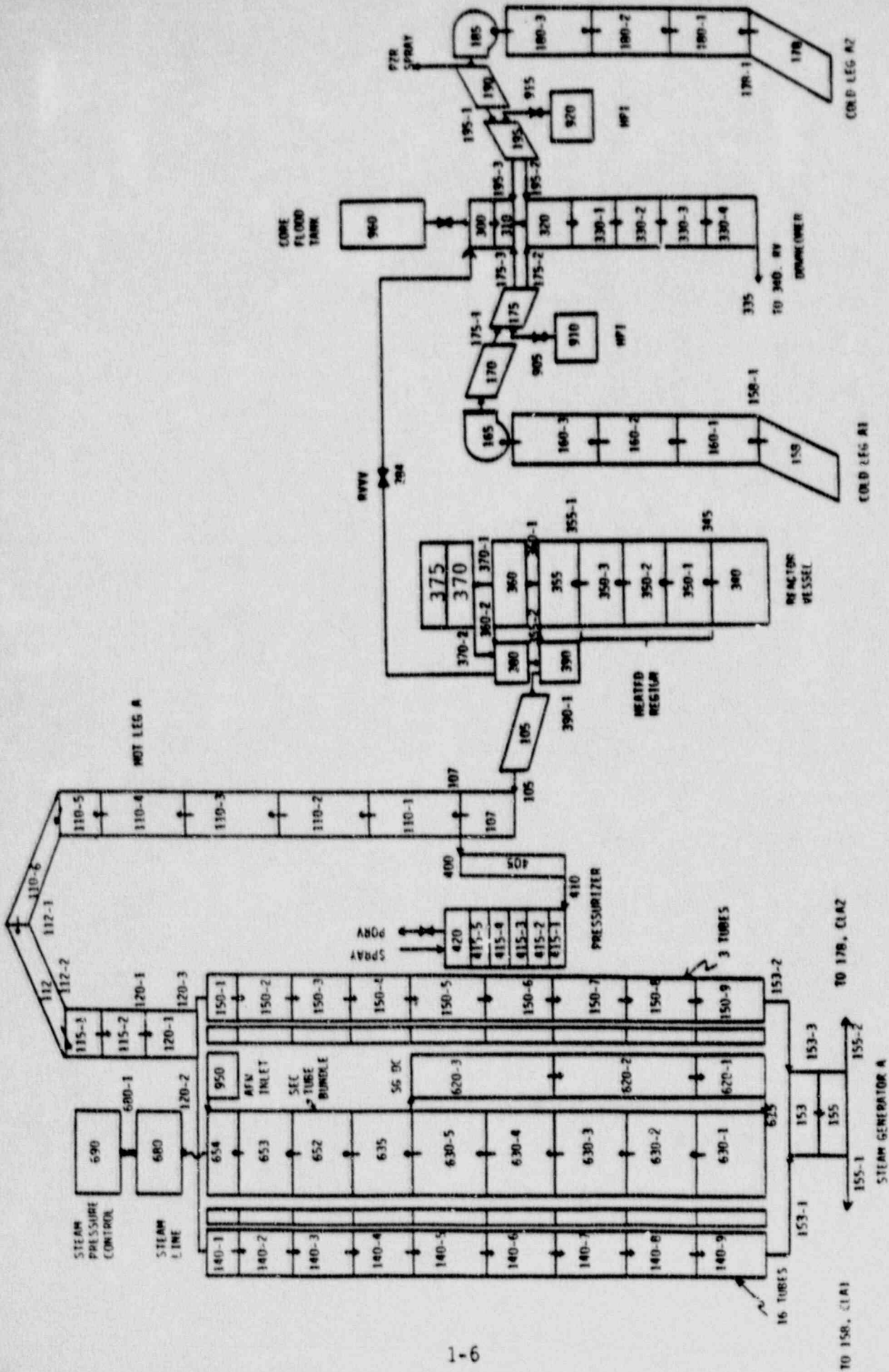
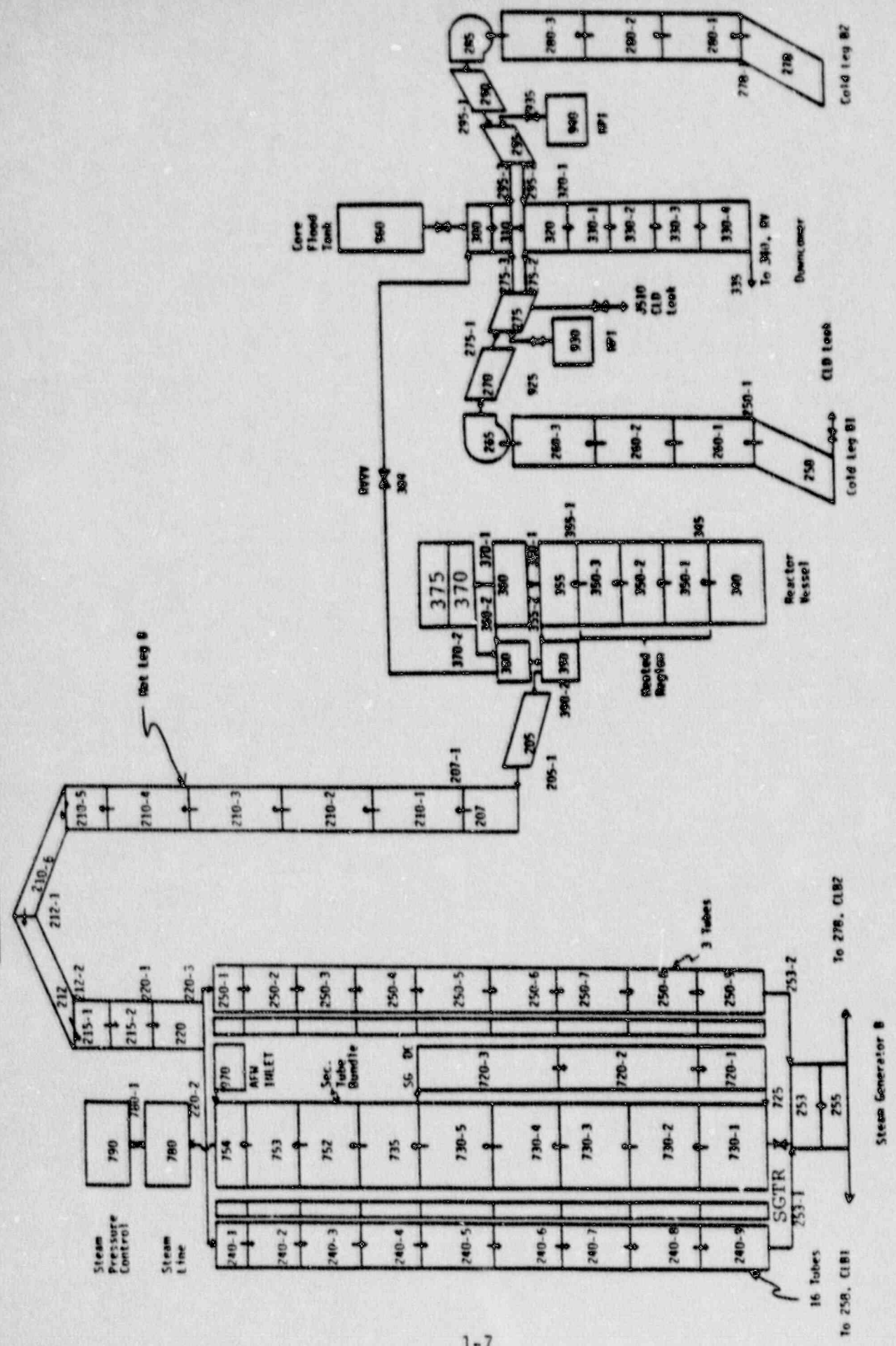
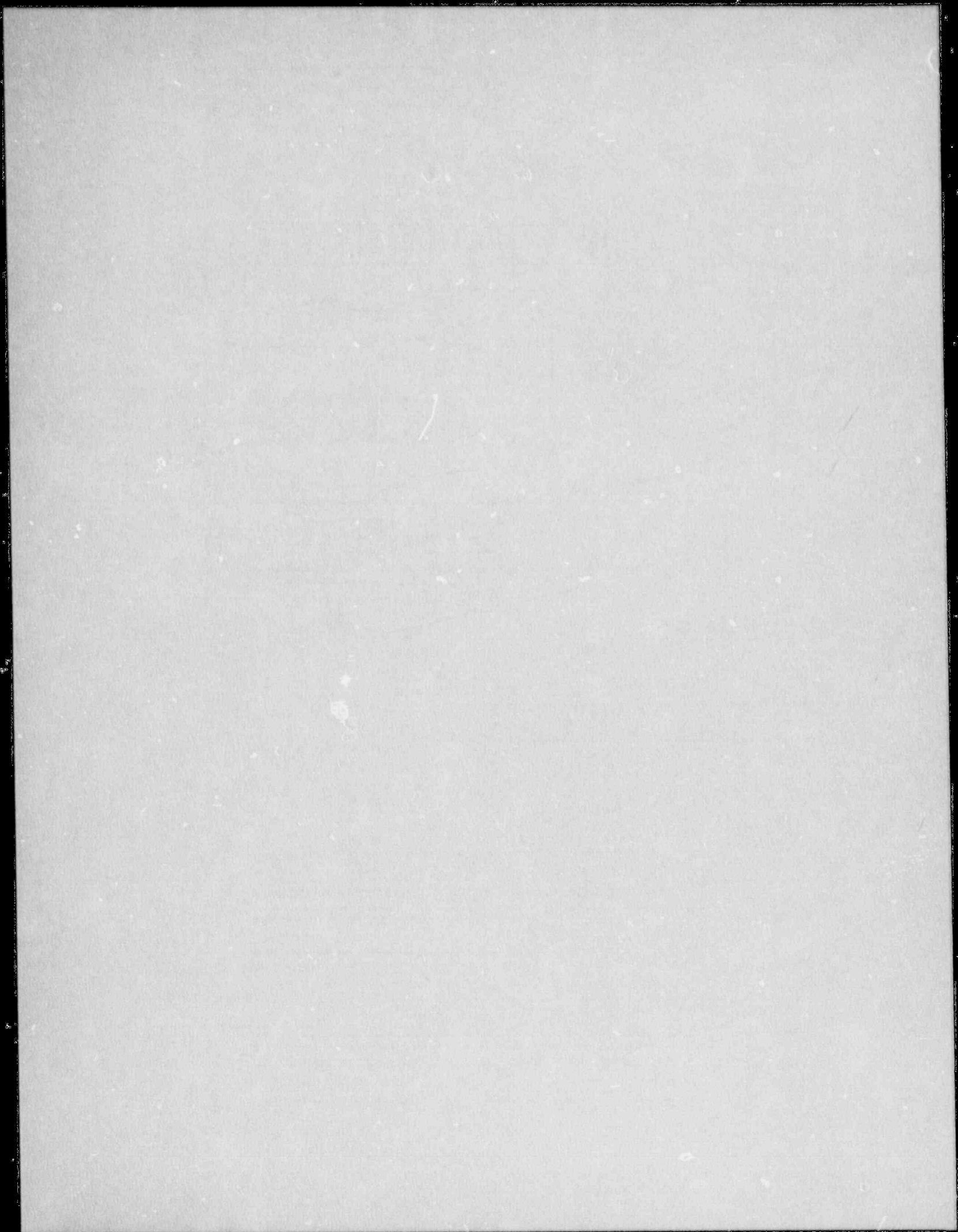


Figure 1.2 RELAP5/MOD2 MIST Loop B Modeling Diagram







## 2. PRETEST PREDICTIONS

One of the best methods for evaluating codes and input models is to perform pretest predictions and then compare those results to the actual test data. For this reason, subtask 4.3 of the Integral System Test (IST) program contained provisions and guidelines for performing various MIST pretest predictions with B&W version 3.0 of RELAP5/MOD2<sup>2</sup>. Three MIST pretest predictions were ultimately performed on tests which were initially designated by the numbers 310000, 320201, and 340302. The facility tests which coincided with these predictions were designated as 3109AA, 320201, and 3406AA respectively. For the sake of discussion, the tests will hereafter be called by the facility designated test numbers.

The first pretest prediction was performed for test 3109AA. This test, called the nominal case, was a scaled 10 cm<sup>2</sup> CLPD break located on the bottom of the pipe several inches downstream of the HPI nozzle. Full flow HPI and auxiliary feedwater (AFW) capacity were utilized with the nominally confined operator actions and controls. A complete test description is given in the MIST Group 31 report. Comparison against the test data and discussion of the results is included in section 2.1 of this report.

The second prediction was performed for test 320201. This test opened a scaled 50 cm<sup>2</sup> CLPD at the same location as the nominal case. "Evaluation model" (EM) HPI capacity was intentionally simulated for the prediction in order to evaluate potential facility limitations. At the time that the prediction was performed, the decision on which HPI capacity would be used had not been made. Unfortunately, the test was ultimately performed with full HPI capacity, invalidating the comparison. Therefore, no discussion of this test will be included in this report. The B&W Owners Group subsequently sponsored a post-test prediction of this test with RELAP5/MOD2.<sup>9</sup>

The final prediction was performed for test 3406AA, a repeat of the scaled double-ended ten tube rupture at the lower tube support plate. Full HPI capacity was used during this test which did not isolate the affected steam generator secondary side. This test is described in the MIST Group 34 report. Comparison against the data is included in section 2.2. of this report.

The pretest prediction model used for the analyses was described in the Preliminary MIST Facility Input Model for the REDBL5 Code<sup>6</sup> and the RELAP5/MOD2 MIST Pretest Prediction reports<sup>4</sup>. Uncompensated localized heat losses were modeled and the core power was augmented to offset those losses. The system was initialized in steady-state natural circulation using high elevation AFW injection. During the initialization, the RVVVs were manually held closed and the system guard heaters were modeled as an adiabatic condition at the outer pipe wall boundary.

The comparison plots shown for the pretest predictions used the preliminary test data. This data is generally very accurate, although the collapsed levels include a slight error. The sign of the absolute pressure correction factor on most differential pressures was incorrect resulting in a slight positive bias to the levels. Generally, the absolute levels are not as important as the rates of level change, therefore, the impact on the comparisons are minimal. The maximum errors in the collapsed levels are approximately one foot in the hot legs or steam generator and less in the shorter components.

## 2.1. MIST Test 3109AA Pretest Prediction

The MIST nominal case, designated as 3109AA, is a scaled 10 cm<sup>2</sup> CLPD break on the bottom of the B1 pipe several inches downstream of the HPI nozzle. The first 4000 seconds (66.7 minutes) of the test was pretest predicted.

### 2.1.1. MIST Test 3109AA Steady-State Conditions

The pretest prediction model was initialized to steady-state conditions shown in Table 2.1.1. The facility initial conditions are also shown within that table. The calculated initial conditions compared reasonably well with the facility steady-state data. The two biggest discrepancies are the initial pressurizer level and the total loop flow rates. The pressurizer level with

respect to the bottom of the component was modified from 2.5 feet to 5.0 feet of liquid inventory during the time between the execution of the pretest prediction and the test operation. Differences in the total loop flows are directly attributed to the steam generator thermal center and loop resistances. RELAP calculated a higher steam generator thermal center and also had too small of a flow resistance for the pump locked rotor and downcomer-core region. As a result the calculated flow was higher than the actual value.

Table 2.1.1. MIST Test 3109AA Calculated and Measured Initial Steady-State Conditions

<u>Parameter</u>	<u>RELAP</u>	<u>Data</u>
Primary Pressure, (psia)	1670.	1739.
SG A Secondary Pressure*, (psia)	1010.	1014.
SG B Secondary Pressure*, (psia)	1010.	1015.
SG A Collapsed Level*, (ft)	5.00	4.65
SG B Collapsed Level*, (ft)	5.00	4.74
Hot Leg Subcooling*, (F)	22.0	23.9
Pressurizer Collapsed Level*, (ft)	21.45	23.17
Core Power into the Fluid*, (% FP)	3.9	3.9
SG Primary Exit Temperatures, (F)	549.2	550.0
Core Exit Temperature, (F)	588.1	592.4
Core Total Mass Flow Rate, (lbm/s)	2.16	1.9
Uncompensated Heat Losses, (% FP)	0.4	0.5

\*Denotes specified condition.

2.1.2. MIST Test 3109AA Transient Comparisons

The leak was opened at a time equal to zero, initiating the test. A detailed discussion of the calculated results can be found in section 3.1 of the pretest prediction report. The second transient initiation step was performed as the hot leg neared saturation. The following actions were to be taken at that time.

1. Initiate the core power decay ramp.
2. Initiate full capacity HPI flow.
3. Reset the secondary control level from 5 to 31.6 feet.
4. Put the RVVVs in automatic control with open and close setpoints of 0.125 and 0.04 psid, respectively.
5. Initiate the synchronous secondary cooldown rate.

In the RELAP calculations these actions were automated and performed when the level in the pressurizer reached a collapsed liquid inventory of one foot. A comparison of the calculated versus test event sequences is contained in Table 2.1.2. The comparison plots are shown in Figures 2.1.1. through 2.1.32.

The lower initial pressurizer level resulted in earlier actuation of the second transient initiation step. After the RVVV opened the loop A hot leg flow interrupted due to the flashing liquid and the steam flow from the pressurizer. RELAP predicted this earlier due to the lower pressurizer inventory. The B loop hot leg flow continued until after the secondary levels reached the 95% mark and shut off the AFW. In the facility, the loop B flow declined sharply about 16 minutes due to the onset of saturation and subsequent reduction of the mixture level in that loop. At 18 minutes, however, the RVVVs closed for 8 minutes resulting in core generated steam accumulation in the reactor vessel upper head. The liquid from this region was displaced into the loops such that loop B circulation was enhanced. When the RVVVs re-opened the circulation in this loop abruptly halted. The RELAP calculations predicted the RVVVs remained open, resulting in much earlier loss of circulation in loop B. The discrepancy between the loop interruption times was evident in the steam generator feed and steam flow rates.

Probably the biggest difference between the calculations and the data was observed slightly after 12 minutes. The test pressure declined rapidly due to a AFW feed cycle high elevation boiler-condenser mode (BCM) of heat transfer in steam generator A. The facility AFW was terminated abruptly as the secondary level reached the control point of 31.6 feet. AFW was not re-established until 2.5 minutes later. At that time, the primary level had

dropped below the AFW injection elevation thus permitting a substantial high elevation BCM.

The RELAP AFW controller was different than its facility counterpart. It did not include automatic termination of the AFW when the level reached the shut-off control point. The level was maintained at or slightly above the control value because the proportional gain was somewhat higher. The higher level delayed the potential high elevation BCM until the loop B and the upper downcomer fluid saturation was predicted. The flashing of these regions allowed the steam generator A primary level to increase above the top of the tubes. As a result no high elevation BCM was calculated. The primary pressure remained approximately 100 psia above the test value. Contributing to these indicated differences was the lower calculated steady-state core exit temperature due to the higher loop flow rates. The RVVVs in the prediction also remained open through-out the simulation allowing the loop B flows to remain interrupted.

From 25 to 47 minutes the prediction matched the basic test behavior. During this period the hot leg and steam generator collapsed levels declined at approximately the same rate with some time shift. The major energy removal mechanism for both was accomplished by the leak-HPI cooling, although the predicted steam generator B feeding and steaming was providing extra cooling which the test did not observe. The AFW controller in the test over-filled the level near 30 minutes. As a result, no AFW flow was needed to control level until 48.5 minutes. The predicted feeding of this loop resulted in additional energy removal which depressurized the system faster than the test. The different rates reduced the earlier pressure discrepancy to within 20 psi at 47 minutes.

At 47 minutes the prediction encountered a feed cycle high elevation BCM in steam generator A. The secondary pressure had repressurized to the control pressure at 41 minutes. The resultant steaming reduced the collapsed level such that AFW was re-established to control level. Since the primary level resided within the tubes, a BCM occurred.

An identical event occurred in the test at 65 minutes. The time was shifted due to a later intersection between the steam generator A secondary pressure and the control pressure. The time shift resulted from the difference in the

secondary pressure behavior. In the prediction a slow repressurization was calculated, while the test slowly depressurized. A leaking steam valve in the facility and steam line heat losses are blamed. The RELAP model did not include these heat losses which were estimated to be as high as several kilowatts.

Both steam generators eventually locked into alternate feed cycle high elevation BCMs both predicted and realized. The resultant condensation accelerated the primary depressurization toward the secondary control pressure. The calculations ended in this mode of cooling.

Table 2.1.2. MIST Test 3109AA Sequence of Events Comparisons

Event	Approximate Test Time (Min)	
	RELAP	Data
Scaled 10-cm <sup>2</sup> CLPD Leak Opened	0.0	0.0
Pressurizer Level to 1.0 ft: Initiate Core Power Ramp, HPI, RVVV Automatic Control, SG Secondary Refill and Depressurization	0.9	2.1
Hot Leg A Flow Interruption	2.5	3.8
SG A High Elevation BCM Started	6.7	8.0
SG Secondary Level to 31.6 Feet	8.3	9.8
Hot Leg B Flow Interruption	13.3	17.0
Complete Loss of Natural Circulation	17.5	26.0
Feed Cycle BCM Started	47.1	65.0
Primary System Refill Began	51.3	66.0
Calculations Terminated	66.7	--

2.1.3. MIST Test 3109AA Pretest Conclusions

The pretest prediction of the nominal test 3109AA was quite reasonable. The major system trends were predicted as expected with the obvious exception of the BCM at 12 minutes. Slight differences in the initial conditions, AFW controller, and the RVVV behavior contributed to this effect. Even during facility reruns of identical MIST 31 series tests, differences similar to

those between the predicted and measured were observed. Given the conditions calculated by RELAP the system behavior appeared reasonable and correct. The timing phase shifts for the later portions of the predictions were a result of secondary boundary conditions which were unknown at the time of the RELAP simulation.

PRETEST BENCHMARK COMPARISONS  
MIST Nominal Test, Observed Vs. Predicted - 3109AA

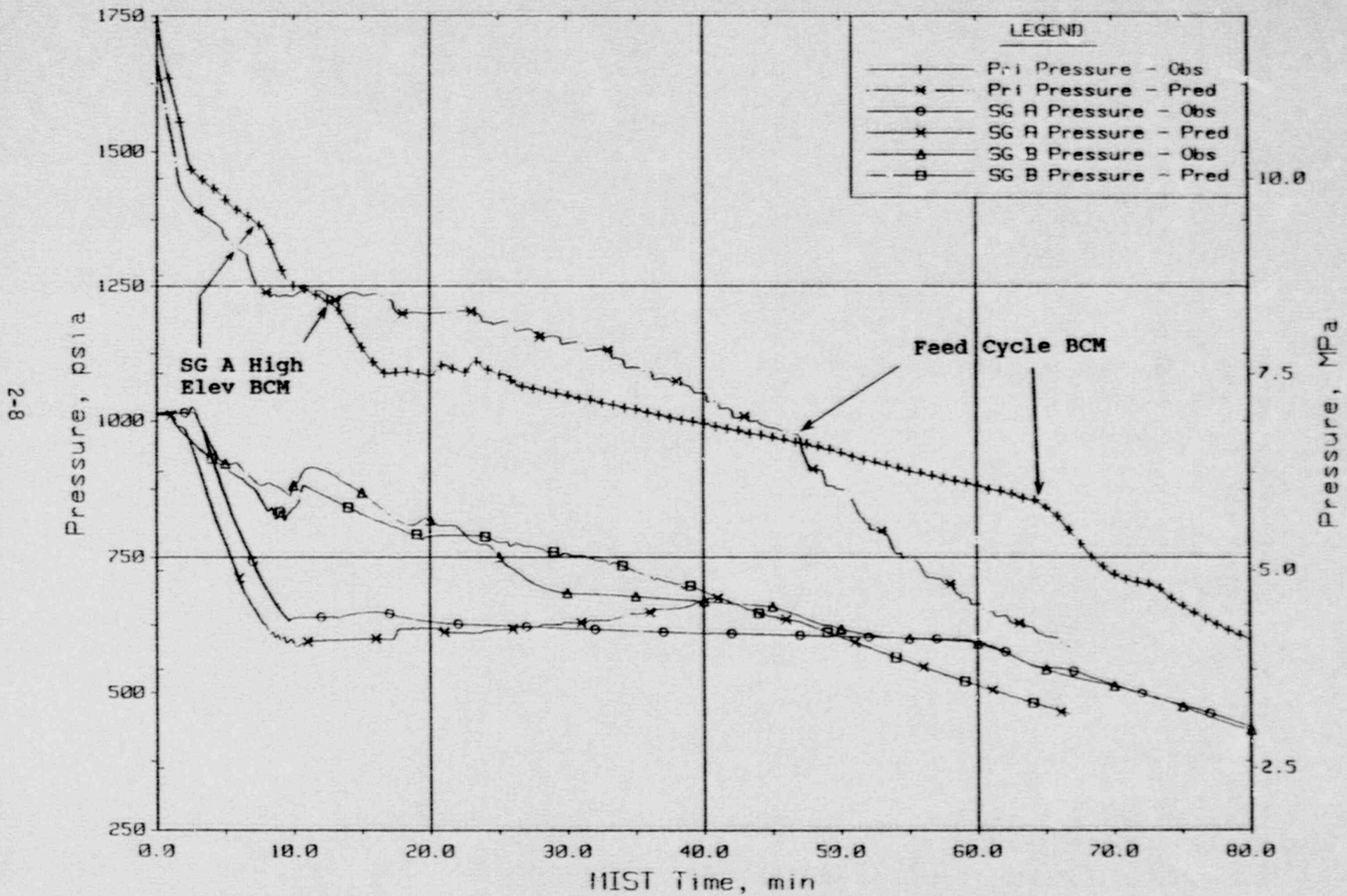


Figure 2.1.1. System Pressures.



PRETEST BENCHMARK COMPARISONS  
MIST Nominal Test, Observed Vs. Predicted - 3109AA

2-9

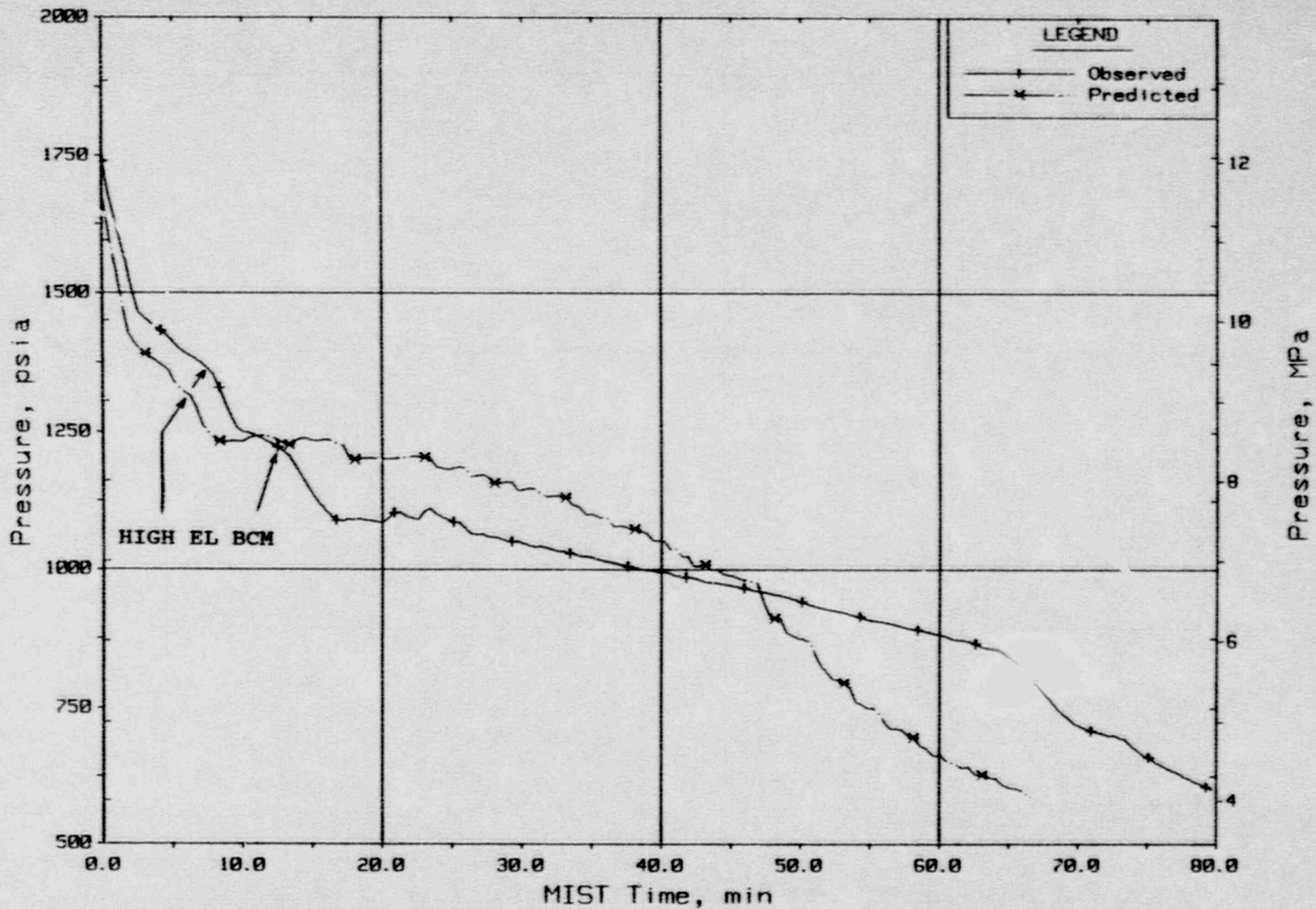


Figure 2.1.2. Reactor Vessel Pressure.

PRETEST BENCHMARK COMPARISONS  
 MIST Nominal Test, Observed Vs. Predicted - 3109AA

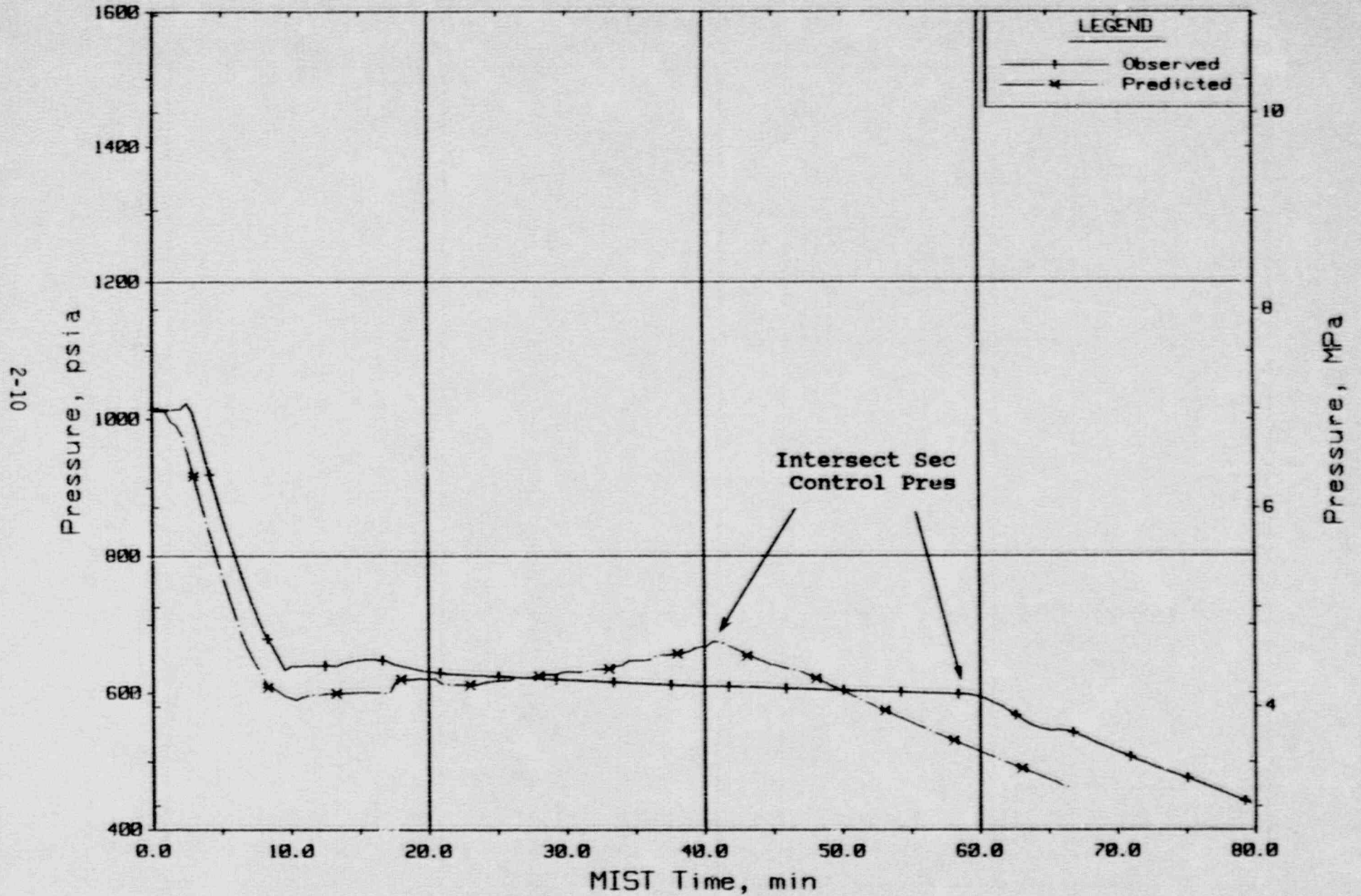


Figure 2.1.3. Steam Generator A Secondary Pressure.

PRETEST BENCHMARK COMPARISONS  
MIST Nominal Test, Observed Vs. Predicted - 3109AA

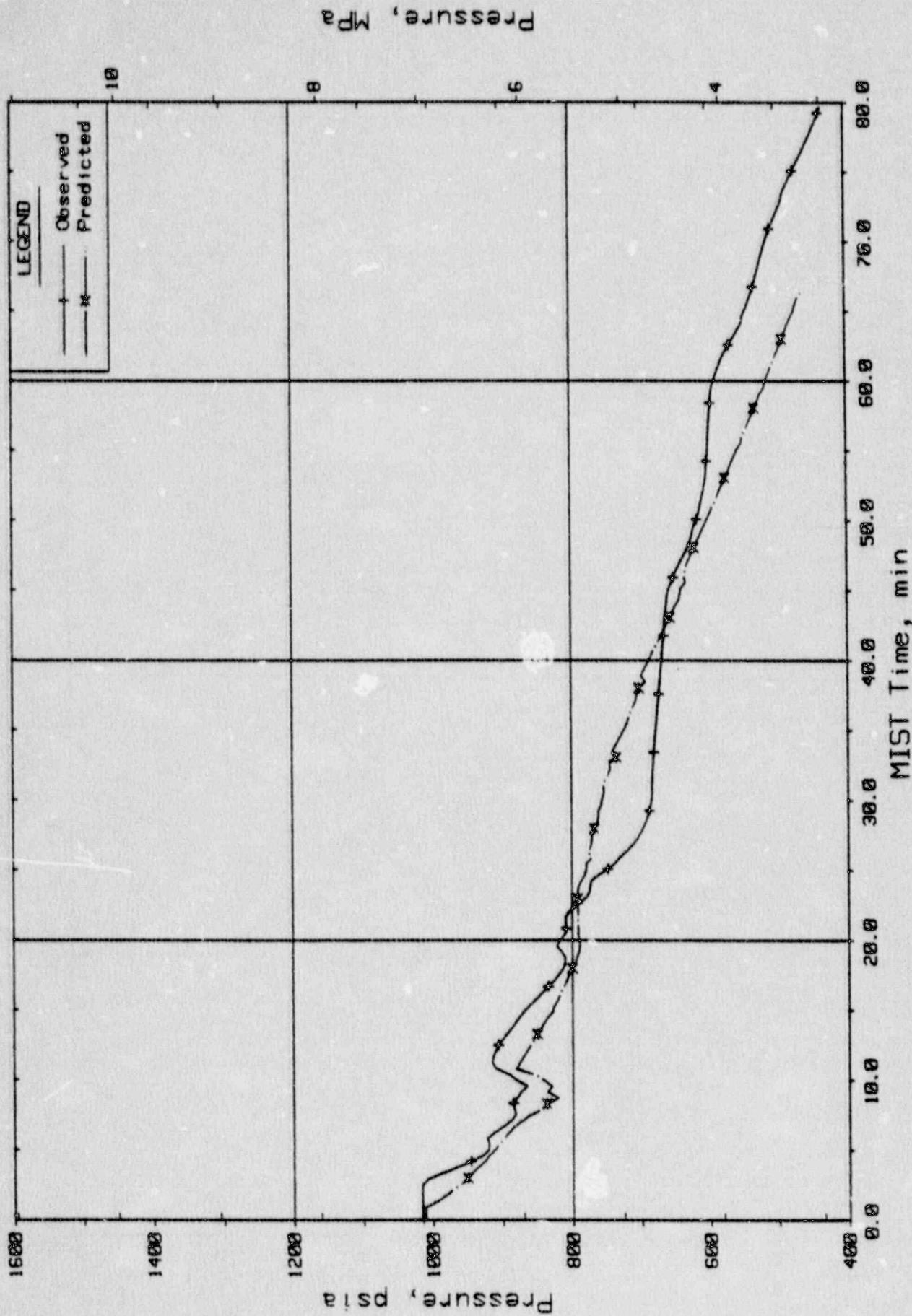


Figure 2.1.4. Steam Generator B Secondary Pressure.

Cs2gp01

Wed Apr 1 19:19:47 1987

PRETEST BENCHMARK COMPARISONS  
MIST Nominal Test, Observed Vs. Predicted - 3109AA

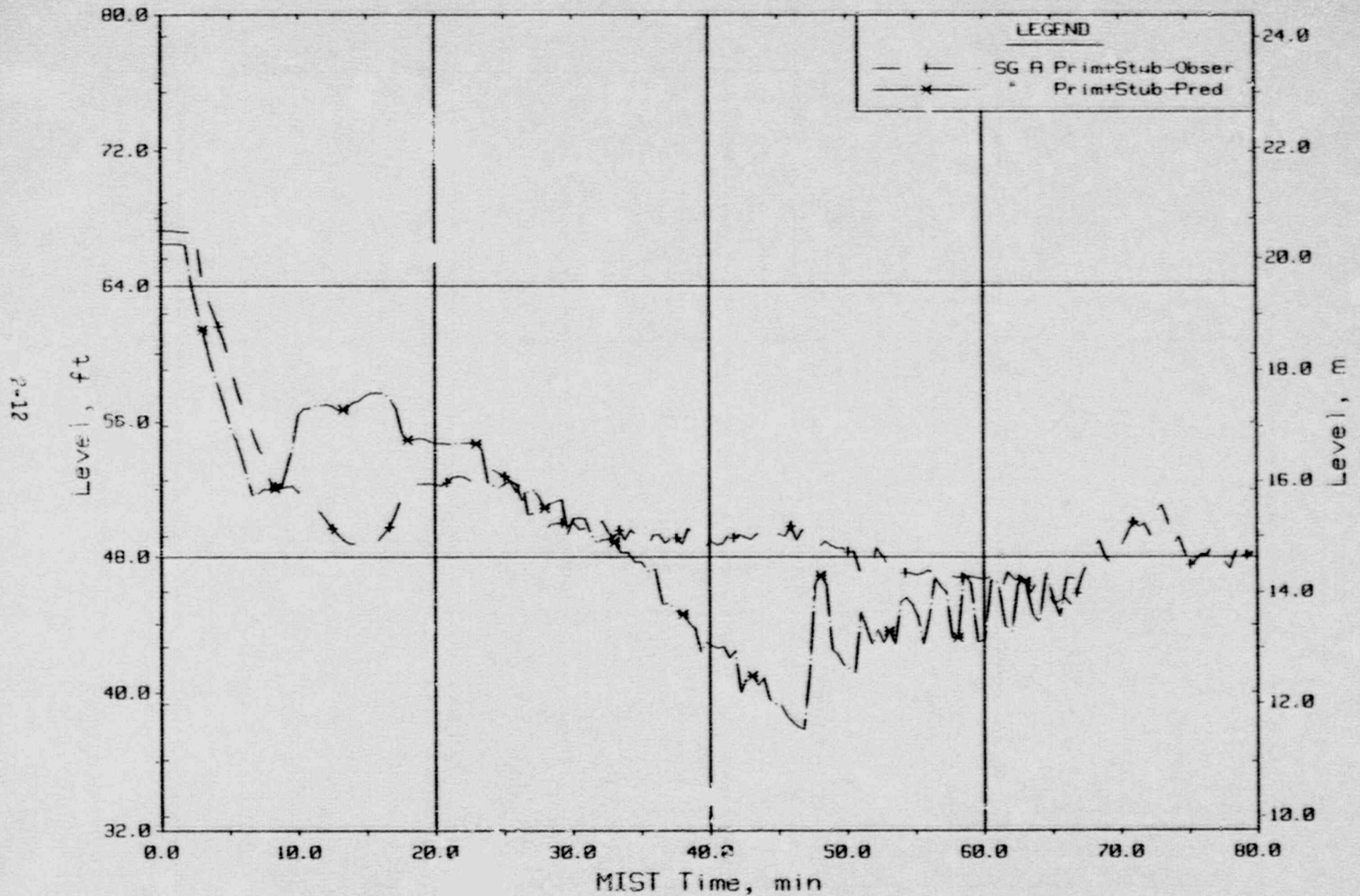


Figure 2.1.5. Steam Generator A Primary + Stub Level.

PRETEST BENCHMARK COMPARISONS  
MIST Nominal Test, Observed Vs. Predicted - 3109AA

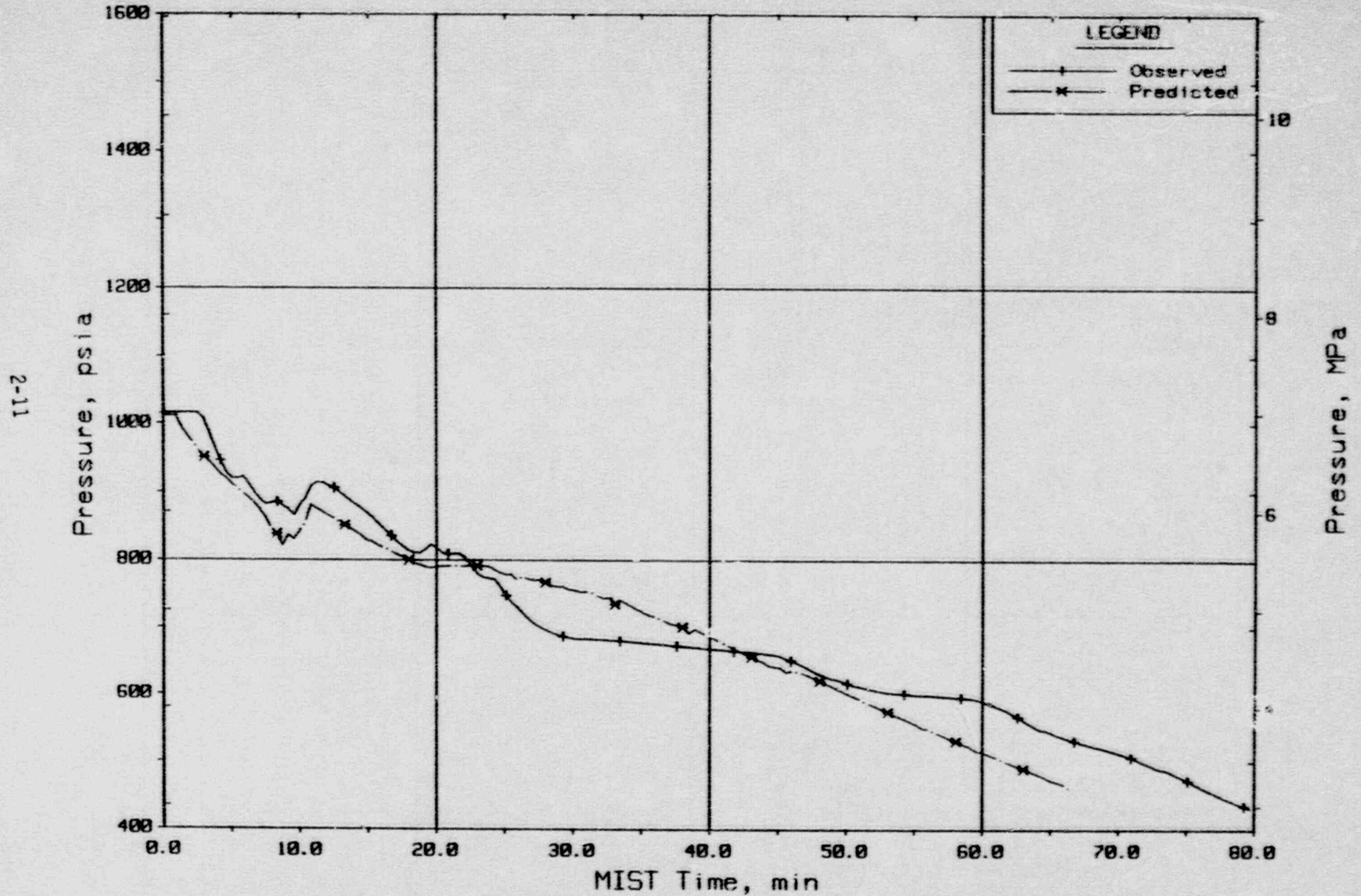


Figure 2.1.4. Steam Generator B Secondary Pressure.

PRETEST BENCHMARK COMPARISONS  
 MIST Nominal Test, Observed Vs. Predicted - 3109AA

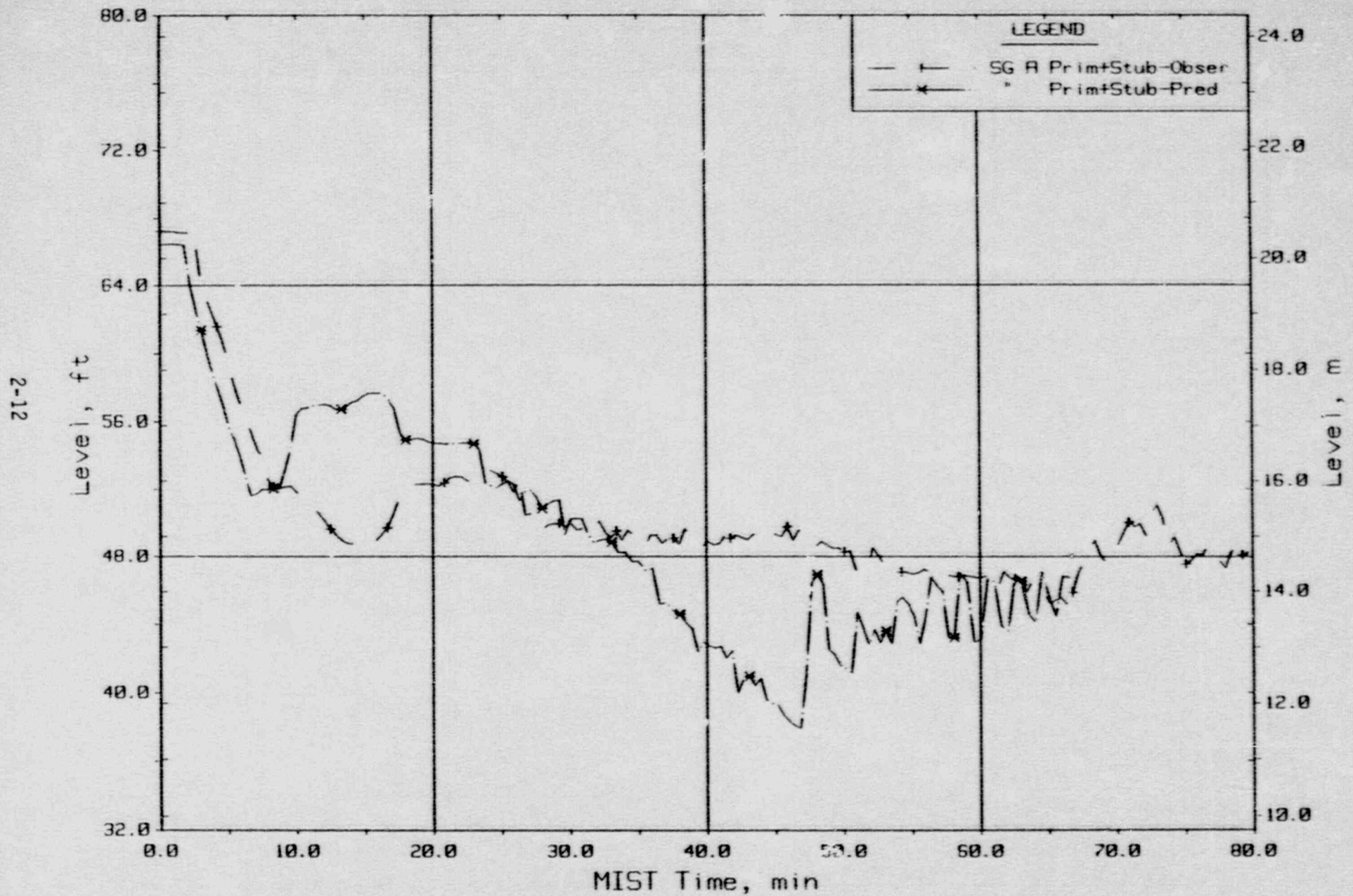


Figure 2.1.5. Steam Generator A Primary + Stub Level.

PRETEST BENCHMARK COMPARISONS  
MIST Nominal Test, Observed Vs. Predicted - 3109AA

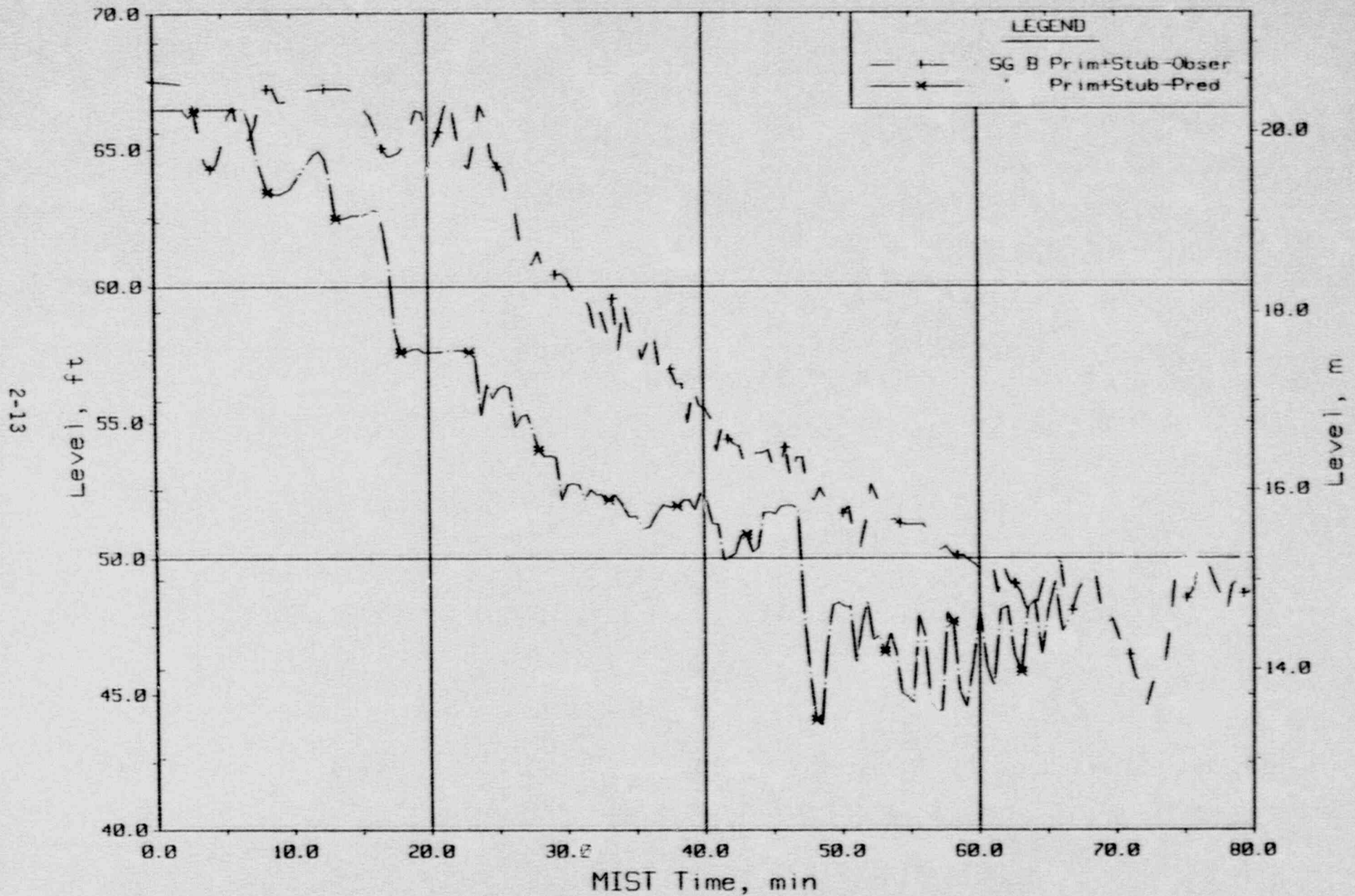


Figure 2.1.6. Steam Generator B Primary + Stub Level.

PRETEST BENCHMARK COMPARISONS  
 MIST Nominal Test, Observed Vs. Predicted - 3109AA

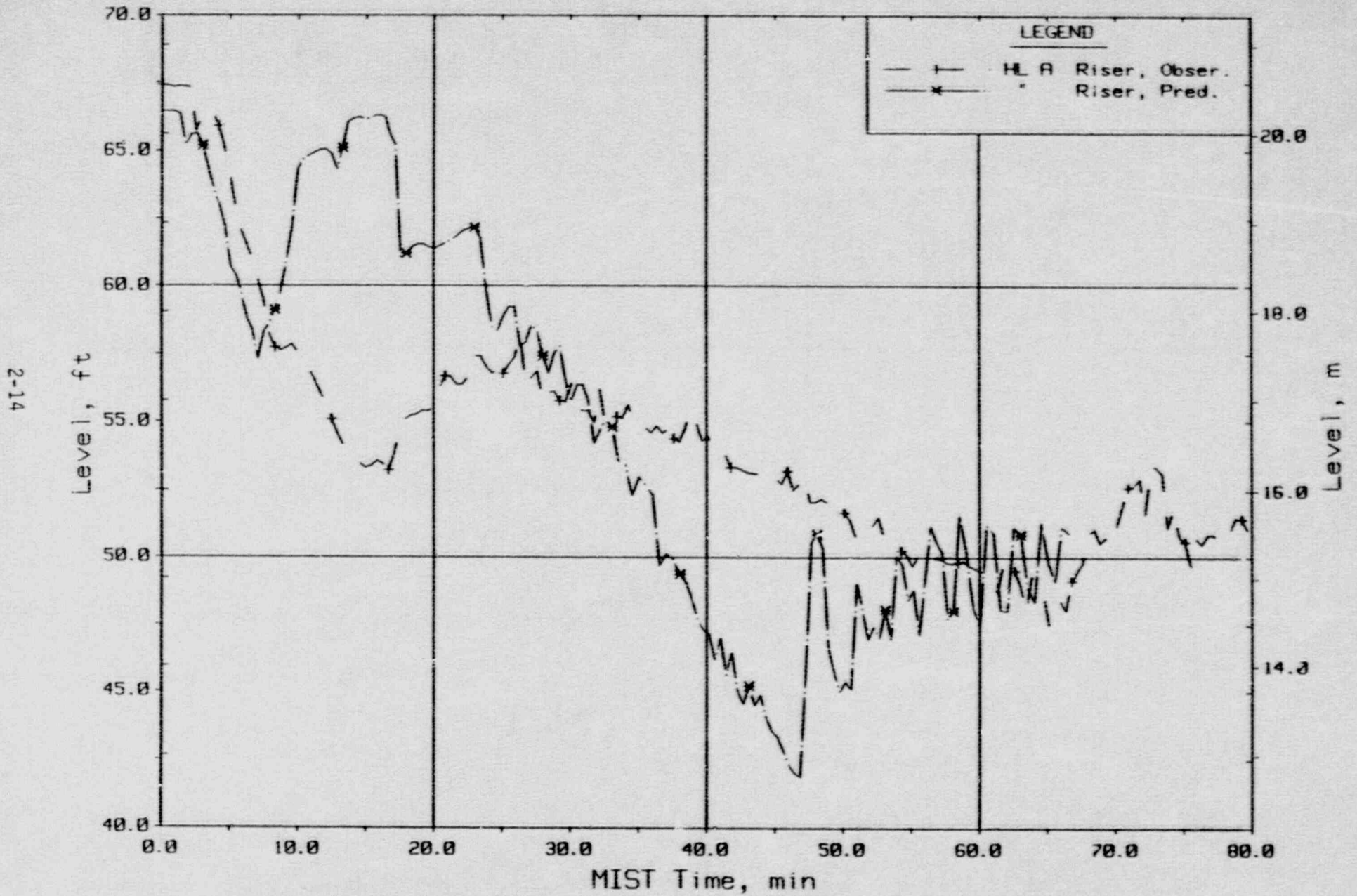


Figure 2.1.7. Hot Leg A Riser Level.



PRETEST BENCHMARK COMPARISONS  
MIST Nominal Test, Observed Vs. Predicted - 3109AA

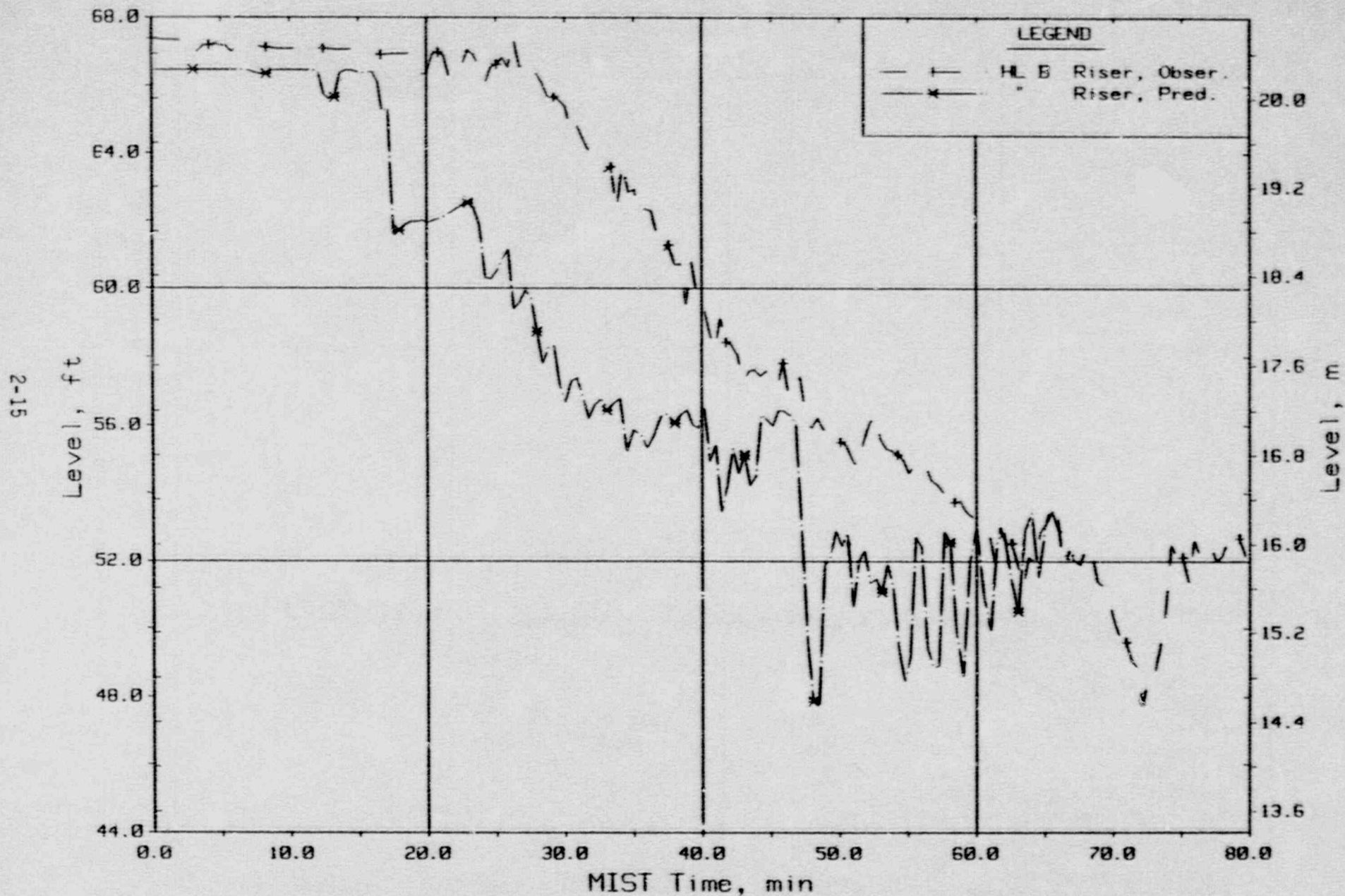


Figure 2.1.8. Hot Leg B Riser Level.

PRETEST BENCHMARK COMPARISONS  
MIST Nominal Test, Observed Vs. Predicted - 3109AA

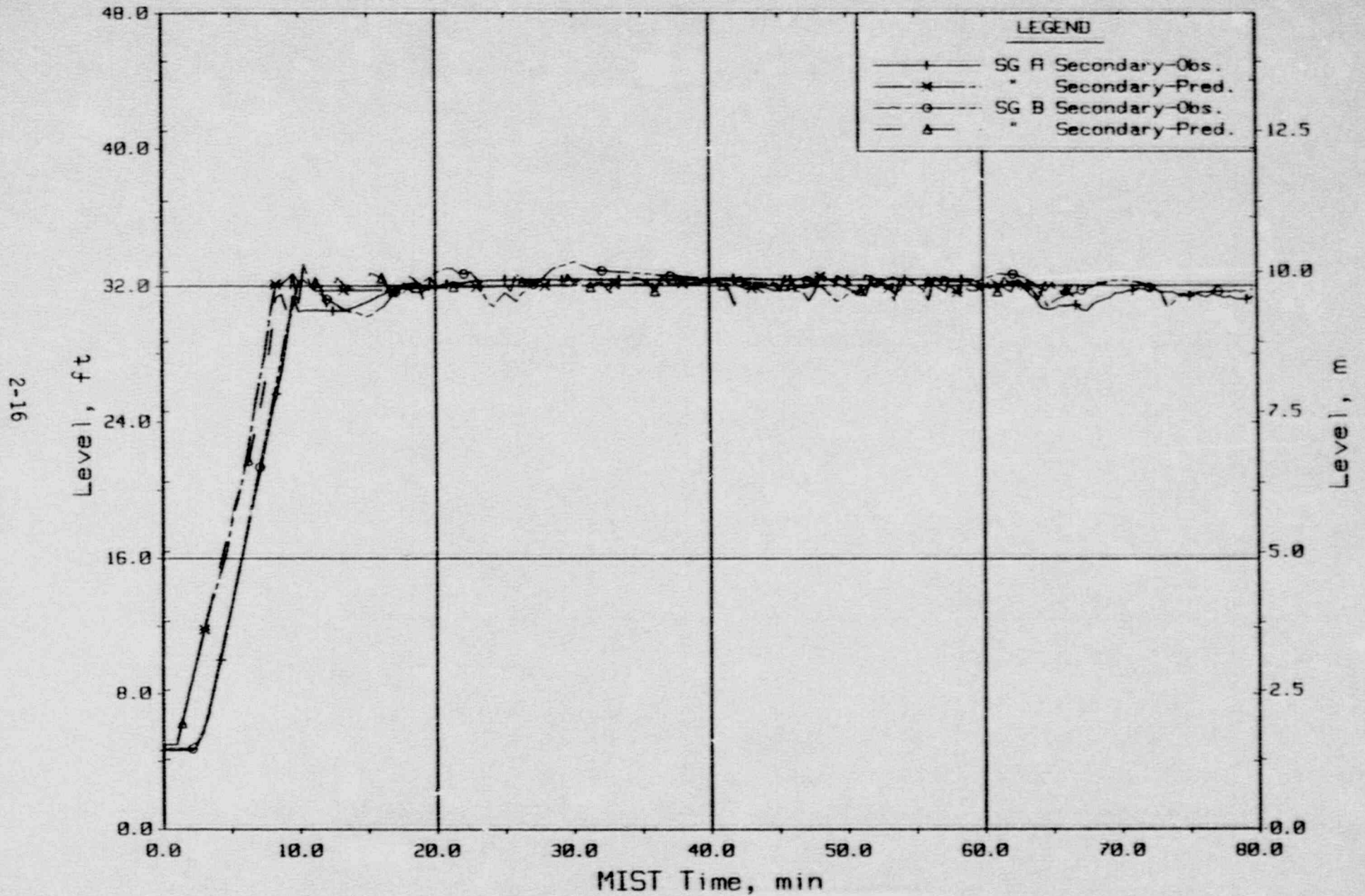


Figure 2.1.9. Steam Generator Sec. Collapsed Liquid Levels.

PRETEST BENCHMARK COMPARISONS  
MIST Nominal Test, Observed Vs. Predicted - 3109AA

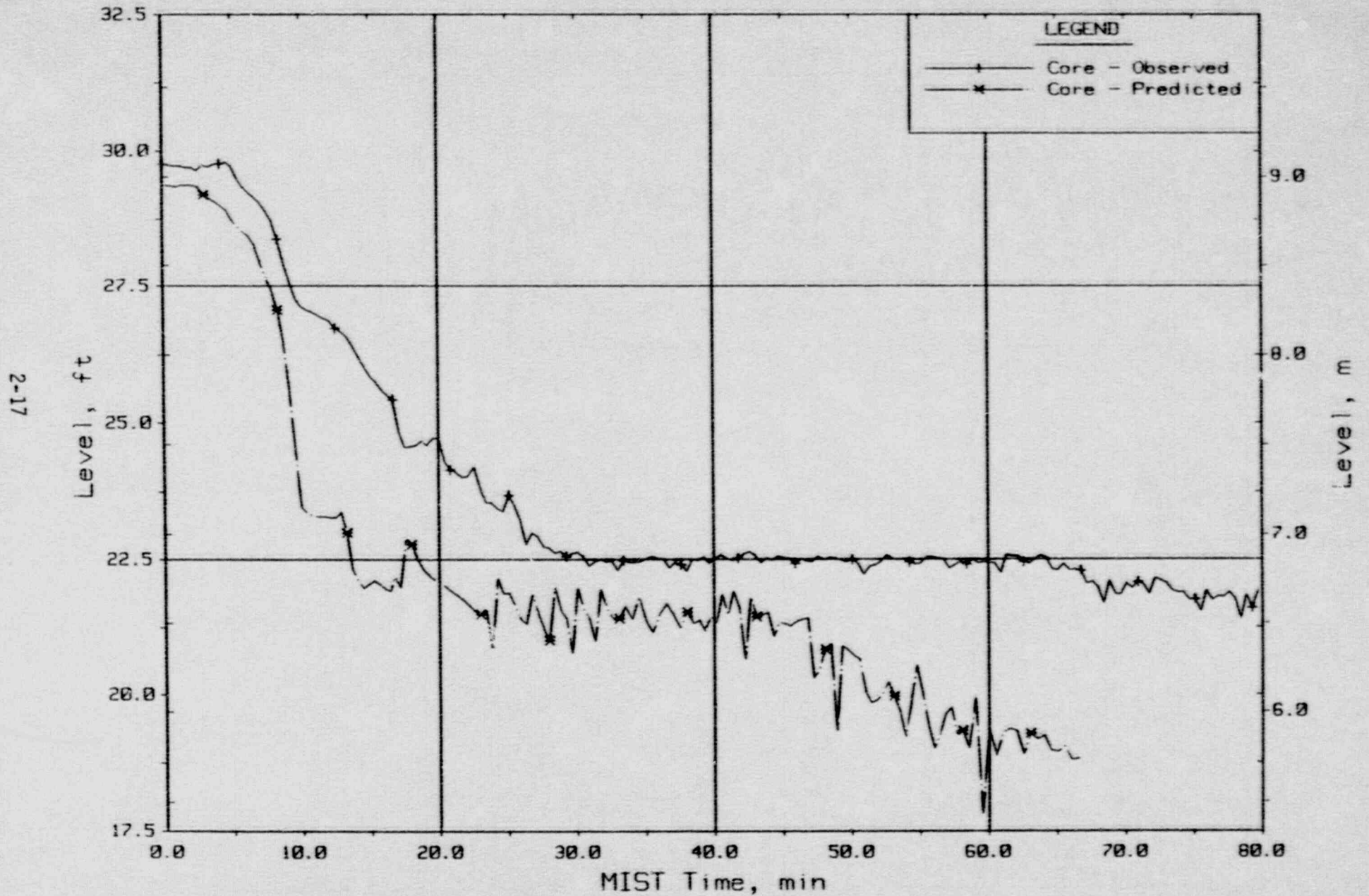


Figure 2.1.10. Core Region Collapsed Liquid Levels.

PRETEST BENCHMARK COMPARISONS  
MIST Nominal Test, Observed Vs. Predicted - 3109AA

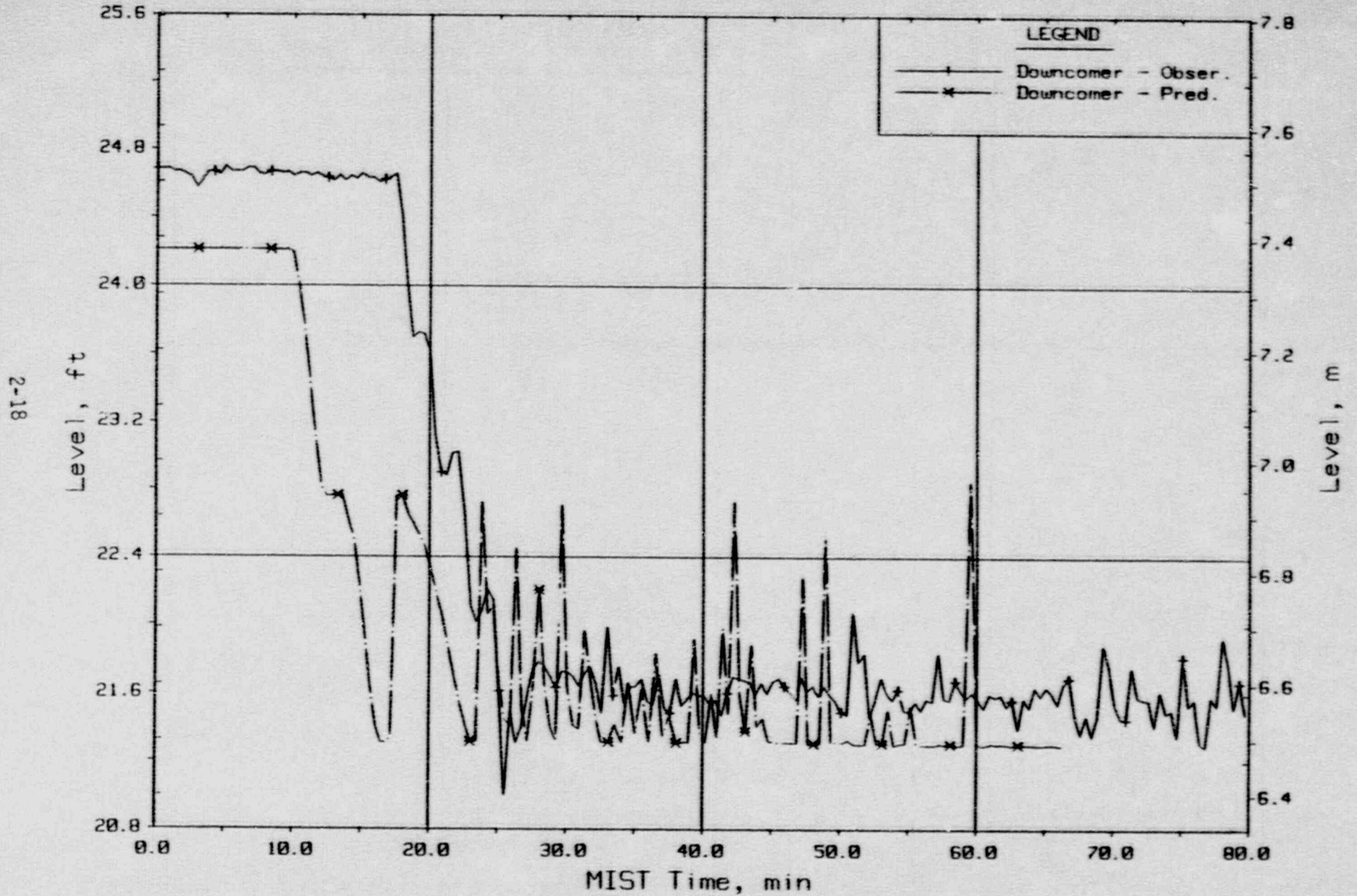


Figure 2.1.11. Core Region Collapsed Liquid Levels.

PRETEST BENCHMARK COMPARISONS  
 MIST Nominal Test, Observed Vs. Predicted - 3109AA

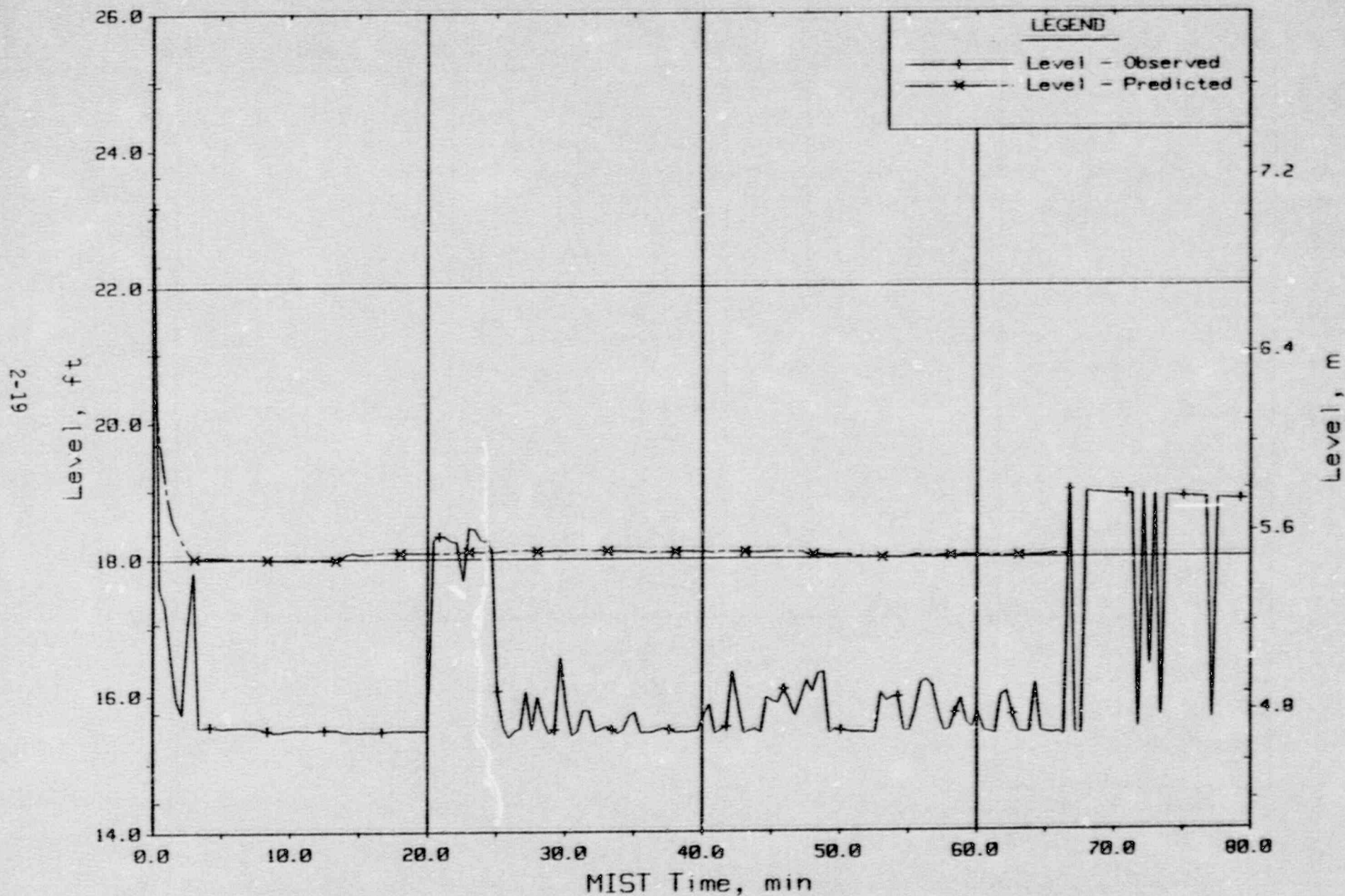


Figure 2.1.12. Pressurizer Collapsed Liquid Level (PZLV20).

PRETEST BENCHMARK COMPARISONS  
 MIST Nominal Test, Observed Vs. Predicted - 3109AA

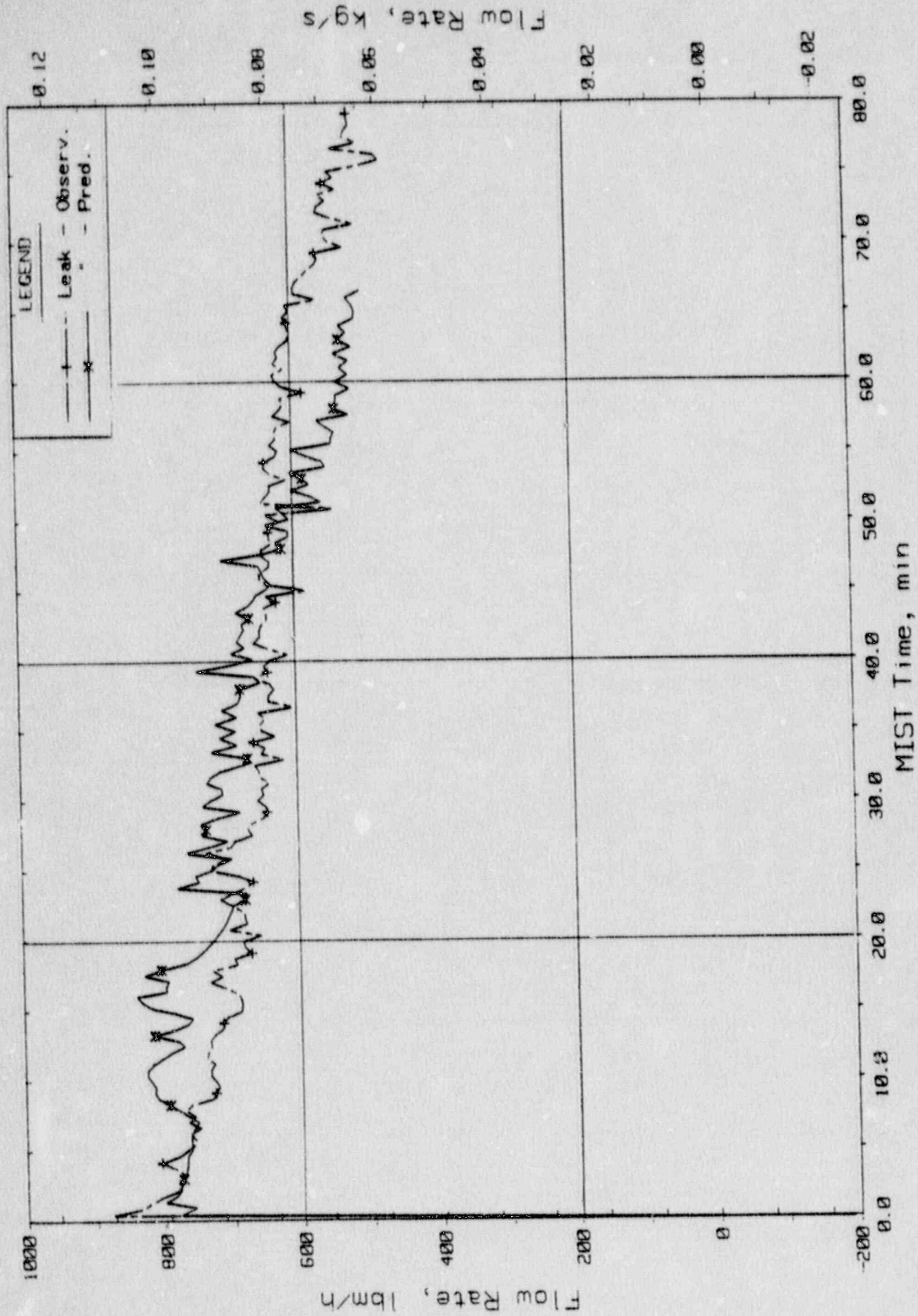


Figure 2.1.13. Primary System Boundary Flow Rates.

PRETEST BENCHMARK COMPARISONS  
 MIST Nominal Test, Observed Vs. Predicted - 3109AA

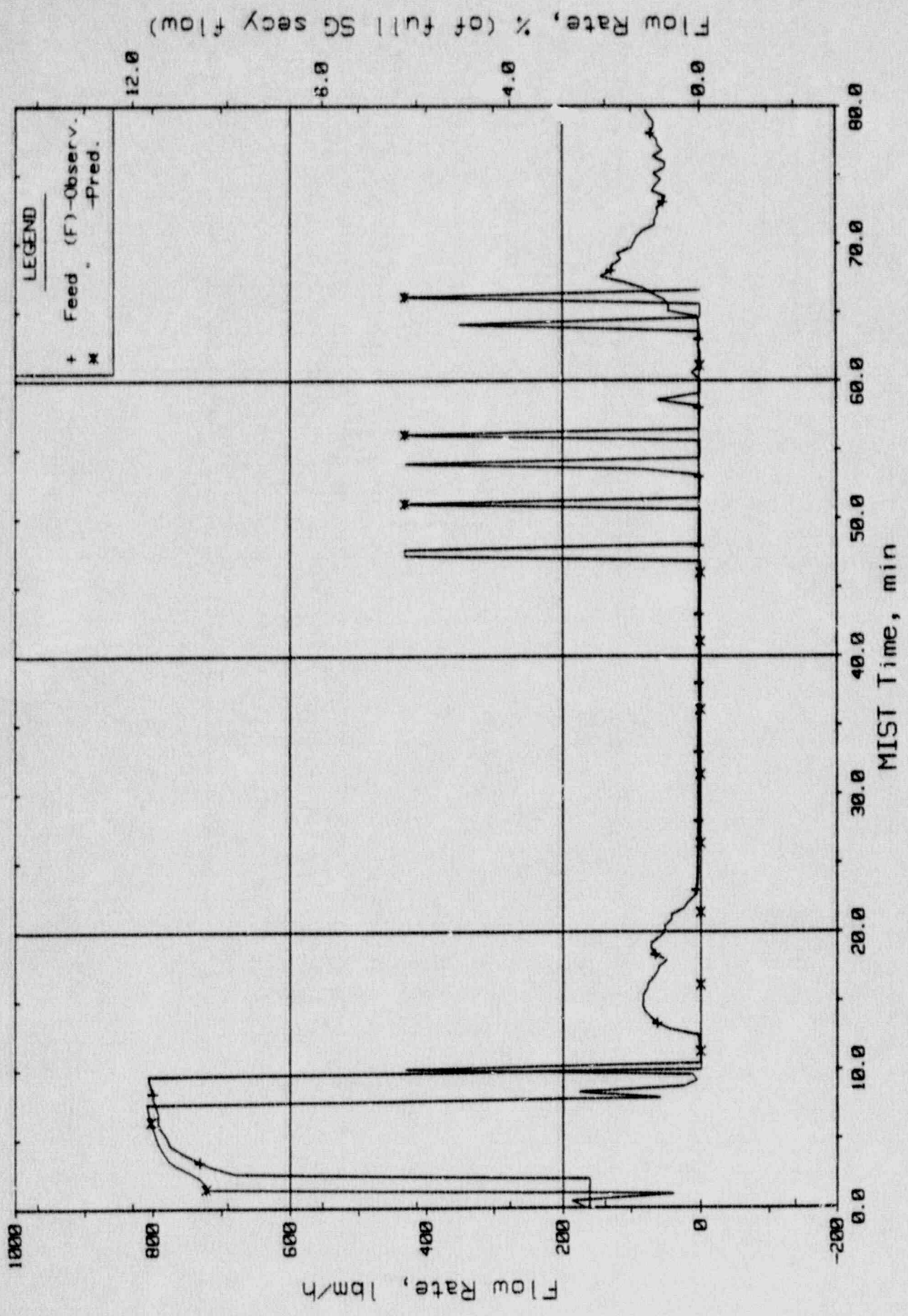


Figure 2.1.14. Steam Generator A Flow Rate (Ssfor20).

PRETEST BENCHMARK COMPARISONS  
 MIST Nominal Test, Observed Vs. Predicted - 3109AA

2-22

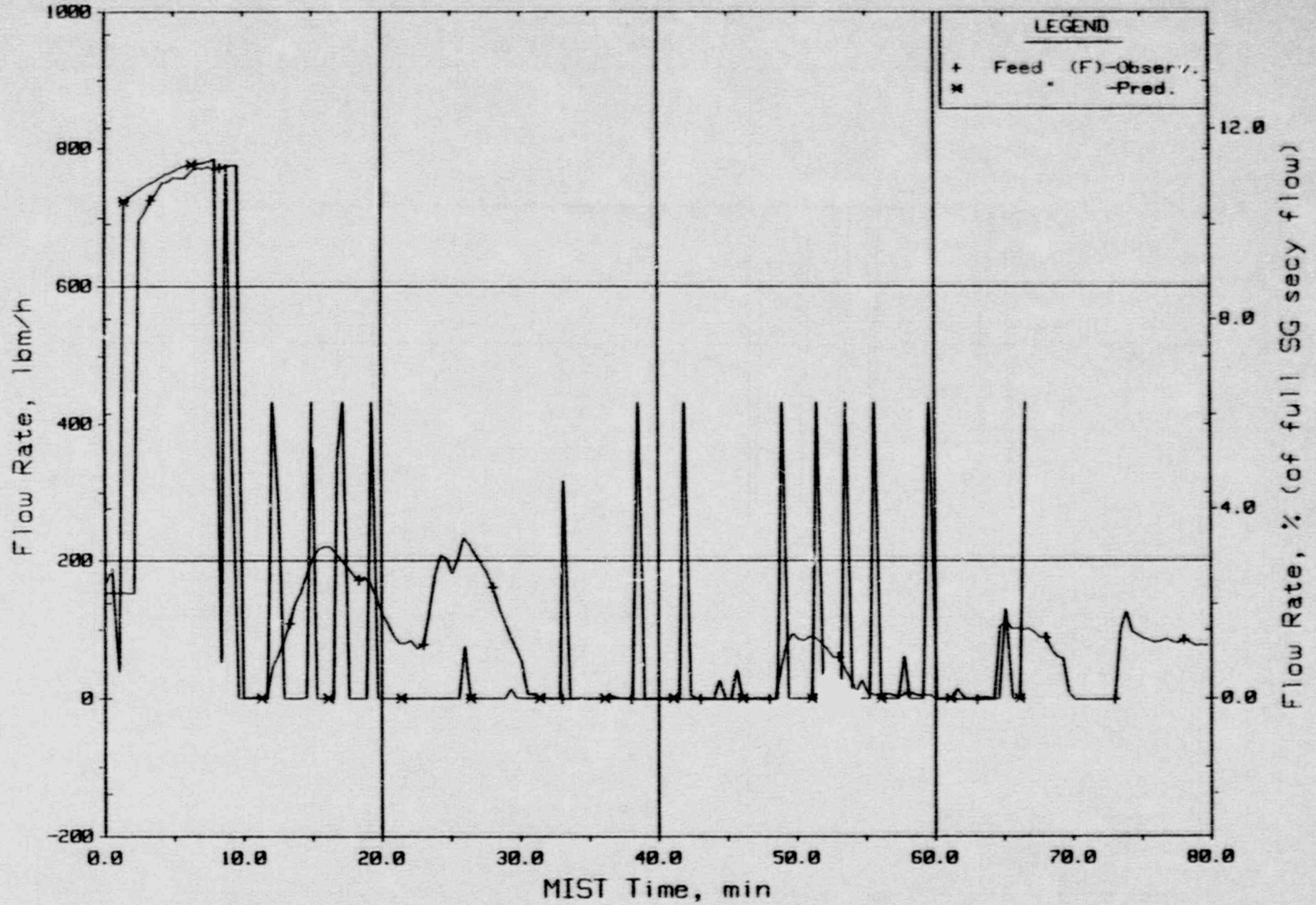


Figure 2.1.15. Steam Generator B Flow Rate (Ssfor21).



PRETEST BENCHMARK COMPARISONS  
MIST Nominal Test, Observed Vs. Predicted - 3109AA

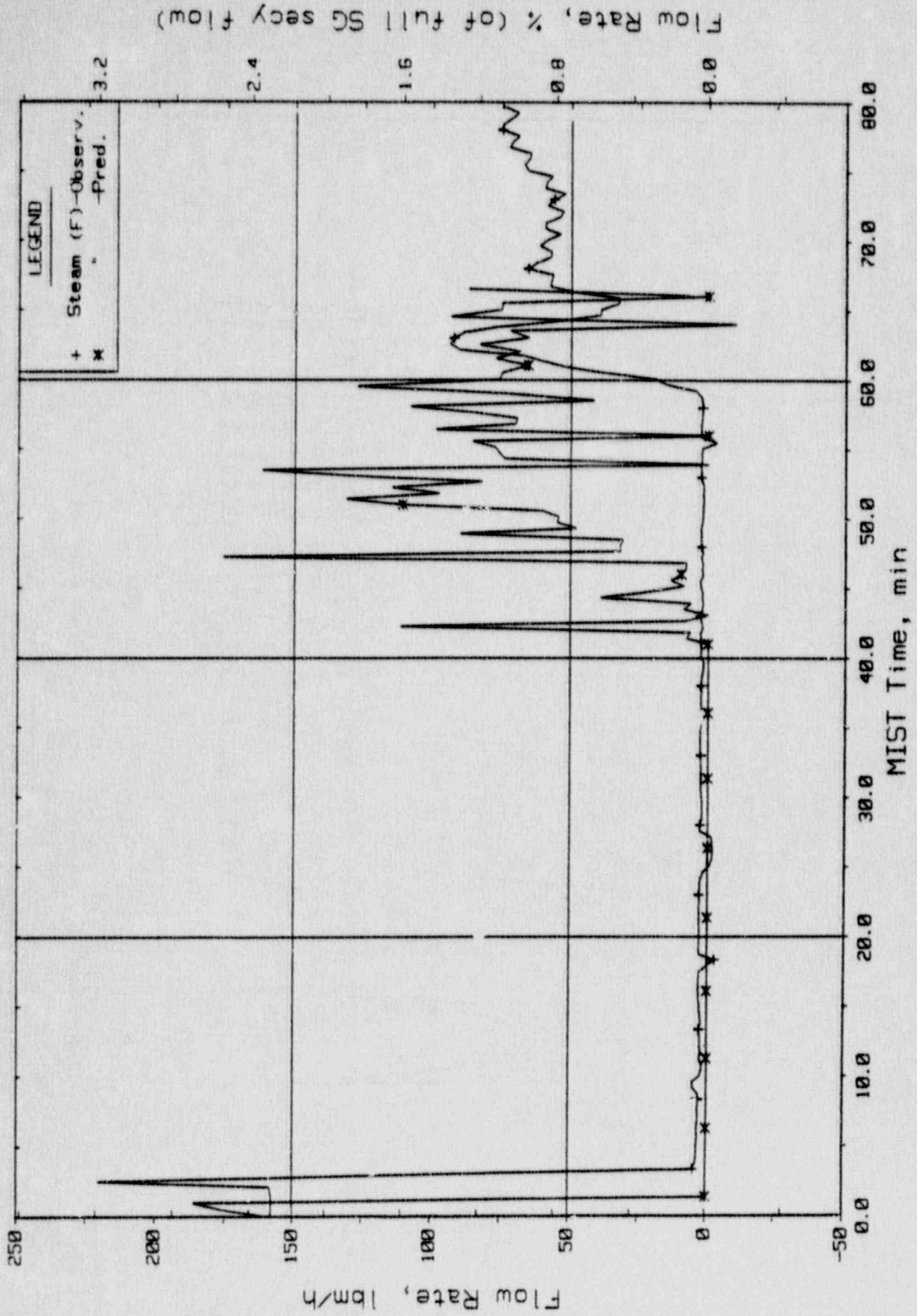


Figure 2.1.16. Steam Generator A Flow Rates (Sssor20).

PRETEST BENCHMARK COMPARISONS  
MIST Nominal Test, Observed Vs. Predicted - 3109AA

2-24

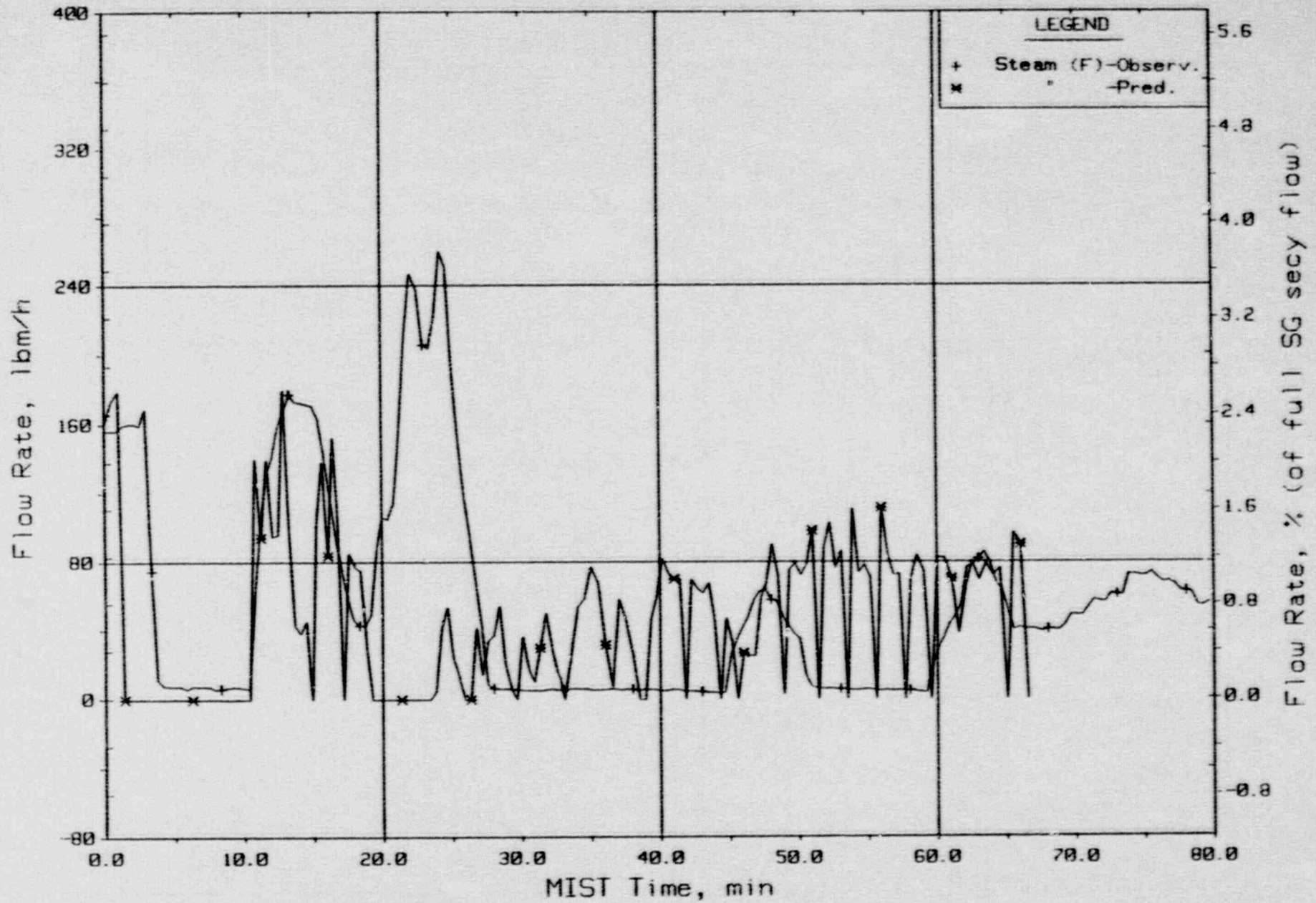


Figure 2.1.17. Steam Generator B Flow Rates (Sssor21).

PRETEST BENCHMARK COMPARISONS  
 MIST Nominal Test, Observed Vs. Predicted - 31090A

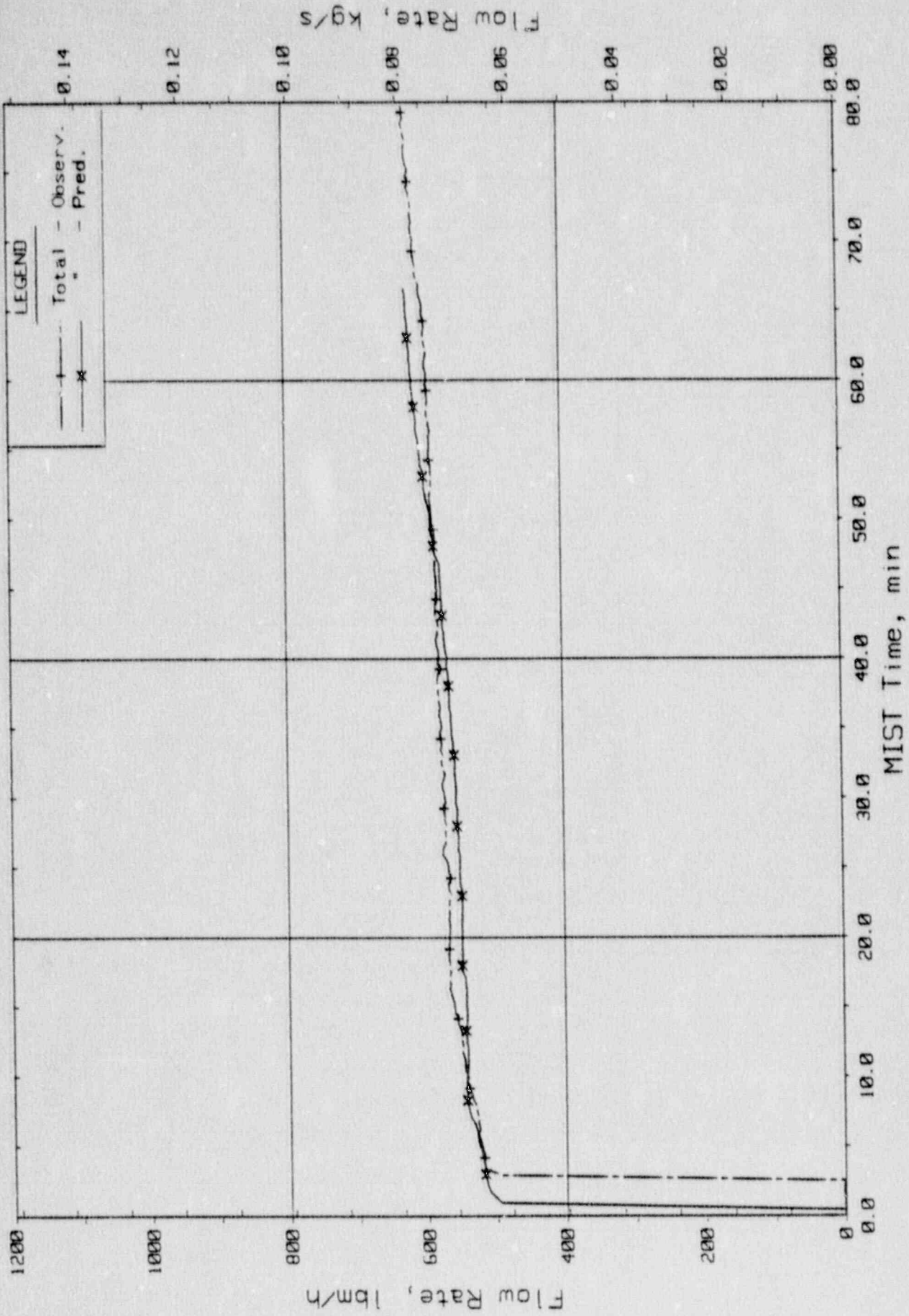


Figure 2.1.18. HPI Total Flow Rates.

PRETEST BENCHMARK COMPARISONS  
MIST Nominal Test, Observed Vs. Predicted - 3109AA

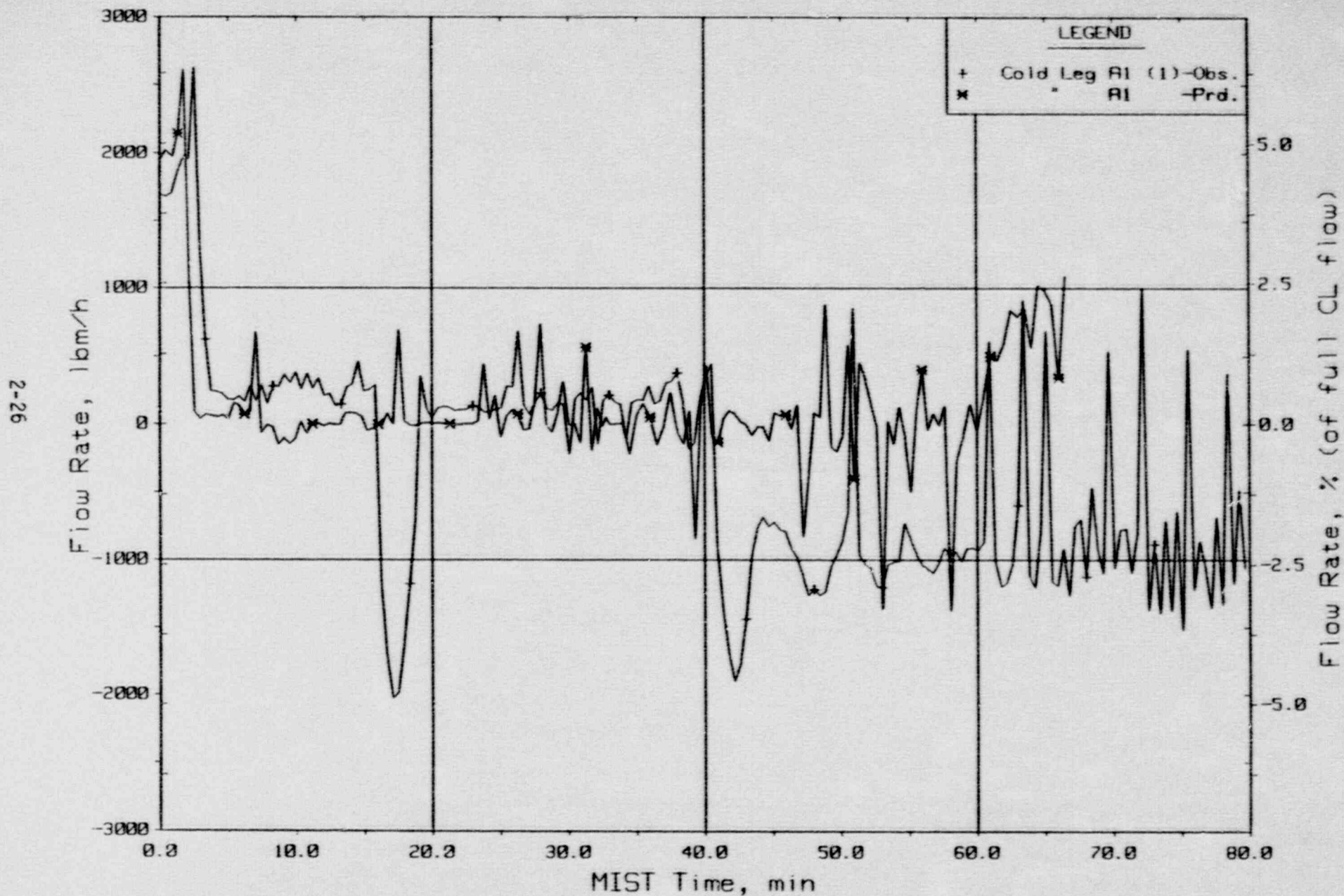


Figure 2.1.19. Loop AI Cold Leg (Venturi) Flow Rate (C1VN20).

PRETEST BENCHMARK COMPARISONS  
 MIST Nominal Test, Observed Vs. Predicted - 3109AA

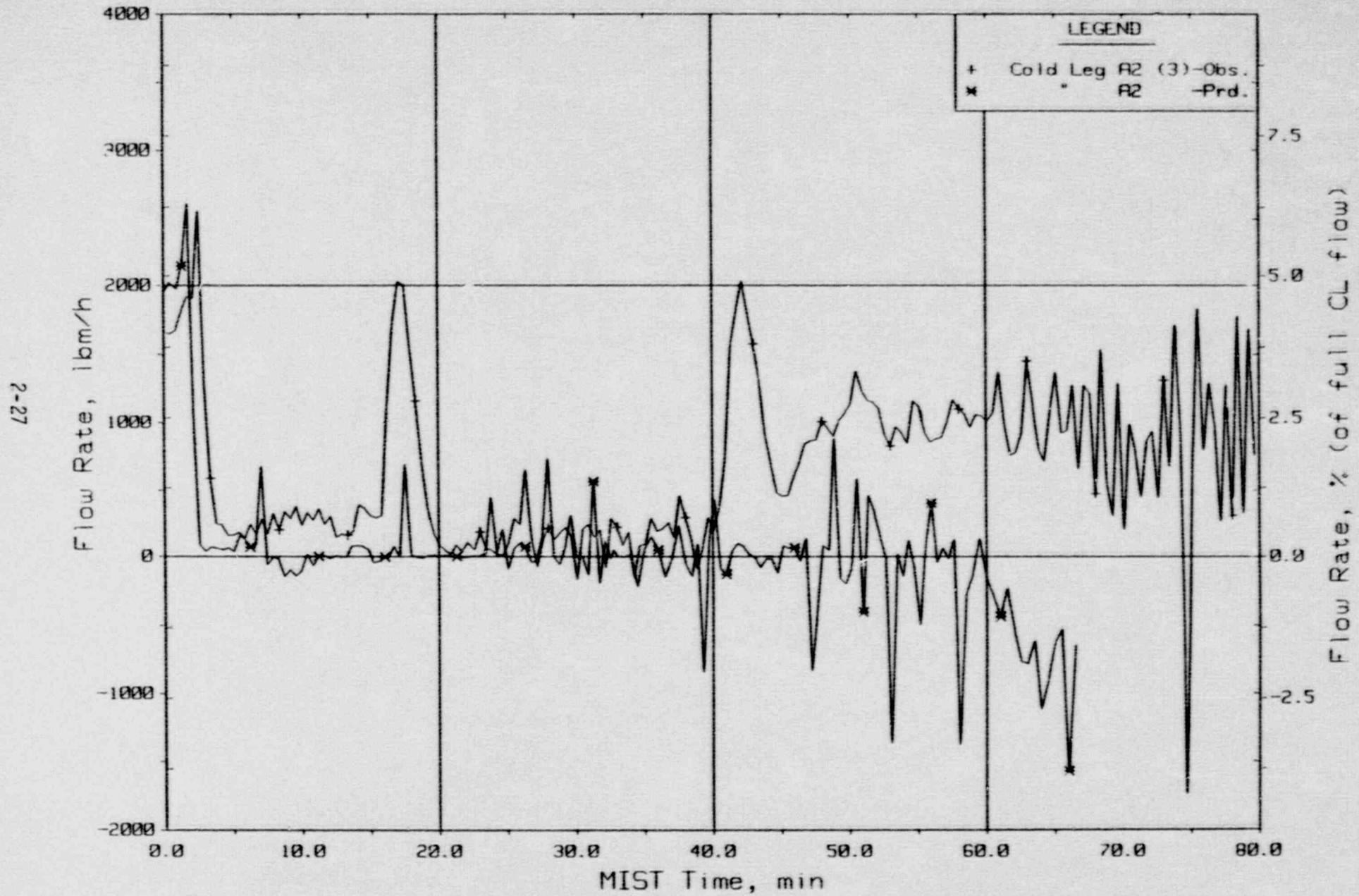


Figure 2.1.20. Loop A2 Cold Leg (Venturi) Flow Rate (C2VN20).

PRETEST BENCHMARK COMPARISONS  
MIST Nominal Test, Observed Vs. Predicted - 3109AA

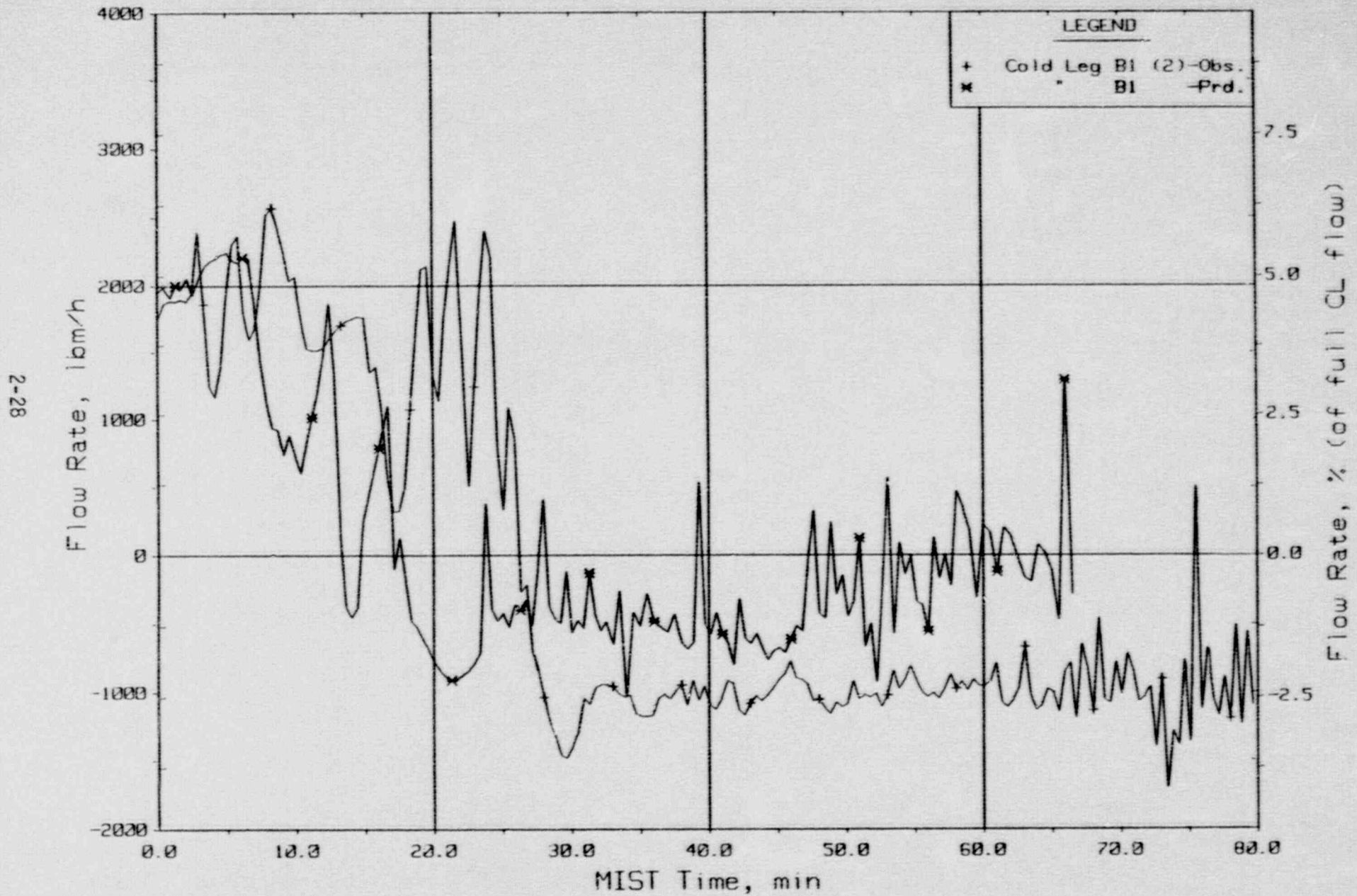


Figure 2.1.21. Loop BI Cold Leg (Venturi) Flow Rate (C1VN20).

PRETEST BENCHMARK COMPARISONS  
MIST Nominal Test, Observed Vs. Predicted - 3109AA

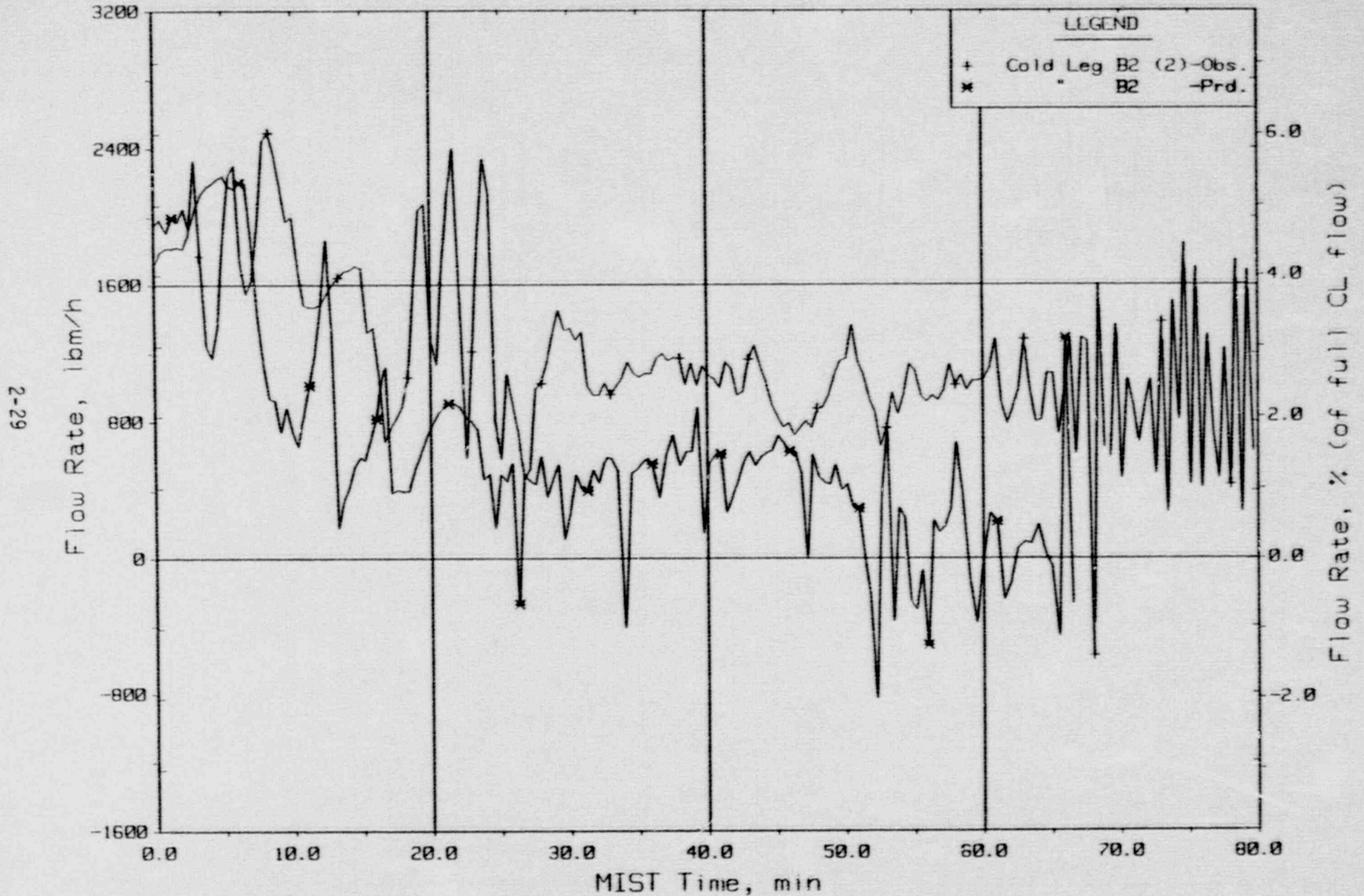


Figure 2.1.22. Loop B2 Cold Leg (Venturi) Flow Rate (C4VN20).

PRETEST BENCHMARK COMPARISONS

MIST Nominal Test, Observed Vs. Predicted - 3109AA

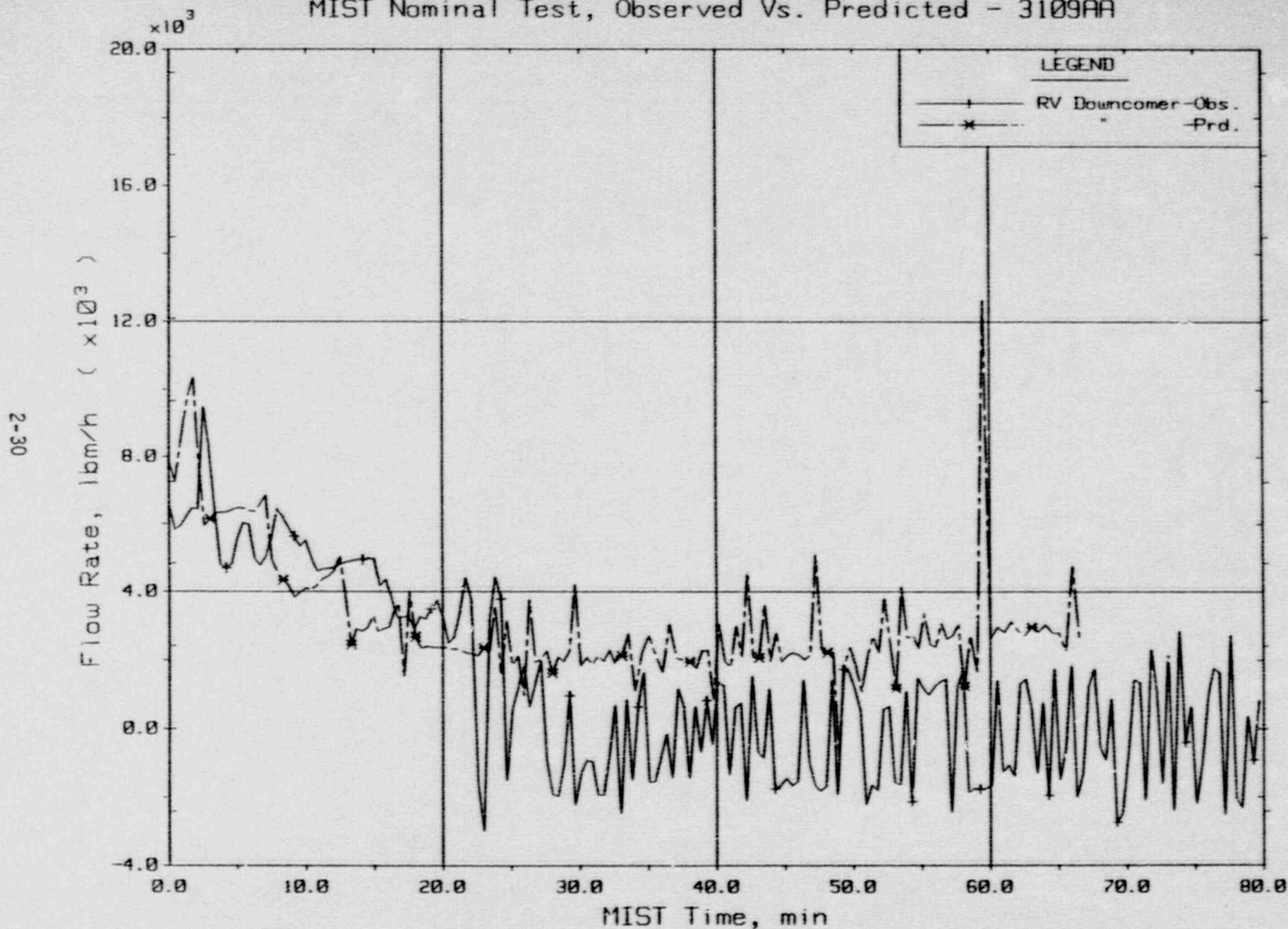


Figure 2.1.23. Primary System Venturi Flow Rates.



PRETEST BENCHMARK COMPARISONS  
 MIST Nominal Test, Observed Vs. Predicted - 3109AA

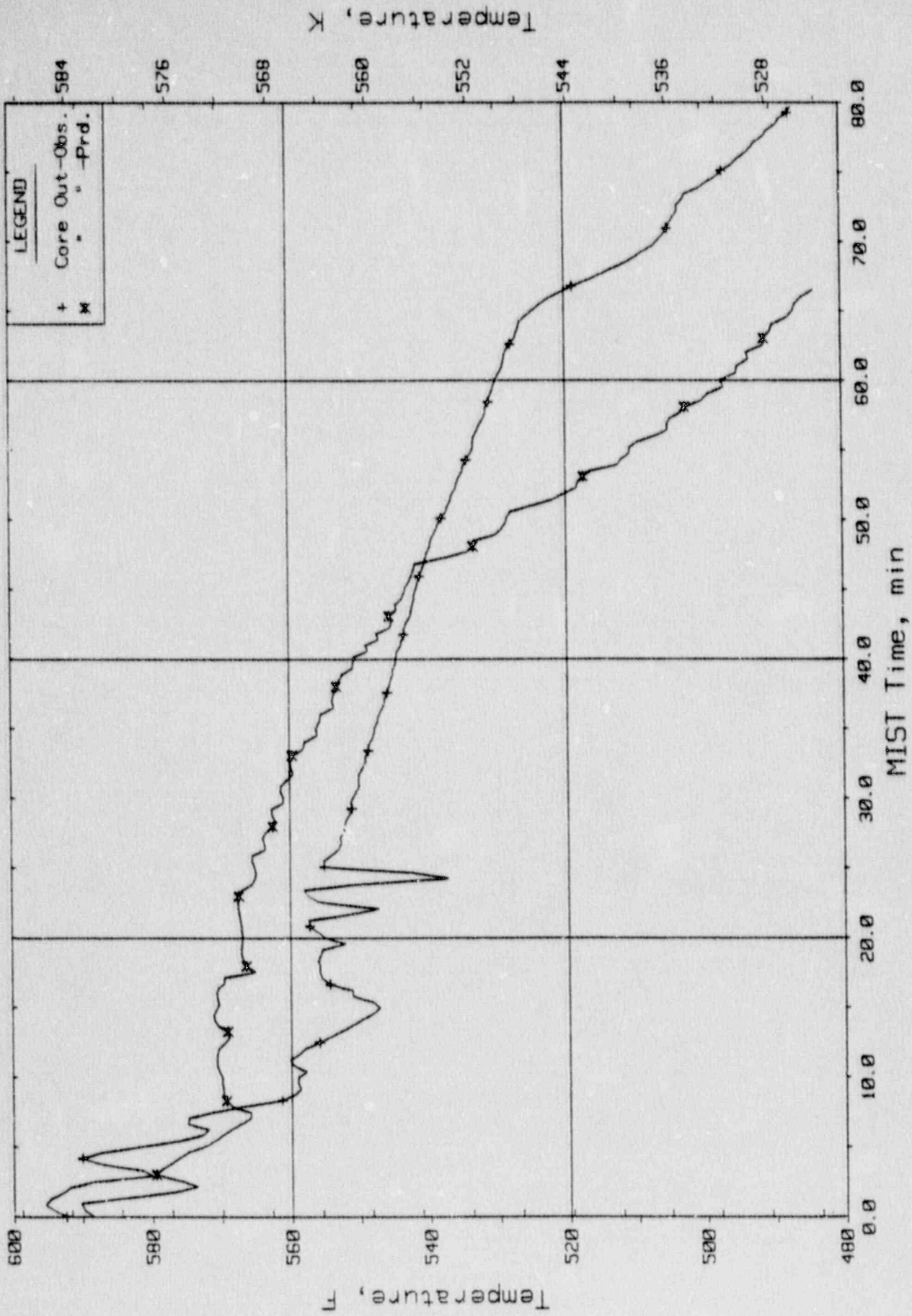


Figure 2.1.24. Core Exit Reactor Vessel Fluid Temperature (RVTC11).

Crvt11

Hard Apr 1 20:20:45 1987

PRETEST BENCHMARK COMPARISONS  
MIST Nominal Test, Observed Vs. Predicted - 3109AA

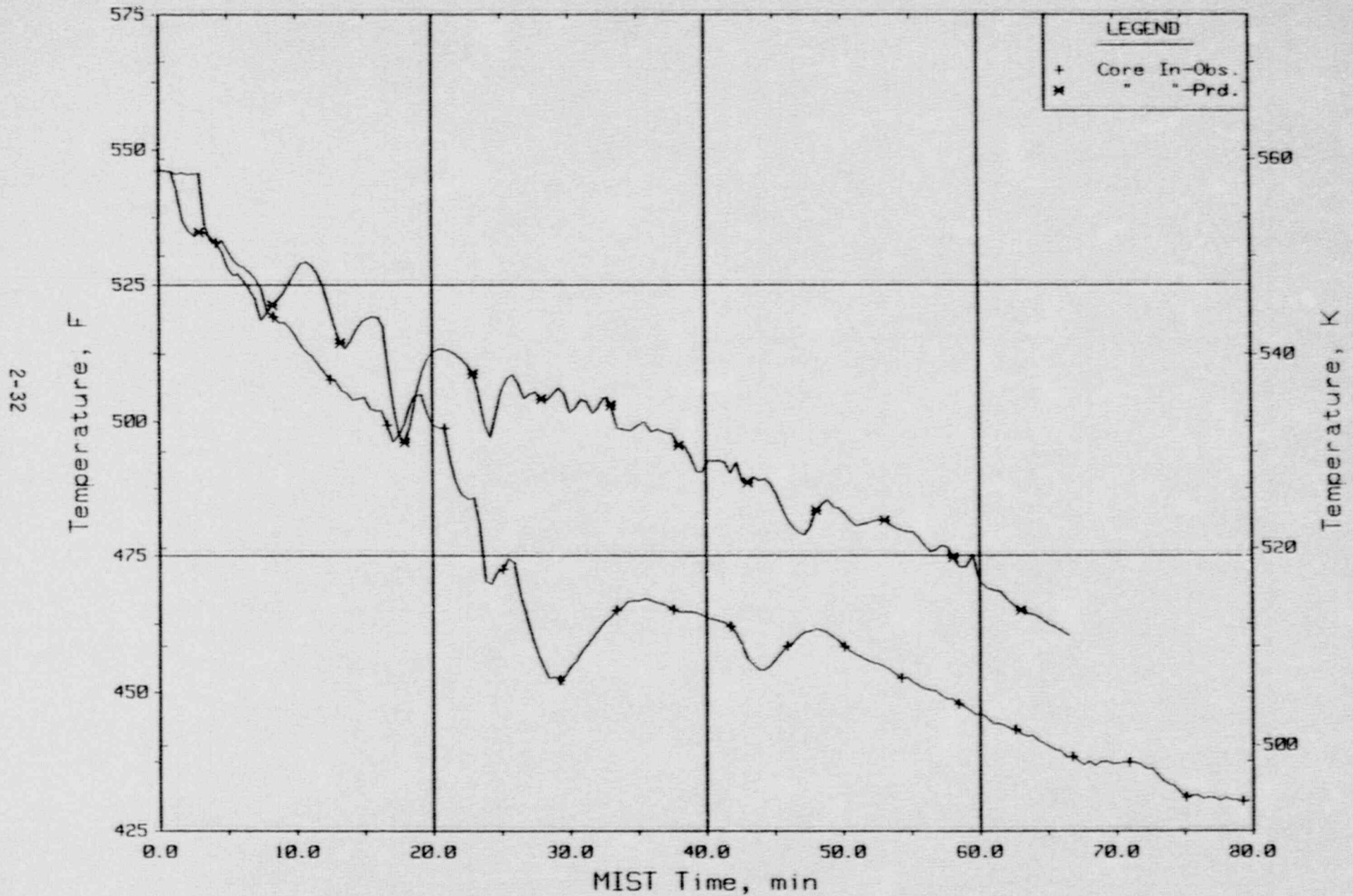


Figure 2.1.25. Core Inlet Reactor Vessel Fluid Temperature (DCRT01).

PRETEST BENCHMARK COMPARISONS  
MIST Nominal Test, Observed Vs. Predicted - 3109AA

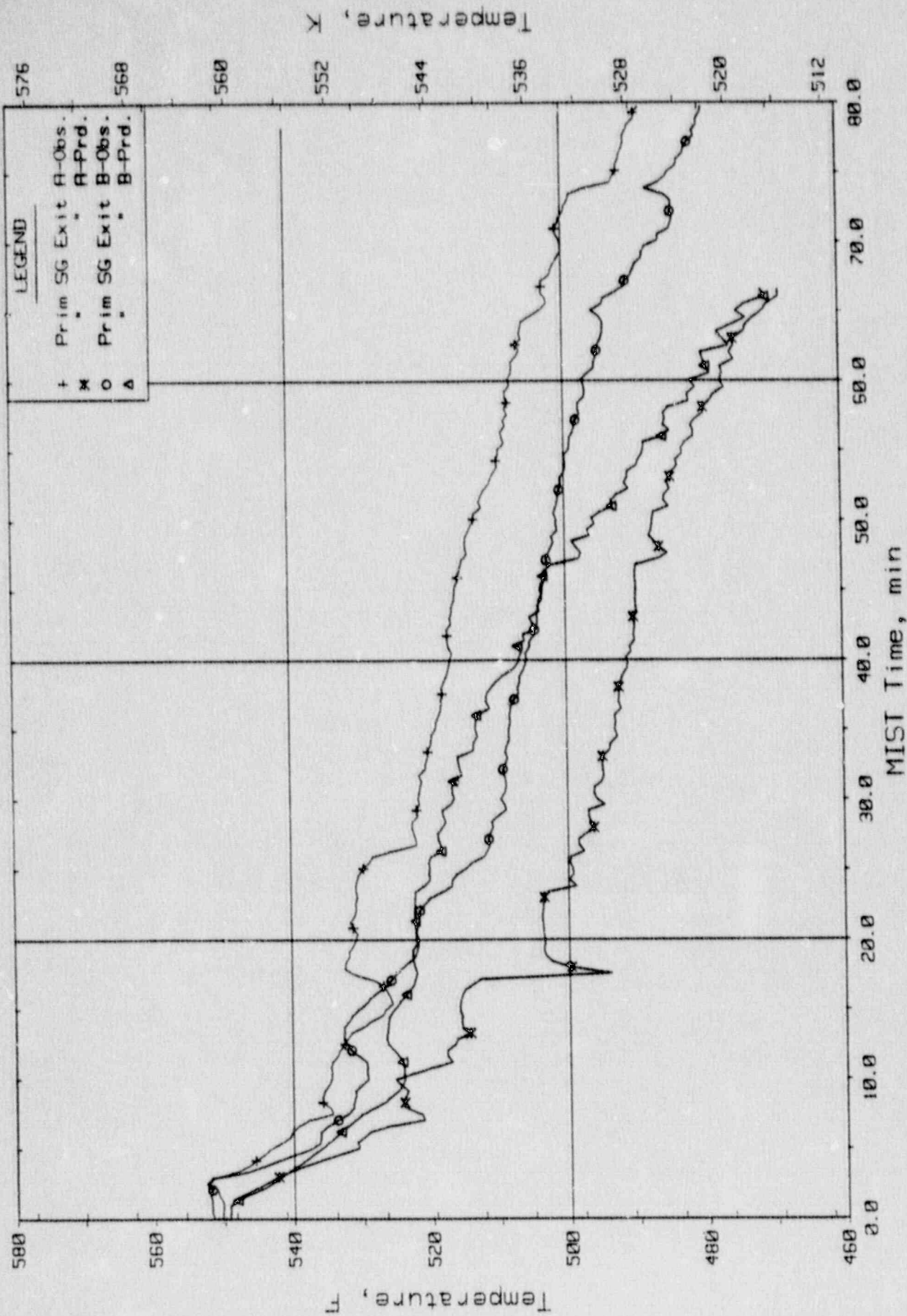


Figure 2.1.26. Loops A/B SG Exit Primary Fluid Temperatures (RIDTs).

PRETEST BENCHMARK COMPARISONS  
 MIST Nominal Test, Observed Vs. Predicted - 3109AA

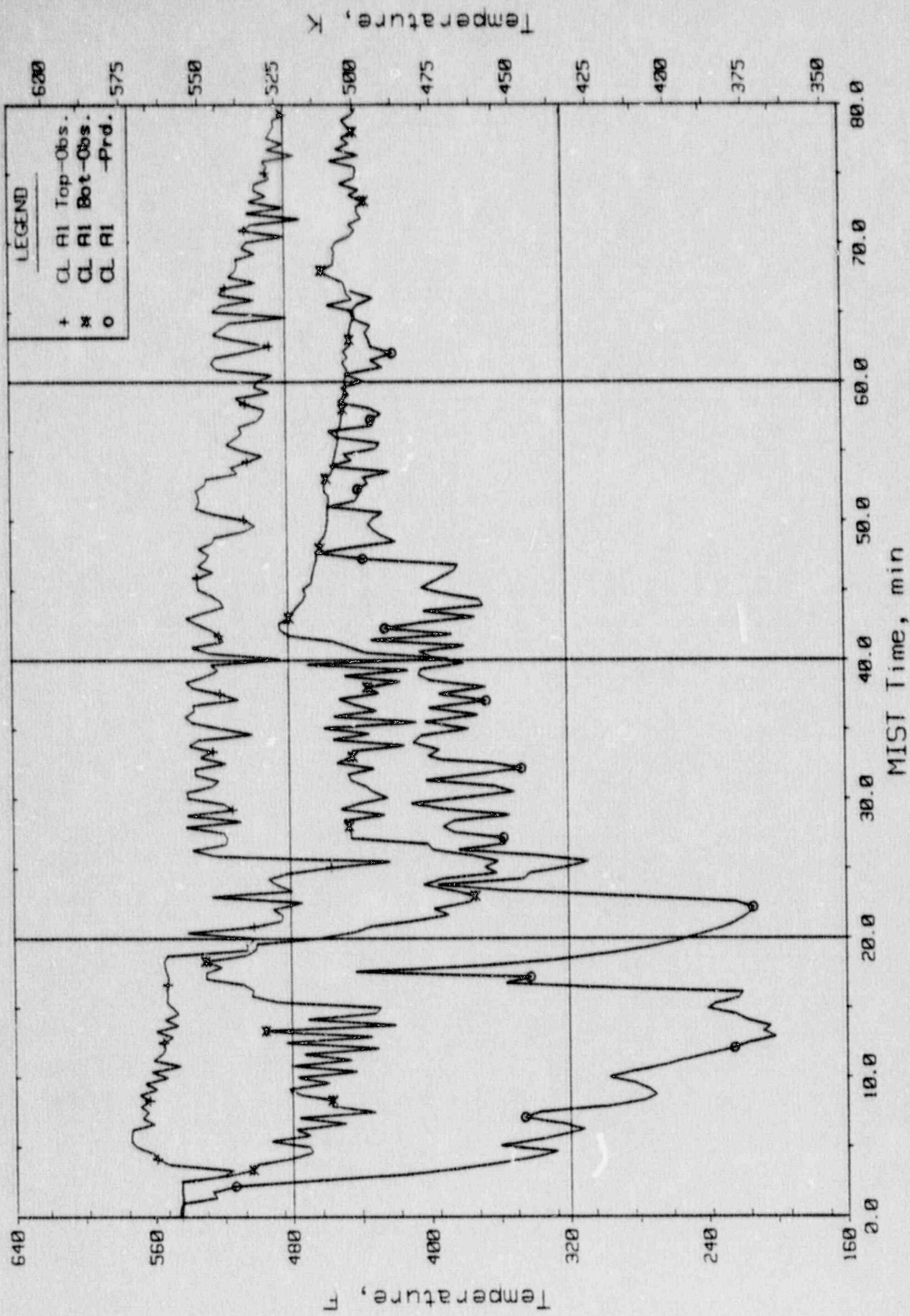


Figure 2.1.27. Cold Leg Nozzle Fluid Temperatures, Top/Bot of Rake (21.3ft, CrTC11/14s).

Wed Apr 1 20:43:44 1987

PRETEST BENCHMARK COMPARISONS  
MIST Nominal Test, Observed Vs. Predicted - 3109AA

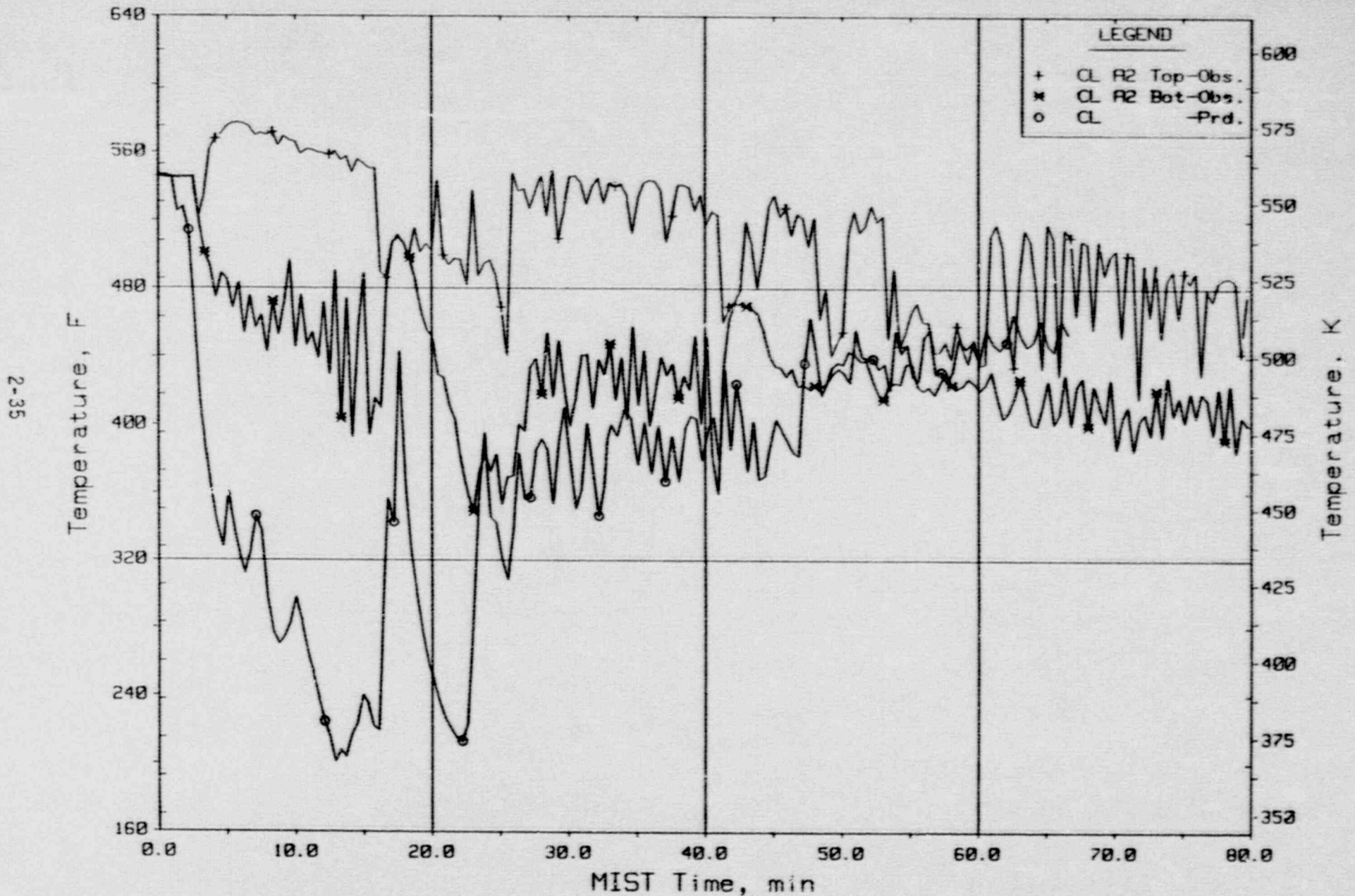


Figure 2.1.28. Cold Leg Nozzle Fluid Temperatures, Top/Bot of Rake (21.3ft, Ccltca2).

PRETEST BENCHMARK COMPARISONS  
MIST Nominal Test, Observed Vs. Predicted - 3109AA

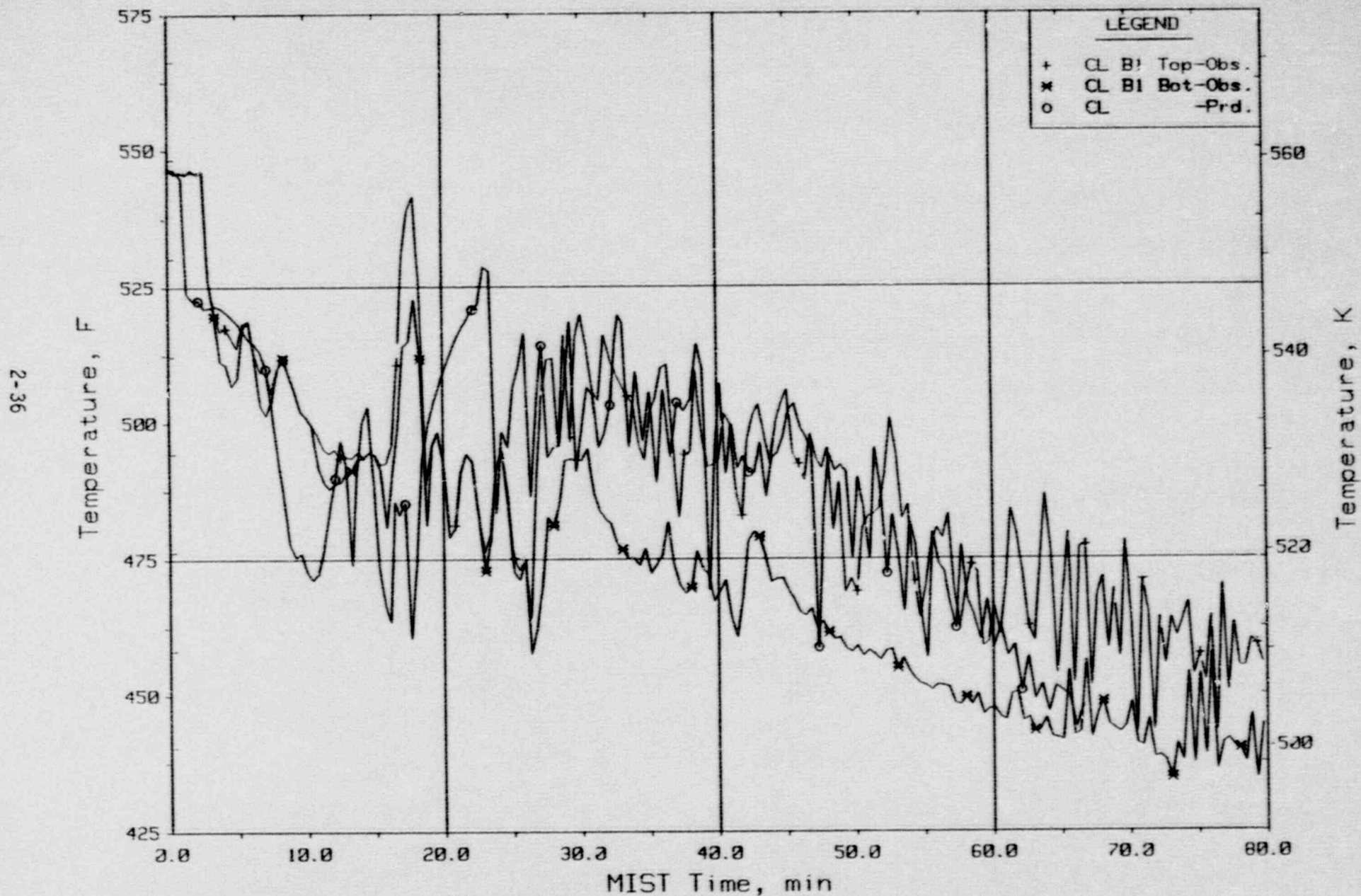


Figure 2.1.29. Cold Leg Nozzle Fluid Temperatures, Top/Bot of Rake (21.3ft, Cc1tcbl).

PRETEST BENCHMARK COMPARISONS  
MIST Nominal Test, Observed Vs. Predicted - 3109AA

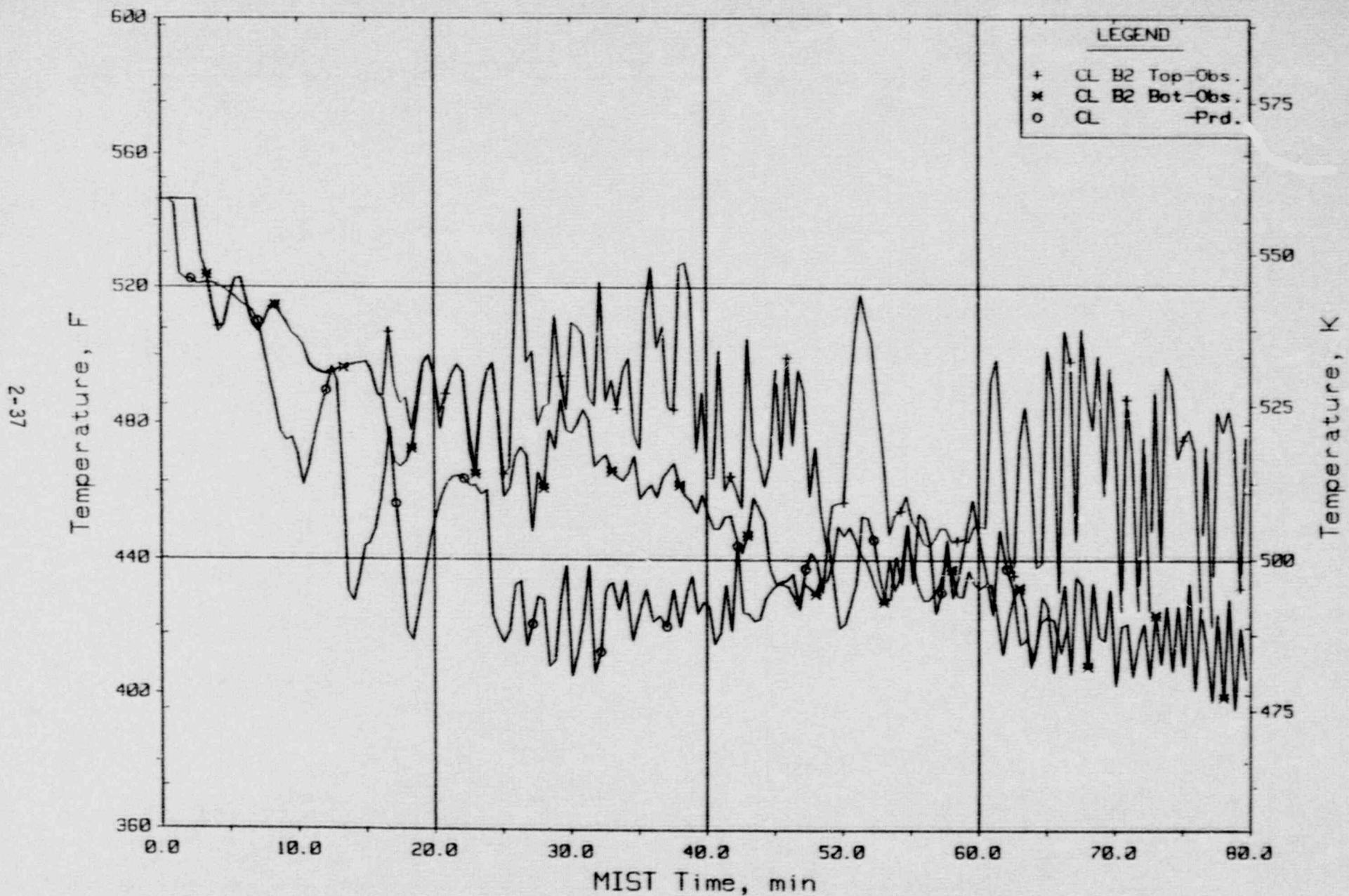


Figure 2.1.30. Cold Leg Nozzle Fluid Temperatures, Top/Bot of Rake (21.3ft, Cc1tcb2).

PRETEST BENCHMARK COMPARISONS  
MIST Nominal Test, Observed Vs. Predicted - 3109AA

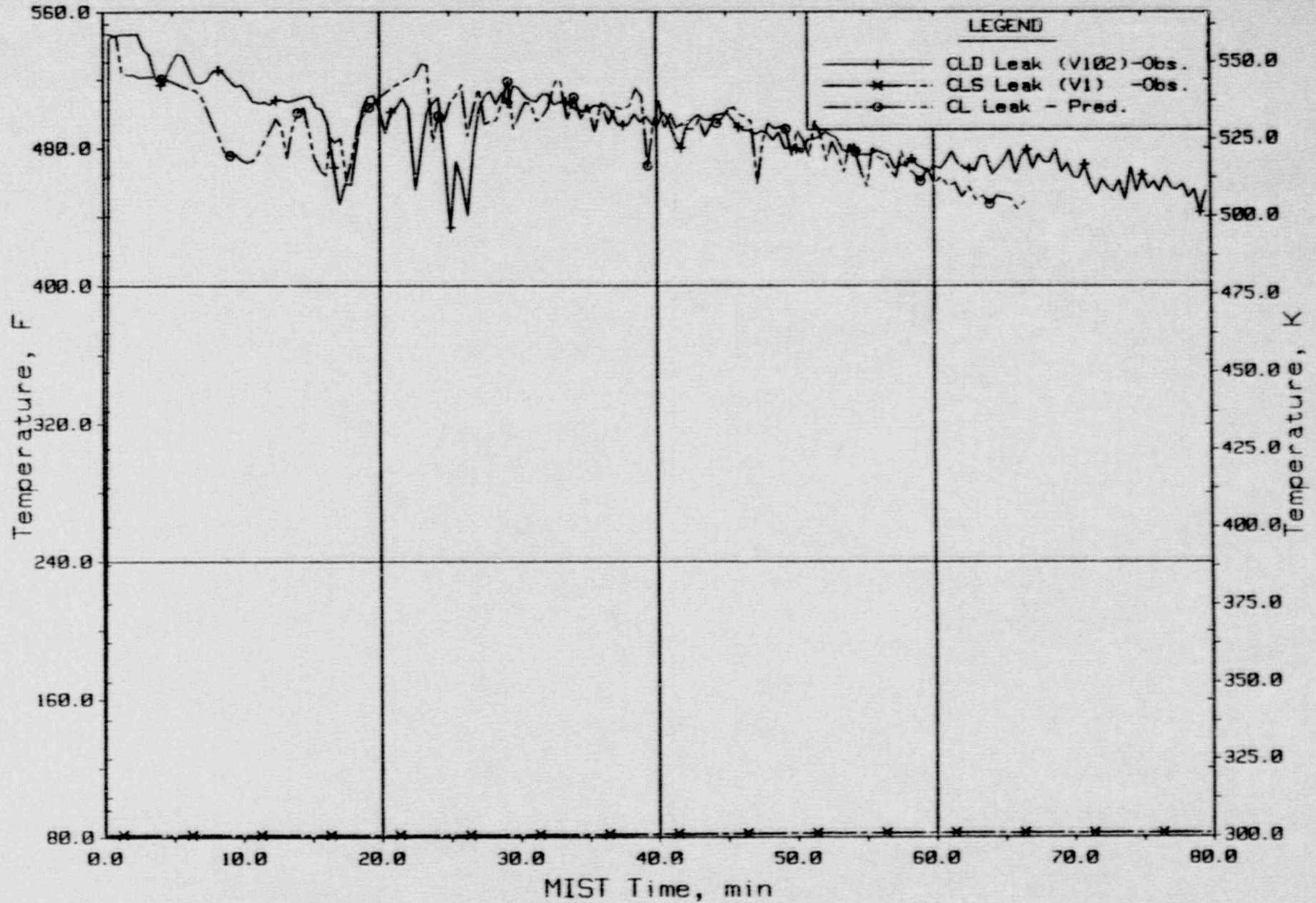


Figure 2.1.31. Single-Phase Discharge Temperatures (VITC01s).



PRETEST BENCHMARK COMPARISONS  
MIST Nominal Test, Observed Vs. Predicted - 3109AA

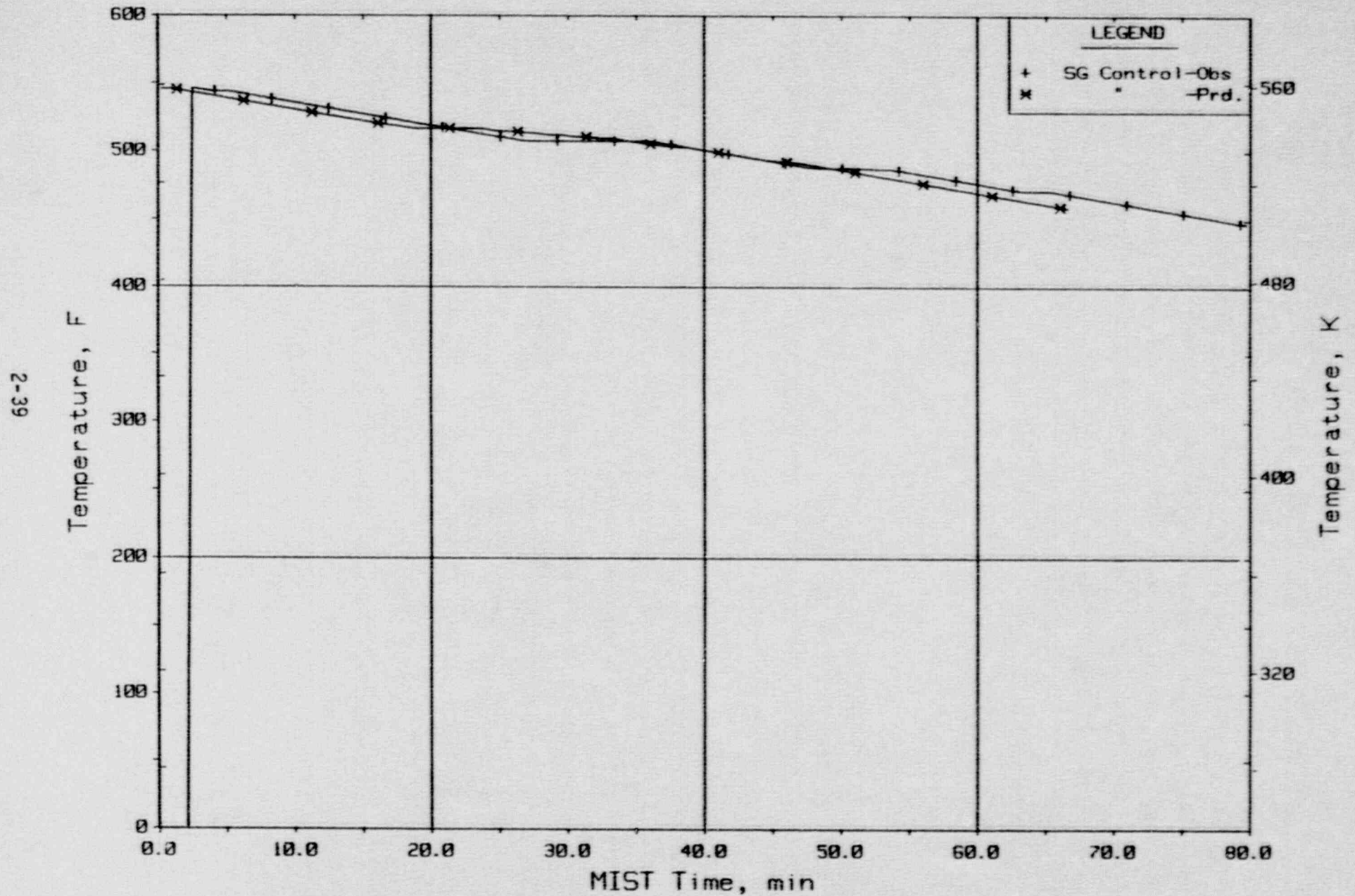


Figure 2.1.32. Steam Generator Secondary Saturation and Control Temperatures.

## 2.2. MIST Test 3406AA Pretest Prediction

MIST test 3406AA was a repeat of the scaled ten tube lower SGTR test 340302. This test opened valves which permitted leak flow between the lower plenum of the steam generator B primary side into the bottom of the secondary side. The leak flow piping contained an orifice which was sized to provide the initial prototypically scaled flow from the double-ended rupture of ten OTSG tubes. Full HPI capacity was used in this test. The secondary side was not isolated. Instead, full steaming was used to attempt to control secondary inventory.

### 2.2.1. MIST Test 3406AA Steady-State Conditions

The pretest prediction model was initialized to steady-state natural circulation conditions shown in Table 2.2.1. The initial conditions for SGTR were modified from the nominal natural circulation initialization by specifying an increased primary pressure of 2150 psia instead of a hot leg subcooling margin. The increased pressure provided a prototypical primary to secondary initial pressure difference.

The change in the initial pressure had little impact on the steady-state natural circulation flows and loop temperatures. Again the calculated loop flows were higher than the observed due to the higher steam generator thermal centers and lower system pressure drops.

Table 2.2.1. MIST Test 3406AA Calculated and Measured  
Initial Steady-State Conditions

<u>Parameter</u>	<u>RELAP</u>	<u>Data</u>
Primary Pressure*, (psia)	2150.	2153.
SG A Secondary Pressure*, (psia)	1010.	1012.
SG B Secondary Pressure*, (psia)	1010.	1013.
SG A Collapsed Level*, (ft)	5.00	5.19
SG B Collapsed Level*, (ft)	5.00	5.11
Hot Leg Subcooling, (F)	57.8	61.9
Pressurizer Collapsed Level*, (ft)	22.95	23.01
Core Power into the Fluid*, (% FP)	3.9	3.9

Table 2.2.1. MIST Test 3406AA Calculated and Measured  
Initial Steady-State Conditions (Cont'd)

Parameter	RELAP	Data
SG Primary Exit Temperatures, (F)	549.2	550.0
Core Exit Temperature, (F)	588.9	593.
Core Total Mass Flow Rate, (lbm/s)	2.15	1.9
Uncompensated Heat Losses, (% FP)	0.4	0.5

\*Denotes specified condition.

### 2.2.2. MIST Test 3406AA Transient Comparisons

The transient was initiated by opening a scaled 30.8 cm<sup>2</sup> leak in the lower SGTR leak circuit. At that time, the RVVV controller was placed in automatic and the core decay heat ramp was started. The primary pressure declined quickly to the point where the core exit subcooling reached 50 F and triggered the second transient initiation step. The actions taken at these conditions included:

1. Actuation of full capacity HPI flow;
2. Resetting the steam generator A secondary level to 31.6 feet (95% on operating range);
3. Termination of AFW to the affected steam generator B;
4. Initiation of the 100 F/hr cooldown rate in the intact steam generator; and
5. Actuation of automatic level control for the affected steam generator.

The broken steam generator level was to be maintained between 10 and 20 feet using the low-flow steam circuit. The high flow (full capacity) circuit was to be used if the level exceed 20 feet to attempt to control secondary level through steaming.

The transient sequence of events are shown in Table 2.2.2. and plotted in Figures 2.2.1. through 2.2.30. Within the first 2.5 minutes in the test and the prediction, the second transient initiation step, full capacity steaming to control level, hot leg A interruption, and the onset of a high elevation

BCM in the A loop had occurred. Interruption of flow in the loop B hot leg occurred between 3.2 and 4.4 minutes. During that time two-phase flow in the broken steam generator steam line was both observed and predicted. By approximately seven minutes an unusual mode of energy removal was achieved by both in the affected steam generator. A high elevation BCM due to the SGTR leak flow and secondary level swell to the top of the tubes provided the cooling once the primary level dropped within the tube region. The primary-to-secondary pressure differential maintained the leak flow and saturation temperature difference which produced the forcing function for continuous leak BCM cooling.

In the 5 to 7 minute time period, a significant loop B secondary pressure difference between the observed and predicted values was begun. During two-phase conditions the predicted full capacity steam flow was too small resulting in a slower secondary depressurization rate. The primary depressurization rate was correspondingly slower due primarily to the decreased leak BCM heat transfer. It should be noted that the two predicted secondary pressures on Figure 2.2.4. correspond to the tube bundle pressure and the pressure just upstream of the full flow control valve. The higher pressure was in tube bundle. The difference between the two were simply the pressure drop through the steam line piping, valves, and metering orifices.

The initial SGTR leak flow prediction was excellent prior to 6 minutes. At that time the primary-to-secondary pressure differential began to diverge between the test and the prediction. Since the low elevation SGTR leak was unchoked the calculated leak flow decreased accordingly. The two leak flows became equal again at 16 minutes as a direct result of a more rapid depressurization from a pool BCM occurring in loop A of the test. The loop A BCM began at 15 minutes and continued until 16.5 minutes when the secondary pressure exceeded the primary value. From that time onward, reverse heat transfer occurred in that loop. The pool BCM enhanced the loop B hot leg flashing rate. The loop A hot leg had just emptied at 16 minutes diverting the most all of the core generated steam into the affected loop. The impact of the increased flashing and diverted steam dropped the primary levels well within the tubes. As a result the leak BCM effectiveness improved, and the enhanced depressurization rate continued until 19 minutes. At that time the

primary level temporarily increased to the top of the tubes halting most of the condensation. The leak and HPI cooling along with the intermittent leak BCM continued to depressurize the test primary system for the remainder of the simulation period.

The calculated results reached a loop A pool BCM at 12.7 minutes. However, at that time the secondary pressure was within 30 psi of the primary and the impact was correspondingly small. The secondary pressure had already increased to nearly the primary value due to earlier primary-to-secondary coupling between 8 and 12 minutes. The predictions also included reverse heat transfer, although the timing of the event was shifted up by eight minutes to 24 minutes. The primary and secondary pressures had been within 10 psi of each since 15 minutes. Since the affected loop secondary steam flows were underpredicted, the primary side was not depressurized as quickly due to a weaker leak BCM coupling. From the 20 to 45 minute period the leak, HPI, and leak BCM depressurized the primary similar to the test. In both cases, the primary pressure followed the affected steam generator secondary pressure within 100 to 150 psi. The under-prediction of the two-phase steaming capacity was the only real divergence which was observed in the prediction.

Table 2.2.2. MIST Test 3406AA Sequence of Events Comparisons

Event	Approximate Test Time (Min)	
	RELAP	Data
Scaled 10 Tube Low SGTR Leak Opened (Start Core Power Ramp and Place RVVV in Automatic Control)	0.0	0.0
Hot Leg Subcooling to 50.0 F: Initiate HPI, Terminate SG B AFW, SG A Secondary Refill and Depressurization	0.9	2.1
SG B Secondary Level Exceeded 20 ft (Start Full Steaming to Control Level)	1.7	2.0
Hot Leg A Flow Interruption	1.8	1.9
SG A High Elevation BCM Started	2.5	2.4
Hot Leg B Flow Interruption	4.4	3.2
Two-Phase Flow into SG B Steam Line	4.1	4.1

Table 2.2.2. MIST Test 3406AA Sequence of Events Comparisons (Cont'd)

Event	Approximate Test Time (Min)	
	RELAP	Data
SG B Leak BCM Began	6.7	7.0
SG A Secondary Level to 31.6 Feet	7.8	8.0
Hot Leg A Empty	23.3	16.0
SG A Reverse Heat Transfer Began	24.4	16.5
Core Flood Tank Flow Started	33.5	20.5
Primary System Refill Began	44.2	55.0
Calculations Terminated	45.0	--

2.2.3. MIST Test 3406AA Pretest Conclusions

The pretest prediction of low elevation SGTR test 3406AA was very reasonable except for the underprediction of the full capacity secondary two-phase steaming flow rates. All major system phenomena such as: high elevation BCM, pool BCM, leak BCM, steam generator reverse heat transfer, hot leg emptying, and loop asymmetries were predicted to occur at approximately the correct time and magnitudes. The system collapsed levels, flows and temperatures behaved similar to the test observations with certain timing shifts related generally to the slower secondary depressurization of the affected steam generator.

SGTR BENCHMARK COMPARISONS  
PRETEST BENCHMARK, Observed Vs. Predicted - Test 3406AA

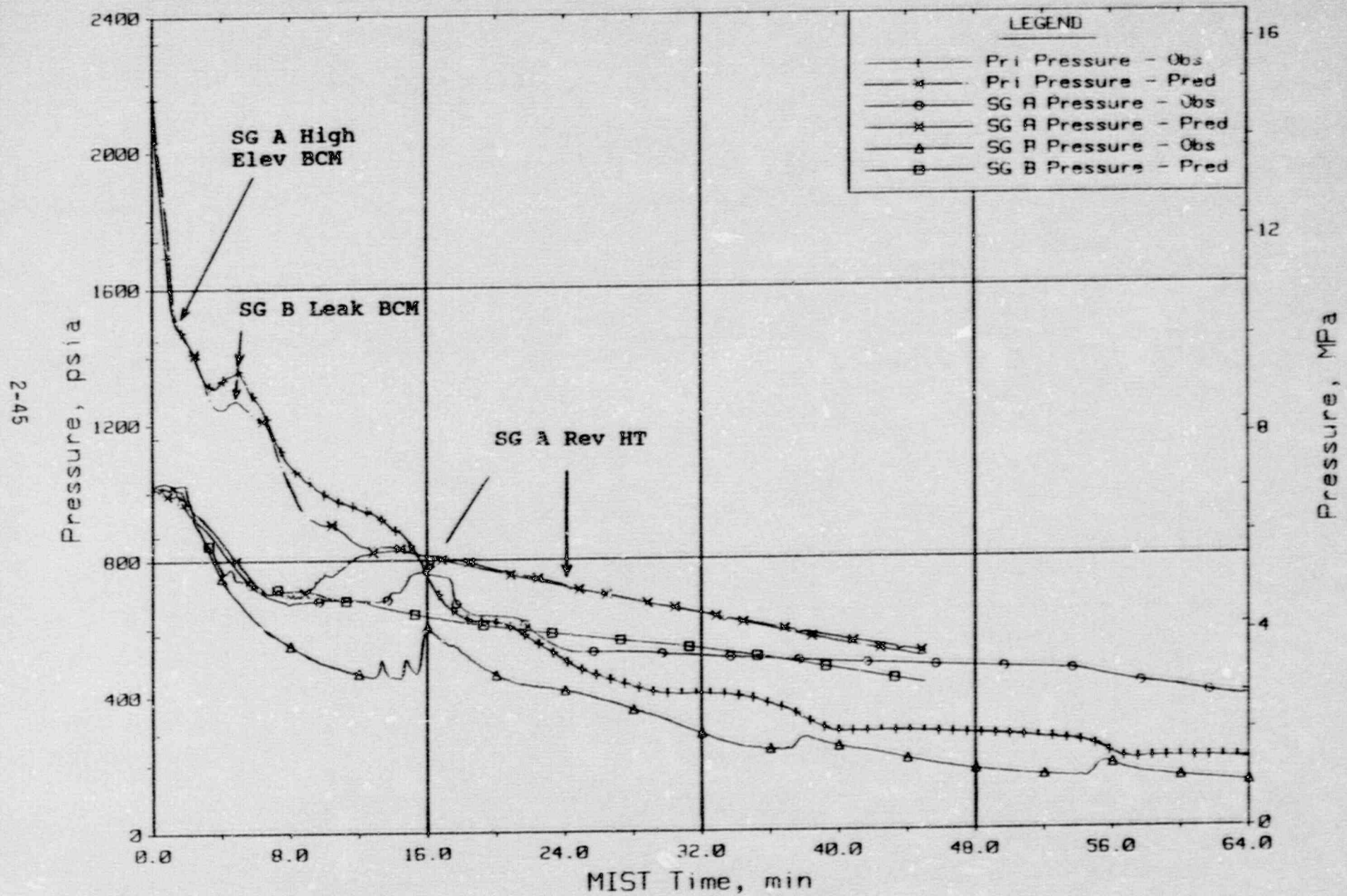


Figure 2.2.1. System Pressures.

SGTR BENCHMARK COMPARISONS  
 PRETEST BENCHMARK, Observed Vs. Predicted - Test 3406AA

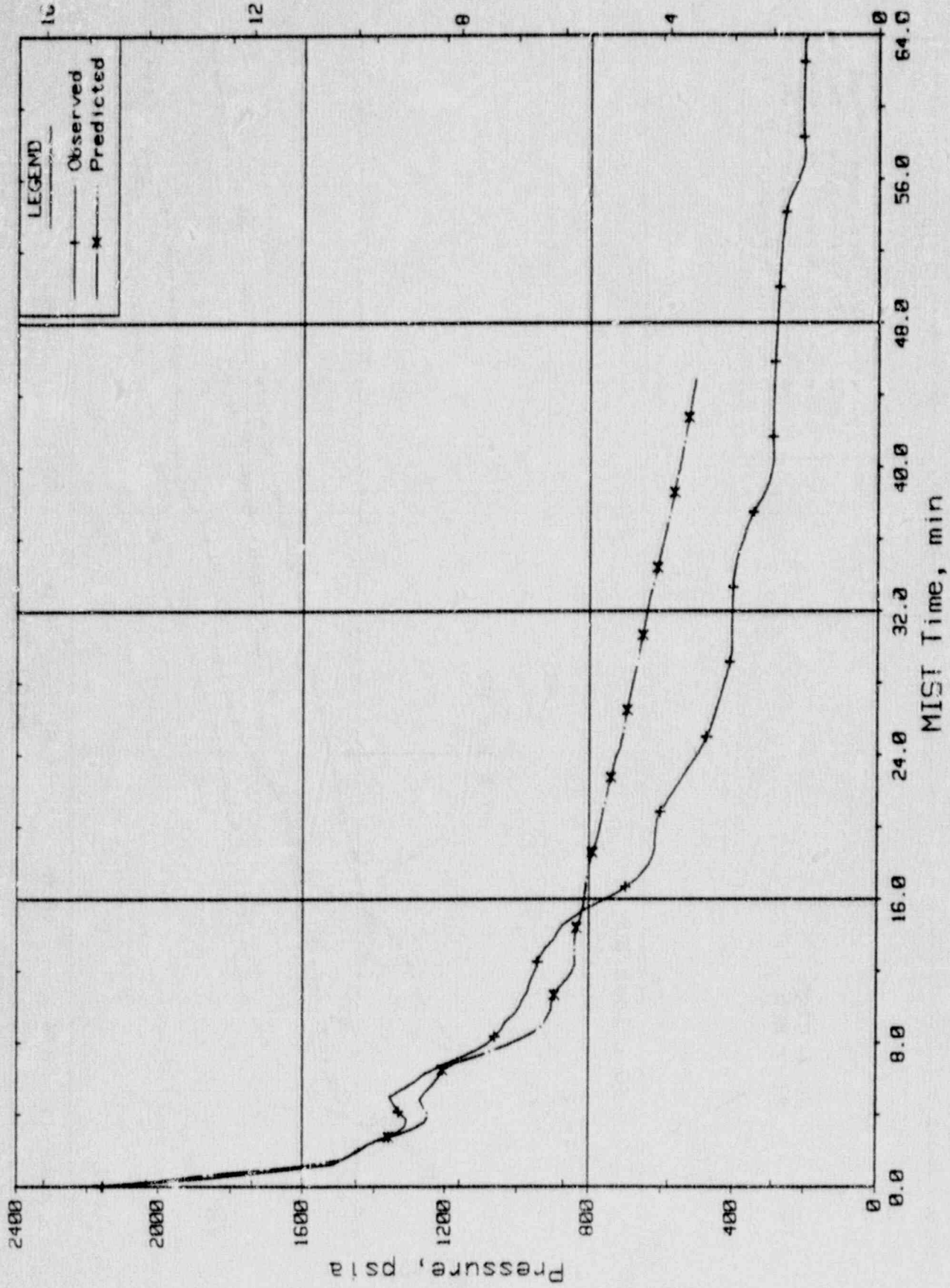


Figure 2.2.2. Reactor Vessel Pressure.



SGTR BENCHMARK COMPARISONS  
 PRETEST BENCHMARK, Observed Vs. Predicted - Test3406AA

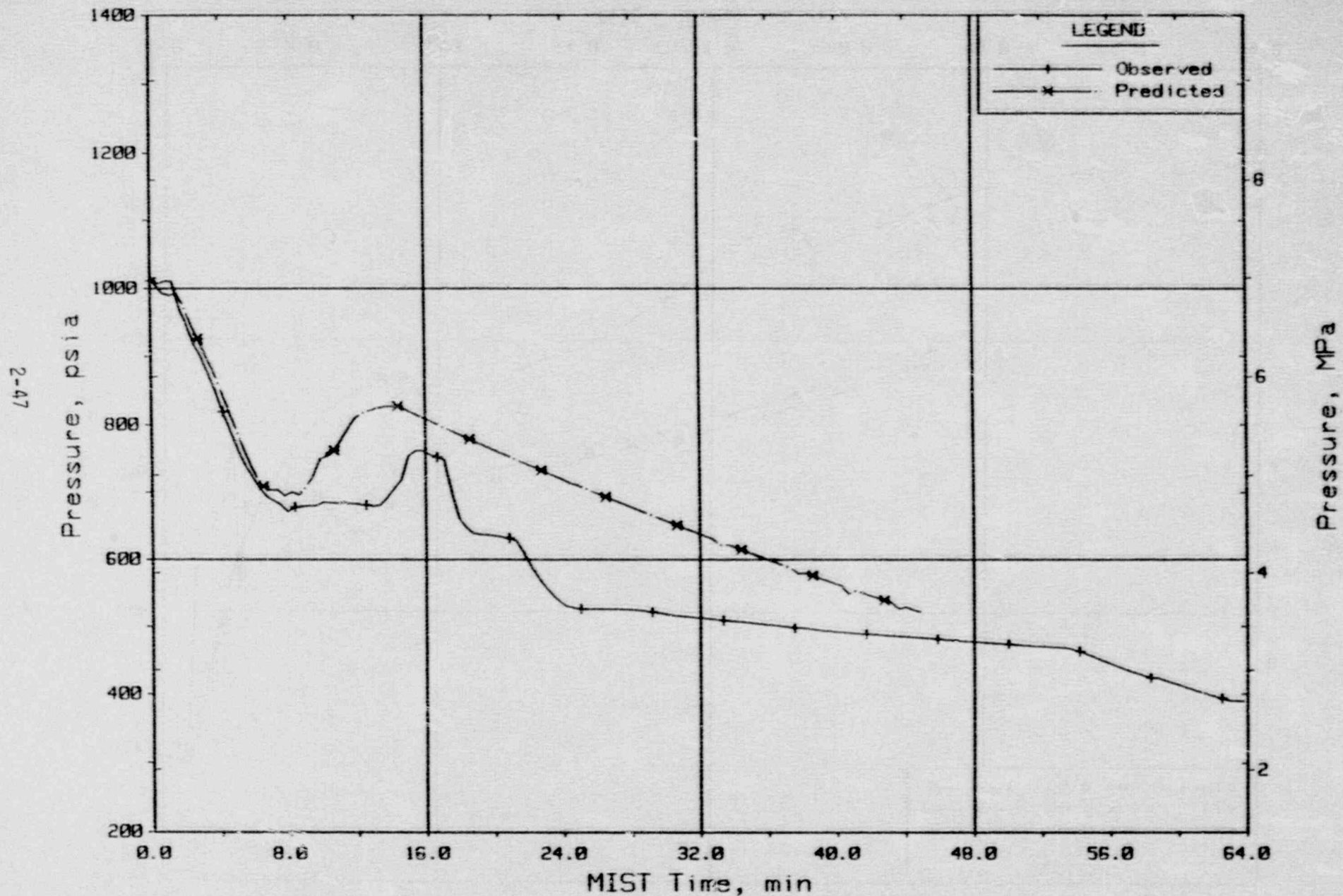


Figure 2.2.3. Steam Generator A Secondary Pressure.

SGTR BENCHMARK COMPARISONS  
 PRETEST BENCHMARK, Observed Vs. Predicted - Test3406AA

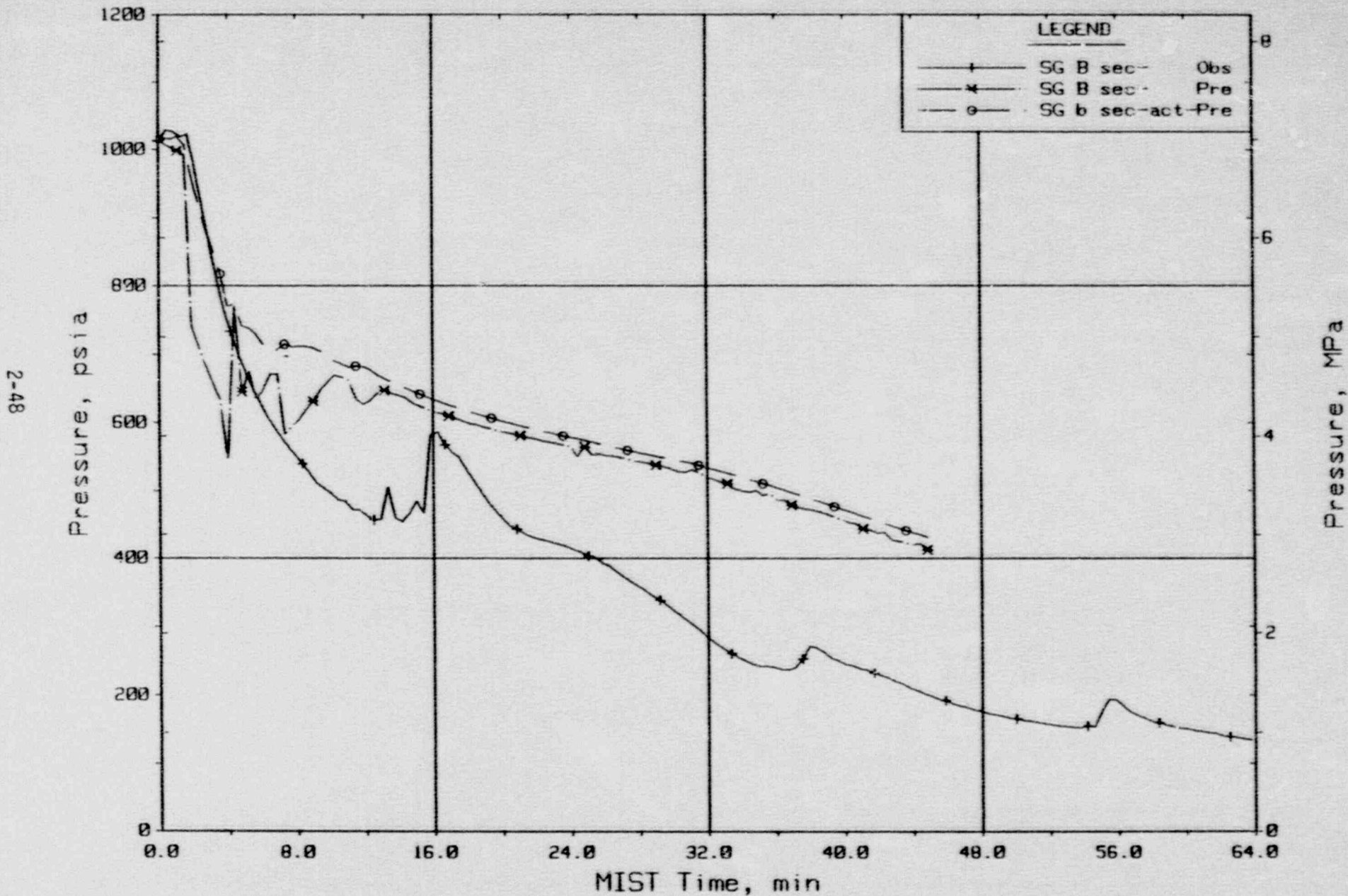


Figure 2.2.4. Steam Generator B Secondary Pressure.

SGTR BENCHMARK COMPARISONS  
 PRETEST BENCHMARK, Observed Vs. Predicted - Test3406AA

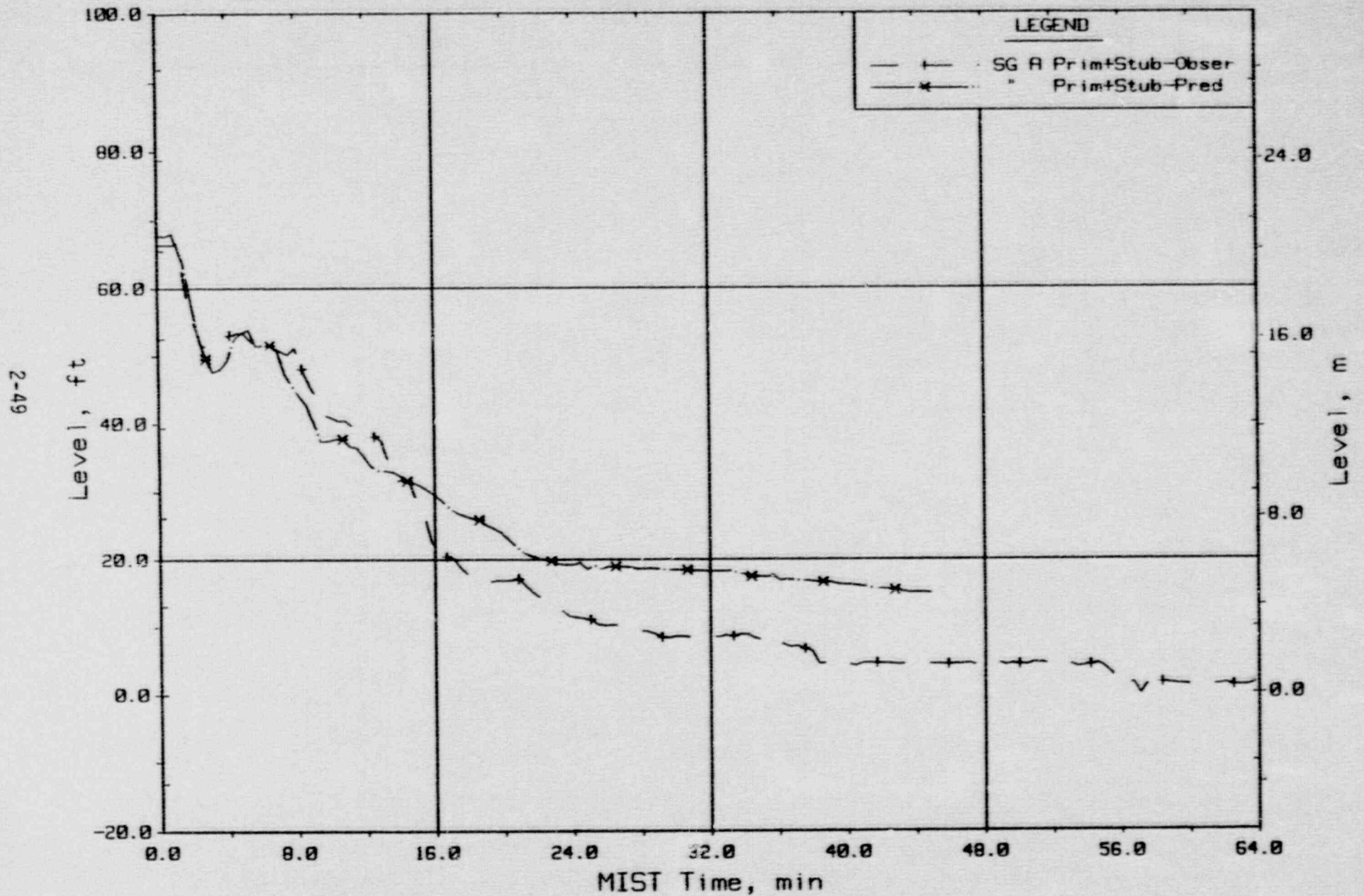


Figure 2.2.5. Steam Generator A Primary + Stub Level.

SGTR BENCHMARK COMPARISONS  
 PRETEST BENCHMARK, Observed Vs. Predicted - Test3406AA

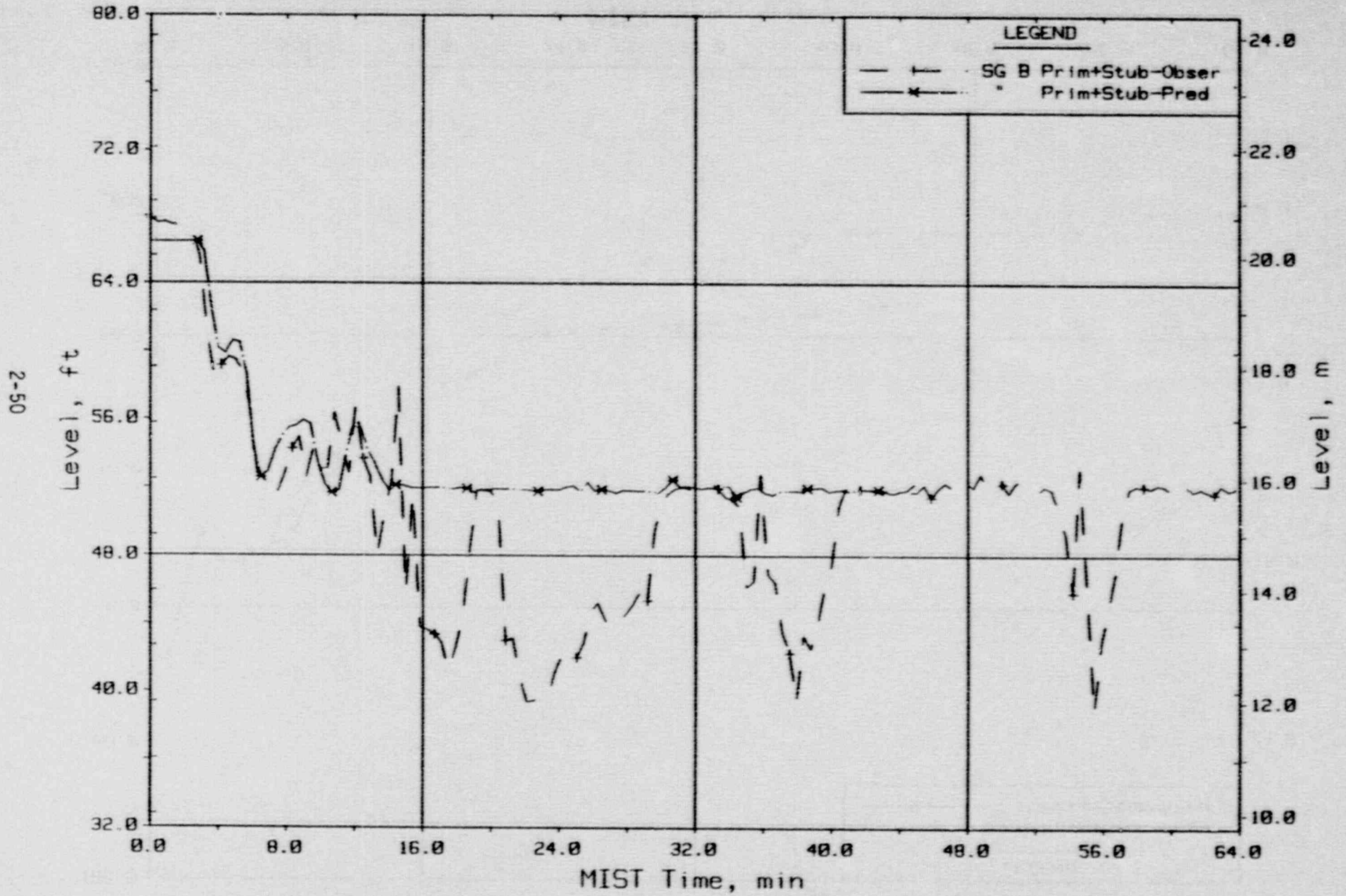


Figure 2.2.6. Steam Generator B Primary + Stub Level.

SGTR BENCHMARK COMPARISONS  
PRETEST BENCHMARK, Observed Vs. Predicted - Test3406AA

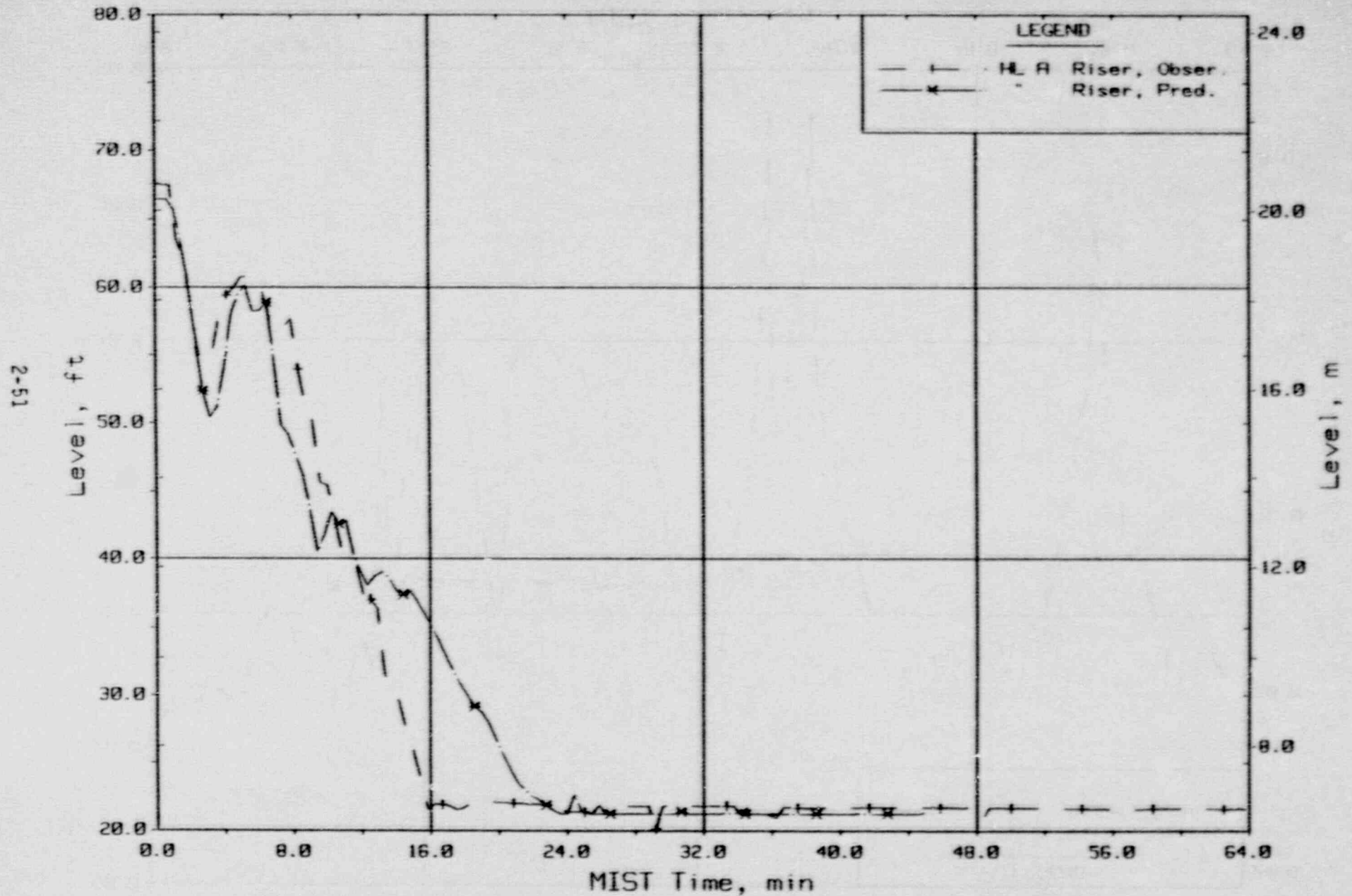


Figure 2.2.7. Hot Leg A Riser Level.

SGTR BENCHMARK COMPARISONS  
 PRETEST BENCHMARK, Observed Vs. Predicted - Test3406AA

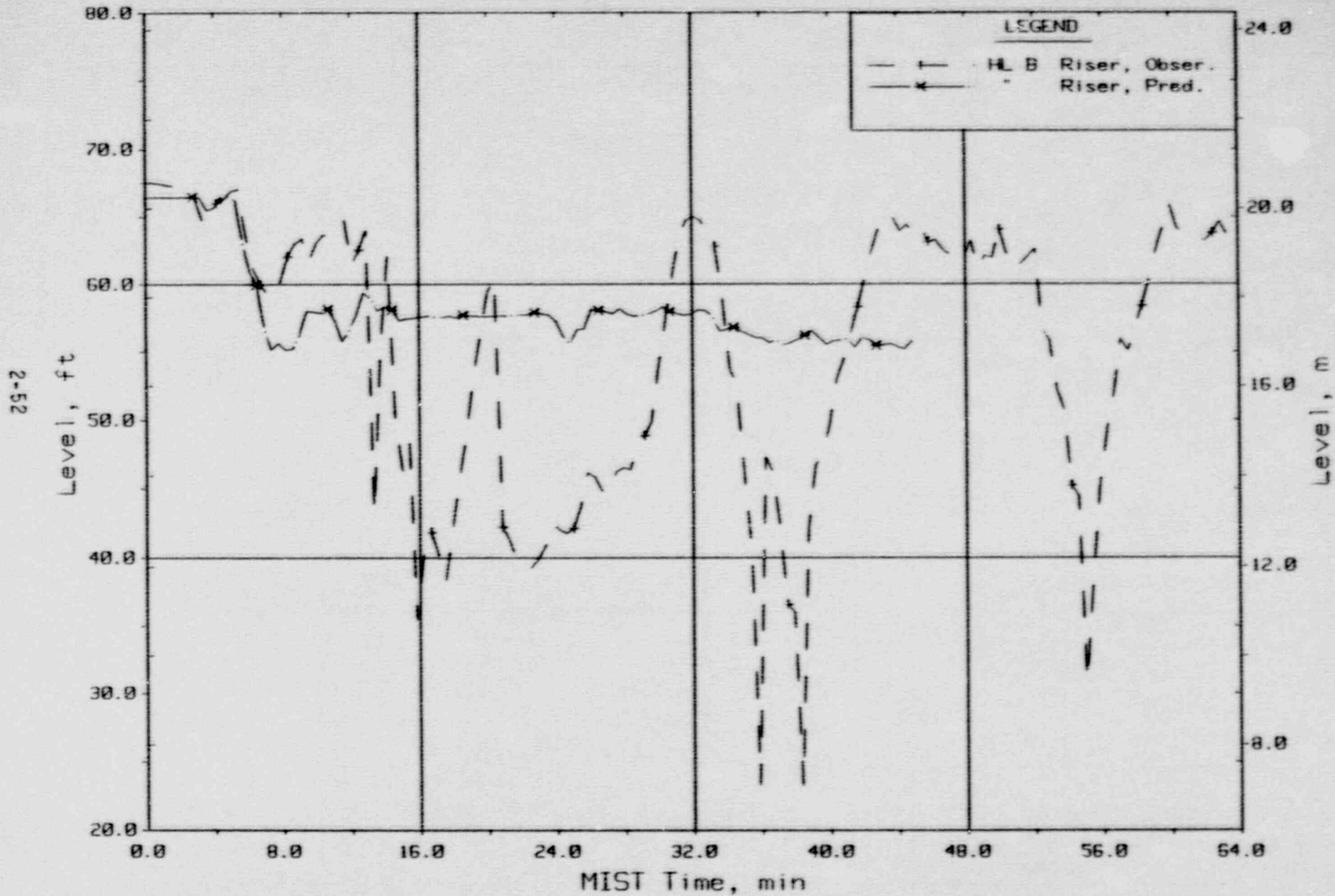


Figure 2.2.8. Hot Leg B Riser Level.

SGTR BENCHMARK COMPARISONS  
 PRETEST BENCHMARK, Observed Vs. Predicted - Test 3406AA

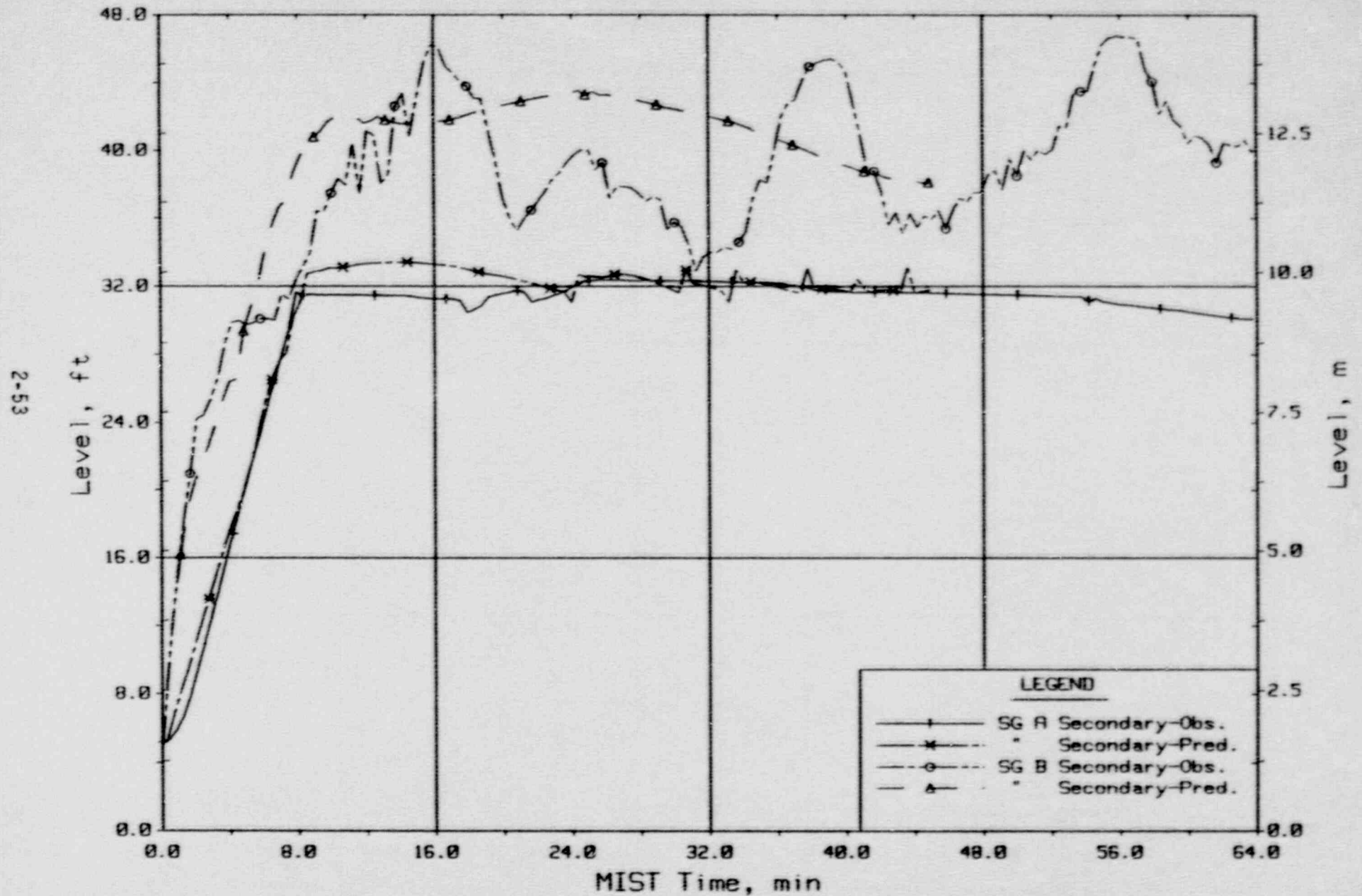


Figure 2.2.9. Steam Generator Sec. Collapsed Liquid Levels.

SGTR BENCHMARK COMPARISONS  
 PRETEST BENCHMARK, Observed Vs. Predicted - Test 3406AA

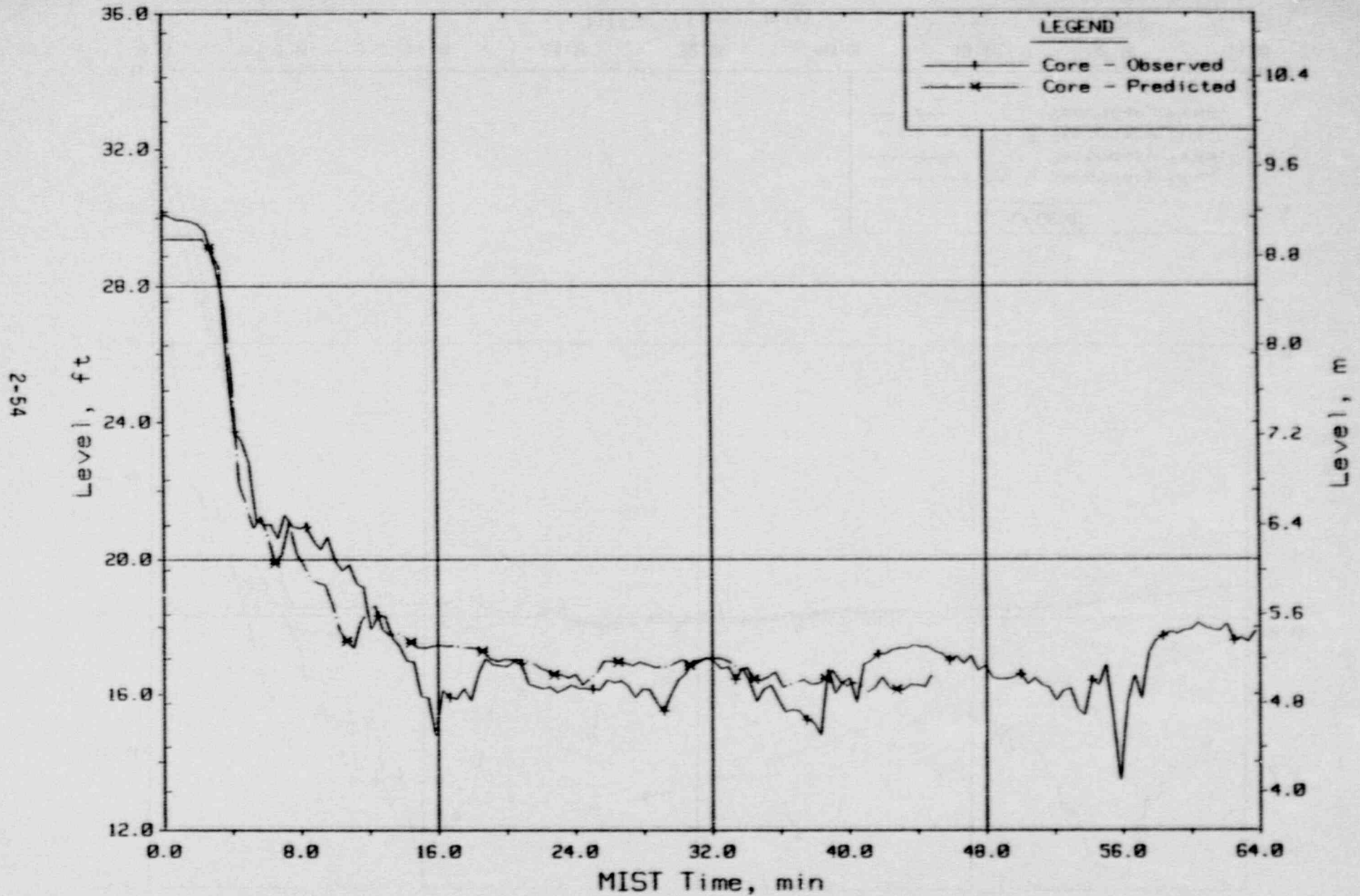


Figure 2.2.10. Core Region Collapsed Liquid Levels.



SGTR BENCHMARK COMPARISONS  
PRETEST BENCHMARK, Observed Vs. Predicted - Test 3406AA

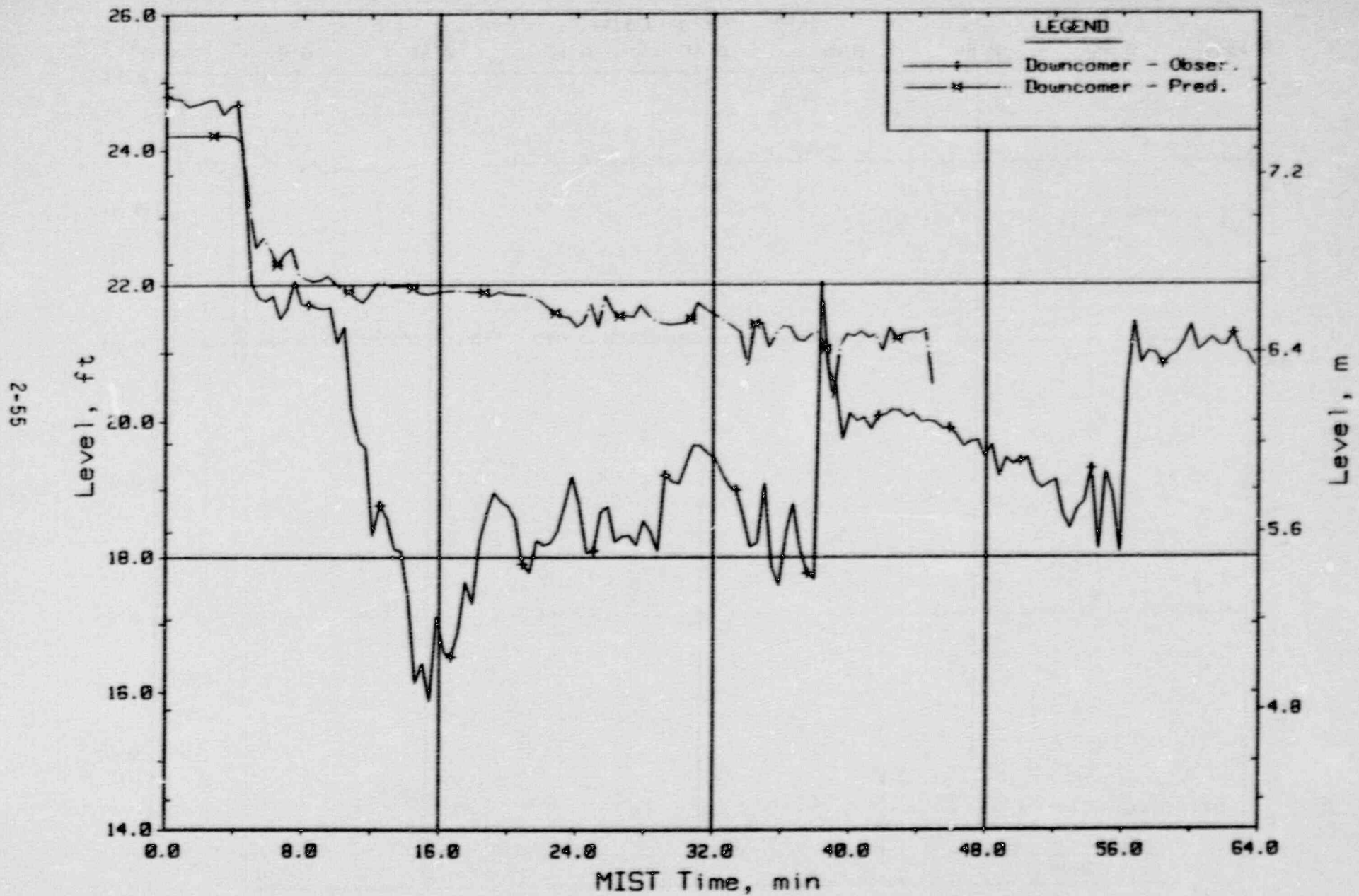


Figure 2.2.11. Core Region Collapsed Liquid Levels.

SGTR BENCHMARK COMPARISONS  
 PRETEST BENCHMARK, Observed Vs. Predicted - Test 3406AA

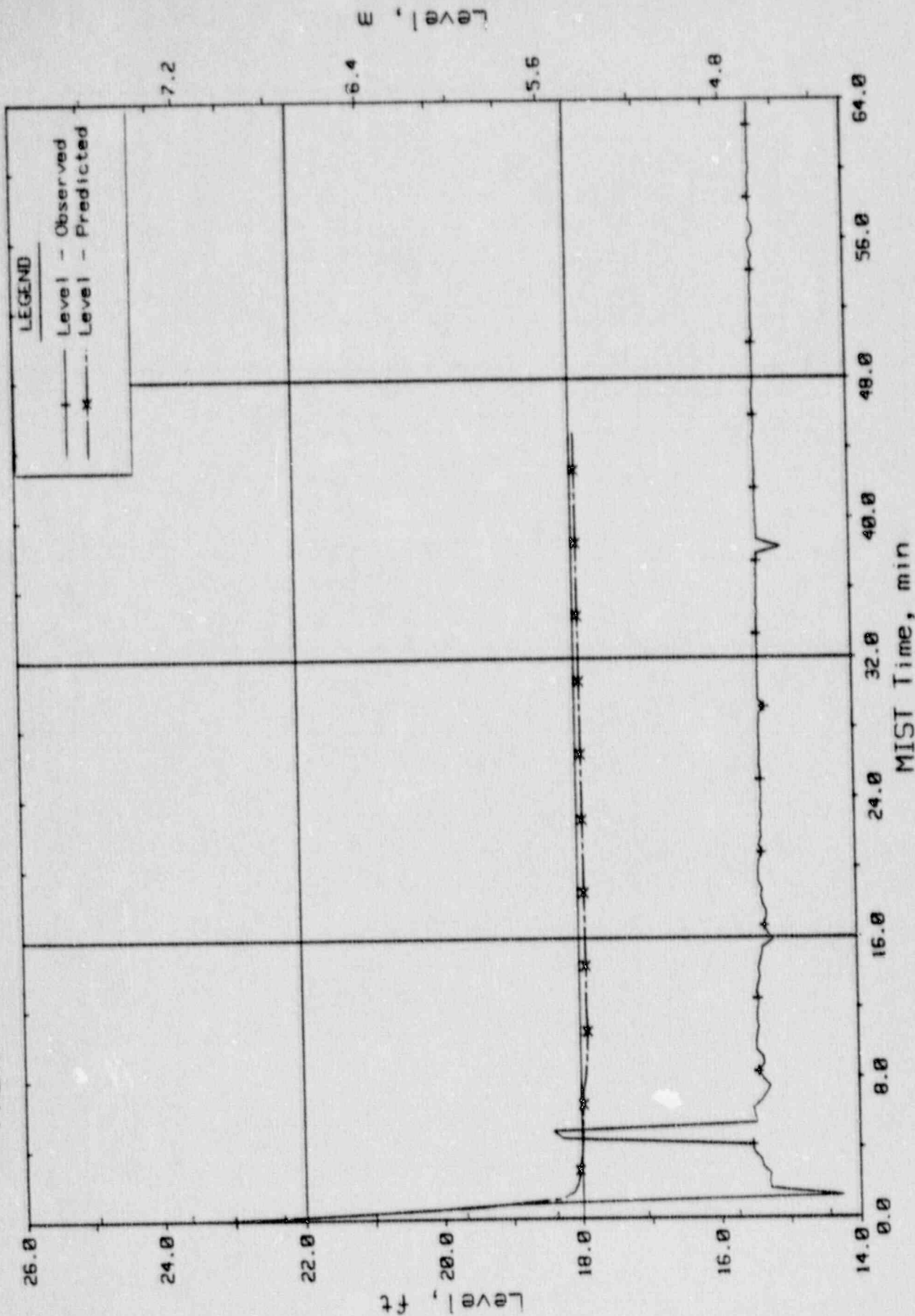


Figure 2.2.12. Pressurizer Collapsed Liquid Level (PZLV20).

SGTR BENCHMARK COMPARISONS  
PRETEST BENCHMARK, Observed Vs. Predicted - Test 3406AA

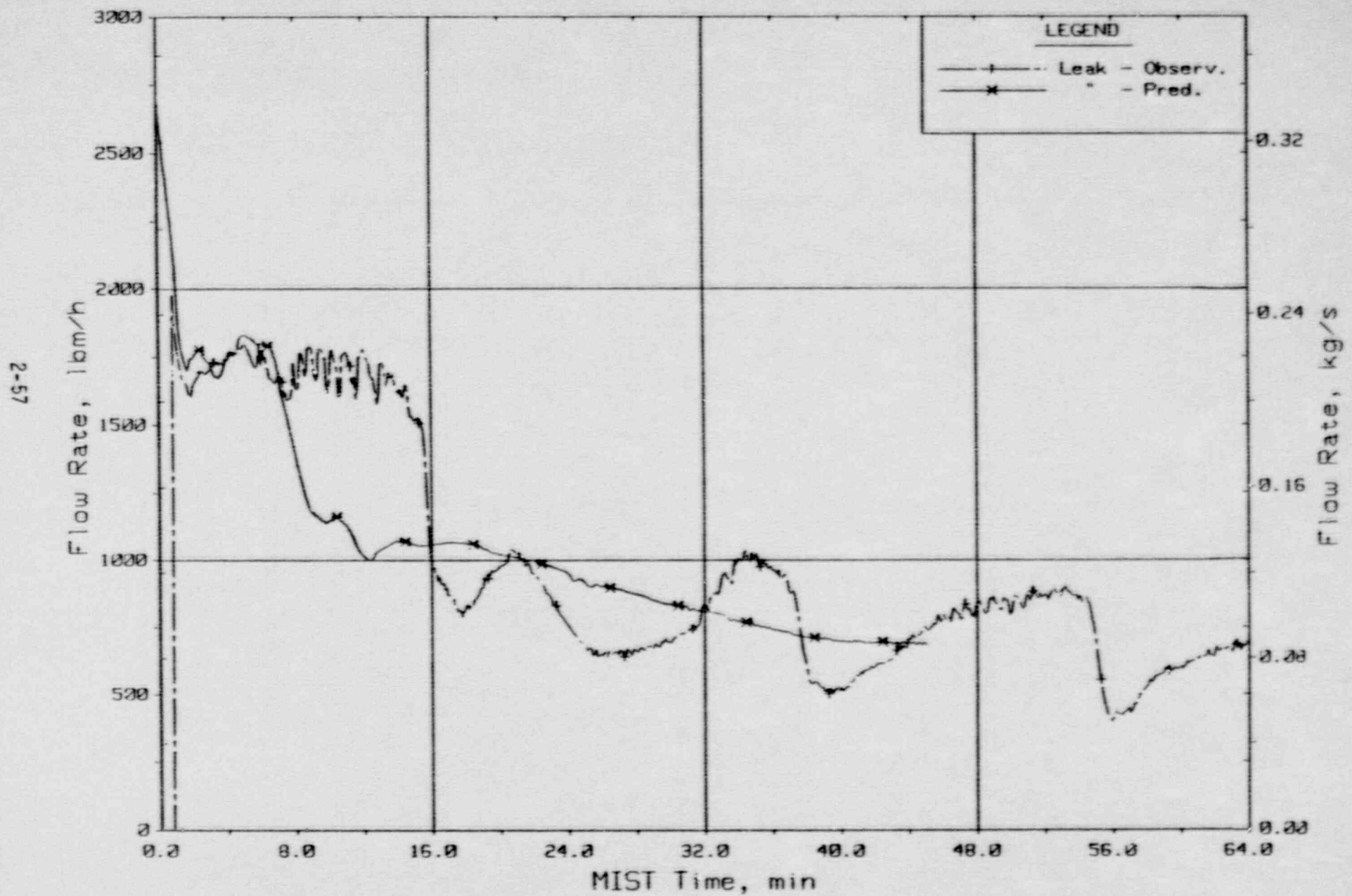


Figure 2.2.13. Leak Flow Rates.

SGTR BENCHMARK COMPARISONS  
 PRETEST BENCHMARK, Observed Vs. Predicted - Test 3406AA

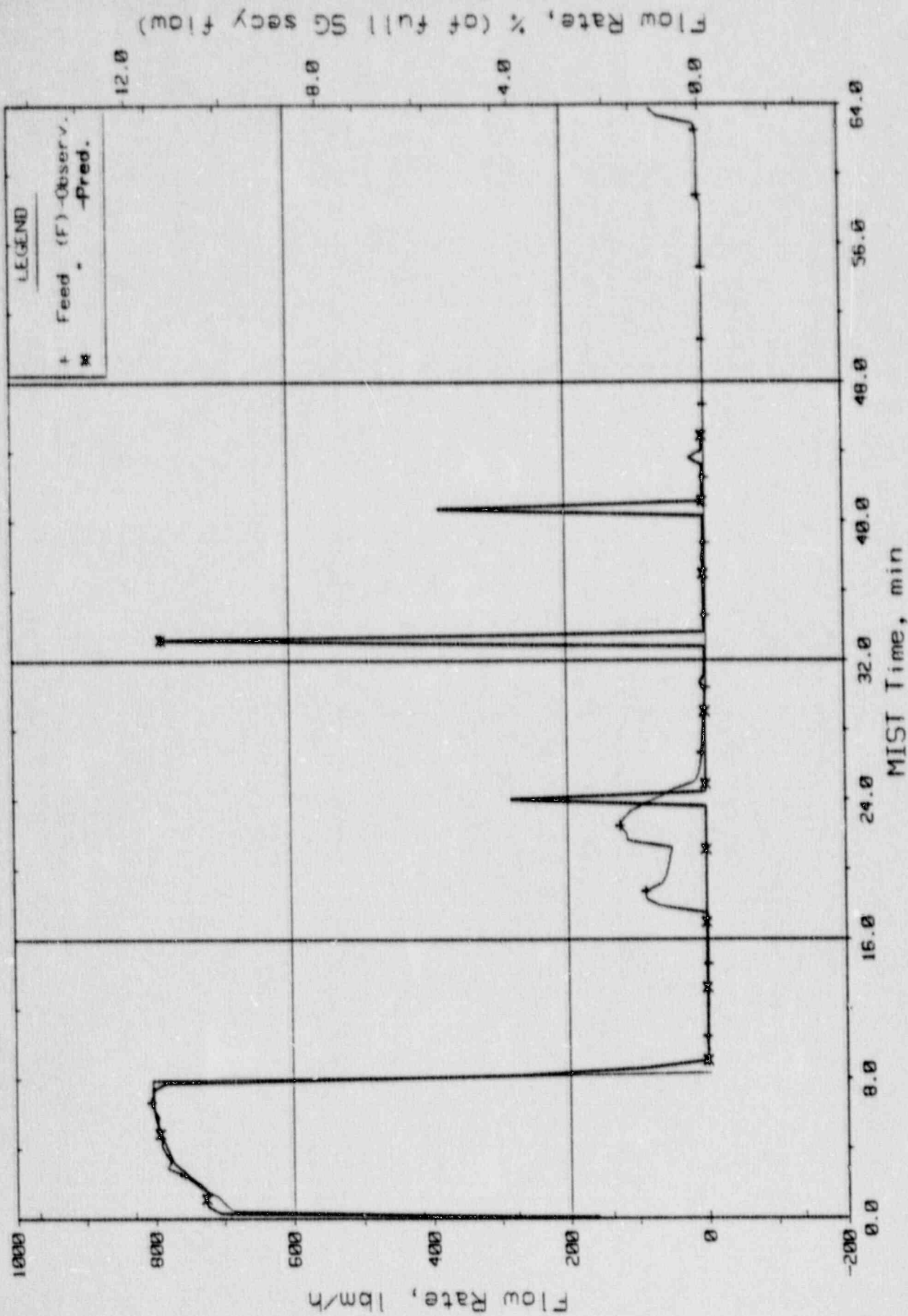


Figure 2.2.14. Steam Generator A Flow Rate (Ssfor20).

Csfor20

SGTR BENCHMARK COMPARISONS  
 PRETEST BENCHMARK, Observed Vs. Predicted - Test 3406AFA

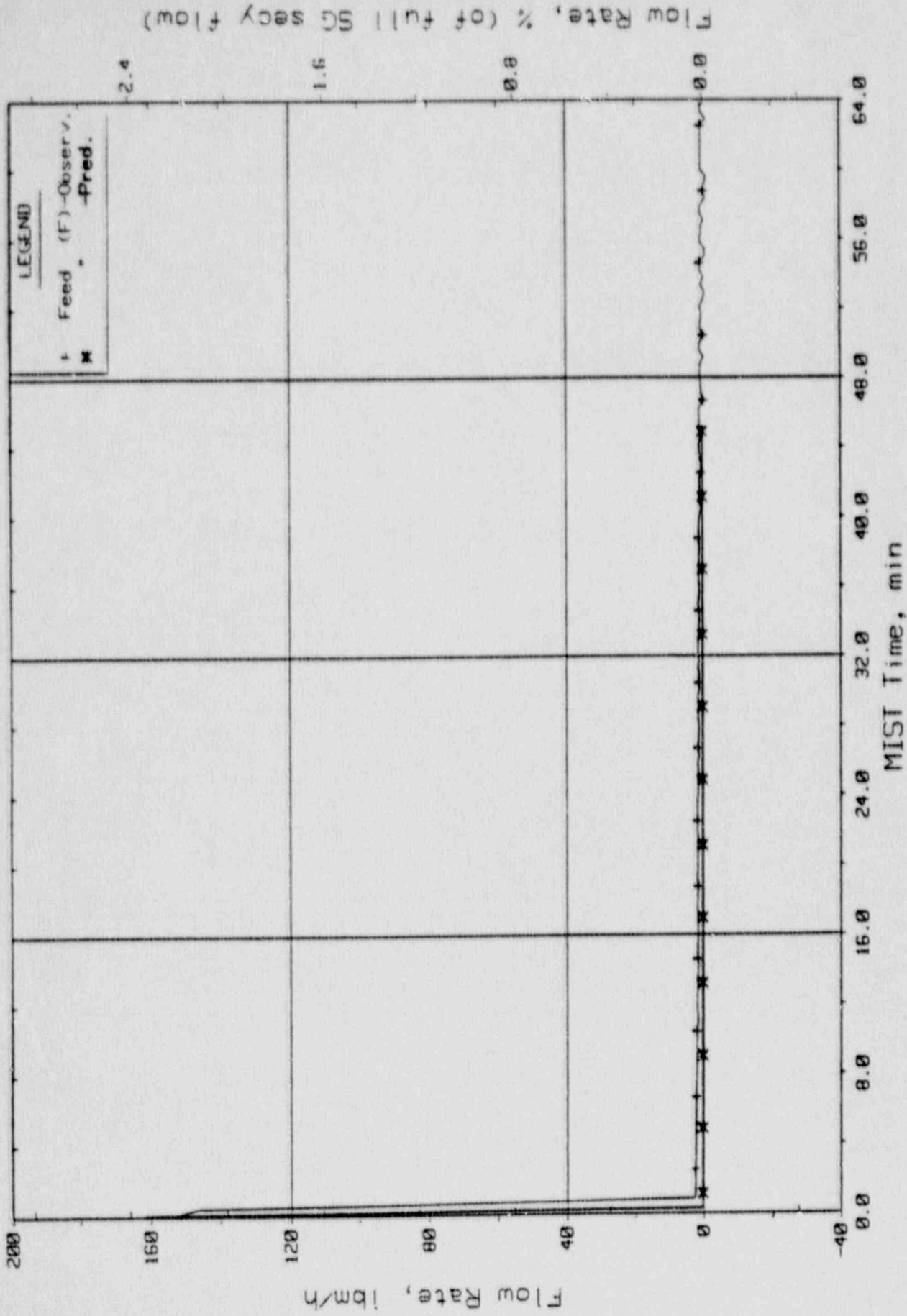


Figure 2.2.15. Steam Generator B Flow Rate (Ssfor21).

SGTR BENCHMARK COMPARISONS  
 PRETEST BENCHMARK, Observed Vs. Predicted - Test 3406A

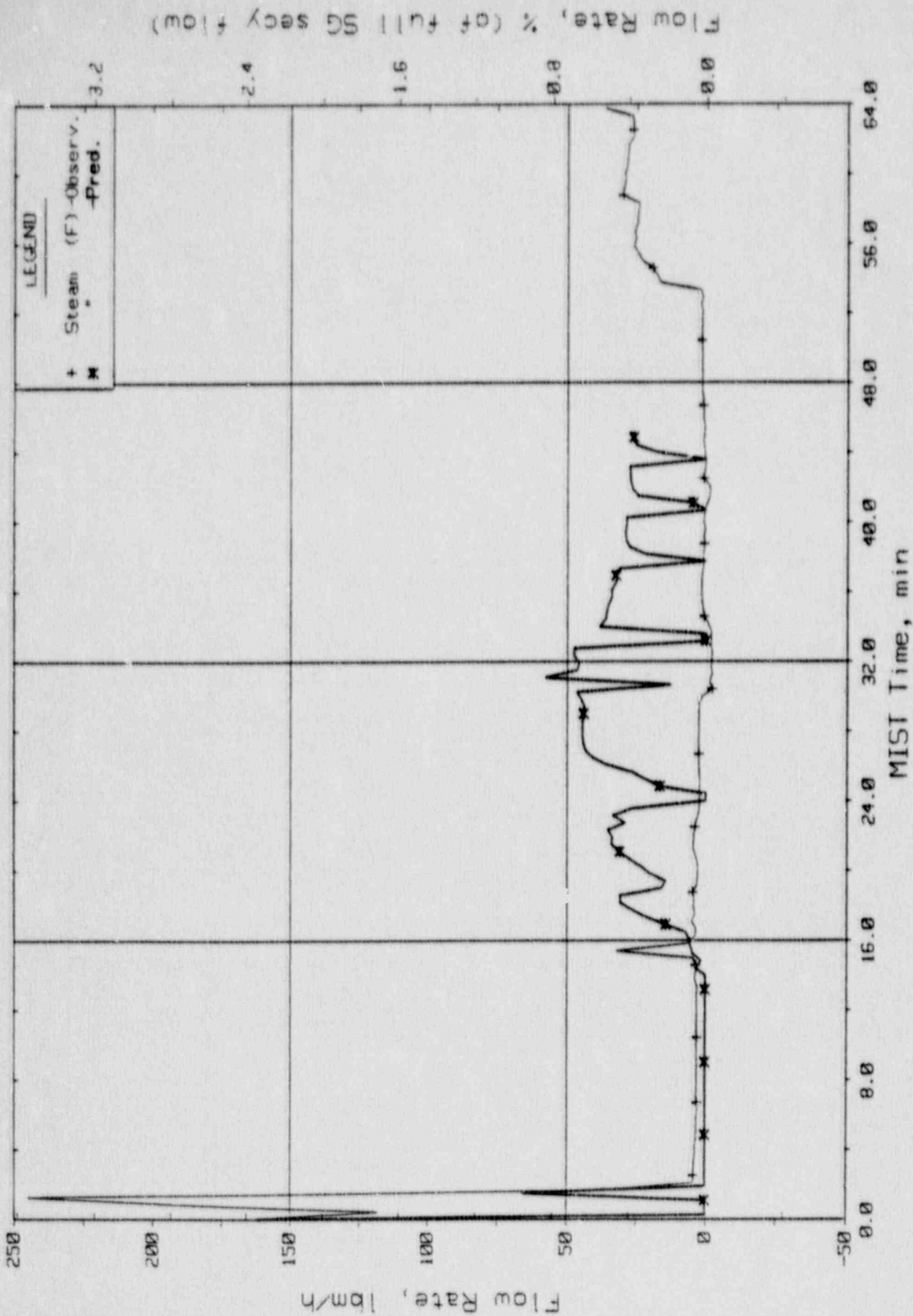


Figure 2.2.16. Steam Generator A Flow Rates (Cссор20).

SGTR BENCHMARK COMPARISONS  
 PRETEST BENCHMARK, Observed Vs. Predicted - Test3406AA

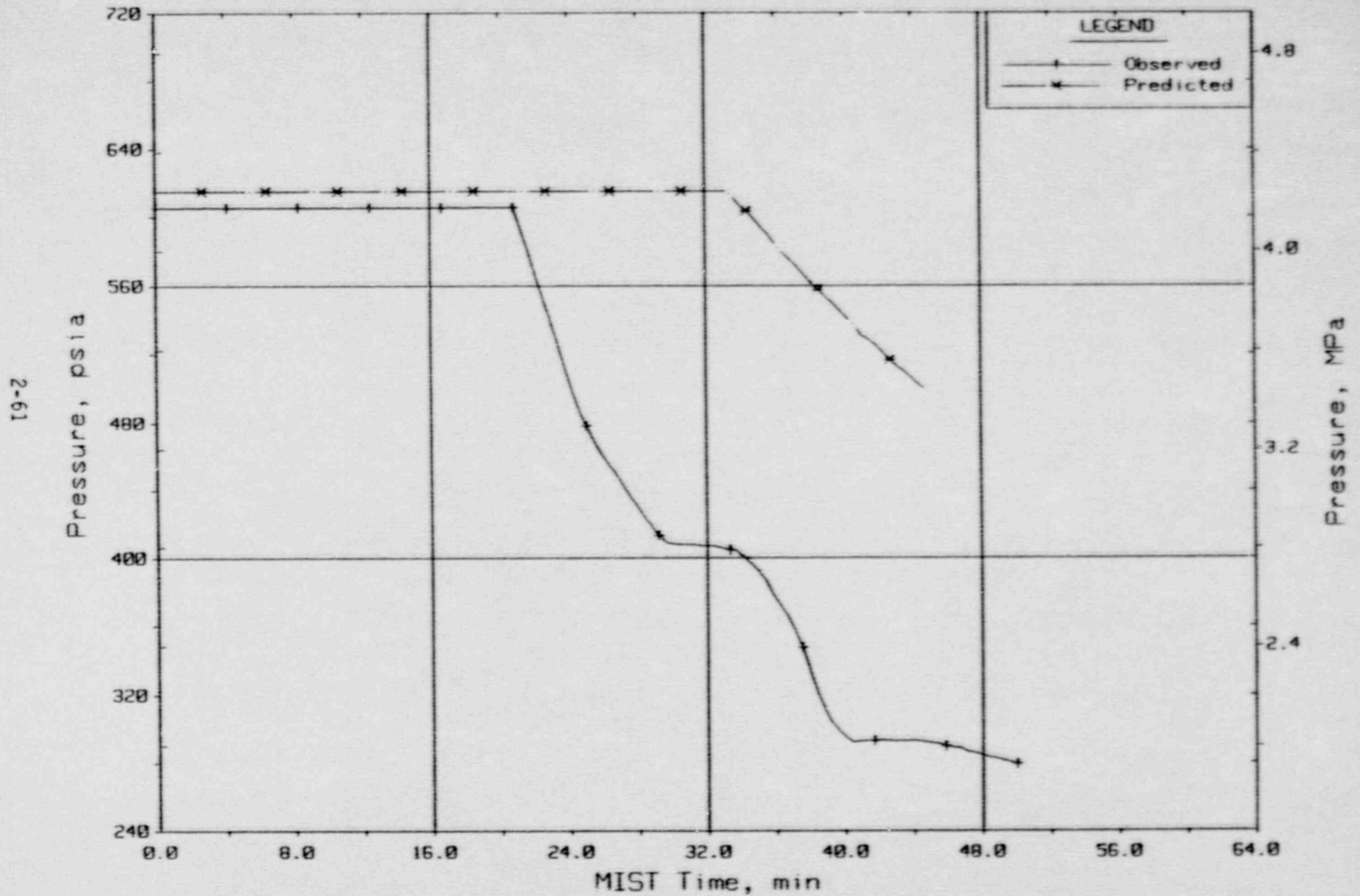


Figure 2.2.17. Core Flood Tank Pressure.

SGTR BENCHMARK COMPARISONS  
 PRETEST BENCHMARK, Observed Vs. Predicted - Test 3406AA

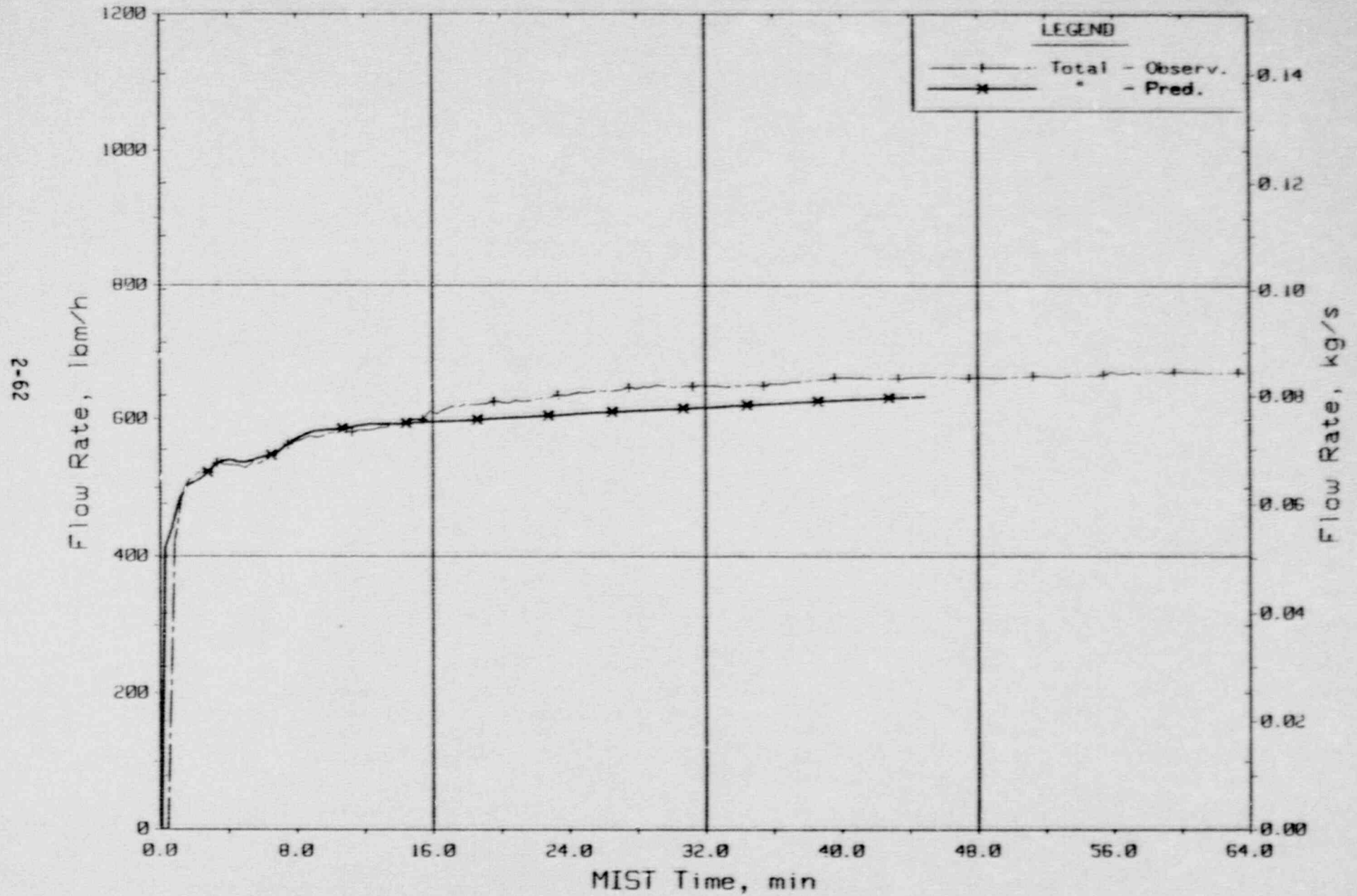


Figure 2.2.18. HPI Total Flow Rates.



SGTR BENCHMARK COMPARISONS  
 PRETEST BENCHMARK, Observed Vs. Predicted - Test 3406AA

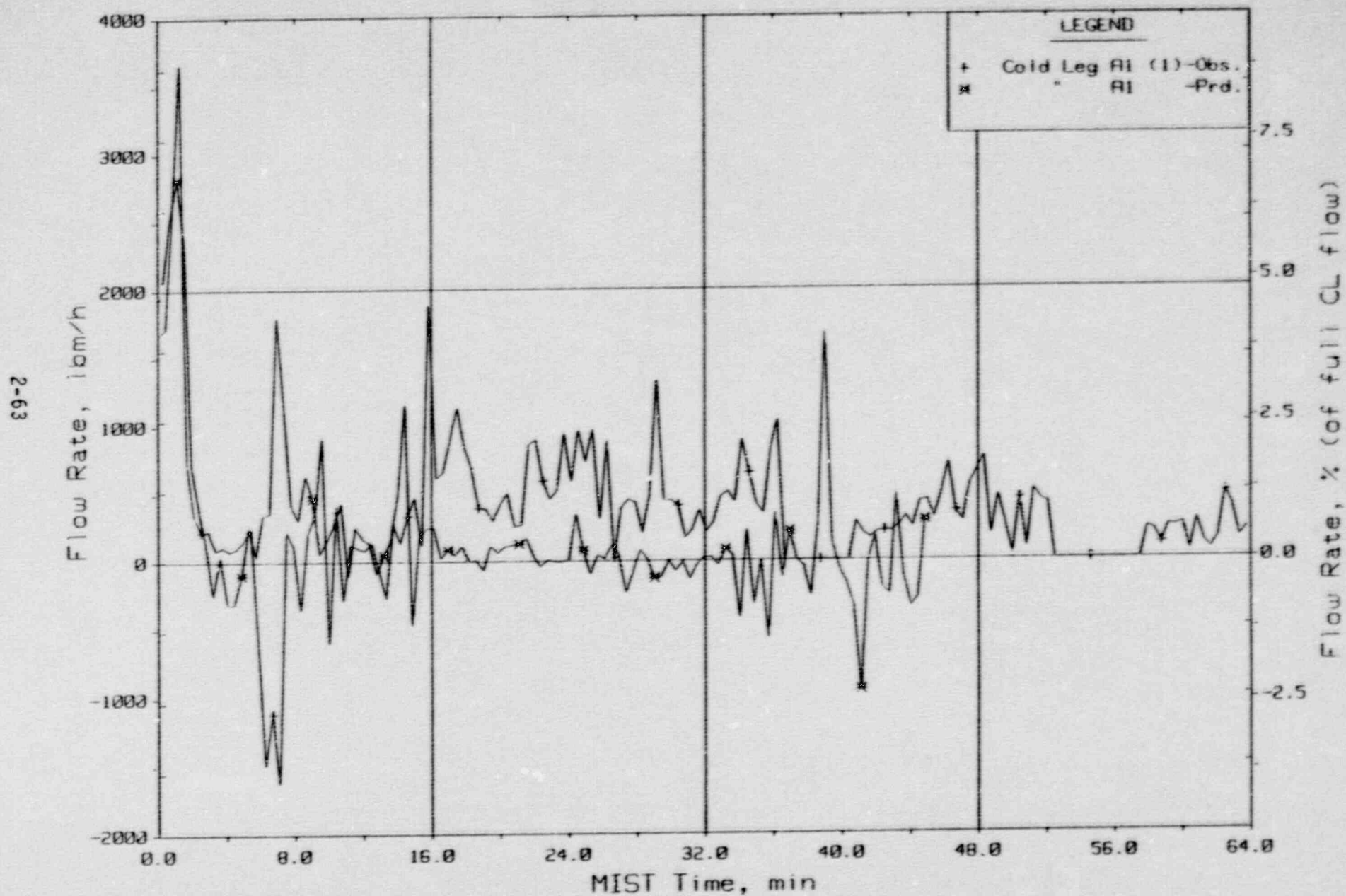


Figure 2.2.19. Loop AI Cold Leg (Venturi) Flow Rate (C1VN20).

SGTR BENCHMARK COMPARISONS  
PRETEST BENCHMARK, Observed Vs. Predicted - Test 3406AA

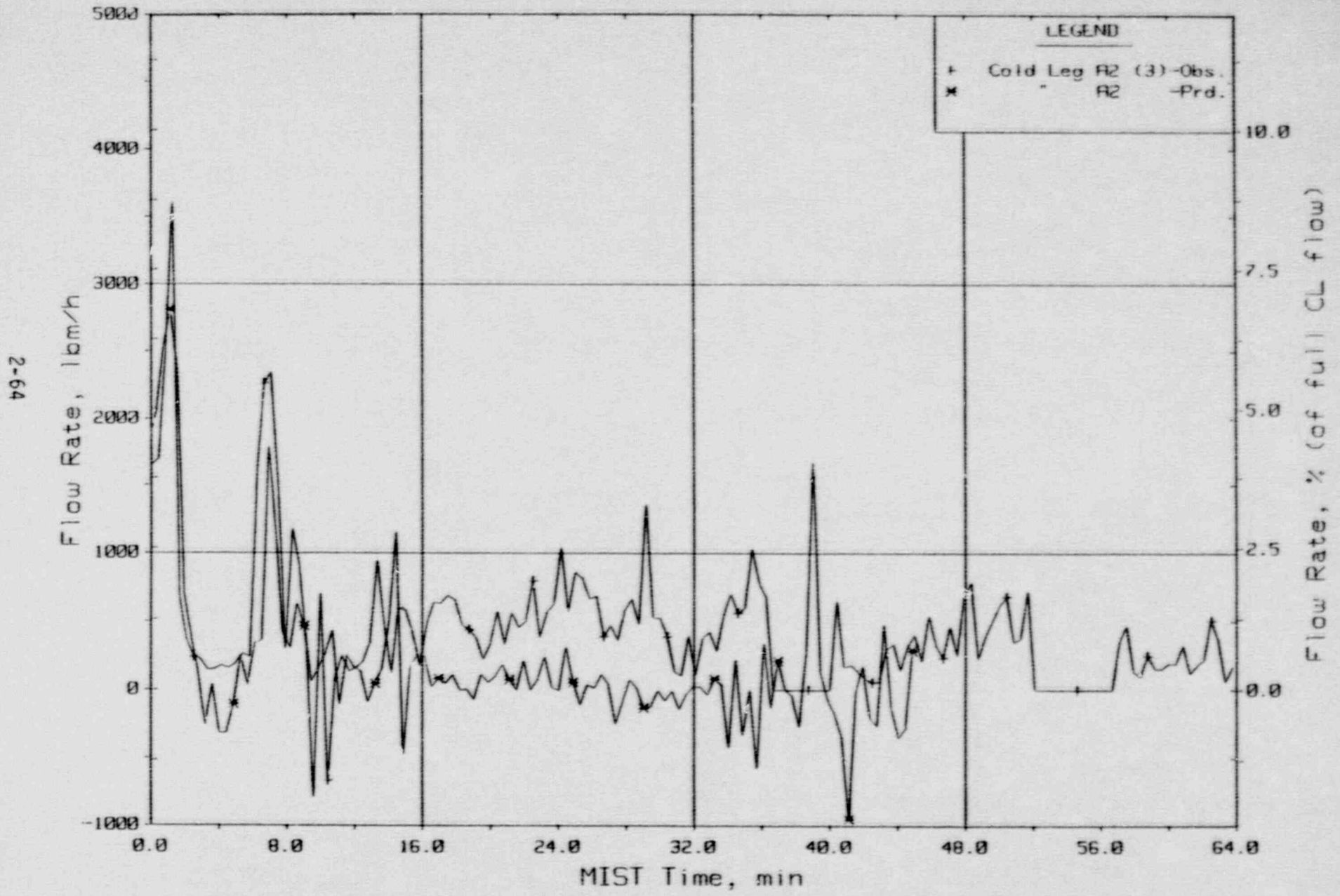


Figure 2.2.20. Loop A2 Cold Leg (Venturi) Flow Rate (C2VN20).

SGTR BENCHMARK COMPARISONS  
 PRETEST BENCHMARK, Observed Vs. Predicted - Test 3406AA

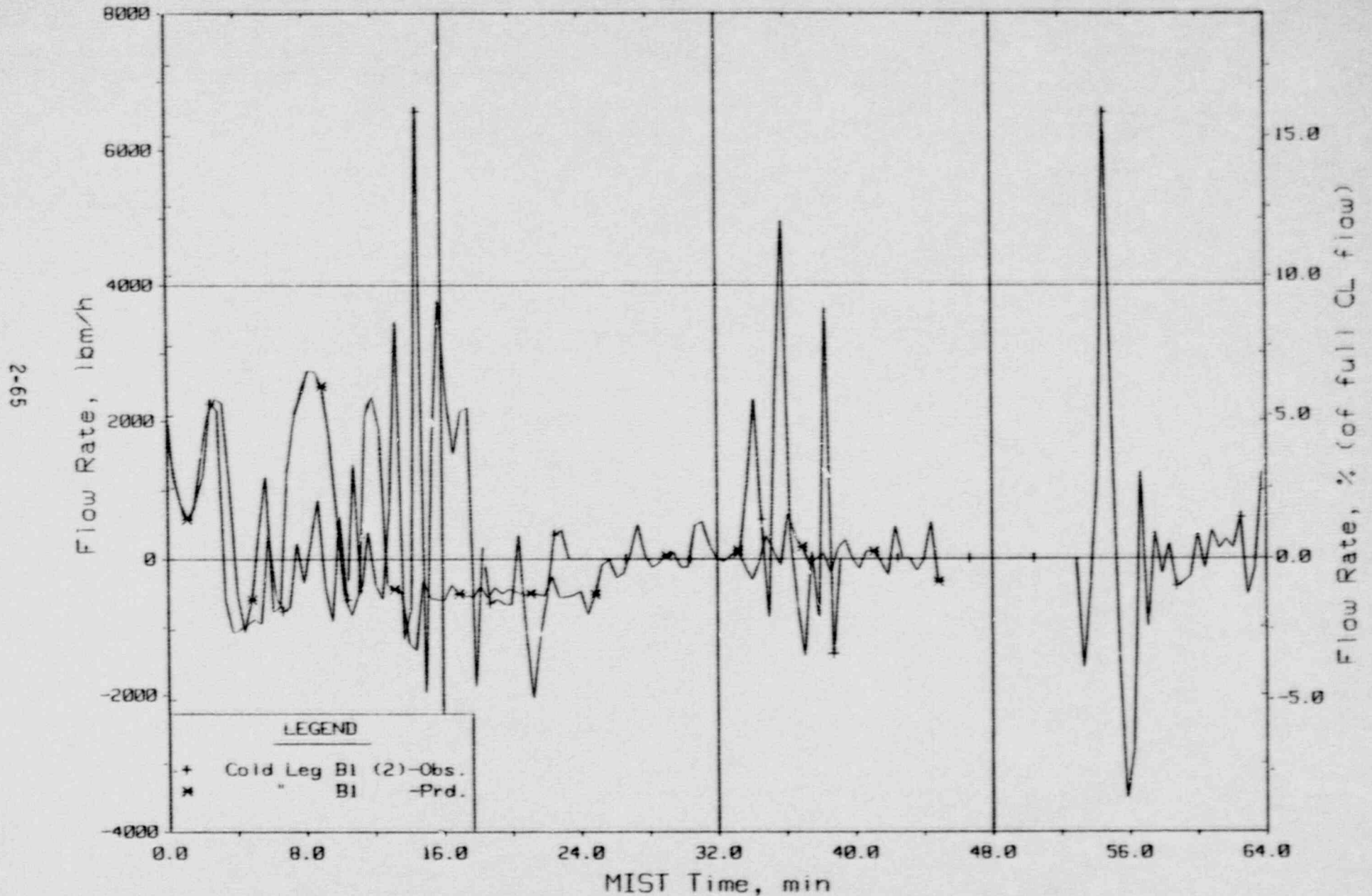


Figure 2.2.21. Loop BI Cold Leg (Venturi) Flow Rate (CIVN20).

SGTR BENCHMARK COMPARISONS  
 PRETEST BENCHMARK, Observed Vs. Predicted - Test 3406AA

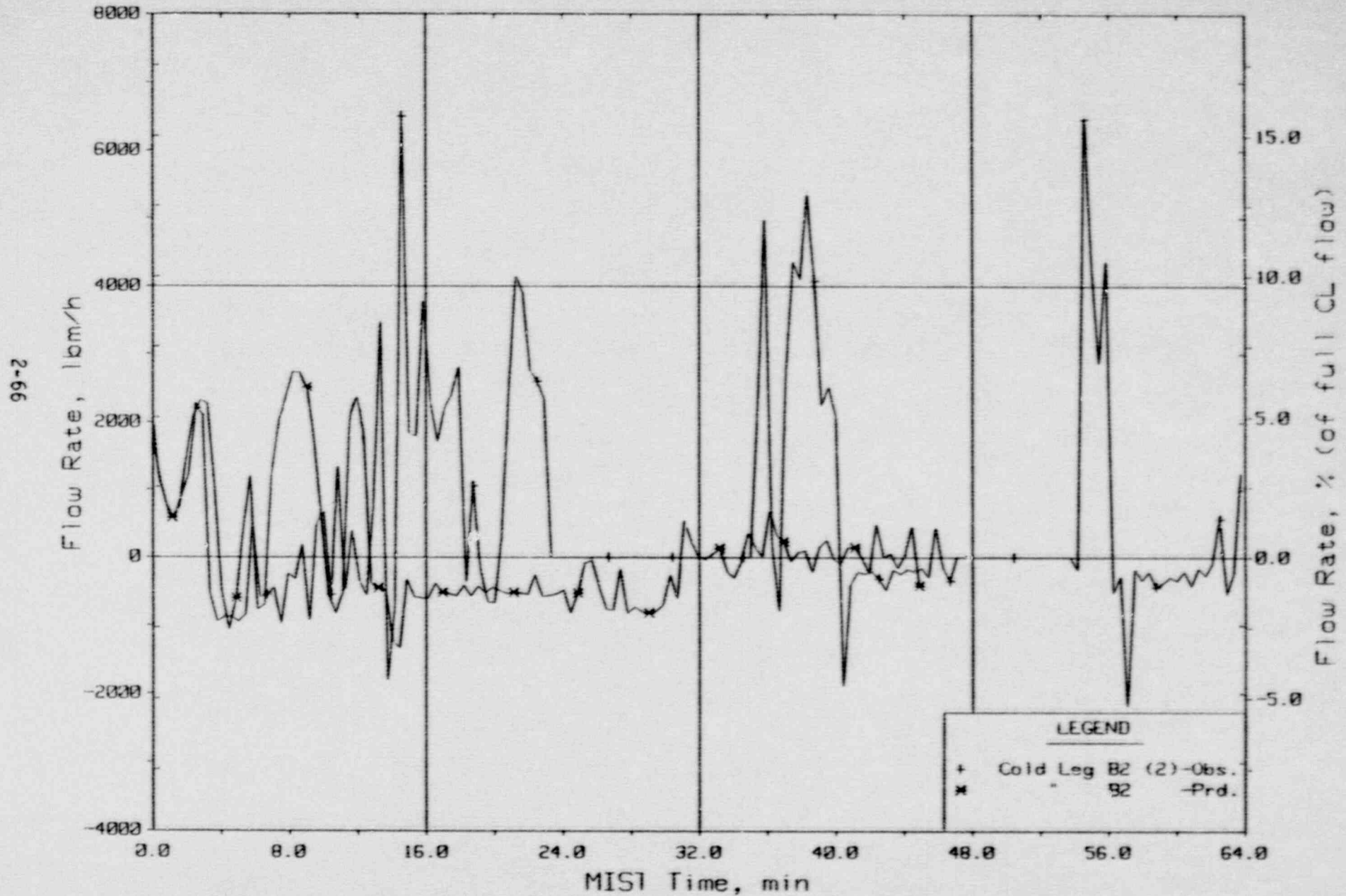


Figure 2.2.22. Loop B2 Cold Leg (Venturi) Flow Rate (C4VN20).

SGTR BENCHMARK COMPARISONS

PRETEST BENCHMARK, Observed Vs. Predicted - Test 3406AA

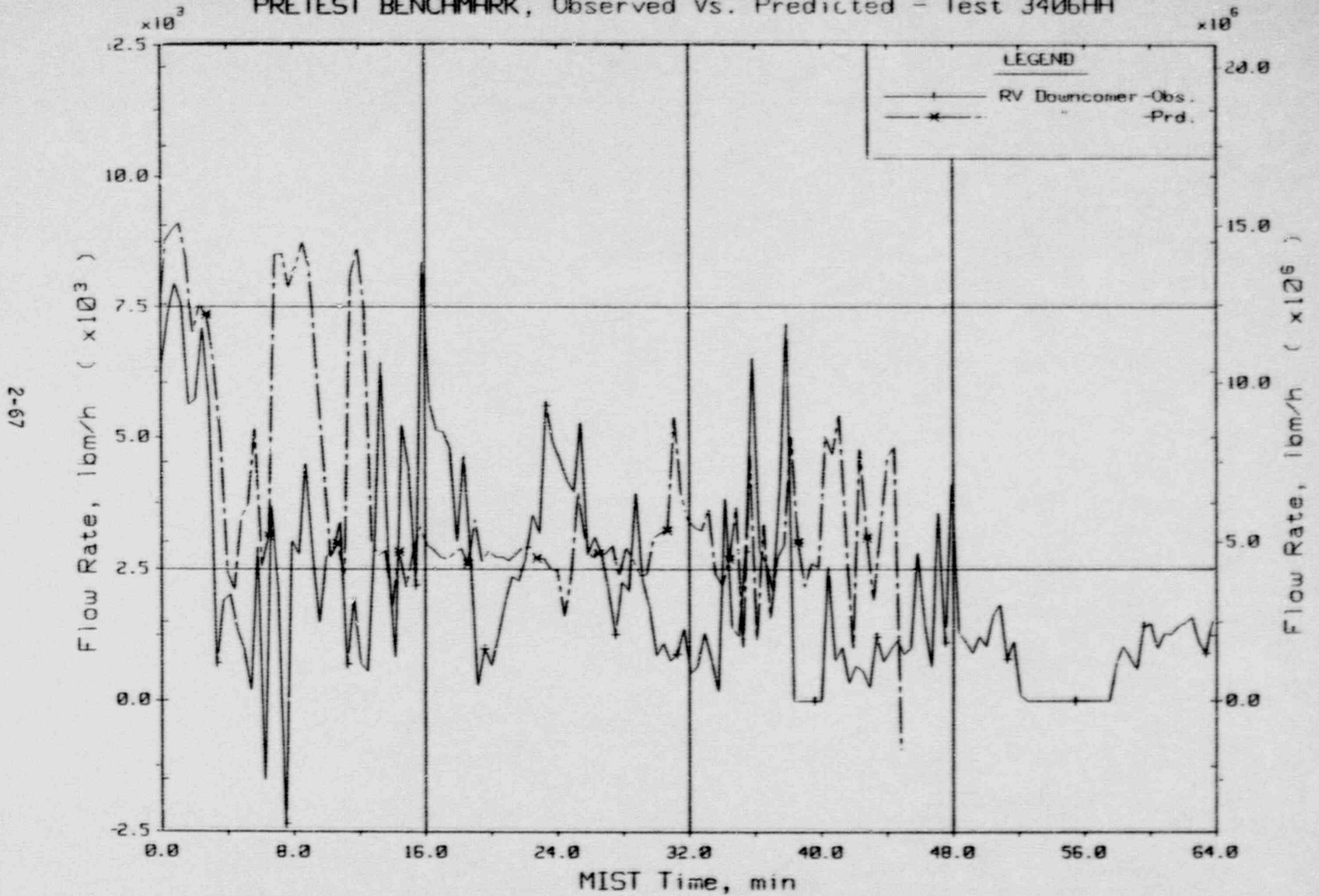


Figure 2.2.23. Primary System Venturi Flow Rates.

SGTR BENCHMARK COMPARISONS  
 PRETEST BENCHMARK, Observed Vs. Predicted - Test 3406AA

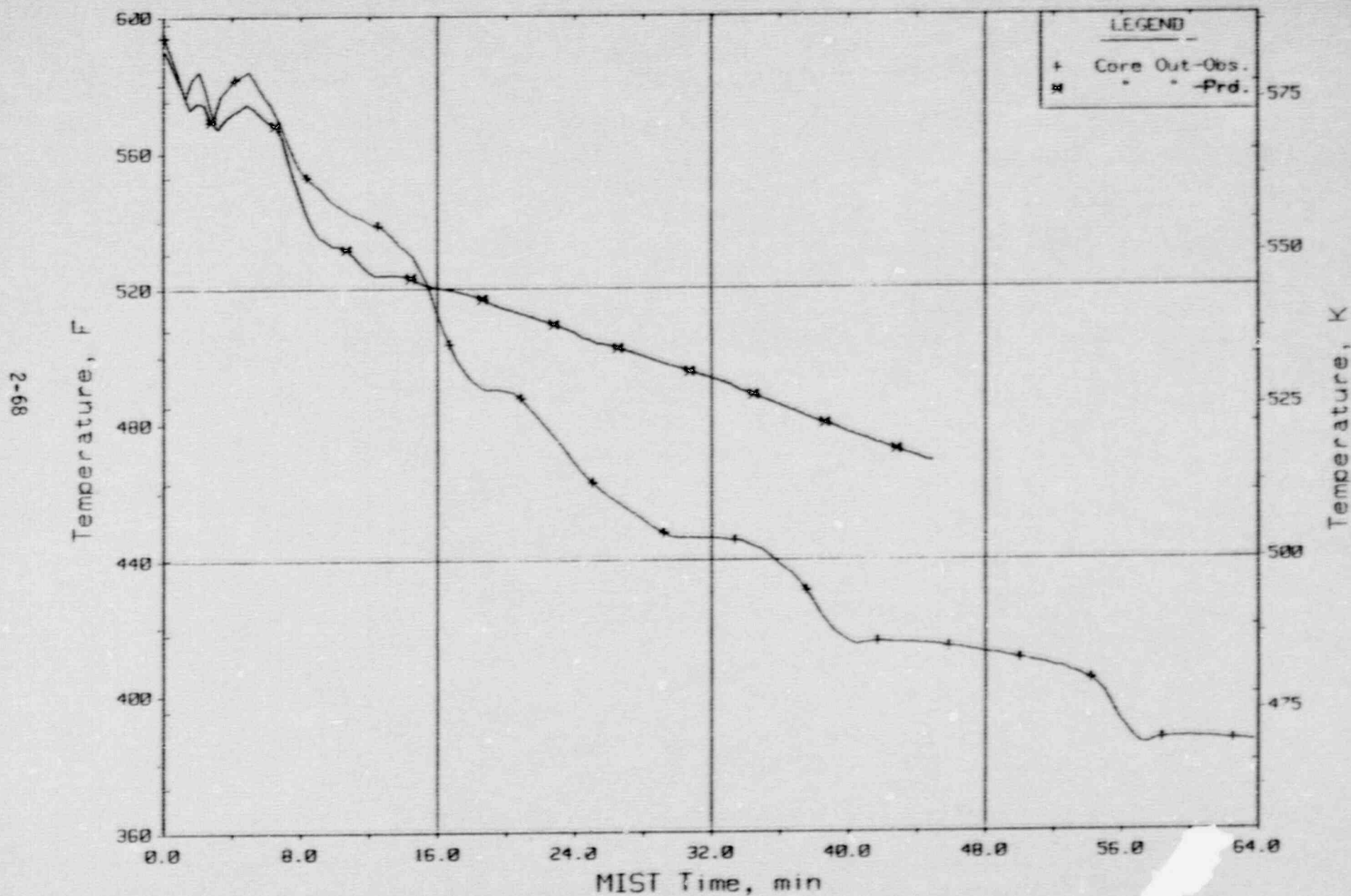


Figure 2.2.24. Core Exit Reactor Vessel Fluid Temperature (RVTC11).

SGTR BENCHMARK COMPARISONS  
 PRETEST BENCHMARK, Observed Vs. Predicted - Test 3406AA

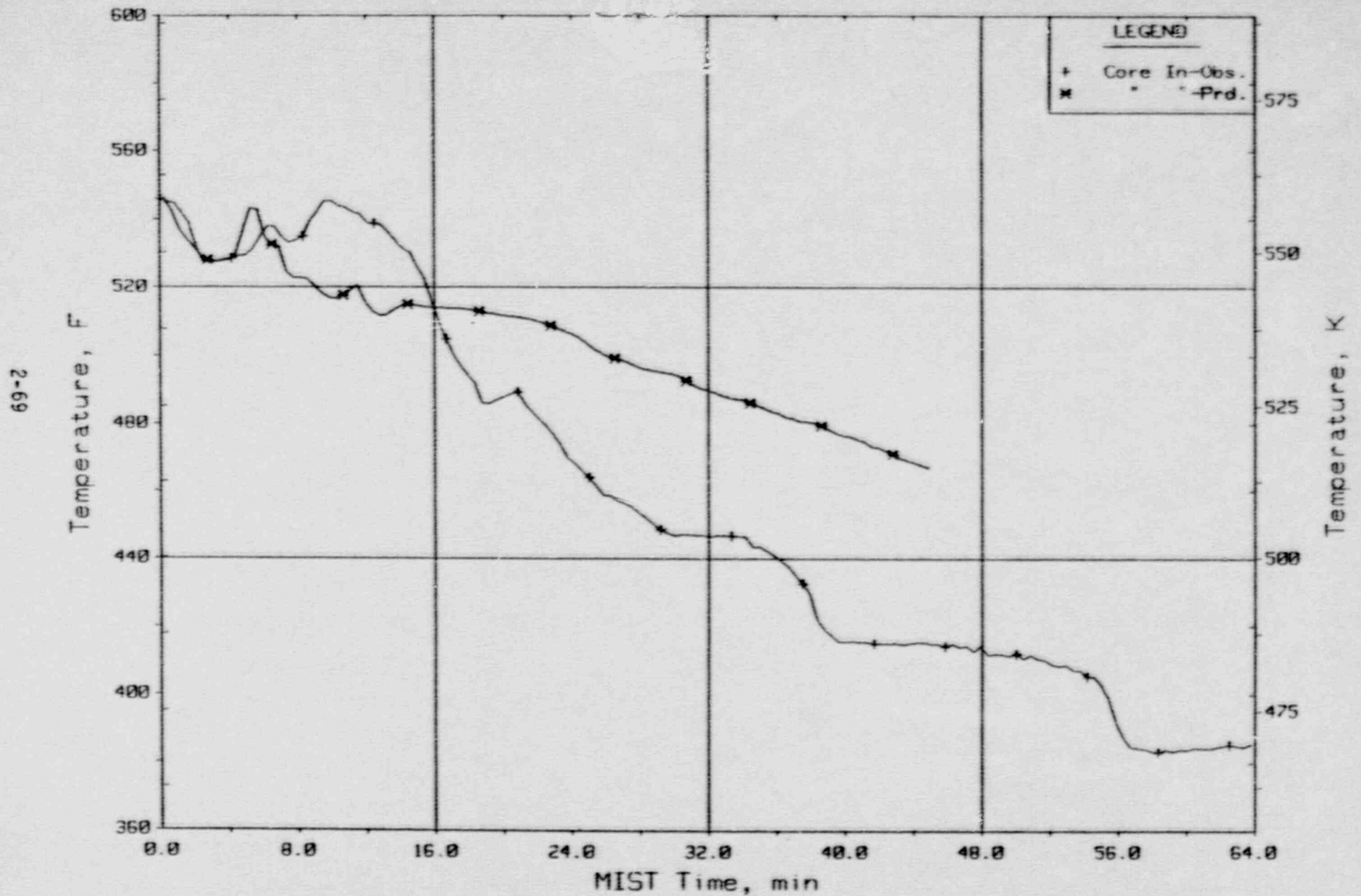


Figure 2.2.25. Core Inlet Reactor Vessel Fluid Temperature (DORT01).

SGTR BENCHMARK COMPARISONS  
 PRETEST BENCHMARK, Observed Vs. Predicted - Test 3406AA

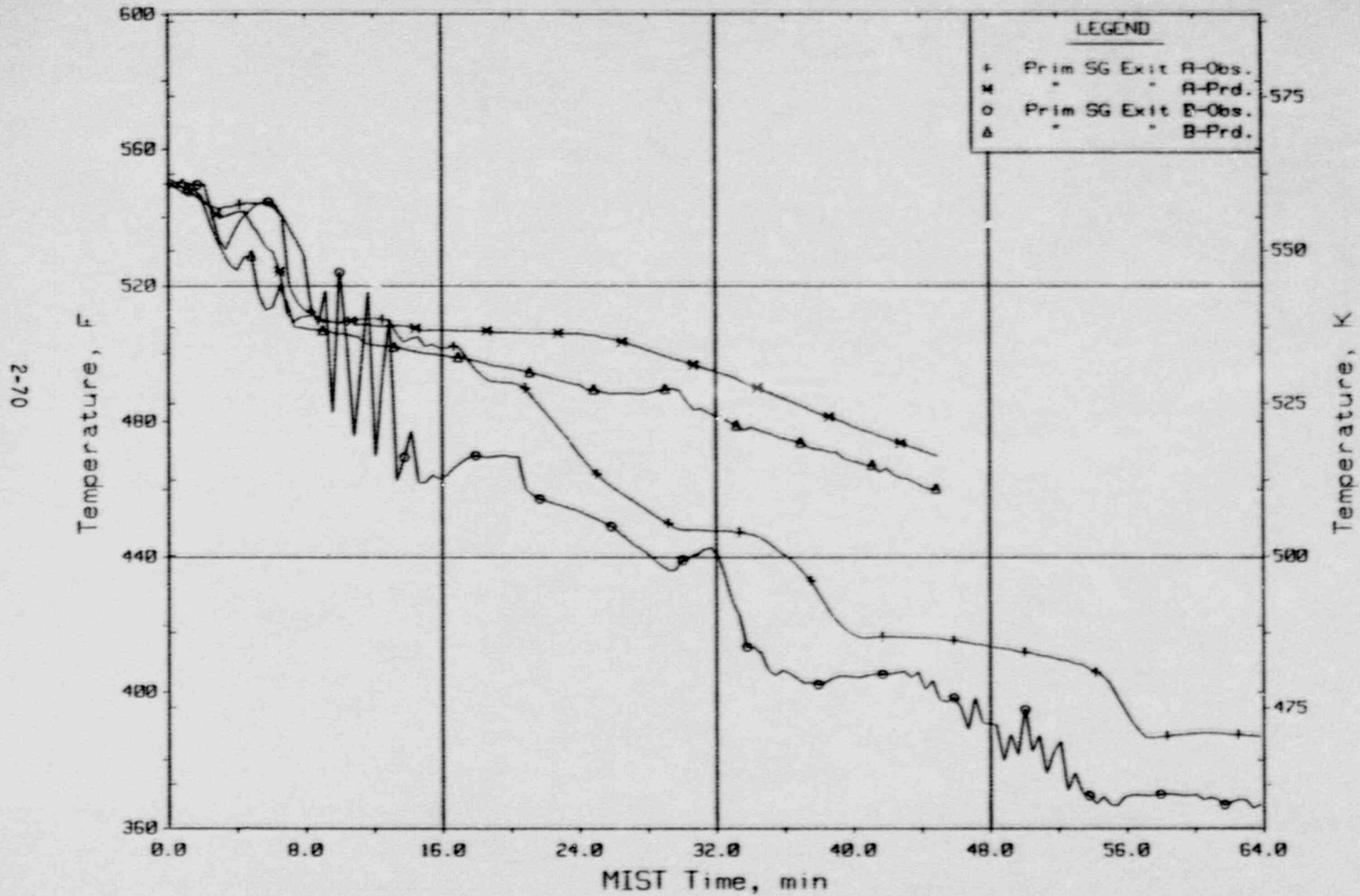


Figure 2.2.26. Loops A/B SG Exit Primary Fluid Temperatures (RTDs).



SGTR BENCHMARK COMPARISONS  
PRETEST BENCHMARK, Observed Vs. Predicted - Test 3406AA

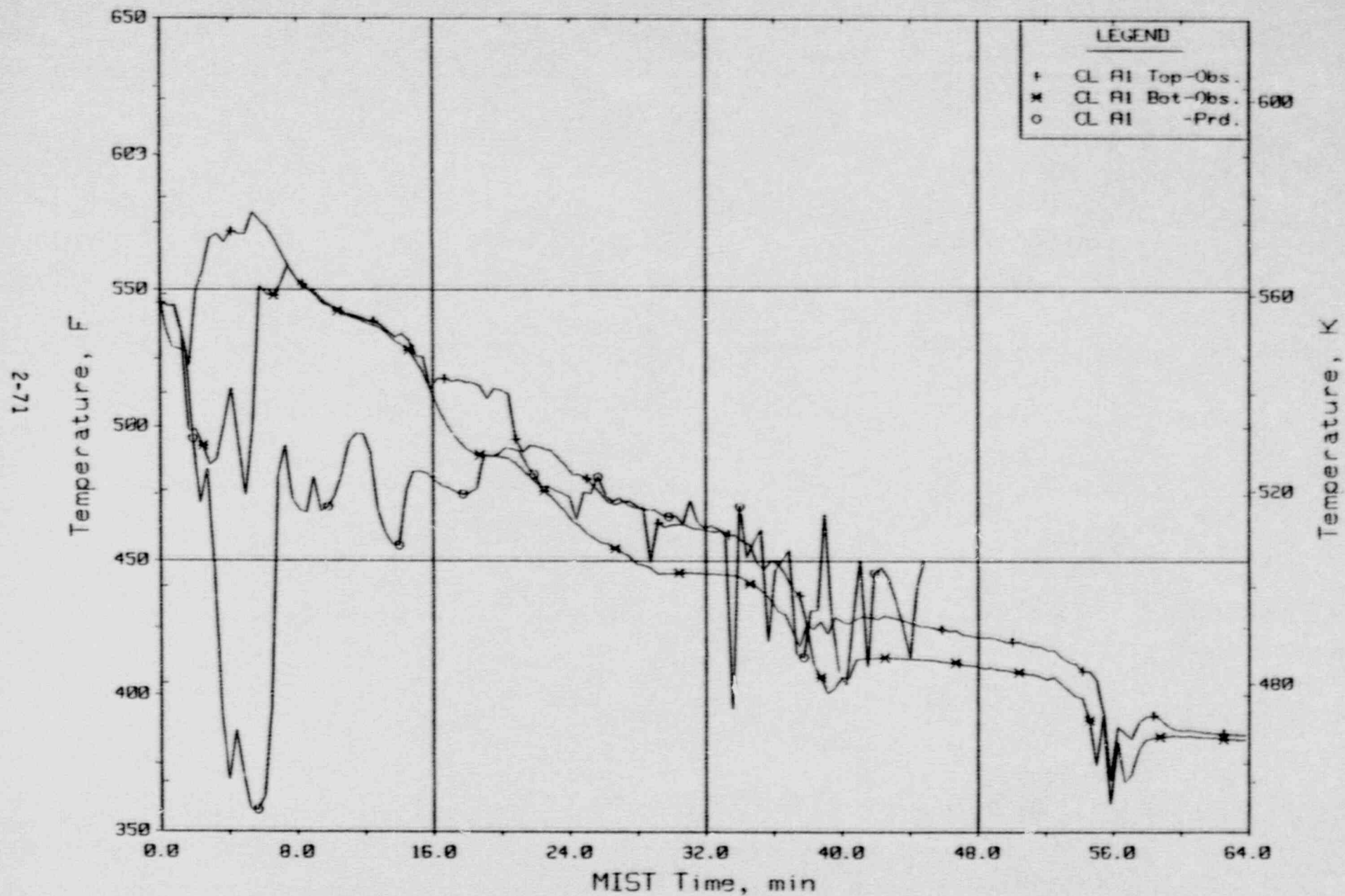


Figure 2.2.27. Cold Leg Nozzle Fluid Temperatures, Top/Bot of Rake (21.3ft, CnTC11/14s).

SGTR BENCHMARK COMPARISONS  
 PRETEST BENCHMARK, Observed Vs. Predicted - Test 3406AA

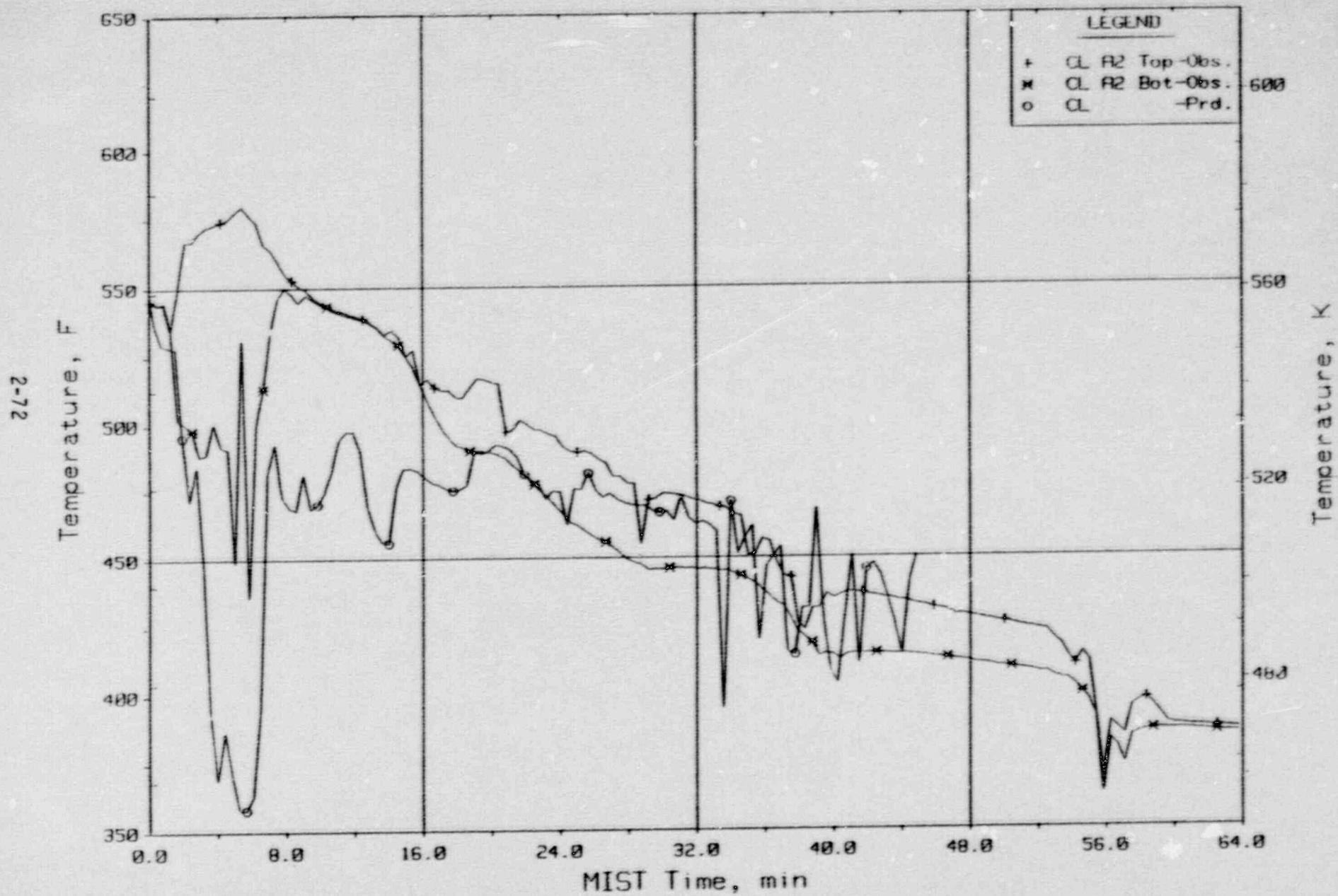


Figure 2.2.28. Cold Leg Nozzle Fluid Temperatures, Top/Bot of Rake (21.3ft, Ccltca2).

SGTR BENCHMARK COMPARISONS  
PRETEST BENCHMARK, Observed Vs. Predicted - Test 3406AA

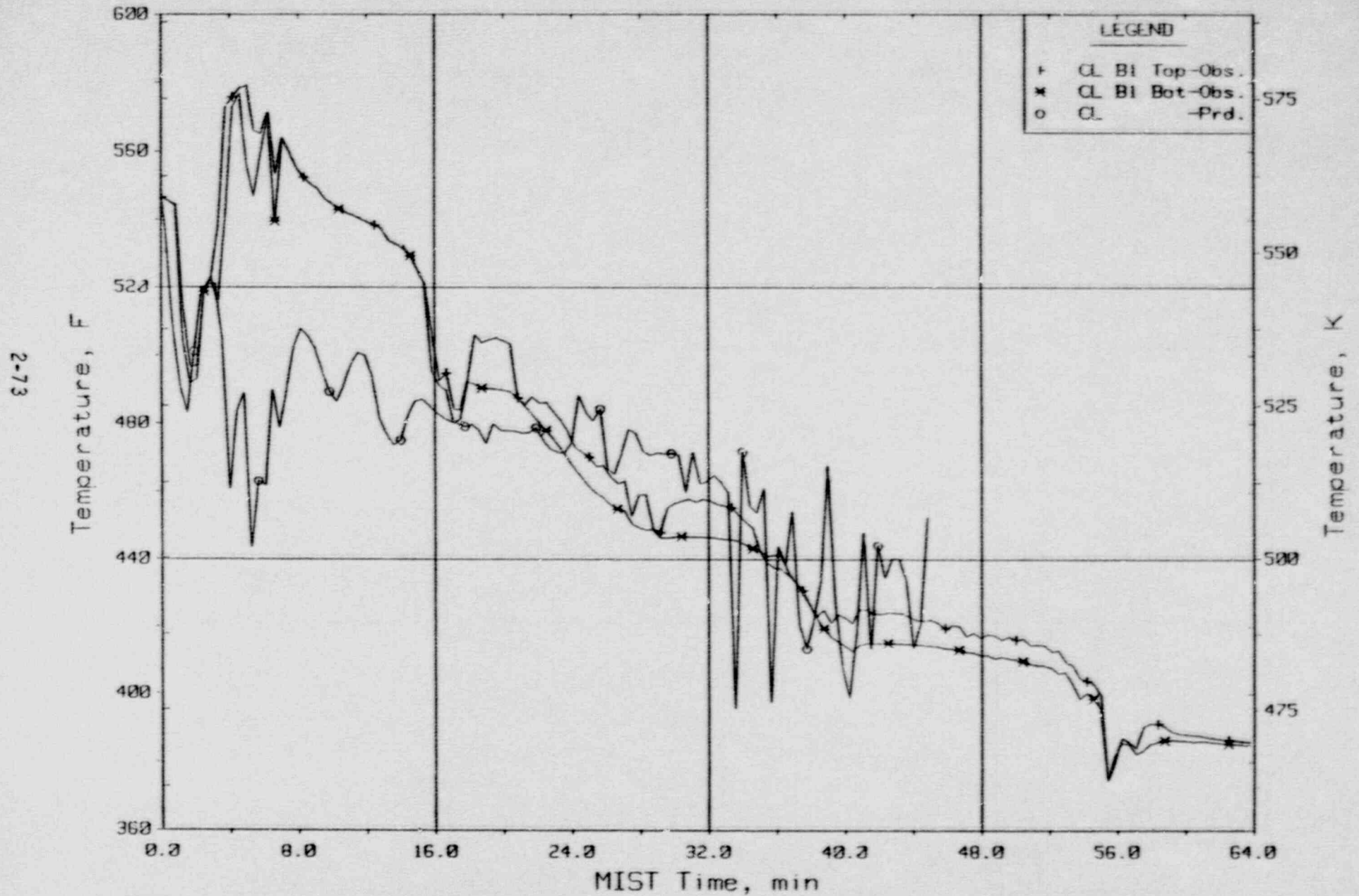


Figure 2.2.29. Cold Leg Nozzle Fluid Temperatures, Top/Bot of Rake (21.3ft, Cc1tcb1).

SGTR BENCHMARK COMPARISONS  
PRETEST BENCHMARK, Observed Vs. Predicted - Test 3406AA

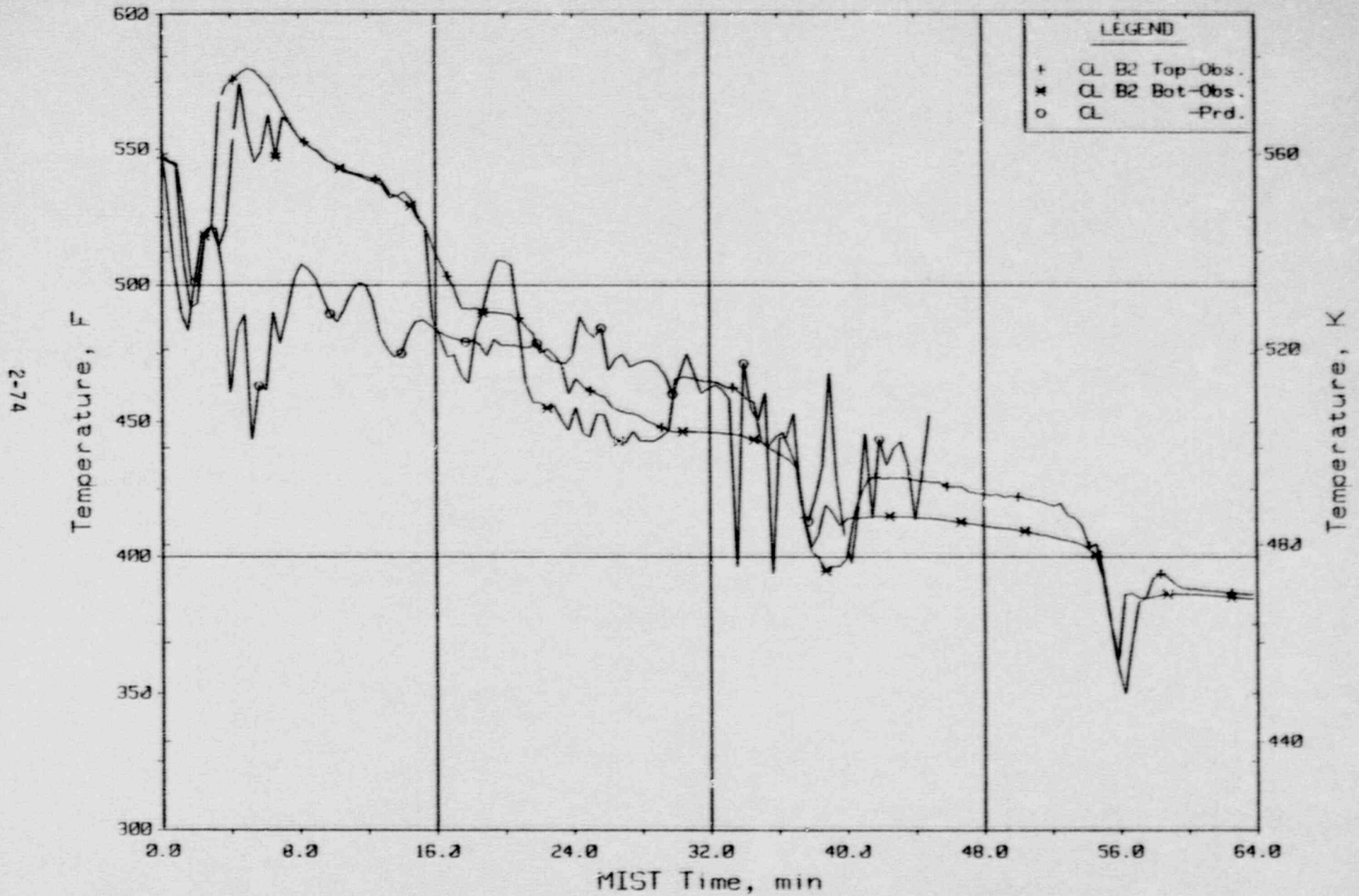


Figure 2.2.30. Cold Leg Nozzle Fluid Temperatures, Top/Bot of Rake (21.3ft, Cc1tcb2).

### 3. POST-TEST PREDICTIONS

The IST program authorized five separate MIST post-test predictions using the latest B&W version of RELAP5/MOD2. The first step in completing these predictions was to upgrade the pretest prediction base deck as necessary. These upgrades were sponsored and funded by the B&W Owners Group and documented in a separate report.<sup>5</sup> The goal of the upgrades was to accurately represent the geometrical and modeling inputs with facility drawings and data such that a new, accurate steady-state could be calculated with minimal tuning of the steam generator tube wetted fractions. Modifications which could improve transient predictions were also included. The steps involved in upgrading the model were completed in the following order:

1. Check the component physical characteristics and volumes and adjust where necessary;
2. Evaluate the estimated facility uncompensated heat losses and adjust the input model values;
3. Adjust the modeled irrecoverable pressure drops through the incorporation of measured surface roughnesses and form loss coefficients; and
4. Make miscellaneous changes such as adding cold leg collapsed level calculations, adjusting the initial core power to include line losses, and modifying the AFW proportional-integral controller gains.

Included in these updates were significant adjustments to the reactor coolant pump and reactor vessel lower head volumes. Removal of the four CLPS cooled thermocouple heat losses, addition of secondary steam line heat losses, and adjustment of the RVVV and reactor coolant pump heat losses provided a better prediction of system uncompensated heat losses. The pump locked rotor, CLPS venturi, and reactor vessel downcomer venturi resistances were each increased to measured values. After completing these changes the new nominal natural circulation steady-state was recalculated. Slight adjustments to the steam

generator AFW wetted fractions altered the steam generator thermal center such that the measured test natural circulation flows were achieved.

Following completion of the model changes the post-test calculations were performed. An agreement was made to use the results directly from the base model without tuning or massaging the answer. In other words, the predictions were performed with the base model plus any boundary system or control changes necessary to accurately model the test. If any significant deviation from the observed results was calculated, then the findings were documented. If the calculations were rendered unusable with the deviation, then any necessary model changes were made and documented accordingly. By using this approach, the true predictive capabilities of the code and input model are easily evaluated, while possibly saving extensive computer resources.

A systematic process<sup>15</sup> was used to select which MIST tests would be benchmarked with RELAP5/MOD2. First, the MIST PMG designated selection criteria to be applied to each test. These criteria included:

- Presence of key phenomena
- Relevance to TAG issues
- Relevance to generic technical bases for ATOG
- Economics
- Provide information about significant code limitations
- One test from each group
- Applicability to full size PWRs
- Characterize accuracy of code component models
- Characterize accuracy of code constitutive relations

Next, B&W applied the first criteria to make a list of observed and TAG phenomena (Table 3.1) and to develop a matrix denoting which phenomena were observed at each test. Finally, using this matrix, B&W applied the rest of the criteria to yield a list of tests which exhibit the largest number of phenomena, would provide the greatest challenge to the code's component models and constitutive relations, which meet as many of the other criteria as possible and would be benchmarked at reasonable expense.

B&W recommended RELAP5/MOD2 calculations of 13 tests (Table 3.2). Also, for most efficient use of the available funding, B&W recommended that the B&W Owners Group sponsor six post-test calculations<sup>9-14</sup> and that the MIST PMG sponsor five post-test calculations. Only the PMG sponsored post-test calculations are discussed in this report.

The first PMG sponsored post-test prediction was performed on MIST test 320503. This test was a repeat of the nominal test with leak isolation at 30 minutes into the test. The second prediction was performed on test 320302, a scaled 10 cm<sup>2</sup> CLPS leak with full HPI capacity. A scaled one tube high SGTR, test 340213, was performed next followed by the noncondensable threshold test 3502CC. The final test prediction was performed on test 3801AA. This test included core uncover and was performed with pumps running. A brief test description, base input model changes required, steady-state comparisons, transient comparisons, and conclusions are included in the following sections for each test.

### 3.1. MIST Test 320503 Post-Test Prediction

MIST test 320503 began as a repeat of the nominal case 3109AA. At 30 minutes into the test, however, the cold leg pump discharge (CLPD) leak in loop B1 was isolated. Following leak isolation, the primary repressurized until it refilled the hot legs and re-established natural circulation. The refill with full high pressure injection flow was accomplished by approximately 50 minutes into the test. Once continuous natural circulation was restored the RELAP calculations were stopped. The RELAP5/MOD2 simulation was performed using the base deck post-test prediction model with several minor changes required to be consistent with test 320503 boundary conditions or operator actions. A detailed test description may be found in the MIST Group 32 Report.

Table 3.1. Phenomena and Observations Considered During  
Test Selection for Code Benchmarking

1. AFW Driven BCM Cooling
2. Pool Driven BCM Cooling
3. Internally Driven SG Instabilities (Alternating BCM)
4. Externally Driven SG Instabilities
5. Cold Leg Flow Oscillations
6. Interruption/Re-Establishment of NC
7. Refill/Collapse Void/Restart
8. RVVV Performance in Single Phase
9. RVVV Performance in 2 Phase
10. Intermittent Saturated Natural Circulation
11. Single Loop NC Cooldown
12. Two Loop NC Cooldown
13. Cooldown with CVL (DB-1 Specific)
14. Intra Loop Circulation
15. TSP Flooding During High Steaming Rate
16. TSP Flooding During High Feedwater Rate
17. Cold Leg Counterflow (Single Phase)
18. Stratified Fluid in Cold Leg (Two Phase)
19. Steam Generator Overfill (Event)
20. Rapid Increase in Subcooling
21. Vapor, Liquid out the PORV (Pre-Surgeline Uncovery)
22. Surgeline Uncovery
23. Effect of AFW Wetting
24. NCG Transport (3 Modes)
25. Core Uncovery (heater temperature greater than  $T_{sat}$ )
26. Steam Line Break
27. RC Pump Bump
28. Continuous Operation of RCP During SBLOCA
29. SG Pool Heat Transfer (Boil-Off Without Feedwater)
30. Steady-State AFW Heat Transfer
31. Steam Generator Overfill (Controlled during SGTR)



Table 3.2. MIST Tests and Sponsors for RELAP5/MOD2 Benchmarks

<u>MIST PMG</u>	<u>B&amp;W Owners Group</u>	<u>Toledo Edison Company</u>
3801AA	3105AA	370199 (pre-test)
3502CC	320604	330499
340213	320201	
320302	3404AA	
320503	350101	
	3601AA	

3.1.1. MIST Test 320503 Base Case Modifications

The RELAP5/MOD2 base input model was modified as follows to allow the transient calculations to be performed as simulated.

1. The break was changed to a trip valve junction with an isolation trip applied to isolate the leak at 30 minutes.
2. The original break area was changed from the scaled 50 cm<sup>2</sup> to a scaled 10 cm<sup>2</sup> break.
3. A control variable to calculate core subcooling margin was added to accommodate HPI throttling at the end of the test.
4. Miscellaneous time step and minor edit variable additions or changes were made to aid in interpreting the test simulation.

These changes are documented in detail in the calculational file for this test.

3.1.2. MIST Test 320503 Transient Comparisons

The initial conditions for the RELAP calculation are consistent with the test conditions just before leak opening at time zero. Table 3.1.1. contains a listing of test and RELAP calculated conditions, while the transient comparison plots are shown in Figures 3.1.1. through 3.1.35. The core power, secondary pressure, secondary collapsed level, hot leg subcooling margin, and pressurizer level were defined for the steady-state initialization. The remainder of the parameters were determined from the spacial heat transfer and thermal-hydraulic system behavior. Table 3.1.2. contains a transient sequence of events.

The primary system depressurized quickly following leak actuation until 2 minutes when the upper regions of the system began to saturate. The observed pressure dropped below the predicted value by approximately 50 psi within the next three or four minutes due to several factors. First of all, the observed loop A hot leg flow did not completely interrupt. Therefore, a higher core flow was obtained, resulting in a delay in the onset of significant core boiling. The slightly earlier actuation of HPI also delayed the beginning of this event as the core fluid cooled quicker than the predicted value. In the prediction, the A loop flow completely interrupted at 4 minutes and remained that way until 9 minutes. As a result, the cold HPI flow mixed with the CLPD fluid cooling it and did not reach the core inlet until after the predicted loop A spill-over flow surge at 9 minutes. This spill-over occurred when the rapid accumulation of steam in the reactor vessel upper head displaced extra liquid into the hot legs increasing the mixture level above the U-bend spill-over elevation.

A spill-over was observed in the B loop at 12 minutes in the test due to the steam accumulation in the reactor vessel upper head. The magnitude of this spill-over was enhanced because the facility RVVVs closed at 13 minutes for two minutes. The RVVVs remained open continuously in the prediction. During the spill-over primary-to-secondary heat transfer was restored and the secondary side repressurized to the control pressure. The impact of the heat transfer on the primary pressure was minimal since the energy was removed from the liquid. The effect of the secondary repressurization was more evident later in the transient, since it allowed the secondary control pressure to decrease.

After 15 minutes the observed and predicted hot leg U-bend flows remained interrupted until the first refill spill-overs were encountered. The hot leg and steam generator primary levels declined at similar rates as system liquid inventory was lost. At 30 minutes, however, the CLPD leak was isolated. The primary system repressurized due to the HPI refill. The predicted rates of repressurization and increase in primary collapsed levels corresponded closely to the observed rates during this period. The small perturbations in the repressurization rates in both cases prior to 48 minutes were due

condensation rate fluctuations associated with variations in the reactor vessel downcomer level.

Between 48 and 51 minutes the hot leg levels increased to the point where U-bend spill-overs and complete refill had occurred. The test spill-overs behaved more symmetrically than the predicted spill-overs, although little impact of this difference was observed. The effect of the steam generator control pressure differences was obvious after the recoupling of the primary-to-secondary heat transfer. Since the steam generator B repressurization at 18 minutes was not predicted, the control pressure was considerably higher when refill spill-overs occurred. Therefore, the predicted secondary pressures had to rise to the control pressure before the secondary steaming and feeding could occur. Without the steaming and feeding, the magnitude of the primary-to-secondary heat transfer would have been significantly reduced resulting in a slower primary system depressurization. For this reason, the calculations were terminated at 52 minutes following the hot leg refill. It should be noted that the core exit subcooling reached 70 F and the automatic HPI throttling had begun just as the calculations were halted.

Table 3.1.1. MIST Test 320503 Calculated and Measured Initial Steady-State Conditions

Parameter	Data	RELAP5
Primary Pressure, (psia)	1732.	1727.
SG A Secondary Pressure*, (psia)	1014.	1010.
SG B Secondary Pressure*, (psia)	1015.	1010.
SG A Secondary Collapsed Level*, (ft)	5.53	4.95
SG B Secondary Collapsed Level*, (ft)	5.57	4.95
Hot Leg Subcooling Margin*, (F)	22.8	22.0
Pressurizer Collapsed Level*, (ft)	22.80	22.95
Core Power into the Fluid*, (Btu/s)	119.5	119.5
Primary Side Mass Inventory	972.0	970.0
SG A Primary Exit Temperature, (F)	550.0	550.3
SG B Primary Exit Temperature, (F)	550.0	550.3
Core Exit Temperature, (F)	593.0	593.4

\*Denotes specified condition.

Table 3.1.2. MIST Test 320503 Sequence of Events Comparisons

Event	Approximate Test Time (Min)	
	RELAP	Data
Scaled 10-cm <sup>2</sup> CLPD Leak Opened	0.0	0.0
Pressurizer Level to 1.0 ft: Initiate Core Power Ramp, HPI, RVVV Automatic Control, SG Secondary Refill and Depressurization	2.8	2.3
First Hot Leg A Flow Interruption	4.0	4.0
SG Secondary Level to 31.6 Feet	10.0	9.0
First Hot Leg B Flow Interruption	9.8	9.5
SG A Primary Level to Top of Tubes	22.2	21.6
SG B Primary Level to Top of Tubes	27.0	27.0
Leak Isolated -- Primary Refill Began	30.0	30.0
Downcomer Level Above Nozzle	33.5	38.5
Downcomer Liquid Full	45.7	46.0
Loop B First Refill Spill-Over	48.5	49.5
Core Exit Subcooling Exceeds 70F	51.8	50.7
Loop A First Refill Spill-Over	50.3	49.5
Both Hot Legs Refilled	49.6	50.3
Calculations Terminated	52.0	--

3.1.3. MIST Test 320503 Post-Test Conclusions

The RELAP5/MOD2 post-test prediction of MIST test 320503 was quite reasonable. All major system trends were predicted at nearly the same time and magnitude as was observed in the test. The most significant deviation was probably due to not predicting the loop B spill-over and RVVV closing near 13 minutes in the test. The secondary control pressure was therefore predicted to remain at 1010 psia until late in the calculations.

10 cm<sup>2</sup> CLPD Break with 30 Minute Isolation  
 MIST Nominal Test, Observed Vs. Predicted - Test 320503

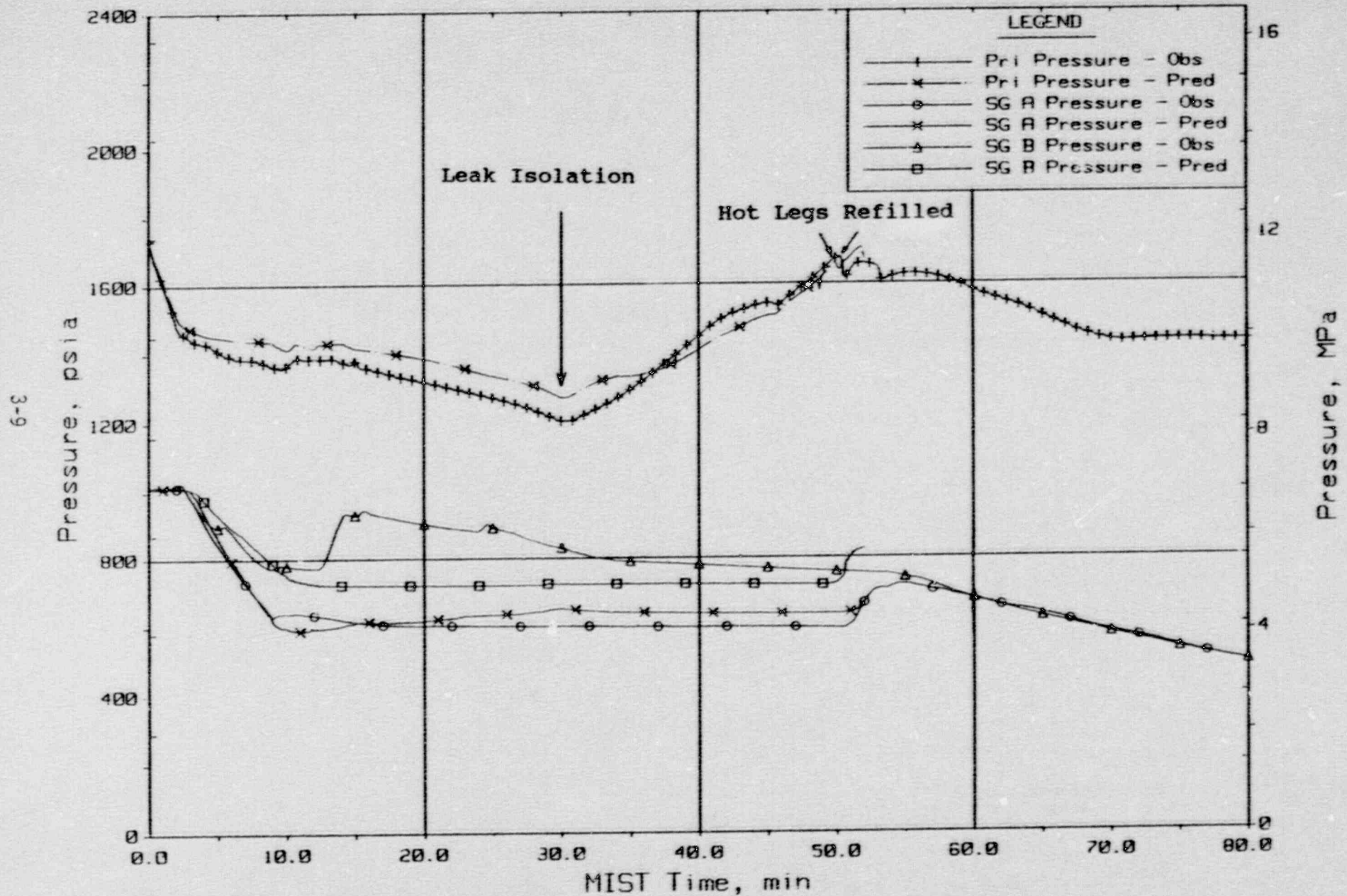


Figure 3.1.1. System Pressures.

10 cm<sup>2</sup> CLPD Break with 30 Minute Isolation  
 MIST Nominal Test, Observed Vs. Predicted - Test 320503

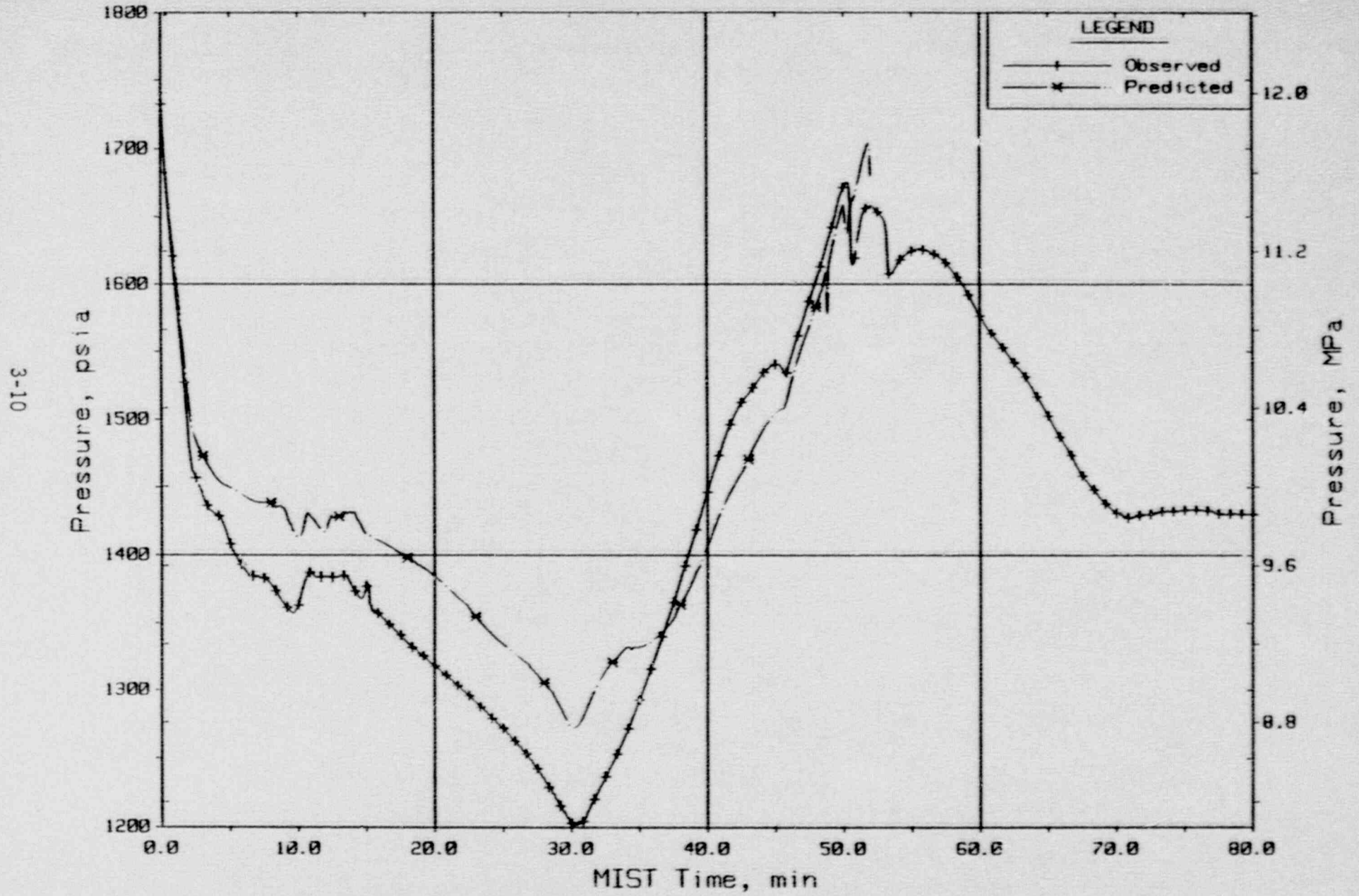


Figure 3.1.2. Reactor Vessel Pressure.

10 cm<sup>2</sup> CLPD Break with 30 Minute Isolation  
 MIST Nominal Test, Observed Vs. Predicted - Test 320503

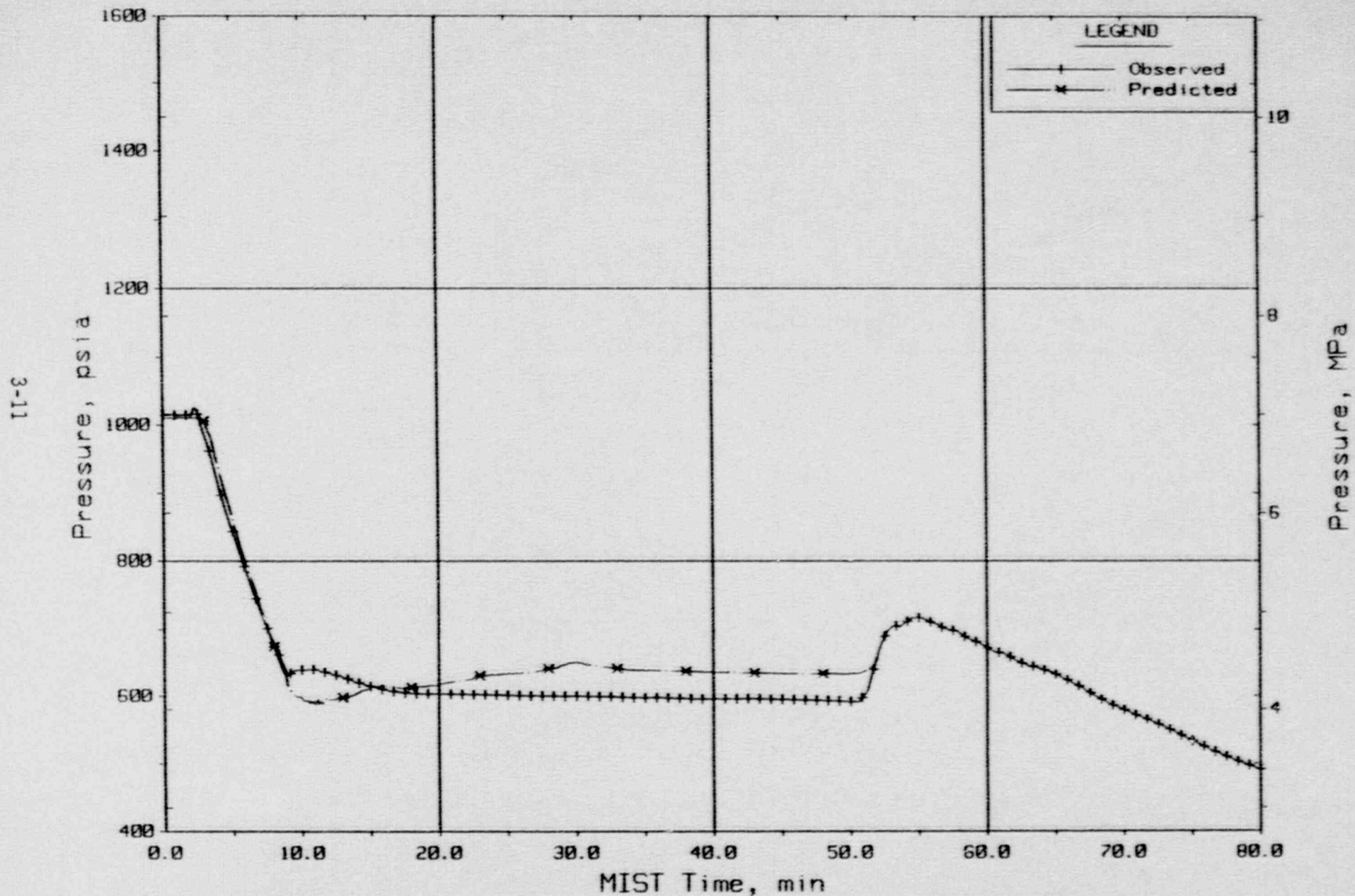


Figure 3.1.3. Steam Generator A Secondary Pressure.

10 cm<sup>2</sup> CLPD Break with 30 Minute Isolation  
MIST Nominal Test, Observed Vs. Predicted - Test 320503

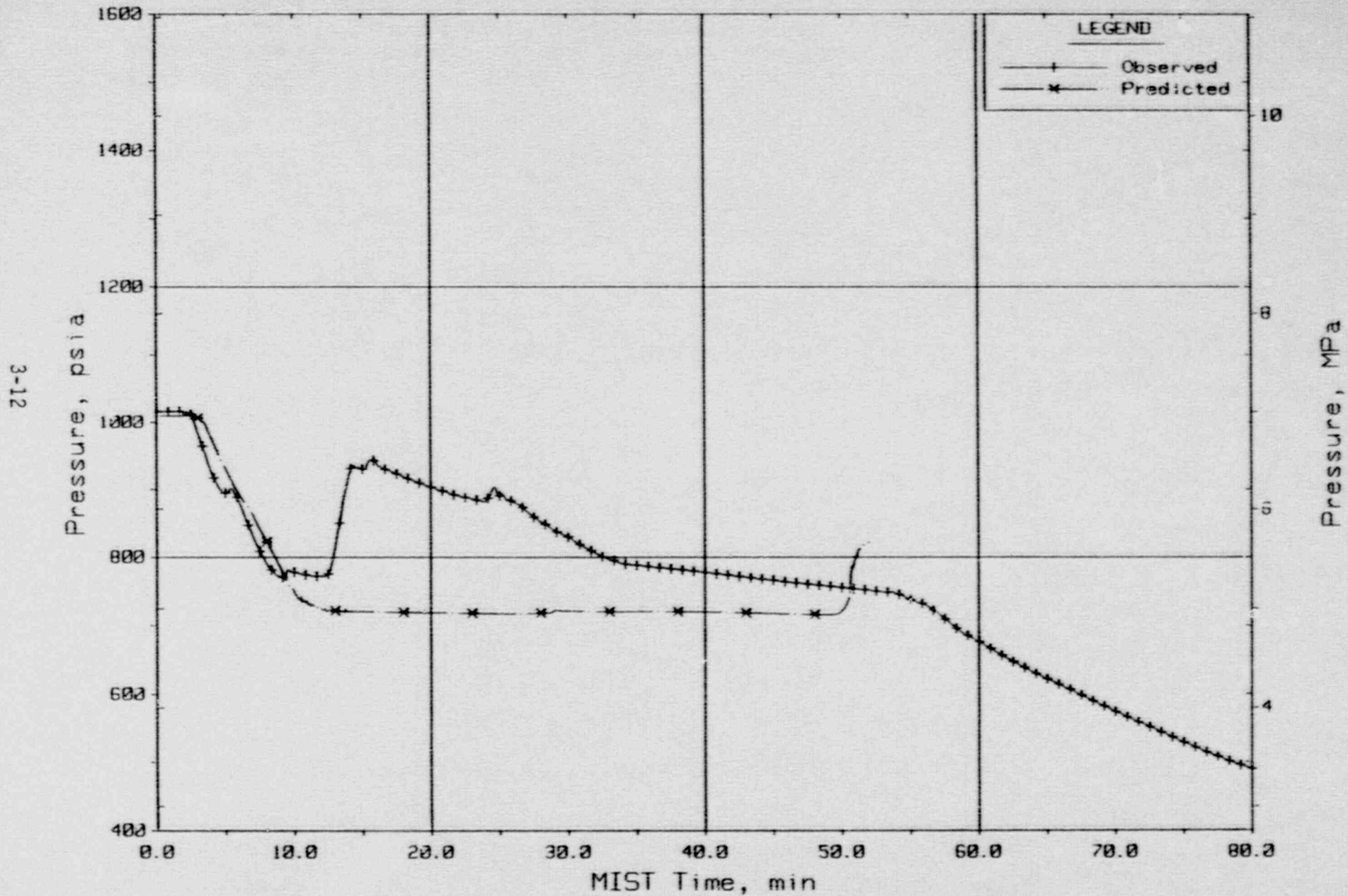


Figure 3.1.4. Steam Generator B Secondary Pressure.



10 cm<sup>2</sup> CLPD Break with 30 Minute Isolation  
 MIST Nominal Test, Observed Vs. Predicted - Test 320503

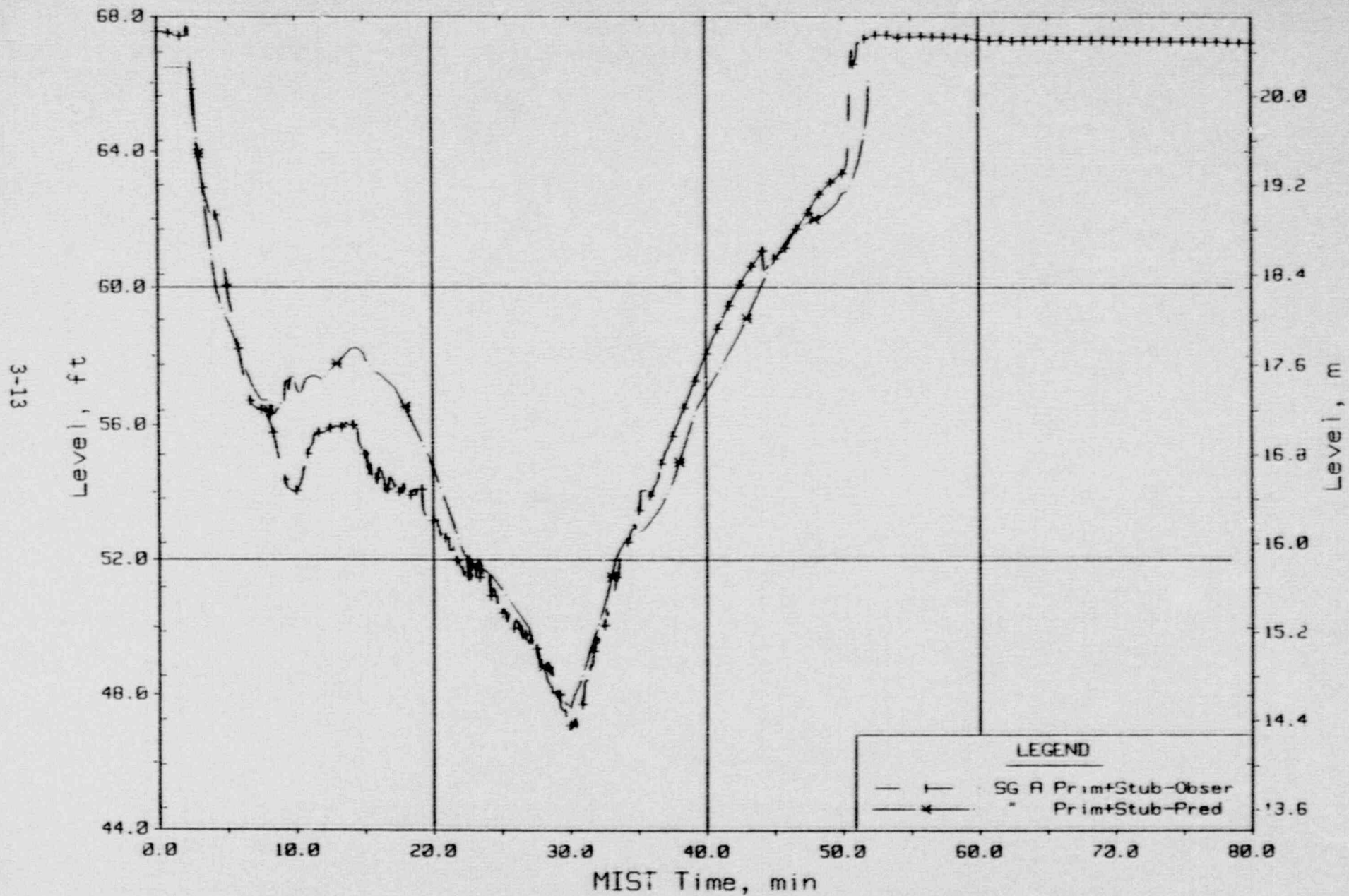


Figure 3.1.5. Steam Generator A Primary + Stub Level.

10 cm<sup>2</sup> CLPD Break with 30 Minute Isolation  
 MIST Nominal Test, Observed Vs. Predicted - Test 320503

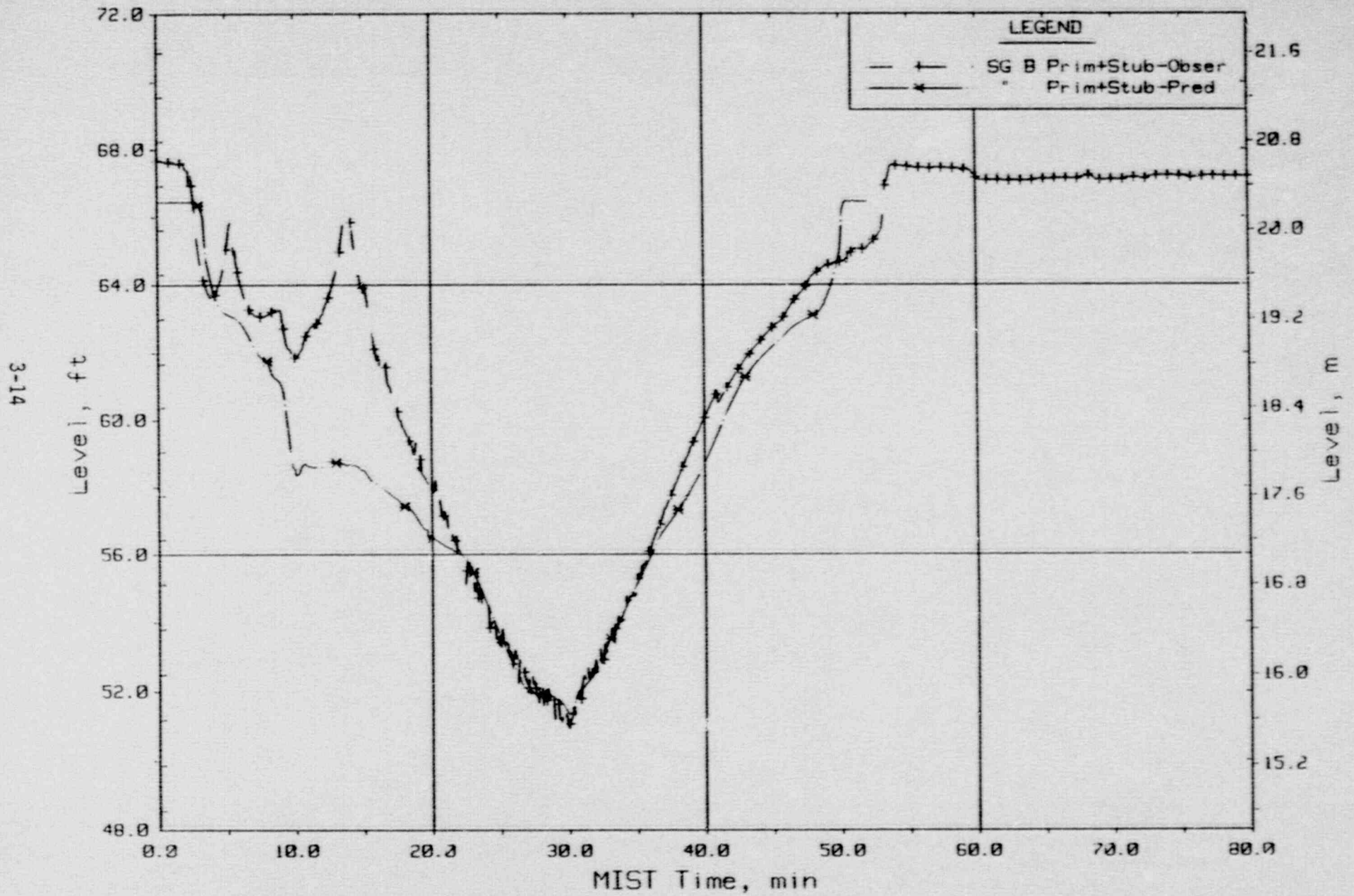


Figure 3.1.6. Steam Generator B Primary + Stub Level.

10 cm<sup>2</sup> CLPD Break with 30 Minute Isolation  
 MIST Nominal Test, Observed Vs. Predicted - Test 320503

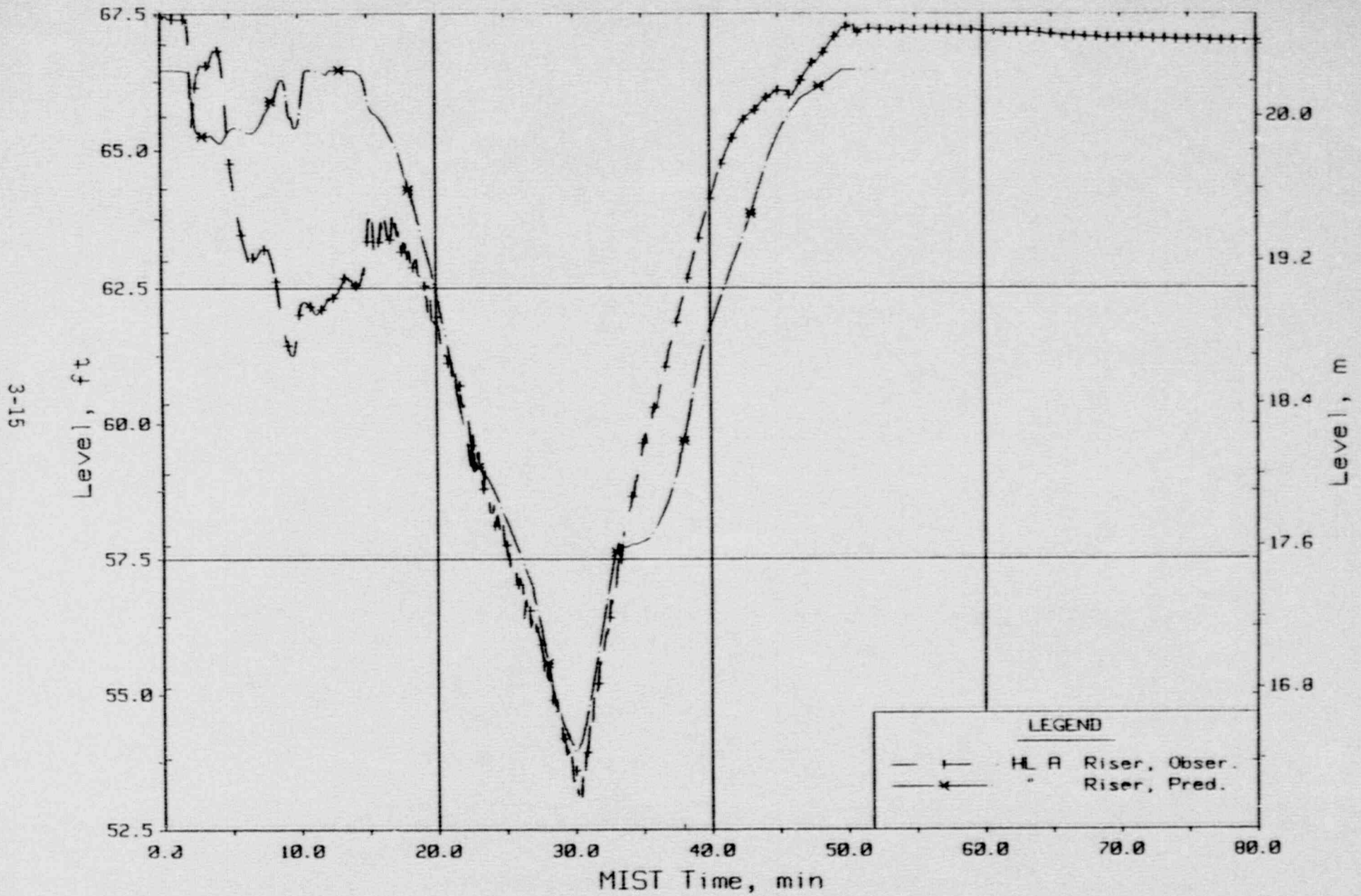


Figure 3.1.7. Hot Leg A Riser Level.

17 cm<sup>2</sup> CLPD Break with 30 Minute Isolation  
 MIST Nominal Test, Observed Vs. Predicted - Test 320503

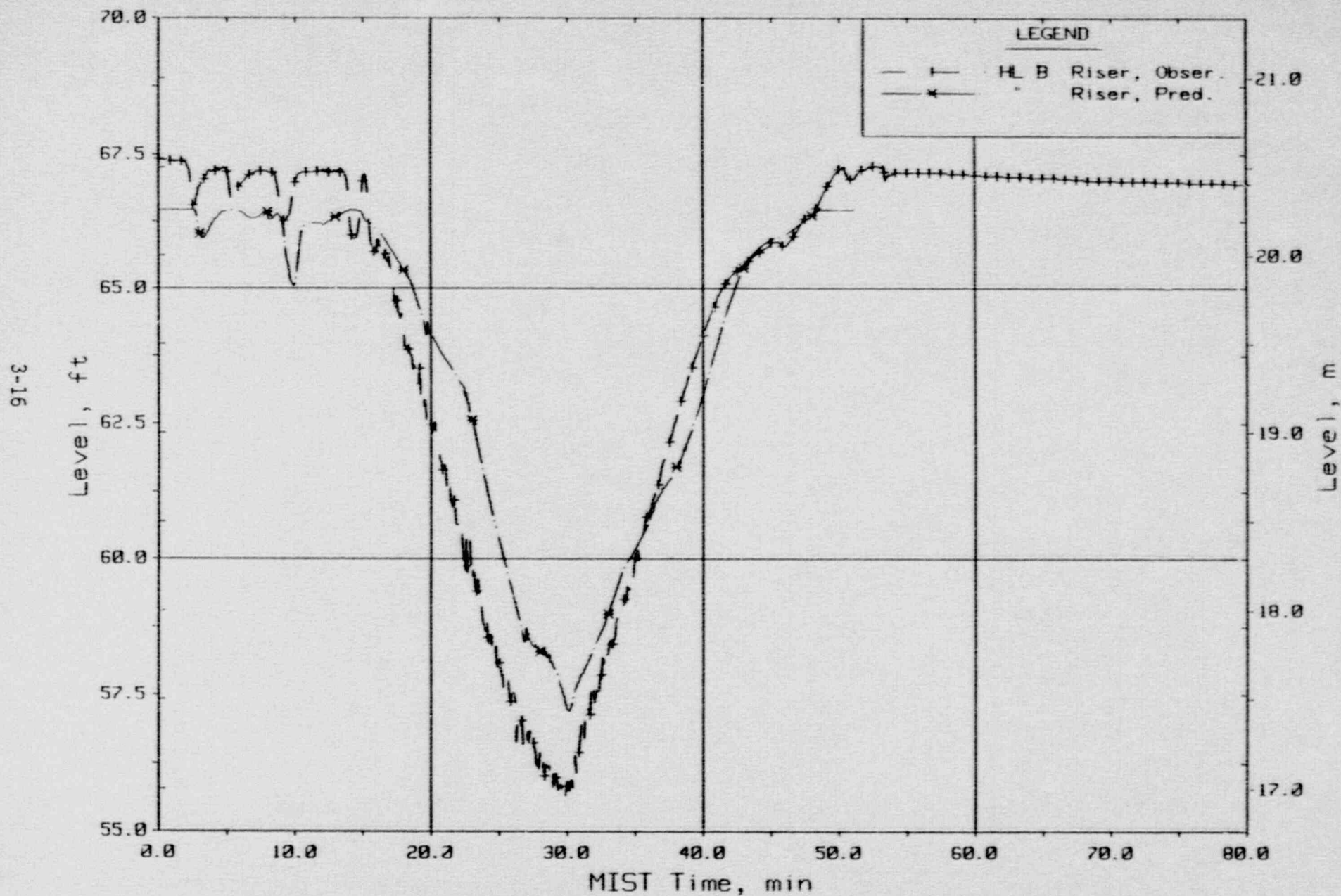


Figure 3.1.8. Hot Leg B Riser Level.

10 cm<sup>2</sup> CLPD Break with 30 Minute Isolation  
 MIST Nominal Test, Observed Vs. Predicted - Test 320503

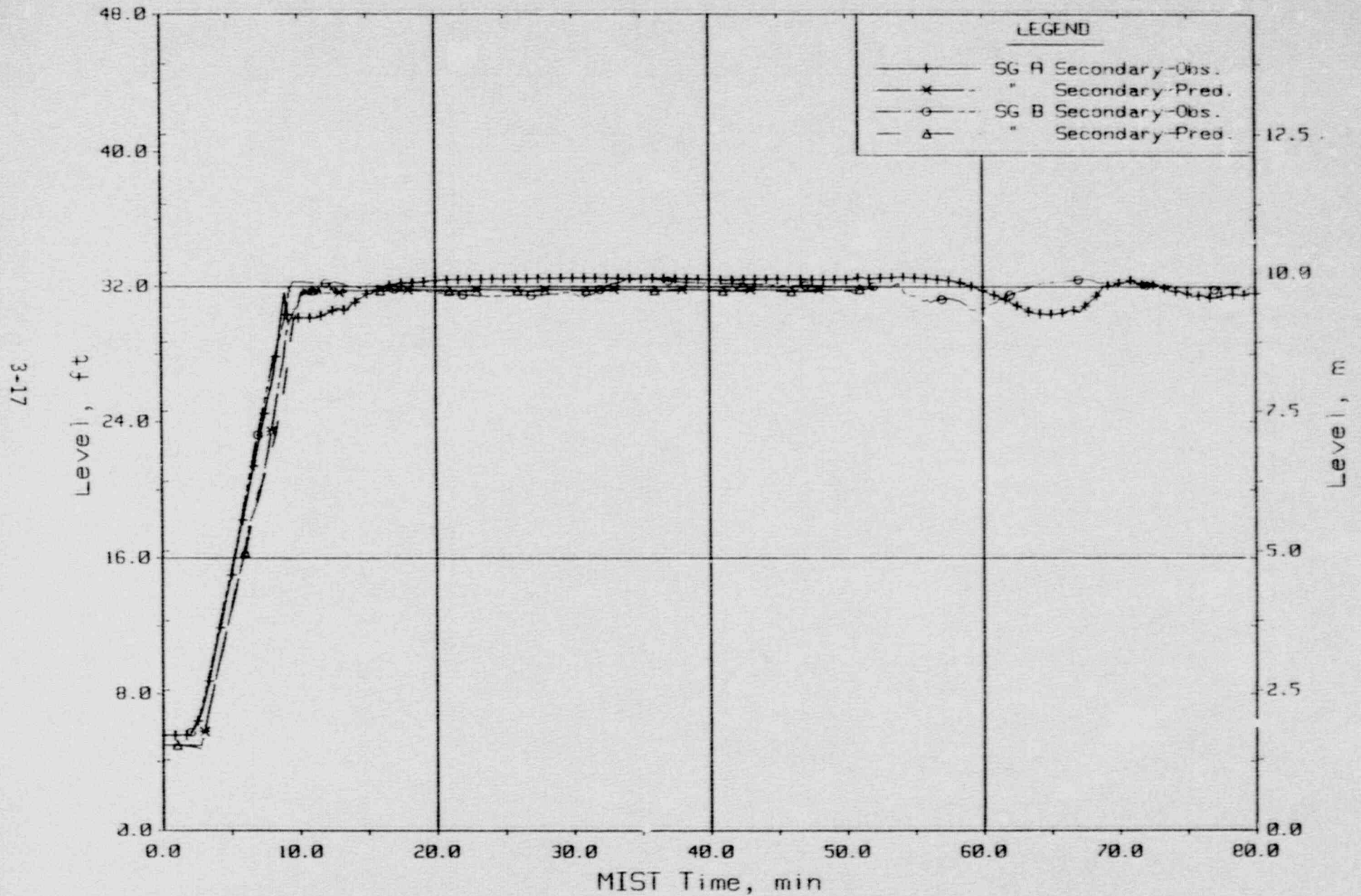


Figure 3.1.9. Steam Generator Sec. Collapsed Liquid Levels.

10 cm<sup>2</sup> CLPD Break with 30 Minute Isolation  
 MIST Nominal Test, Observed Vs. Predicted - Test 320503

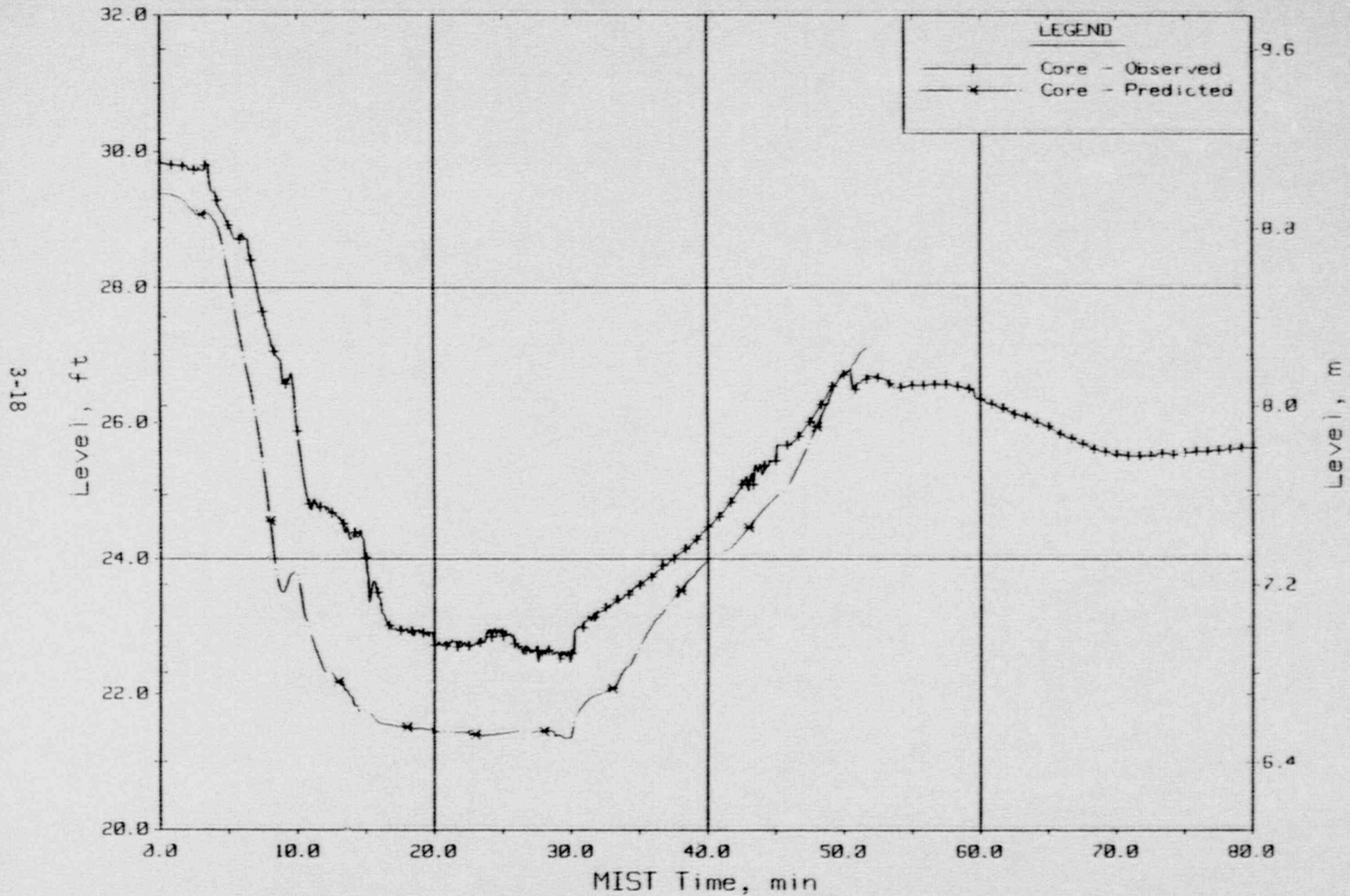


Figure 3.1.10. Core Region Collapsed Liquid Levels.

10 cm<sup>2</sup> CLPD Break with 30 Minute Isolation  
 MIST Nominal Test, Observed Vs. Predicted - Test 320503

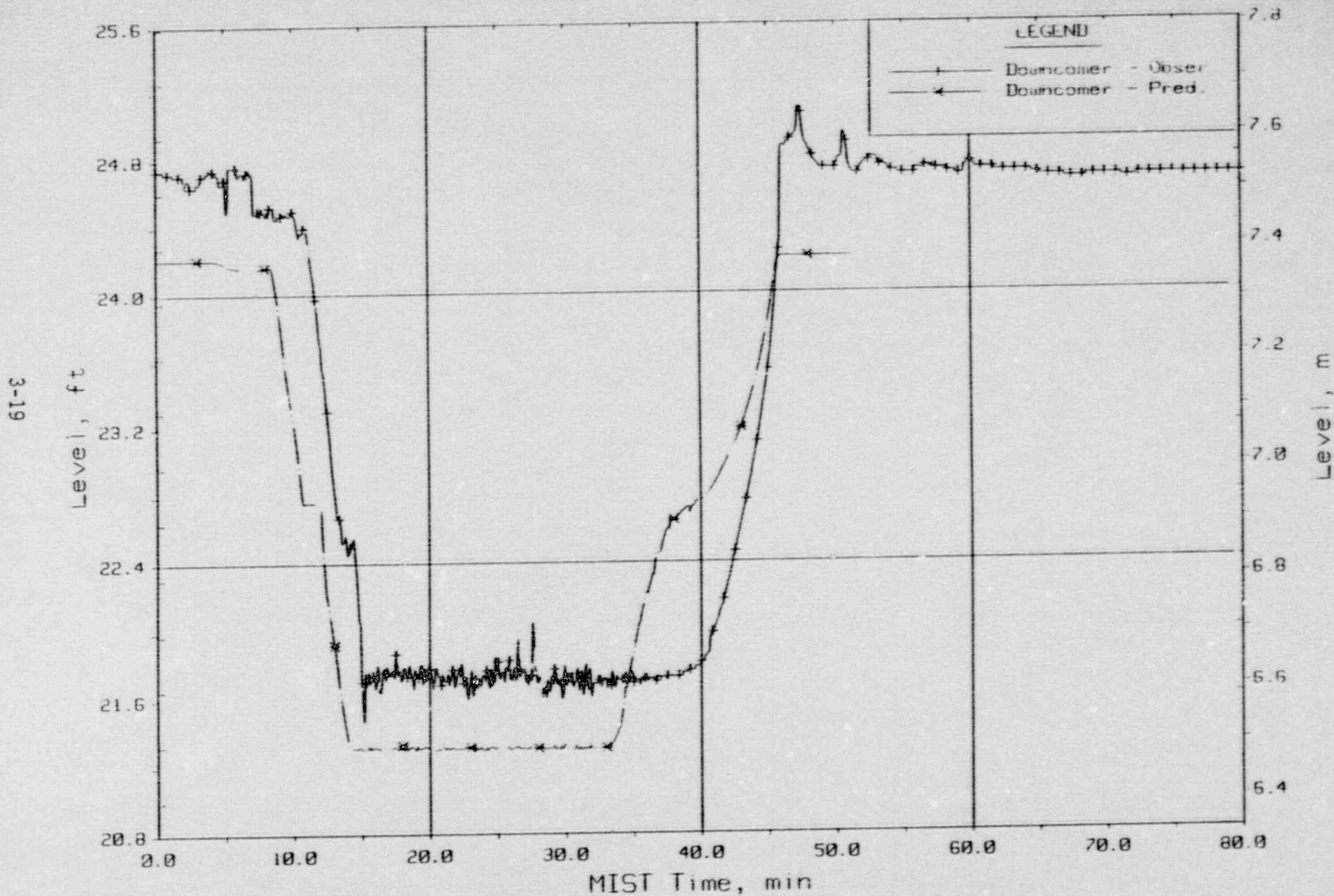


Figure 3.1.11. Core Region Collapsed Liquid Levels.

10 cm<sup>2</sup> CLPD Break with 30 Minute Isolation  
 MIST Nominal Test, Observed Vs. Predicted - Test 320503

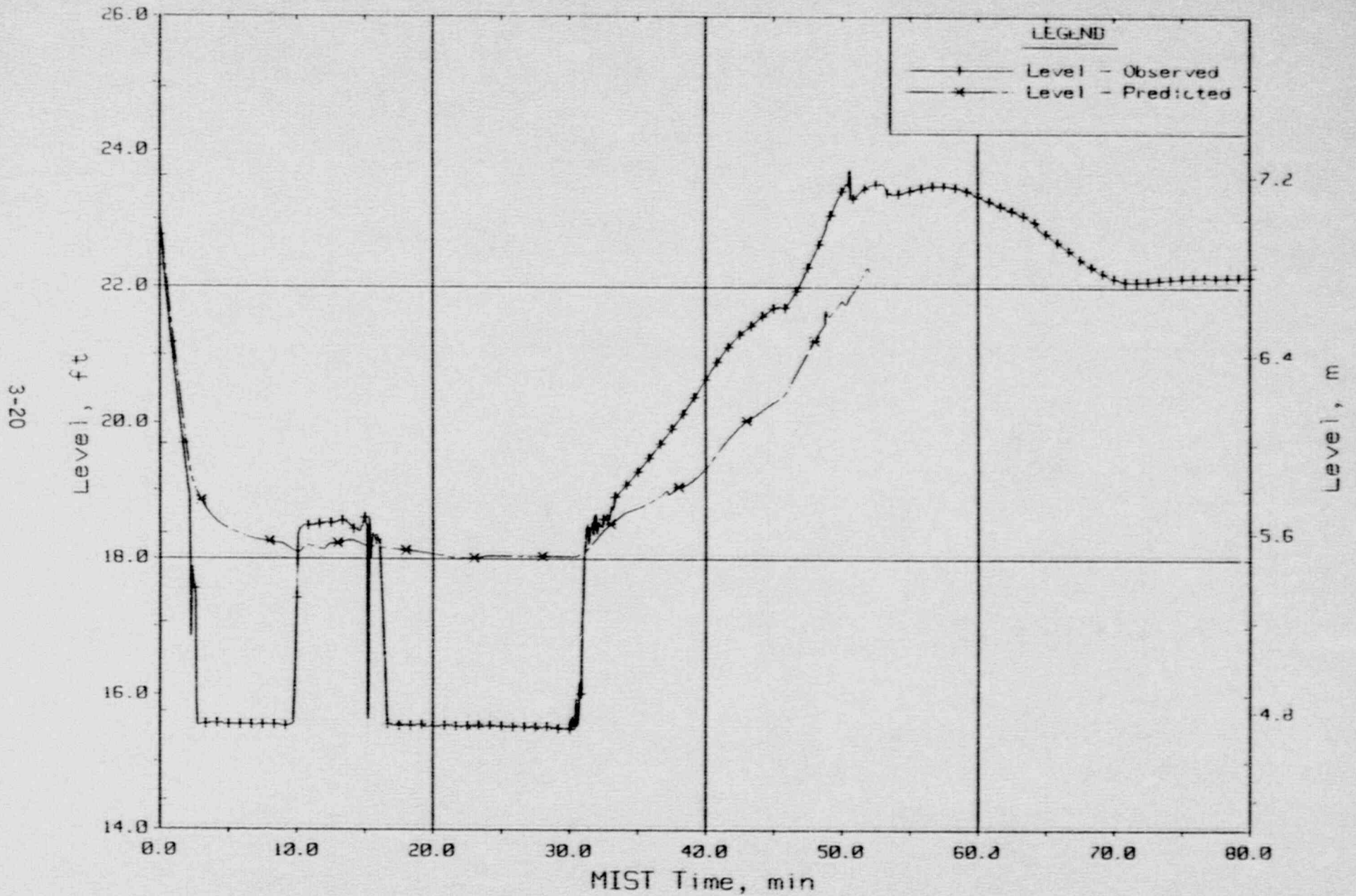


Figure 3.1.12. Pressurizer Collapsed Liquid Level (PZLV20).



10 cm<sup>2</sup> CLPD Break with 30 Minute Isolation  
 MIST Nominal Test, Observed Vs. Predicted - Test 320523

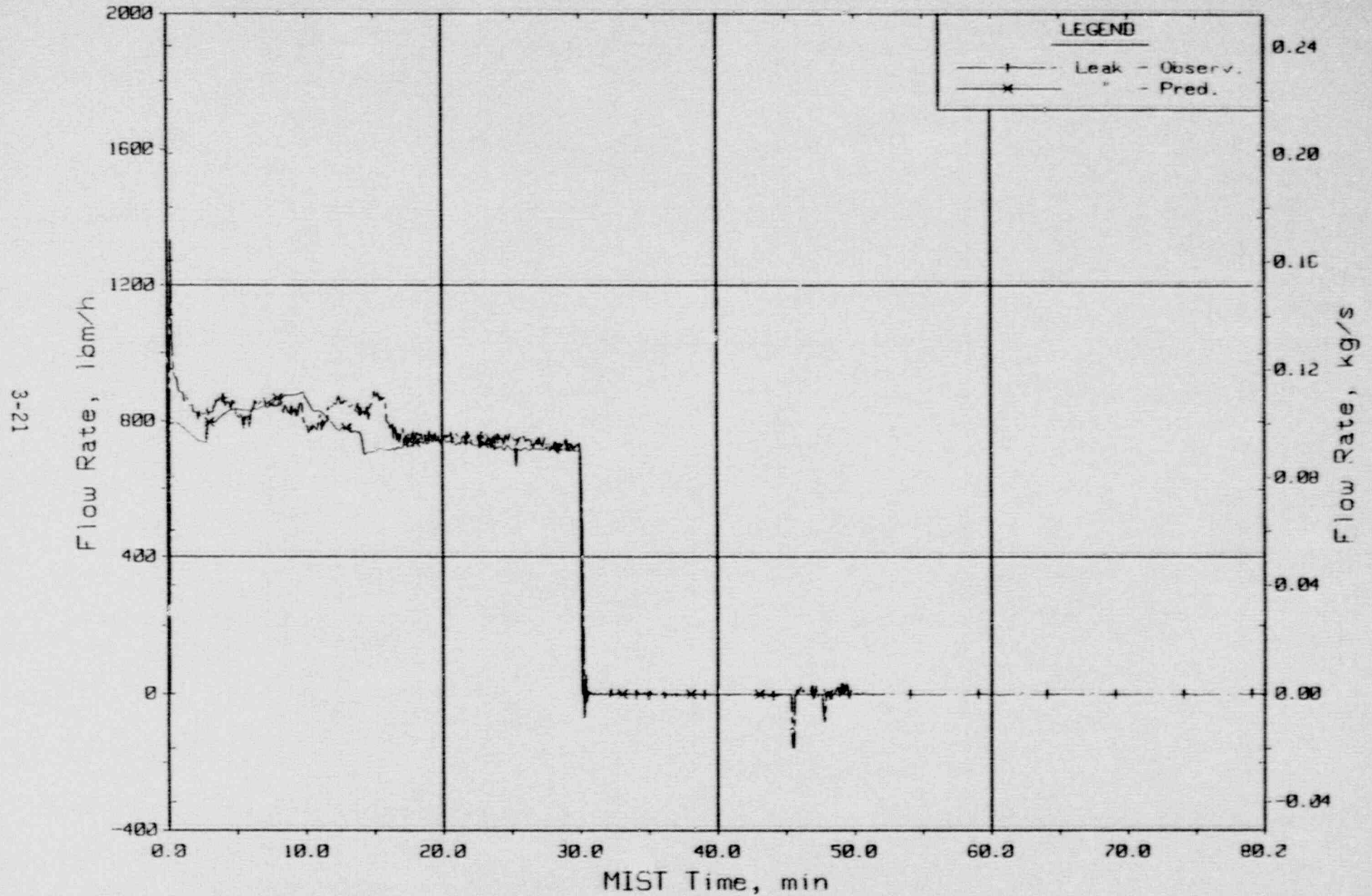


Figure 3.1.13. Leak Flow Rates.

10 cm<sup>2</sup> CLPD Break with 30 Minute Isolation  
MIST Nominal Test, Observed Vs. Predicted - Test 320503

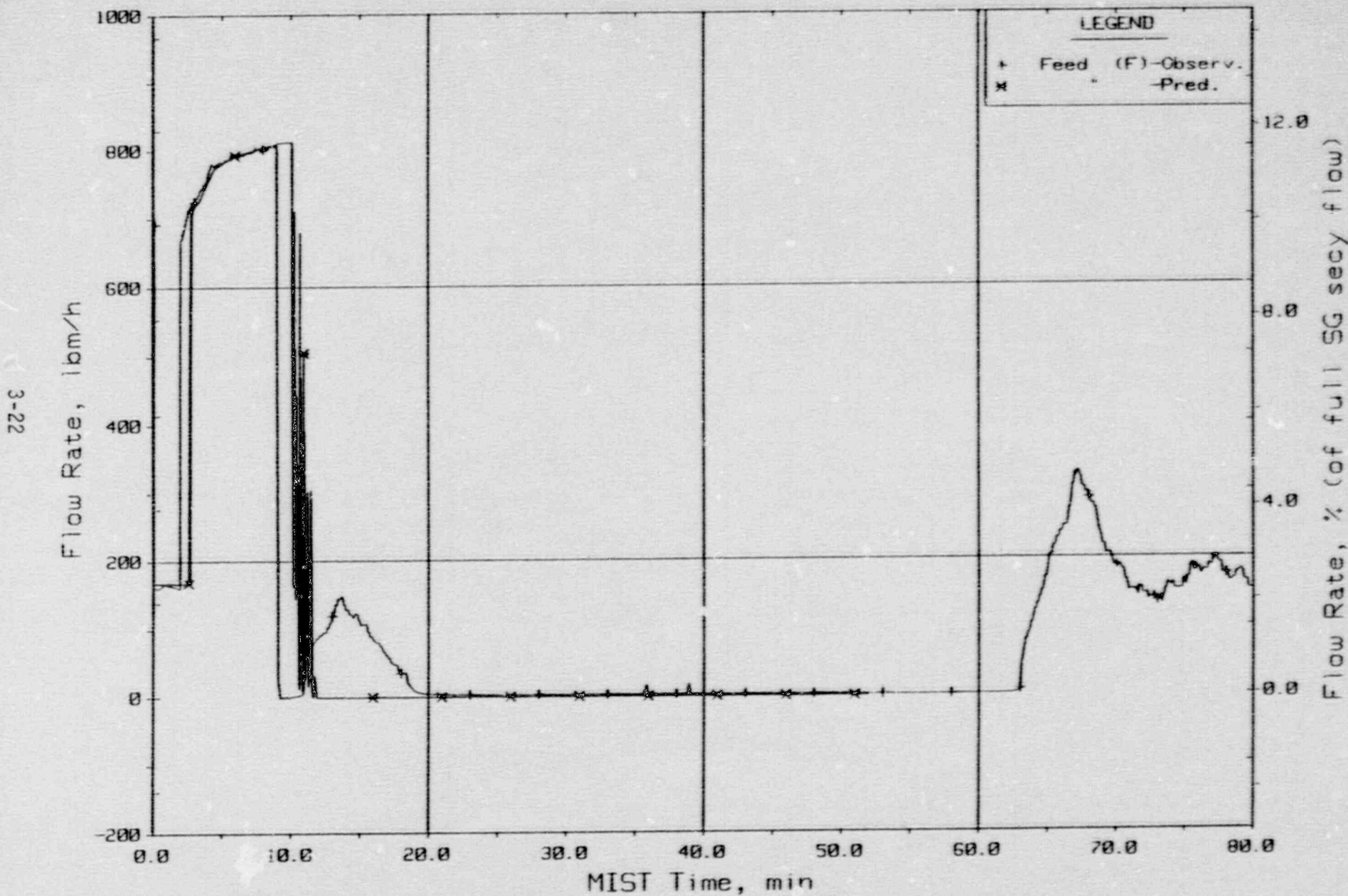


Figure 3.1.14. Steam Generator A Flow Rate (Ssfcr20).

10 cm<sup>2</sup> CLPD Break with 30 Minute Isolation  
 MIST Nominal Test, Observed Vs. Predicted - Test 320503

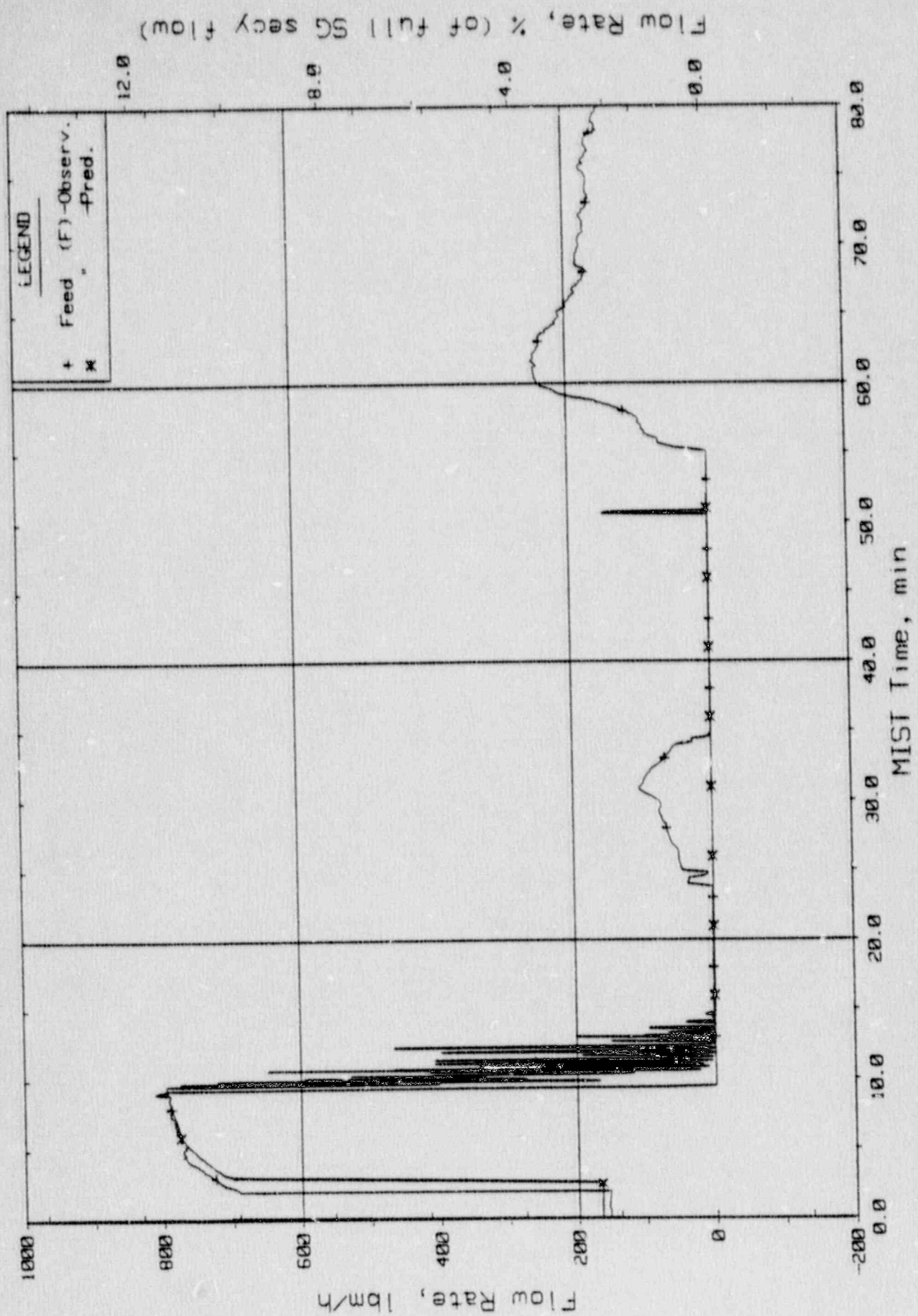


Figure 3.1.15. Steam Generator B Flow Rate (Ssfcr21).

Csfor21

10 cm<sup>2</sup> CLPD Break with 30 Minute Isolation  
 MIST Nominal Test, Observed Vs. Predicted - Test 320503

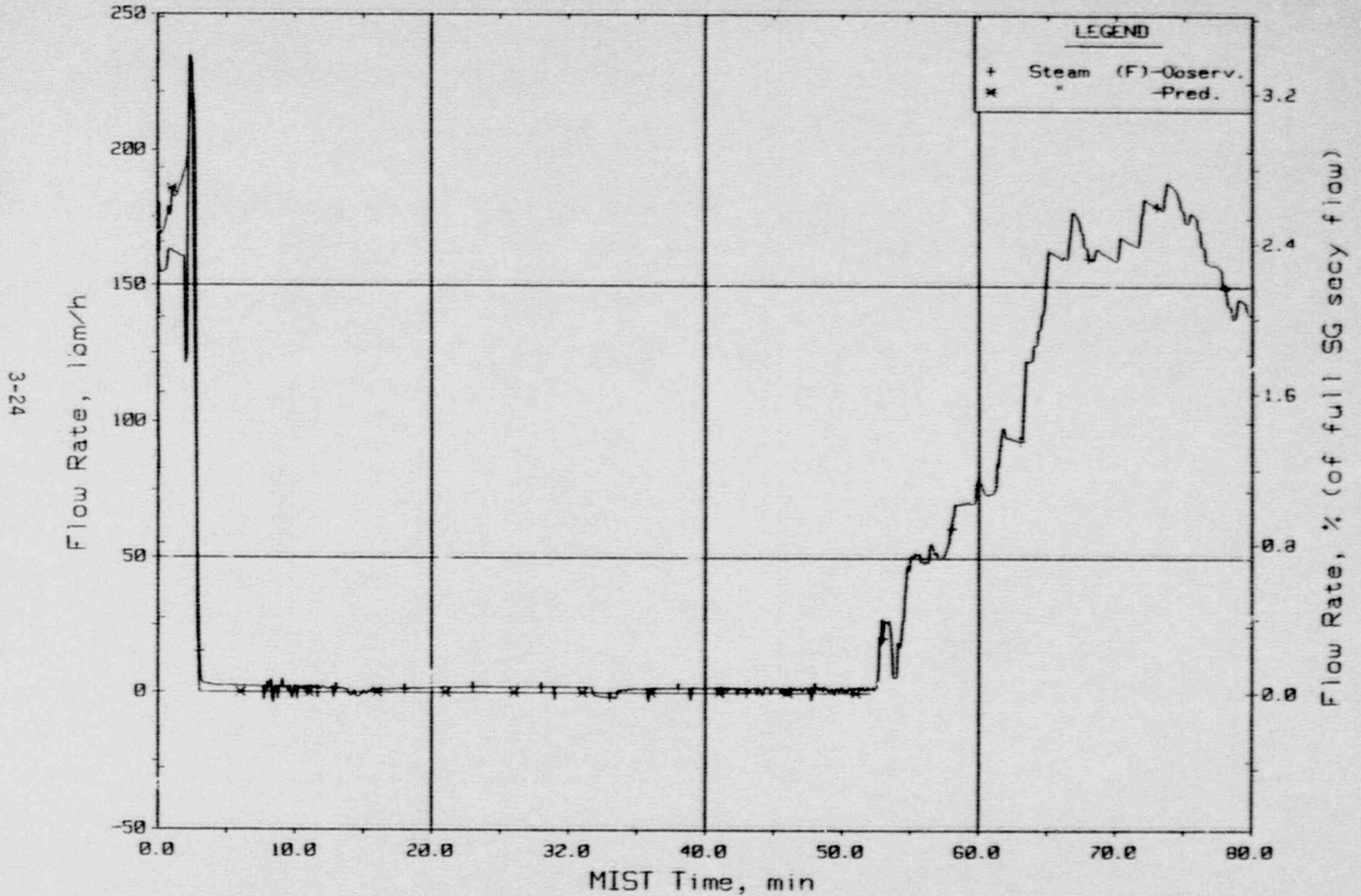


Figure 3.1.16. Steam Generator A Flow Rates (Cssor22).

10 cm<sup>2</sup> CLPD Break with 30 Minute Isolation  
 MIST Nominal Test, Observed Vs. Predicted - Test 320503

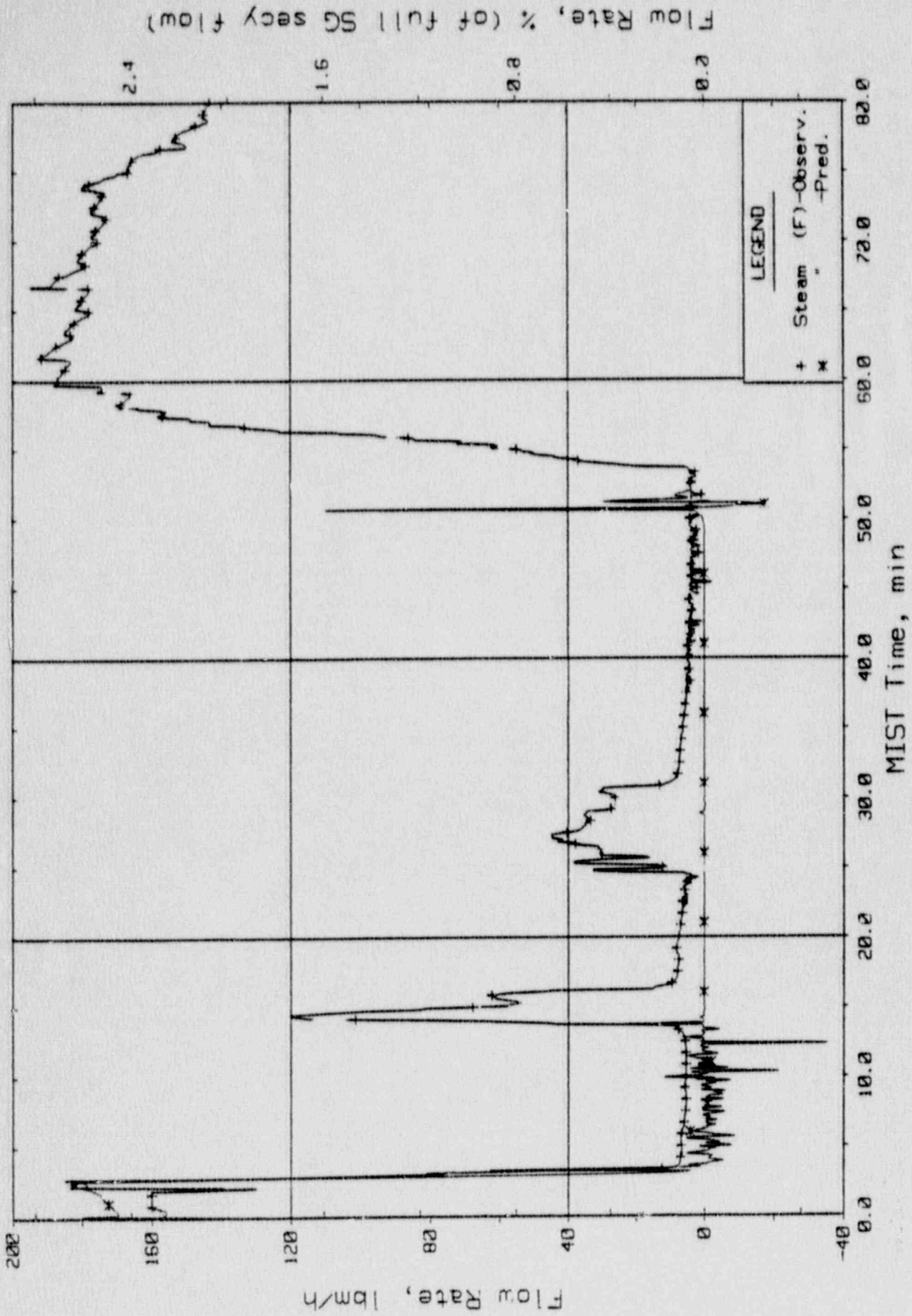


Figure 3.1.17. Steam Generator B Flow Rates (Sssor21).

10 cm<sup>2</sup> CLPD Break with 30 Minute Isolation  
 MIST Nominal Test, Observed Vs. Predicted - Test 320503

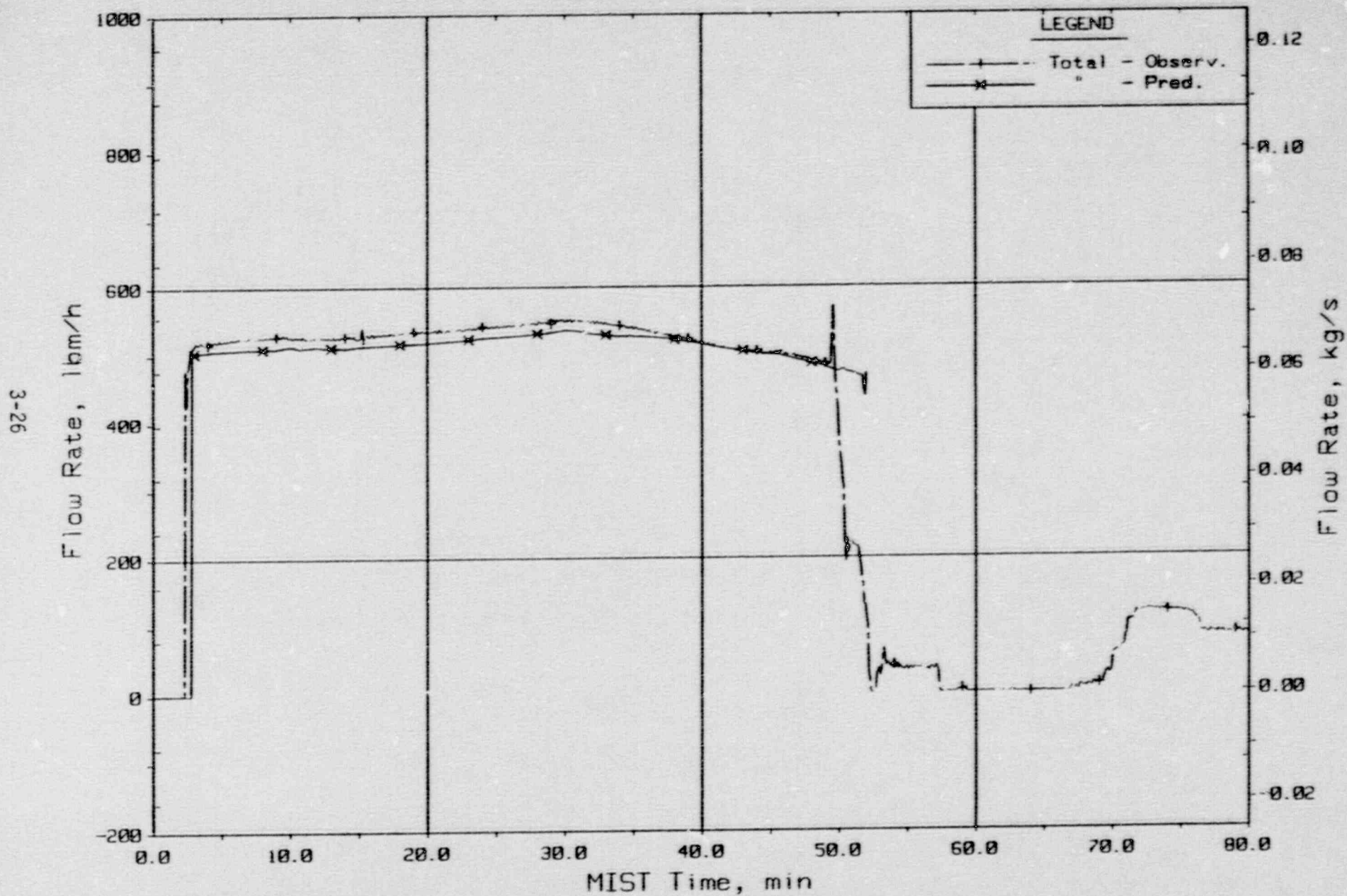


Figure 3.1.18. HPI Total Flow Rates.

10 cm<sup>2</sup> CLPD Break with 30 Minute Isolation  
 MIST Nominal Test, Observed Vs. Predicted - Test 320503

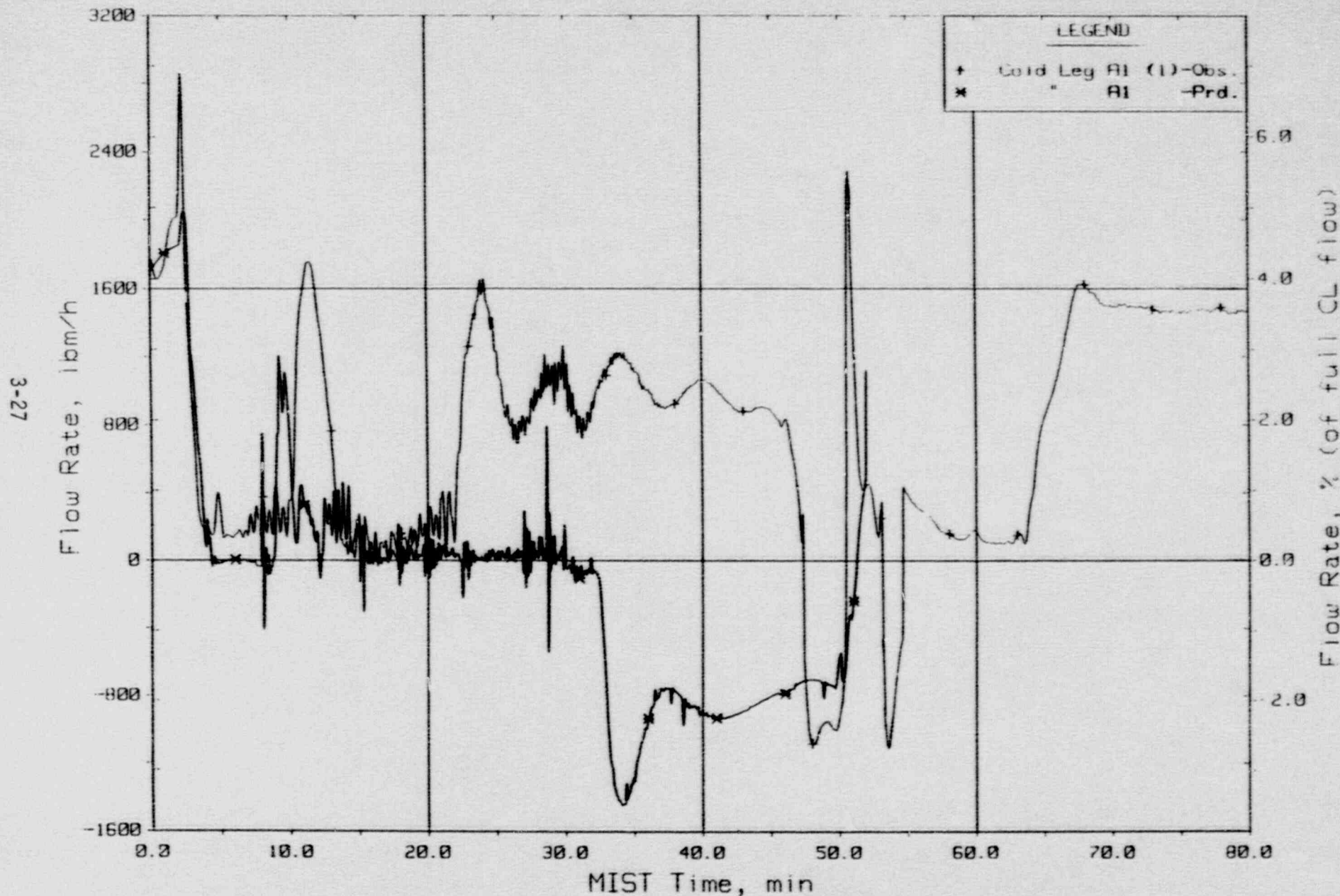


Figure 3.1.19. Loop AI Cold Leg (Venturi) Flow Rate (C1VN20).

10 cm<sup>2</sup> CLPD Break with 30 Minute Isolation  
 MIST Nominal Test, Observed Vs. Predicted - Test 320503

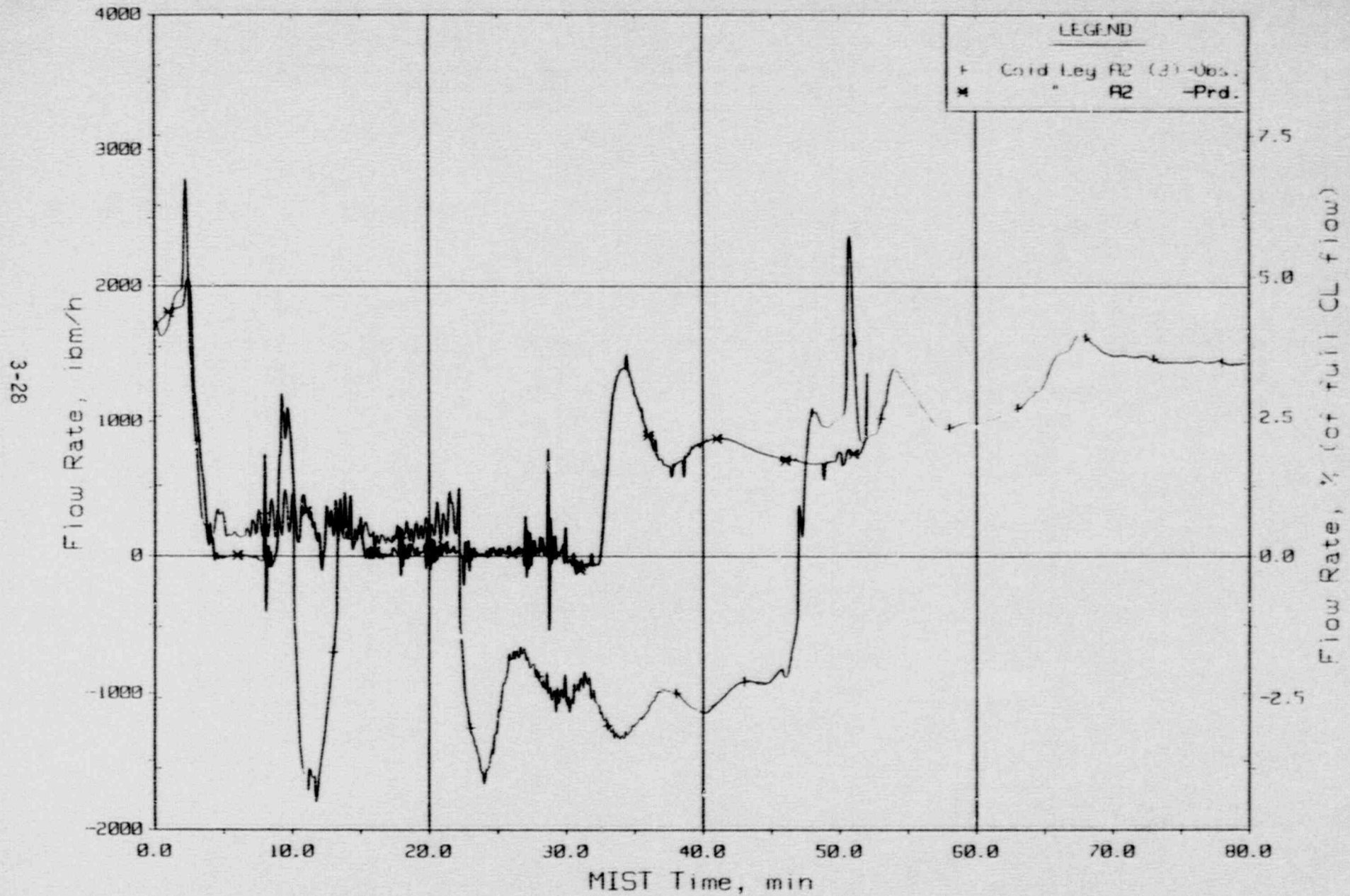


Figure 3.1.20. Loop A2 Cold Leg (Venturi) Flow Rate (C2VN20).



10 cm<sup>2</sup> CLPD Break with 30 Minute Isolation  
 MIST Nominal Test, Observed Vs. Predicted - Test 320503

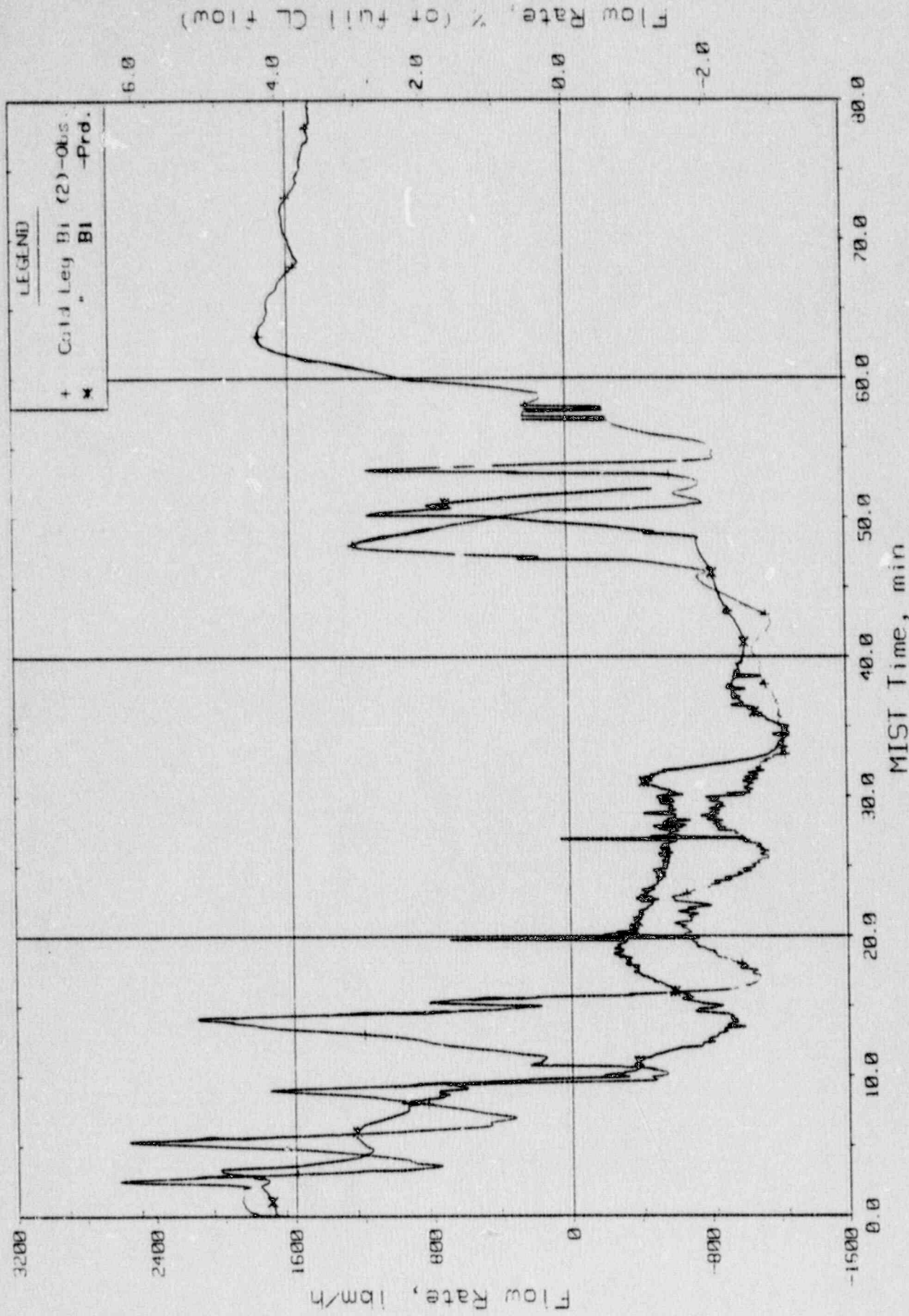


Figure 3.1.21. Loop BI Cold Leg (Venturi) Flow Rate (CIVN20).

Cc2vm20

10 cm<sup>2</sup> CLPD Break with 30 Minute Isolation  
 MIST Nominal Test, Observed Vs. Predicted - Test 320503

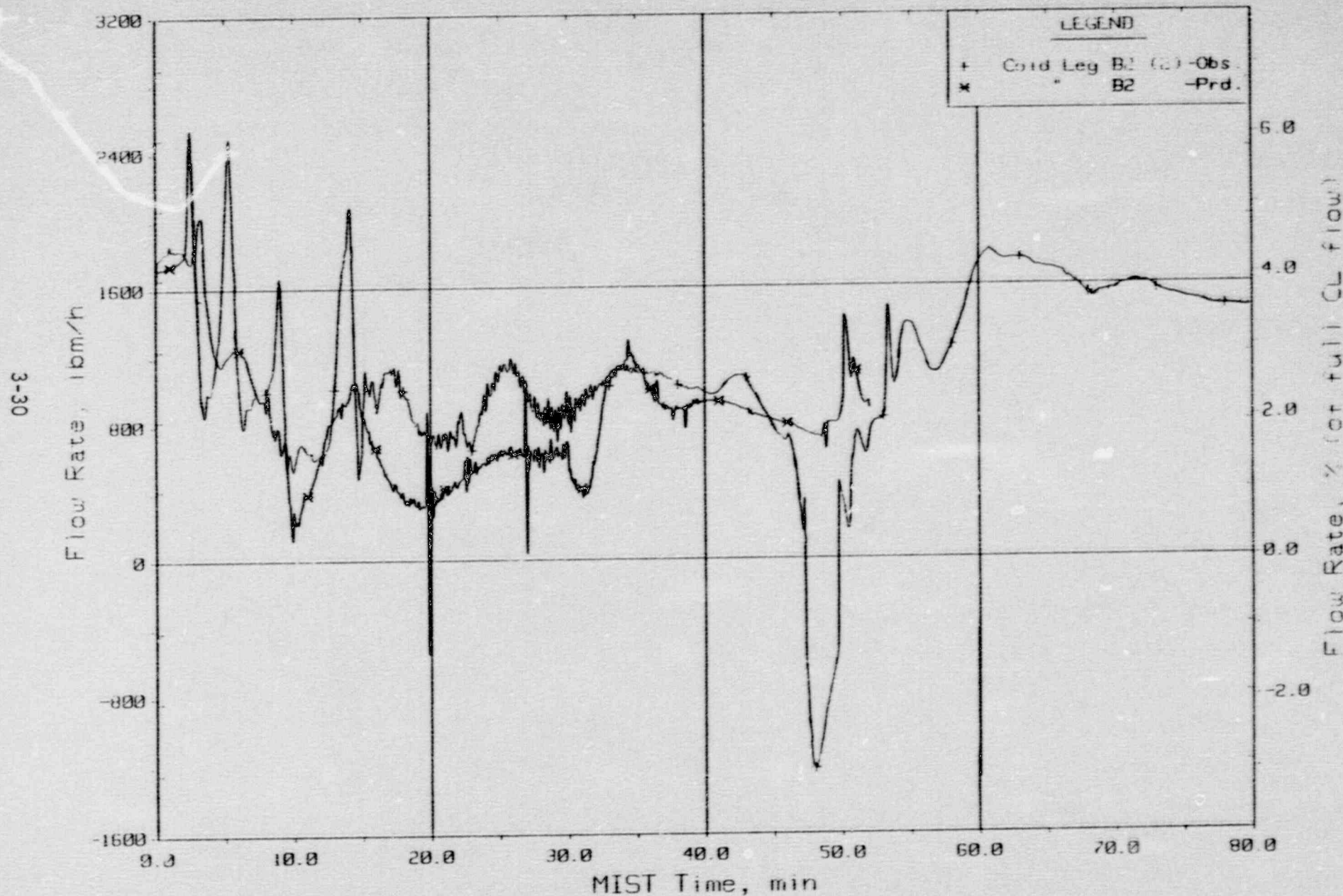


Figure 3.1.22. Loop B2 Cold Leg (Venturi) Flow Rate (C4VN20).

10 cm<sup>2</sup> CLPD Break with 30 Minute Isolation  
 MIST Nominal Test, Observed Vs. Predicted - Test 320503

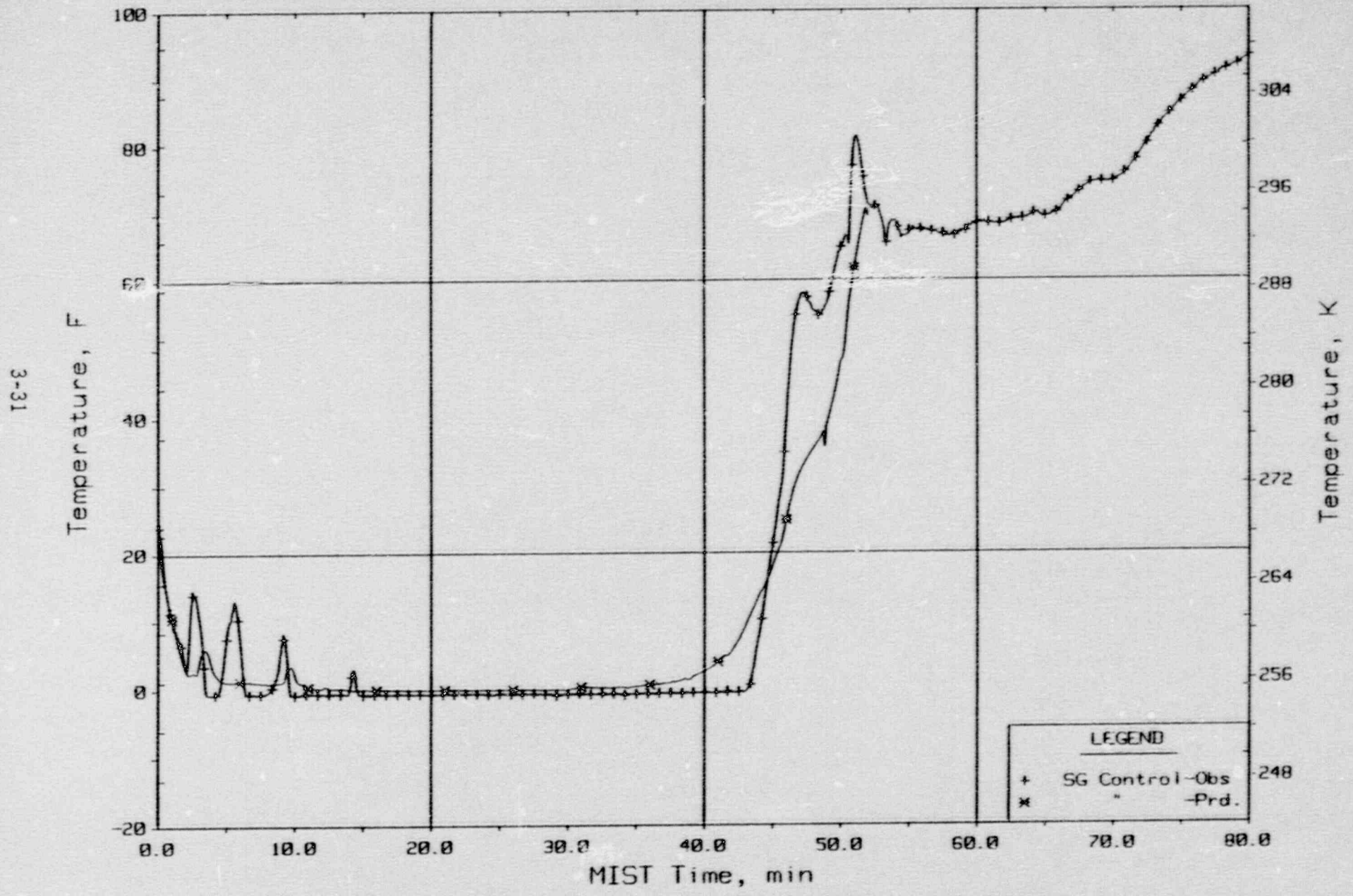


Figure 3.1.23. Reactor Core Exit Subcooling Margin.

10 cm<sup>2</sup> CLPD Break with 30 Minute Isolation  
 MIST Nominal Test, Observed Vs. Predicted - Test 320503

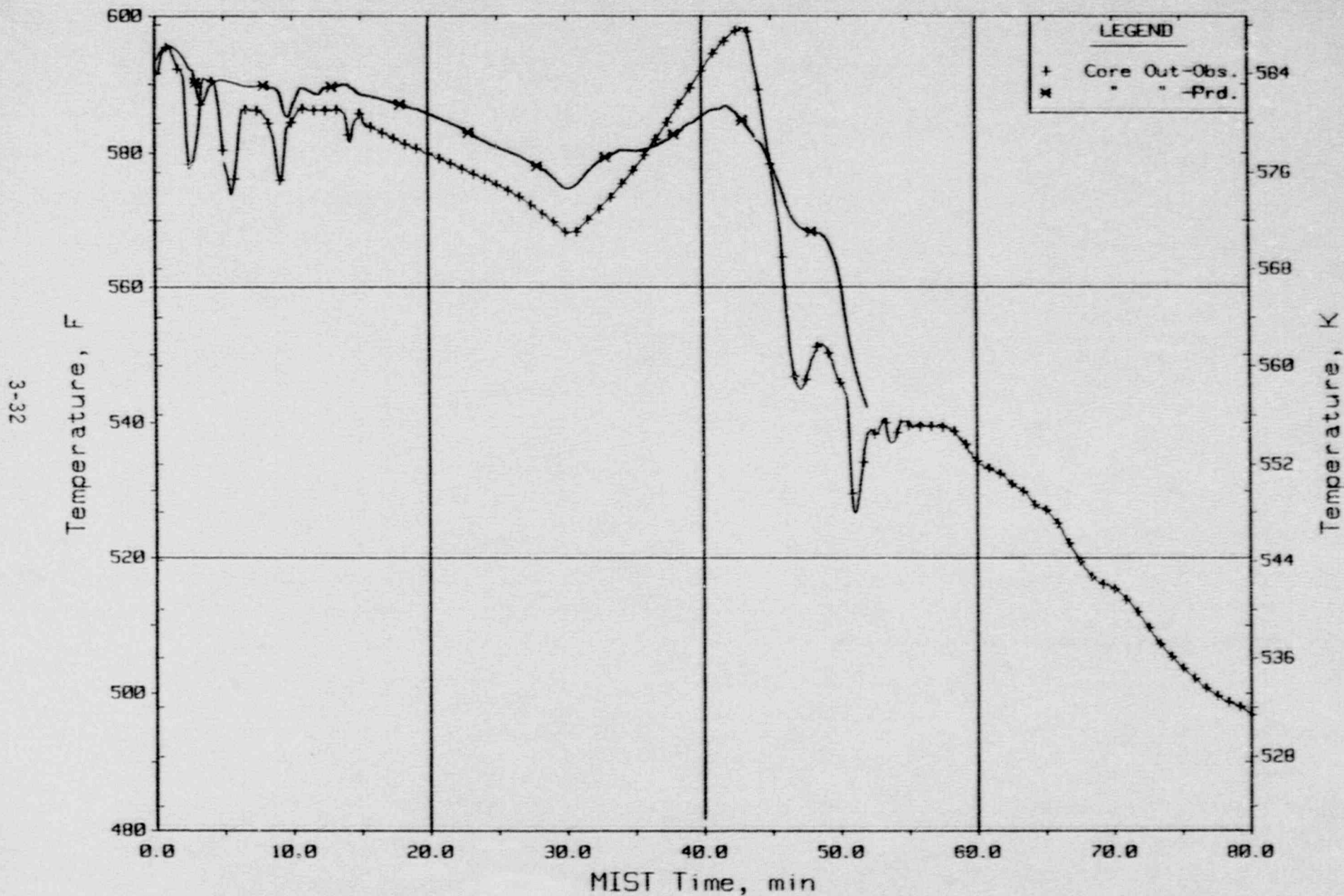


Figure 3.1.24. Core Exit Reactor Vessel Fluid Temperature (RVTc11).

10 cm<sup>2</sup> CLPD Break with 30 Minute Isolation  
 MIST Nominal Test, Observed Vs. Predicted - Test 320503

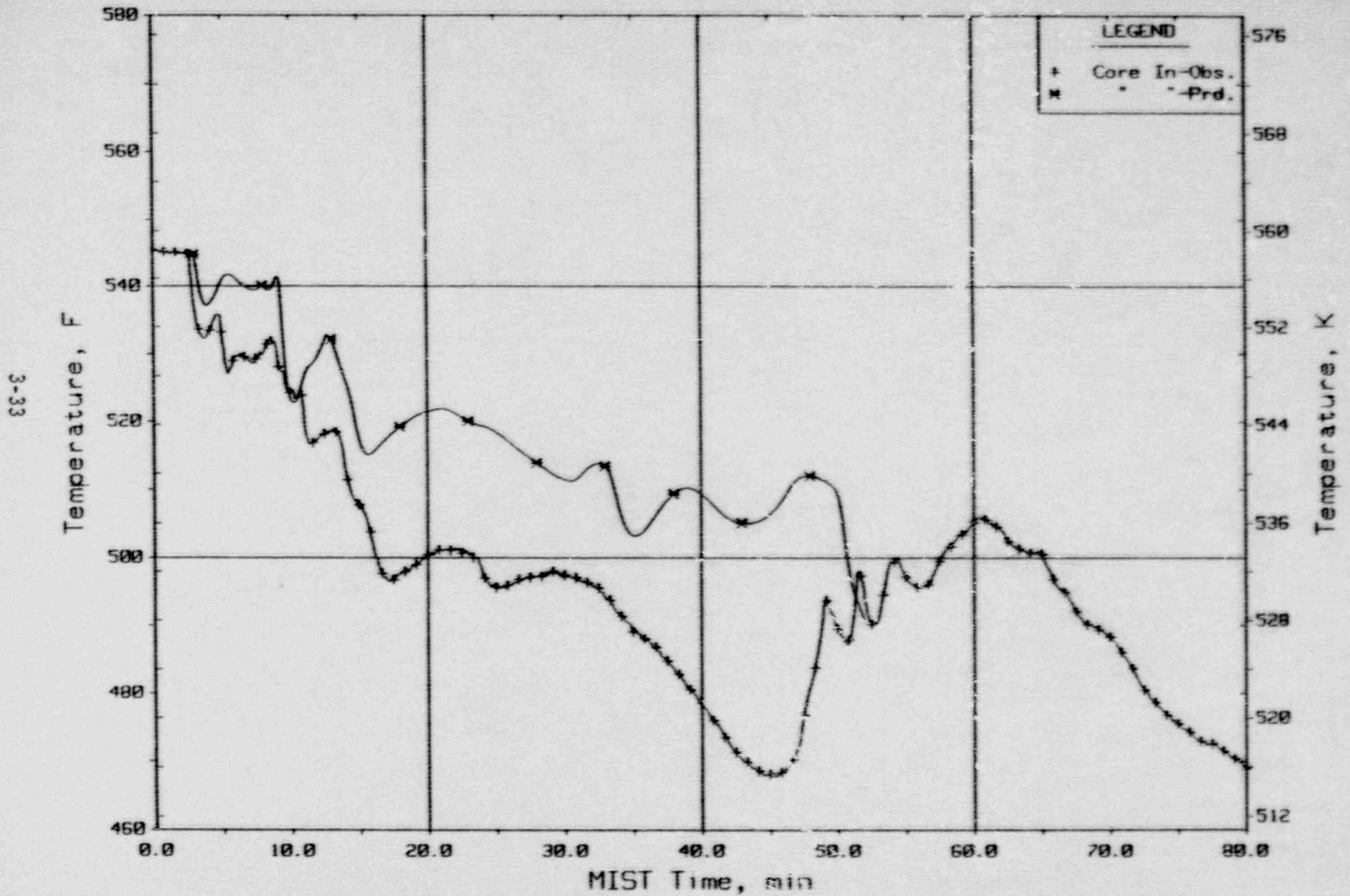


Figure 3.1.25. Core Inlet Reactor Vessel Fluid Temperature (DCRT01).

10 cm<sup>2</sup> CLPD Break with 30 Minute Isolation  
 MIST Nominal Test, Observed Vs. Predicted - Test 320503

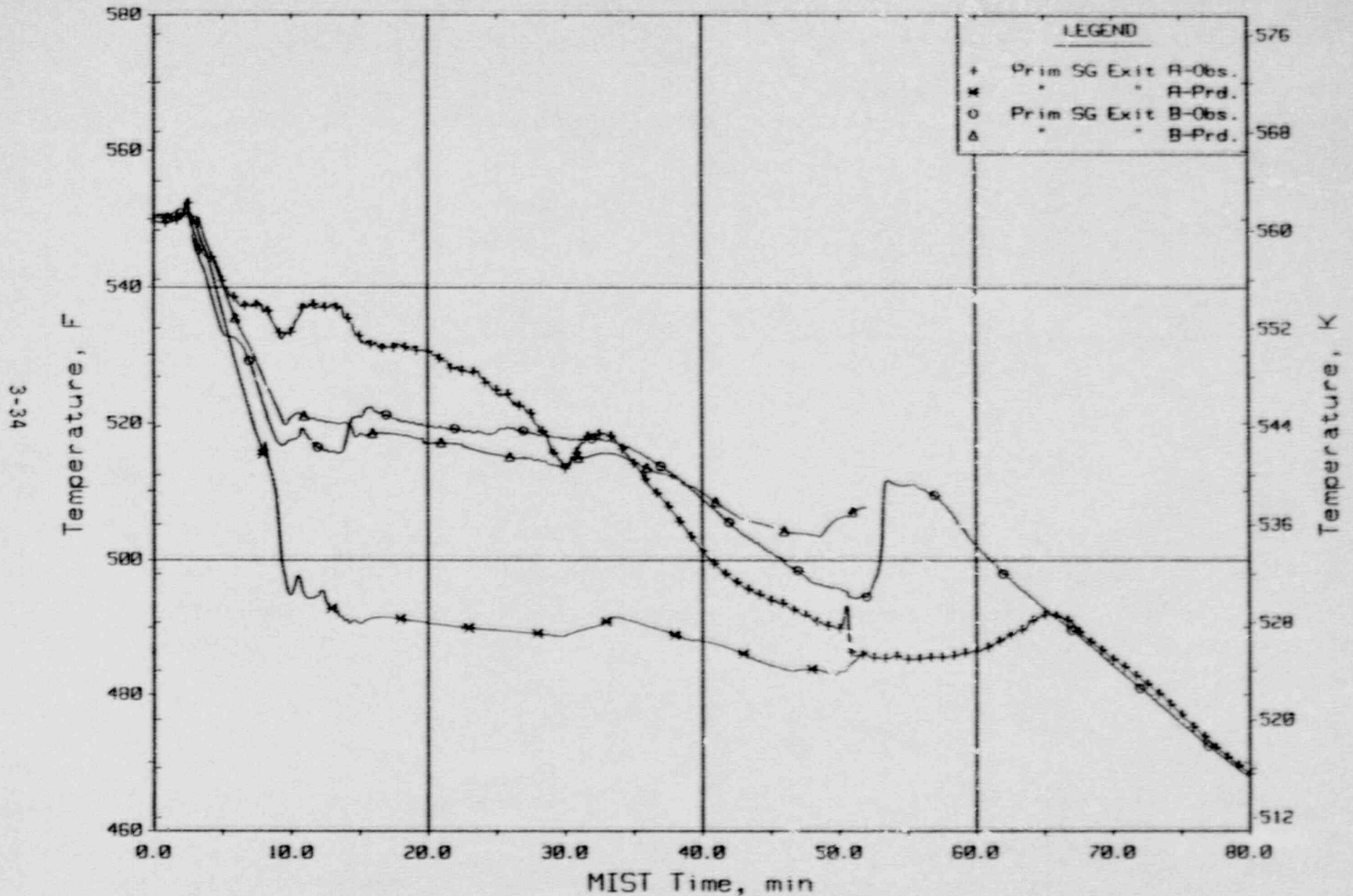


Figure 3.1.26. Loops A/B SG Exit Primary Fluid Temperatures (RTDs).

10 cm<sup>2</sup> CLPD Break with 30 Minute Isolation  
 MIST Nominal Test, Observed Vs. Predicted - Test 320503

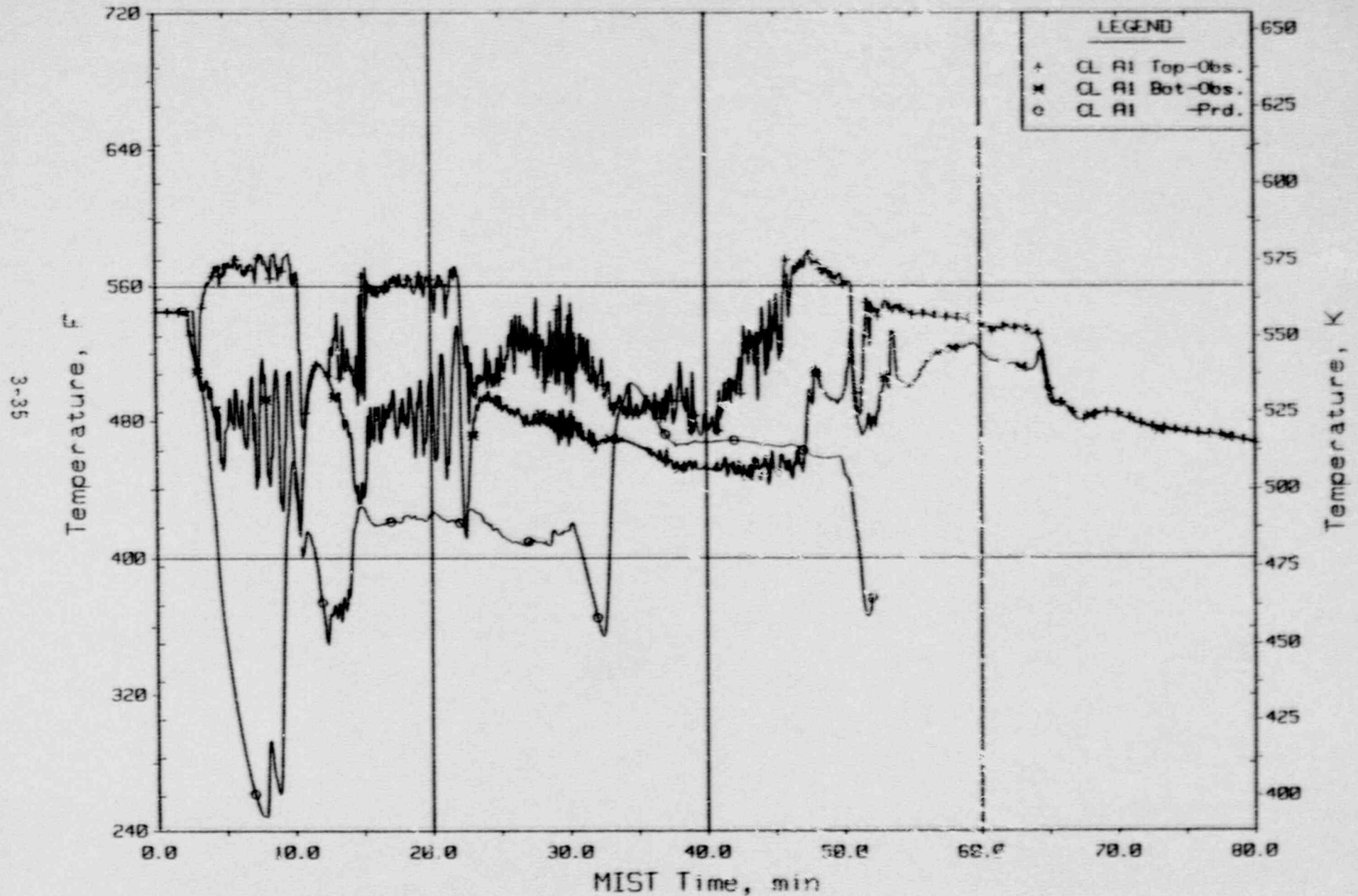


Figure 3.1.27. Cold Leg Nozzle Fluid Temperatures, Top/Bot of Rake (21.3ft., CnFC11/14s).

10 cm<sup>2</sup> CLPD Break with 30 Minute Isolation  
 MIST Nominal Test, Observed Vs. Predicted - Test 320503

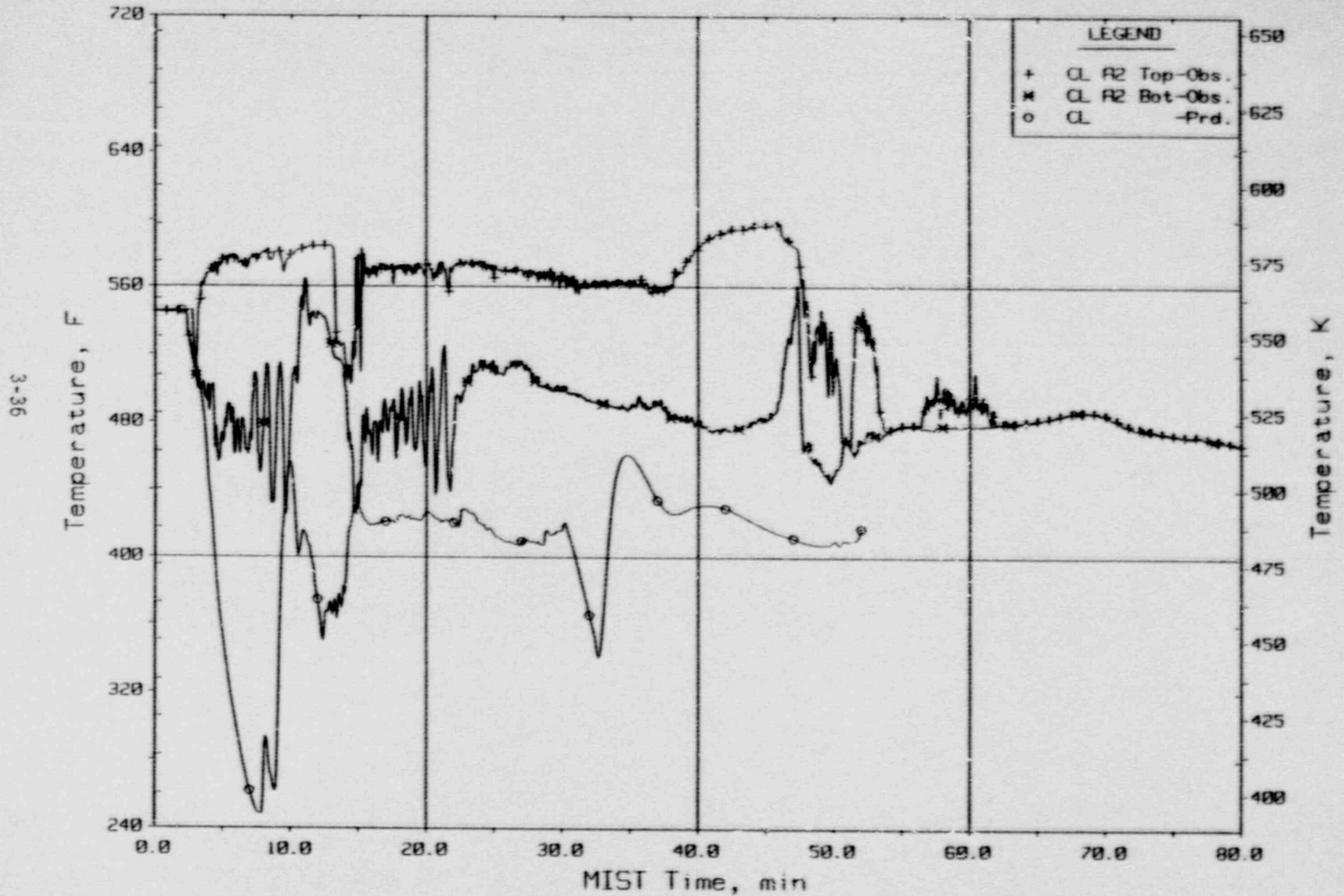


Figure 3.1.28. Cold Leg Nozzle Fluid Temperatures, Top/Bot of Rake (21.3ft, Ccltca2).



10 cm<sup>2</sup> CLPD Break with 30 Minute Isolation  
 MIST Nominal Test, Observed Vs. Predicted - Test 320503

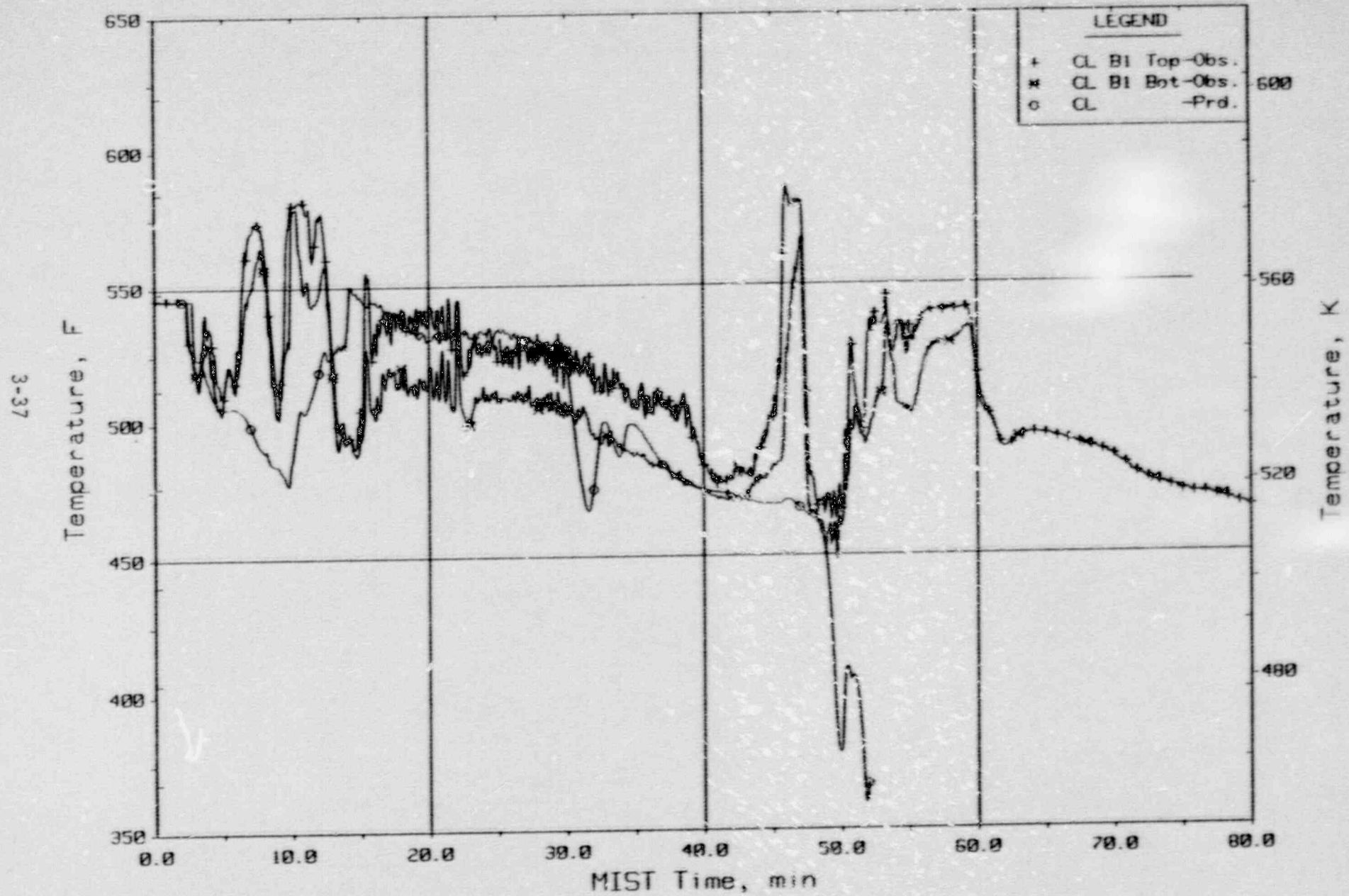


Figure 3.1.29. Cold Leg Nozzle Fluid Temperatures, Top/Bottom of Rake (21.3ft, Cc1tcbl).

Cc1tcbl

10 cm<sup>2</sup> CLPD Break with 30 Minute Isolation  
 MIST Nominal Test, Observed Vs. Predicted - Test 320503

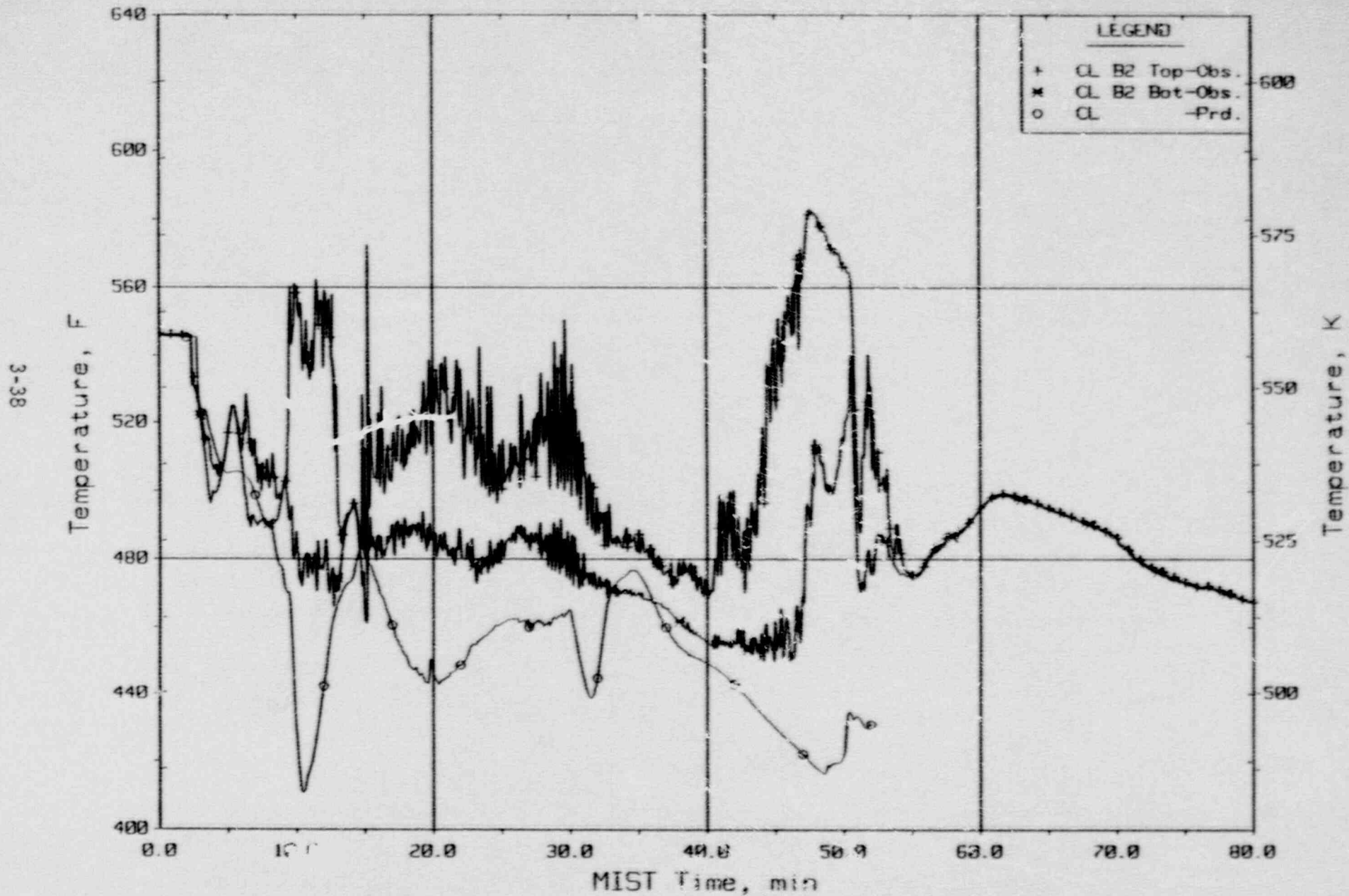


Figure 3.1.30. Cold Leg Nozzle Fluid Temperatures, Top/Bot of Rake (21.3ft, Ccltcb2).

10 cm<sup>2</sup> CLPD Break with 30 Minute Isolation  
 MIST Nominal Test, Observed Vs. Predicted - Test 320503

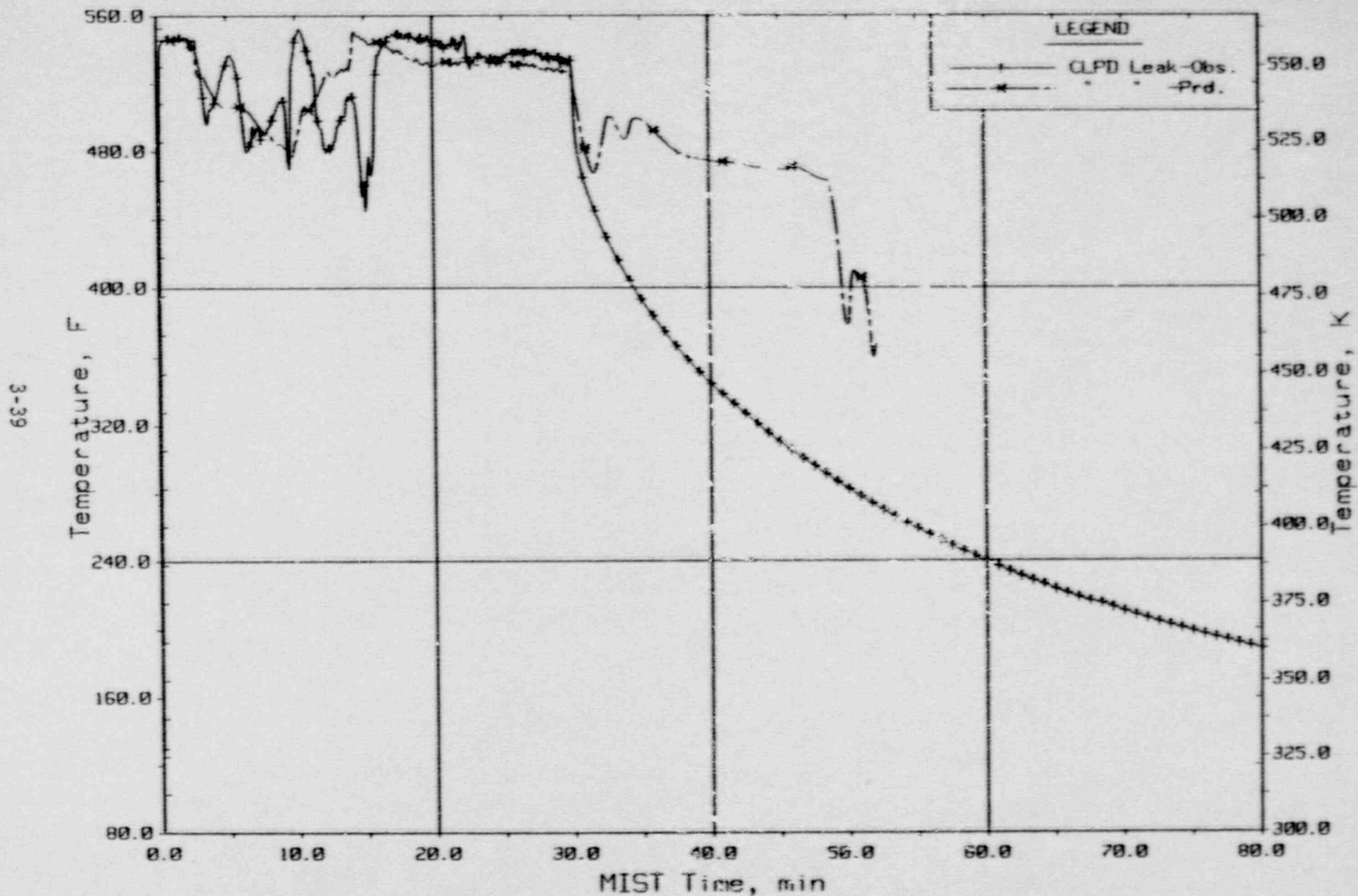


Figure 3.1.31. CLPD Leak Fluid Temperature (TC01s).

10 cm<sup>2</sup> CLPD Break with 30 Minute Isolation  
 MIST Nominal Test, Observed Vs. Predicted - Test 320503

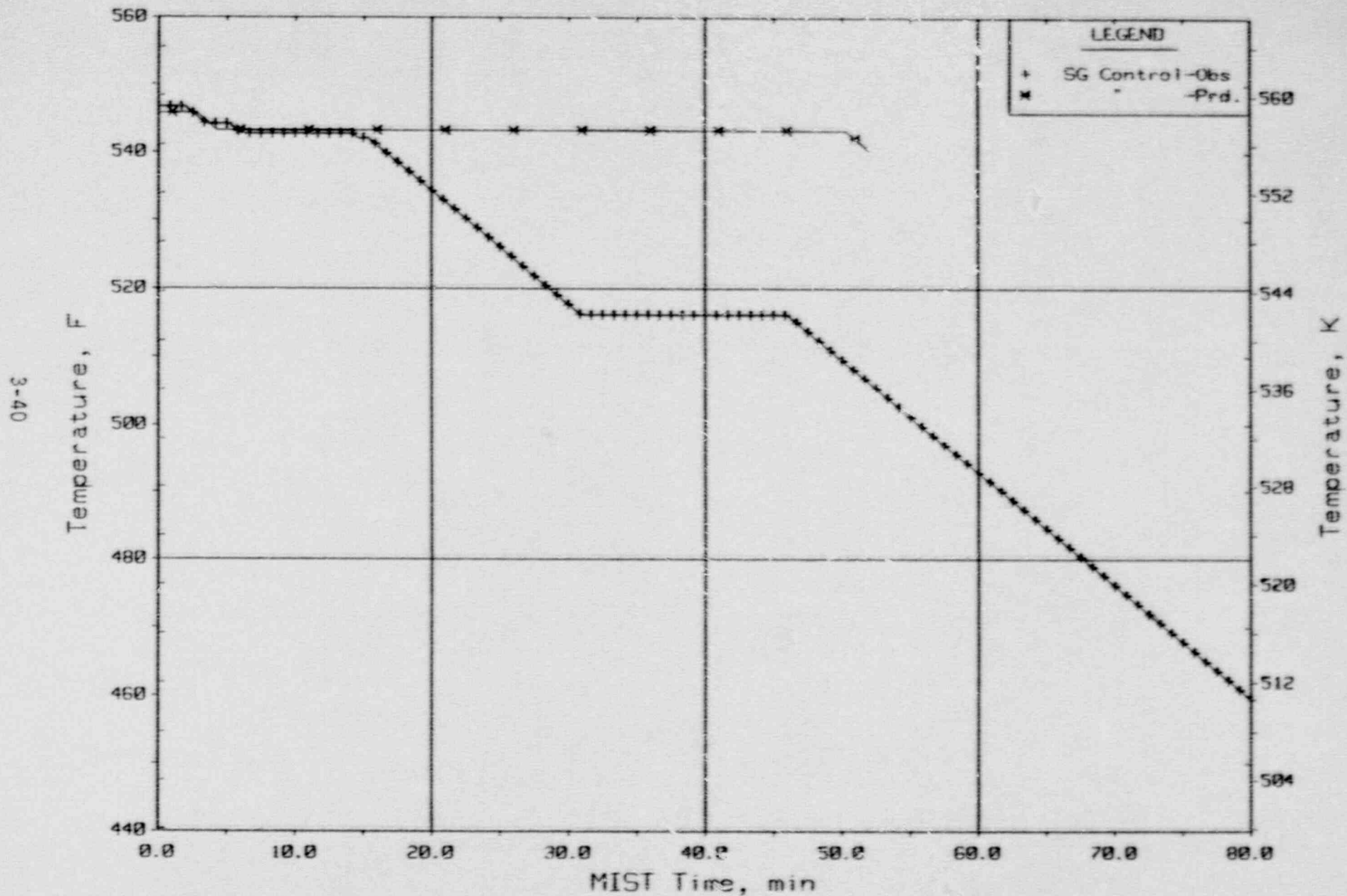


Figure 3.1.32. Steam Generator Secondary Saturation and Control Temperatures.

10 cm<sup>2</sup> CLPD Break with 30 Minute Isolation  
 MIST Nominal Test, Observed Vs. Predicted - Test 320503

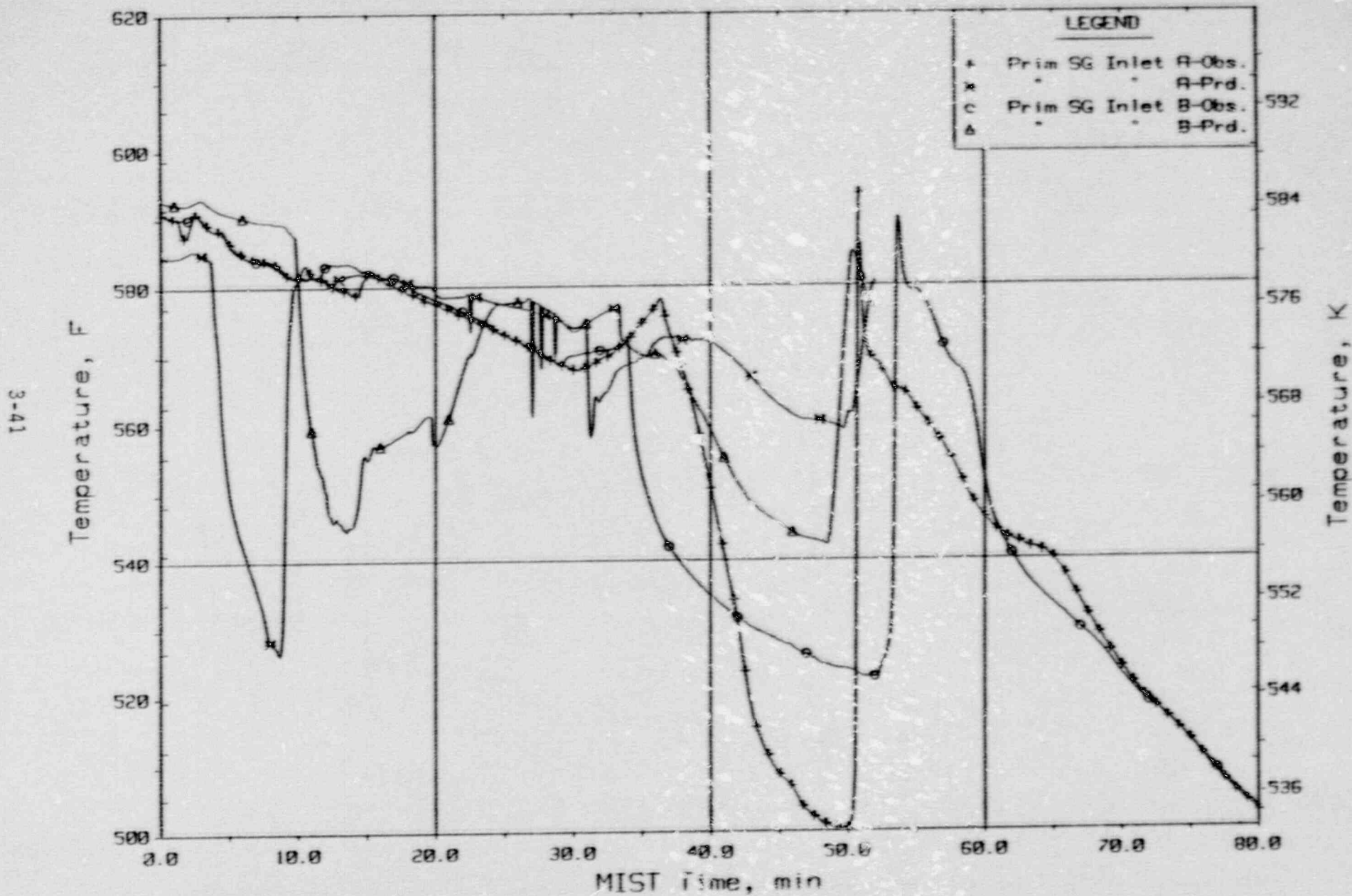


Figure 3.1.33. Loops A/B SG Primary Inlet Fluid Temperatures (RTDs).

10 cm<sup>2</sup> CLPB Break with 30 Minute Isolation  
 MIST Nominal Test, Observed Vs. Predicted - Test 320503

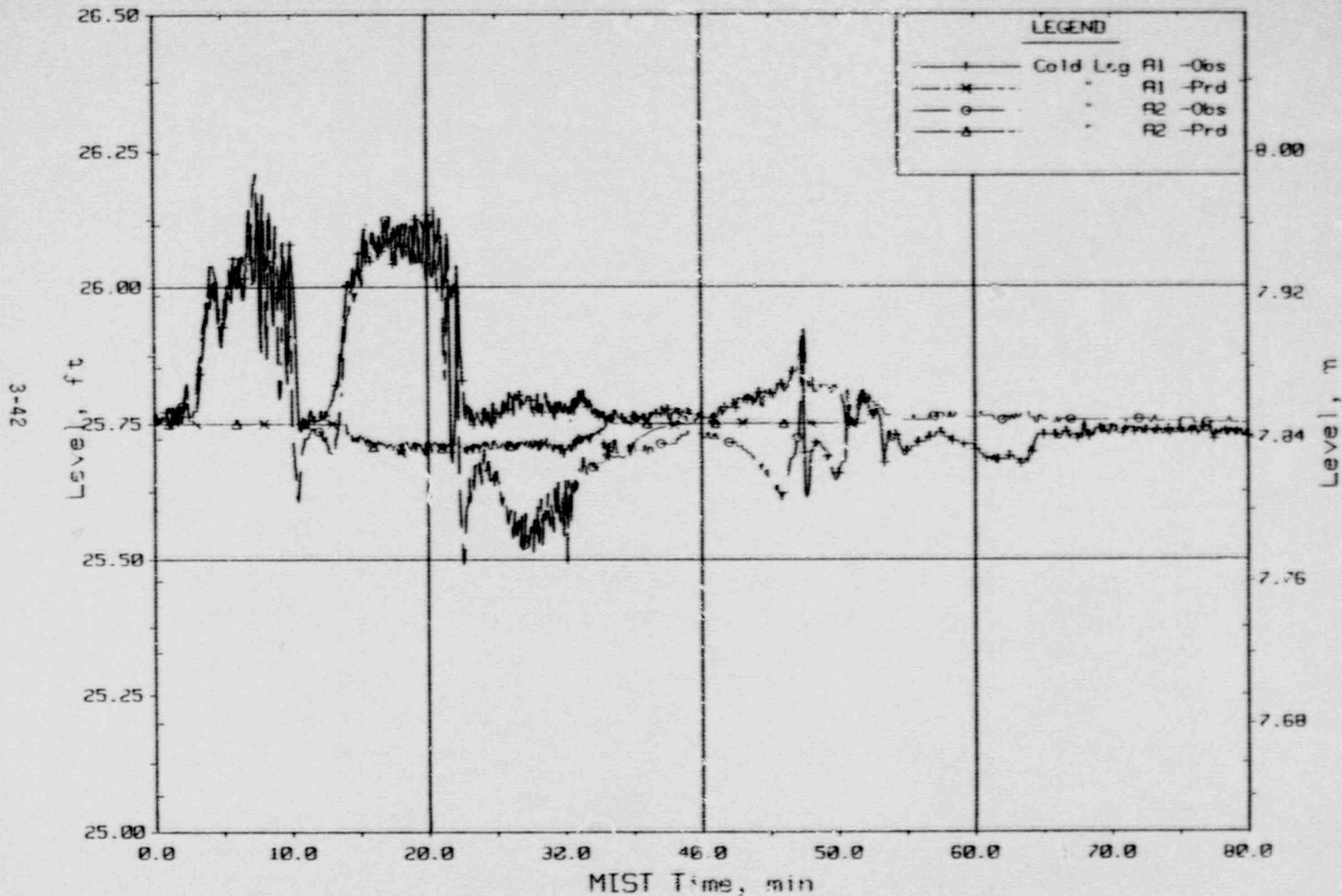


Figure 3.1.34. Cold Leg A Discharge Collapsed Liquid Levels (CnLV23s).

10 cm<sup>2</sup> CLPD Break with 30 Minute Isolation  
 MIST Nominal Test, Observed Vs. Predicted - Test 320503

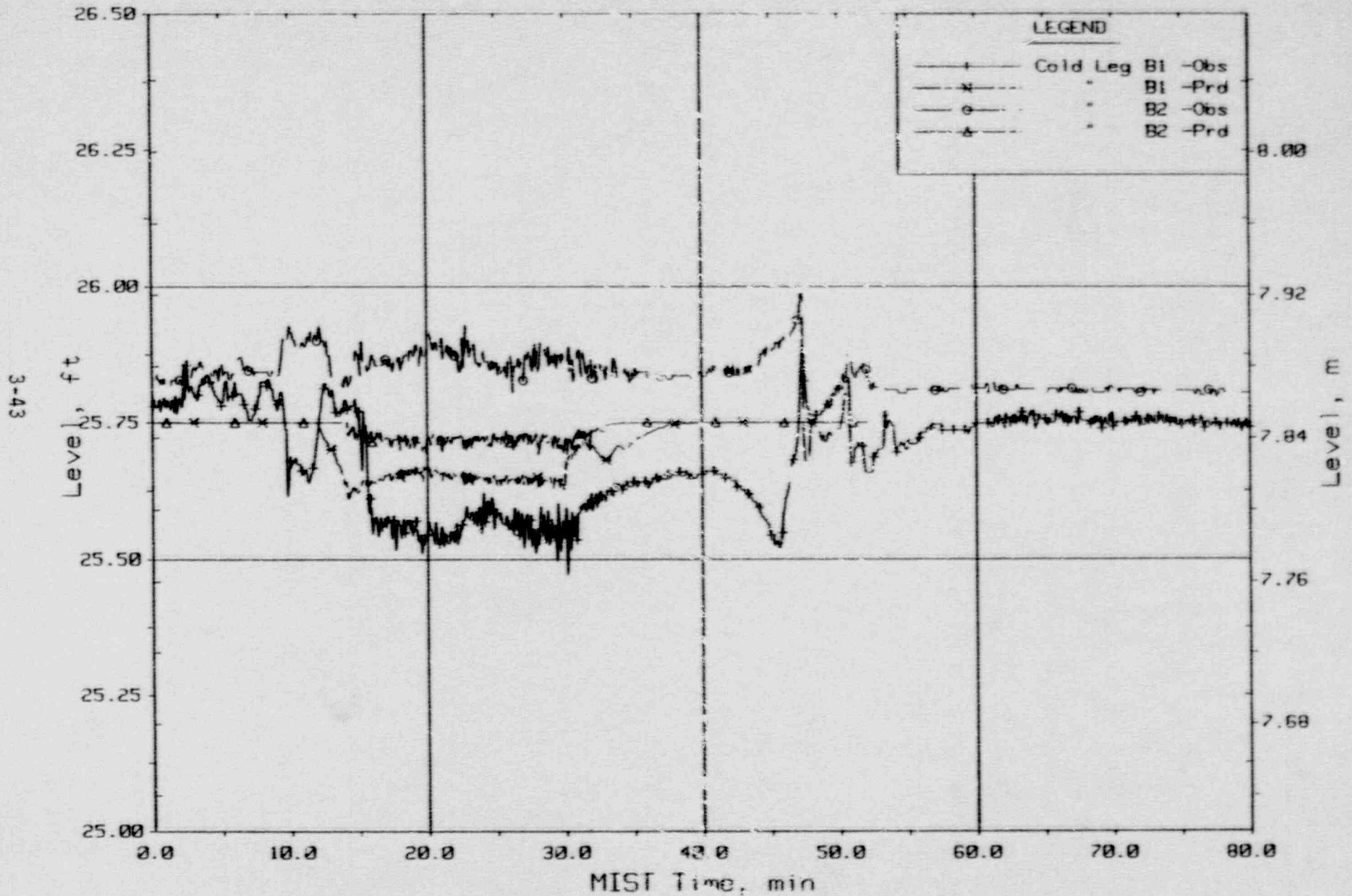


Figure 3.1.35. Cold Leg B Discharge Collapsed Liquid Levels (CnLV23s).

### 3.2. MIST Test 320302 Post-Test Prediction

MIST test 320302 is a 10 cm<sup>2</sup> cold leg pump suction (CLPS) leak in B1 loop with full high pressure injection (HPI). All other controls are nominal during the first hour and one-half which is the time period calculated for this test. The RELAP5/MOD2 simulation was performed using the MIST base deck model with several minor changes required to be consistent with test 320302 boundary conditions or operator actions. A detailed test description may be found in the MIST Group 32 Report.

#### 3.2.1. MIST Test 320302 Base Case Modifications

The RELAP5/MOD2 base input model was modified as follows to allow the transient calculations to be performed as simulated.

1. The CLPS break was actuated and all control variables which integrate the flows or energies were modified accordingly.
2. The original CLPD break was isolated.
3. A control variable to calculate core subcooling margin was added.
4. Miscellaneous time step and minor edit variable additions or changes were made to aide in interpreting the test simulation.

These changes are documented in detail in the calculational file for this test.

#### 3.2.2. MIST Test 320302 Transient Comparisons

The initial conditions for the RELAP calculation are consistent with the test conditions just before leak opening at time zero. Table 3.2.1. contains a listing of test and RELAP calculated steady-state initial conditions, while the transient comparison plots are shown in Figures 3.2.1. through 3.2.33. The core power, secondary pressure, secondary collapsed level, hot leg subcooling margin, and pressurizer level were defined for the steady-state initialization. The remainder of the parameters were determined from the spacial heat transfer and thermal-hydraulic behavior of the facility. Table 3.2.2. summarizes the transient progression through a tabular sequence of events list.

The initial rapid depressurization following leak actuation ended as the upper regions of the primary saturated. In the time period between 6 and 10



minutes the observed primary pressure dropped below the predicted value by approximately 50 psi. The loop A hot leg flows did not completely interrupt in the test while the predicted loop A flow was completely interrupted. The reduced loop flow delayed the time required for the HPI fluid to reach the core inlet, and therefore, resulted in earlier significant core boiling. As a result the primary pressure during this period was over-predicted.

At 14 minutes in the test, the loop B hot leg mixture level increased above the bottom of the U-bend and a spill-over occurred. The rapid accumulation of steam in the reactor vessel upper head had displaced enough liquid into this loop to bolster the level. Closing of the RVVVs just as the spill-over began enhanced the magnitude of the spill-over and recoupled the primary-to-secondary heat transfer. The secondary repressurized from this coupling until the control pressure value was reached and the 100F/hr cooldown was initiated. Since the calculations did not predict this spill-over and subsequent secondary repressurization, the RELAP secondary cooldown was not initiated until almost twenty minutes later. The effect of this delay was observed in the secondary pressure differential after 55 minutes.

The effect of the earlier test secondary steaming resulted in inventory loss which required additional AFW to maintain a constant level. At 44 minutes a feed cycle produced a high elevation BCM in loop B. The prediction had not reached the control pressure yet, therefore, this event was delayed. This delay provided enough time for the leak to drain the steam generator tube levels below the secondary level. When this happened at 51 minutes, a pool and subsequent high elevation BCM was predicted. At 57 minutes the test loop A secondary pressure reached the control pressure. By 66 minutes AFW flow was needed to maintain a constant secondary level. The AFW injection resulted in a feed cycle BCM. When the calculations were terminated both the test and prediction were continuously feeding and steaming the secondary side of the generators. The primary pressures responded by following the secondary control pressures as the cooldown rates continued.

Table 3.2.1. MIST Test 320302 Calculated and Measured  
Initial Steady-State Conditions

<u>Parameter</u>	<u>Data</u>	<u>RELAP5</u>
Primary Pressure, (psia)	1727.	1727.
SG A Secondary Pressure*, (psia)	1015.	1010.
SG B Secondary Pressure*, (psia)	1014.	1010.
SG A Secondary Collapsed Level*, (ft)	4.76	5.02
SG B Secondary Collapsed Level*, (ft)	5.12	5.02
Hot Leg Subcooling Margin*, (F)	22.5	21.5
Pressurizer Collapsed Level*, (ft)	23.13	23.00
Core Power into the Fluid*, (Btu/s)	119.5	119.5
Primary Side Mass Inventory	972.0	970.0
SG A Primary Exit Temperature, (F)	550.0	550.3
SG B Primary Exit Temperature, (F)	550.0	550.3
Core Exit Temperature, (F)	594.0	593.4
Core Total Mass Flow Rate, (lbm/s)	1.87	1.96

\*Denotes specified condition.

Table 3.2.2. MIST Test 320302 Sequence of Events Comparisons

<u>Event</u>	<u>Approximate Test Time (Min)</u>	
	<u>RELAP</u>	<u>Data</u>
Scaled 10 cm <sup>2</sup> CLPS Leak Opened	0.0	0.0
Pressurizer Level to 1.0 ft: Initiate Core Power Ramp, HPI, RVVV Automatic Control, SG Secondary Refill and Depressurization	2.2	2.6
First Hot Leg A Flow Interruption	3.0	3.4
SG Secondary Level to 31.6 Feet	9.0	9.5
First Hot Leg B Flow Interruption	10.0	9.0

Table 3.2.2. MIST Test 320302 Sequence of Events Comparisons (Cont'd)

Event	Approximate Test Time (Min)	
	RELAP	Data
SG A Primary Level to Top of Tubes	18.0	22.0
SG B Primary Level to Top of Tubes	22.0	28.0
SG B Feed Cycle High Elevation BCM	--	44.0
Pool and High Elevation BCM	51.0	--
Primary Refill Began	57.6	54.0
SG A Feed Cycle High Elevation BCM	--	66.0
Core Flood Tank Flow Began	68.5	69.5
Calculations Terminated	90.0	--

3.2.3. MIST Test 320302 Post-Test Conclusions

The prediction of MIST test 320302 was very reasonable. Probably the most significant difference between the test and the prediction was related to the calculated leak flow rate. The predicted leak flow with a discharge coefficient of one exceeded that measured in the test by approximately ten percent. Increased inventory loss because of the excessive leak flow resulted in a lower primary system mass. The discrepancies in the rates of decline between the predicted and observed hot leg and steam generator tube levels were also related to the leak flow differences. Lower steam generator tube levels and lack of repressurization in the loop B secondary side at 14 minutes, provided the mechanism whereby the pool BCM was predicted instead of the observed feed cycle BCM. However, even with these discrepancies, the predicted, governing phenomena and trends still occurred at nearly the same time and magnitude as those observed in the test.

10 C12 Cold Leg Suction Break  
 Test 320302 - Observed Vs. Predicted

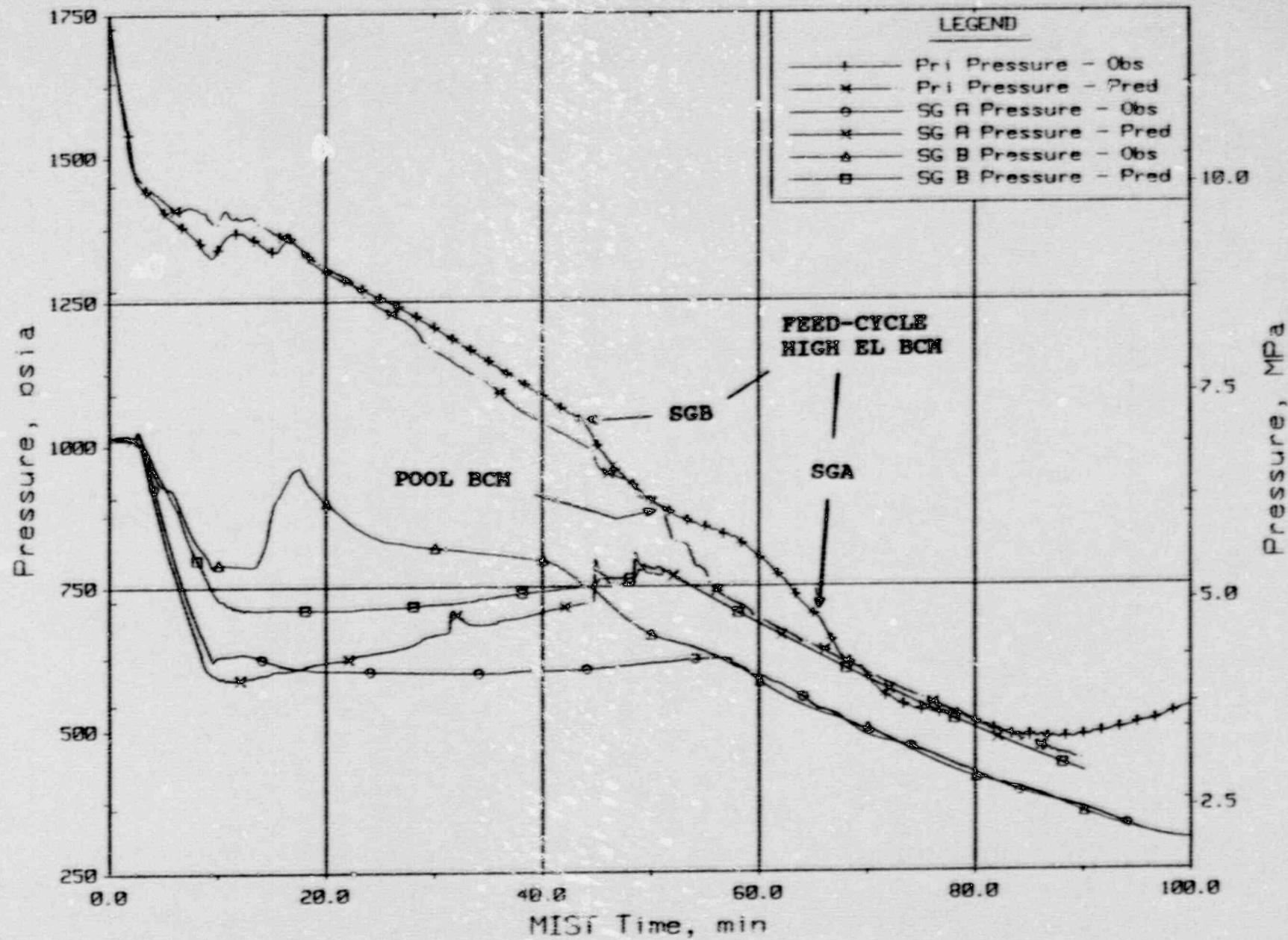


Figure 3.2.1. System Pressures.

18 CM2 Cold Leg Suction Break  
Test 320302 - Observed Vs. Predicted

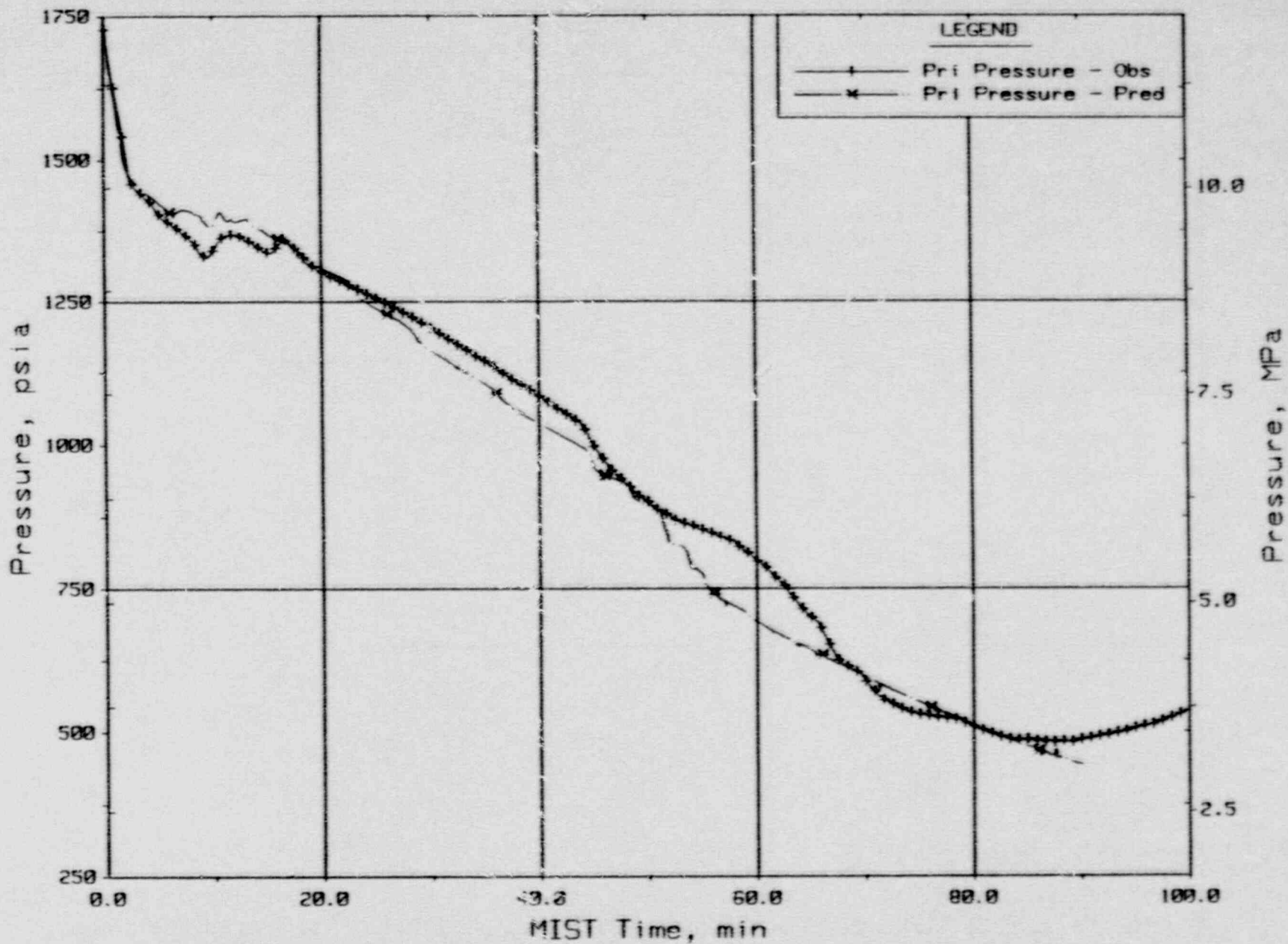


Figure 3.2.2. Primary Pressure.

10 CM2 Cold Leg Suction Break  
 Test 320302 - Observed Vs. Predicted

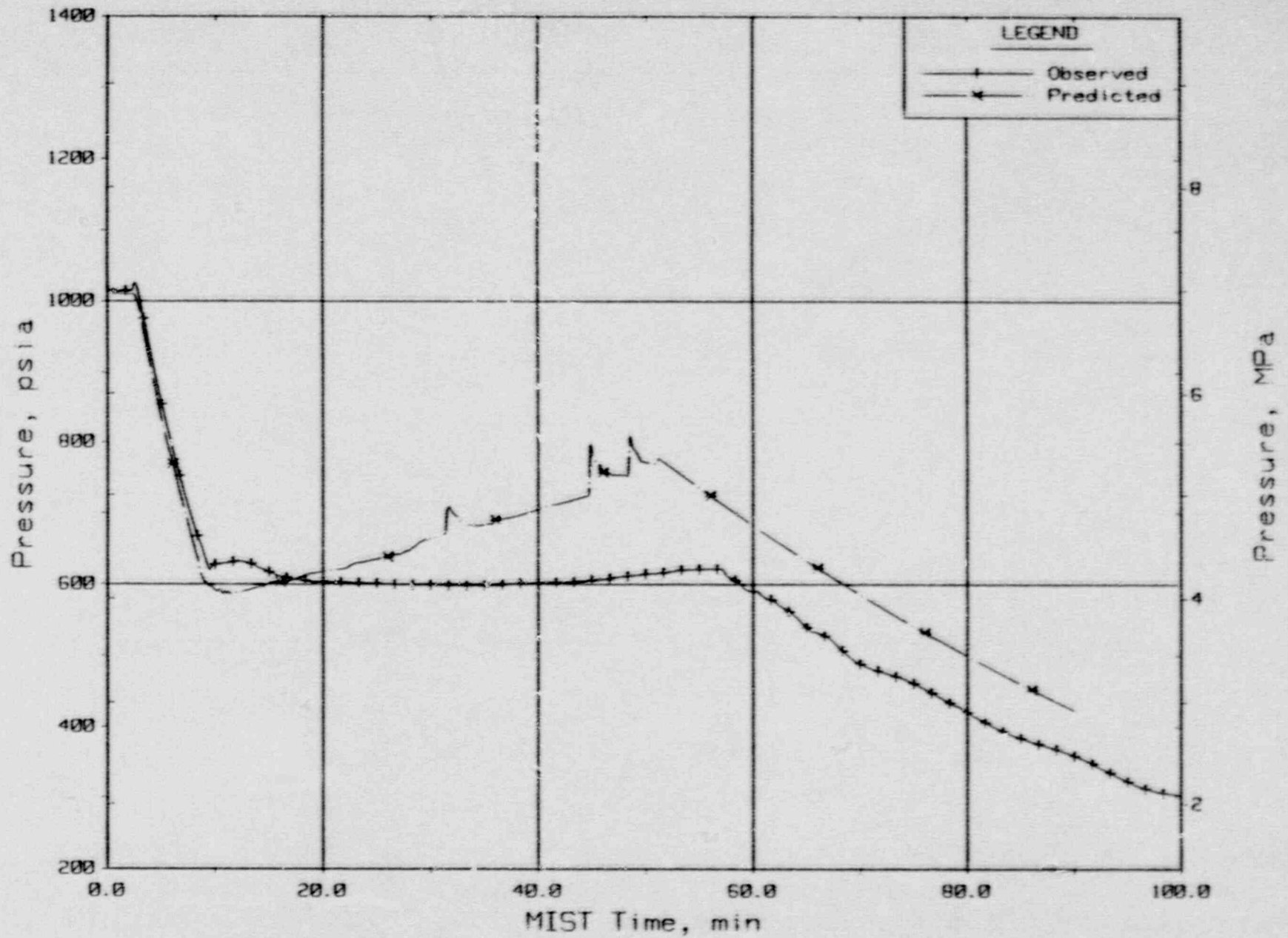


Figure 3.2.3. Steam Generator R Secondary Pressure.

10 CM2 Cold Leg Suction Break  
 Test 329302 - Observed Vs. Predicted

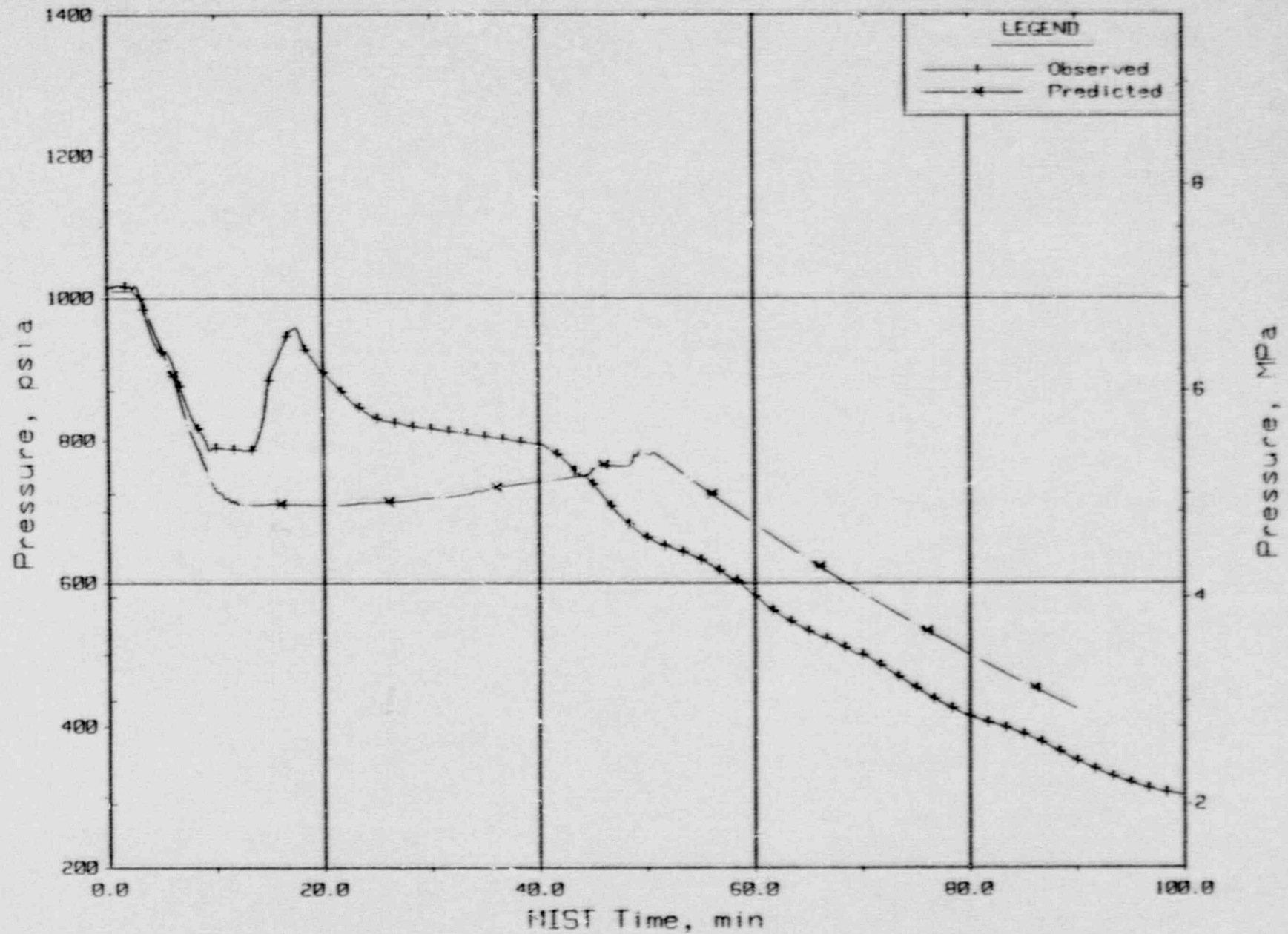


Figure 3.2.4. Steam Generator B Secondary Pressure.

10 CM2 Cold Leg Suction Break  
Test. 320302 - Observed Vs. Predicted

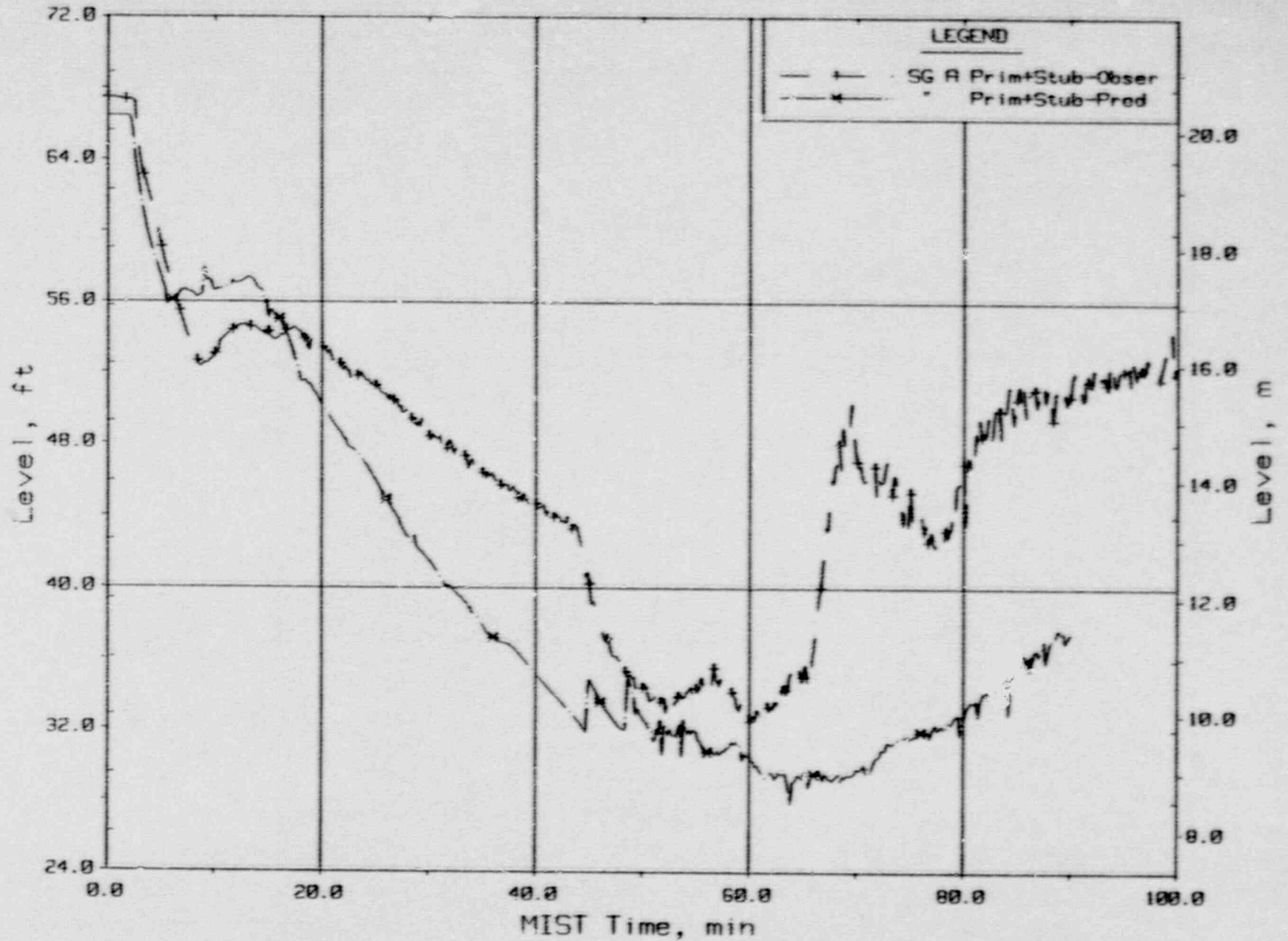


Figure 3.2.5. Steam Generator A Primary + Stub Level.



10 CM2 Cold Leg Suction Break  
 Test 320302 - Observed Vs. Predicted

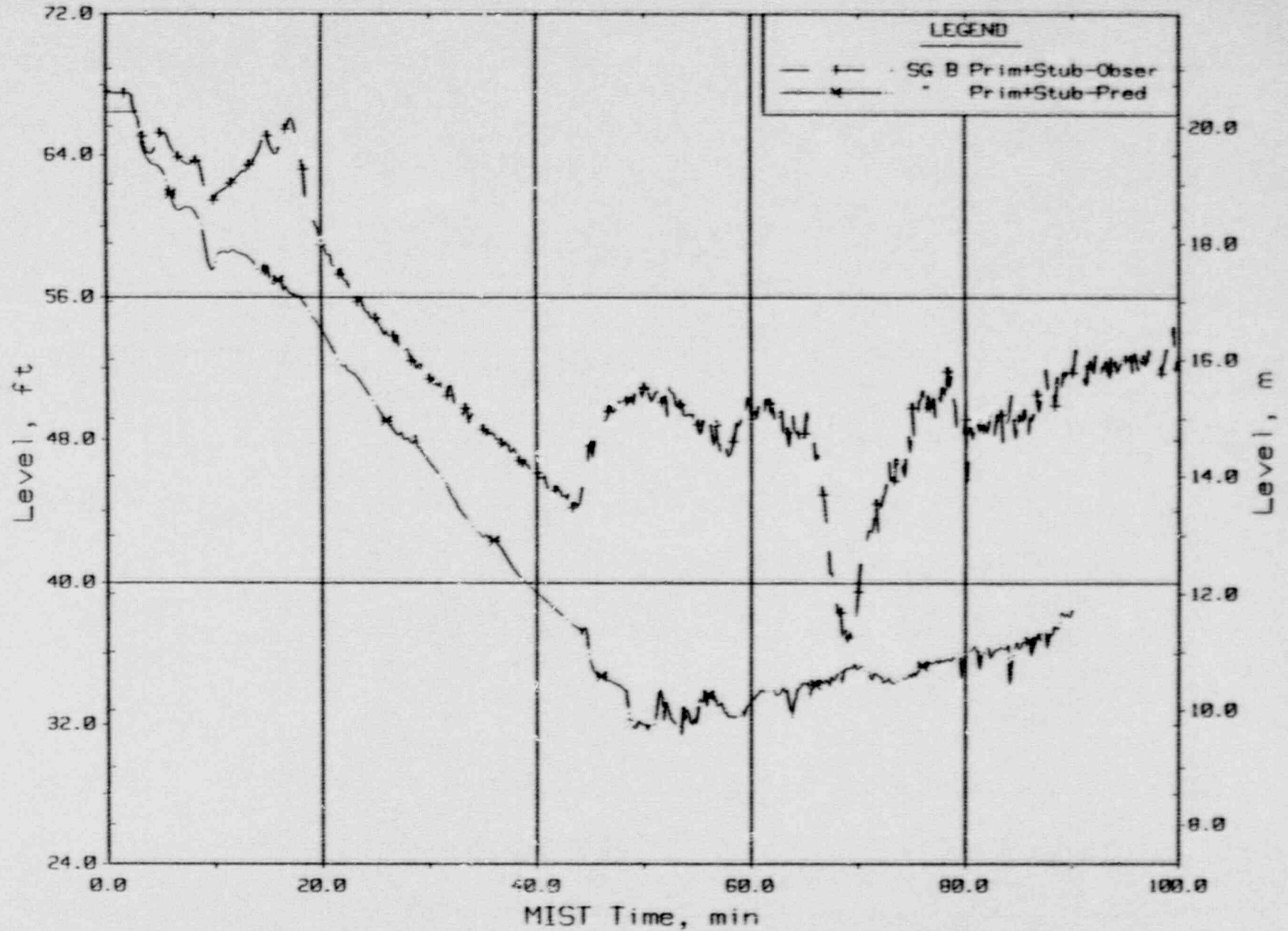


Figure 3.2.6. Steam Generator B Primary + Stub Level.

10 CM2 Cold Leg Suction Break  
Test 320302 - Observed Vs. Predicted

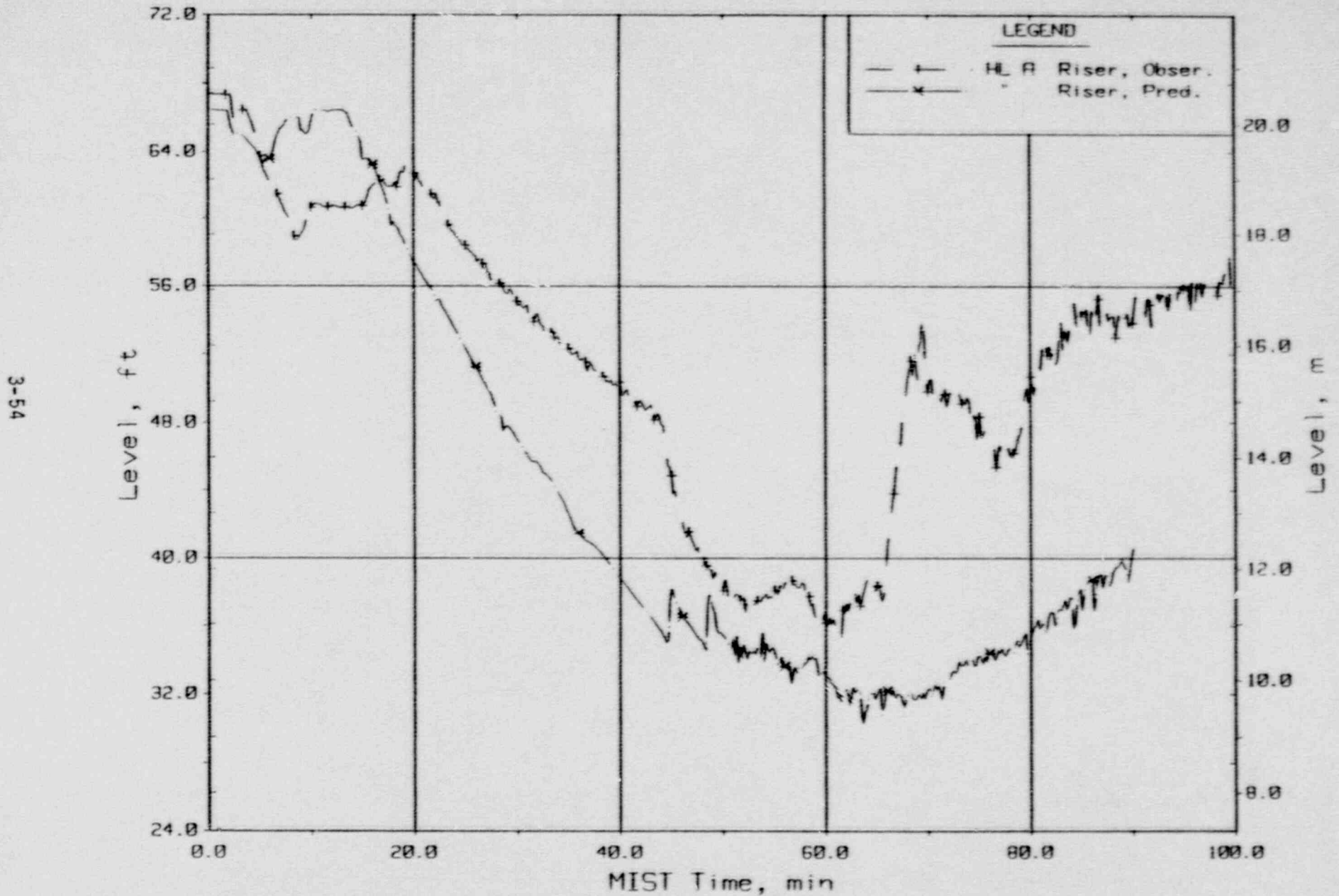


Figure 3.2.7. Hot Leg A Riser Level.

10 CM2 Cold Leg Suction Break  
 Test 320302 - Observed Vs. Predicted

3-55

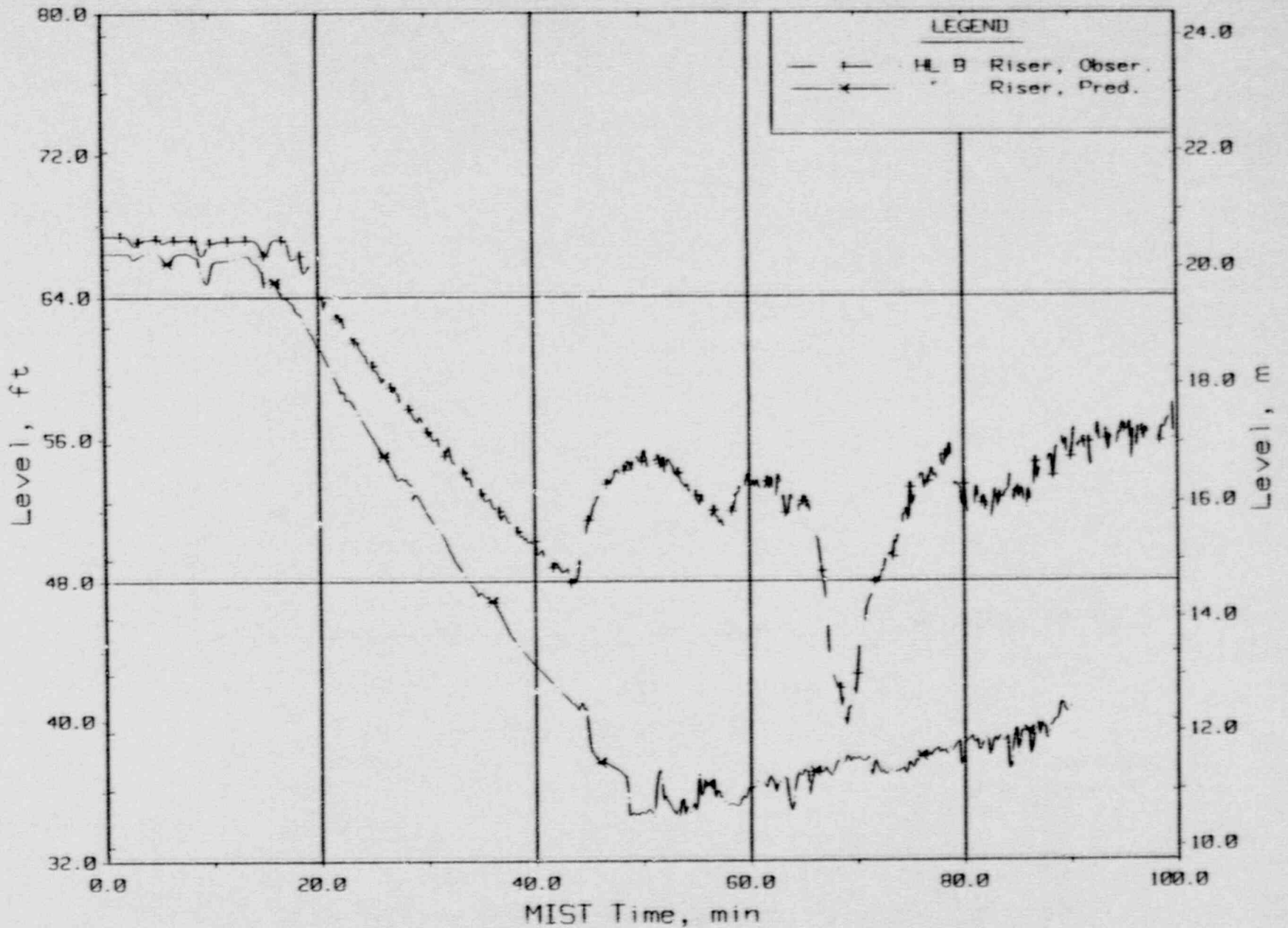


Figure 3.2.8. Hot Leg B Riser Level.

10 CM2 Cold Leg Suction Break  
 Test 320302 - Observed Vs. Predicted

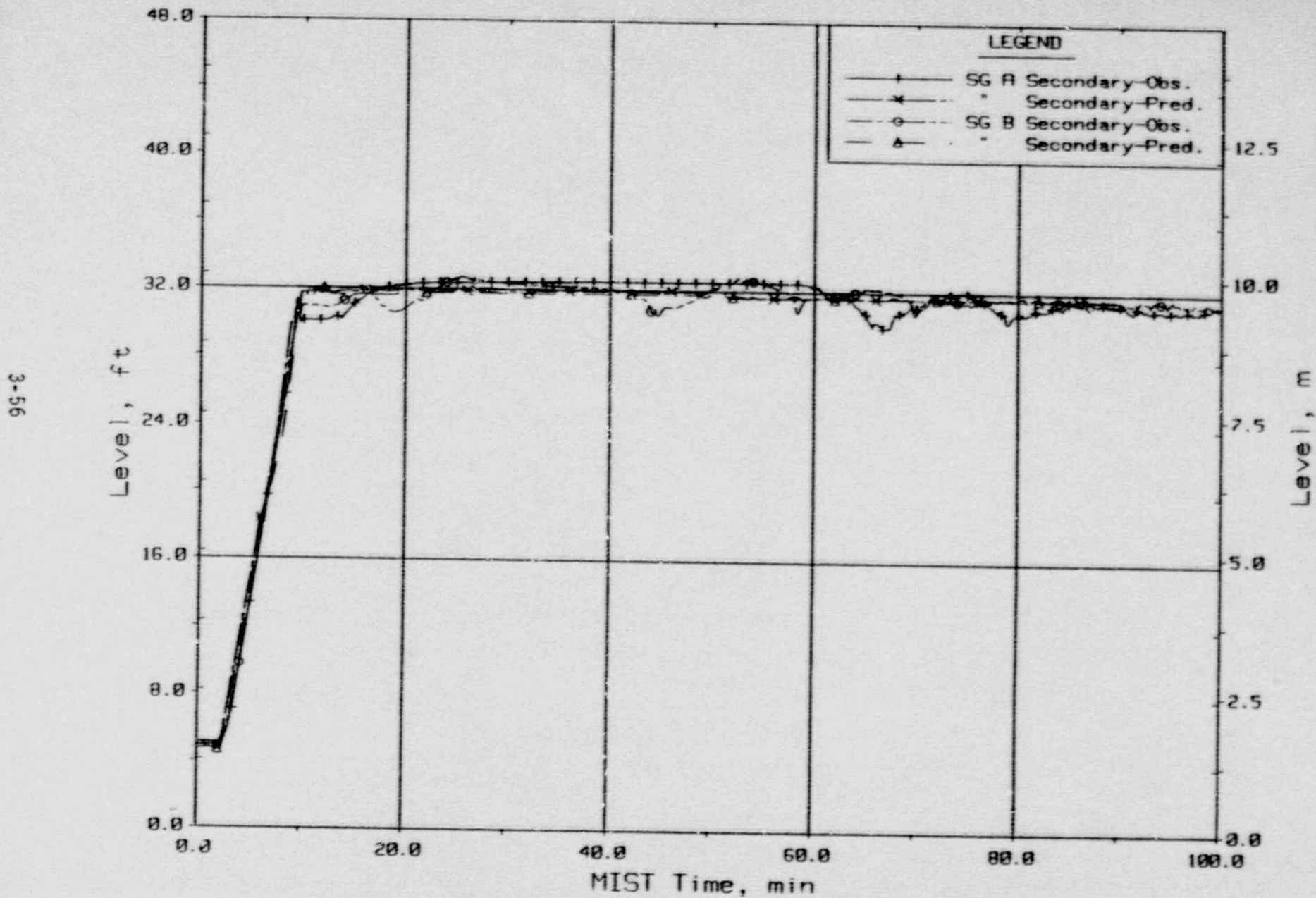


Figure 3.2.9. Steam Generator Sec. Collapsed Liquid Levels.

10 CM2 Cold Leg Suction Break  
Test 320302 - Observed Vs. Predicted

3-57

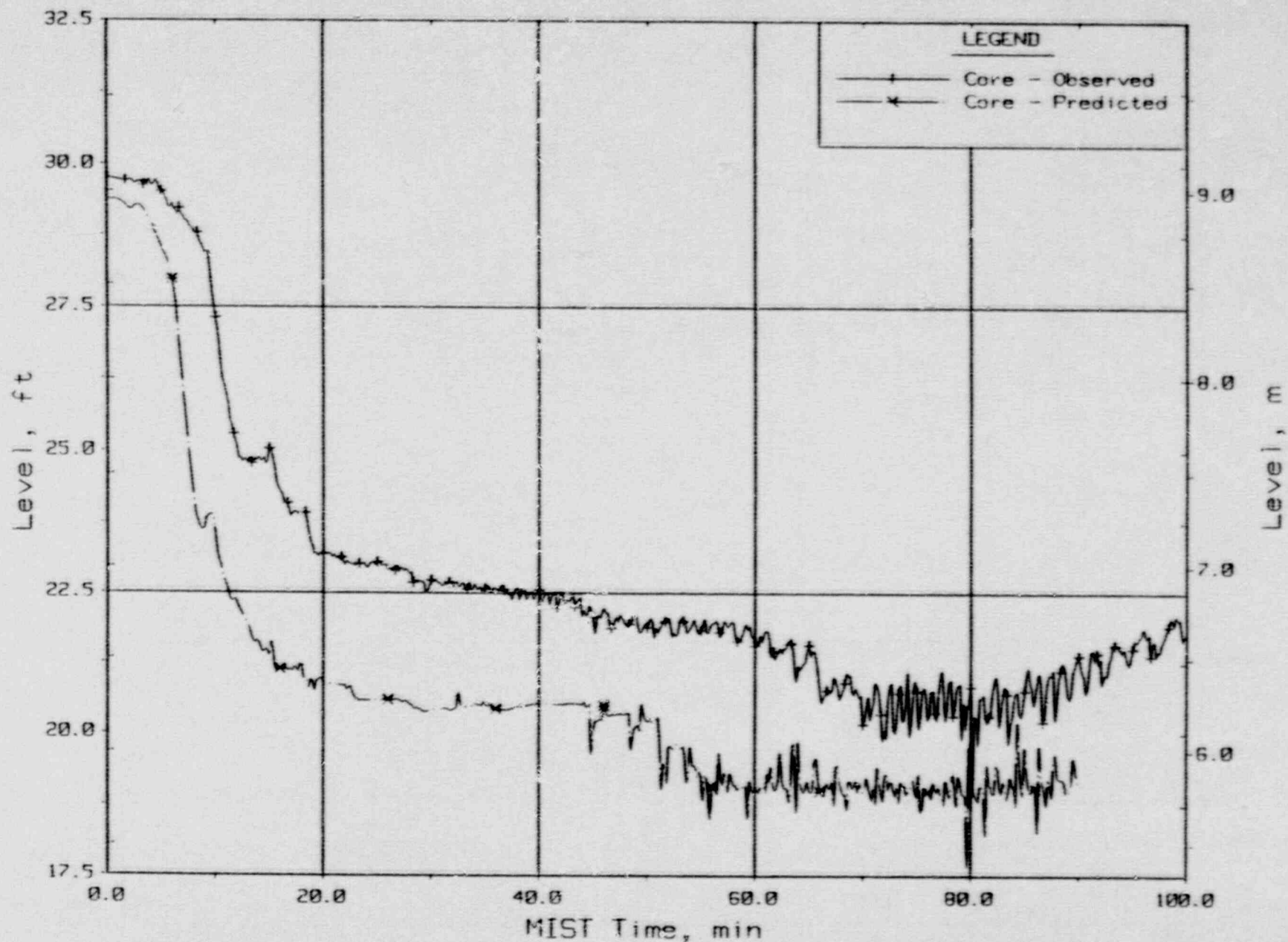


Figure 3.2.10. Core Region Collapsed Liquid Levels.

10 CM2 Cold Leg Suction Break  
 Test 320302 - Observed Vs. Predicted

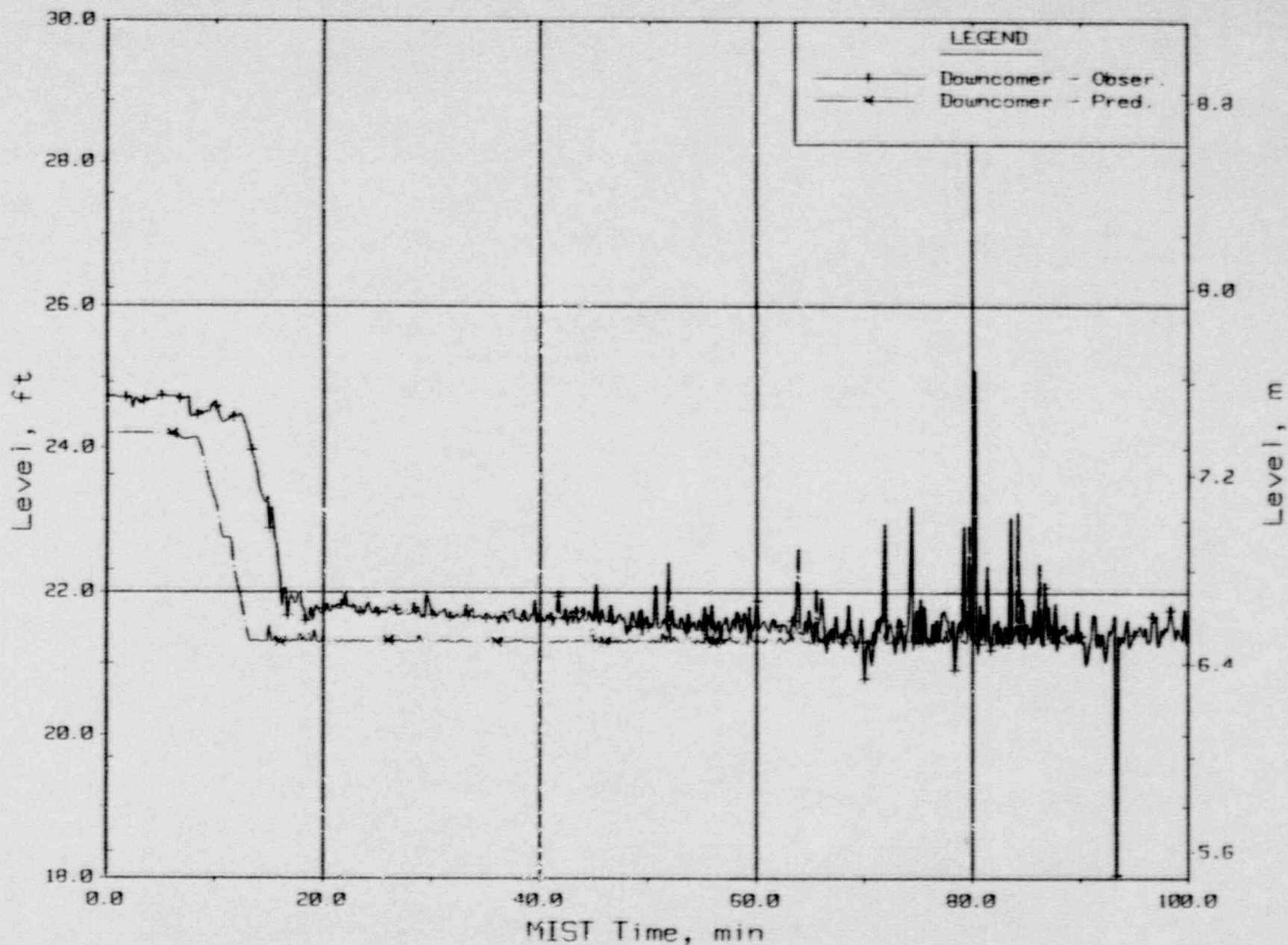


Figure 3.2.11. Core Region Collapsed Liquid Levels.

10 CM2 Cold Leg Suction Break  
Test 320302 - Observed Vs. Predicted

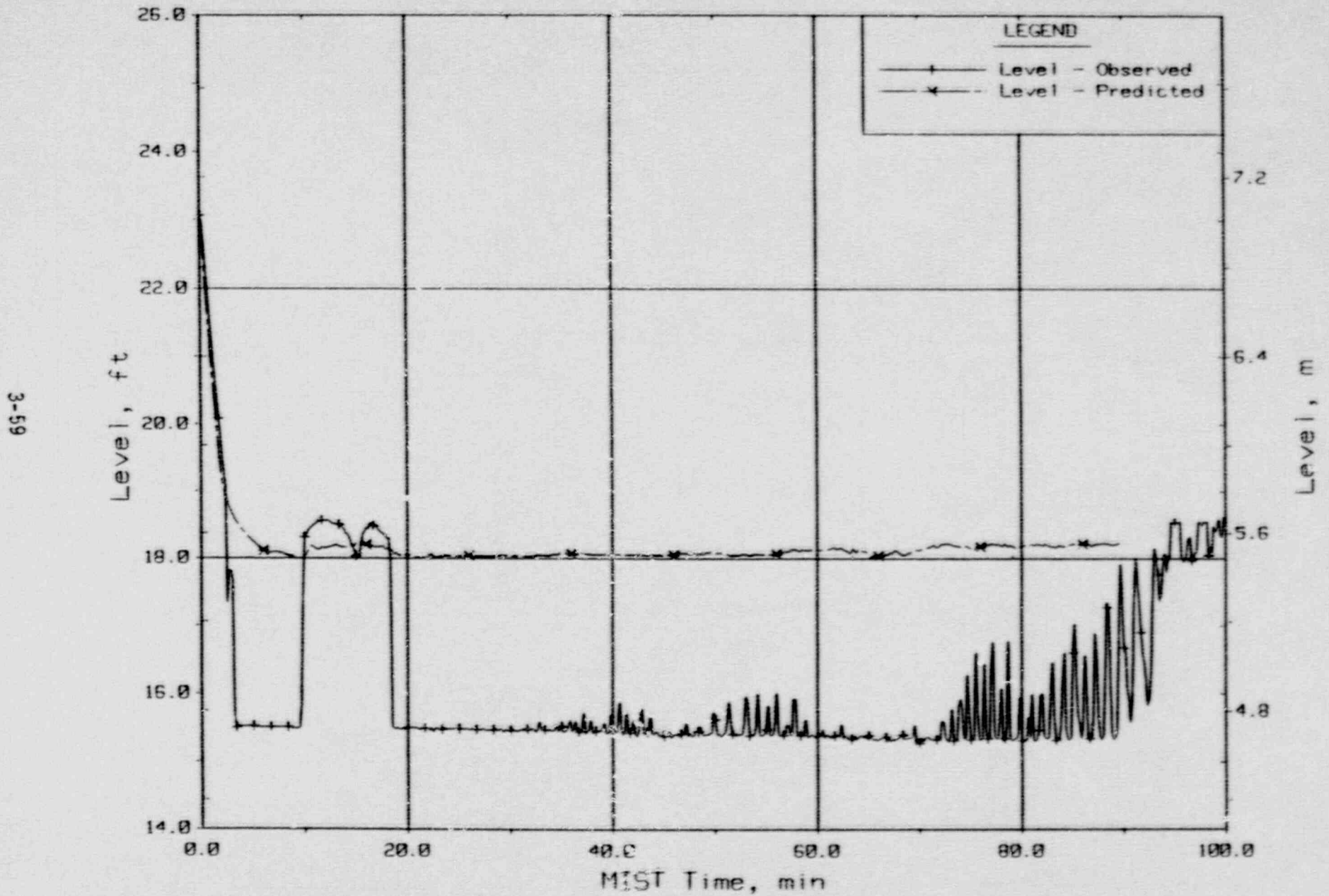


Figure 3.2.12. Pressurizer Collapsed Liquid Level (PZLV20).

10 CM2 Cold Leg Suction Break  
 Test 320302 - Observed Vs. Predicted

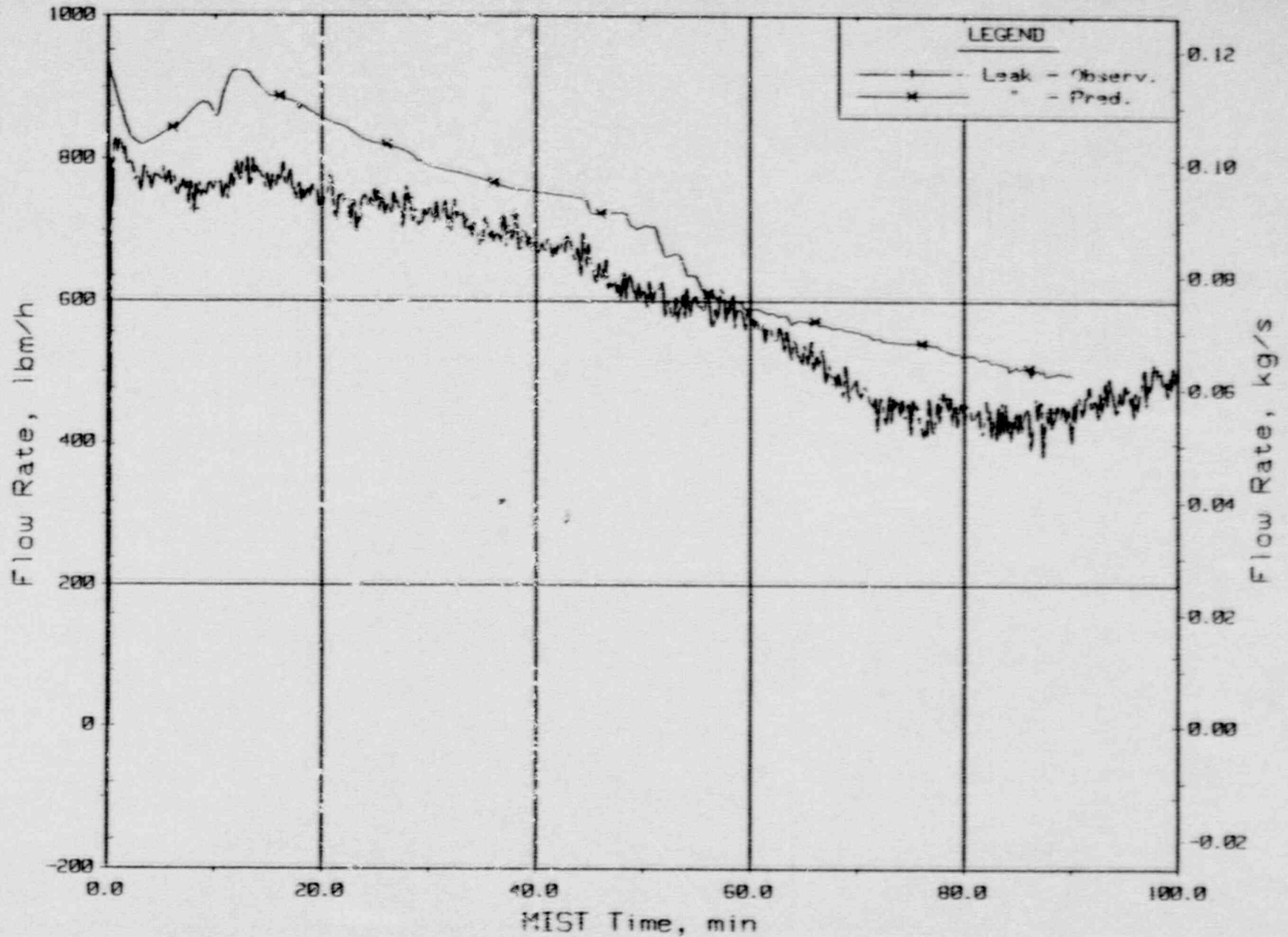


Figure 3.2.13. Leak Flow Rates.



10 CM2 Cold Leg Suction Break  
 Test 320302 - Observed Vs. Predicted

19-6  
 3-61

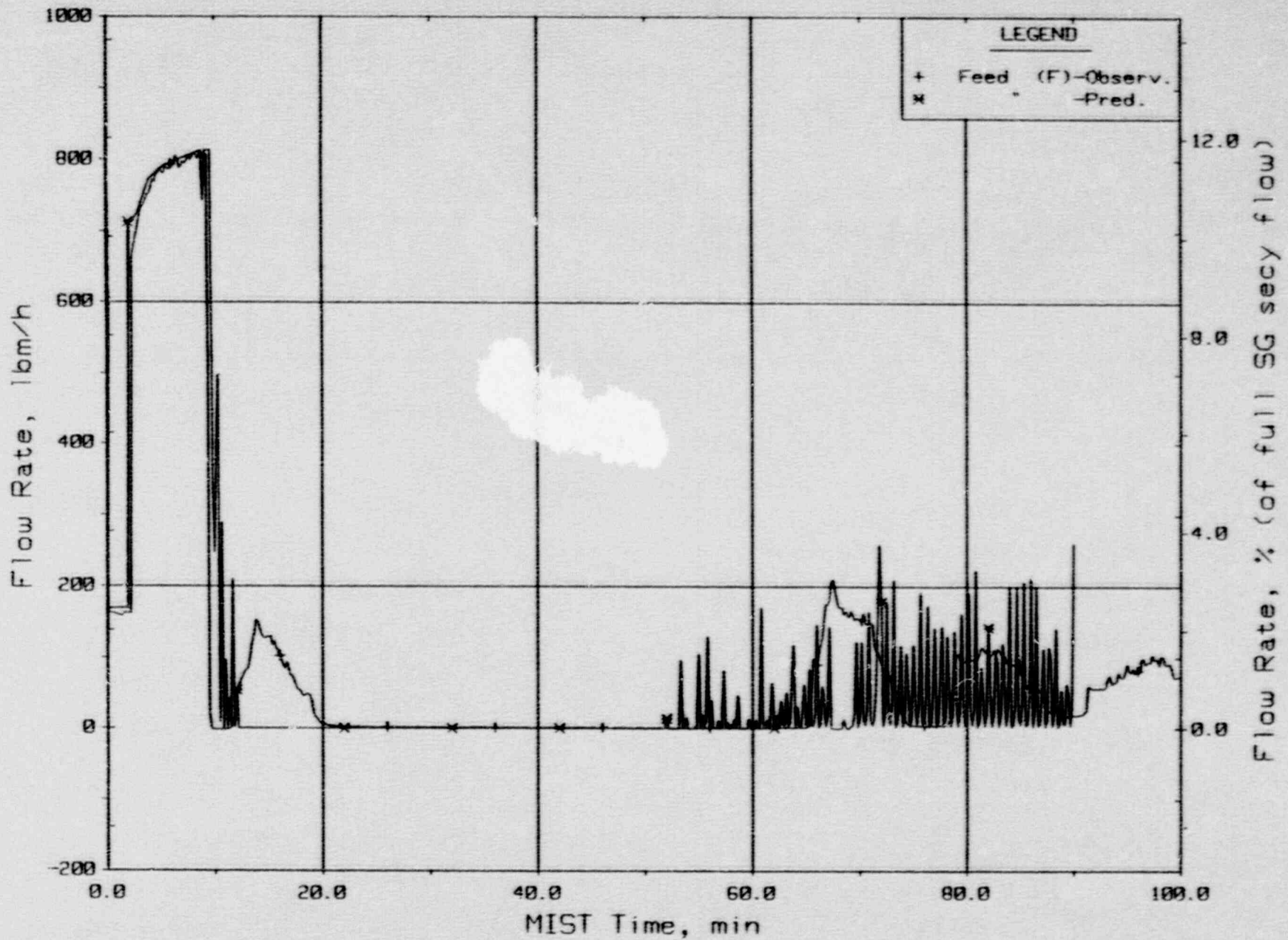


Figure 3.2.14. Steam Generator A Flow Rate (Ssfor20).

10 CM2 Cold Leg Suction Break  
Test 320302 - Observed Vs. Predicted

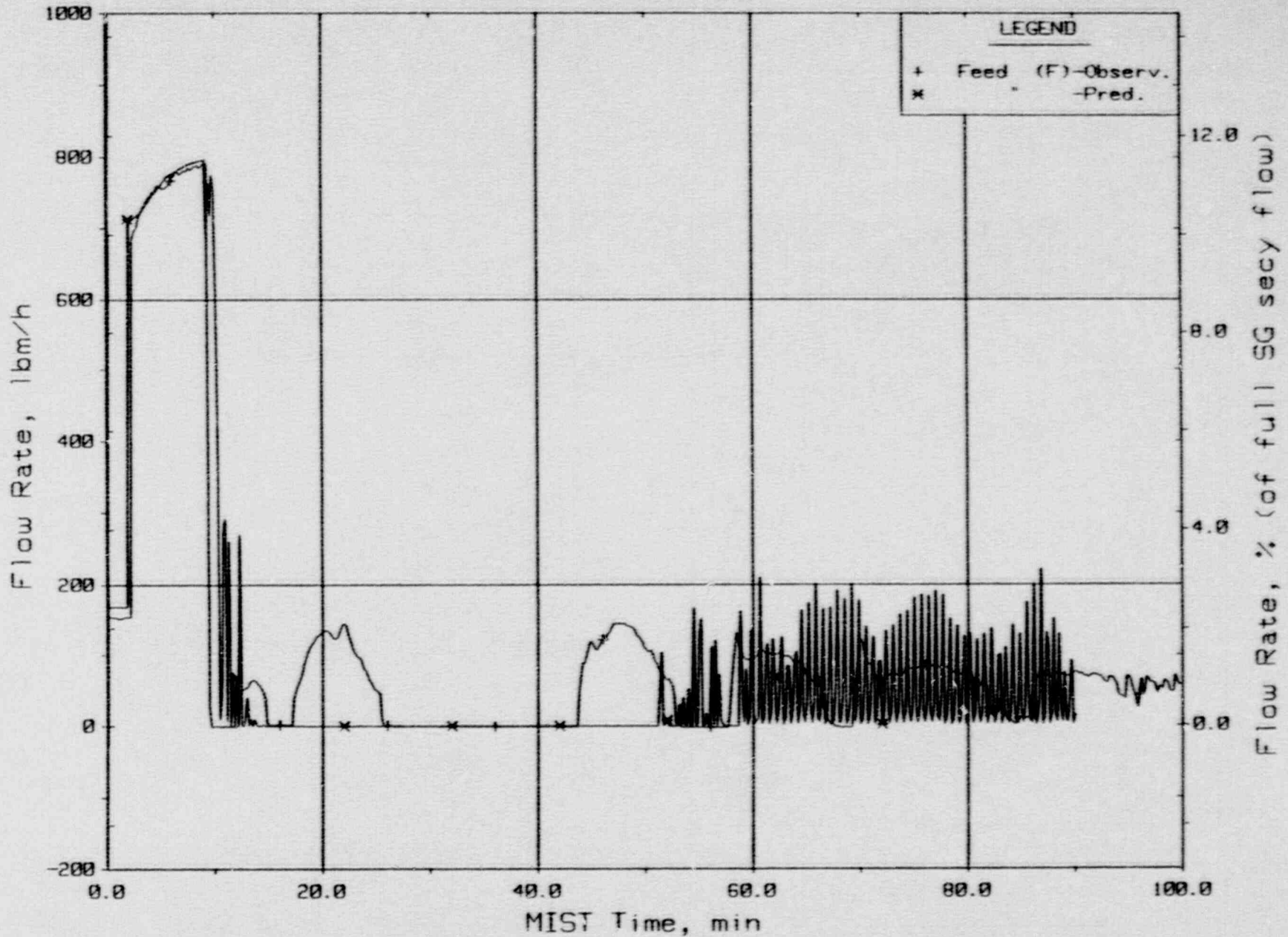


Figure 3.2.15. Steam Generator B Flow Rate (Ssfor21).

10 CM2 Cold Leg Suction Break  
 Test 320302 - Observed Vs. Predicted

3-63

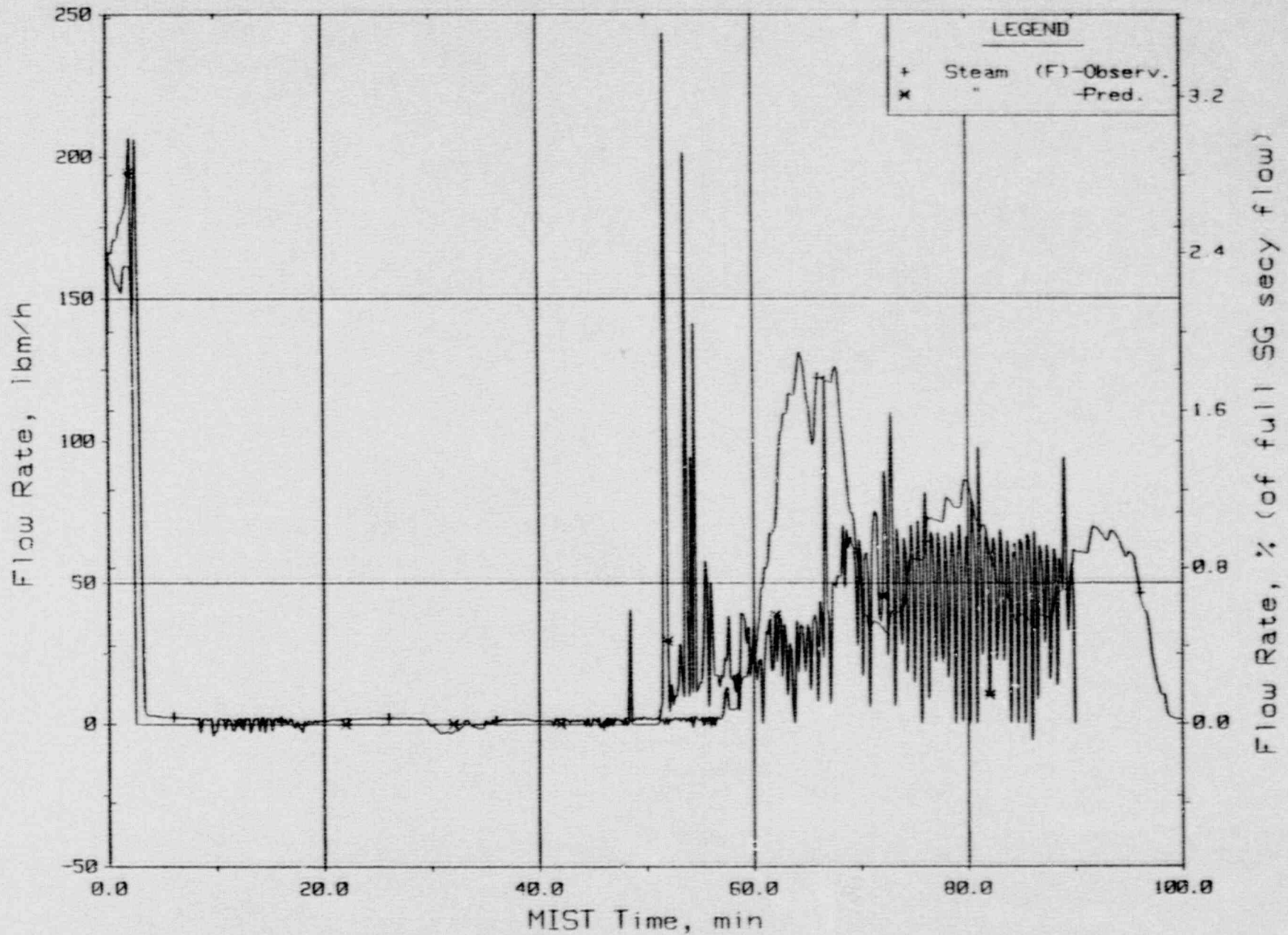


Figure 3.2.16. Steam Generator A Flow Rates (Cссор20).

10 CM2 Cold Leg Suction Break  
 Test 320302 - Observed Vs. Predicted

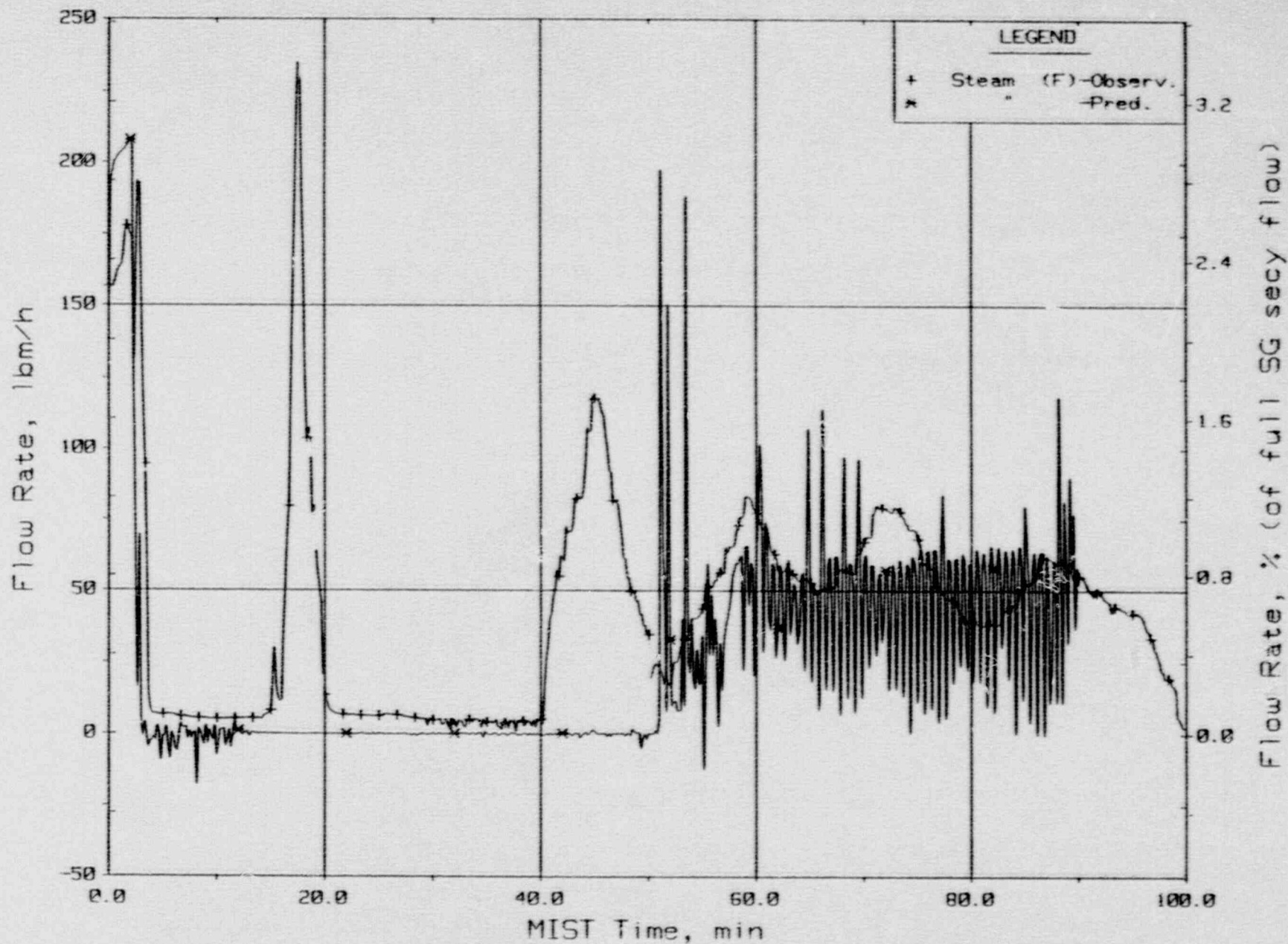


Figure 3.2.17. Steam Generator B Flow Rates (Sssor21).

10 CM2 Cold Leg Suction Break  
 Test 320302 - Observed Vs. Predicted

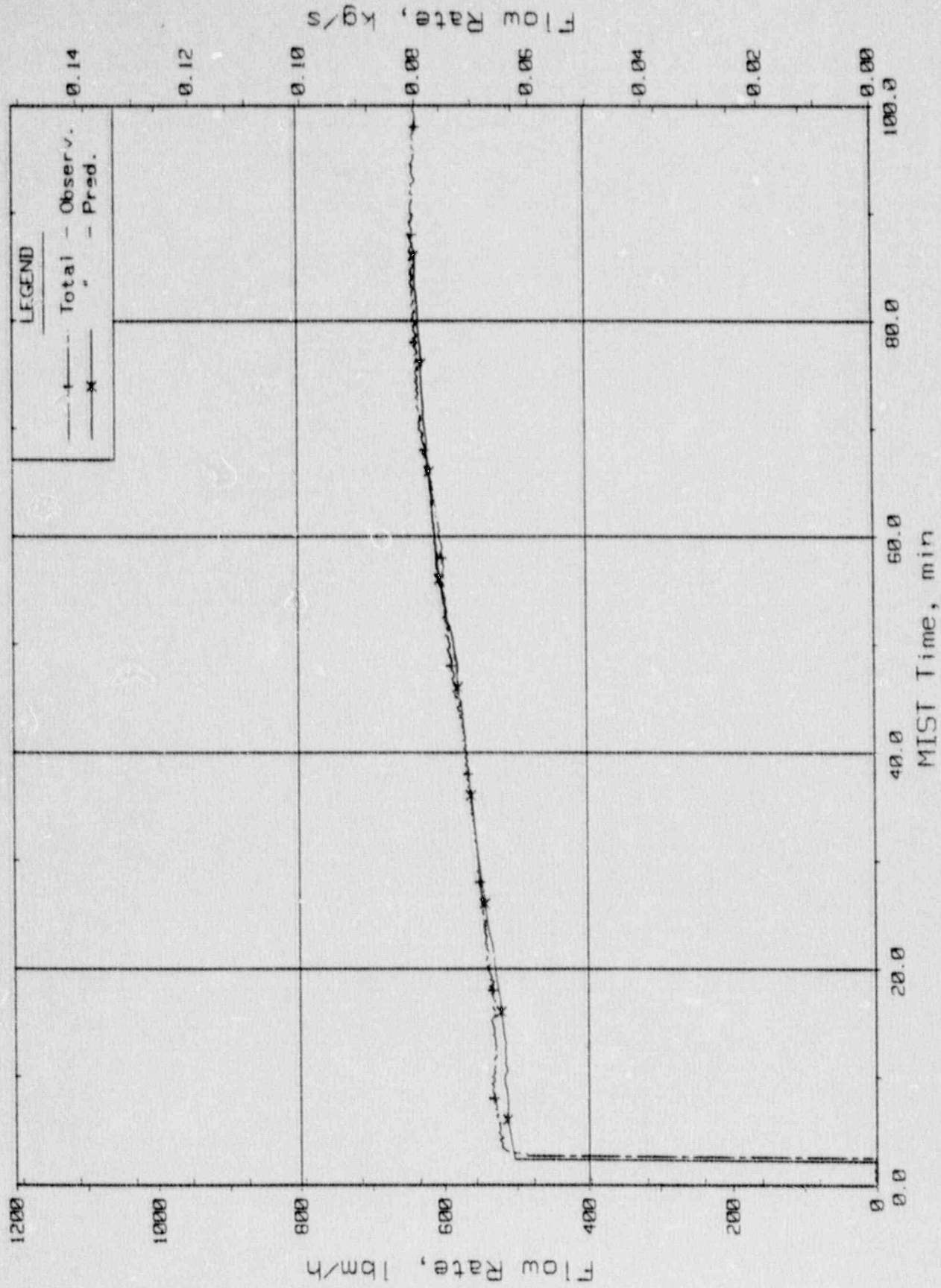


Figure 3.2.18. HPI Total Flow Rates.

10 CM2 Cold Leg Suction Break  
Test 320302 - Observed Vs. Predicted

3-66

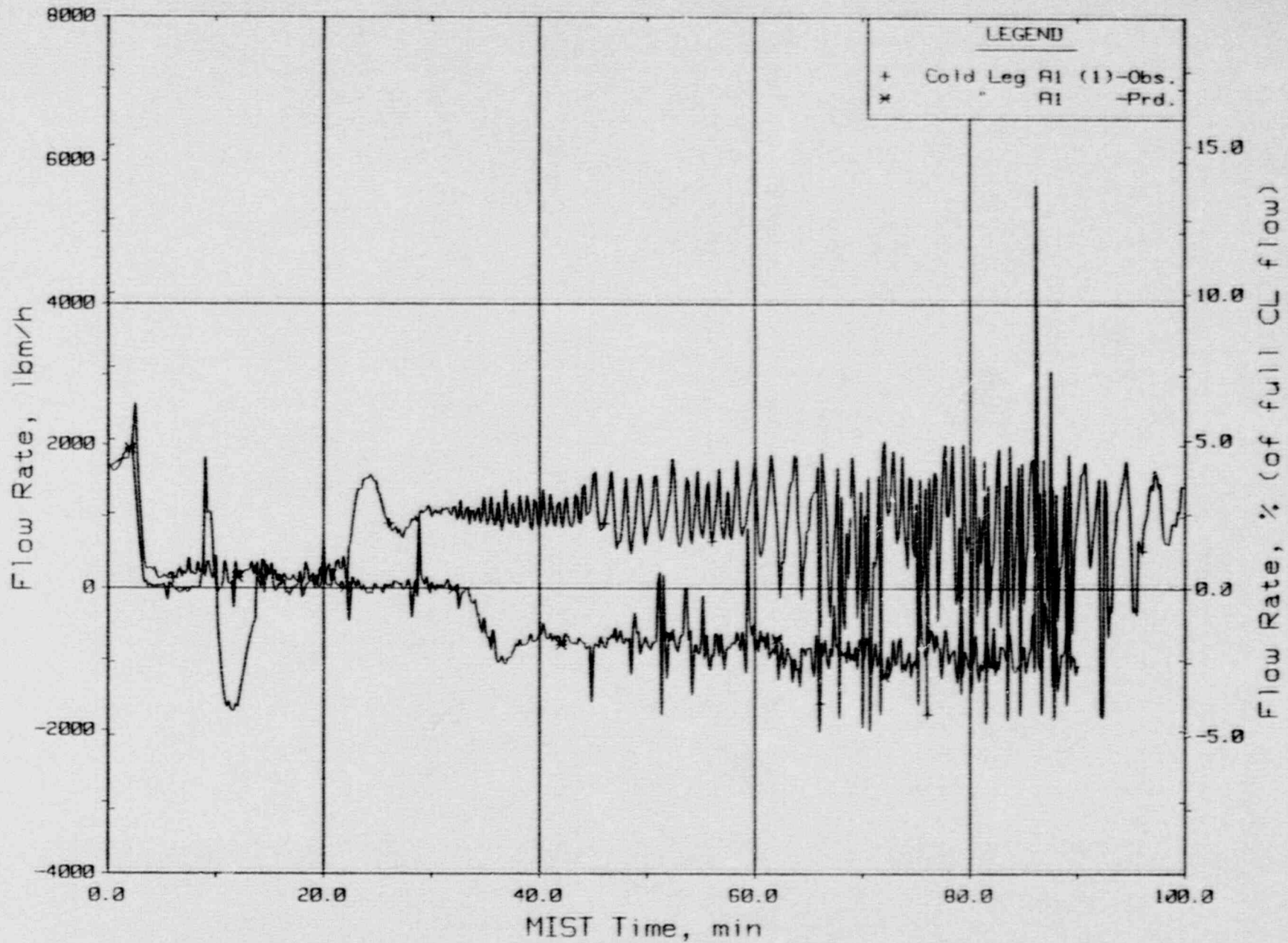


Figure 3.2.19. Loop AI Cold Leg (Venturi) Flow Rate (C1VN20).

10 CM2 Cold Leg Suction Break  
 Test 320302 - Observed Vs. Predicted

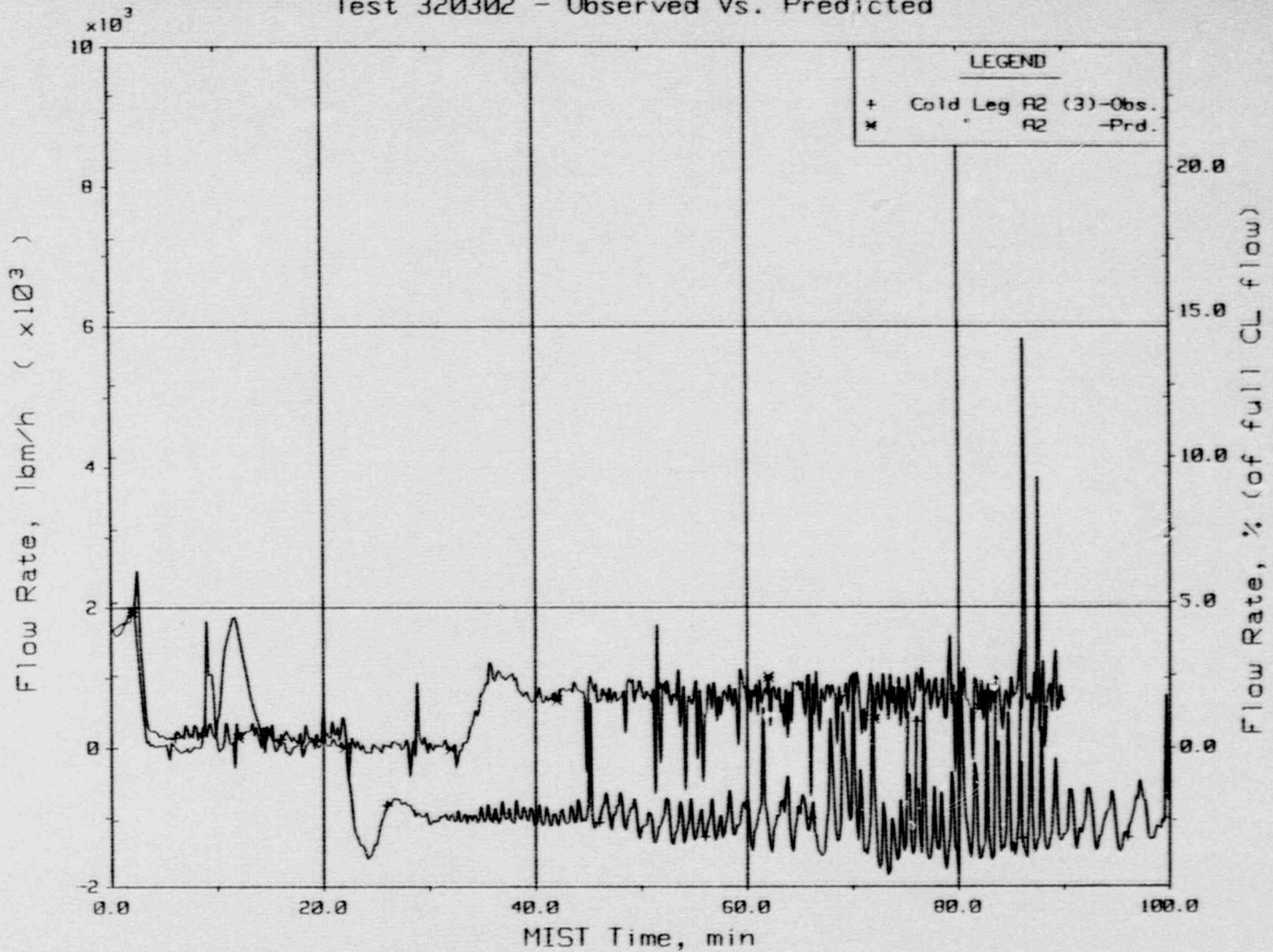


Figure 3.2.20. Loop A2 Cold Leg (Venturi) Flow Rate (C2VN20).

3-67

10 CM2 Cold Leg Suction Break  
 Test 320302 - Observed Vs. Predicted

3-68

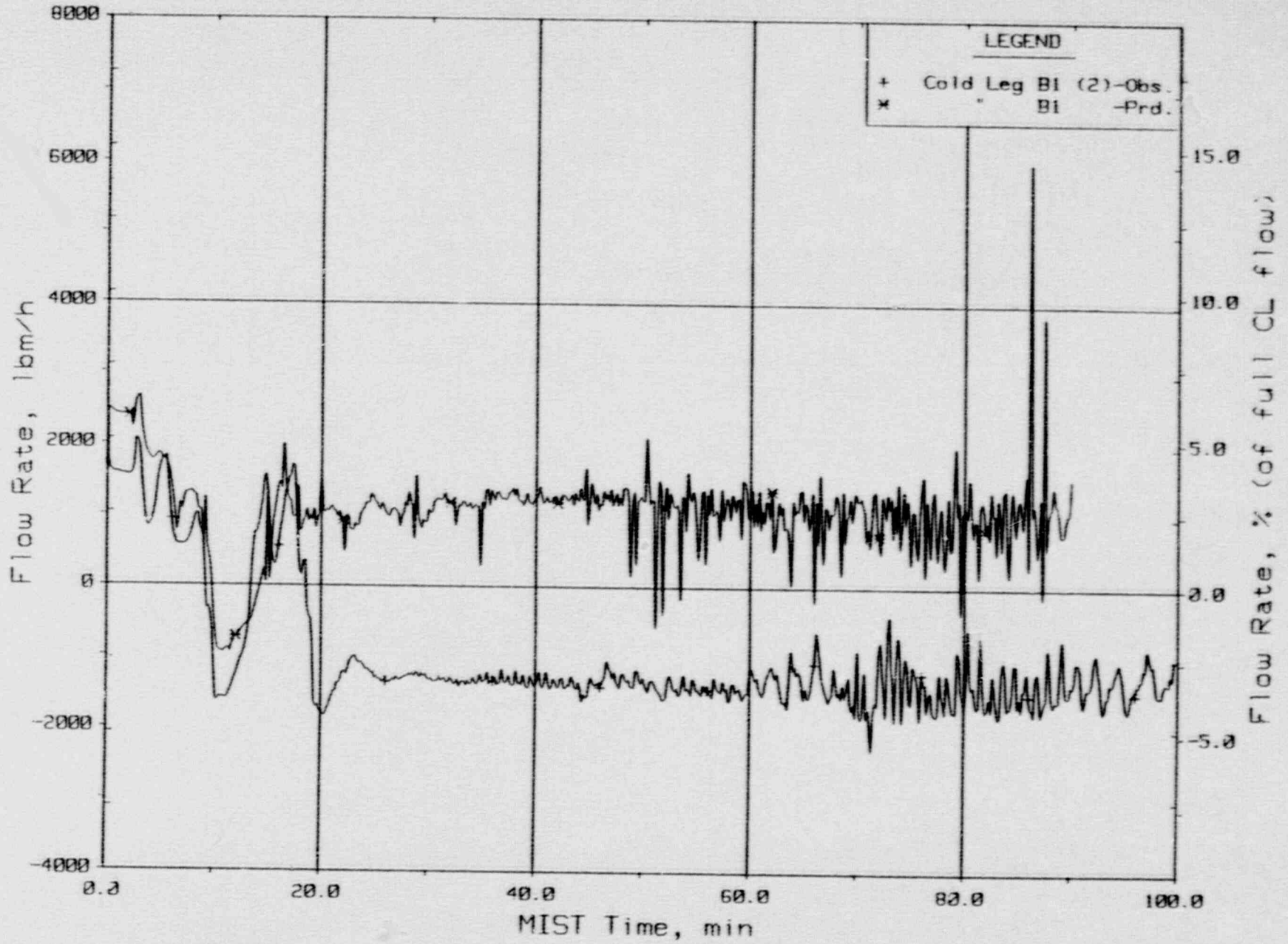


Figure 3.2.21. Loop BI Cold Leg (Venturi) Flow Rate (C1VN20).



10 CM2 Cold Leg Suction Break  
 Test 320302 - Observed Vs. Predicted

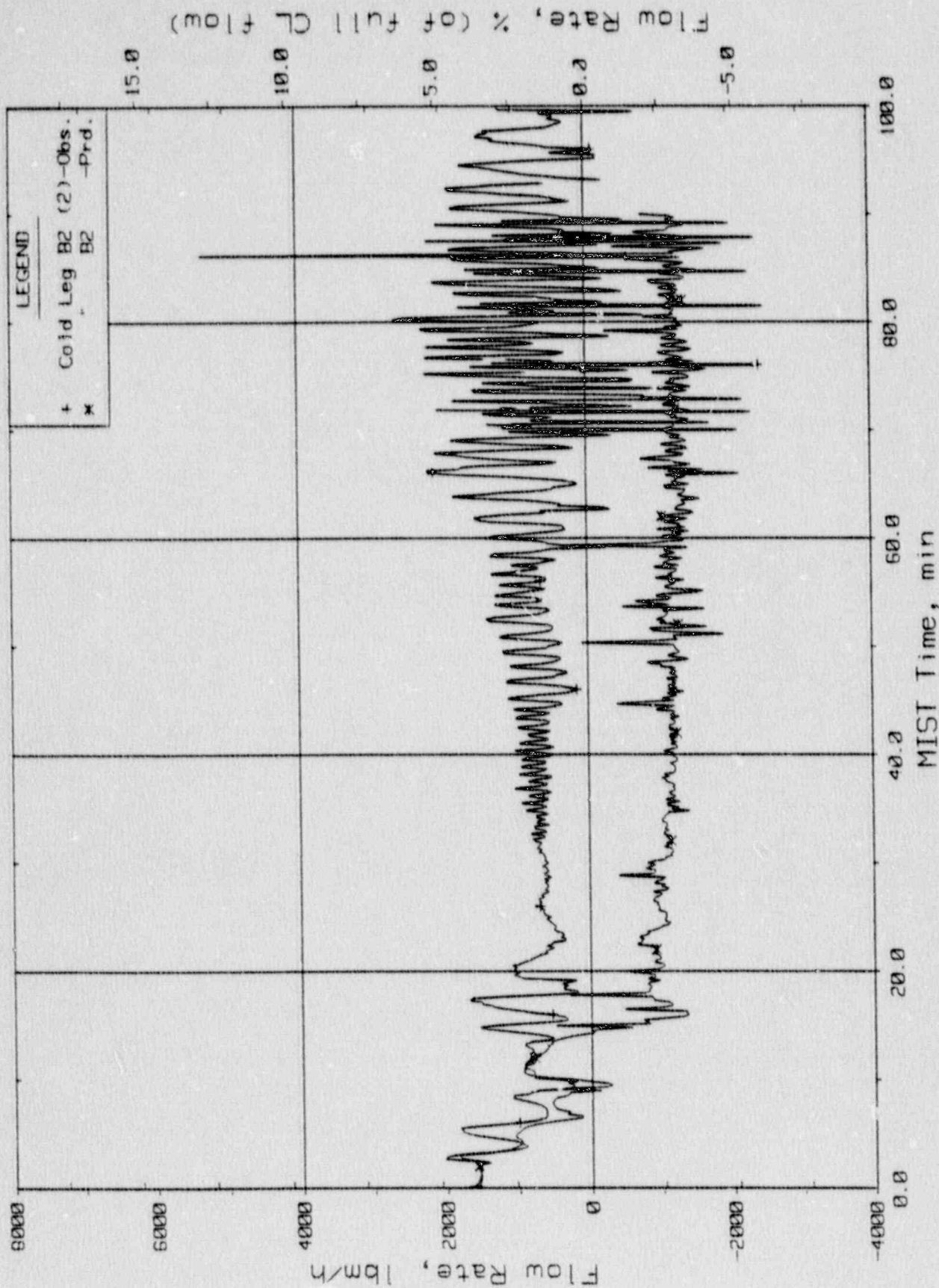


Figure 3.2.22. Loop B2 Cold Leg (Venturi) Flow Rate (C4VN20).

10 CM2 Cold Leg Suction Break  
Test 320302 - Observed Vs. Predicted

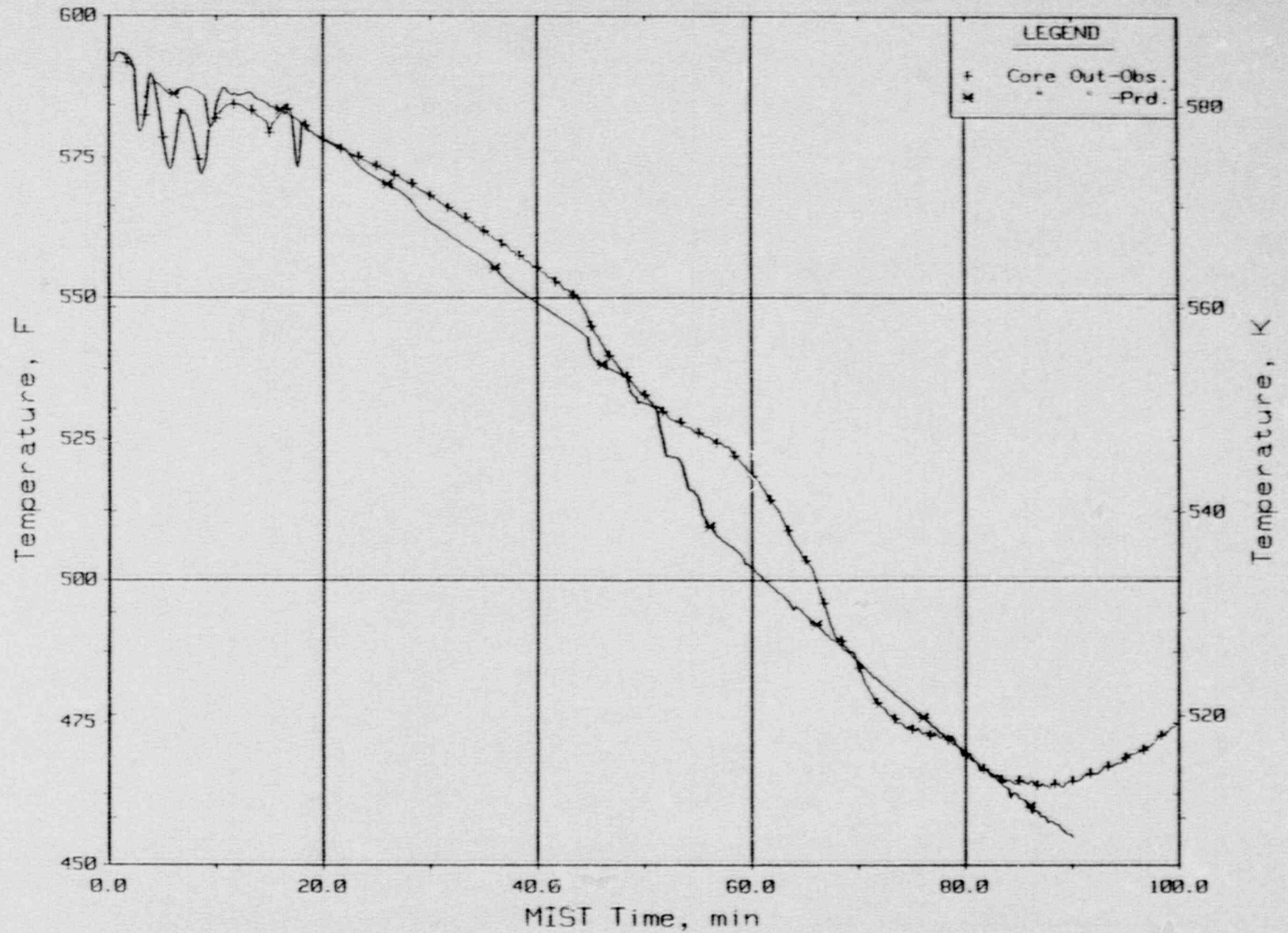


Figure 3.2.23. Core Exit Reactor Vessel Fluid Temperature (RVTC11).

10 CM2 Cold Leg Suction Break  
 Test 320302 - Observed Vs. Predicted

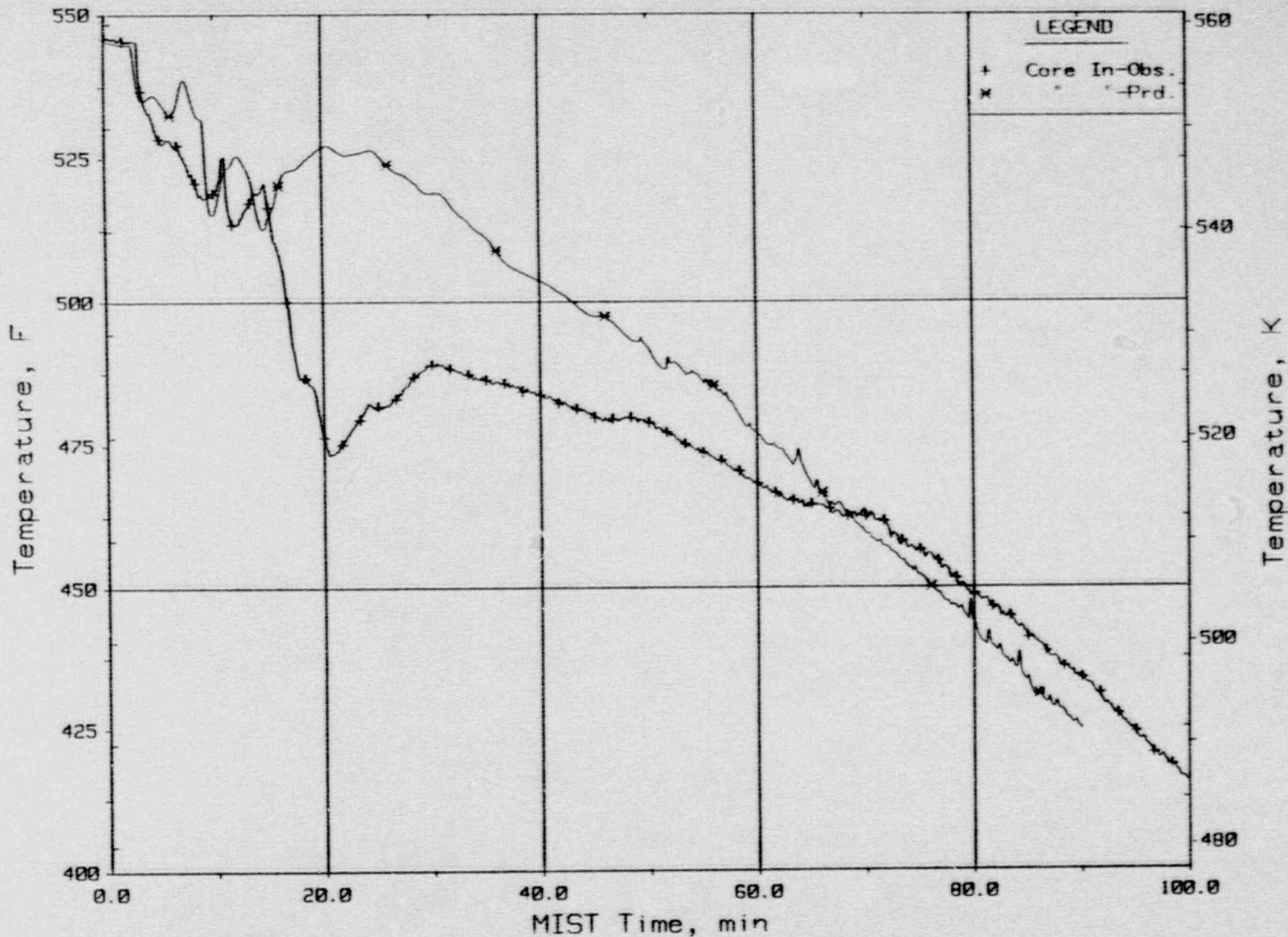


Figure 3.2.24. Core Inlet Reactor Vessel Fluid Temperature (DCRT01).

10 CM2 Cold Leg Suction Break  
 Test 320302 - Observed Vs. Predicted

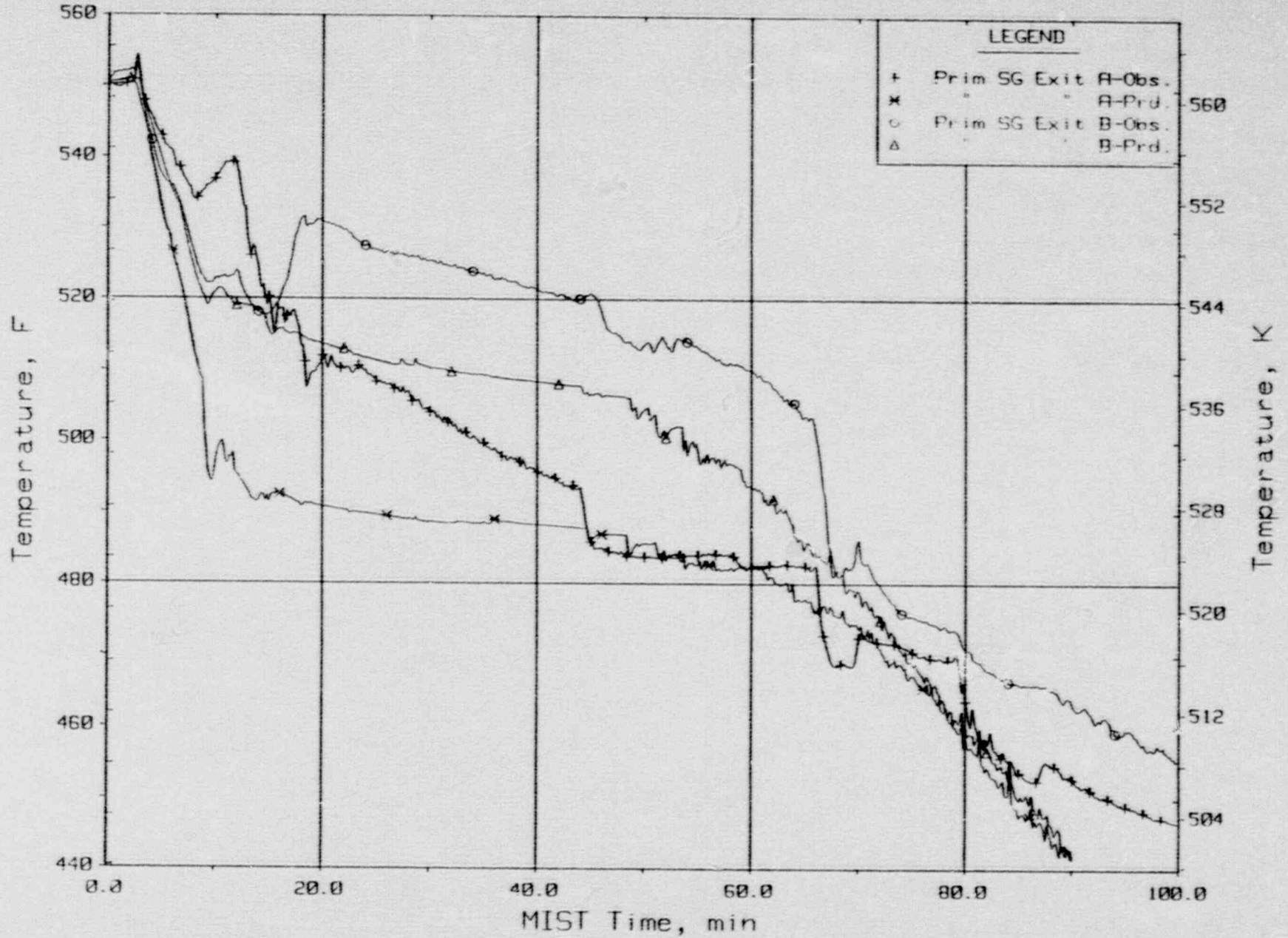
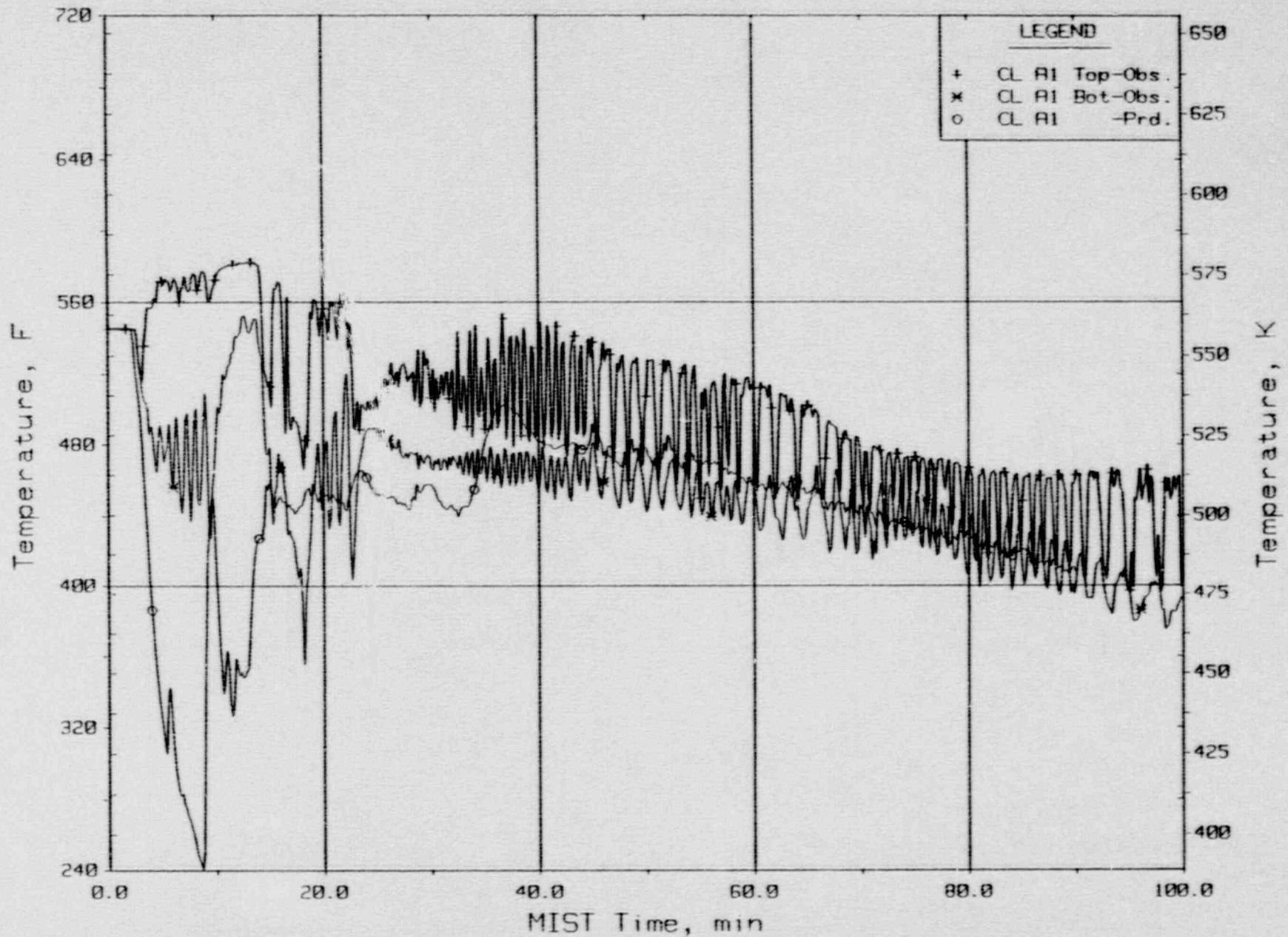


Figure 3.2.25. Loops A/B SG Exit Primary Fluid Temperatures (RTDs).

10 CM2 Cold Leg Suction Break  
 Test 320302 - Observed Vs. Predicted



3-73

Figure 3.2.26. Cold Leg Nozzle Fluid Temperatures, Top/Bot of Rake (21.3ft, CnTC11/14s).

10 CM2 Cold Leg Suction Break  
 Test 320302 - Observed Vs. Predicted

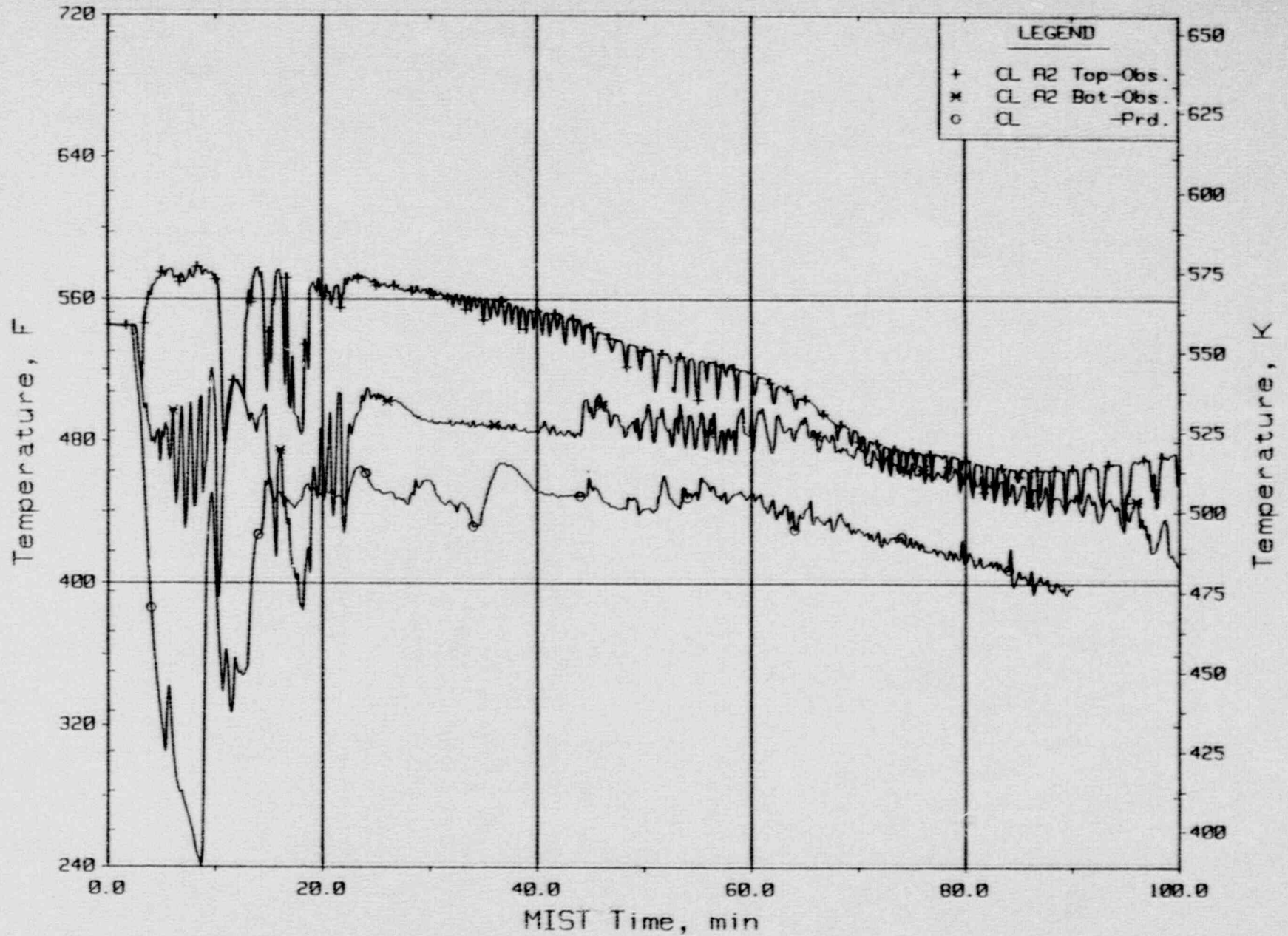


Figure 3.2.27. Cold Leg Nozzle Fluid Temperatures, Top/Bot of Rake (21.3ft, Ccltca2).

10 CM2 Cold Leg Suction Break  
 Test 320302 - Observed Vs. Predicted

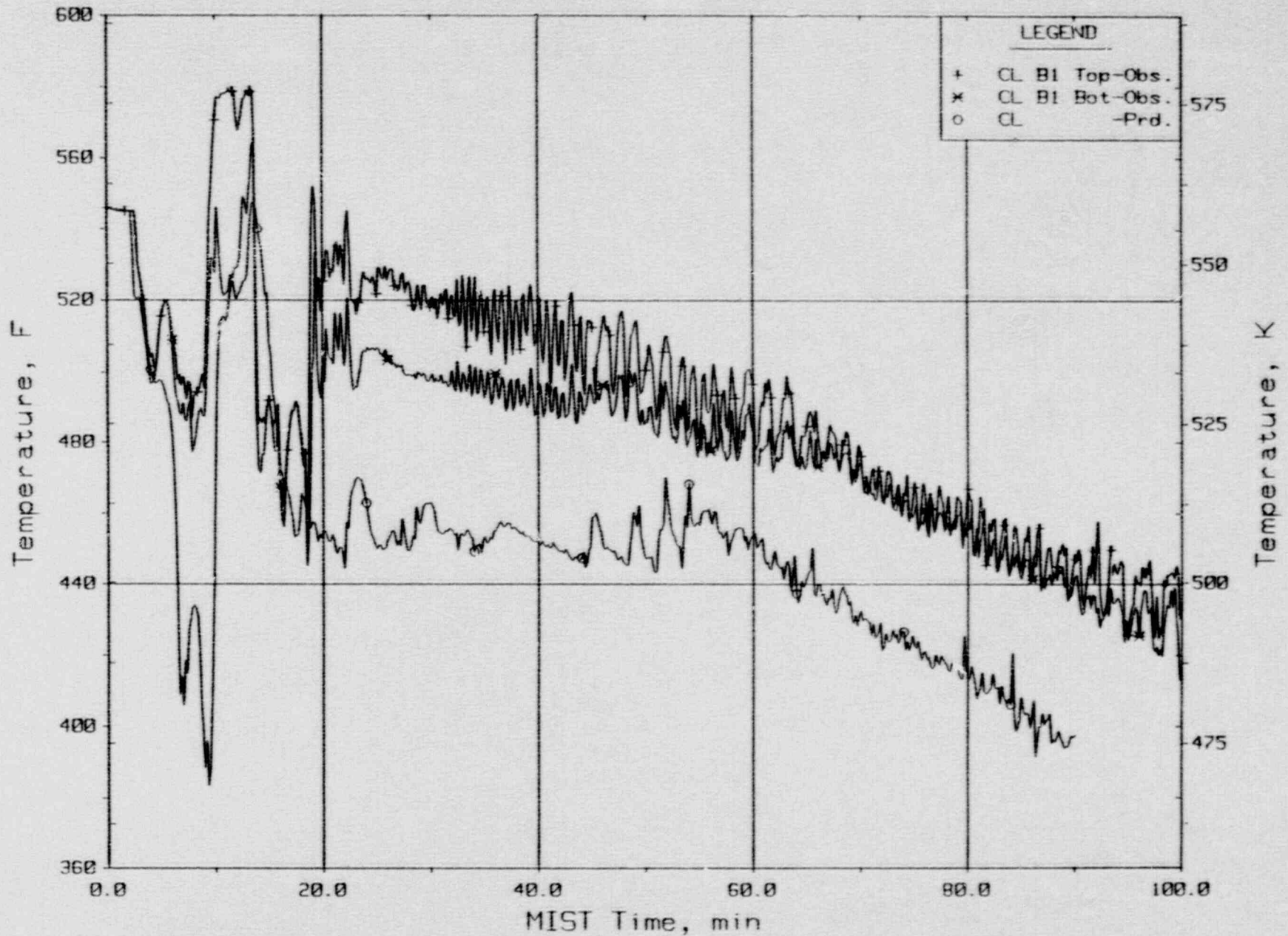


Figure 3.2.28. Cold Leg Nozzle Fluid Temperatures, Top/Bot of Rake (21.3ft, Cc1tcb1).

10 CM2 Cold Leg Suction Break  
 Test 320302 - Observed Vs. Predicted

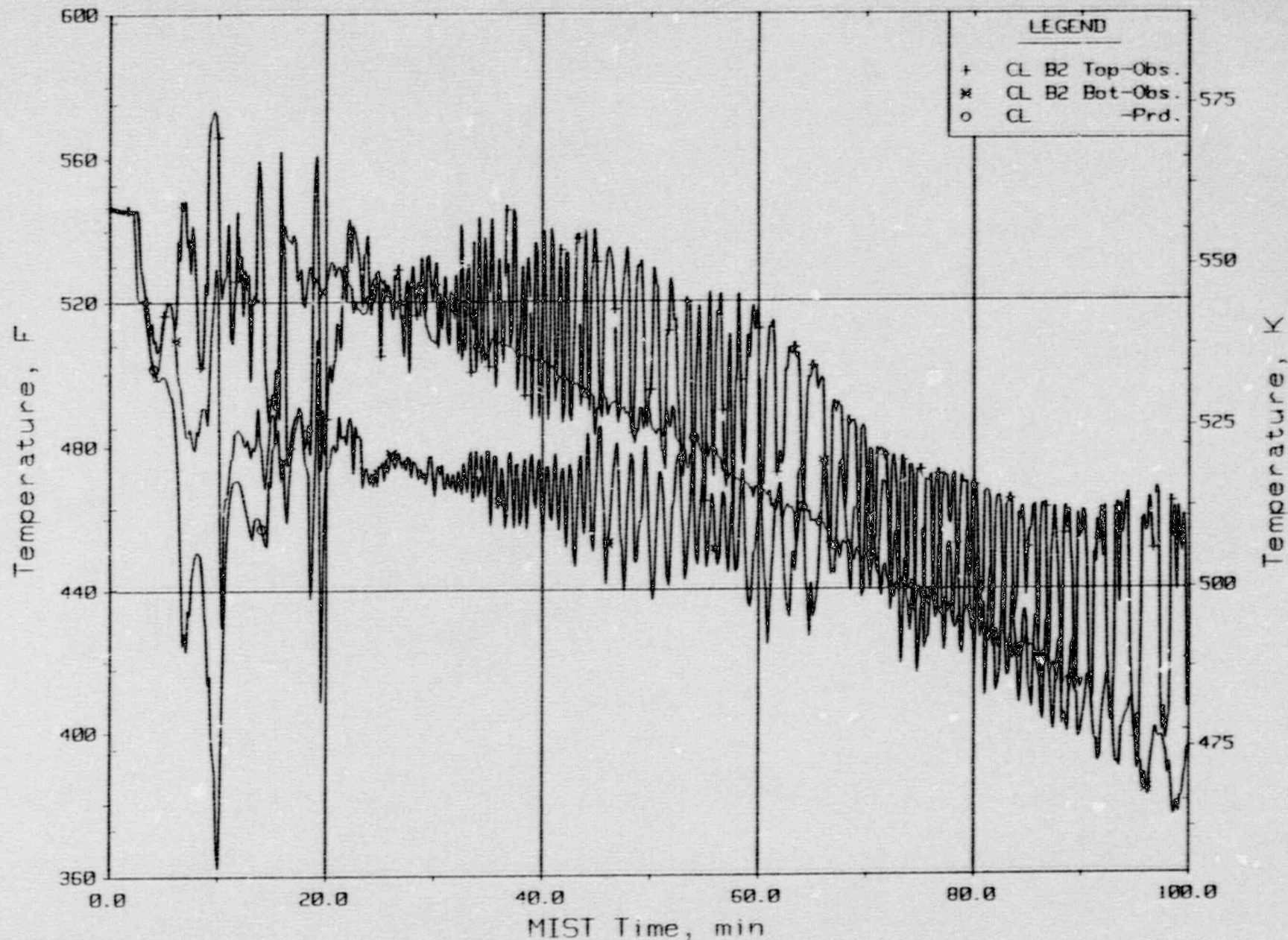


Figure 3.2.29. Cold Leg Nozzle Fluid Temperatures, Top/Bot of Rake (21.3ft, Cc1tcb2).



10 CM2 Cold Leg Suction Break  
 Test 320302 - Observed Vs. Predicted

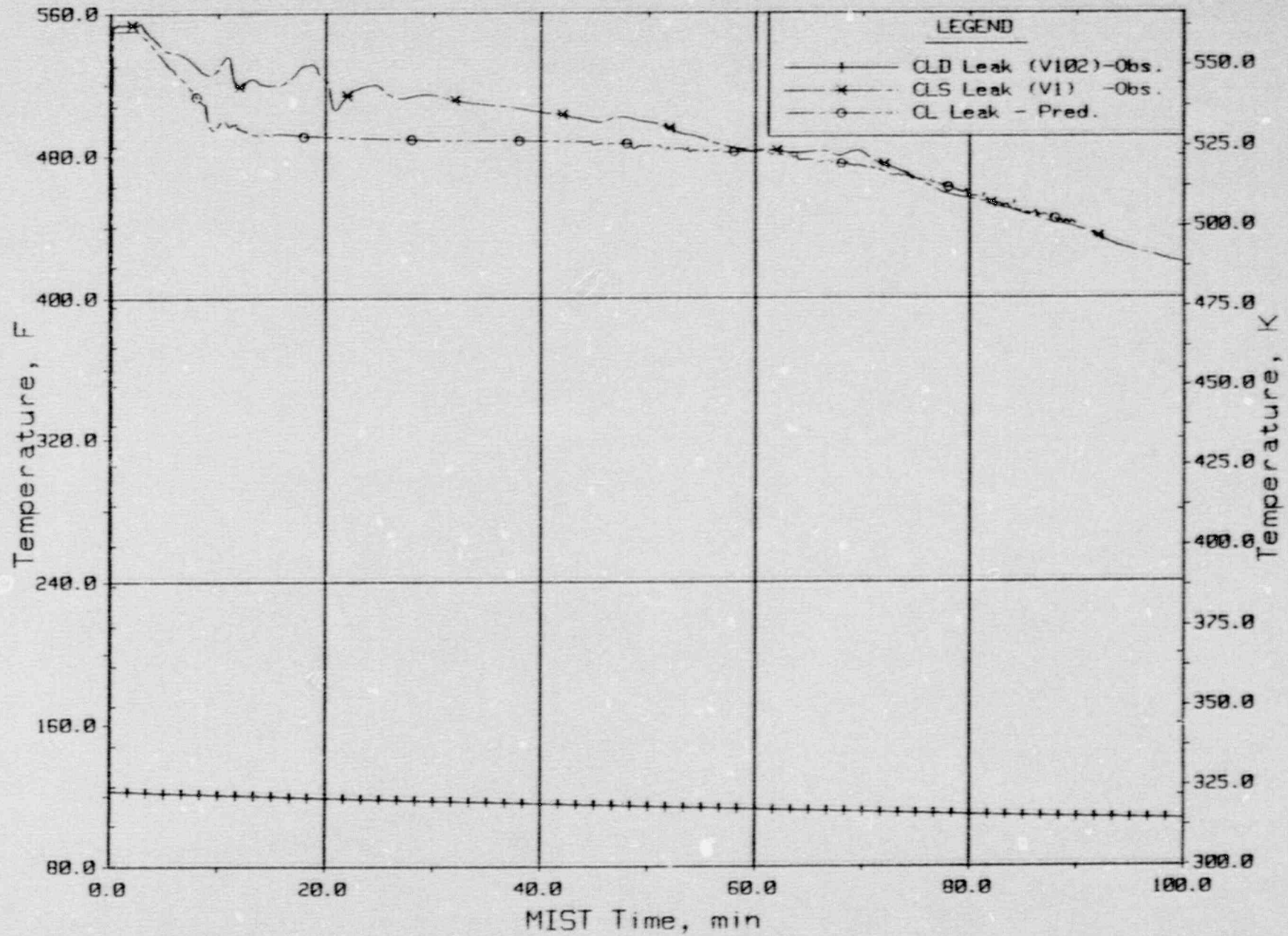


Figure 3.2.30. Single-Phase Discharge Temperatures (VITC01s).

10 CM2 Cold Leg Suction Break  
 Test 320302 - Observed Vs. Predicted

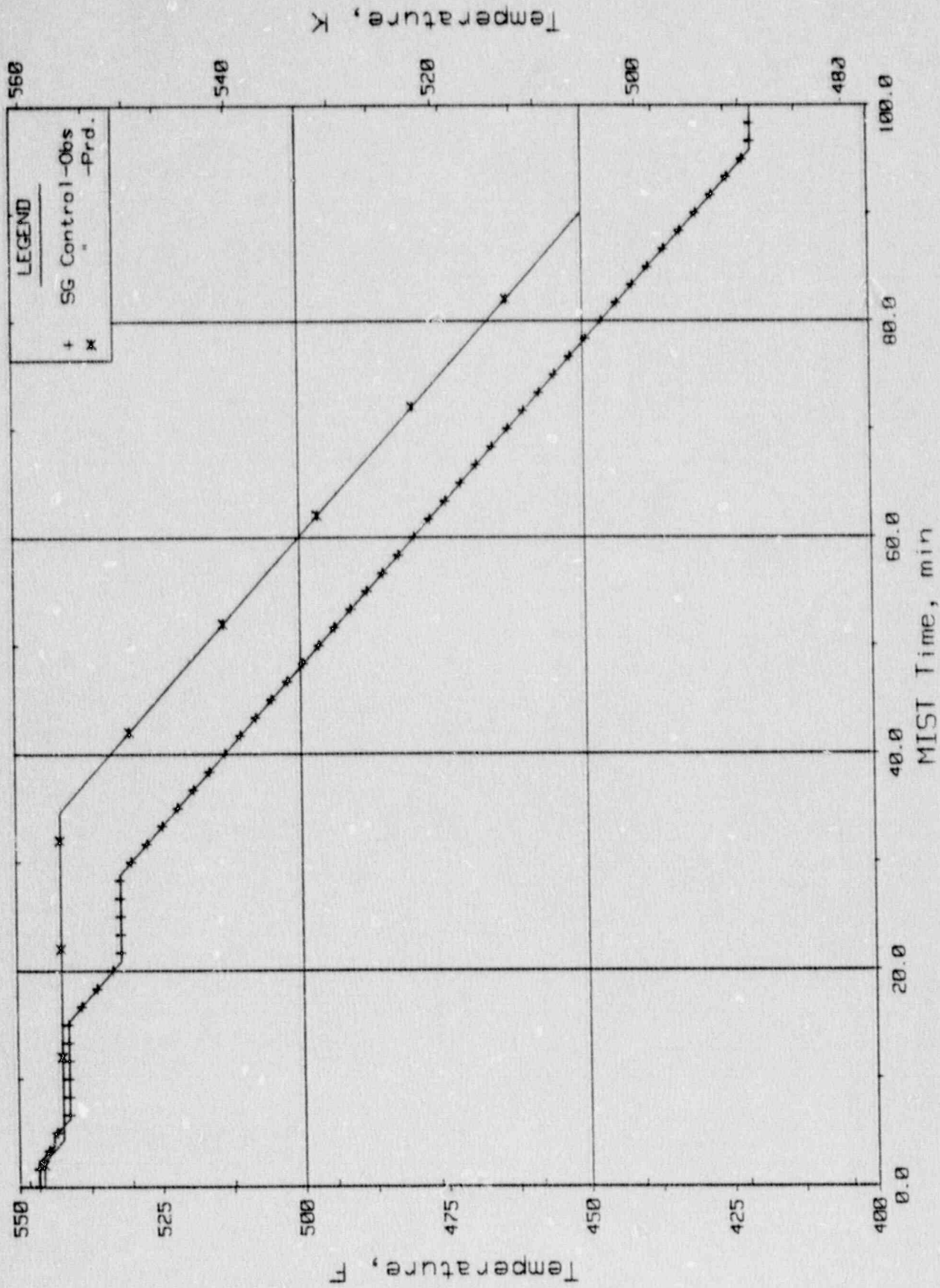


Figure 3.2.31. Steam Generator Secondary Saturation and Control Temperatures.

10 CM2 Cold Leg Suction Break  
 Test 320302 - Observed Vs. Predicted

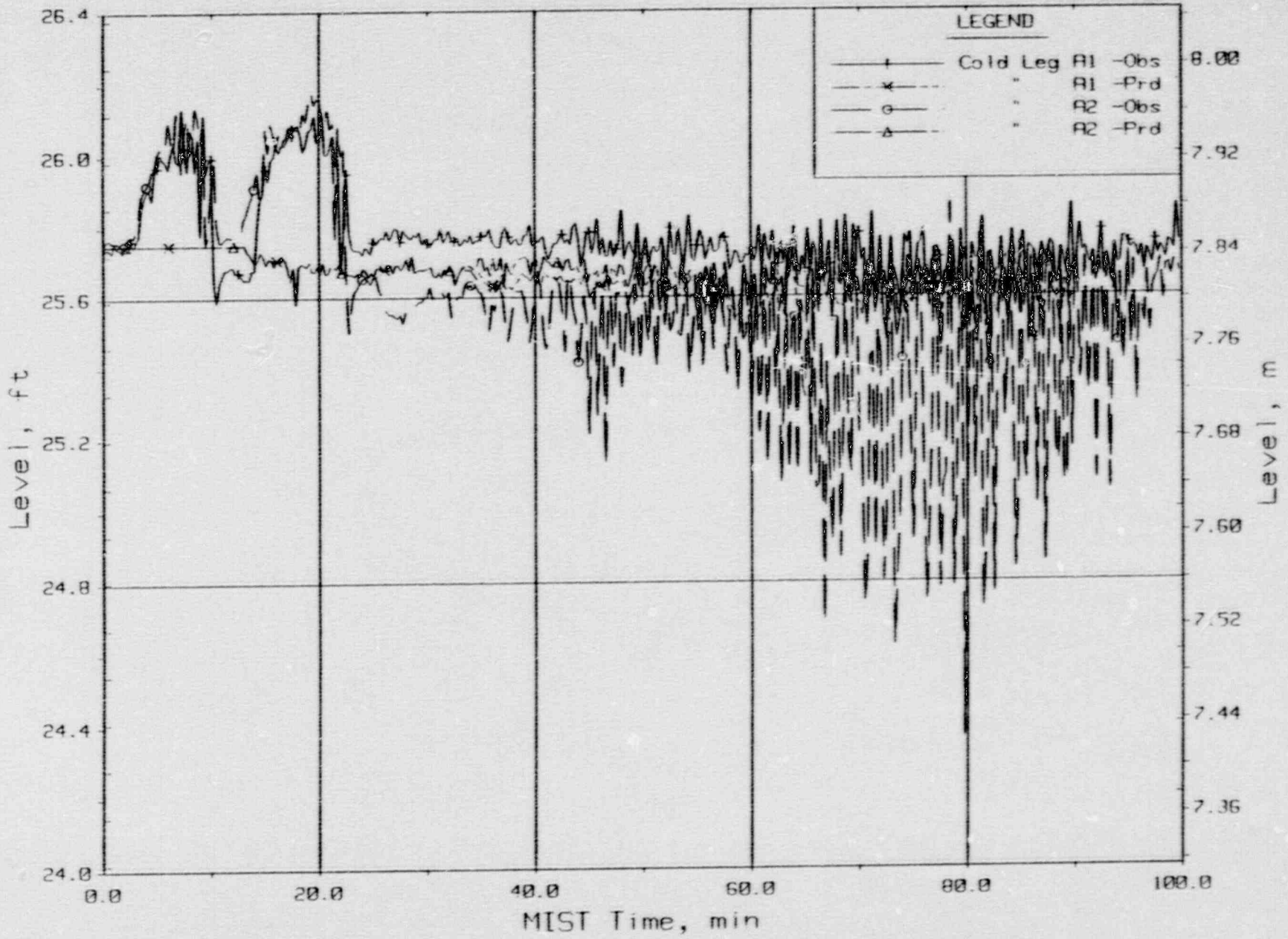


Figure 3.2.32. Cold Leg A Discharge Collapsed Liquid Levels (CnLV23s).

10 CM2 Cold Leg Suction Break  
 Test 320302 - Observed Vs. Predicted

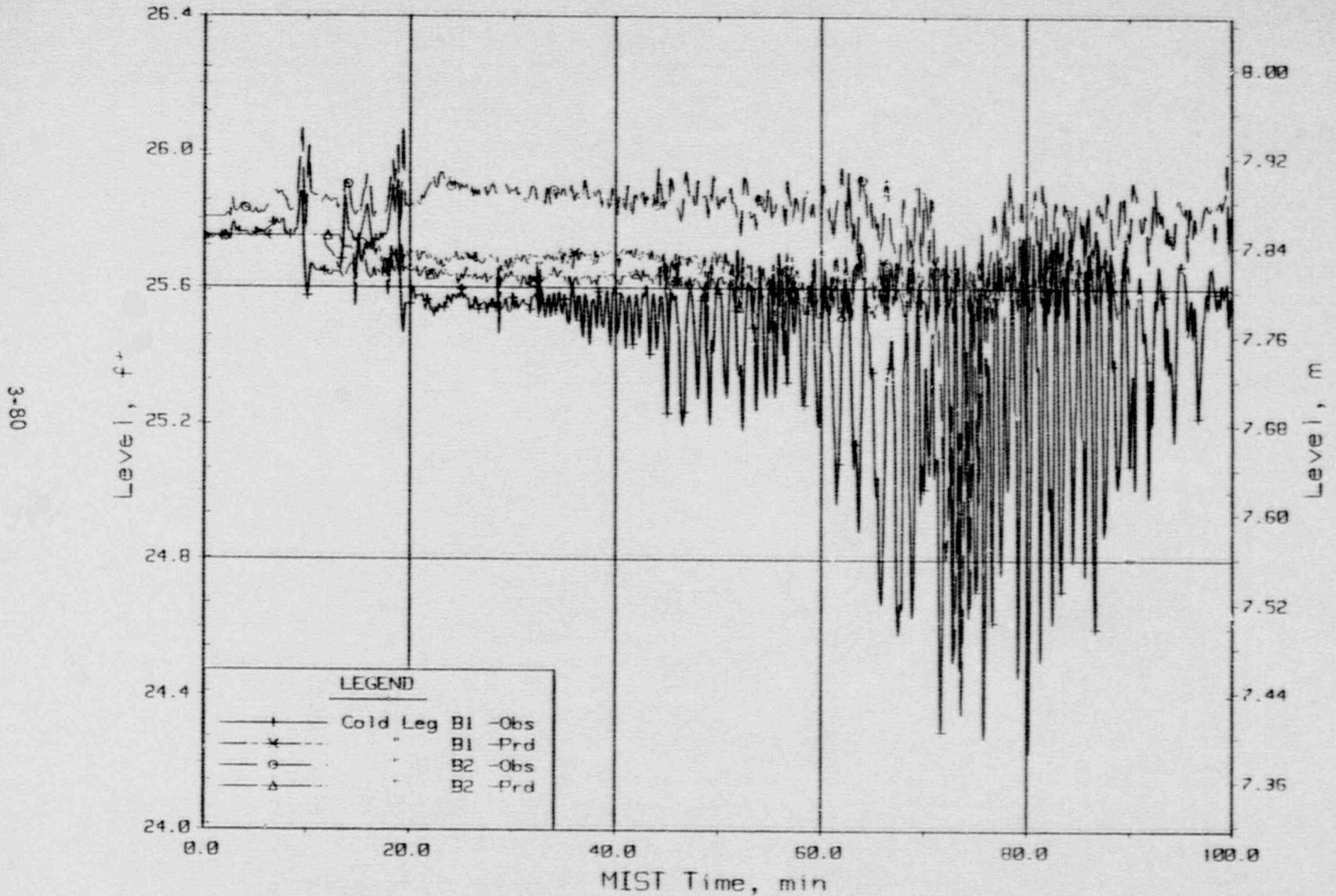


Figure 3.2.33. Cold Leg B Discharge Collapsed Liquid Levels (CnLV23s).

### 3.3. MIST Test 340213 Post-Test Prediction

MIST test 340213 is a scaled one tube steam generator tube rupture (SGTR) at the upper tube support plate in loop B. Since the leak is not large enough to quickly depressurize the system, additional primary cooldown mechanisms were utilized. The additional cooldown mechanisms used for this test were the steam generator secondary cooldown and a controlled PORV-HPI feed and bleed. The controlled feed and bleed opened the PORV when the core exit subcooling reached 75 F and held it open until the subcooling was reduced to 50 F. At 50 F subcooling the PORV was closed. The HPI was throttled to control pressurizer level between 20 and 21 feet. The secondary pressures were reduced at a rate of 100F/hr until the primary pressure reached 950 psia. At that time the broken loop steam generator was isolated and a single loop cooldown with the intact generator was continued. The secondary collapsed levels were initially filled to 20.7 feet and controlled at that value until steam generator isolation. A detailed test write-up is contained in the MIST Group 34 Report.

#### 3.3.1. MIST Test 340213 Base Case Modifications

The RELAP5/MOD2 simulation was performed using the base deck model with several minor changes required to be consistent with test 340213 boundary conditions or operator actions. The changes included the following modifications.

1. The SGTR leak was added and all control variables which integrate the flows or energies were modified accordingly.
2. The original CLPD break was removed.
3. A control variable to calculate core subcooling margin was added.
4. The steam generator secondary depressurization and level control logic was modified.
5. Pressurizer heaters were added with appropriate control logic.
6. The PORV and HPI control logic was modified.
7. The control variables and logic to calculate an unchoked SGTR flow using a Bernoulli formulation and control logic to switch to an unchoked junction was added.

8. Miscellaneous time step and minor edit variable additions or changes were made to aide in interpreting the test simulation.

These changes are documented in detail in the calculational file for this test.

### 3.3.2. MIST Test 340213 Transient Comparisons

The initial conditions for the RELAP calculation are consistent with the test conditions just before leak opening at time zero. Table 3.3.1. contains a listing of test and RELAP calculated steady-state initial conditions, while the transient comparison plots are shown in Figures 3.3.1. through 3.3.35. The core power, secondary pressure, secondary collapsed level, hot leg subcooling margin, and pressurizer level were defined for the steady-state initialization. The remainder of the parameters were determined from the spacial heat transfer and thermal-hydraulic behavior of the facility. Table 3.3.2 summarizes the transient progression through a tabular sequence of events list.

After the SGTR leak was actuated the primary side began a slow depressurization. The loss of primary inventory drained the pressurizer level below 21 feet thus initiating HPI to maintain a constant level. Initiation of the HPI and earlier shut-off of AFW started a slight repressurization in the prediction. The facility also over-filled the secondary level providing additional cooling which allowed the observed transient pressure to continue its initial decline. Between 5 and 6 minutes, however, both the predicted and observed core exit subcooling reached 75 F. Opening of the PORV quickly depressurized the primary until a 32 F core exit subcooling was achieved. The remainder of the cycles isolated the PORV at a value of 50 F. At 5.5 minutes the observed leak flow decreased by approximately one half. Apparently a piece of foreign material became lodged in the leak orifice. The predicted leak flow area was decreased correspondingly, although the leak flow remained high by approximately twenty percent.

Following the first PORV cycle the predicted and observed repressurization rates differed slightly due to HPI and AFW flow differences. The observed HPI had actuated prior to the pressurizer level reaching 21 feet resulting in an HPI shut-off. The HPI remained off between 6 and 11 minutes to allow the level to drop below 21 feet. The AFW had also terminated during this period

to allow the secondary inventory to boil-off following the over-fill. The combination of the slightly reduced heat transfer and no HPI slowed the observed repressurization rate. Differences between the HPI and AFW flows generally accounted for most all of the small repressurization rate changes following the PORV cycles.

At approximately 30 minutes into the test the reactor vessel upper head fluid reached saturated conditions. The depressurizations during the PORV cycles flashed the liquid in this region causing the trapped bubble to grow in size. A PORV cycle caused the prediction to form a bubble after 29 minutes, however, the steam was recondensed during the subsequent primary repressurization. This pattern was repeated for the remainder of the transient.

The primary pressure dropped below 950 psia triggering isolation of the affected steam generator in RELAP and the facility at 58.5 and 69.5 minutes respectively. The isolation times were shifted by the offset in the PORV cycles. Following secondary side isolation the level and pressure in both cases increased from the primary-to-secondary leak flow. The predicted rate of level increase was higher due to a slightly larger leak flow rate.

Several notes on the comparison plots are in order for this test. The hot legs and cold legs remained liquid full and subcooled through-out the first 100 minutes of this test. The data indicated decreases in the level, however, the levels registered above the top of the U-bend piping. The decline simply represented the reduction of the absolute pressure error multiplicative factor which was incorrectly included in the preliminary data. It should also be noted that several of the prediction plots were shown only to 75 minutes. The plot file from 75 to 98.5 minutes was inadvertently erased. The calculated information during that period was lost for the secondary, cold leg, and downcomer flow rates.

Table 3.3.1. MIST Test 340213 Calculated and Measured Initial Steady-State Conditions

Parameter	Data	RELAP5
Primary Pressure*, (psia)	2154.	2150.
SG A Secondary Pressure*, (psia)	1012.	1010.
SG B Secondary Pressure*, (psia)	1011.	1010.
SG A Secondary Collapsed Level*, (ft)	5.10	5.03
SG B Secondary Collapsed Level*, (ft)	5.50	5.03
Hot Leg Subcooling Margin, (F)	52.9	52.9
Pressurizer Collapsed Level*, (ft)	23.15	23.00
Core Power into the Fluid*, (Btu/s)	119.5	119.5
Primary Side Mass Inventory	972.0	970.0
SG A Primary Exit Temperature, (F)	545.2	551.0
SG B Primary Exit Temperature, (F)	545.2	551.0
Core Exit Temperature, (F)	593.5	592.9
Core Total Mass Flow Rate, (lbm/s)	1.87	1.86

\*Denotes specified condition.

Table 3.3.2. MIST Test 340213 Sequence of Events Comparisons

Event	Approximate Test Time (Min)	
	RELAP	Data
Scaled 1 Tube High SGTR Leak Opened; Initiated Core Power Ramp, HPI, RVVV Automatic Control, SG Secondary Refill and Depressurization	0.0	0.0
First PORV Cycle Began	5.5	5.5
SG B Secondary Level to 20.7 Feet	4.7	4.2
SG A Secondary Level to 20.7 Feet	4.7	5.2
SGTR Leak Partially Plugged	5.5	5.5



Table 3.3.2. MIST Test 340213 Sequence of Events Comparisons (Cont'd)

Event	Approximate Test Time (Min)	
	RELAP	Data
Reactor Vessel Upper Head Voiding Began	29.0	30.0
Primary Pressure Below 950 psia, Isolate SG B Secondary Side	58.5	69.5
Calculations Terminated	98.5	--

3.3.3. MIST Test 340213 Post-Test Prediction

The prediction of the scaled one tube SGTR case with affected steam generator isolation and single loop cooldown was very reasonable. The overall system cooldown rates generally followed the observed system behavior. Since the predicted SGTR leak flow was high, more HPI flow was required to maintain the pressurizer liquid level at its specified limit. The additional leak flow kept the reactor vessel upper head fluid slightly cooler, thereby minimizing the amount of flashing which occurred during the PORV cycles.

Single Tube High Elevation SGTR  
 Test 340213 - Observed Vs. Predicted

3-86

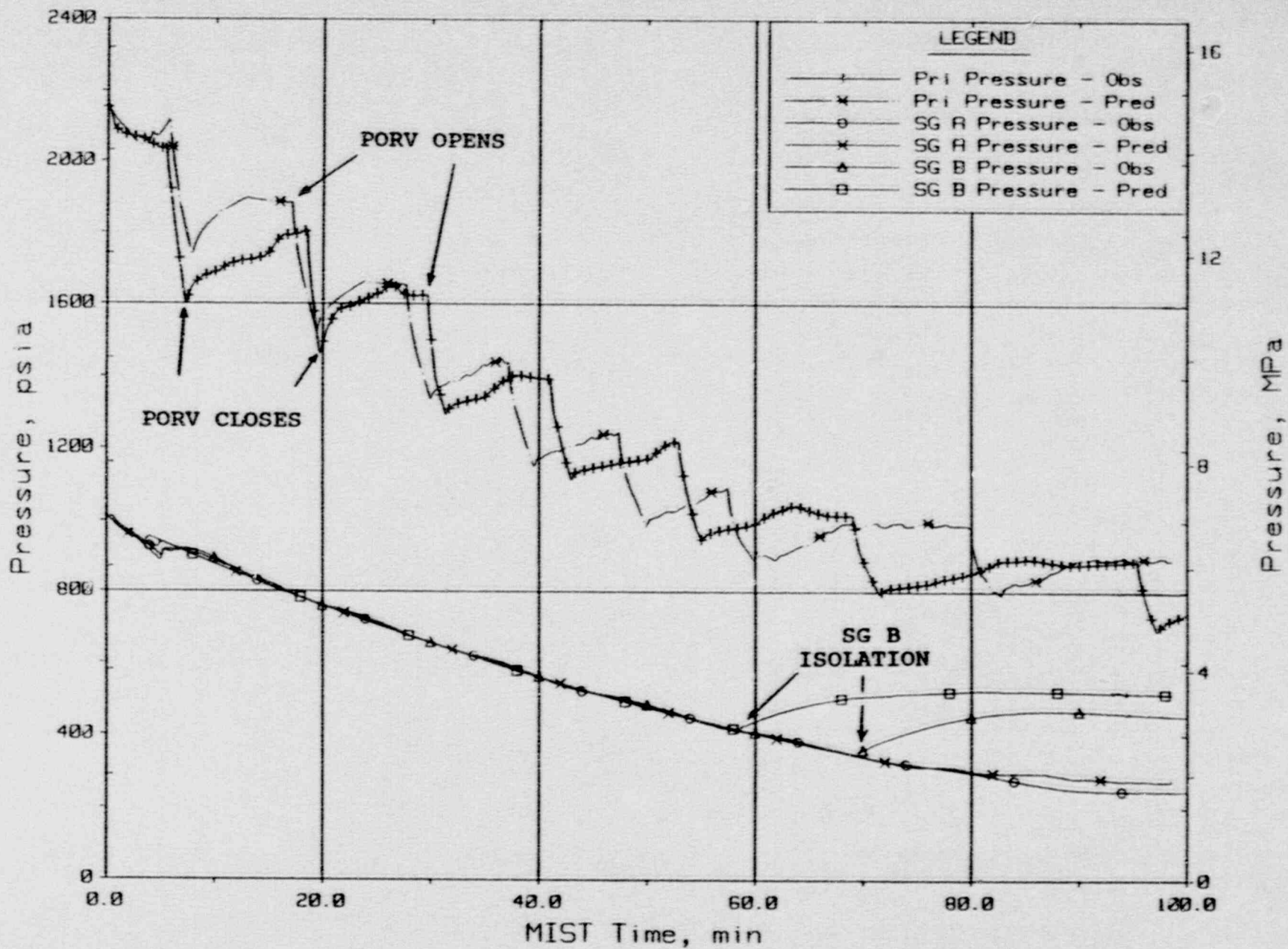


Figure 3.3.1. System Pressures.

Single Tube High Elevation SGTR  
 Test 340213 - Observed Vs. Predicted

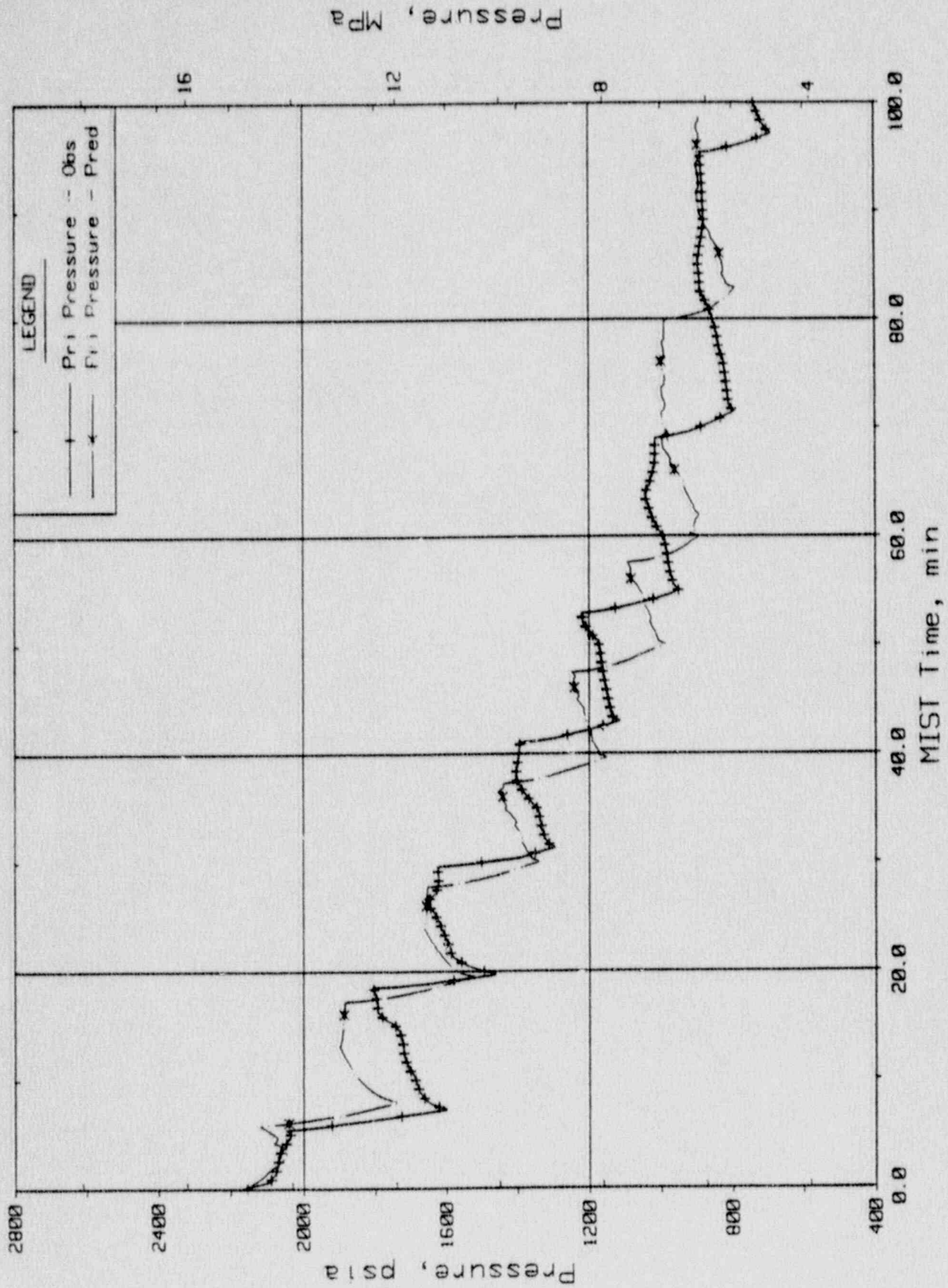
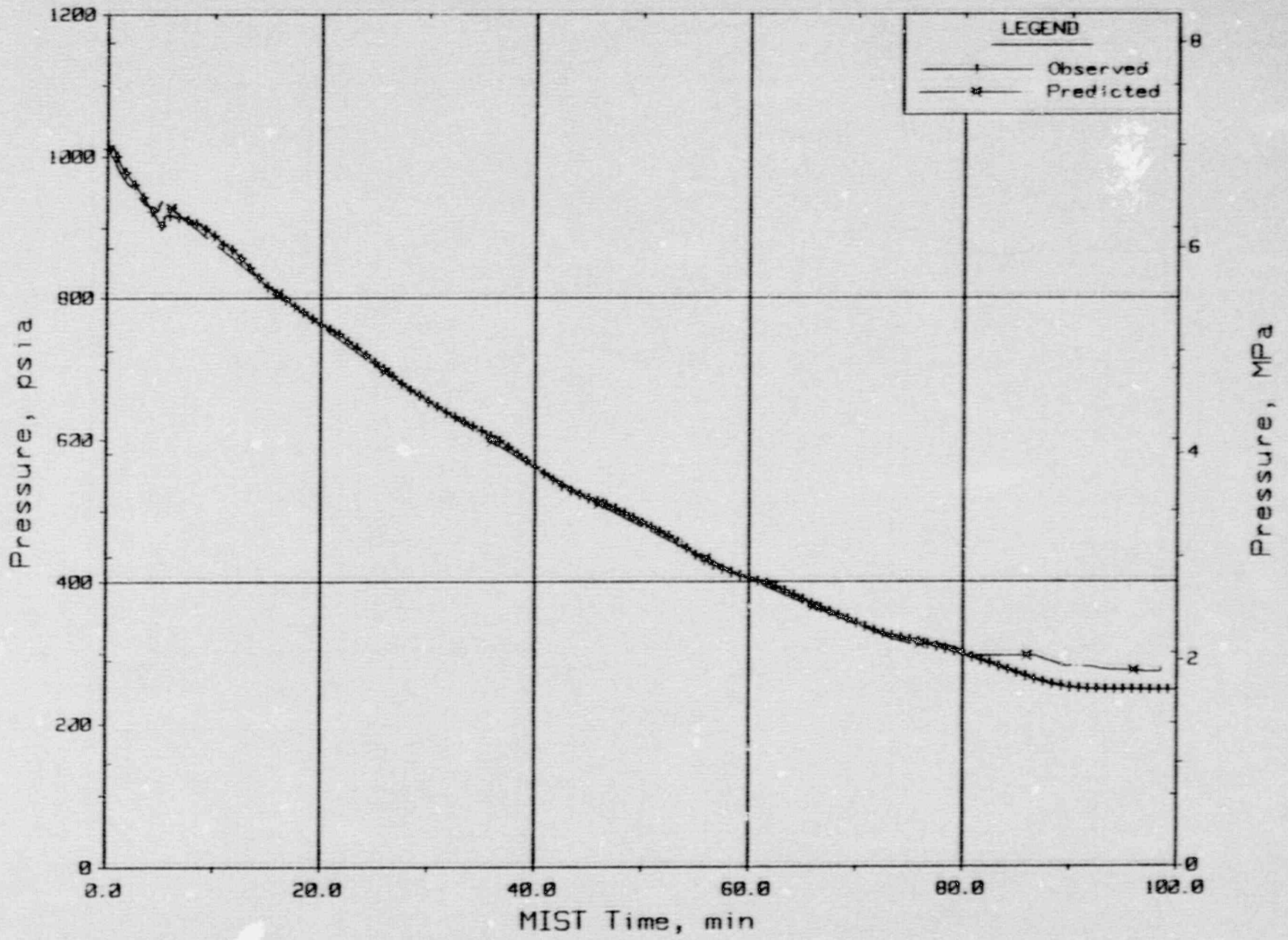


Figure 3.3.2. Primary Pressure.

Single Tube High Elevation SGTR  
Test 340213 - Observed Vs. Predicted



88-3

Figure 3.3.3. Steam Generator A Secondary Pressure.

Single Tube High Elevation SGTR  
 Test 340213 - Observed Vs. Predicted

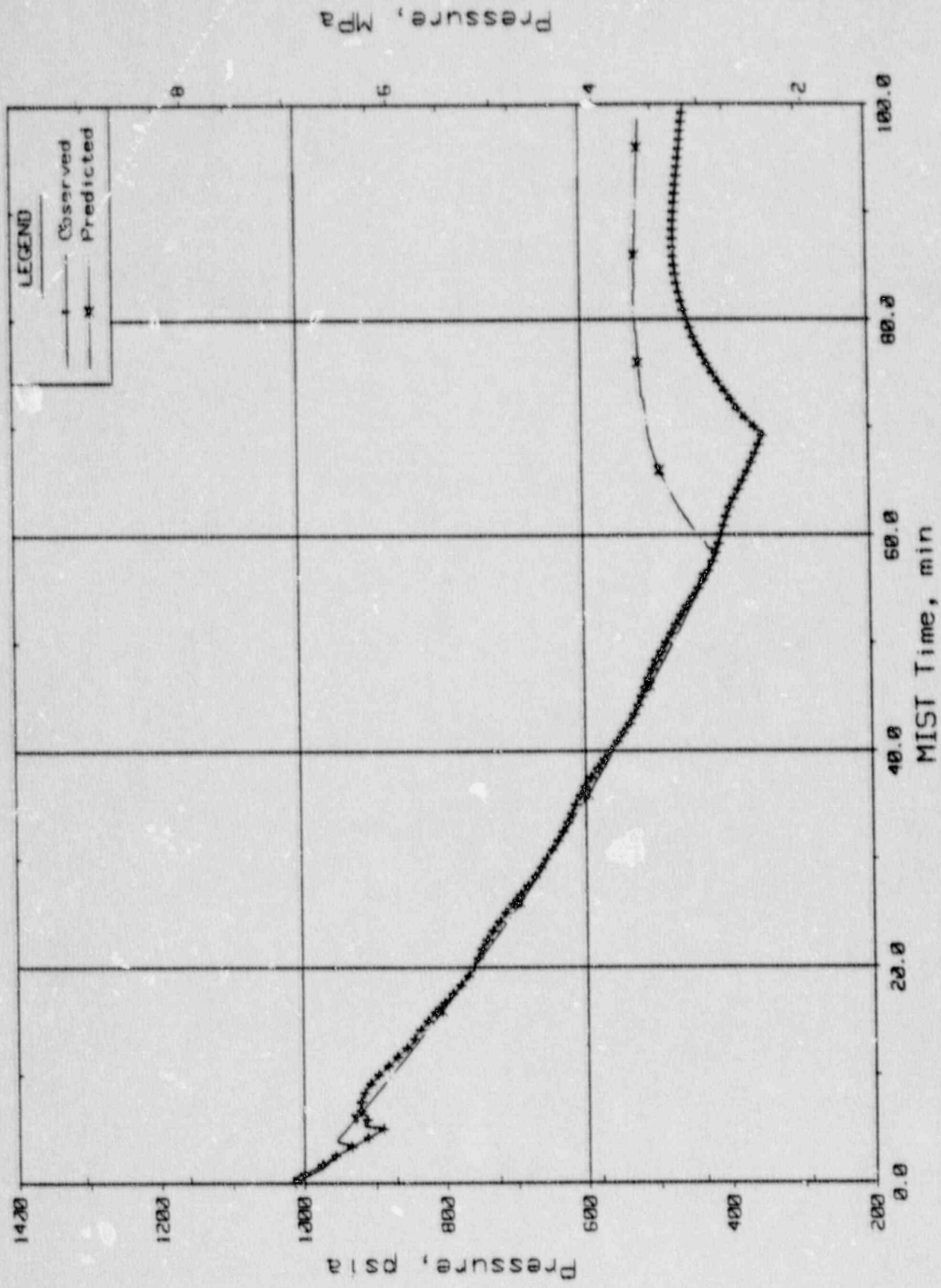


Figure 3.3.4. Steam Generator B Secondary Pressure.

Cs2gp01

Single Tube High Elevation SGTR  
 Test 340213 - Observed Vs. Predicted

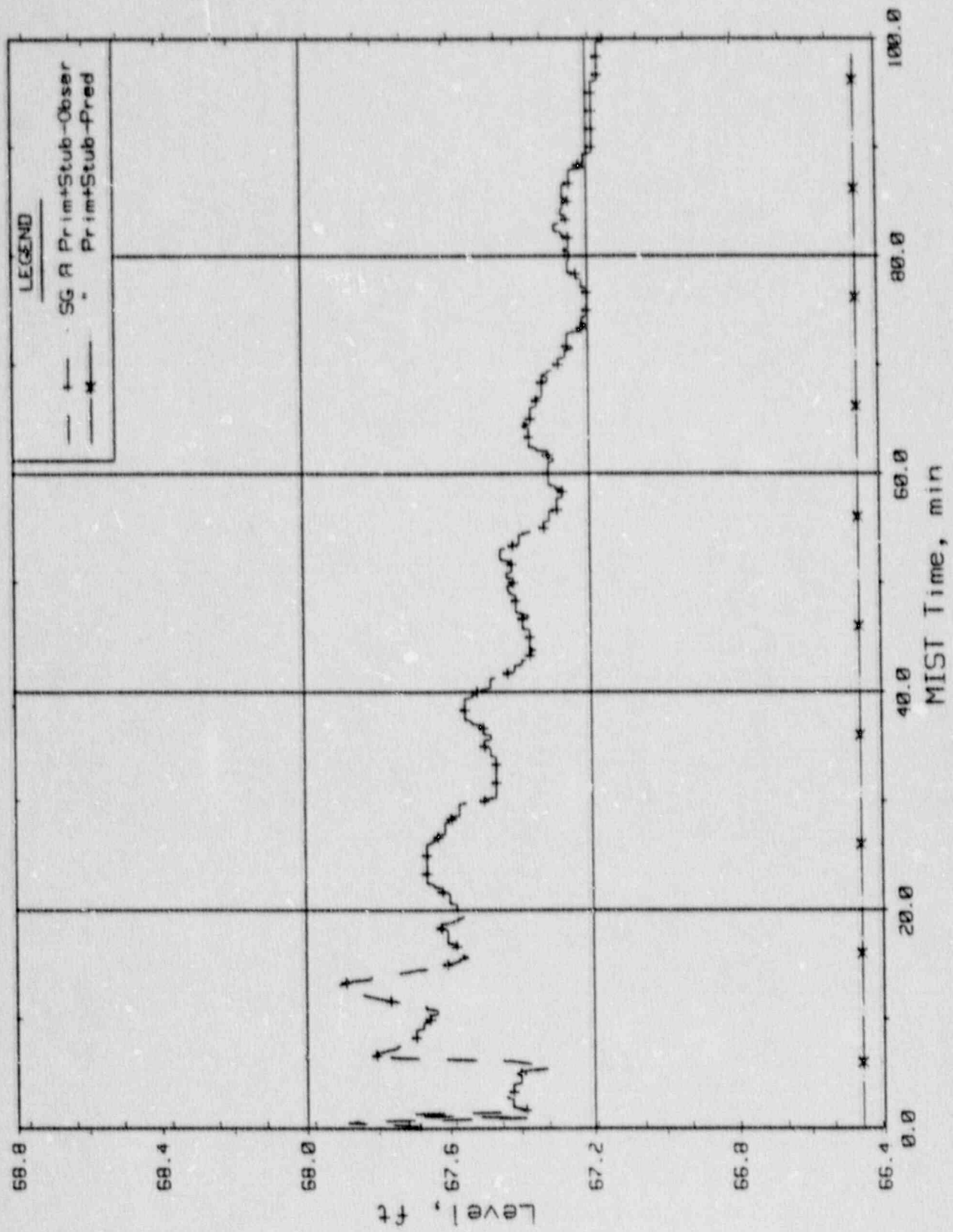


Figure 3.3.5. Steam Generator A Primary + Stub Level.

Czsgpl

Single Tube High Elevation SGTR  
 Test 340213 - Observed Vs. Predicted

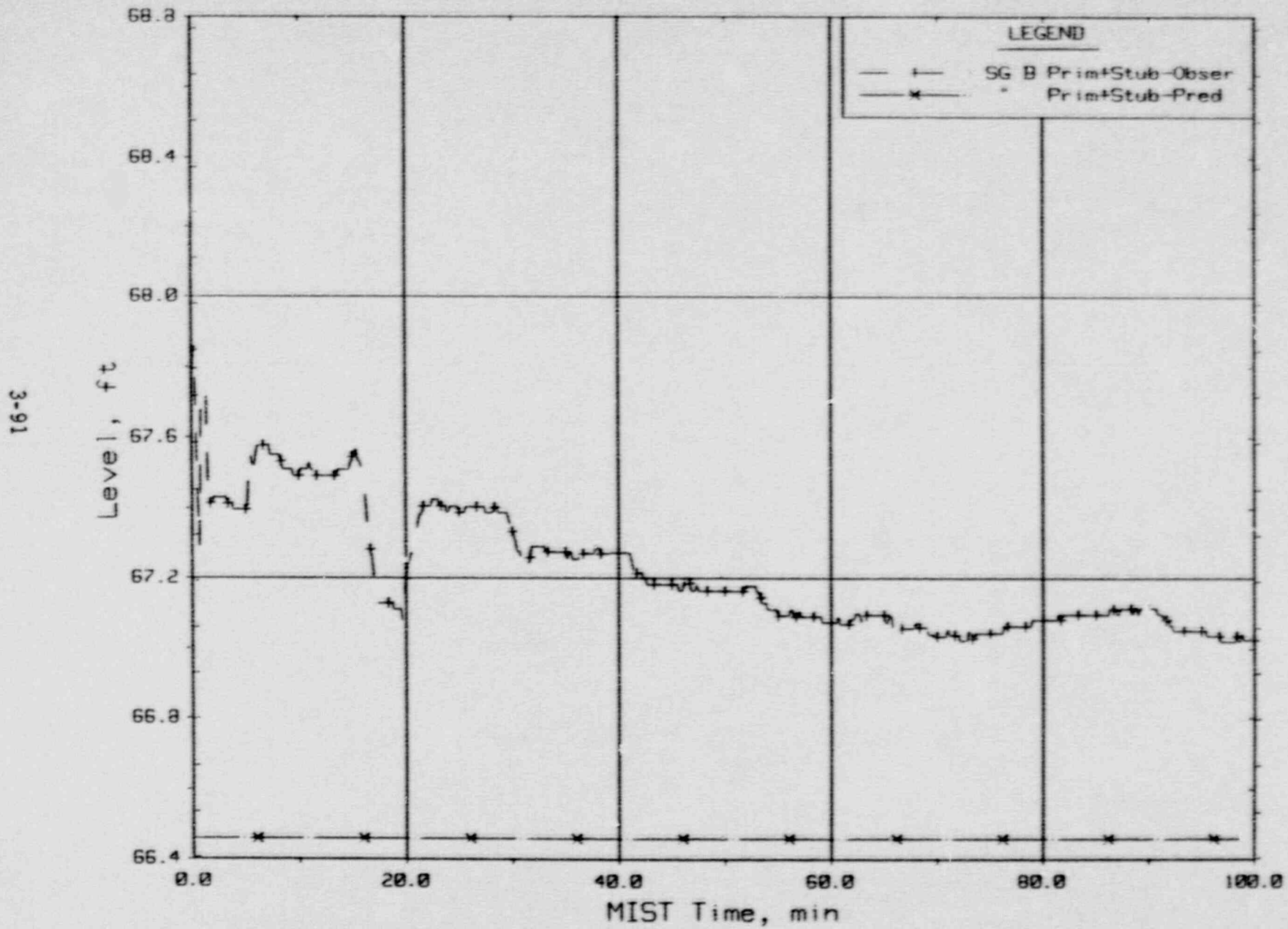


Figure 3.3.6. Steam Generator B Primary + Stub Level.

Single Tube High Elevation SGTR  
 Test 340213 - Observed Vs. Predicted

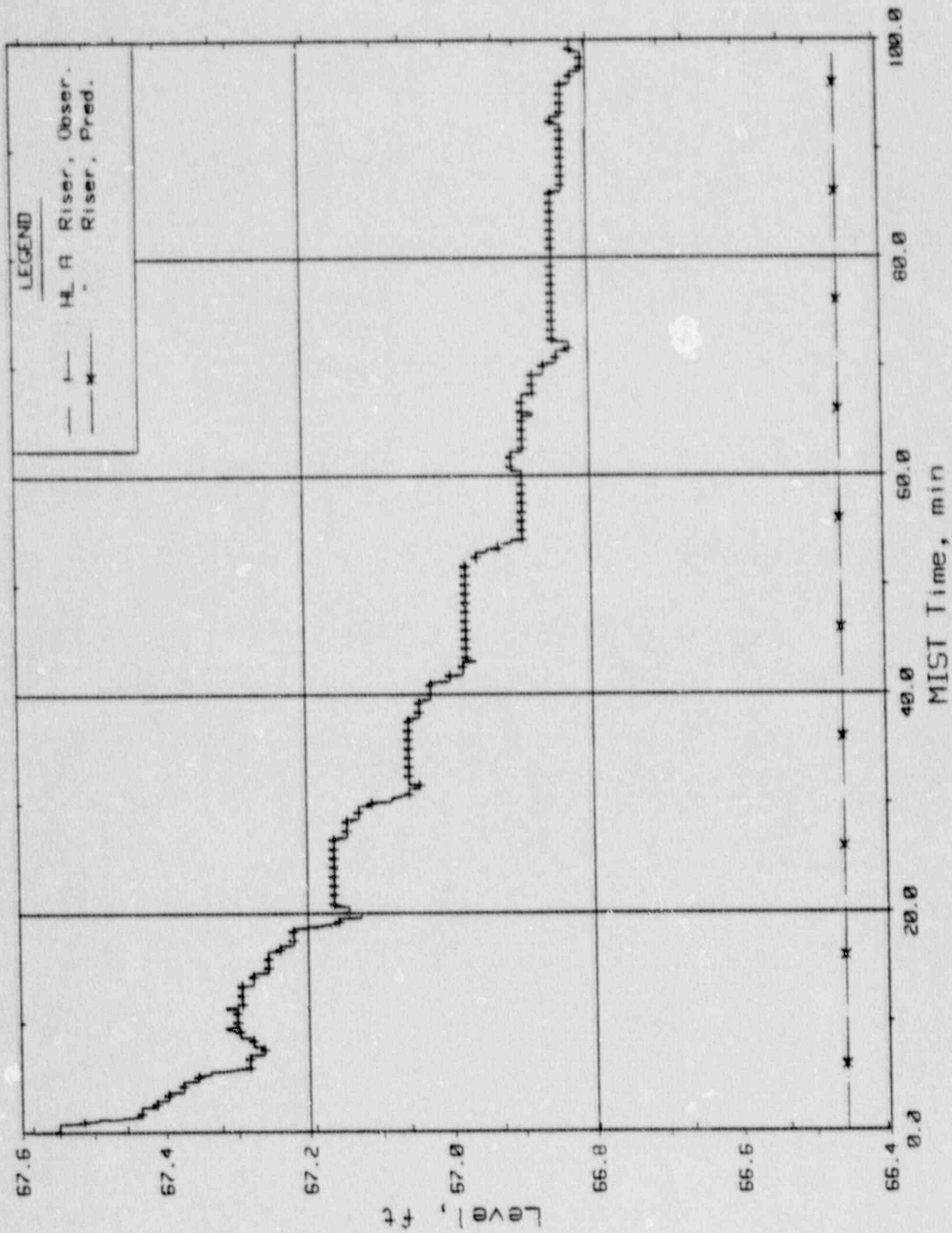


Figure 3.3.7. Hot Leg A Riser Level.

Ch1R21HL



Single Tube High Elevation SGTR  
 Test 340213 - Observed Vs. Predicted

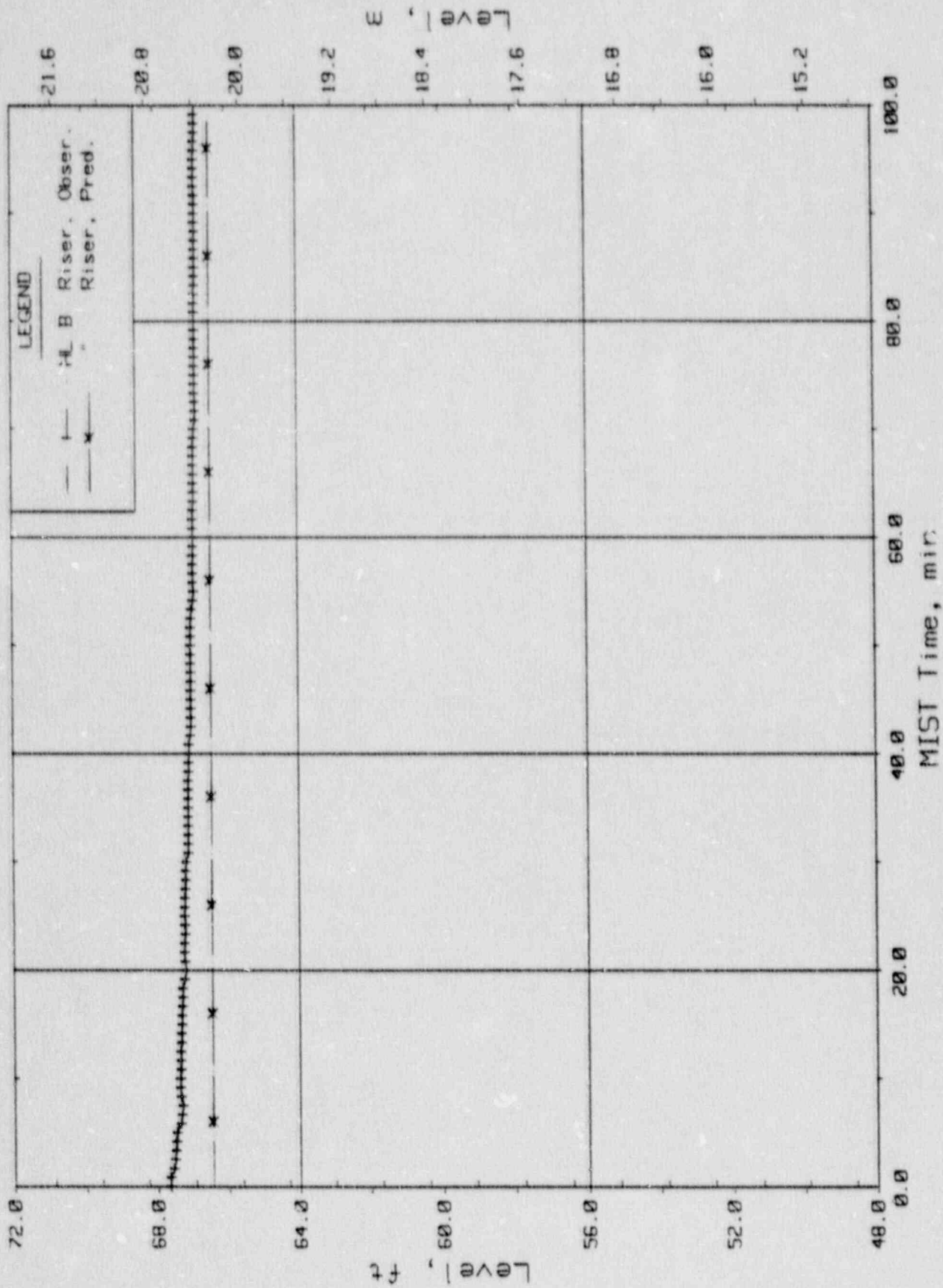


Figure 3.3.8. Hot Leg B Riser Level.

Single Tube High Elevation SGIR  
 Test 340213 - Observed Vs. Predicted

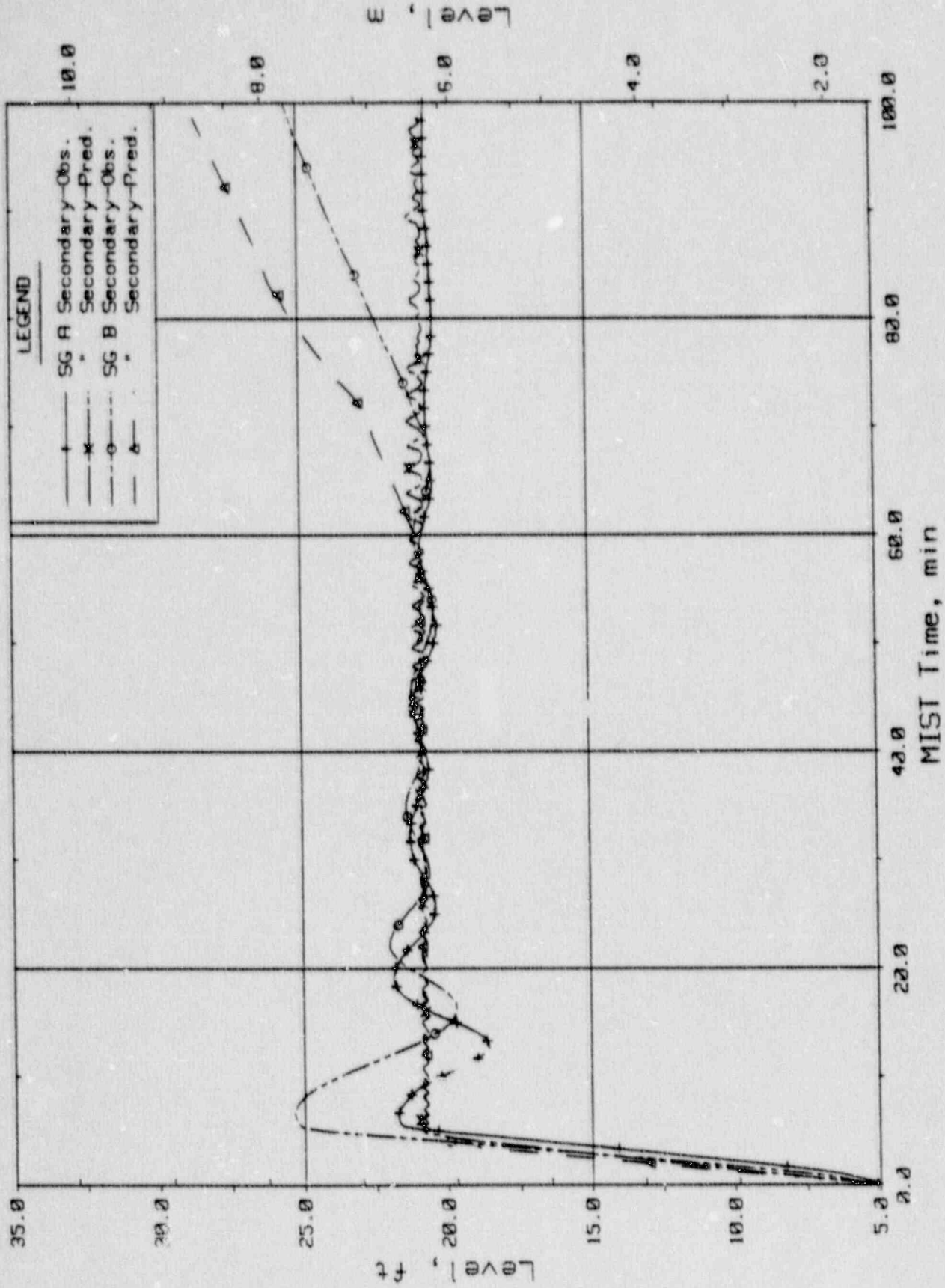


Figure 3.3.9. Steam Generator Sec. Collapsed Liquid Levels.

Single Tube High Elevation SGIR  
 Test 340213 - Observed Vs. Predicted

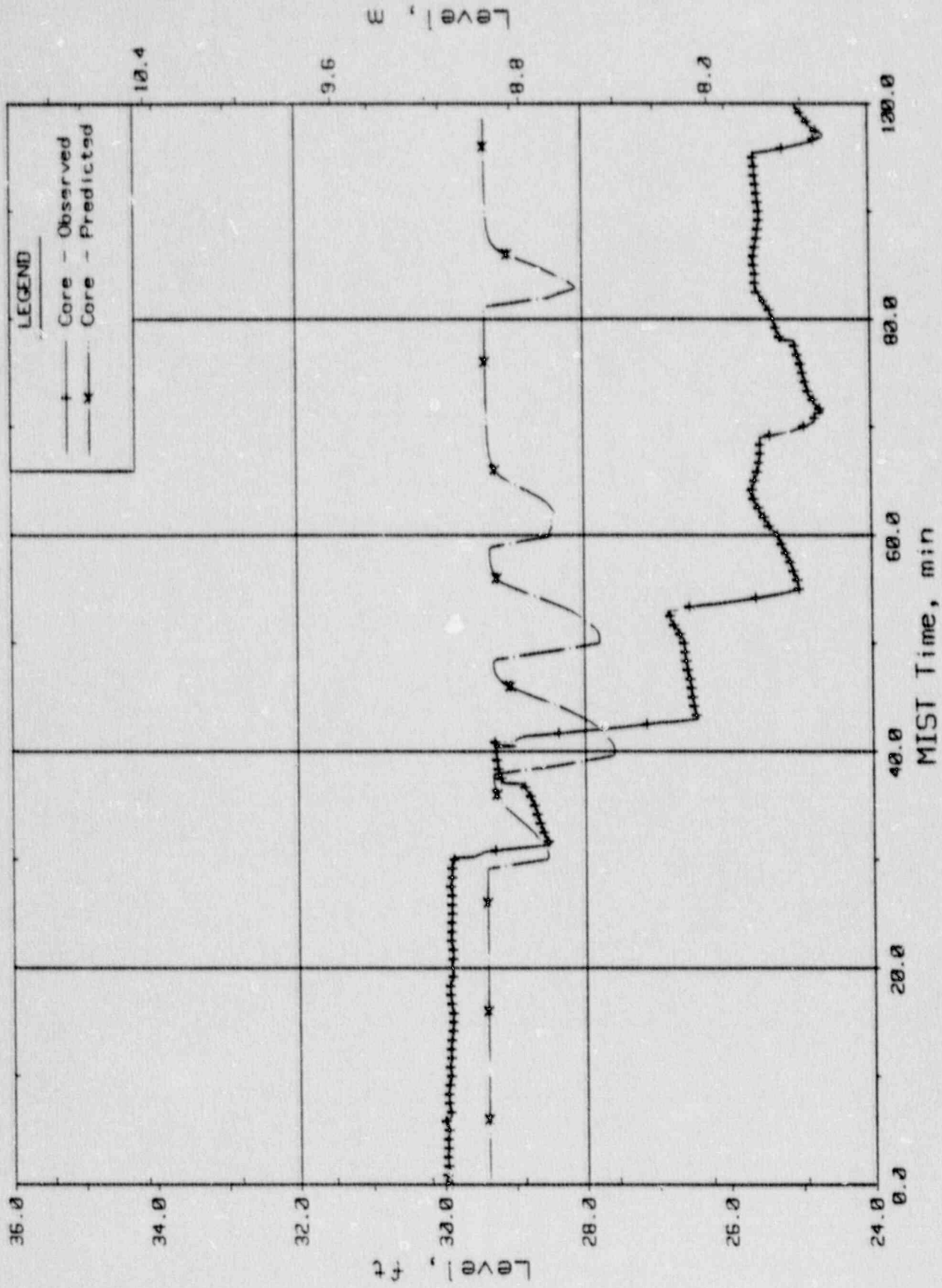


Figure 3.3.10. Core Region Collapsed Liquid Levels.

single Tube High Elevation SGTR  
 Test 340213 - Observed Vs. Predicted

3-96

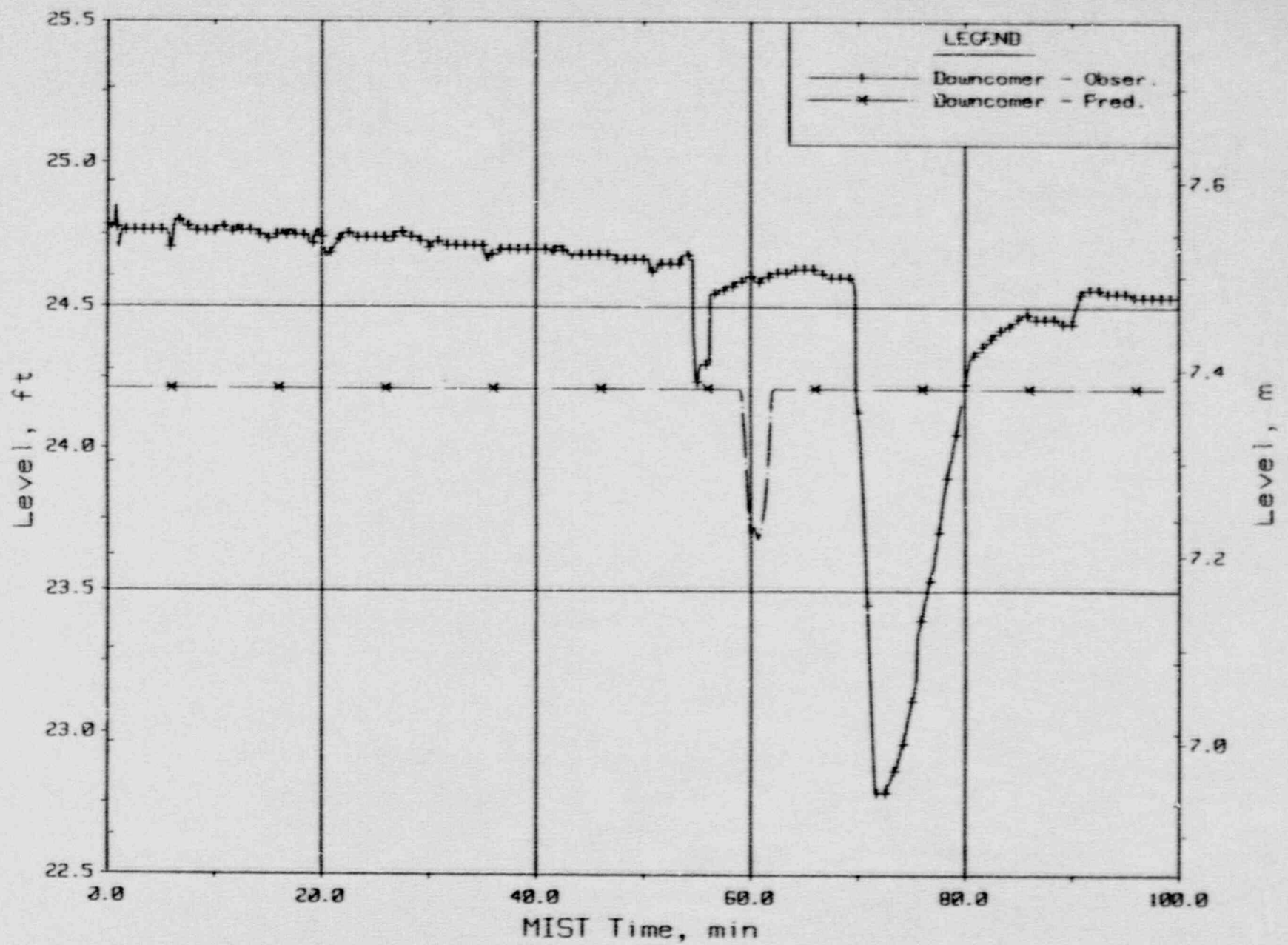


Figure 3.3.11. Core Region Collapsed Liquid Levels.

Single Tube High Elevation SGTR  
 Test 340213 - Observed Vs. Predicted

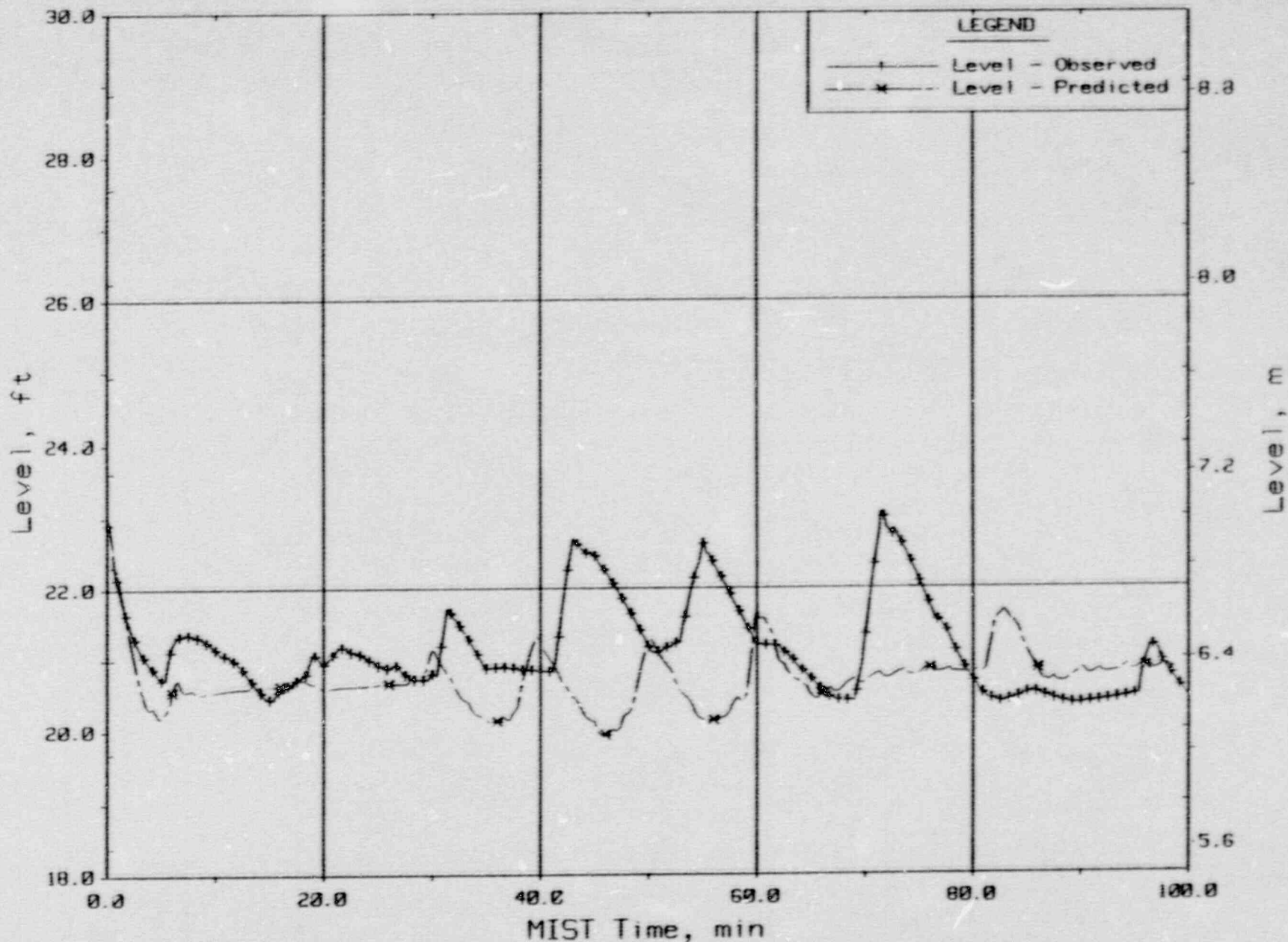


Figure 3.3.12. Pressurizer Collapsed Liquid Level (PZLV20).

Single Tube High Elevation SGTR  
 Test 340213 - Observed Vs. Predicted

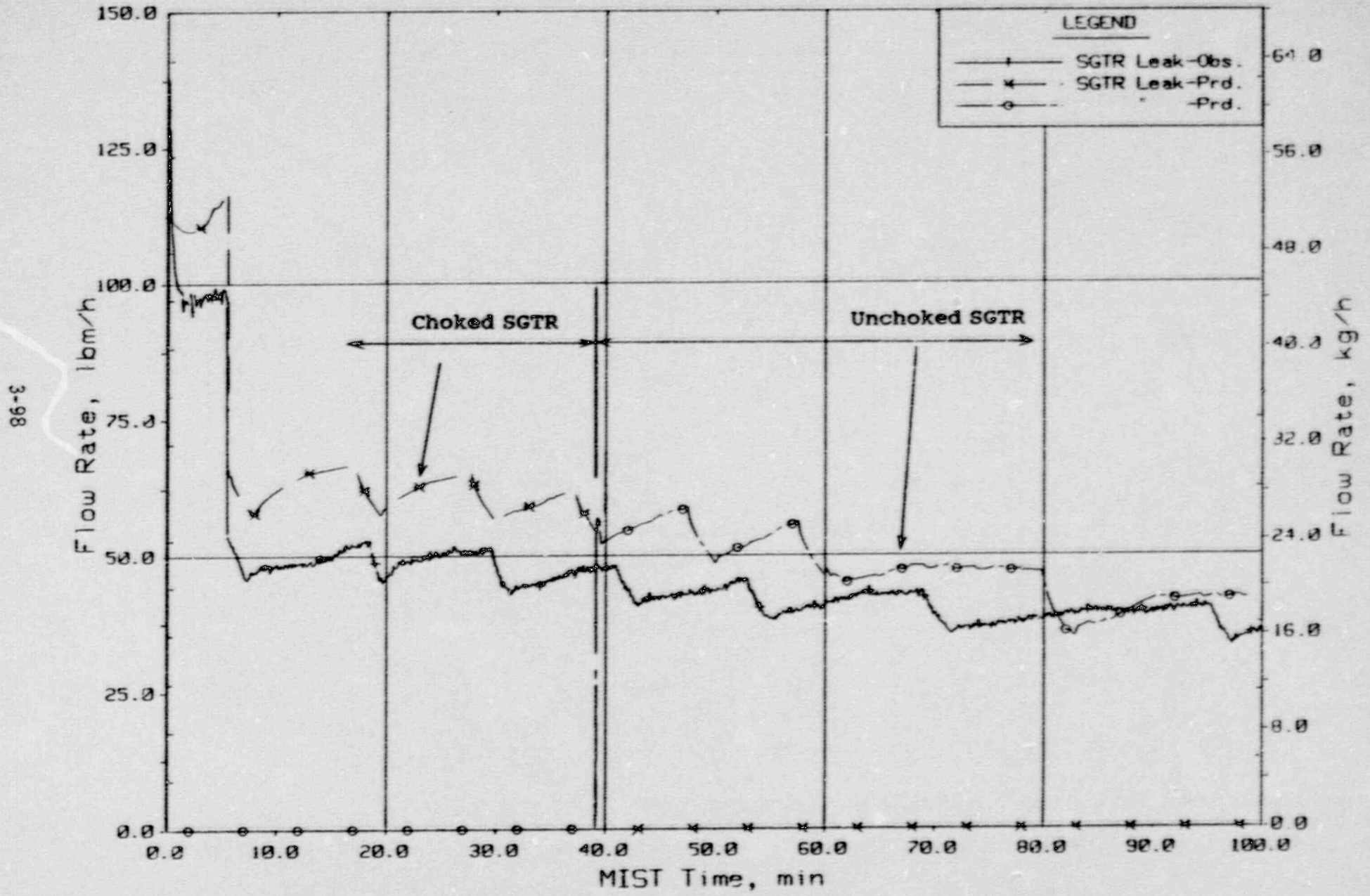


Figure 3.3.13. Primary System SGTR Leak Flow Rates.

Single Tube High Elevation SGTR  
 Test 340213 - Observed Vs. Predicted

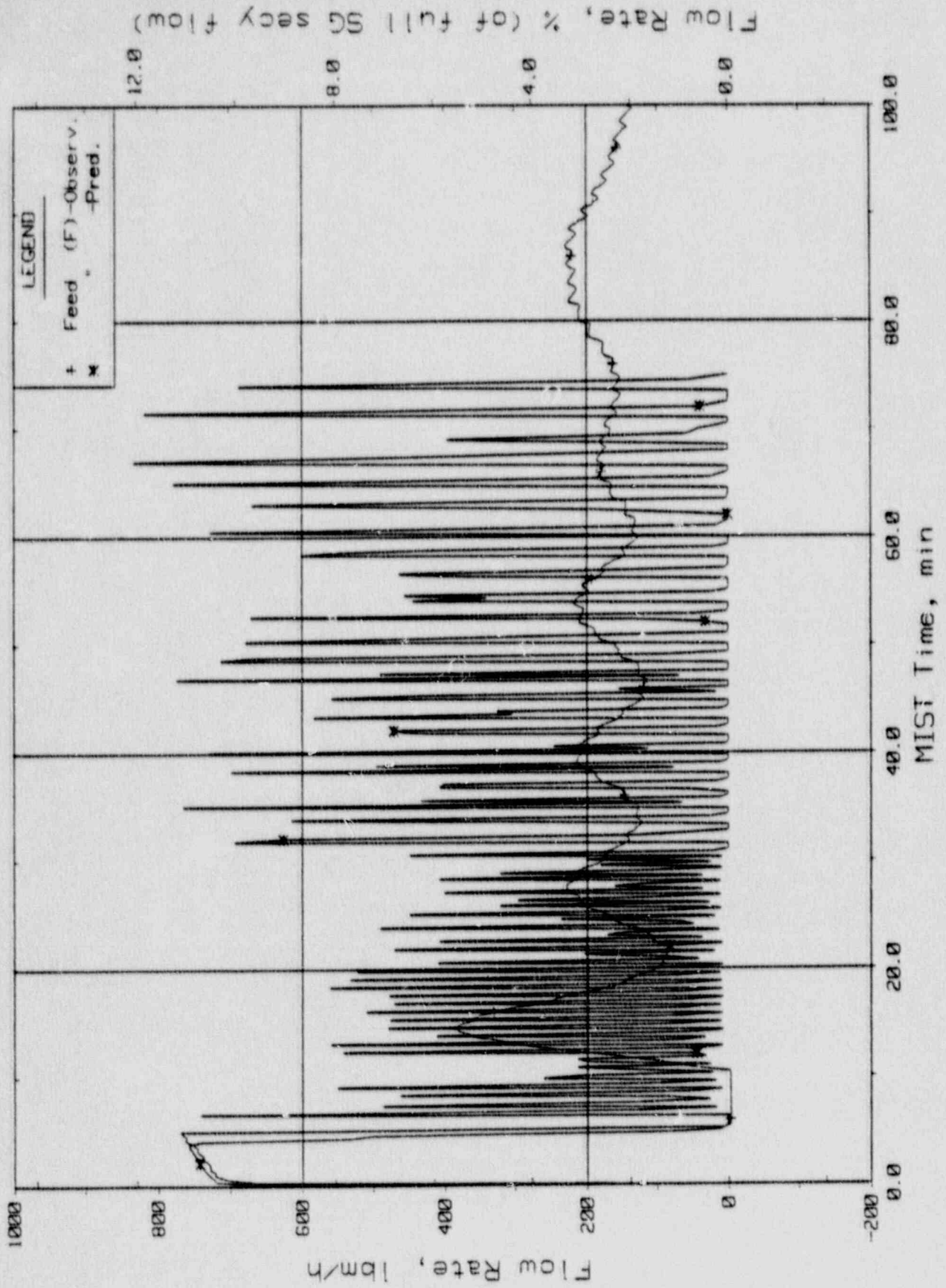


Figure 3.3.14. Steam Generator A Flow Rate (Ssfor20).

Single Tube High Elevation SGTR  
 Test 340213 - Observed Vs. Predicted

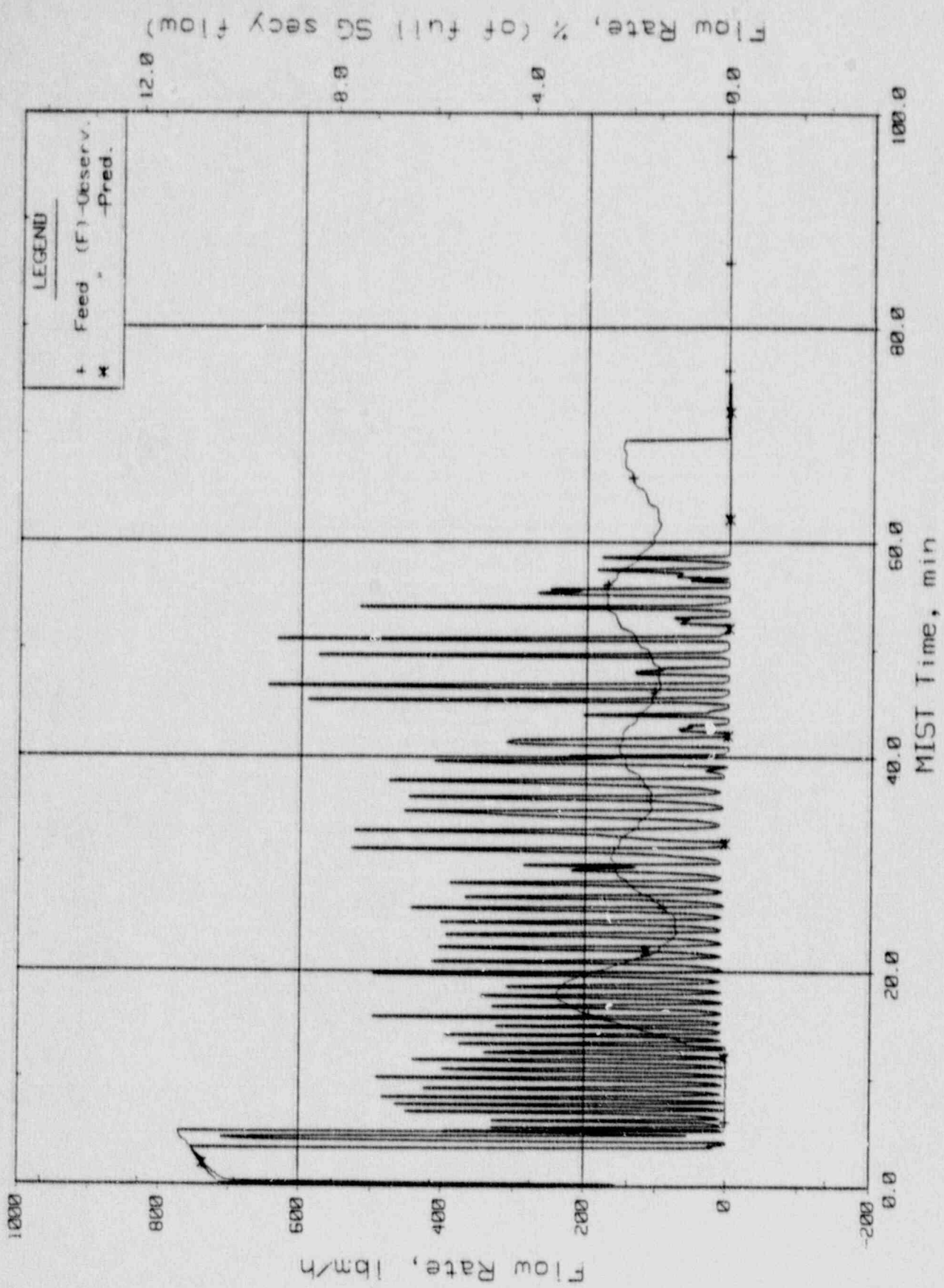


Figure 3.3.15. Steam Generator B Flow Rate (Ssfor21).



Single Tube High Elevation SGTR  
 Test 340213 - Observed Vs. Predicted

3-101

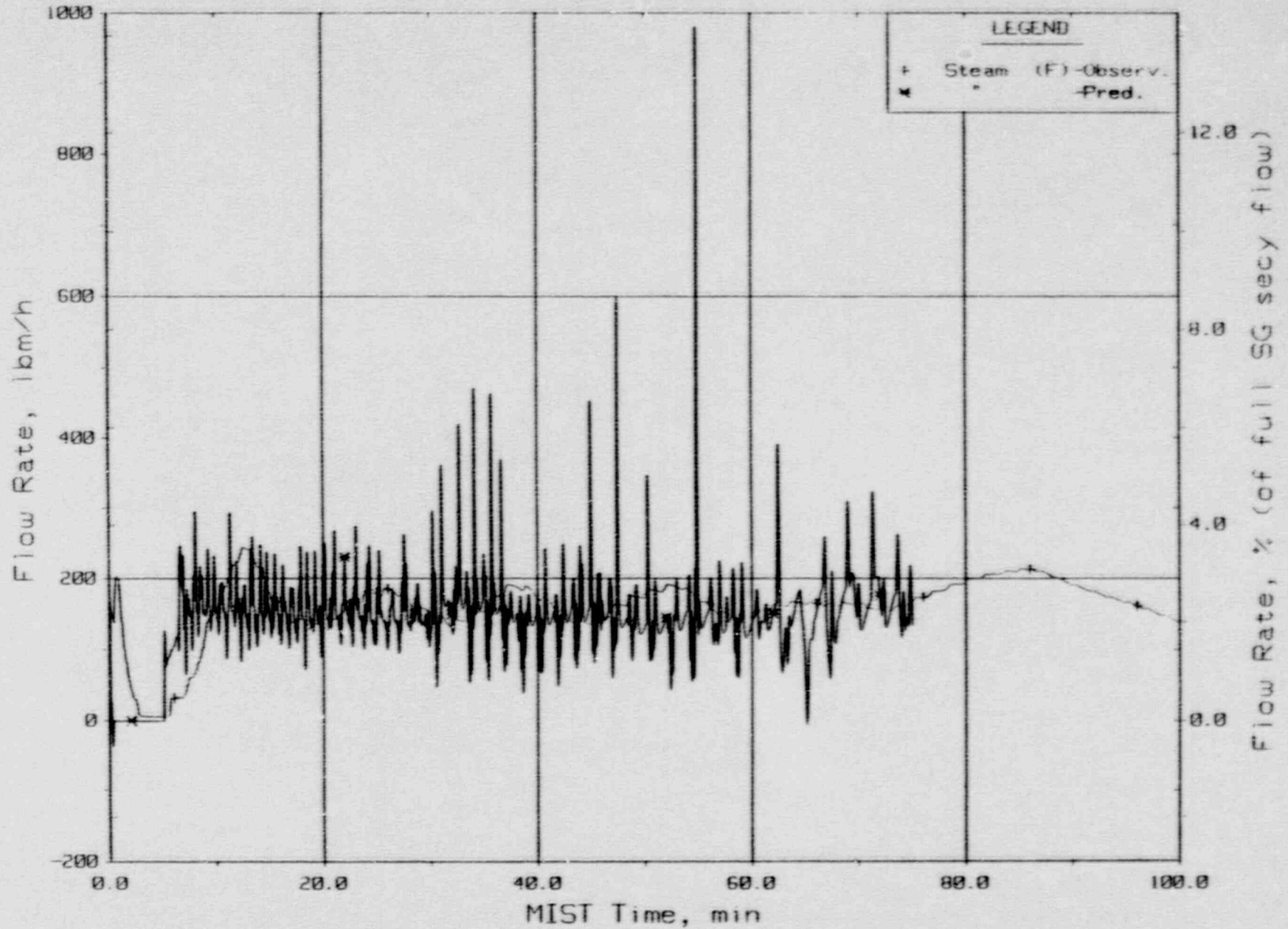


Figure 3.3.16. Steam Generator A Flow Rates (C55020).

Single Tube High Elevation SGTR  
 Test 340213 - Observed Vs. Predicted

3-102

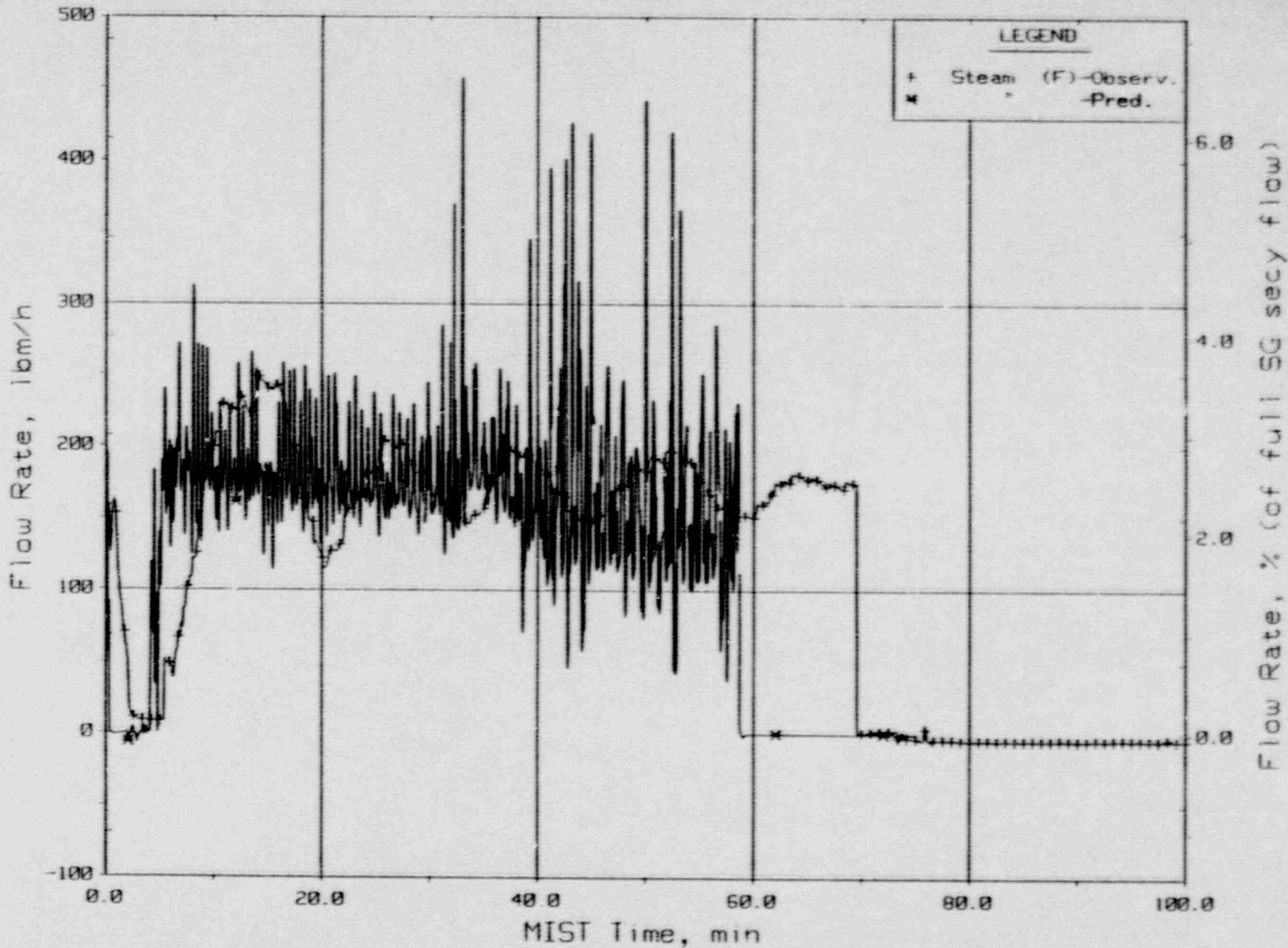


Figure 3.3.17. Steam Generator B Flow Rates (Sssor21).

Single Tube High Elevation SGTR  
Test 340213 - Observed Vs. Predicted

3-103

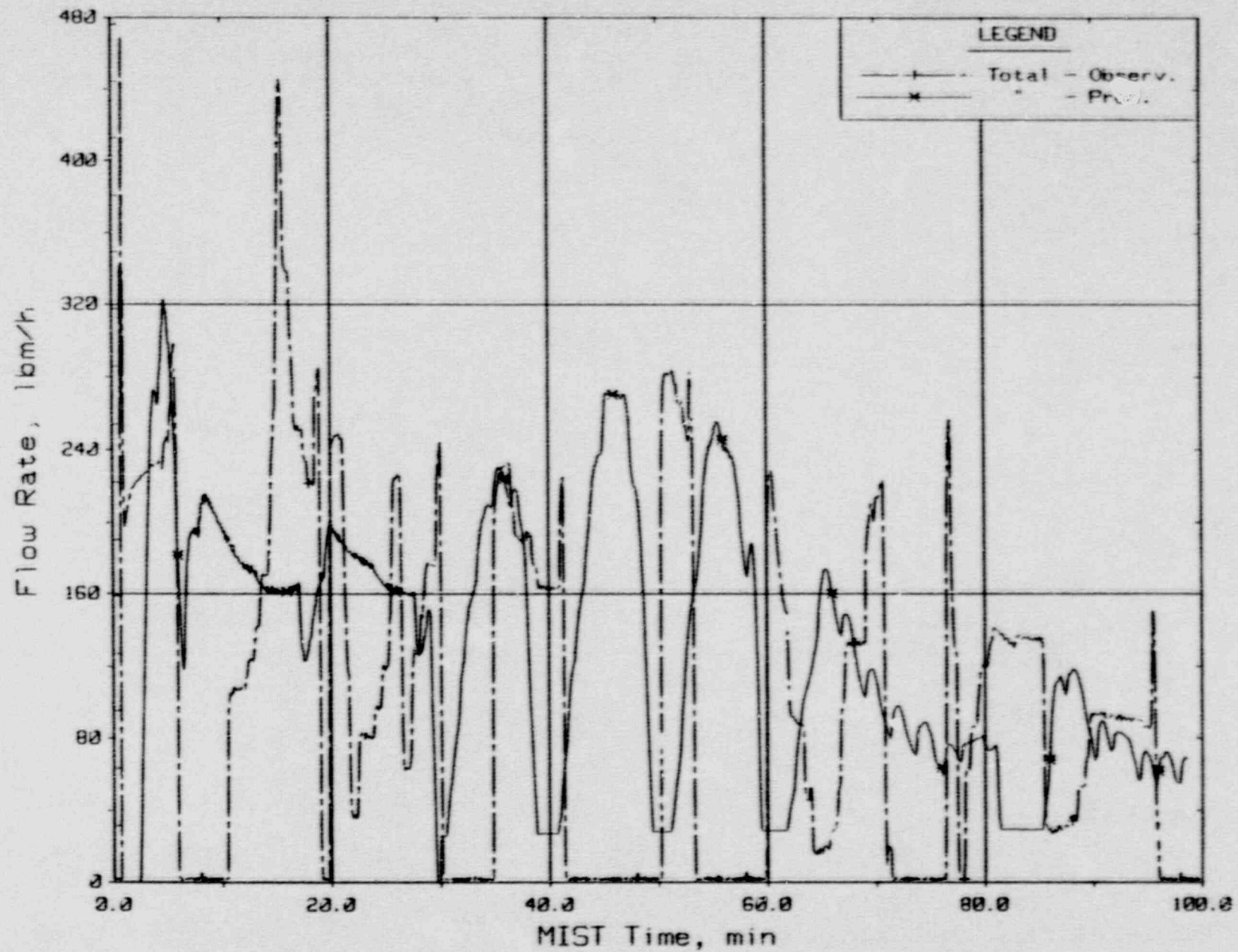


Figure 3.3.18. HPI Total Flow Rates.

Single Tube High Elevation SGTR  
 Test 340213 - Observed Vs. Predicted

3-104

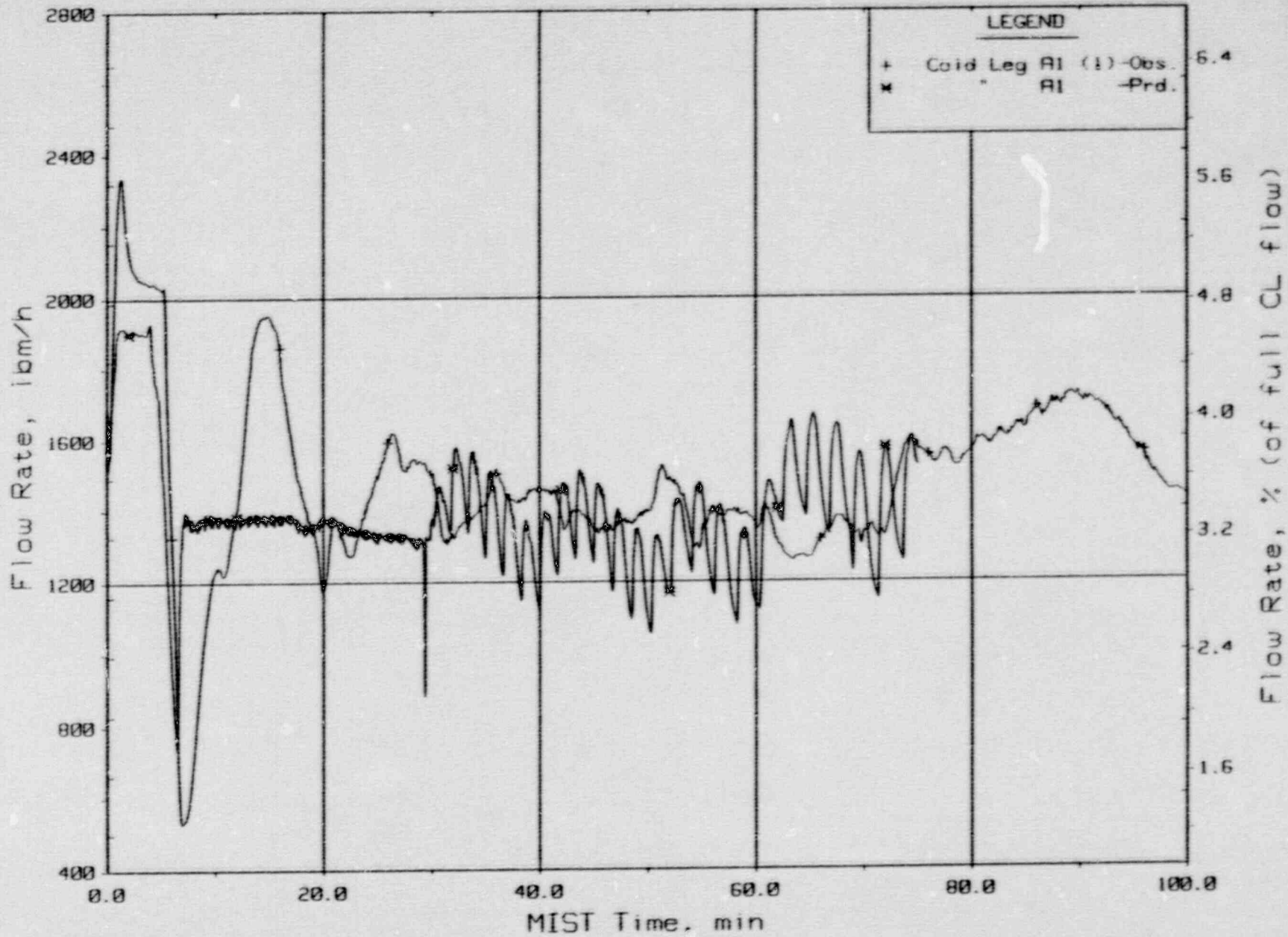


Figure 3.3.19. Loop AI Cold Leg (Venturi) Flow Rate (C1VN20).

Single Tube High Elevation SGTR  
 Test 340213 - Observed Vs. Predicted

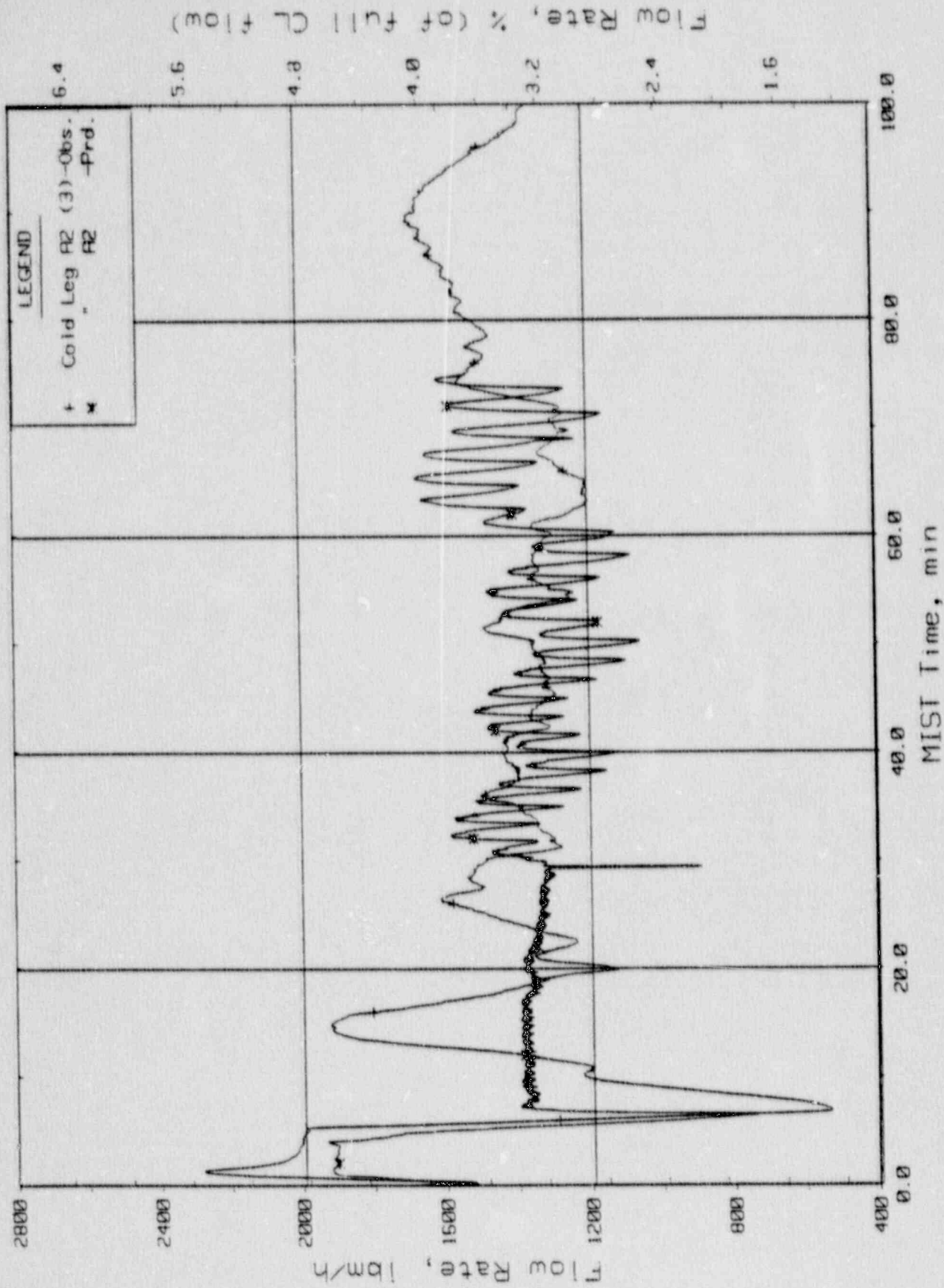


Figure 3.3.20. Loop R2 Cold Leg (Venturi) Flow Rate (C2VN20).

Cc3vn20

Single Tube High Elevation SGTR  
 Test 340213 - Observed Vs. Predicted

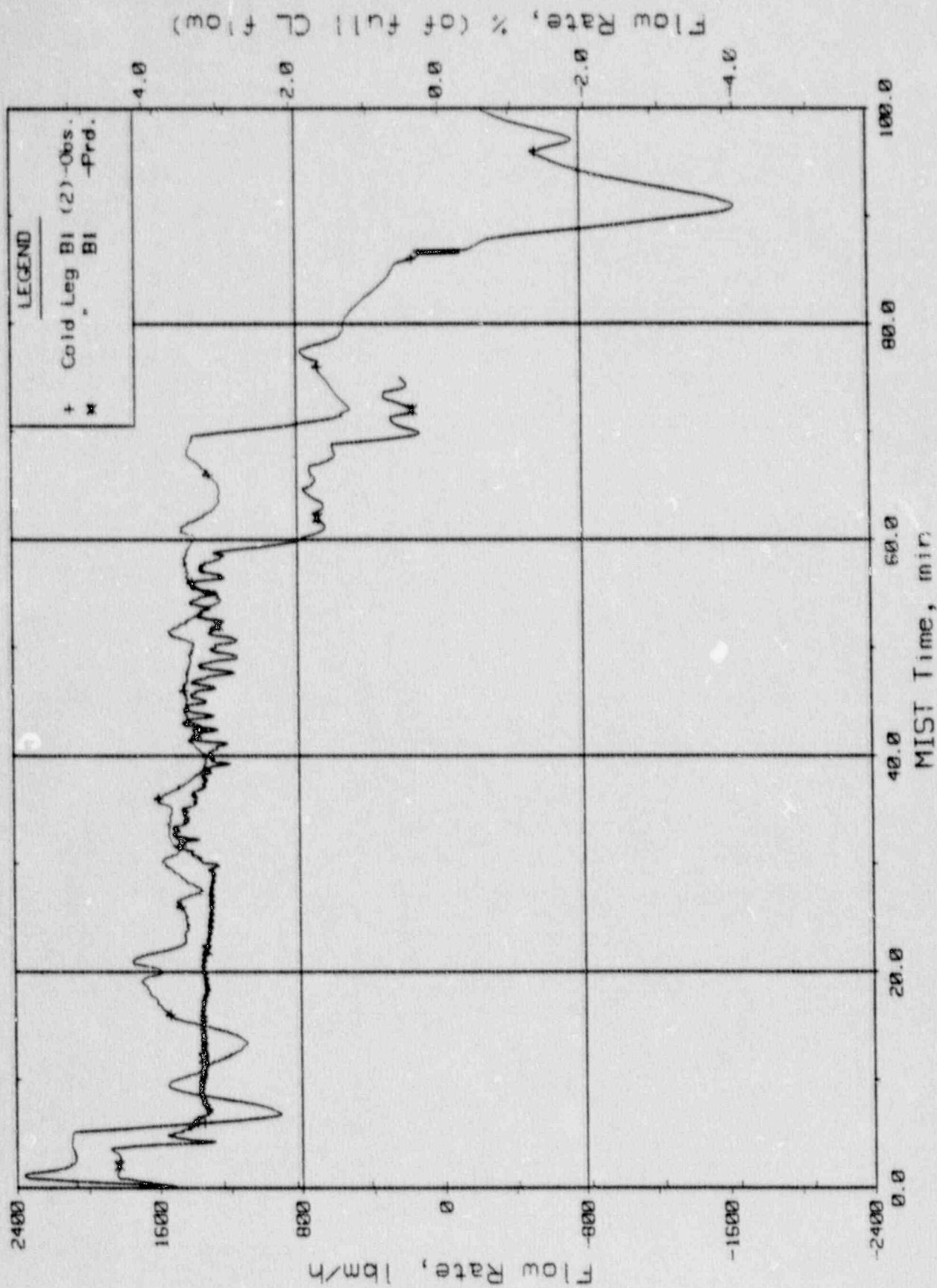


Figure 3.3.21. Loop BI Cold Leg (Venturi) Flow Rate (CIVN20).

Single Tube High Elevation SGTR  
 Test 340213 - Observed Vs. Predicted

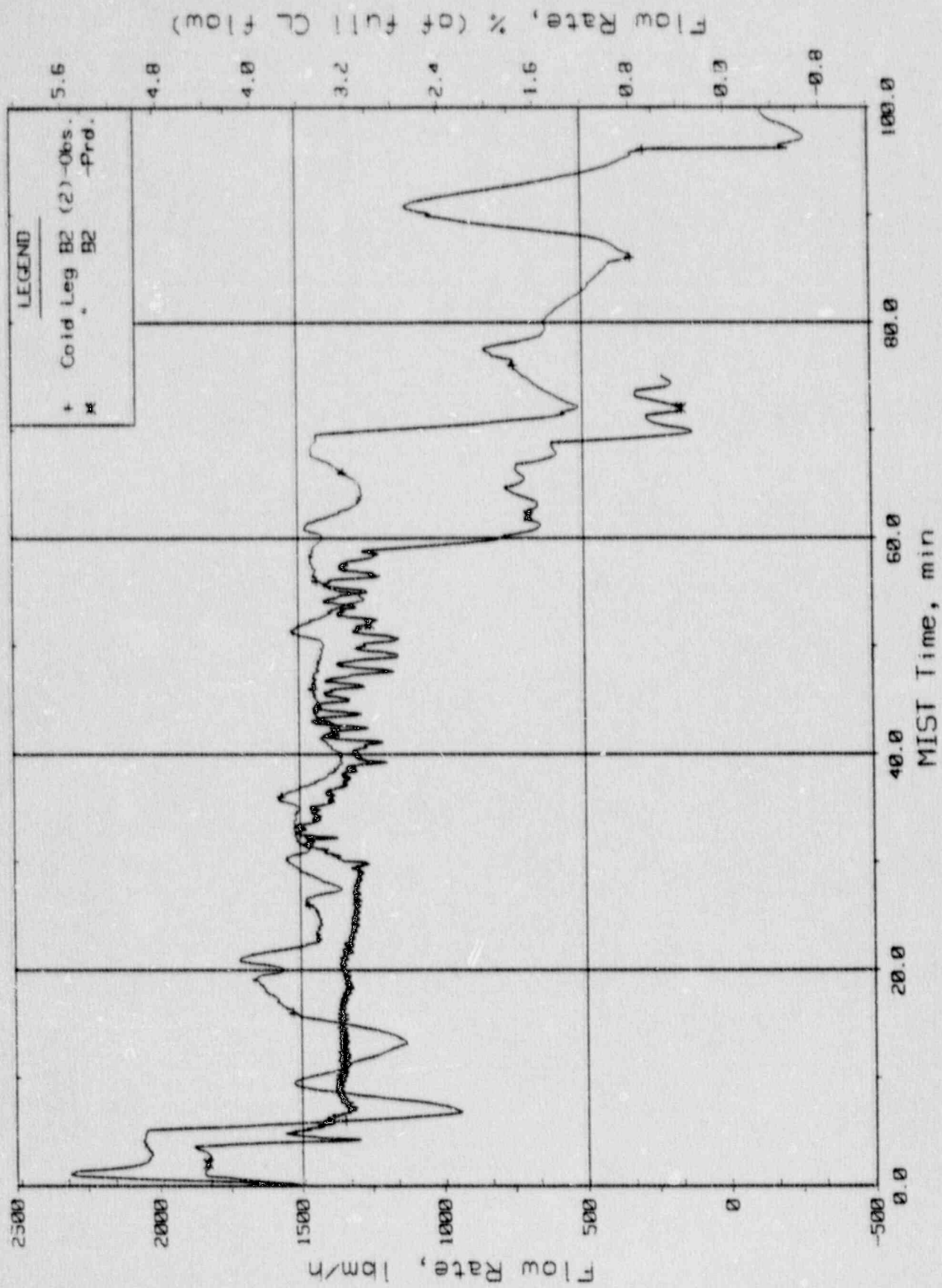


Figure 3.3.22. Loop B2 Cold Leg (Venturi) Flow Rate (C4VN20).

Cc4vm20

Had Sep 30 08:13:05 1987

Single Tube High Elevation SGTR  
 Test 340213 - Observed Vs. Predicted

3-108

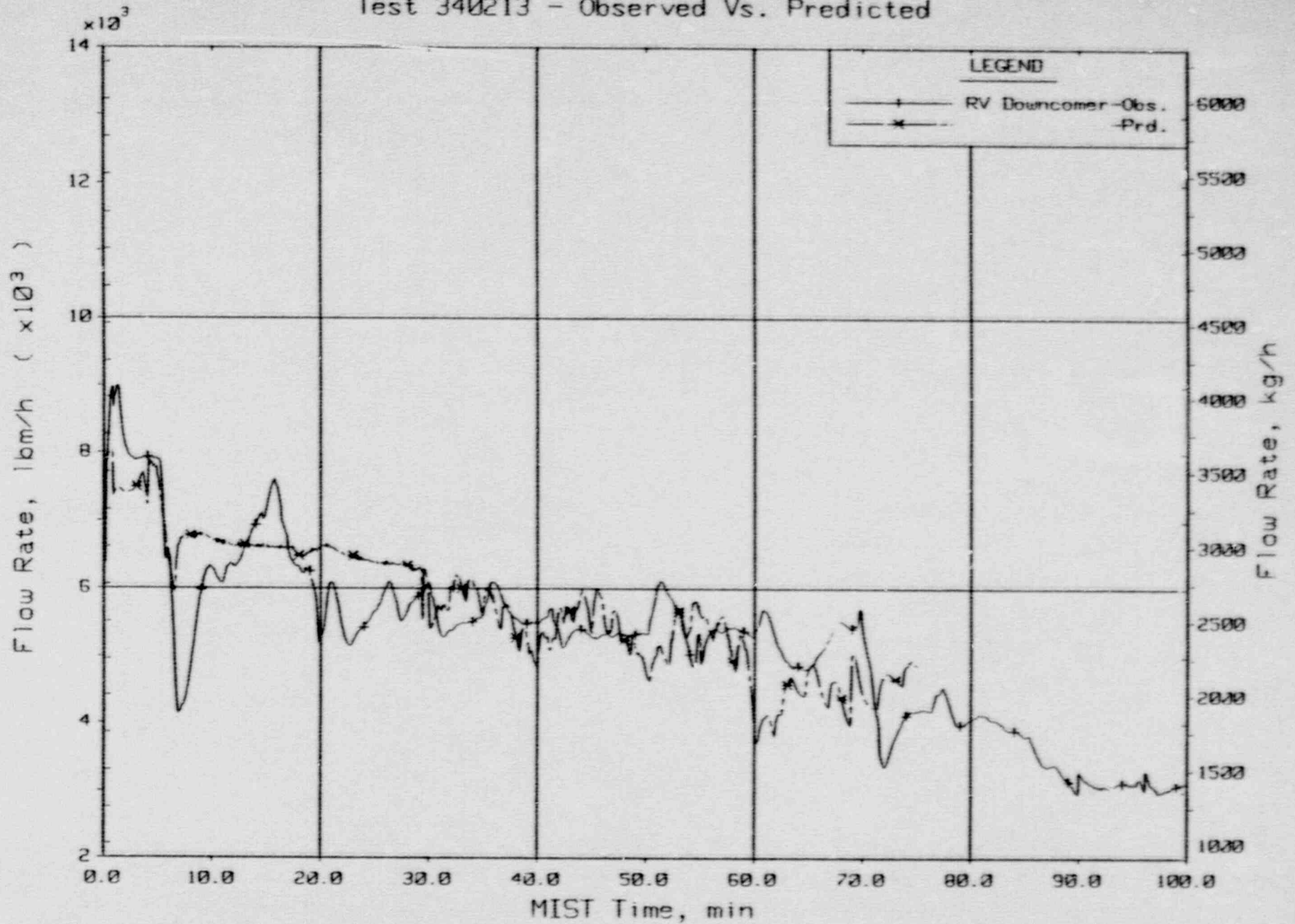


Figure 3.3.23. Primary System Venturi Flow Rates.



Single Tube High Elevation SGTR  
Test 340213 - Observed Vs. Predicted

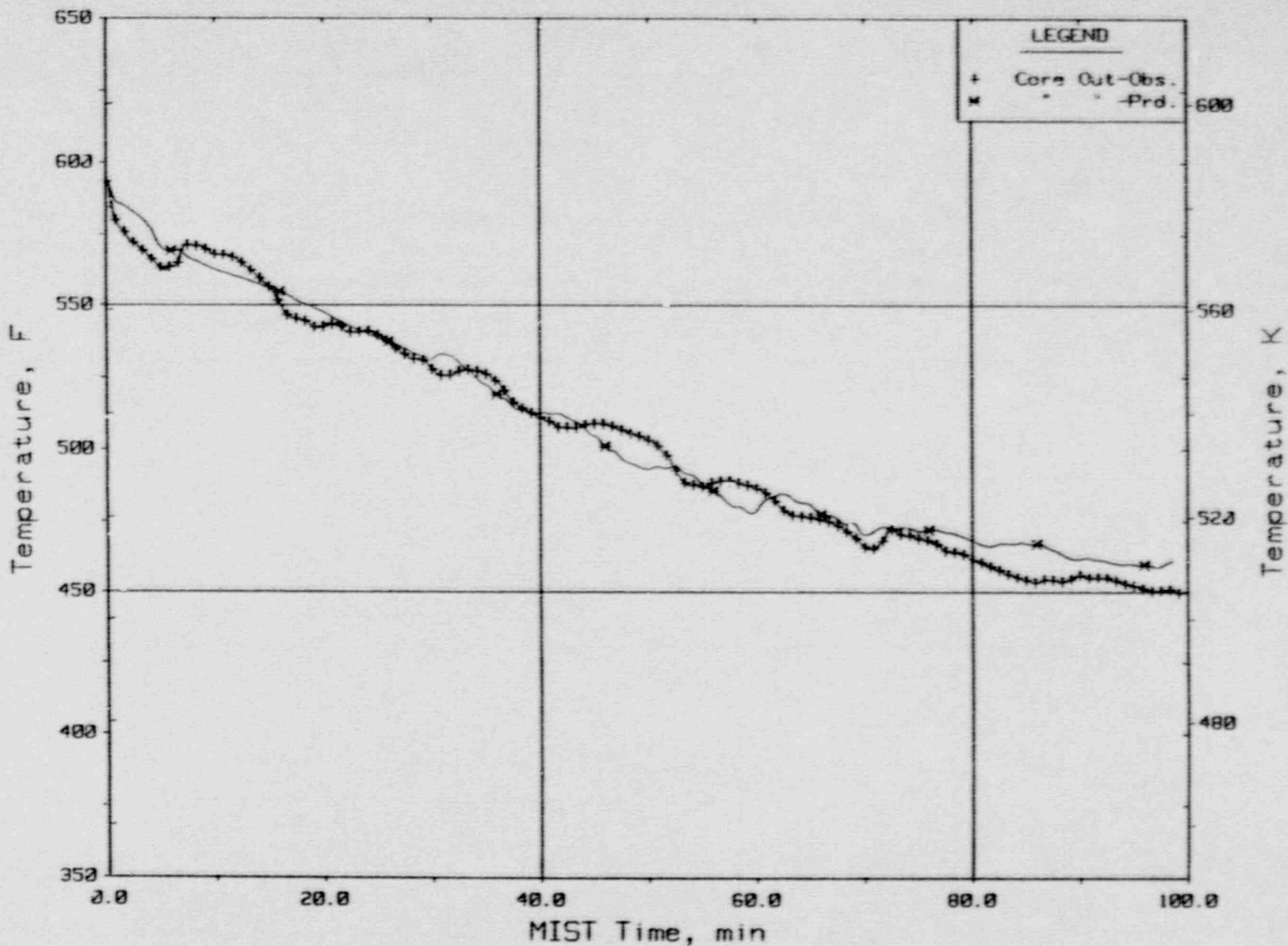


Figure 3.3.24. Core Exit Reactor Vessel Fluid Temperature (RVTCl1).

3-109

Single Tube High Elevation SGTR  
 Test 340213 - Observed Vs. Predicted

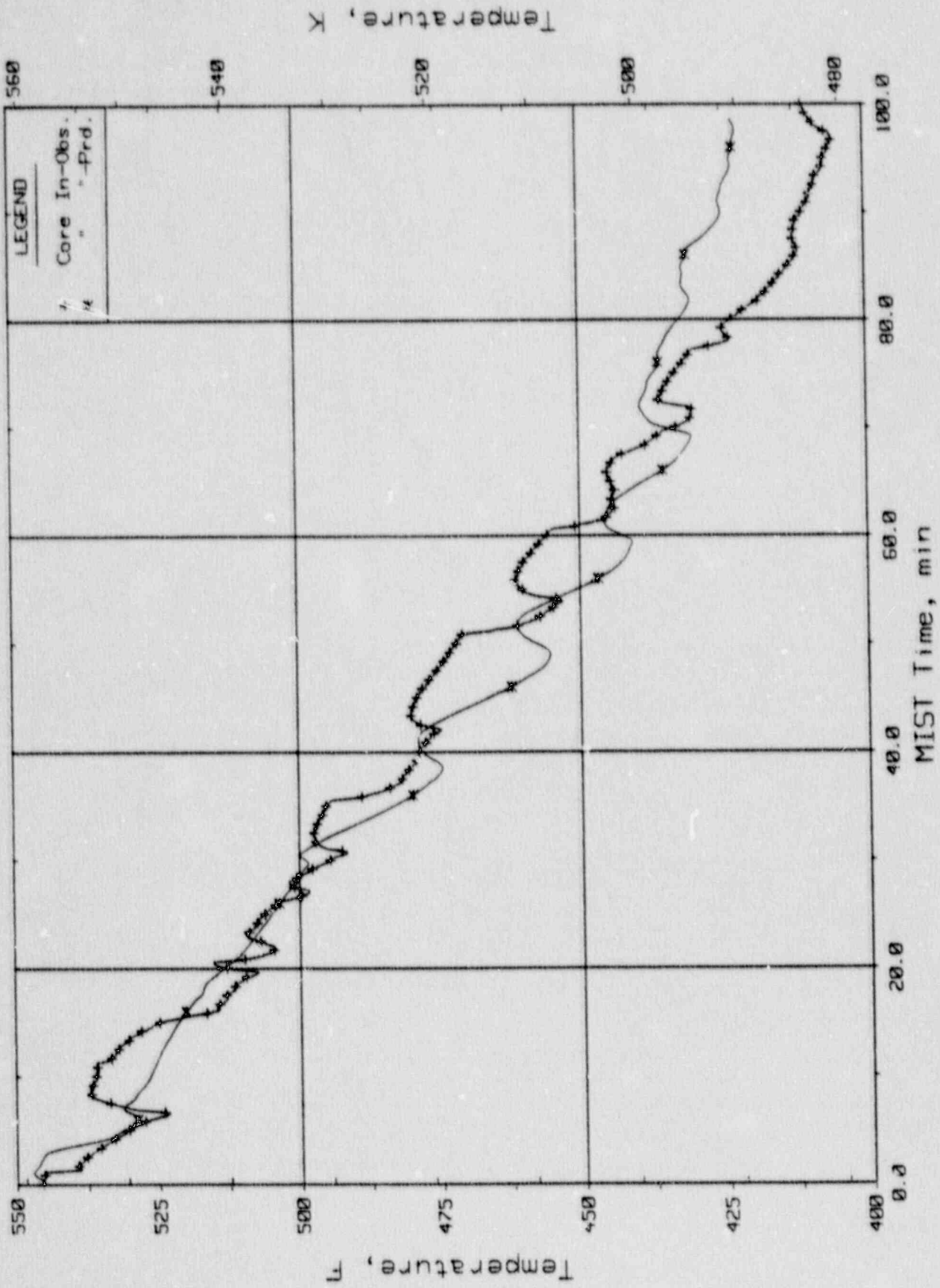


Figure 3.3.25. Core Inlet Reactor Vessel Fluid Temperature (DCRT01).

Cdcrt01

Single Tube High Elevation SGTR  
 Test 340213 - Observed Vs. Predicted

3-111

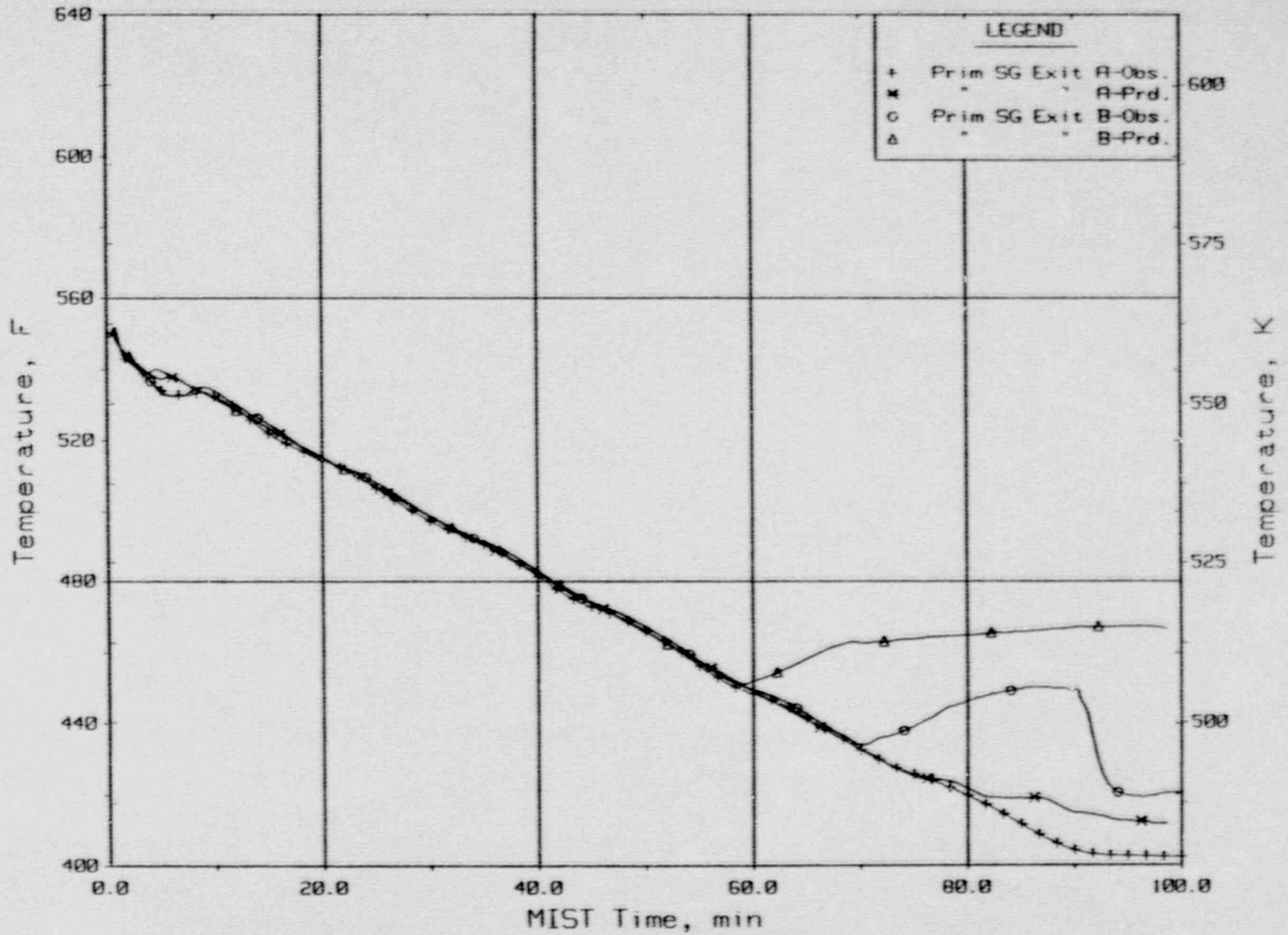


Figure 3.3.26. Loops A/B SG Exit Primary Fluid Temperatures (RTDs).

Single Tube High Elevation SGTR  
 Test 340213 - Observed Vs. Predicted

3-112

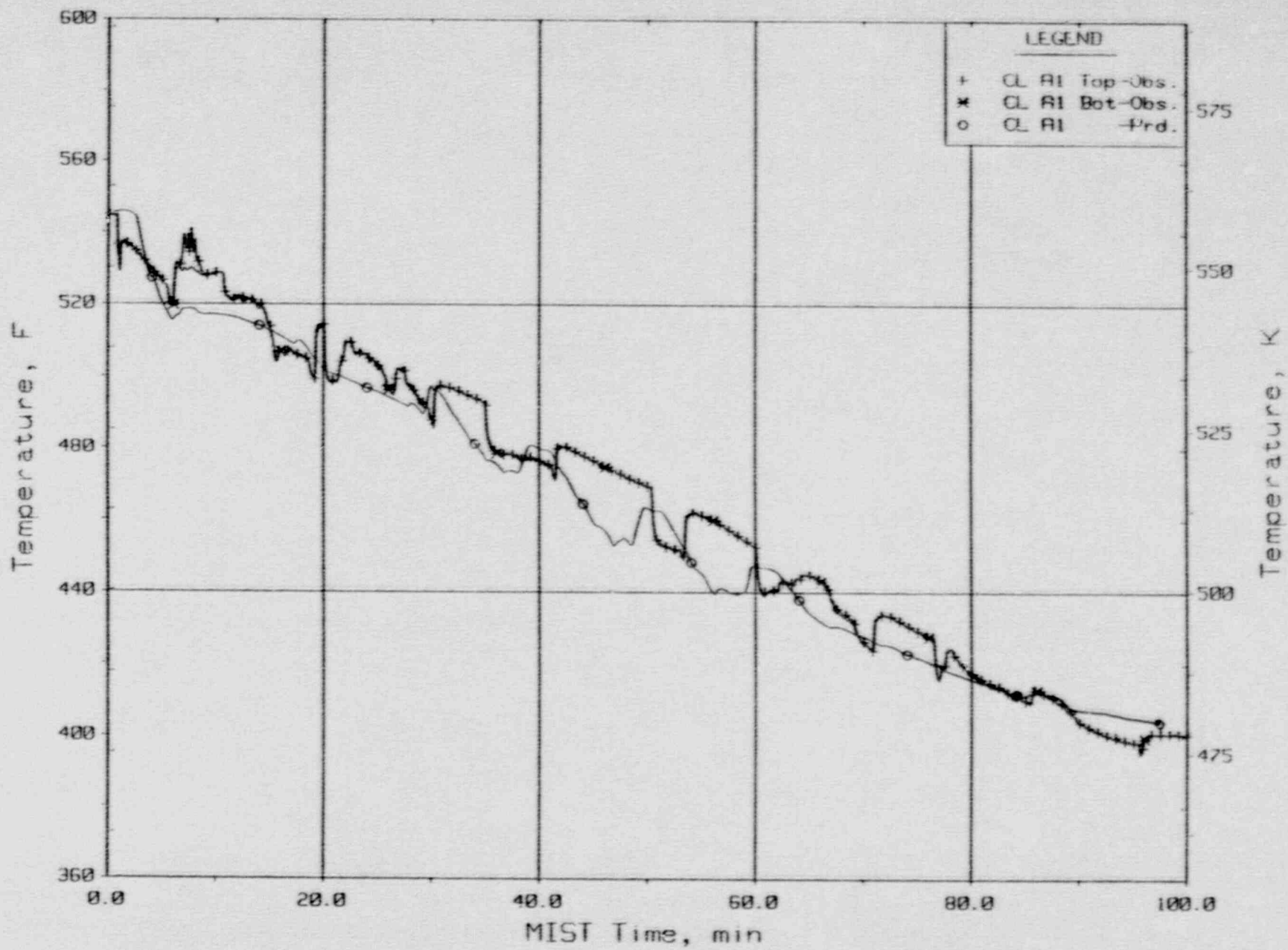


Figure 3.3.27. Cold Leg Nozzle Fluid Temperatures, Top/Bot of Rake (21.3ft, CnTC11/14s).

Single Tube High Elevation SGTR  
 Test 340213 - Observed Vs. Predicted

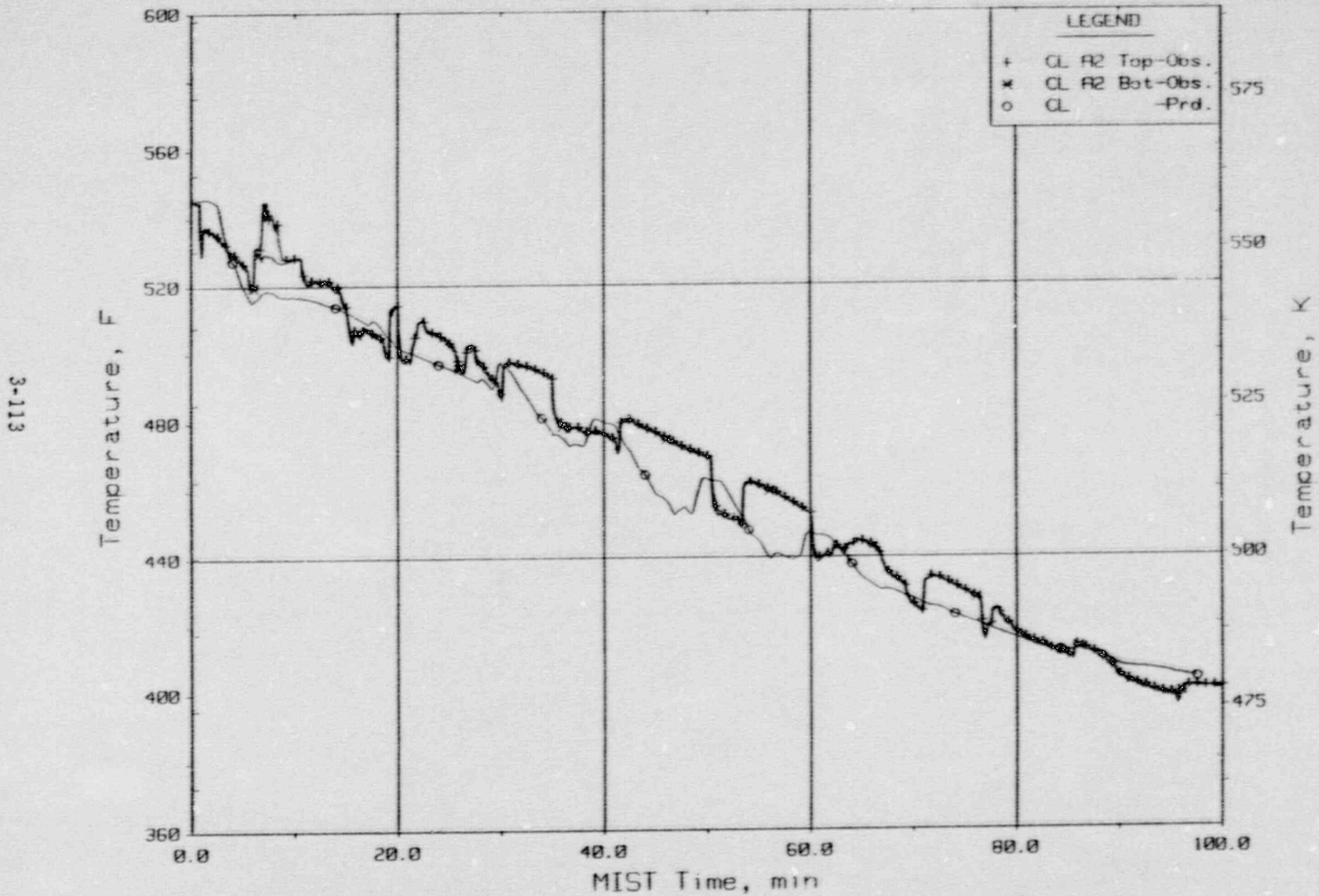


Figure 3.3.28. Cold Leg Nozzle Fluid Temperatures, Top/Bot of Rake (21.3ft, Cc1tca2).

Single Tube High Elevation SGTR  
 Test 340213 - Observed Vs. Predicted

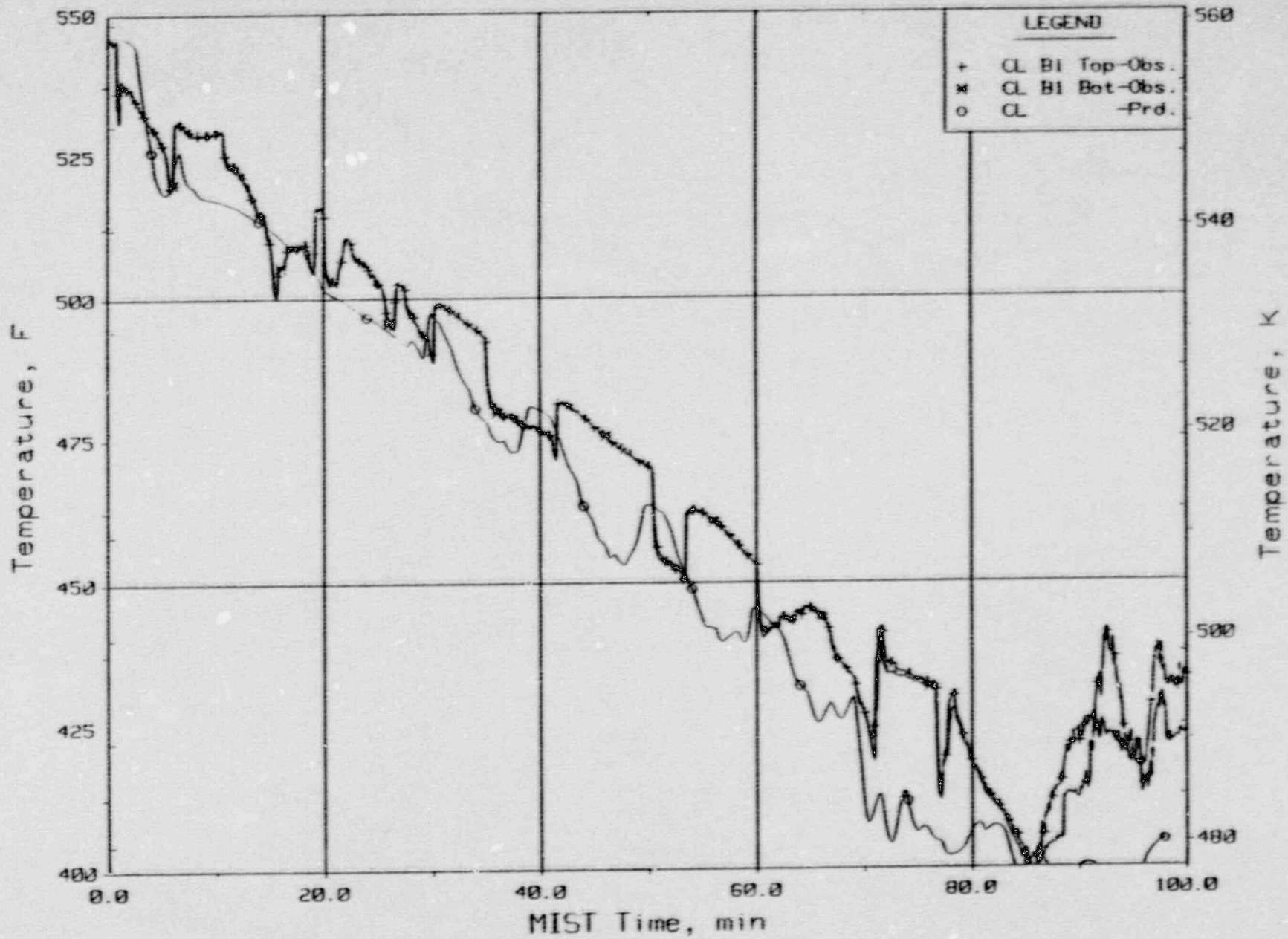


Figure 3.3.29. Cold Leg Nozzle Fluid Temperatures, Top/Bot of Rake (21.3ft, Cc1tcbl).

3-114

Single Tube High Elevation SGTR  
 Test 340213 - Observed Vs. Predicted

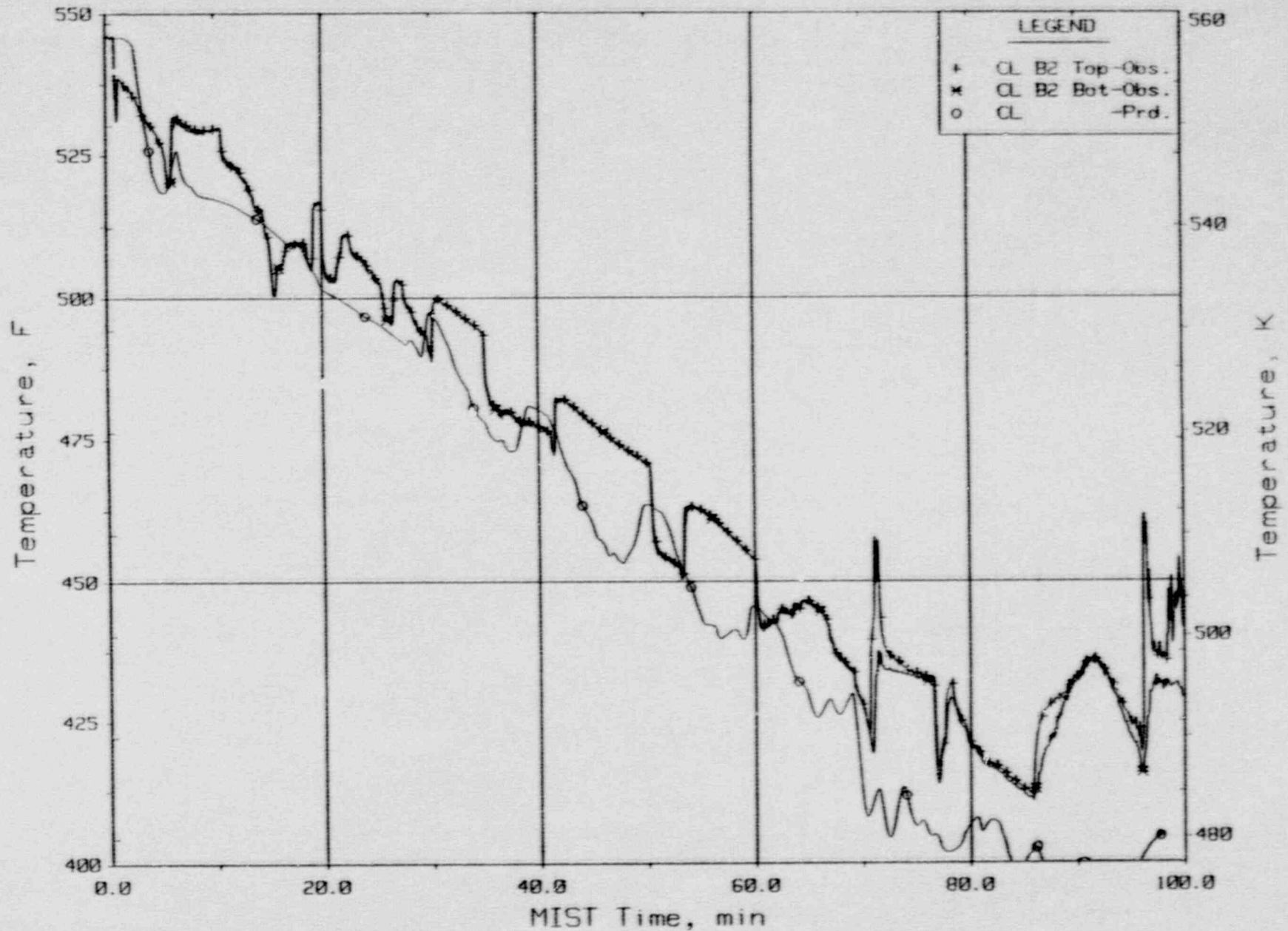


Figure 3.3.30. Cold Leg Nozzle Fluid Temperatures, Top/Bot of Rake (21.3ft, Cc1tcb2).

Single Tube High Elevation SGTR  
 Test 340213 - Observed Vs. Predicted

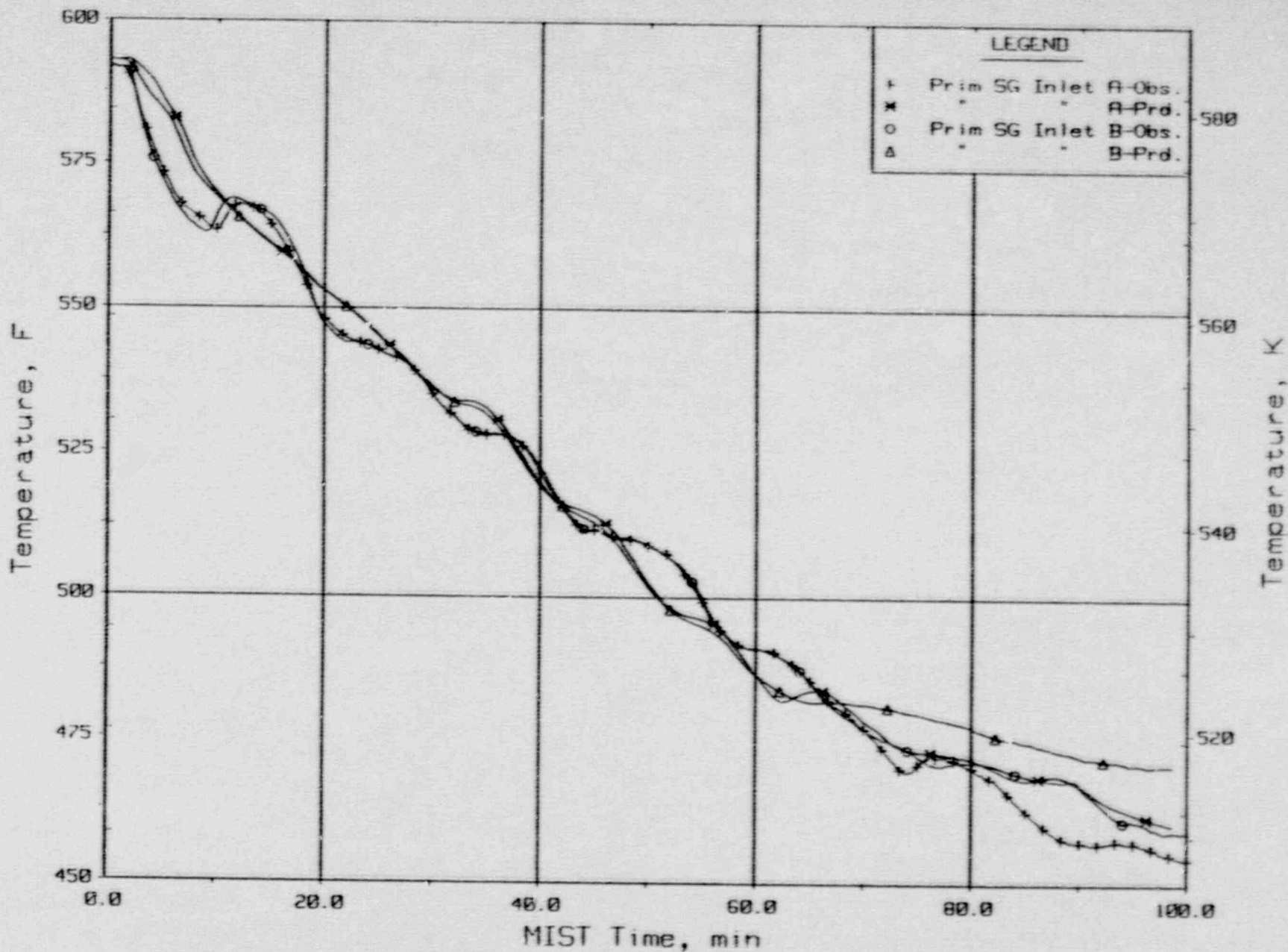


Figure 3.3.31. Loops A/B SG Primary Inlet Fluid Temperatures (RTDs).



Single Tube High Elevation SGTR  
 Test 340213 - Observed Vs. Predicted

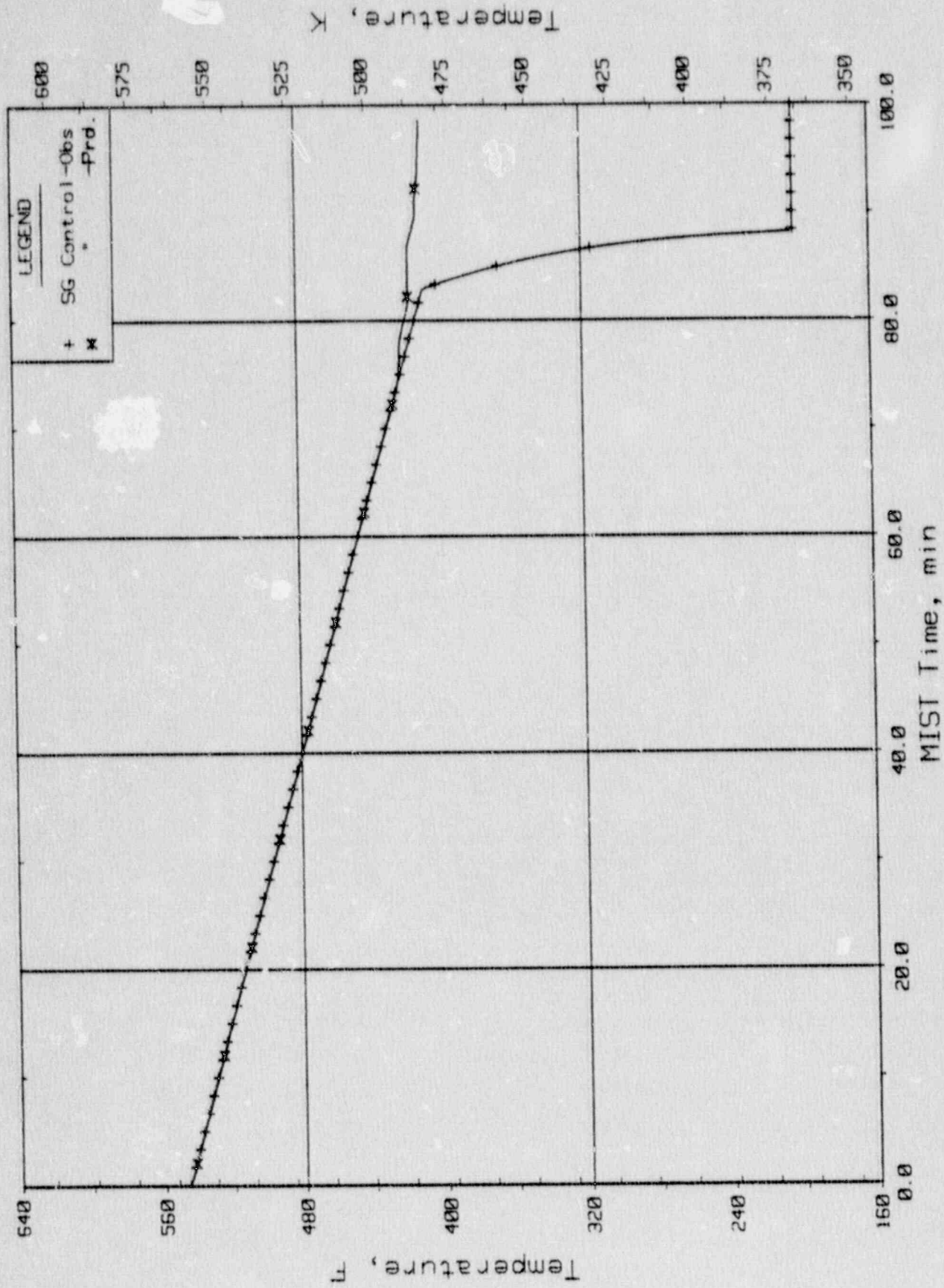


Figure 3.3.32. Steam Generator Secondary Saturation and Control Temperatures.

Single Tube High Elevation SGTR  
 Test 340213 - Observed Vs. Predicted

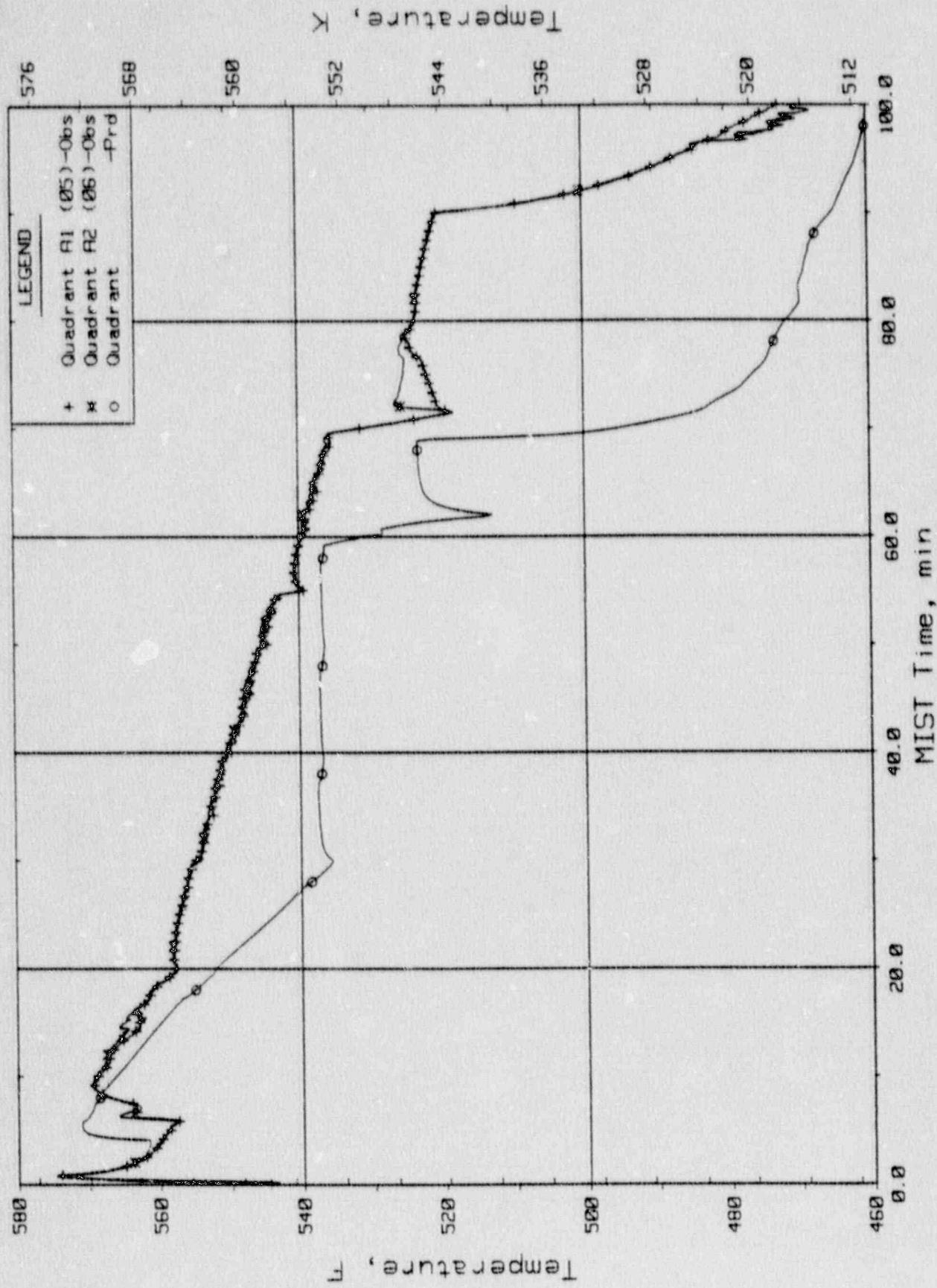


Figure 3.3.33. Downcomer A Fluid Temperatures Below RWVs, Elev. 23.8 ft (DCTCs).

Single Tube High Elevation SGIR  
 Test 340213 - Observed Vs. Predicted

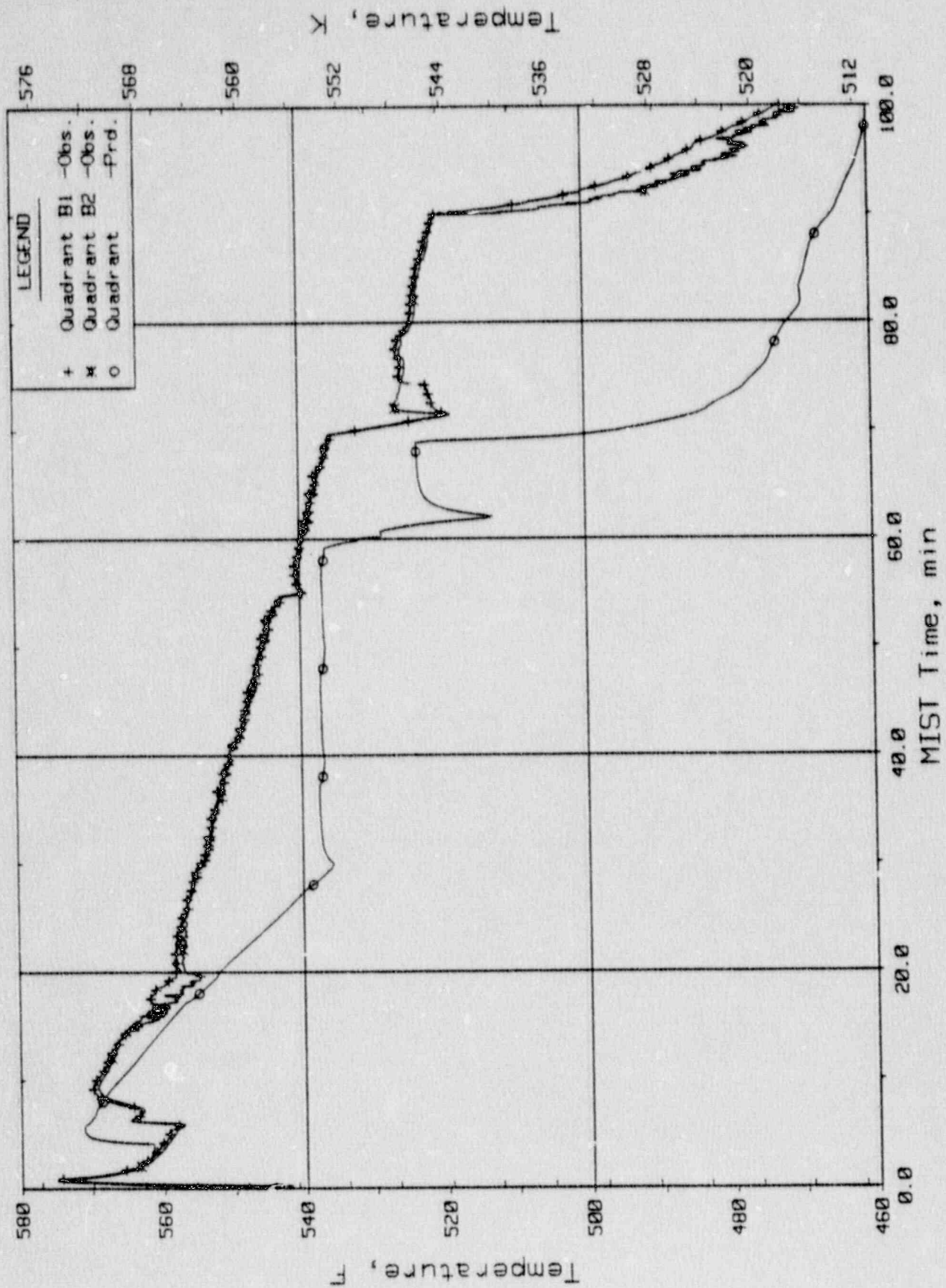


Figure 3.3.34. Downcomer B Fluid Temperatures Below RWVs, Elev. 23.8 ft (DCTCs).

Single Tube High Elevation SGTR  
 Test 340213 - Observed Vs. Predicted

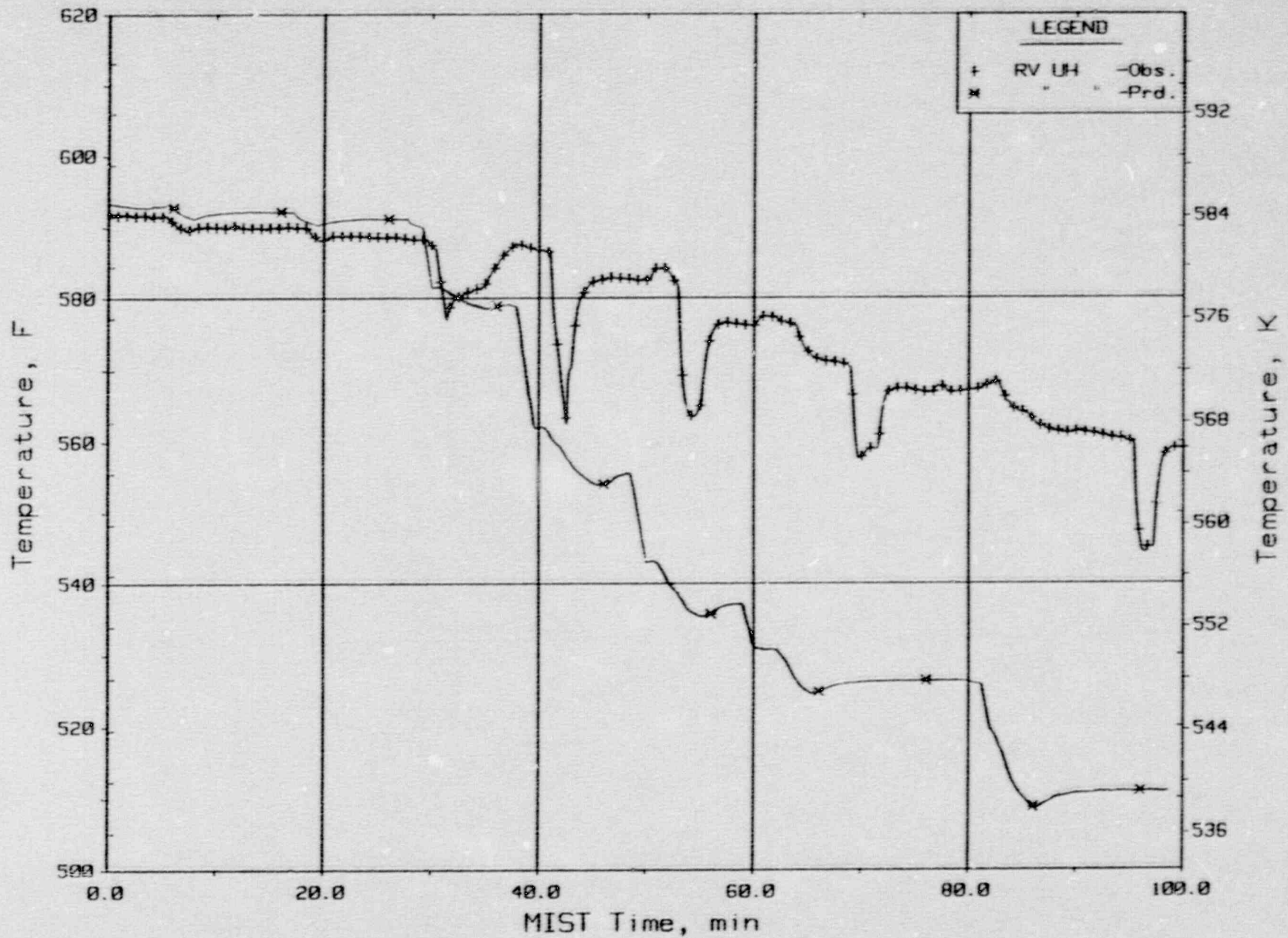


Figure 3.3.35. Reactor Vessel Upper Head Fluid Temperatures (RVTC23).

### 3.4. MIST Test 3502CC Post-Test Prediction

MIST test 3502CC was termed the noncondensable gas (NCG) threshold test. In this test the primary system was drained to approximately 62% of the initial mass inventory. A stable pool and high elevation boiler-condenser mode (BCM) of cooling was established and controlled at steady-state. Upon achieving these system conditions, the leak was isolated and the high pressure injection (HPI) flow was left in the off condition. The new steady-state, which is defined in Table 3.4.1., was maintained for approximately forty minutes. At 267 minutes into the test, helium gas injection into the reactor vessel lower plenum was begun. The NCG was injected at a rate of 20 standard cubic feet per hour (SCF) and continued for three hours. The NCG migrated to the steam generator tubes and interrupted primary side condensation which resulted in a relatively constant repressurization rate. A detailed test description may be found in the MIST Group 35 Report.

The effects of the NCG heat transfer degradation was the emphasis of this post-test prediction. In order to minimize the computer time required for the code simulation, the base post-test prediction model was re-initialized at the conditions present at the time of the helium injection. The steady-state effort required several base case modifications which will be described in the next subsection. Upon completion of these modifications the final steady-state and subsequent transient calculations were begun.

#### 3.4.1. MIST Test 3502CC Base Case Modifications

The RELAP5/MOD2 base input model was modified as follows to allow the new steady-state and transient calculations to be performed.

1. Input helium as the NCG;
2. Modify the nominal second transient initiation step (trip 510) so that the decay heat ramp, secondary depressurization, and HPI do not initiate;
3. Add the NCG addition volume and junction and include control variables to track the NCG addition and migration;
4. Modify the RVVV model to hold open one of the four valves over the duration of the test;
5. Change the secondary control level to 31.6 feet;

6. Maintain a constant core power of 46.5kw;
7. Adjust the initial conditions to be consistent with the test conditions at 267 minutes into the test;
8. Make miscellaneous time step and minor edit variable additions or changes; and
9. Make a slight modification to the steam generator volume heights near the pool level to minimize the crossing of the volume boundary during the steady-state calculations.

These changes are documented in detail in the calculational file for this test. In addition to these changes a temporary code version was utilized. The temporary code version included simple modifications to the conditionally certified version 7.0B of RELAP5/MOD2. These modifications included: high AFW heat transfer model restart capability, a user input option to neglect the liquid velocity direction as a criteria for high AFW heat transfer mode, and additional under-relaxation of the interface heat transfer coefficients. Each of these modifications have been included in the subsequent version 8.0 of RELAP5/MOD2 which was ultimately conditionally certified. These changes provided the capability to smooth the steam generator heat transfer during the steady-state calculations such that moderate oscillations were given additional damping.

#### 3.4.2. MIST Test 3502CC Transient Comparisons

The initial conditions for the RELAP calculation are consistent with the test conditions at 267 minutes. Table 3.4.1. contains a listing of test and RELAP calculated initial conditions. It should be noted that the RELAP analysis began at a time of zero. The first minute of the analysis allowed the transient initialization terms to die out prior to full NCG injection. On all final comparison plots the RELAP time has been adjusted such that one minute coincides with 267 minutes from the actual test time.

The core power, secondary pressure, and the secondary collapsed level were the only defined parameters at 267 minutes. The remainder of the parameters were determined from the transient history prior to that time. All cold leg pump discharge piping was nearly completely voided. The pump suction piping was at the pump spill-over elevation.

The most significant difference between the RELAP initialization and the test conditions is the steady-state steam generator heat load distribution. The previous transient history produced facility conditions that allowed the loop A steam generator to consistently remove approximately seventy percent of the core power. The RELAP calculations oscillated when these conditions were imposed perturbing the steady-state. Therefore, to minimize these oscillations the benchmark was set-up in a symmetrical mode. The impact of this difference was very minimal. The only real effect was to increase the loop B primary steam generator exit temperature a few degrees. Since the loop flows were near zero, the effect of this temperature difference was never observed.

The initial conditions of this test were obviously quite different from the nominal natural circulation initialization. The calculations began with a steam generator high and pool BCM heat transfer. Although the facility found a rather stable steady-state, RELAP did not observe the same success. The RELAP calculations resulted in a pseudo-steady oscillatory behavior. As the steady-state calculations were executed for longer periods the oscillations often became more erratic. They were typically initiated by steam generator primary mixture levels crossing volume interfaces. Since the pool regions of both the primary and secondary are moderately subcooled, a significant primary side condensation potential existed. Downward fluctuations in the primary mixture level from small system perturbations (i.e. hot leg nozzle steam flows, heat transfer, loop asymmetries, etc.) sometimes caused the level to descend into the next lower control volume. The interface heat transfer condensed steam to bring the liquid toward saturated conditions. The result was a sharp primary pressure reduction. The rise in the primary liquid temperature induced more primary-to-secondary heat transfer and more steam condensation. The primary condensation increased the tube mixture levels, which usually resulted in small spill-overs of subcooled liquid from the pump suction piping into the voided discharge piping and even more steam condensation. Fairly large primary pressure reductions would be encountered during these periods, which would eventually halt as the primary mixture levels returned into the original upper-most two-phase control volume. This cycle would repeat itself periodically, especially after the levels returned

to the upper volume and the primary pool once again cooled to near the secondary saturation temperature.

In order to avoid these oscillations, the levels were adjusted slightly to minimize these cycles for the beginning of the transient calculations. The transient began one minute into the RELAP calculations (267 minutes test time) to allow one of these cycles time to run its course. Following NCG injection, the condensation degradation was expected to minimize the heat transfer oscillations which was believed to be the most obvious contributor to these cycles. Unfortunately, the NCG accumulation in the steam generator was unable to preclude a cycle at 269 minutes. The effects of this cycle can be seen in the attached comparison plots shown in Figures 3.4.1. through 3.4.34. These plots used the MIST final revised test data. The sequence of events for this calculation is shown in Table 3.4.2.

At 268.9 minutes the primary mixture level of both steam generators descended from the sixth axial level into the fifth axial level. A pressure decline of approximately 30 psi was observed during this period which lasted 45 seconds. Following this period, the primary pressure started a slow repressurization due to the NCG retarding of the condensation in the steam generators. As the system repressurized, the amounts of steam and NCG in the hot leg and upper steam generator tubes gradually increased. The vapor accumulation slowly displaced the steam generator primary mixture level downward. The displaced liquid continuously spilled-over the pump bottom elevation until 282.7 minutes. At that time, the mixture level in the tubes temporarily receded from the fifth to the fourth axial volume in both steam generators. The associated interface heat transfer resulted in rapid steam condensation and a 35 psi drop in system pressure. The depressurization duration was one minute. Afterward, the calculations produced a primary system repressurization rate similar to the test data. Another depressurization cycle was beginning at 292 minutes. This cycle appeared to begin with a pump liquid spill-over which condensed steam in the cold leg pump discharge piping, thus inducing more liquid spill-over. The loss of the cold leg pump suction liquid inventory decreased the steam generator tube levels into the next lower control volume. The result would probably be a cycle similar to the previous two.



Table 3.4.1. MIST Test 3502CC Calculated and Measured  
Initial Steady-State Conditions

Parameter	Data	RELAP5
Primary Pressure, (psia)	1219.	1210.
SG A Secondary Pressure*, (psia)	1015.	1010.
SG B Secondary Pressure*, (psia)	1016.	1010.
SG A Secondary Collapsed Level*, (ft)	30.05	31.62
SG B Secondary Collapsed Level*, (ft)	30.25	31.61
SG A Primary Collapsed Level, (ft)	30.71	32.95
SG B Primary Collapsed Level, (ft)	30.52	31.80
Hot Leg A Collapsed Level, (ft)	25.77	29.51
Hot Leg B Collapsed Level, (ft)	24.92	28.03
Reactor Vessel Collapsed Level, (ft)	18.50	16.84
Downcomer Collapsed Level, (ft)	18.66	17.48
Pressurizer Collapsed Level, (ft)	18.67	17.96
Core Power*, (Btu/s)	43.79	44.07
Primary Side Mass Inventory	610.0	616.8
SG A Primary Exit Temperature, (F)	533.1	538.0
SG B Primary Exit Temperature, (F)	498.6	508.4
Core Inlet Temperature, (F)	559.3	559.3

\*Denotes specified condition.

Table 3.4.2. MIST Test 3502CC Sequence of Events Comparisons

Event	Time (Minutes)	
	Test Data	RELAP
RELAP Calculations Begin	--	266.0
NCG Injection Begins	267.0	267.0
Primary Side Mixture Level	--	268.9
Declined into the Next Lower	--	282.7
Control Volume	--	292.3
RELAP Calculations Stopped	--	292.6

3.4.3. MIST Test 3502CC Post-Test Conclusions

RELAP tended to calculate the observed repressurization rate during the intervals where the primary mixture levels resided continuously within the confines of the fifth axial control volume. This behavior indicates that the transport and condensation degradation of the helium are reasonable for this type of application. Problems are encountered when the primary mixture levels cross control volume boundaries. During these intervals the calculations diverge significantly from expected behavior. This problem is magnified in cases like test 3502CC, where the primary fluid within the pool region remains at or below the secondary saturation temperature. Any pressure differential between the primary and secondary results in the generation of a significant primary steam condensation potential on the subcooled primary liquid within the pool region. As volume boundaries are crossed, the code interface heat and mass transfer condense steam as it brings the liquid within that control volume toward saturation conditions. RELAP obviously over-predicts these terms in the presence of NCGs. These terms should be more fully degraded, similar to the wall heat and mass transfer.

One method for utilizing the code with its present formulation is to devise noding schemes which utilize larger steam generator volumes. With fewer control volumes, the boundaries will not be traversed as often. Unfortunately, transient history may need to be known prior to beginning the calculation such that the interfaces may be appropriately determined. If boundaries are

still traversed, the interface condensation will be worse because of the larger liquid mass. Also, a more coarse noding arrangement may not give adequate detail for other applications (i.e. high power and flow, natural circulation, interrupted flow, etc. transients).

On the other hand, a finer discretization may minimize the amount of steam condensation due to the smaller mass content per volume. The detail may also provide smoother behavior for other transients as well. However, the higher nodal densities are not desirable from an economic viewpoint. Also, in transients such as 3502CC with oscillatory levels, additional volumes mean that the number of interface crossings will be greater. The likely result would probably be similar in nature, however, more depressurization cycles would be encountered resulting in too much interface heat transfer. The over-prediction of the interface heat transfer in the presence of NCGs is still encountered. Therefore, a code formulation change seems to be needed to correct this problem.

# MIST NCG Threshold - Test 3502CC

## Observed Vs. Predicted

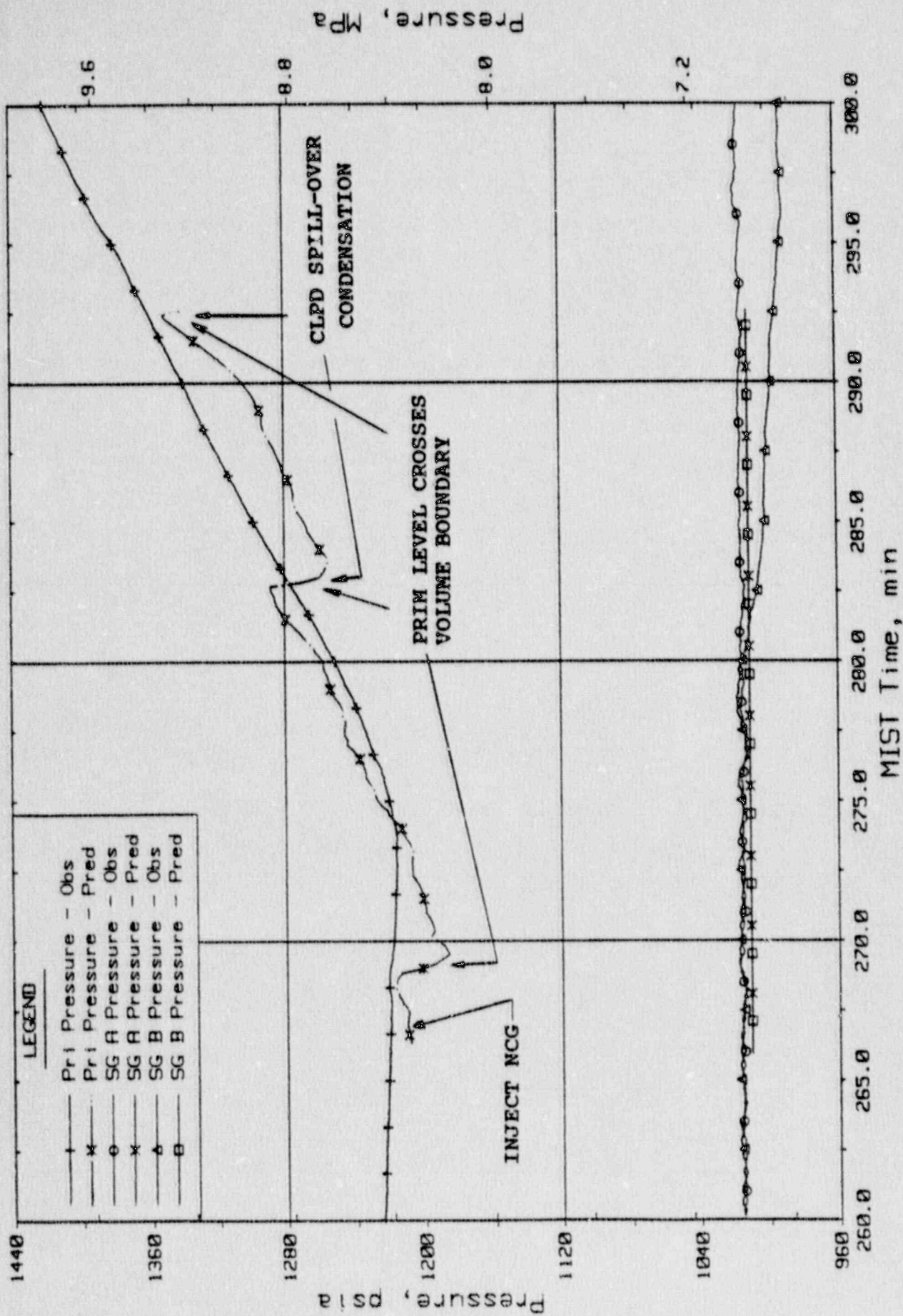


Figure 3.4.1. System Pressures.

# MIST NCG Threshold - Test 3502CC

## Observed Vs. Predicted

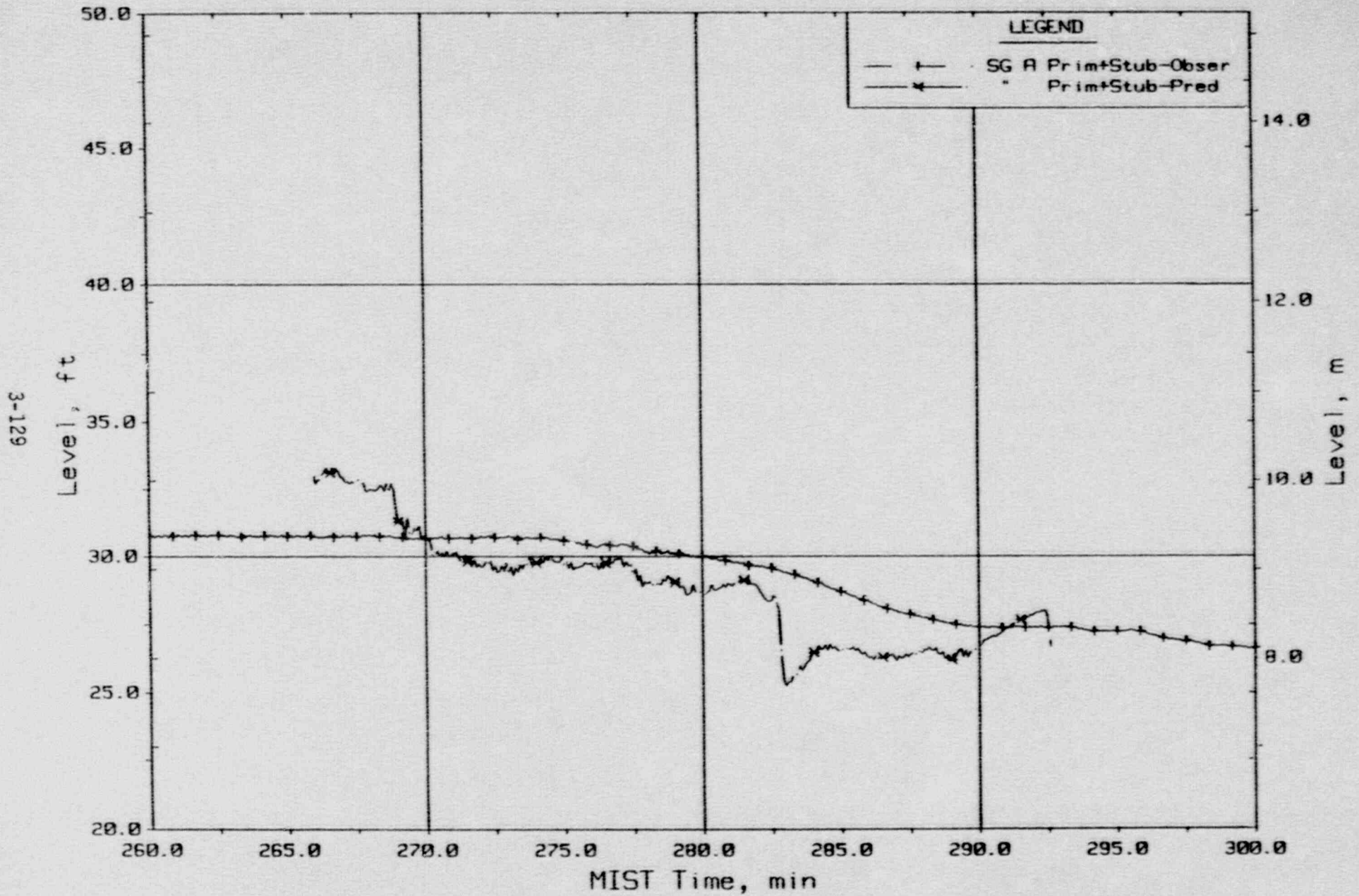


Figure 3.4.2. Steam Generator A Primary + Stub Level.

MIST NCG Threshold - Test 3502CC  
Observed Vs. Predicted

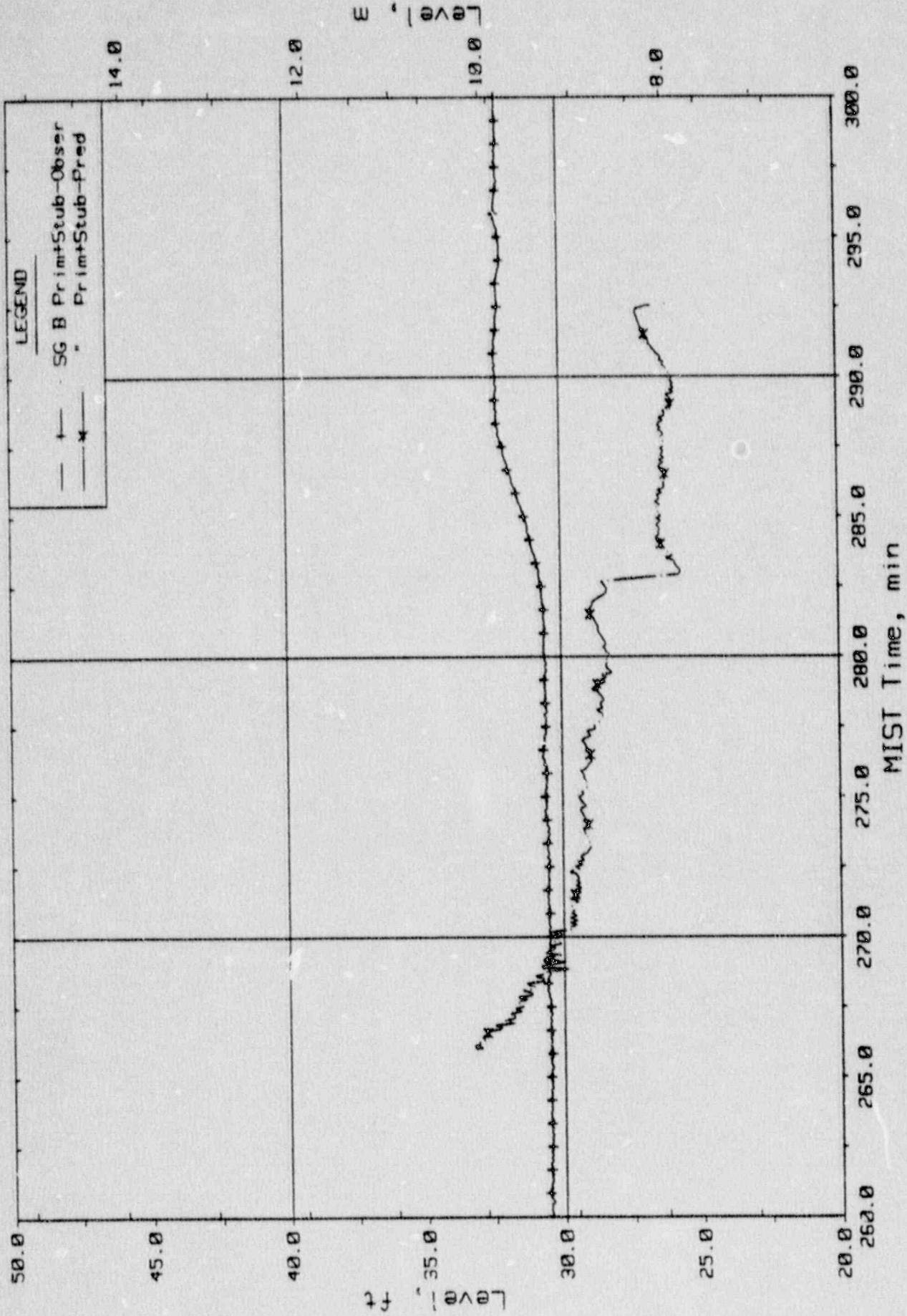


Figure 3.4.3. Steam Generator B Primary + Stub Level.

MIST NCG Threshold - Test 3502CC  
Observed Vs. Predicted

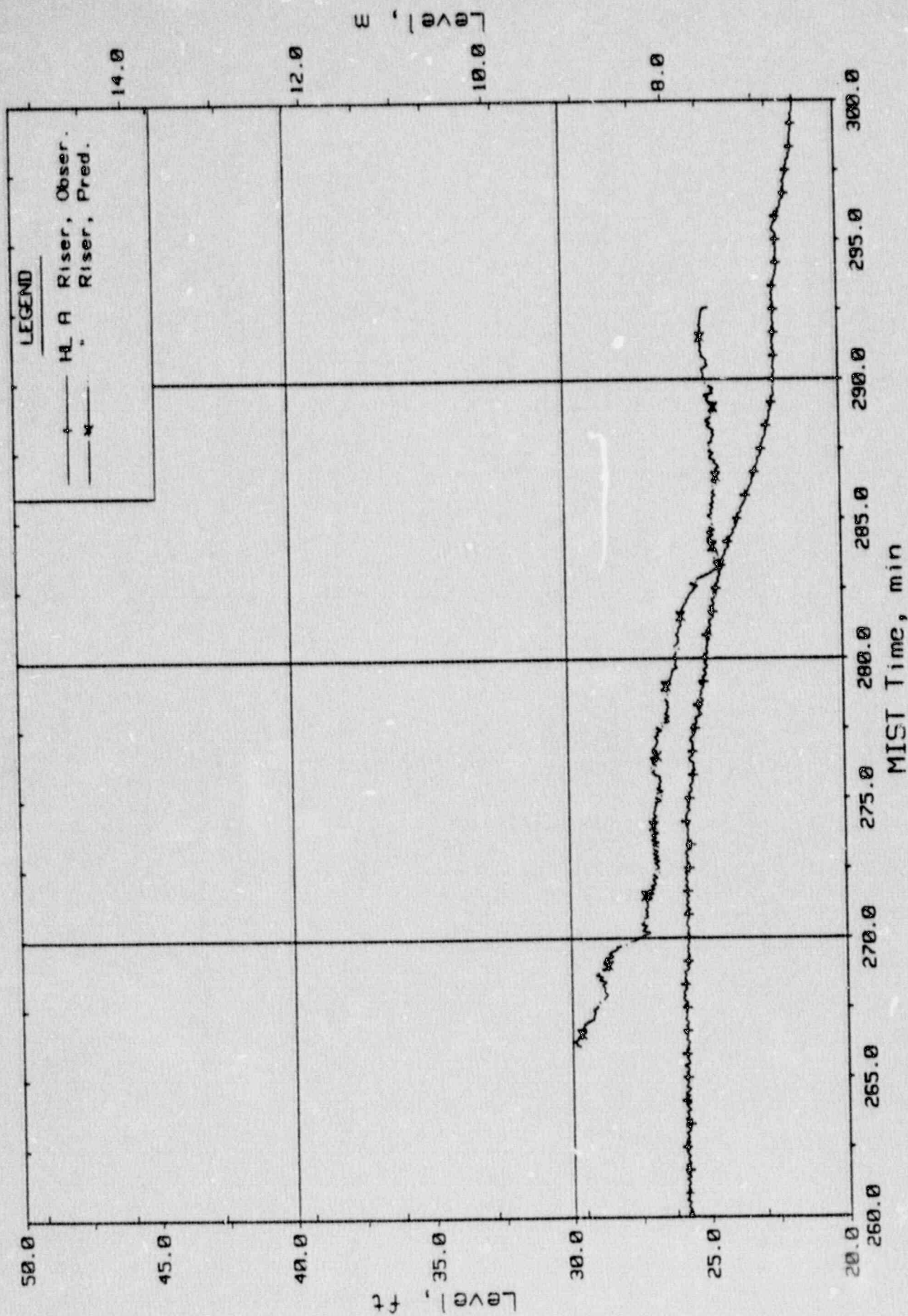


Figure 3.4.4. Hot Leg A Riser Level.

MIST NCG Threshold - Test 3502CC  
 Observed Vs. Predicted

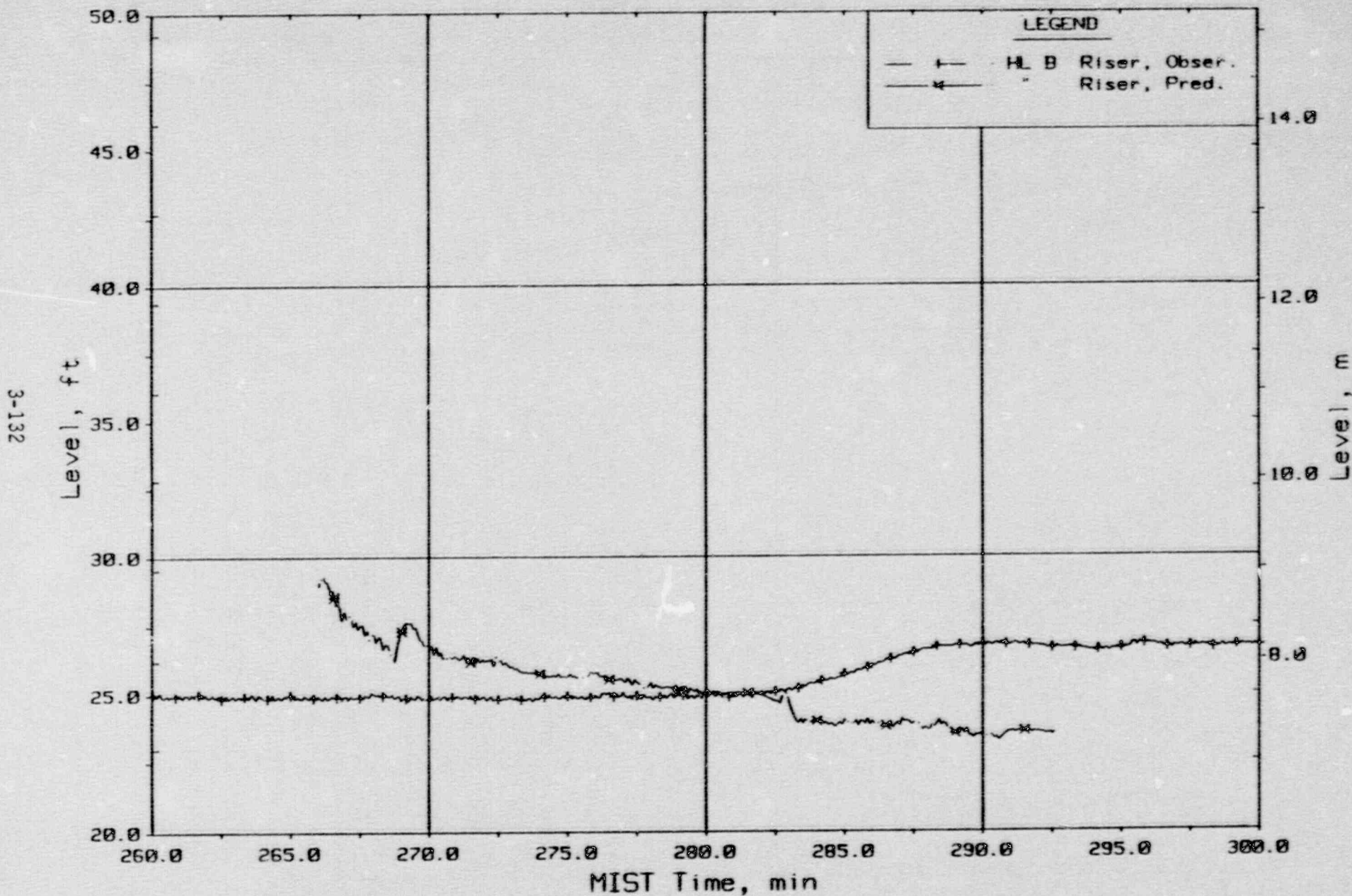


Figure 3.4.5. Hot Leg B Riser Level.



MIST NCG Threshold - Test 3502CC  
Observed Vs. Predicted

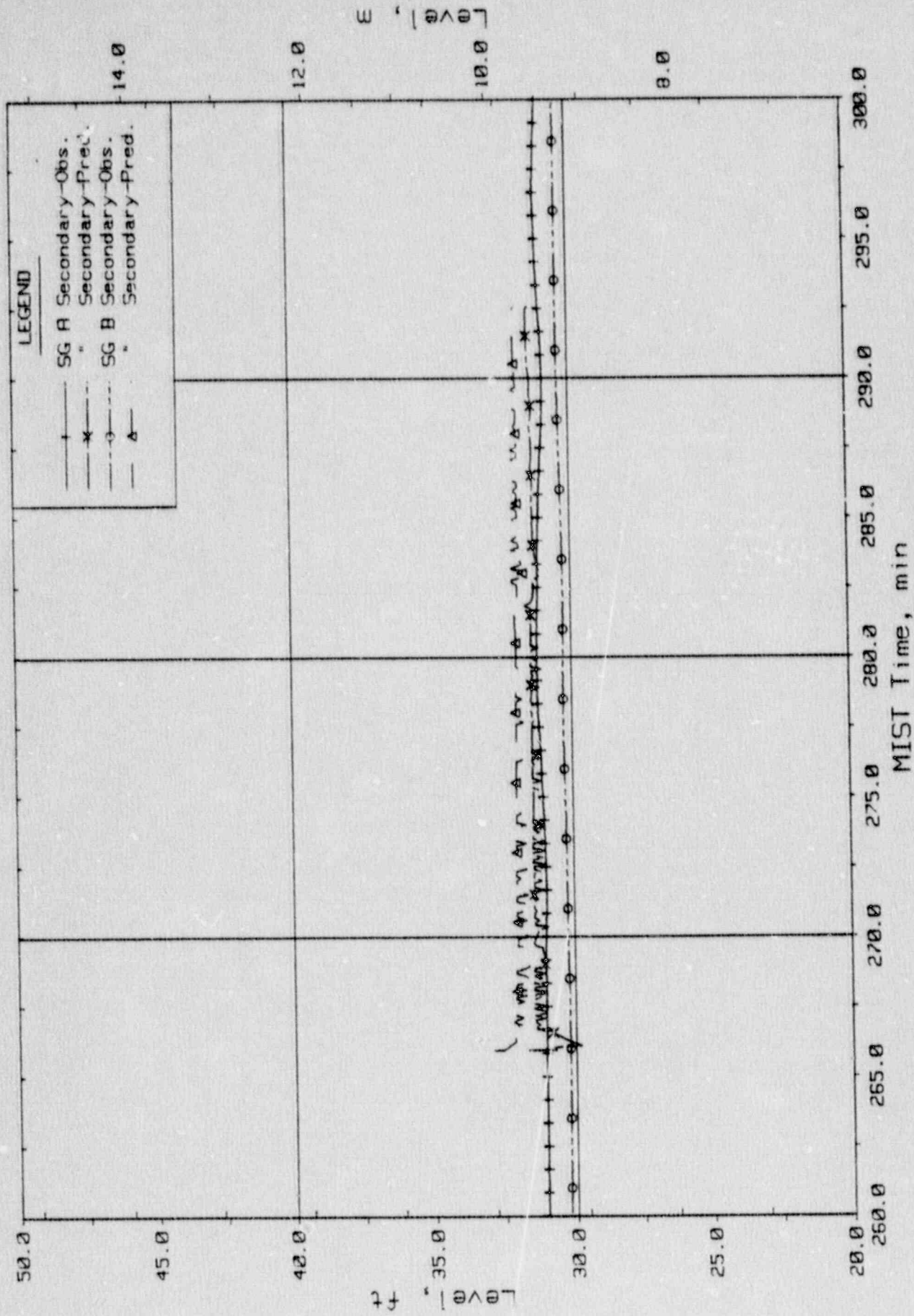


Figure 3.4.6. Steam Generator Sec. Collapsed Liquid Levels.

MIST NCG Threshold - Test 3502CC  
Observed Vs. Predicted

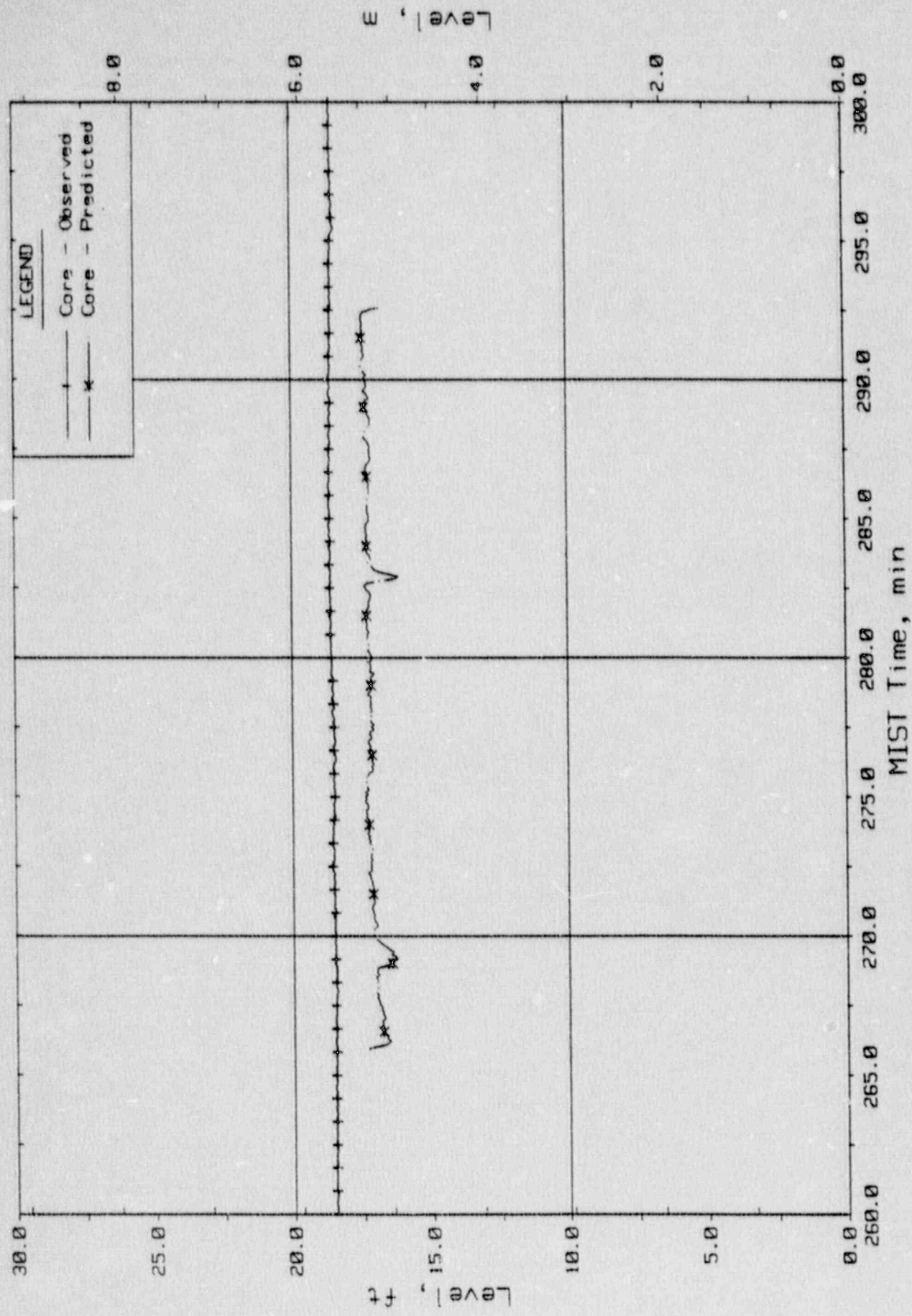
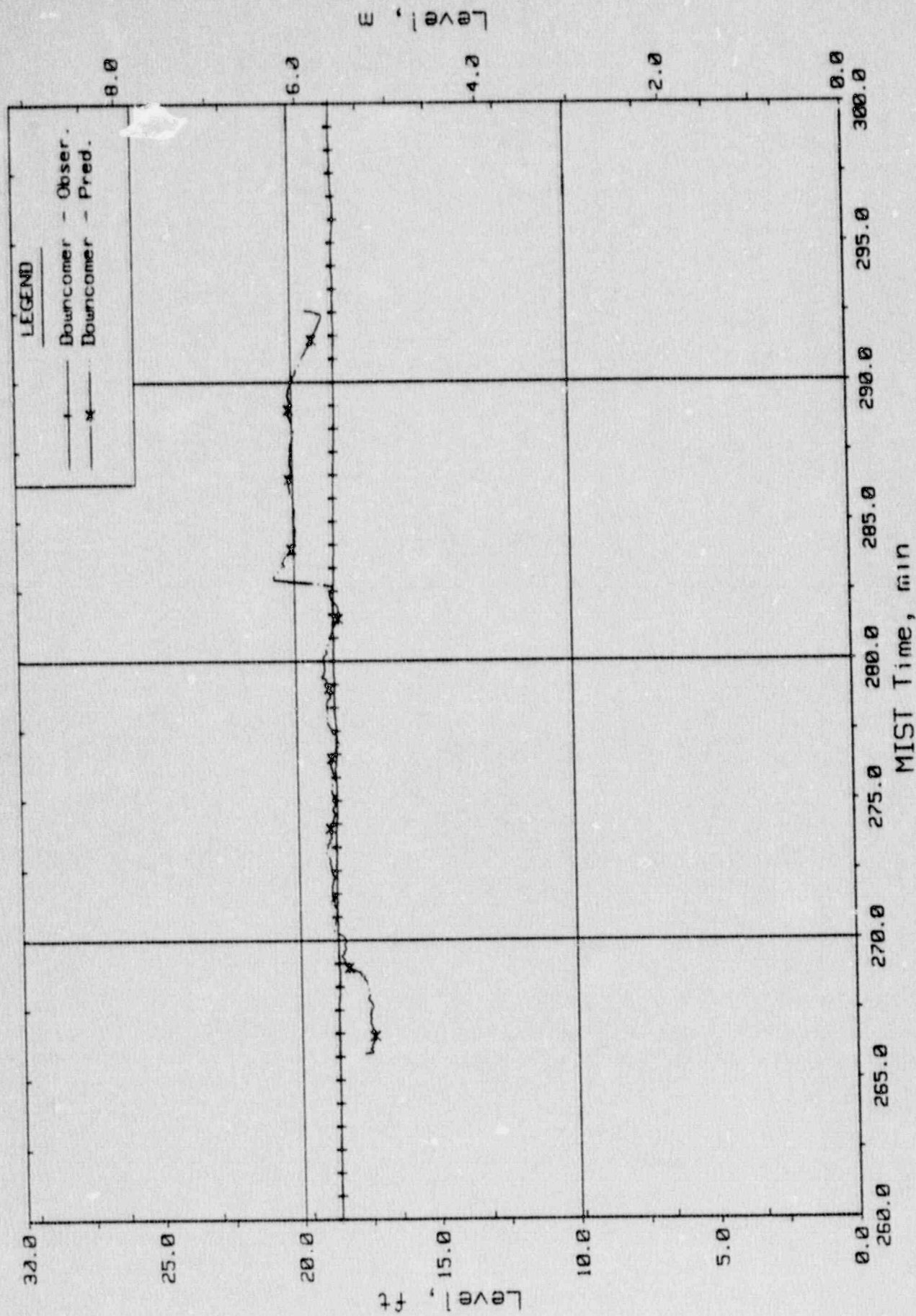


Figure 3.4.7. Core Region Collapsed Liquid Levels.

MIST NCG Threshold - Test 3502CC  
Observed Vs. Predicted



3-135

Figure 3.4.8. Core Region Collapsed Liquid Levels.

# MIST NCG Threshold - Test 3502CC

## Observed Vs. Predicted

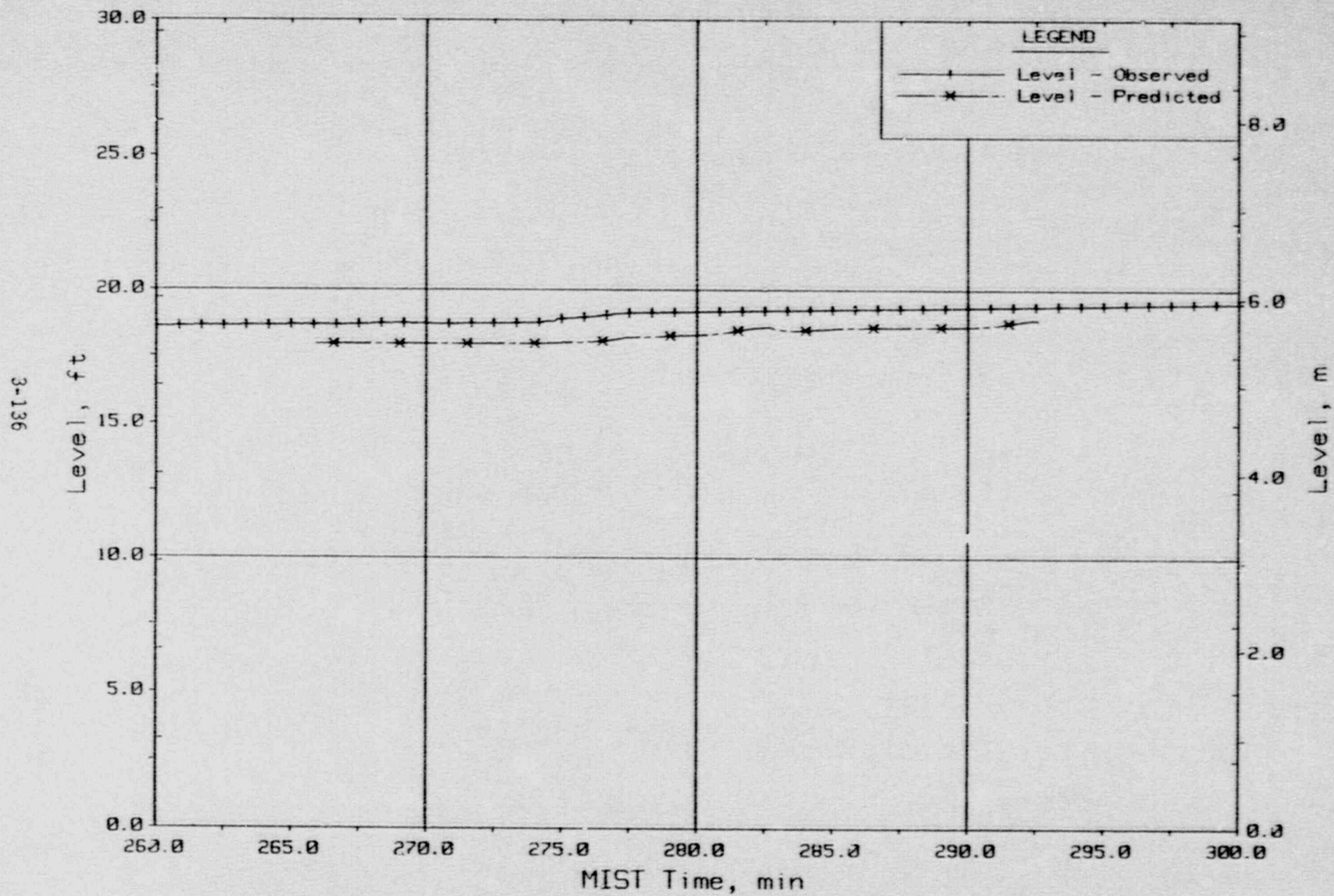


Figure 3.4.9. Pressurizer Collapsed Liquid Level (PZLV20).

MIST NCG Threshold - Test 3502CC  
 Observed Vs. Predicted

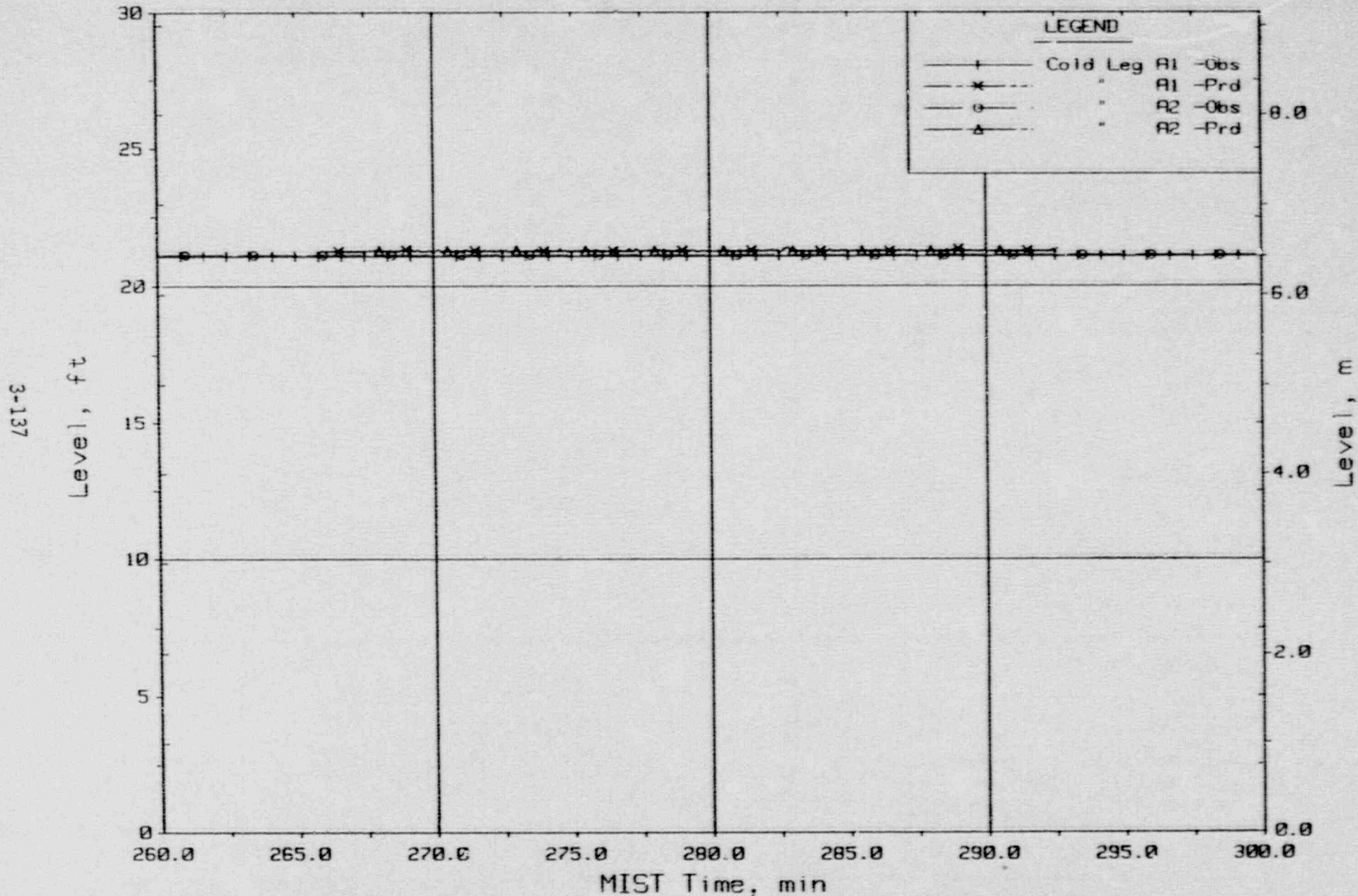


Figure 3.4.10. Cold Leg A Discharge Collapsed Liquid Levels (Cr'V23s).

MIST NCG Threshold - Test 3502CC  
 Observed Vs. Predicted

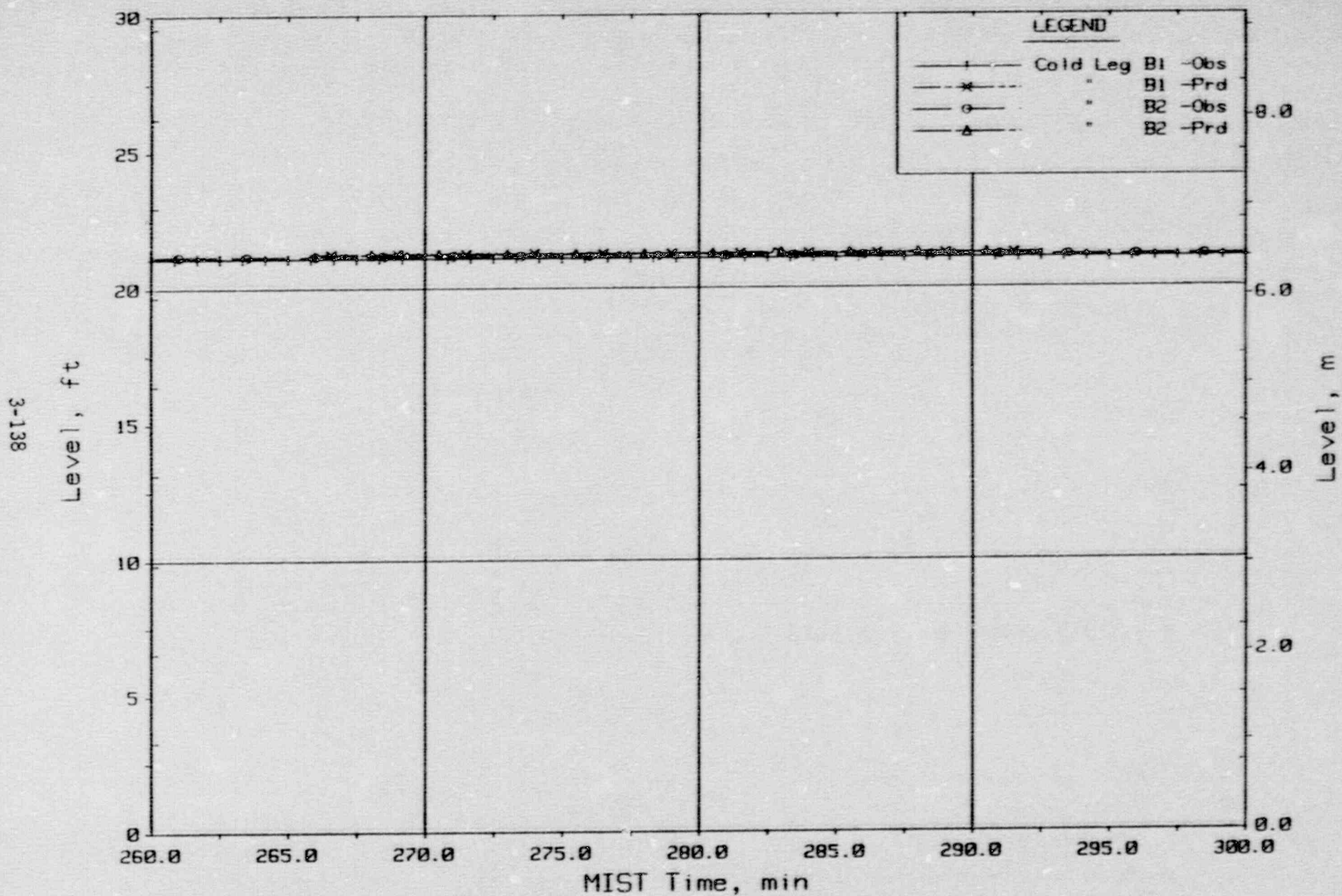


Figure 3.4.11. Cold Leg B Discharge Collapsed Liquid Levels (CnLY23s).

MIST NCG Threshold - Test 3502CC  
Observed Vs. Predicted

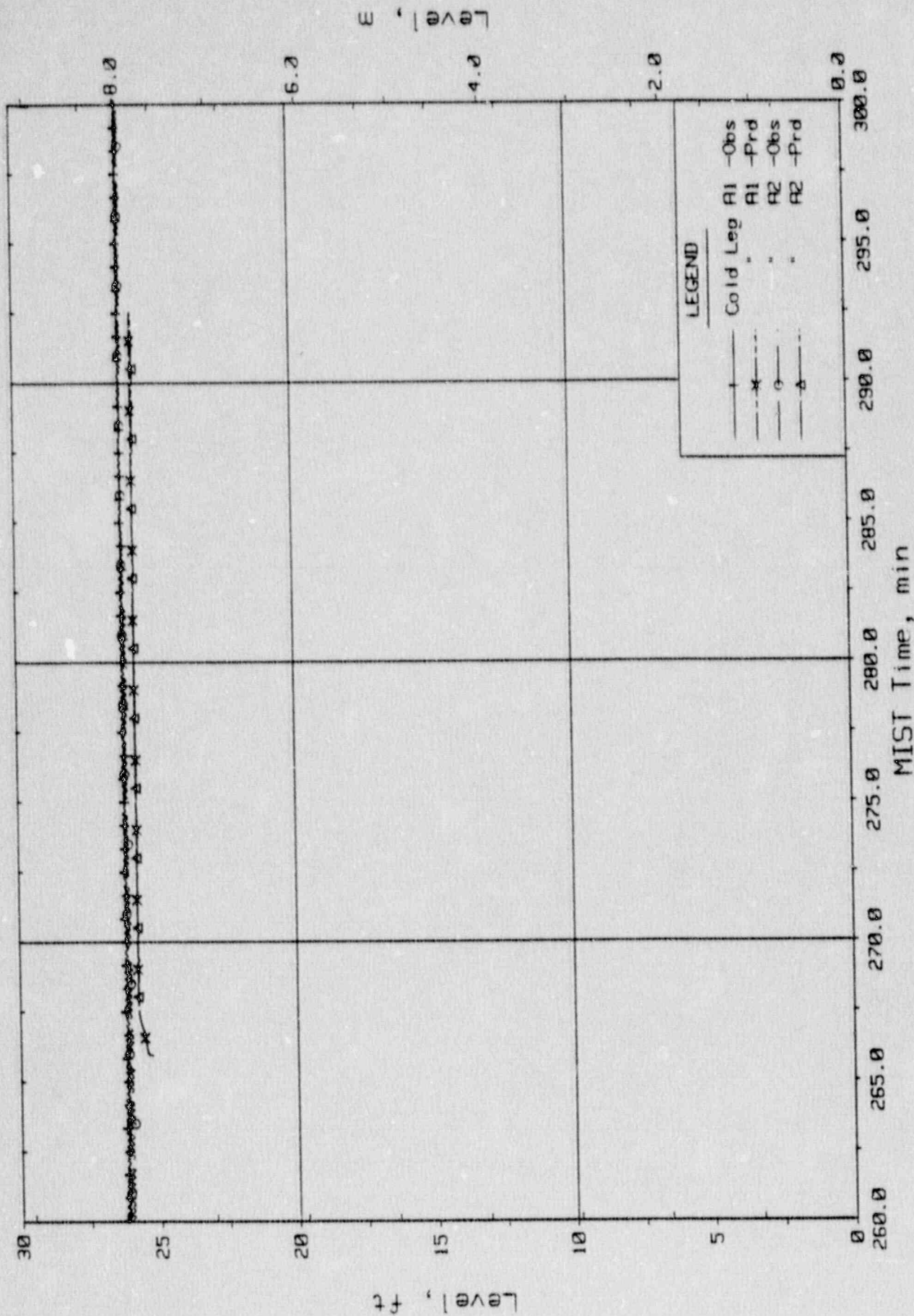


Figure 3.4.12. Cold Leg A Suction Collapsed Liquid Levels (CnLV22s).

MIST NCG Threshold - Test 3502CC  
 Observed Vs. Predicted

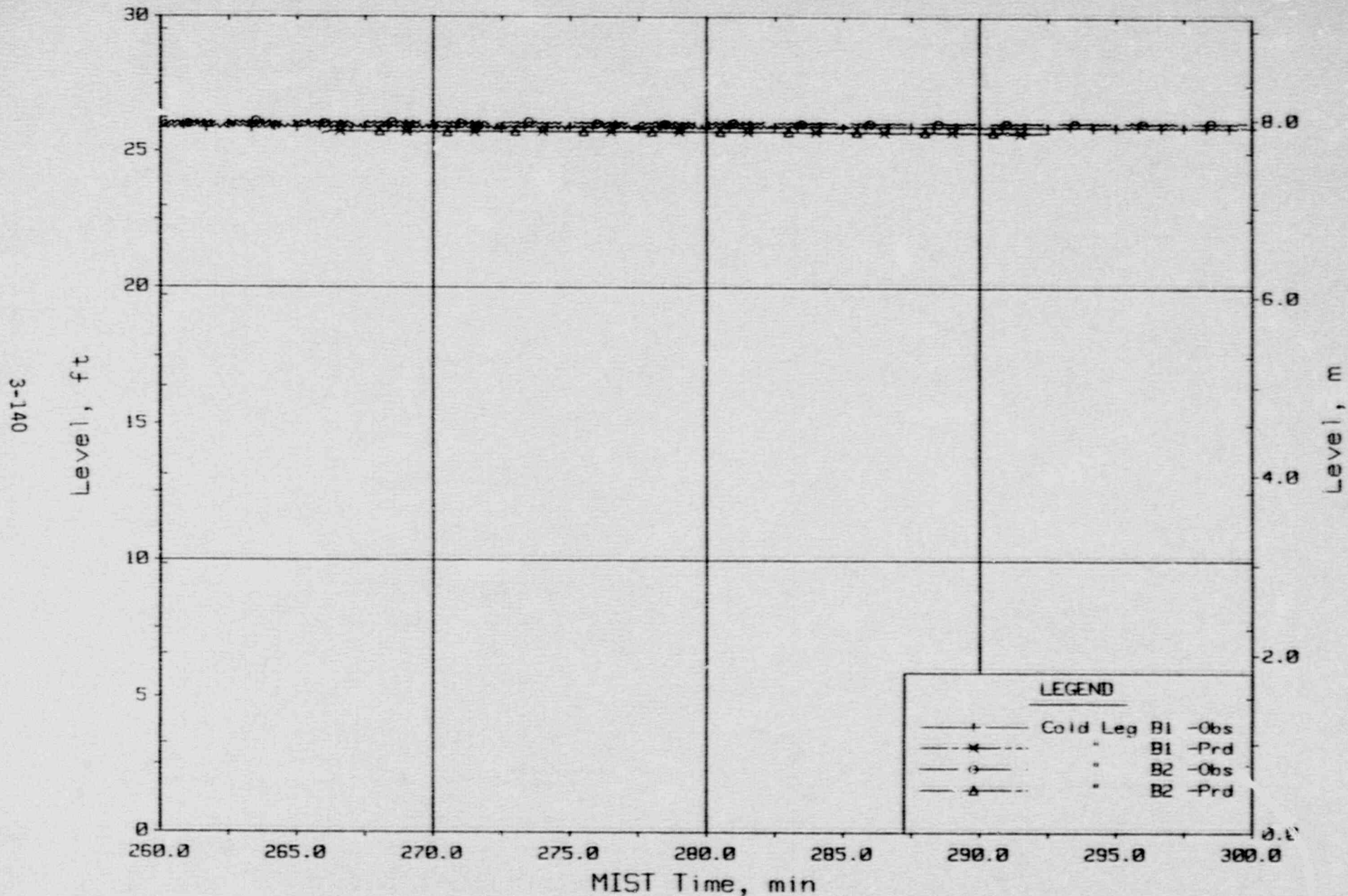


Figure 3.4.13. Cold Leg B Suction Collapsed Liquid Levels (CnLV22s).



MIST NCG Threshold - Test 3522CC  
Observed Vs. Predicted

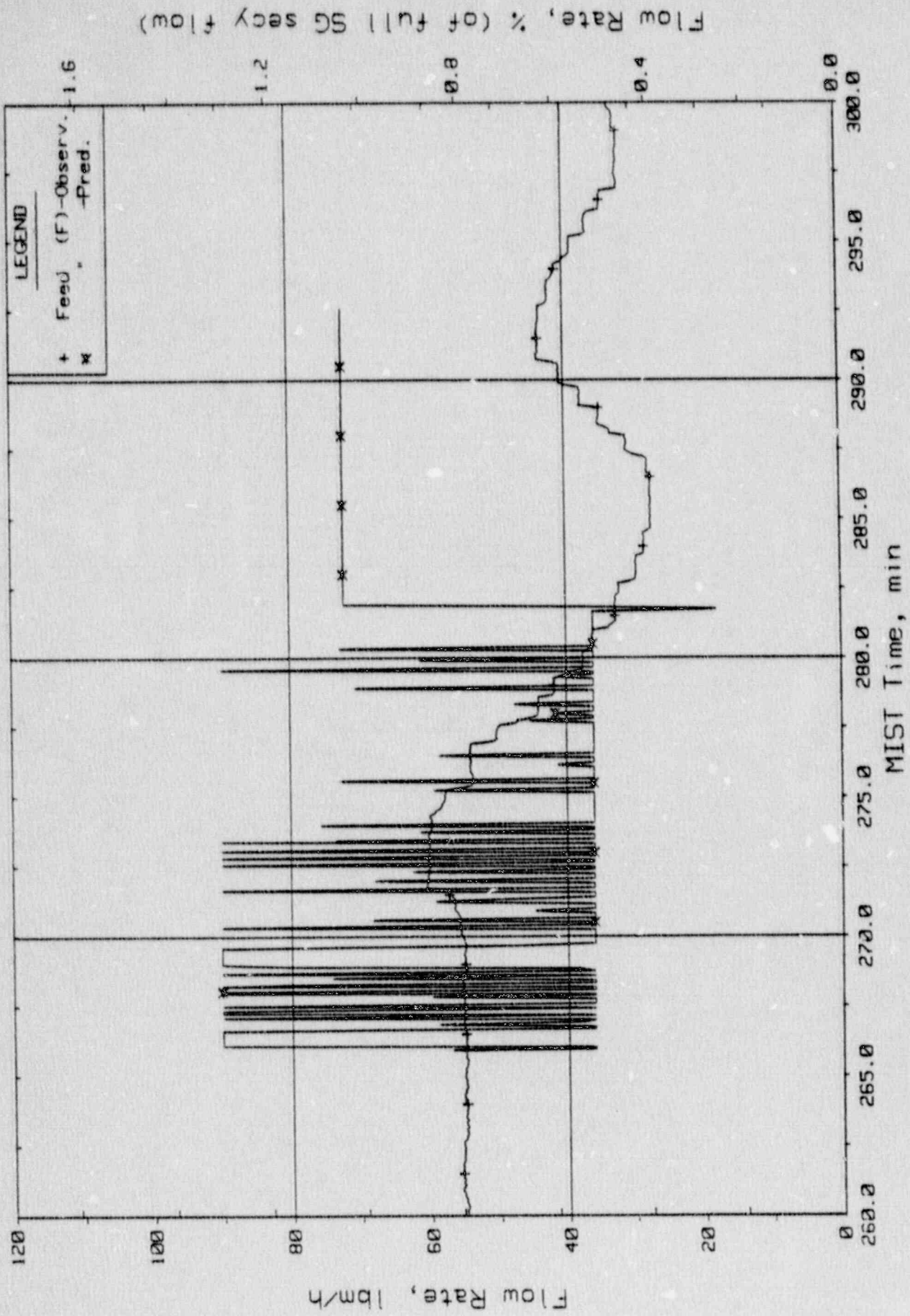


Figure 3.4.14. Steam Generator A Flow Rate (Ssfor20).

Csfor20

MIST NCG Threshold - Test 3502CC  
Observed Vs. Predicted

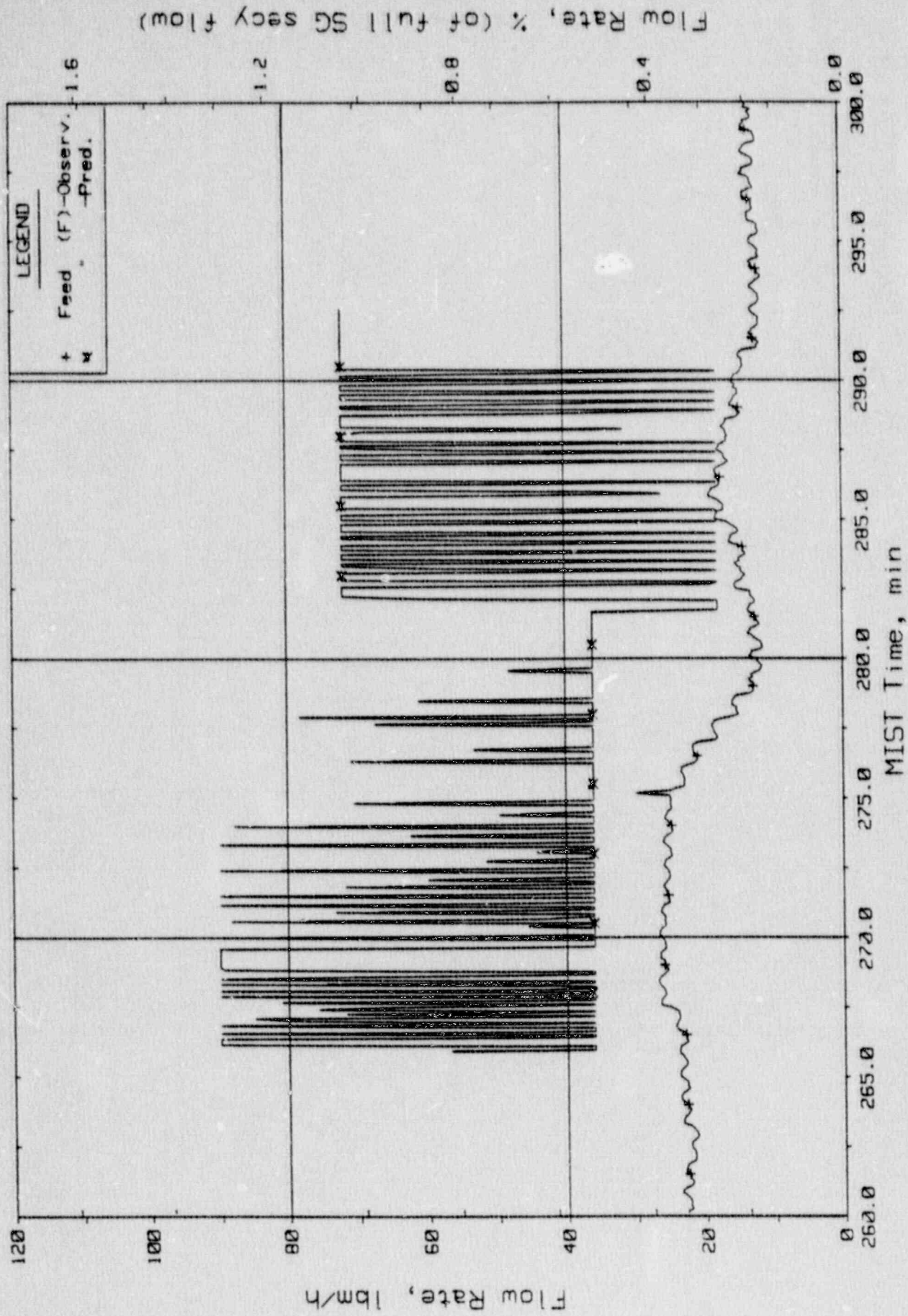


Figure 3.4.15. Steam Generator B Flow Rate (Ssfor21).

MIST NCG Threshold - Test 3502CC  
Observed Vs. Predicted

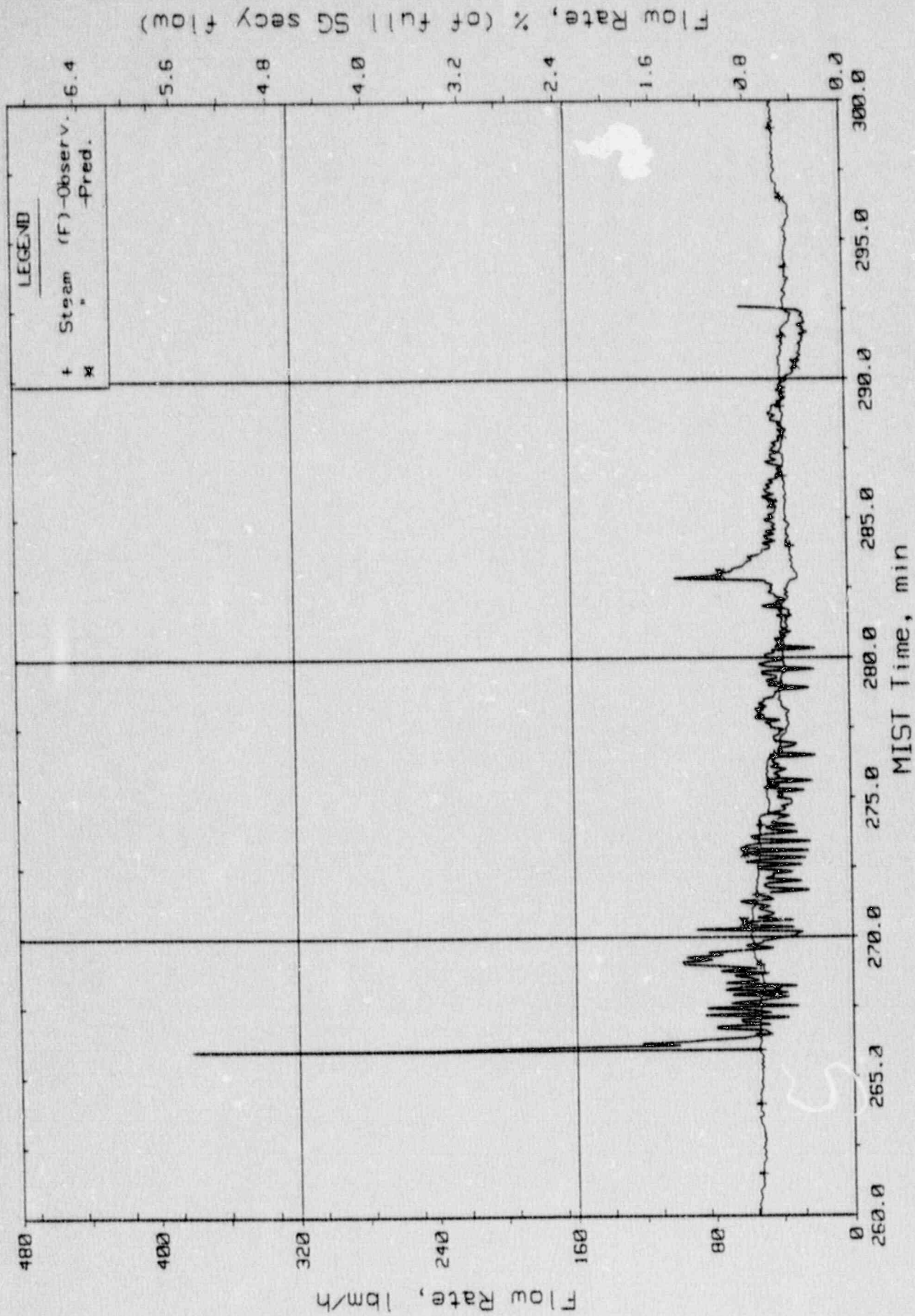


Figure 3.4.16. Steam Generator A Flow Rates (Cссор20).

Cссор20

MIST NCG Threshold - Test 3502CC  
Observed Vs. Predicted

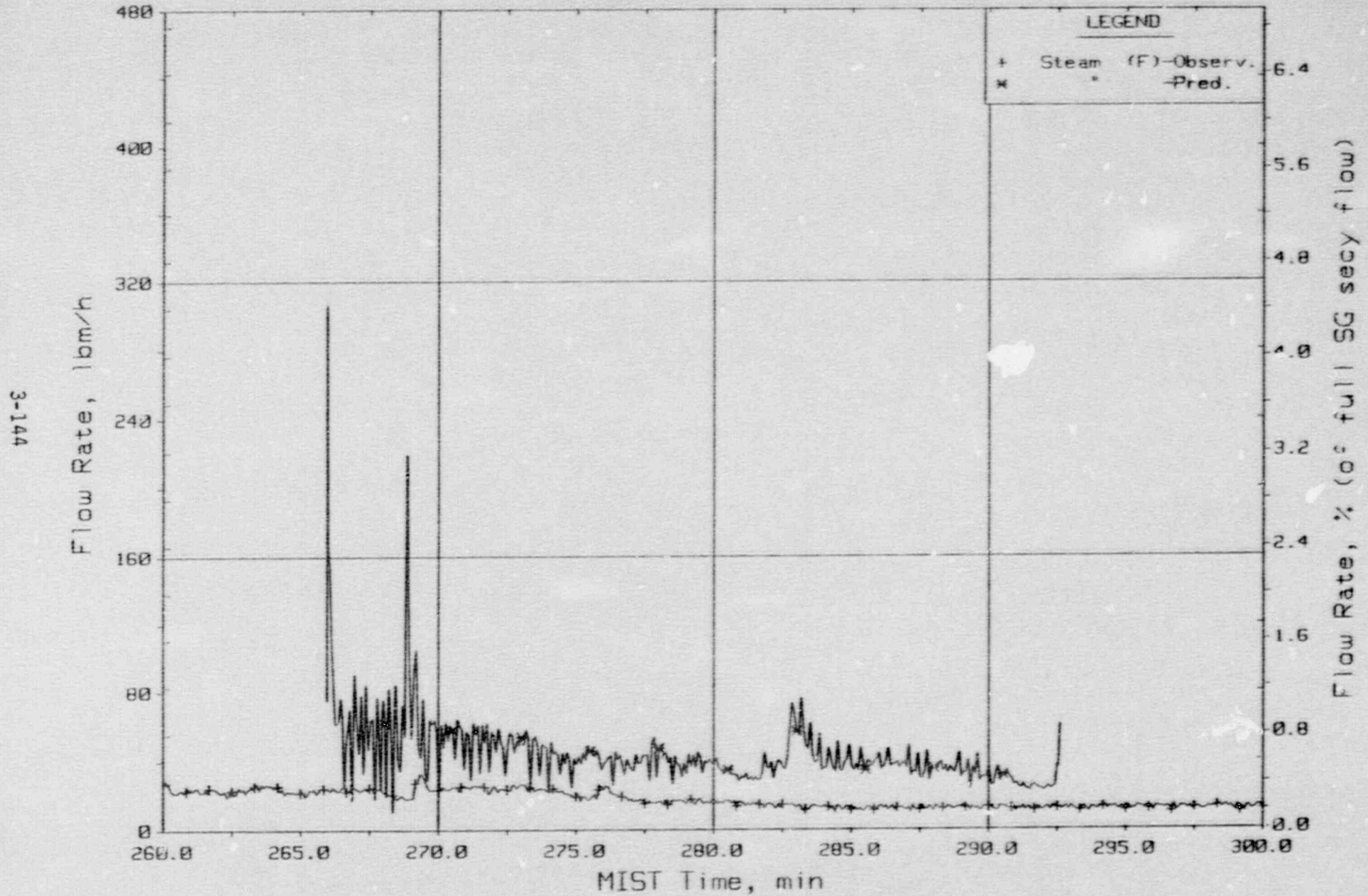


Figure 3.4.17. Steam Generator B Flow Rates (Sssor21).

MIST NCG Threshold - Test 35.320C  
Observed Vs. Predicted

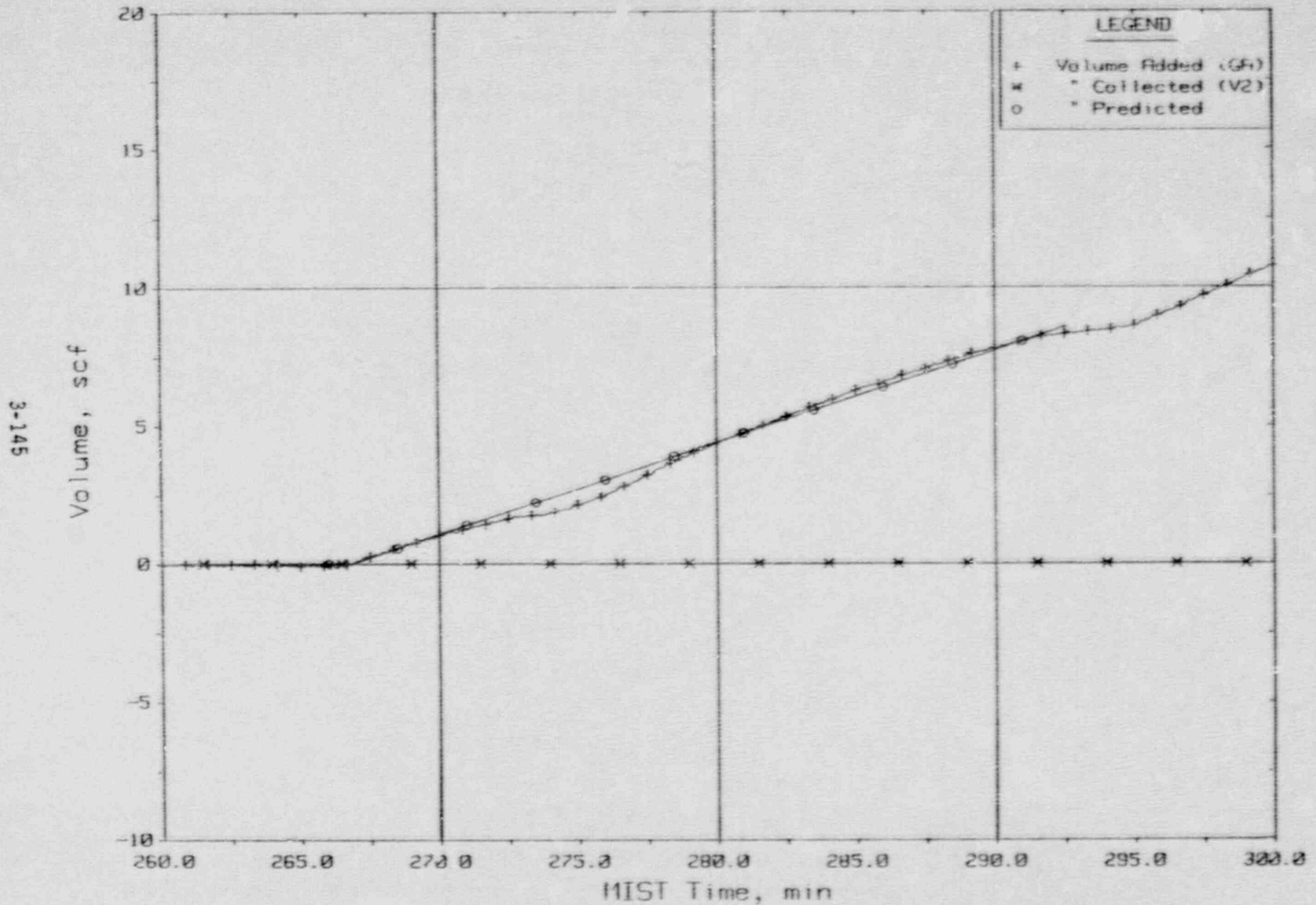


Figure 3.4.18. Noncondensibles Gas Volumes.

MIST NCG Threshold - Test 3502CC  
Observed Vs. Predicted

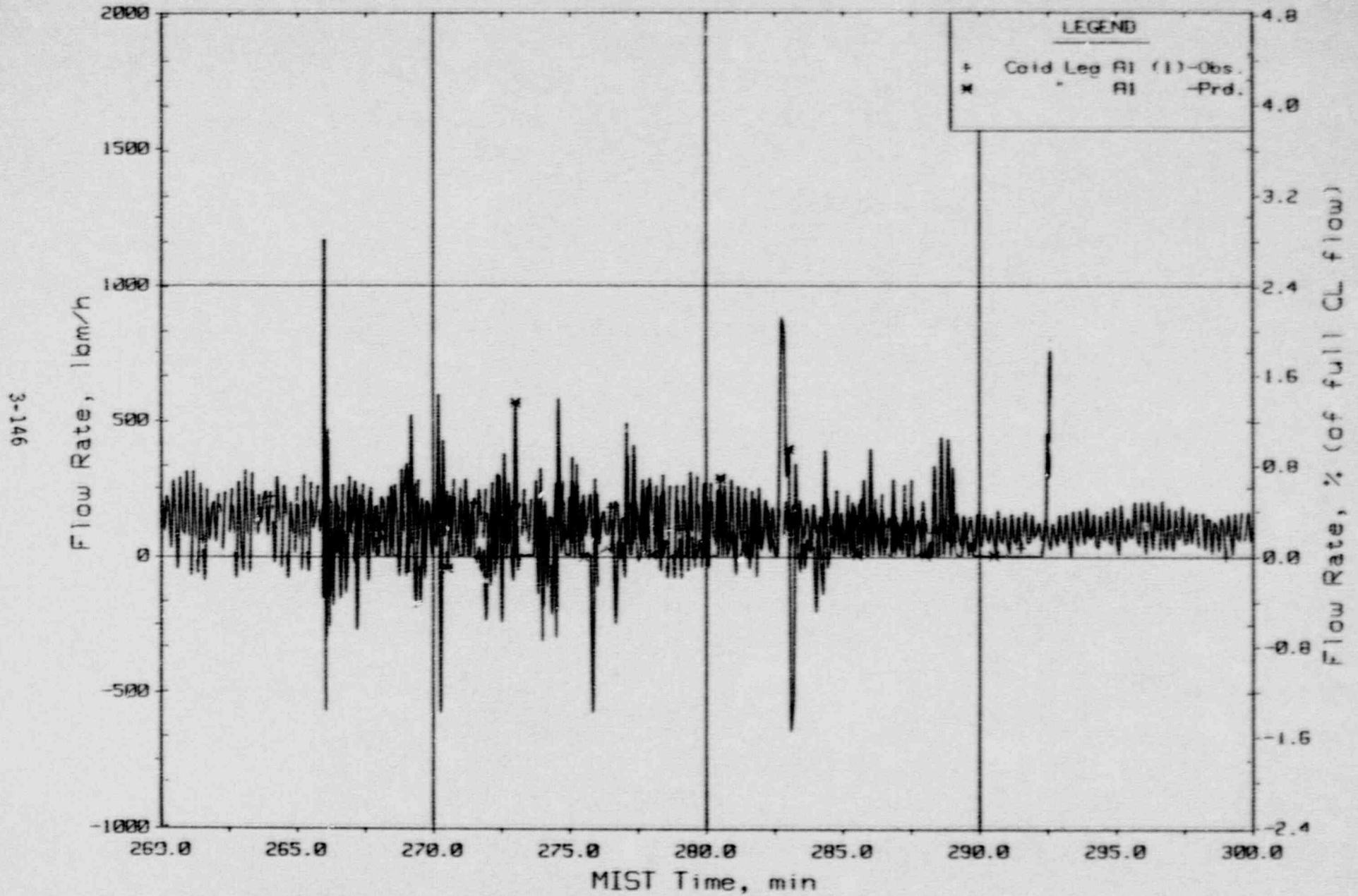


Figure 3.4.19. Loop AI Cold Leg (Venturi) Flow Rate (CIVN20).

MIST NCG Threshold - Test 3502CC  
Observed Vs. Predicted

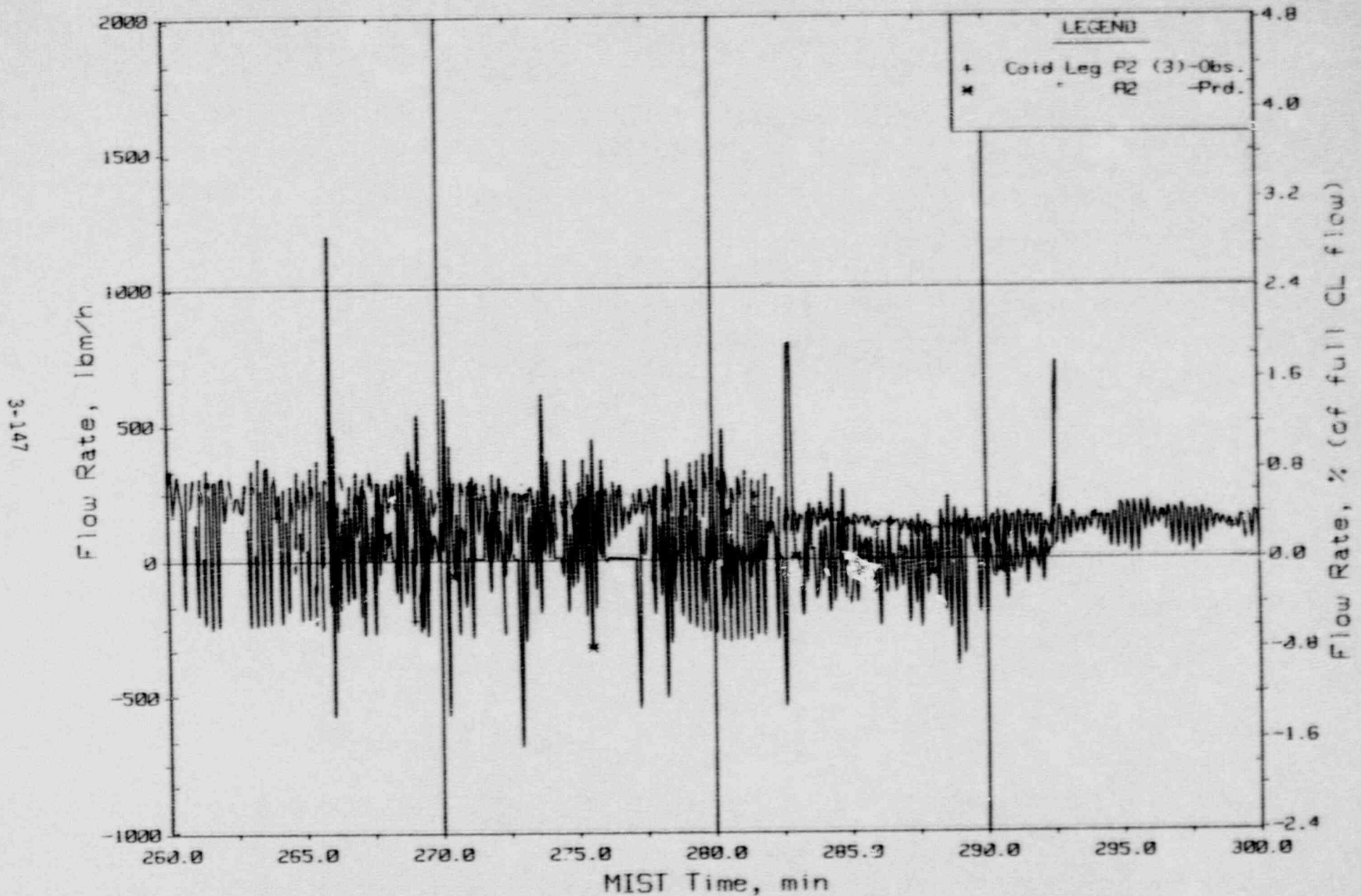


Figure 3.4.20. Loop R2 Cold Leg (Venturi) Flow Rate (C2VN20).

MIST NCG Threshold - Test 35200  
Observed Vs. Predicted

3-148

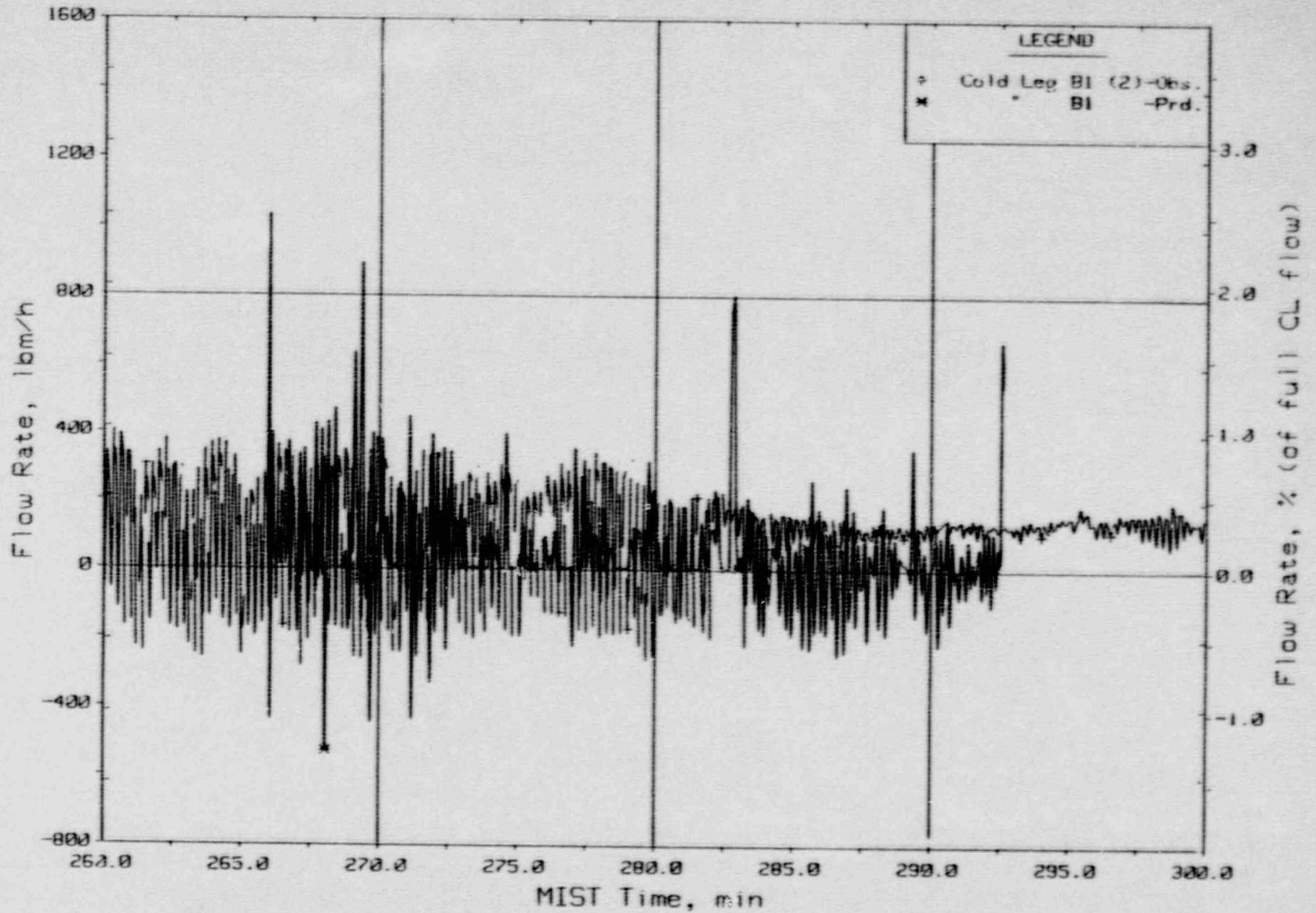


Figure 3.4.21. Loop BI Cold Leg (Venturi) Flow Rate (CIVN20).



MIST NCG Threshold - Test 3502CC  
Observed Vs. Predicted

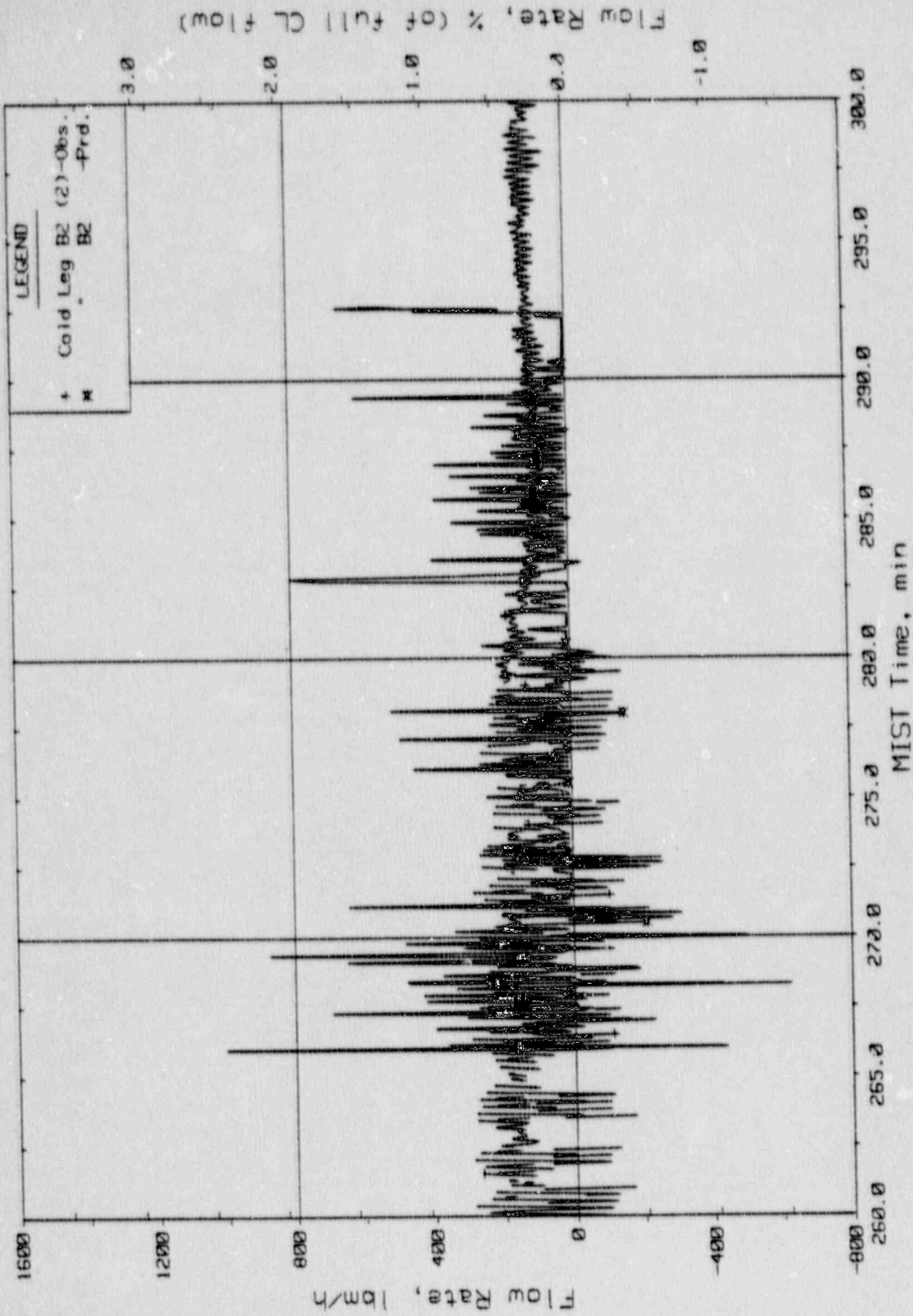


Figure 3.4.22. Loop B2 Cold Leg (Venturi) Flow Rate (C4VN20).

Cc4vn20

MIST NCG Threshold - Test 3502CC  
Observed Vs. Predicted

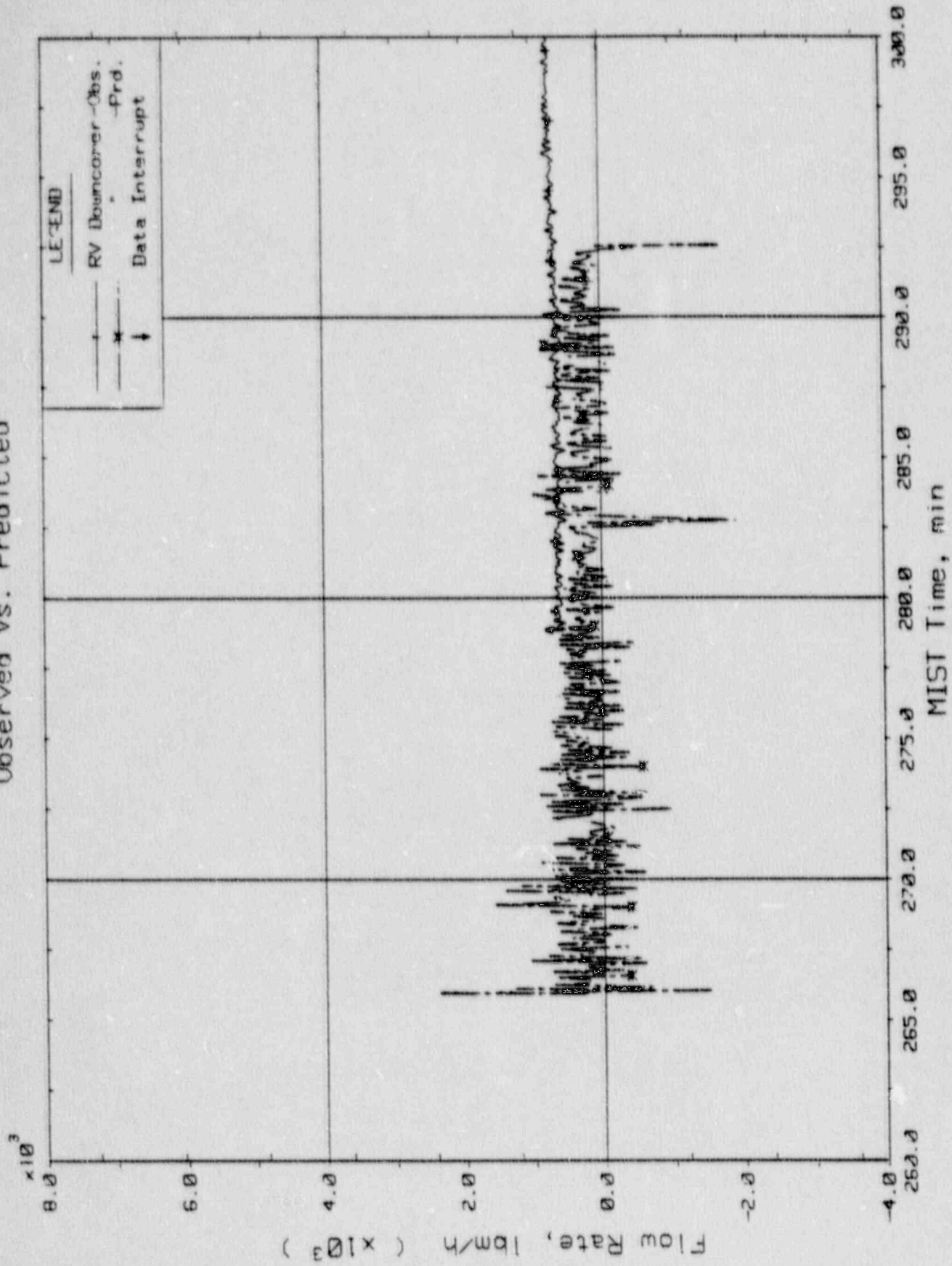


Figure 3.4.23. Primary System Venturi Flow Rates.

MIST NCG Threshold - Test 3502CC  
 Observed Vs. Predicted

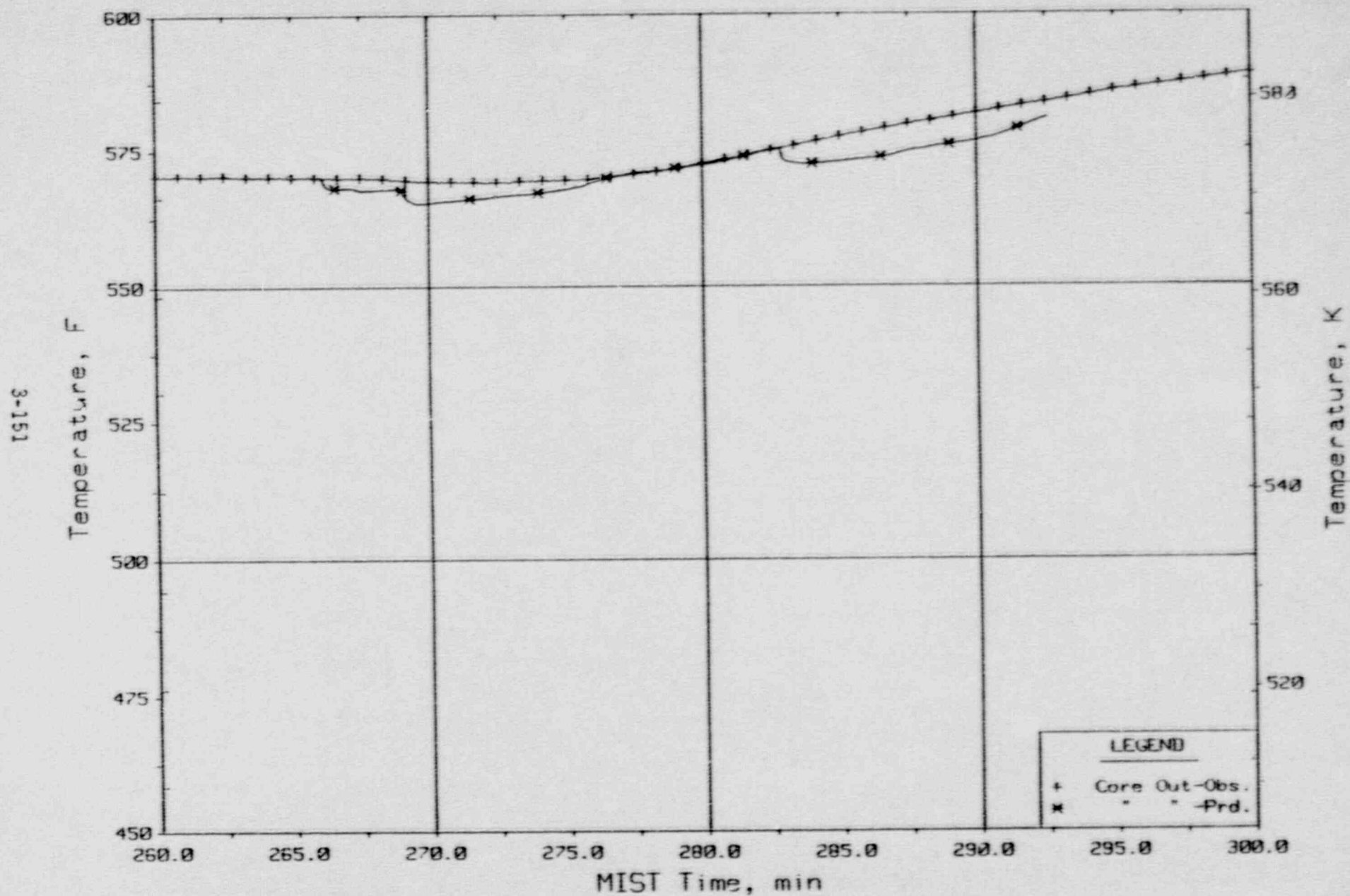


Figure 3.4.24. Core Exit Reactor Vessel Fluid Temperature (RVTC11).

MIST NCG Threshold - Test 3502CC  
Observed Vs. Predicted

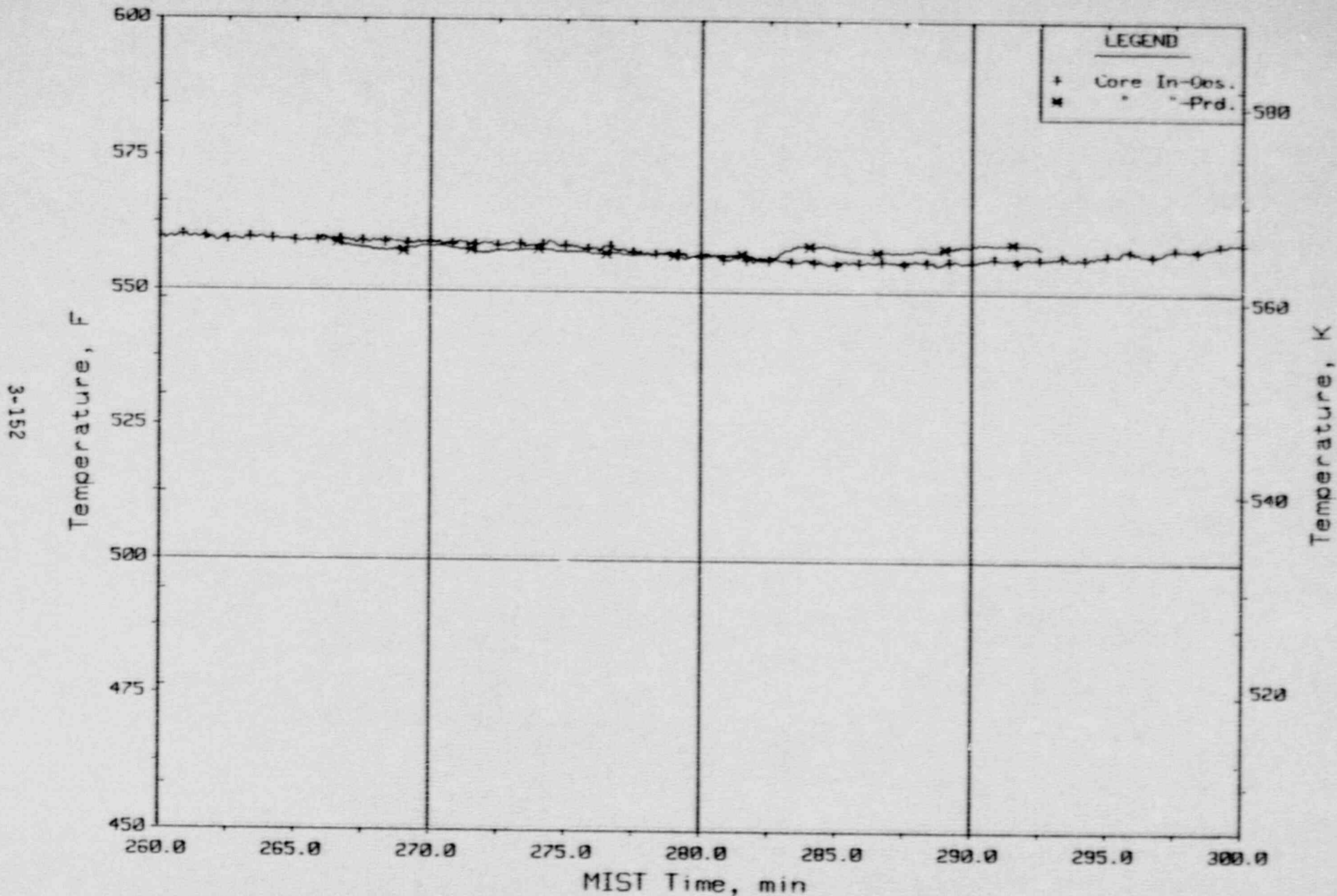


Figure 3.4.25. Core Inlet Reactor Vessel Fluid Temperature (DCRT01).

MISI NCG Threshold - Test 3502CC  
Observed Vs. Predicted

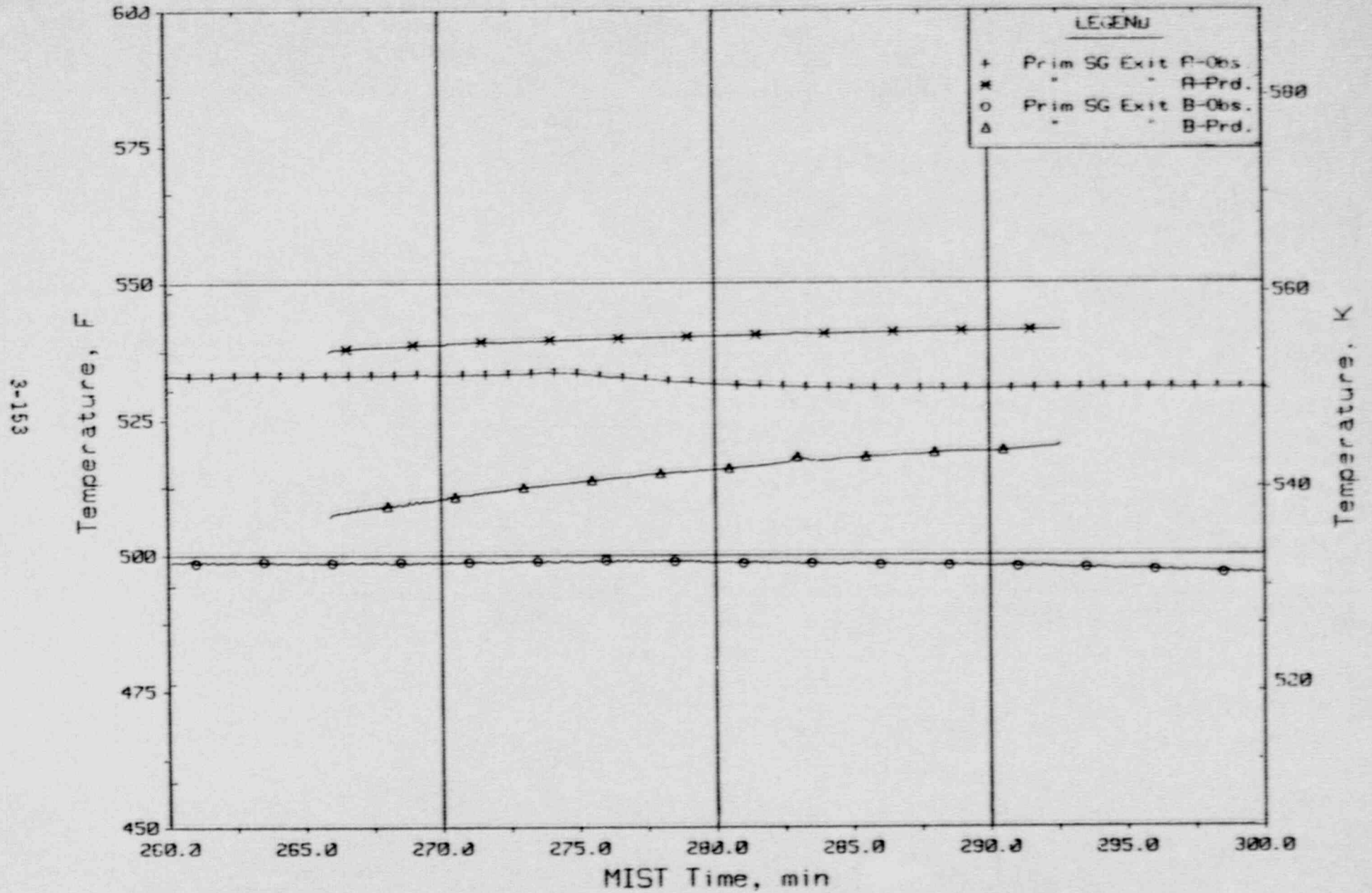


Figure 3.4.26. Loops A/B SG Exit Primary Fluid Temperatures (RTDs).

MIST NCG Threshold - Test 3502CC  
Observed Vs. Predicted

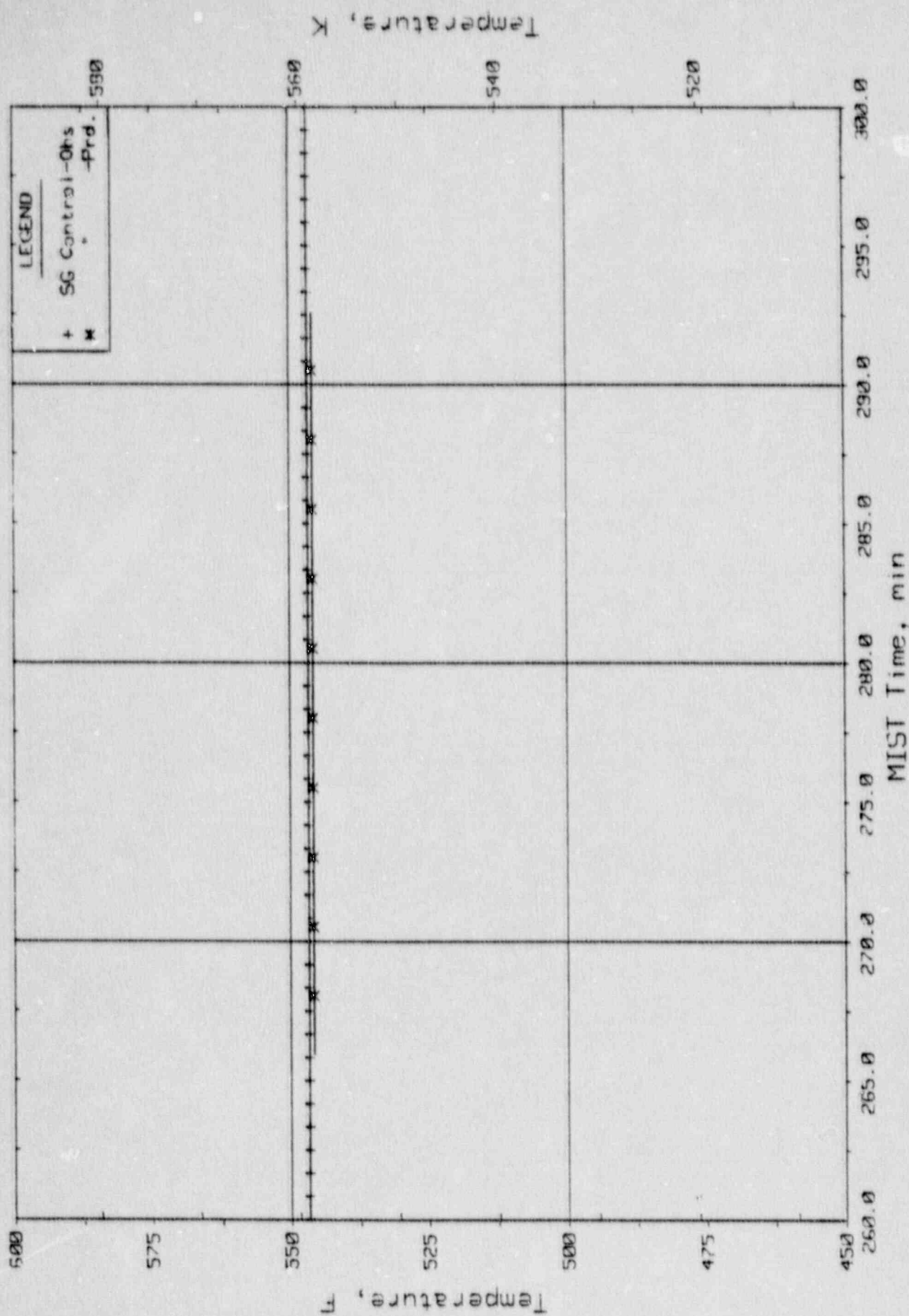


Figure 3.4.27. Steam Generator Secondary Saturation and Control Temperatures.

### 3.5. MIST Test 3801AA Post-Test Prediction

MIST test 3801AA was called the core uncover test with reactor coolant pumps running. This test was designed to uncover the core due to primary system inventory depletion via throttled HPI, a scaled 3 cm<sup>2</sup> CLPS leak, and a stuck open PORV. During the first 73 minutes of the test the reactor coolant pumps were running. AFW was terminated initially and then actuated to maintain levels below 10 feet up to 101 minutes. The items of interest for the benchmark included the continuous two-phase pump performance, primary system inventory depletion, and ultimate core uncover. A detailed discussion of the test can be found in the Immediate Report for MIST Test 3801AA.

#### 3.5.1. MIST Test 3801AA Base Case Modifications

The RELAP5/MOD2 base MIST input model was modified as follows to allow the transient calculations to be performed.

1. Reactor coolant pumps were energized and the rated pump torque was increased from 1 ft-lbf to 32 ft-lbf.
2. The cold leg venturi form loss coefficients were eliminated. The cold leg venturis were replaced by turbine meters for MIST tests in which the reactor coolant pumps were energized.
3. The AFW wetting model was not implemented, and not of major significance since the pumps remained energized throughout the test.
4. The downcomer venturi flow resistance was reduced in order to match system flow rate test data.
5. The initial core power was increased to 10% scaled full power which was the maximum MIST power available.
6. The PORV flow area was increased to a scaled 10 cm<sup>2</sup> with subcooled and two-phase discharge coefficients of 1.4 and 0.85 respectively.

These changes are documented in detail in the calculational file for this post-test prediction.

#### 3.5.2. MIST Test 3801AA Transient Comparisons

The initialization for this test was different from the nominal natural circulation conditions. In this test the pumps were initially running at 100% rated flow and the core power was at 10% of full power. The rated pump torque was increased from 1 ft-lbf to 32 ft-lbf in order to obtain the

correct energy addition to the primary system. Forced primary flow required the reduction in downcomer flow resistance in order to match the observed pump differential pressure increase as well as the observed primary system flow.

Test 3801 was initialized with high elevation AFW injection into each steam generator controlling to a level of approximately 10 feet. Elimination of the RELAS/MOD2 AFW wetting model was required in order to maintain secondary levels at their control settings. With the scaled reactor coolant pumps energized and the AFW wetting model implemented, the secondary level setpoint was reached without sufficient primary-to-secondary energy transfer to maintain steady-state conditions. Subsequent elimination of the AFW wetting model resulted in adequate secondary level control as well as primary-to-secondary heat transfer. The calculated and observed facility steady-state conditions are summarized in Table 3.5.1.

The transient was initiated by opening the scaled 3 cm<sup>2</sup> CLPS leak, terminating AFW to both steam generators, and resetting the secondary pressure control to 1050 and 1000 psia in loops A and B respectively. The core decay heat ramp and HPI were initiated at one minute into the transient. The secondary pressures fluctuated about the specified values and had a significant influence on the overall system behavior. Therefore, in order to replicate the behavior, the observed steam generator pressure was specified as the control value for the prediction during the first 28 minutes. The AFW flow for steam generator B was also specified from the observed value during this time interval since the collapsed level was near zero. A tabular sequence of events for this test was shown in Table 3.5.2. The plotted comparison against the test data was shown in Figures 3.5.1. through 3.5.35.

The primary pressure dropped rapidly following the PORV and CLPS leak opening. Within five minutes the secondary inventories were nearly gone and the hotter regions of the system were beginning to saturate. The cold leg flows began to decline as voiding progressed to the pump inlets. The loss of secondary heat removal forced the primary pressure to begin a slow increase which lasted until 8 minutes when AFW flow was restored to maintain minimal levels in the steam generators. Two-phase conditions were detected at the



PORV by 7 minutes due to the level swell in the pressurizer. At 10 minutes the HPI flow was decreased to a value less than 10 lbm/hr.

The secondary energy removal associated with the restored AFW began to depressurize the primary side at 8 minutes. Steam generator B, which had a lower secondary pressure, became much more active than its counterpart in the A loop. This asymmetric behavior led to wild secondary pressure oscillations in loop B which in turn affected the AFW flow and the amount of primary-to-secondary heat removal. During the first major feed cycle, the facility pump A2 inlet void fraction increased abruptly toward one and the registered flow in that cold leg declined to zero. RELAP predicted a similar behavior in this pump during the fifth cycle approximately 5 minutes later. Both the observed and predicted flows in loop A1 increased sharply at the time that the loop A2 pump became fully degraded.

The undegraded pump inlet void fractions increased in an oscillatory fashion driven by the continued loop B AFW feed cycles. The voiding in the two loop B pumps oscillated out of phase with the A1 pump. At approximately 18 minutes the facility pump B2 became fully degraded. The next pump lost in the predictions was the B1 pump at 24.5 minutes. This pump was lost just after the loop A steam generator AFW flow began to refill to a higher level and before the loop B AFW flow initiated. The observed flow in loop B1 declined sharply at this time, however, the flow increased to the original magnitude after the AFW in loop B began. When the AFW shut-off in loop A the facility lost pump A1. At this time the predicted loop flow in cold leg A1 declined sharply as the void fraction increased, however, the pump did not fully degrade until much later. The observed degradation of pump B1 finally occurred at 32.5 minutes during an off-cycle of the AFW in that steam generator.

At 28 minutes the prediction switched to a constant secondary control pressure and smoother AFW flow model. These changes were made primarily to improve code execution run-time, which was severely limited by the significant AFW flow and secondary pressure swings which caused primary flow surges. Prior to that time, the secondary pressure and AFW flow was specified to attempt to provide the same system forcing functions as the facility. Since the prediction had already diverged somewhat from the observed conditions it

was felt that the impact would be relatively insignificant. Upon further investigation, it may have been more dramatic than expected. The smooth AFW flows removed the forcing function for the pump inlet void oscillations which apparently lead to full pump degradation. The effects can be seen in the predicted behavior of pumps B2 and A1. After 28 minutes the void fractions increase smoothly to 26% and 42% respectively by 50 minutes. The other two pumps which were calculated to degrade did so at void fractions of between 15% and 20% similar to each of the observed pumps.

The two pumps which continued to circulate fluid in the prediction after 33 minutes produced a significant divergence in the system mass inventory. Pump A1 continued to circulate two-phase fluid in the A loop hot leg. The well mixed two-phase fluid entered the pressurizer surge line and maintained a frothy mixture in the pressurizer. Since the phase exiting the PORV contained more steam, the flow rate was much lower. The CLPS leak flow rate also suffered a similar fate. Contributing to this calculated mass imbalance was the fact that the CLPS leak flow discharge coefficient was probably too small prior to this time. The continued loop flows also caused the primary pressure to remain more closely coupled to the secondary pressure. Pump A1 became fully degraded at 54 minutes into the predictions. The fluid phase entering the pressurizer surge line was finally similar to the observed conditions. However, the discrepancy in the mass inventory had reached a value of 155 lbm out of a total observed inventory of 540 lbm. This additional inventory must be discarded and the last pump must be degraded prior to reaching conditions which would permit core uncovering. Because of these significant differences, the calculations were halted at 55 minutes into the test prediction.

Table 3.5.1. MIST Test 3801AA Calculated and Measured Initial Steady-State Conditions

Parameter	RELAP5	Test
Primary Pressure*, psia	2200.	2199.
Secondary Pressure*, psia	1202.	1202.
Hot Leg Subcooling, F	75.	73.
Pressurizer Level*, Ft	22.2	22.7

Table 3.5.1. MIST Test 3801AA Calculated and Measured Initial Steady-State Conditions (Cont'd)

Parameter	RELAP5	Test
Core Power*, % Full Power	10.0	10.0
SG A Secondary Level*, Ft	10.3	10.4
SG B Secondary Level*, Ft	10.3	9.6
Downcomer Mass Flow, lbm/s	52.0	53.9

\*Denotes specified condition.

Table 3.5.2. MIST Test 3801AA Sequence of Events Comparisons

Event	Approximate Test Time (Min)	
	RELAP	Data
Scaled 3 cm <sup>2</sup> CLPS Leak Opened, AFW terminated, SG secondary control pressure adjusted	0.0	0.0
Initiate Core Power Ramp, HPI, Open PORV	1.0	1.0
RCP B2	5.1	5.1
RCP B1	5.5	5.4
Pump Inlet Voiding Began	6.2	5.2
RCP A1	6.2	6.2
RCP A2	6.2	6.2
Liquid Flow out of PORV	7.0	7.2
AFW Restored to Both SG	8.0	8.0
HPI Flow Decreased to 10 lbm/hr	10.0	10.0
PORV Discharge Coefficient Increased to 1.2	11.2	--
RCP A1	13.7	8.7
RCP B2	--	18.0
Pump Flow Approached Zero	24.5	32.5
RCP B1	24.5	32.5
RCP A1	54.2	29.2

Table 3.5.2. MIST Test 3801AA Sequence of Events Comparisons (Cont'd)

Event	Approximate Test Time (Min)	
	RELAP	Data
SG A/B Secondary Level Raised to Constant Value of 2.2/ 3.2 ft	24.0	24.0
Secondary Pressure Held Constant	28.0	--
Secondary Level Raised to _____ ft	--	47.0
Calculations Terminated	55.0	--

3.5.3. MIST Test 3801AA Post-Test Conclusions

MIST test 3801AA presented a major challenge to the RELAP5/MOD2 code and base input model. This test included two-phase pump performance with scaled pumps which had not been adequately characterized for two-phase behavior. Therefore, for lack of a better model, the SEMISCALE pump degradation model was used for this test prediction. This model performed reasonable well compared to the data when similar system conditions existed.

The prediction of the over-all system pressure response was quite reasonable for this test. The biggest discrepancy between the calculated and observed parameters concerned the primary system mass inventory. This mismatch was primarily due to leak fluid phase differences associated with the predicted pump performance. A significant impact on the pump performance may have been caused by the secondary boundary condition modelling techniques after 28 minutes. Either the difference in the system conditions or the two-phase pump performance could be responsible for the over-all divergence in calculated behavior. During the first 28 minutes of the prediction the calculations were quite reasonable. However, a gradual primary mass imbalance was begun which may have affected the system conditions enough that the divergence could not be avoided. Better prediction of the leak flows during this period would have helped answer what mechanism caused the most significant difference between the prediction and the data.

# MIST TEST 3801AA POST TEST PREDICTION

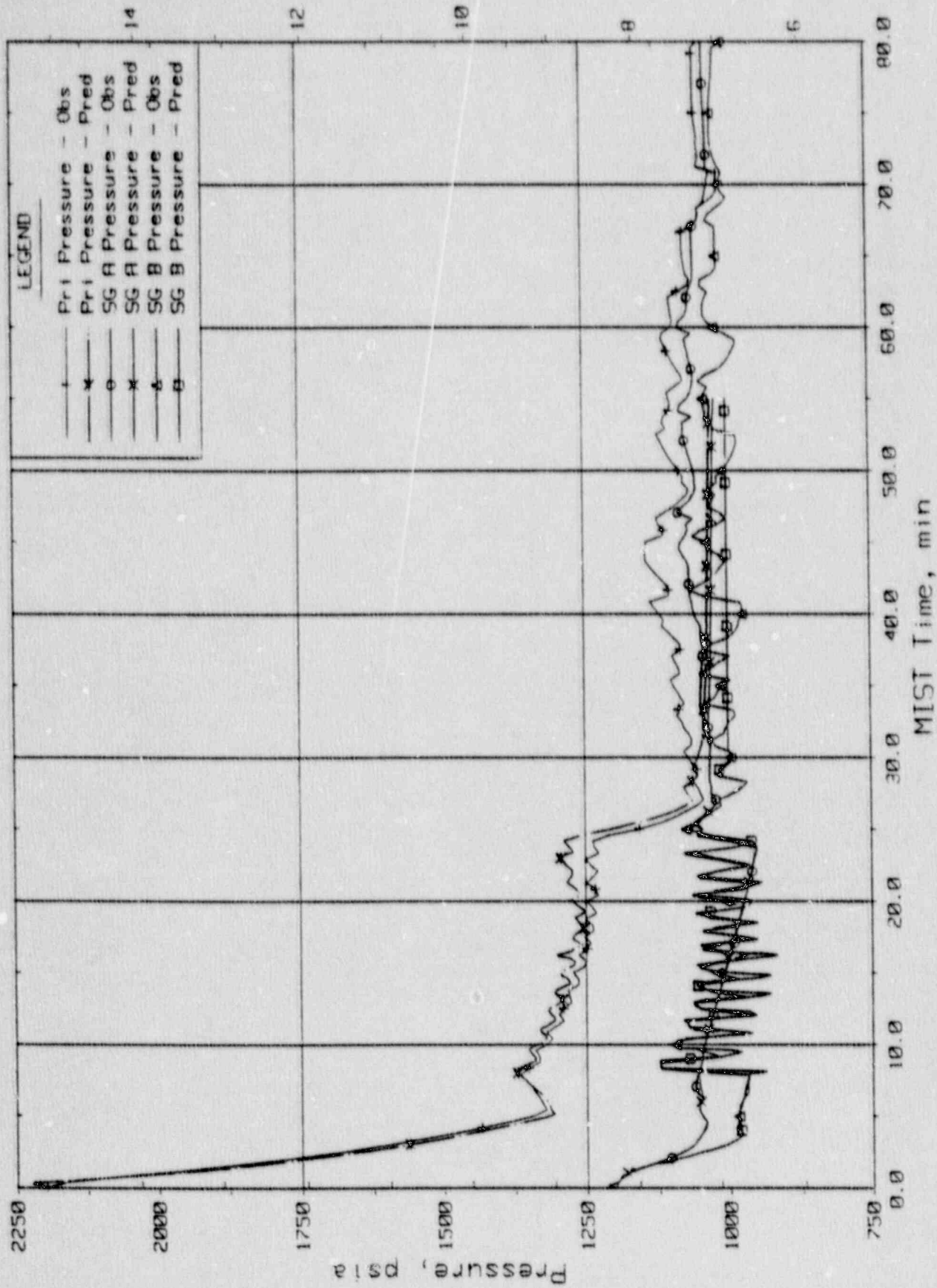


Figure 3.5.1. System Pressure.

Cr-2001

Tue Feb 22 00:07:07 1993

MIST TEST 3801AA POST TEST PREDICTION

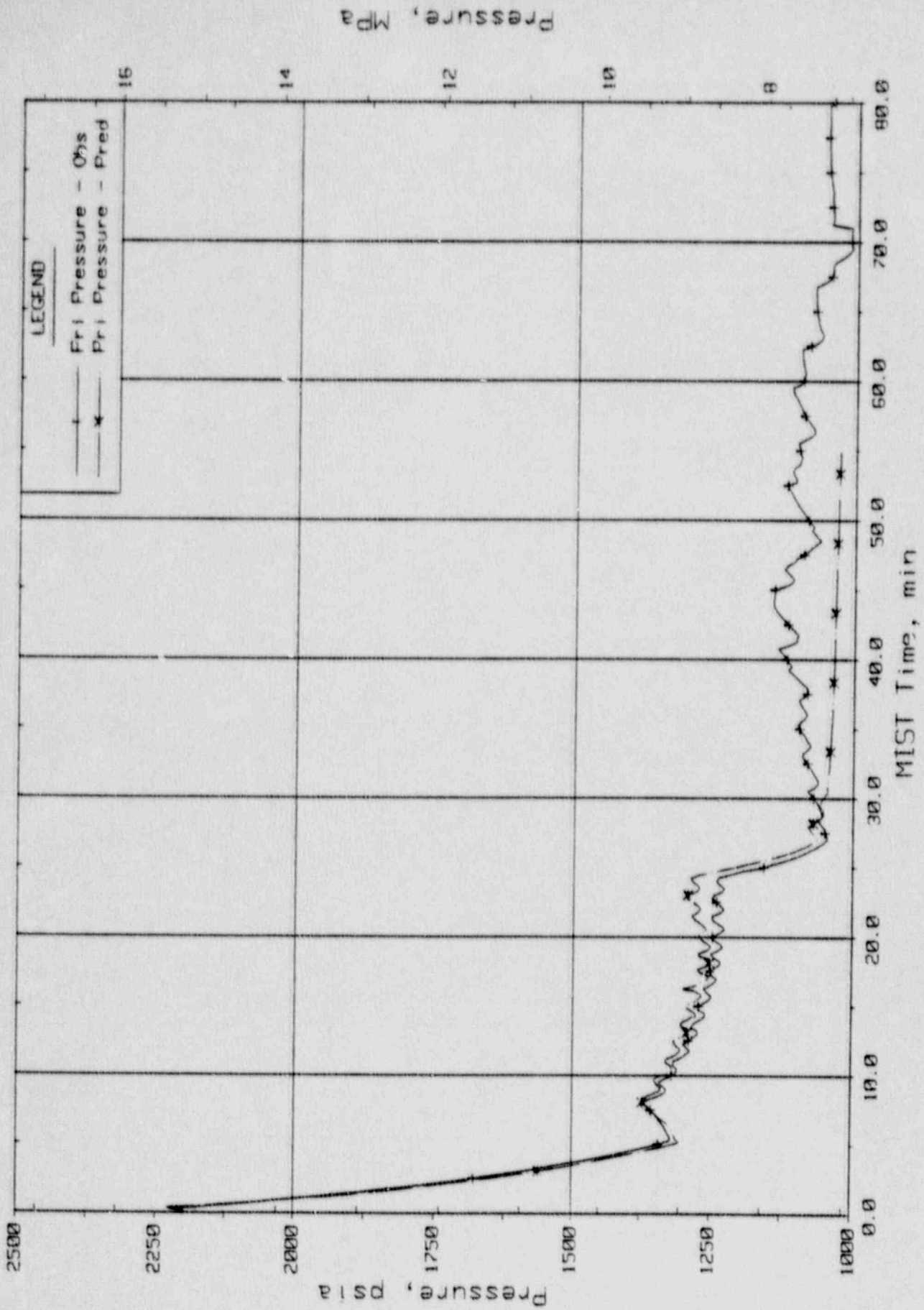


Figure 3.5.2. Reactor Vessel Pressure.

MIST TEST 3801AA POST TEST PREDICTION

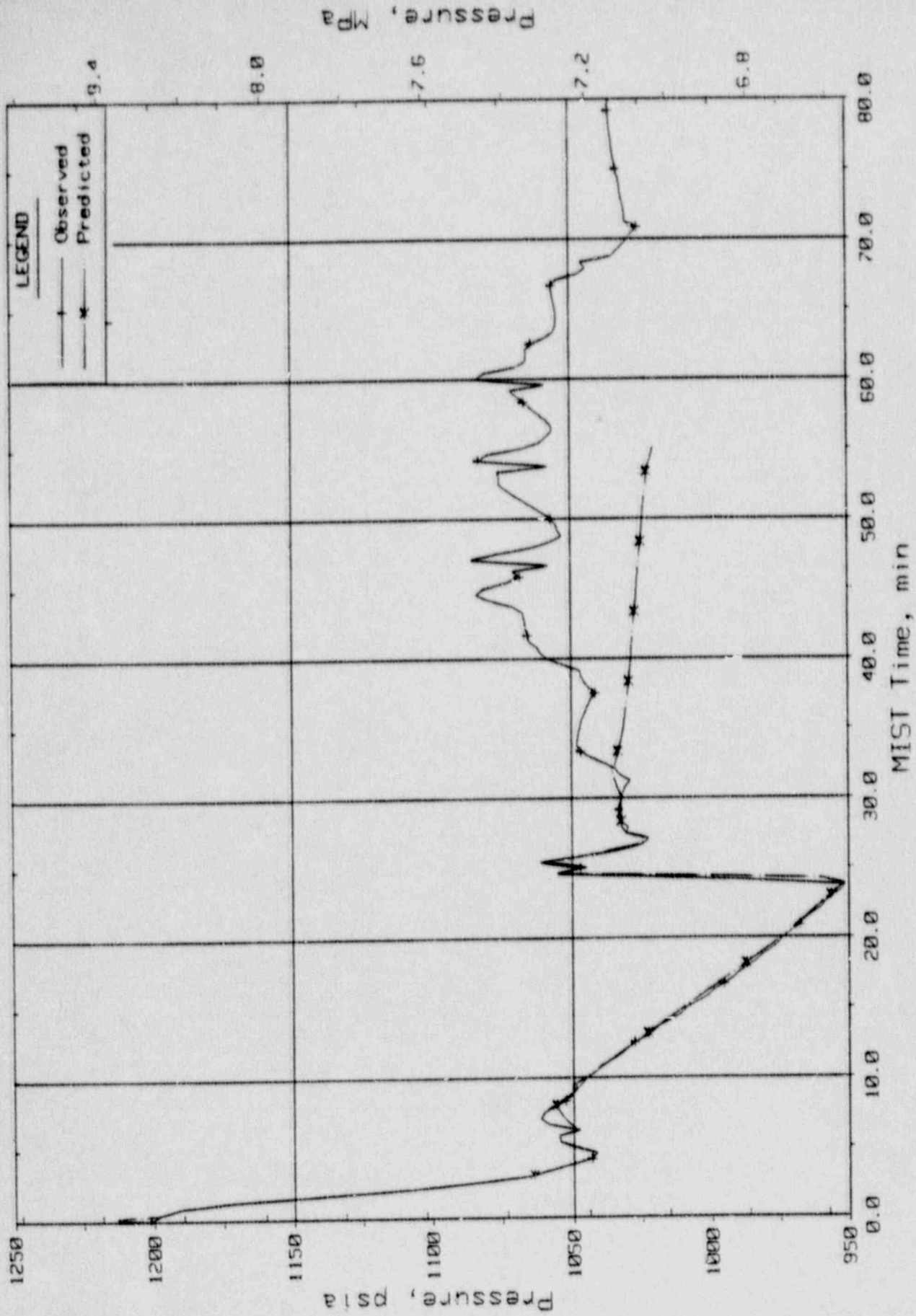


Figure 3.5.3. Steam Generator A Secondary Pressure.

MIST TEST 3801AA POST TEST PREDICTION

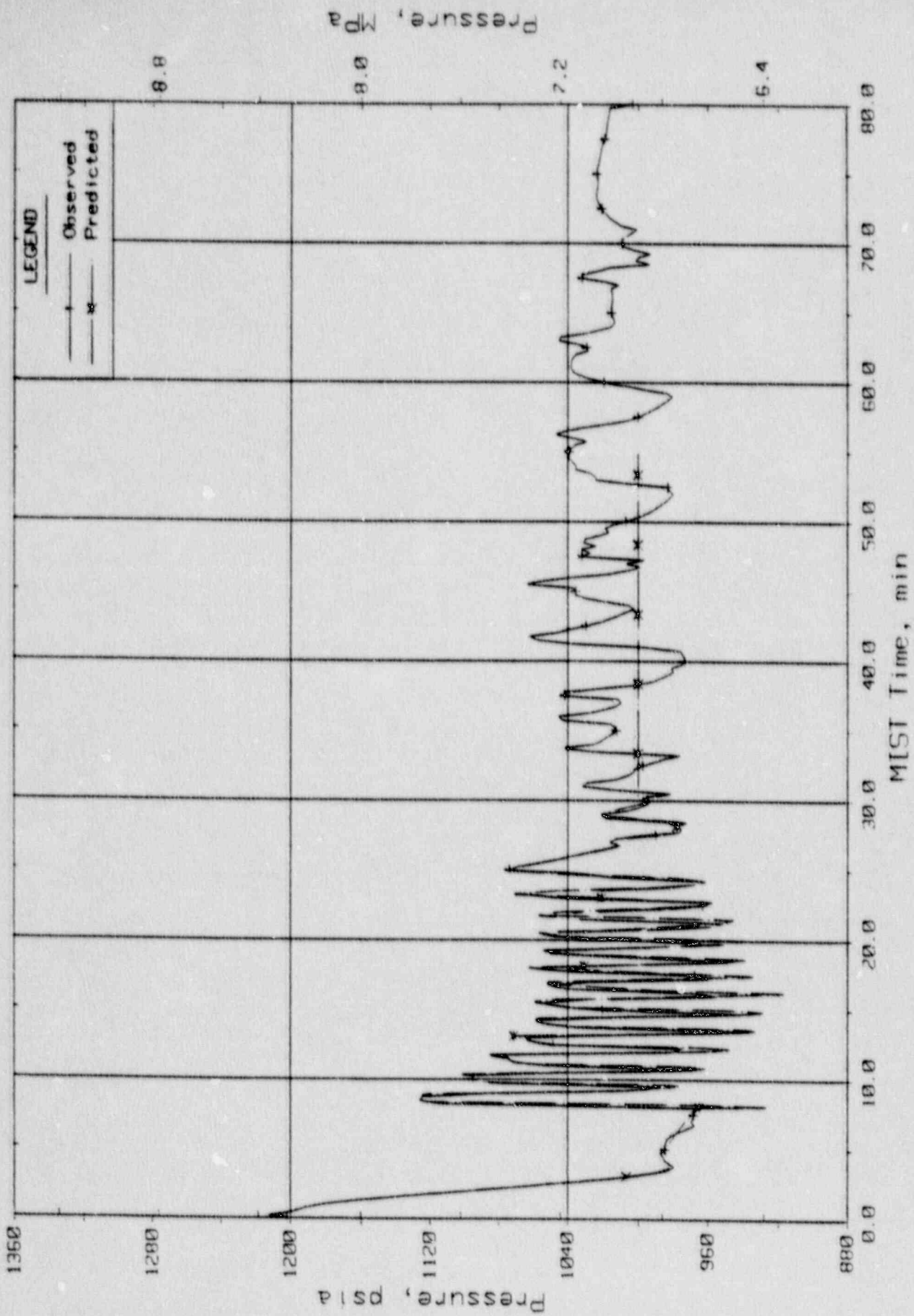


Figure 3.5.4. Steam Generator B Secondary Pressure.



MIST TEST 3801AA POST TEST PREDICTION

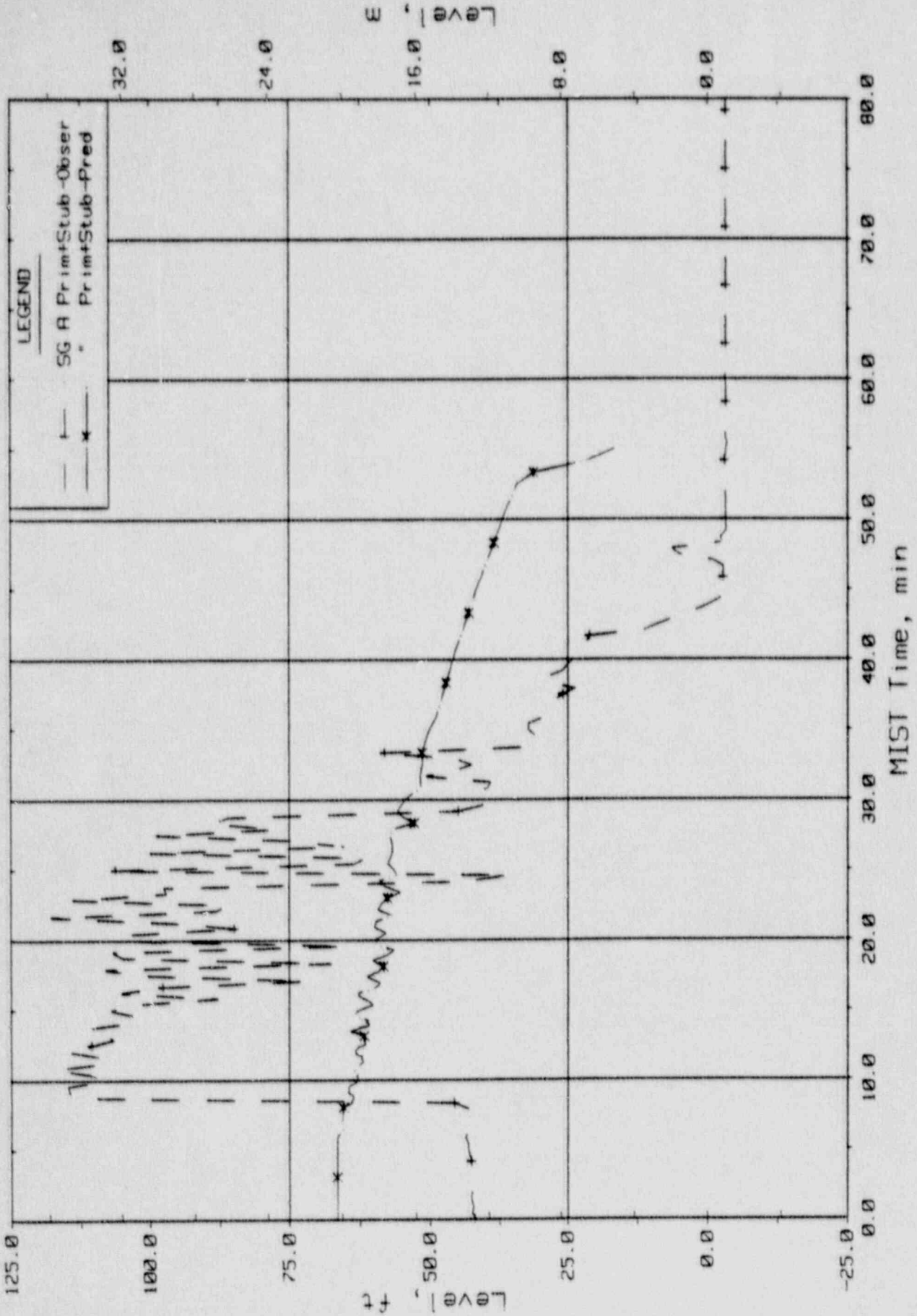


Figure 3.5.5. Steam Generator A Primary + Stub Level.

MIST TEST 3801AA POST TEST PREDICTION

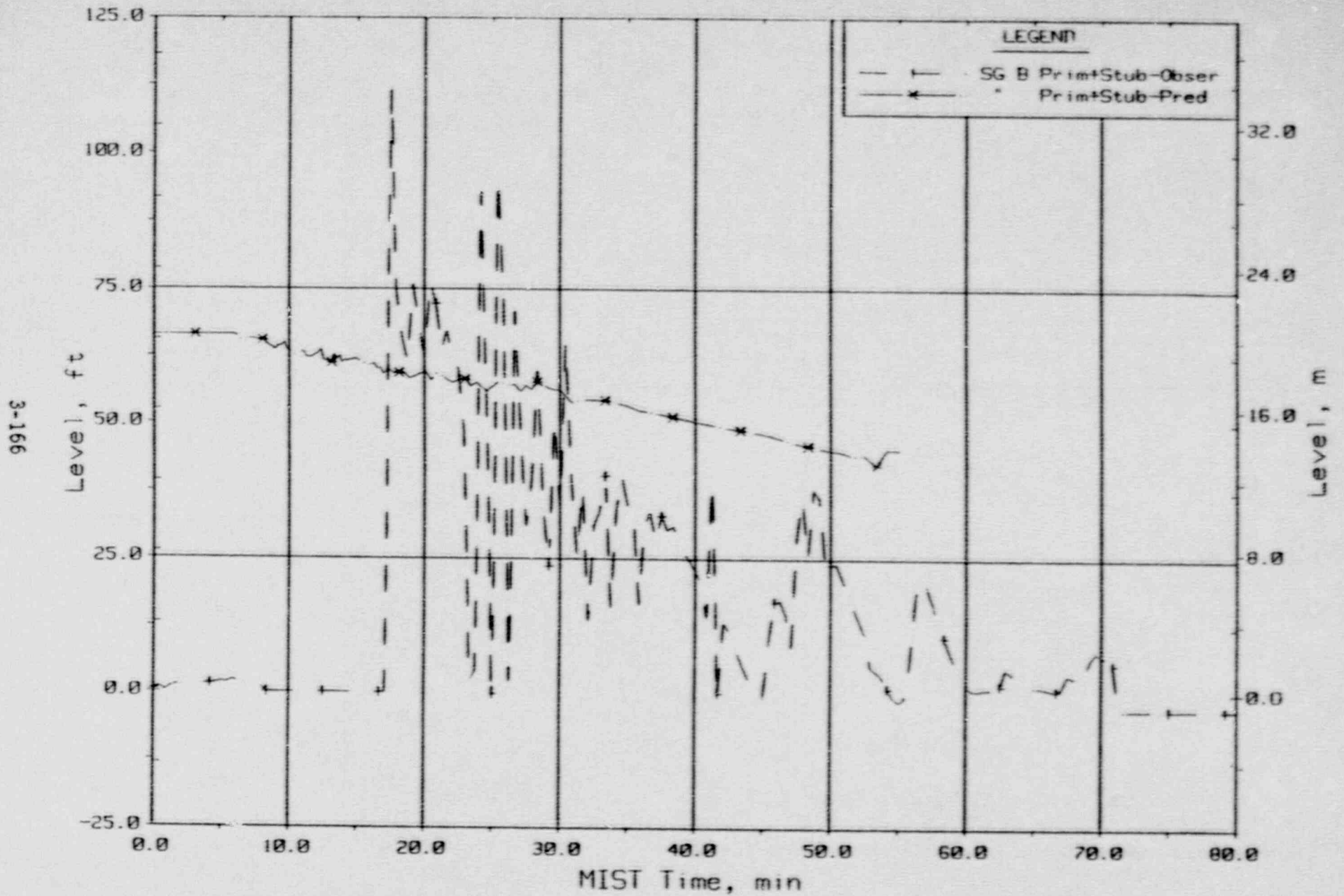


Figure 3.5.6. Steam Generator B Primary + Stub Level.

MIST TEST 3801A POST TEST PREDICTION

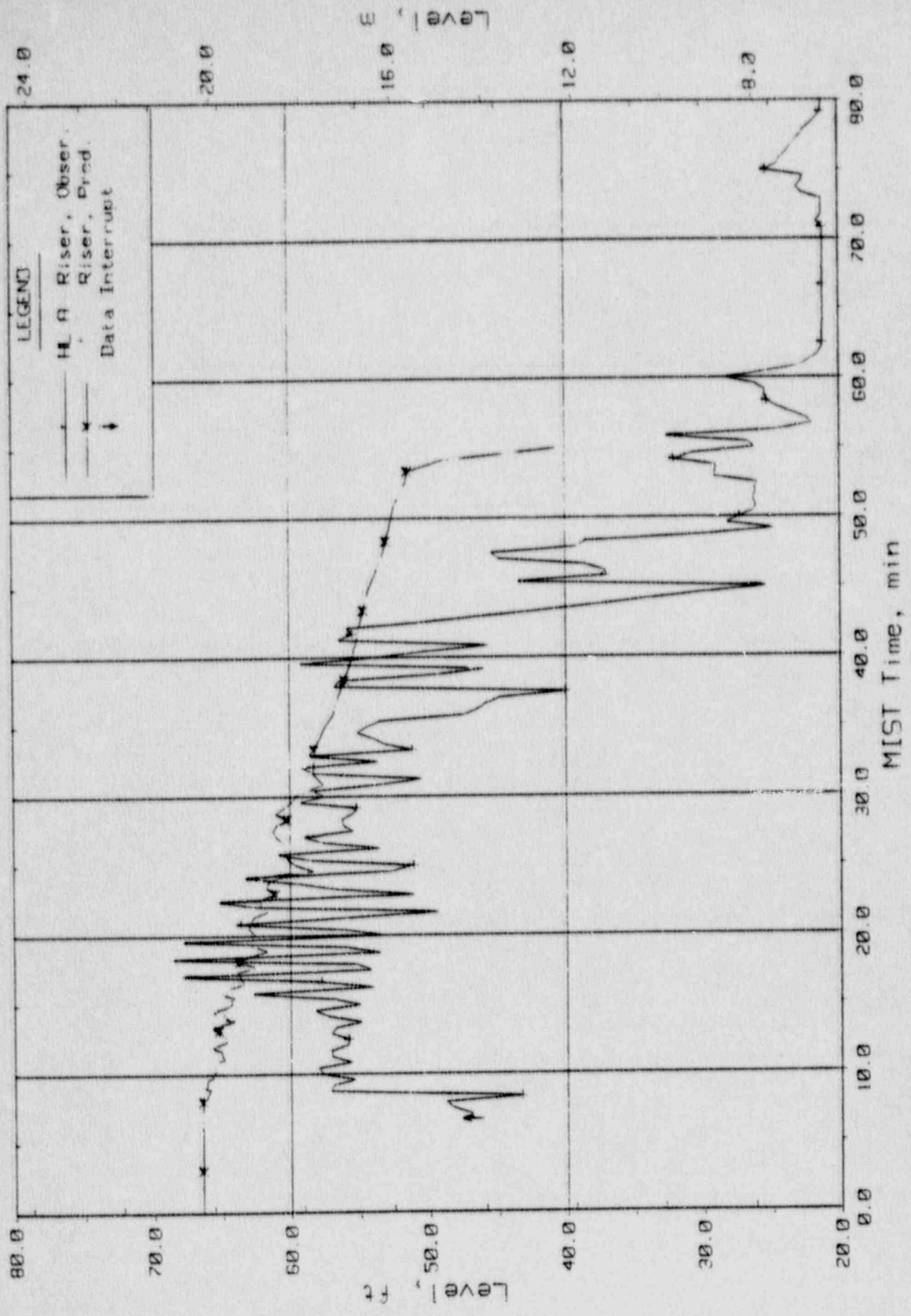


Figure 3.5.7. Hot Leg A Riser Level.

# MIST TEST 3801AA POST TEST PREDICTION

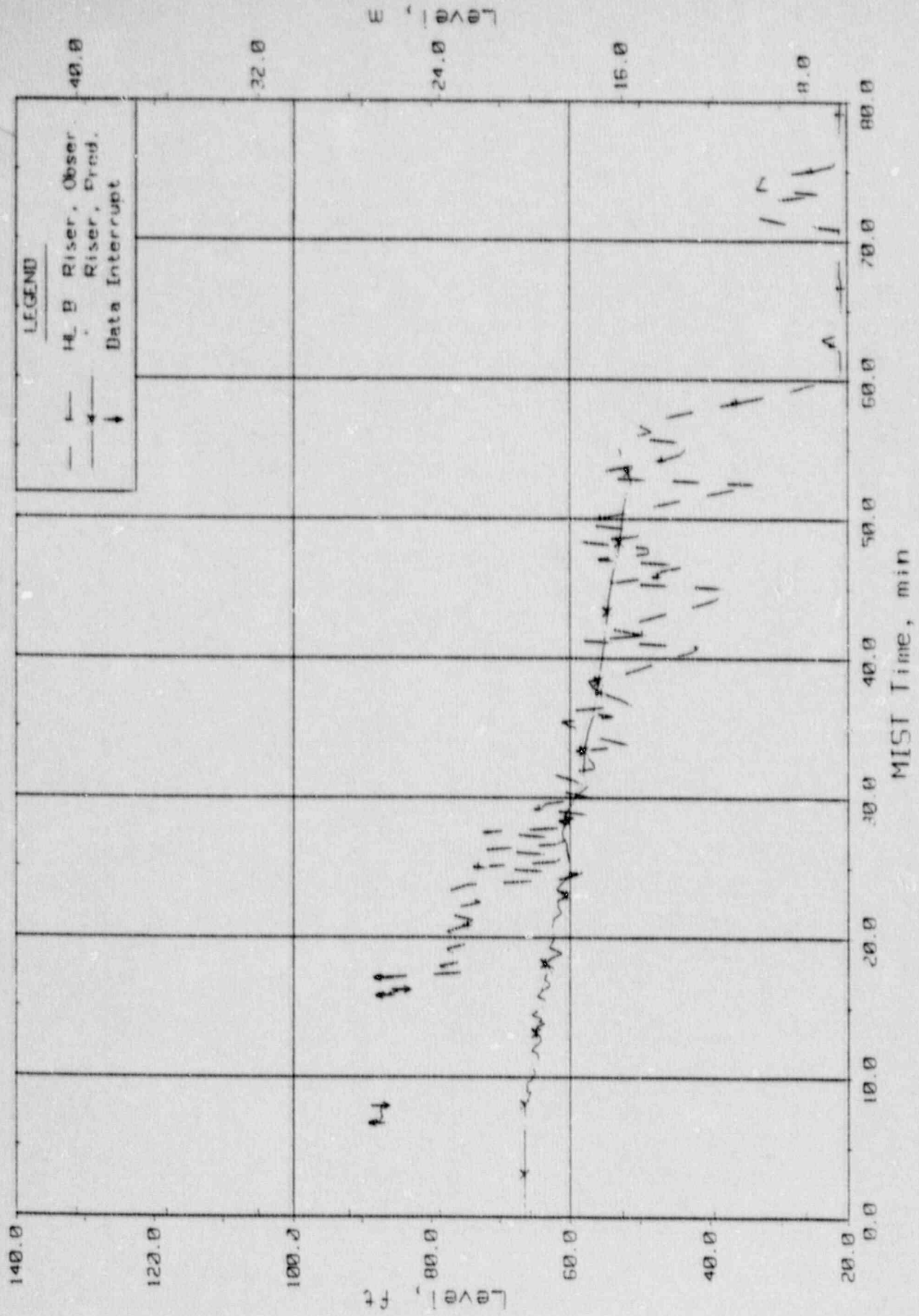


Figure 3.5.8. Hot Leg B Riser Level.

# MIST TEST 3821AA POST TEST PREDICTION

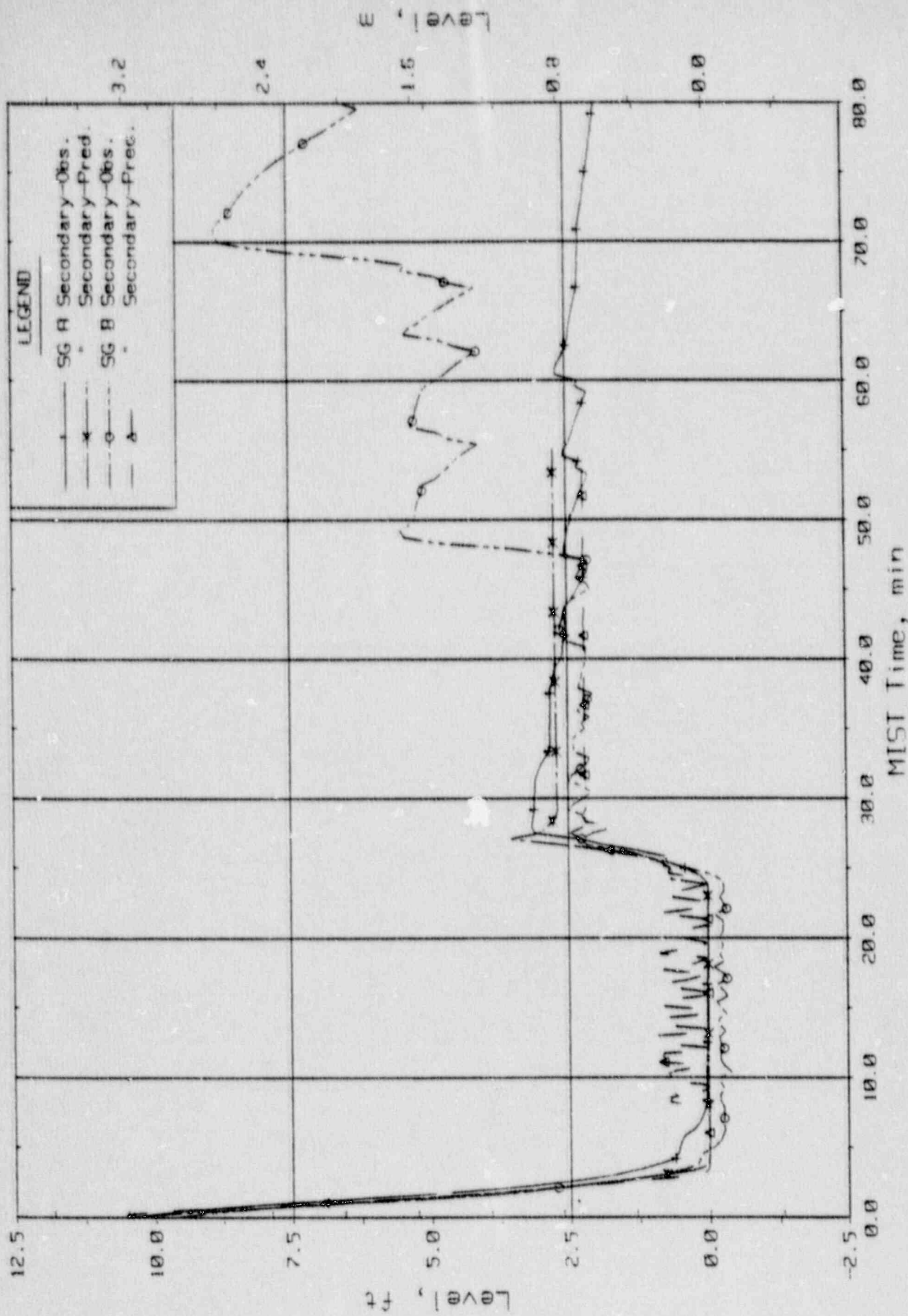


Figure 3.5.9. Steam Generator Sec. Collapsed Liquid Levels.

Csclv2

Top Feb 27 14:49:05 1989

# MIST TEST 3801AA POST TEST PREDICTION

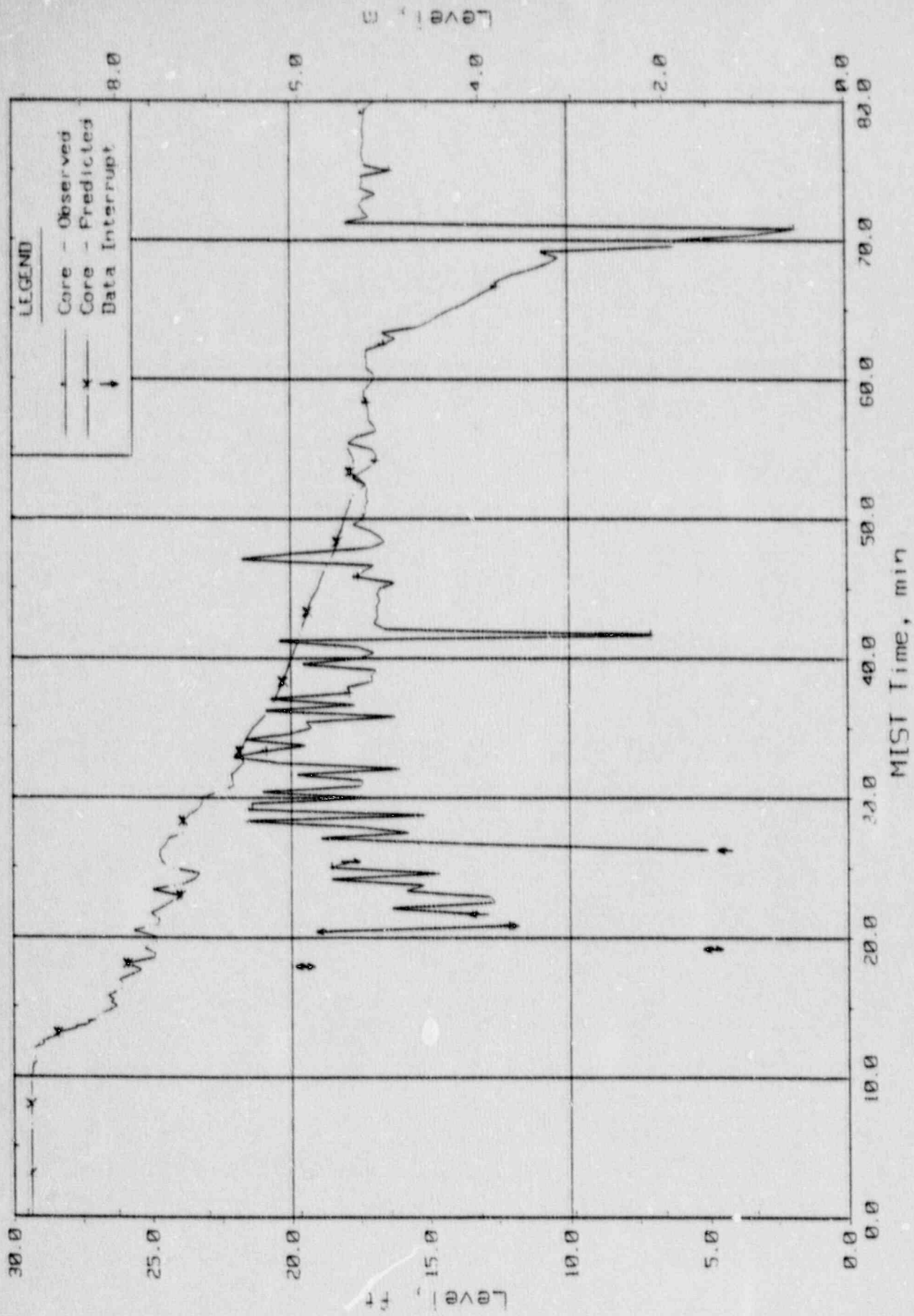


Figure 3.5.10. Core Region Collapsed Liquid Levels.

For Use in 3801AA Post Test

Gr 1.00

MIST TEST 38010A POST TEST PREDICTION

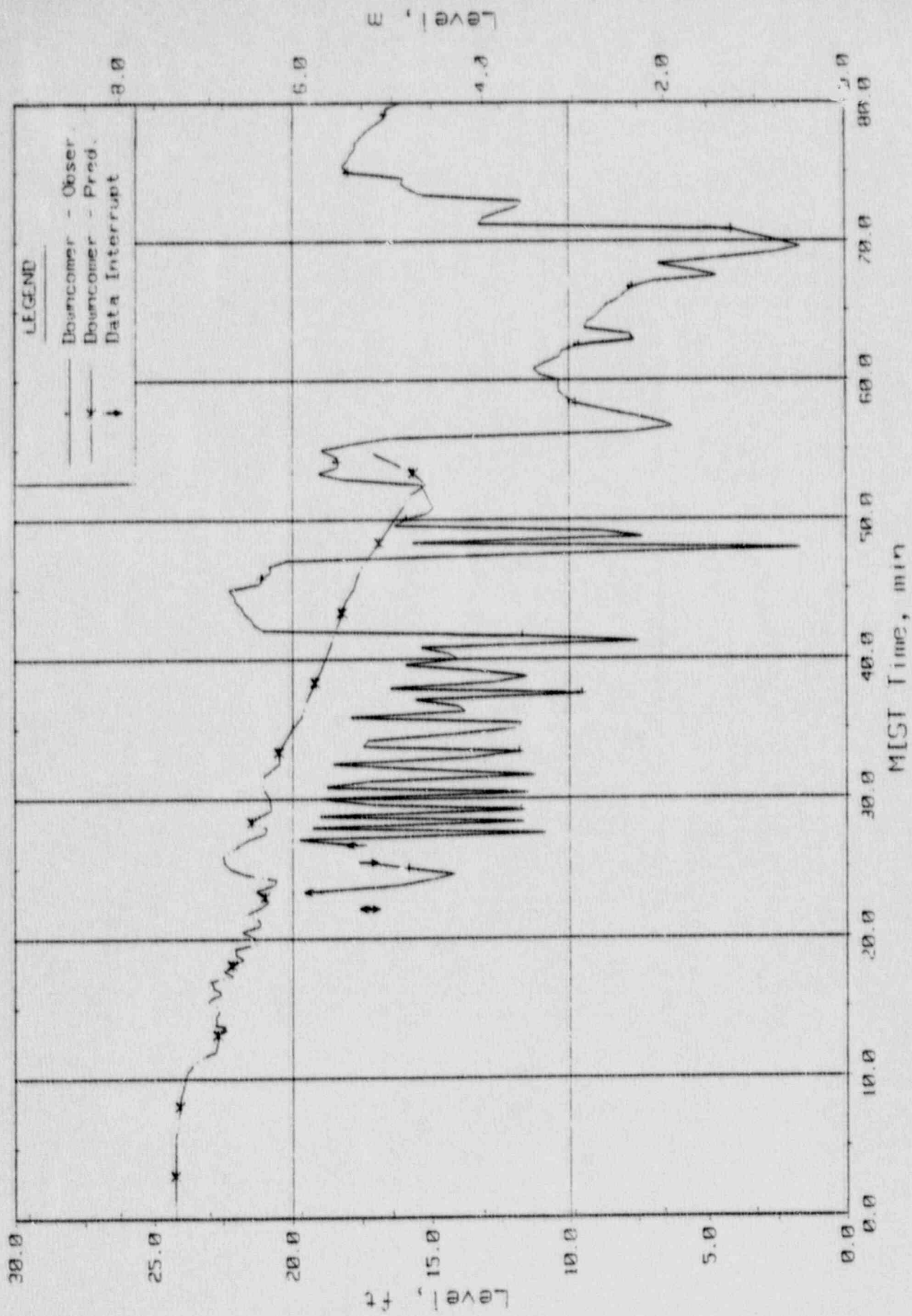


Figure 3.5.11. Core Region Collapsed Liquid Levels.

# MIST TEST 3801AA POST TEST PREDICTION

3-172

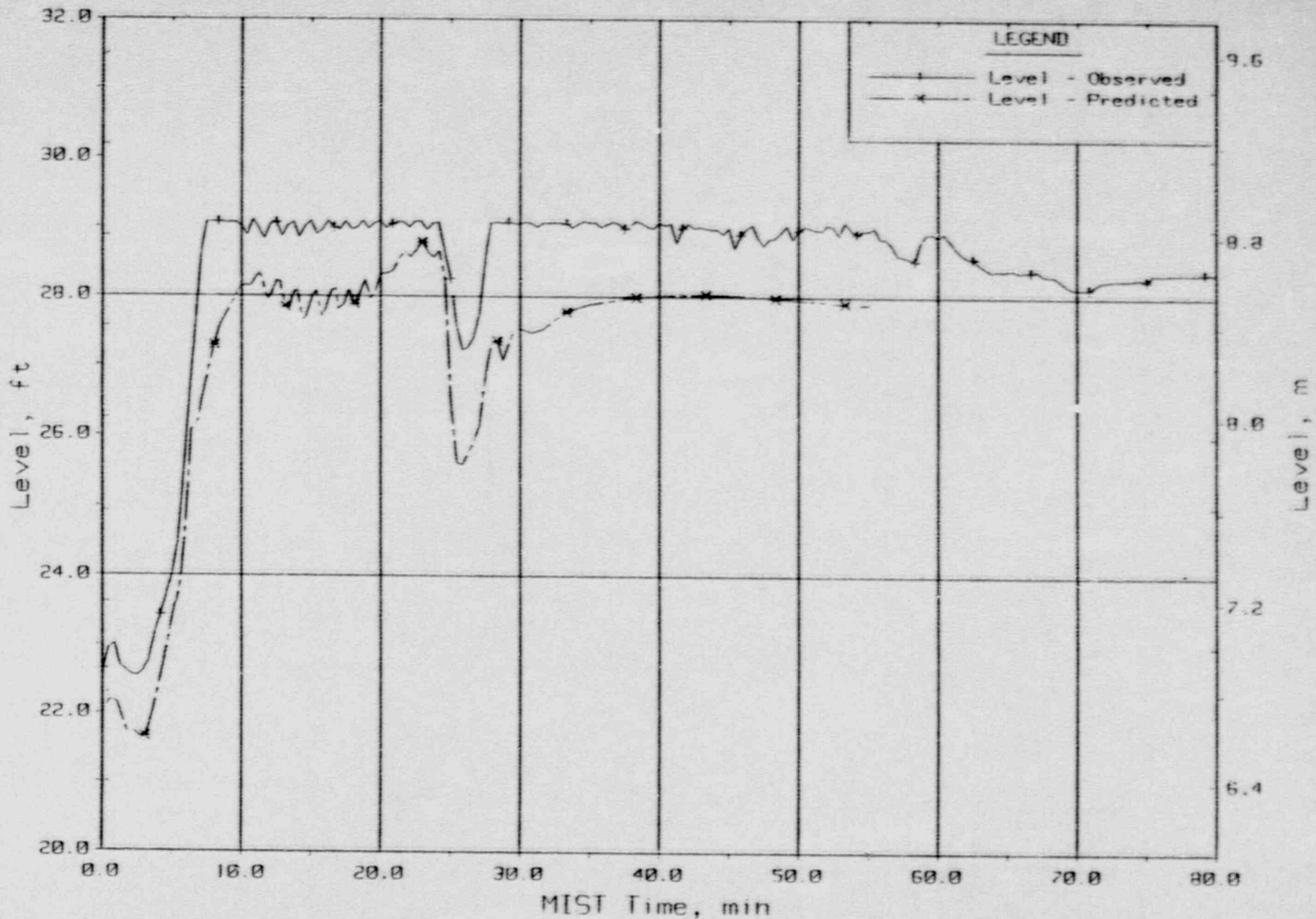


Figure 3.5.12. Pressurizer Collapsed Liquid Level (PZLV20).



# MIST TEST 3801AA POST TEST PREDICTION

3-173

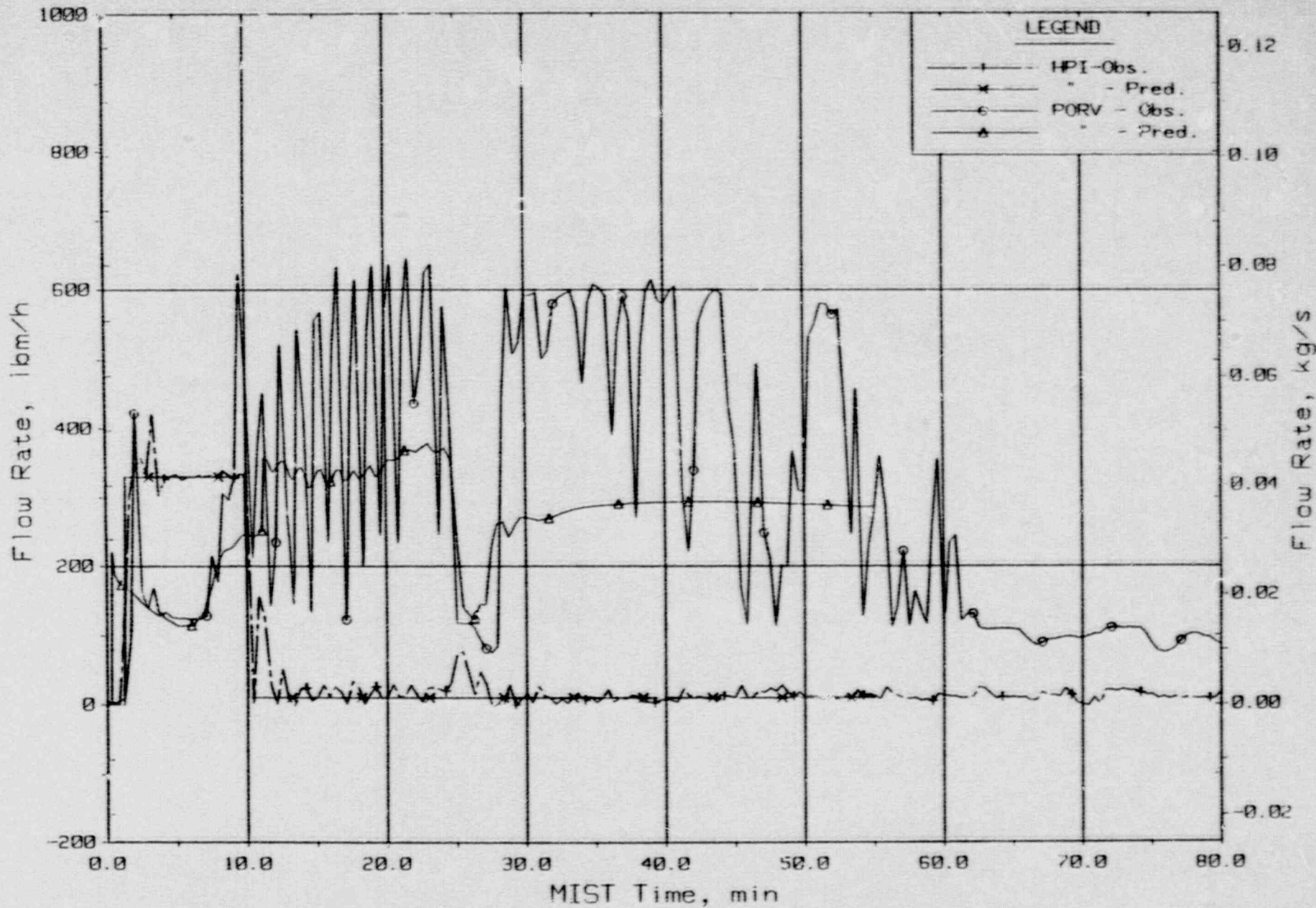


Figure 3.5.13. Primary System Boundary Flow Rates.

# MIST TEST 3801AA POST TEST PREDICTION

3-174

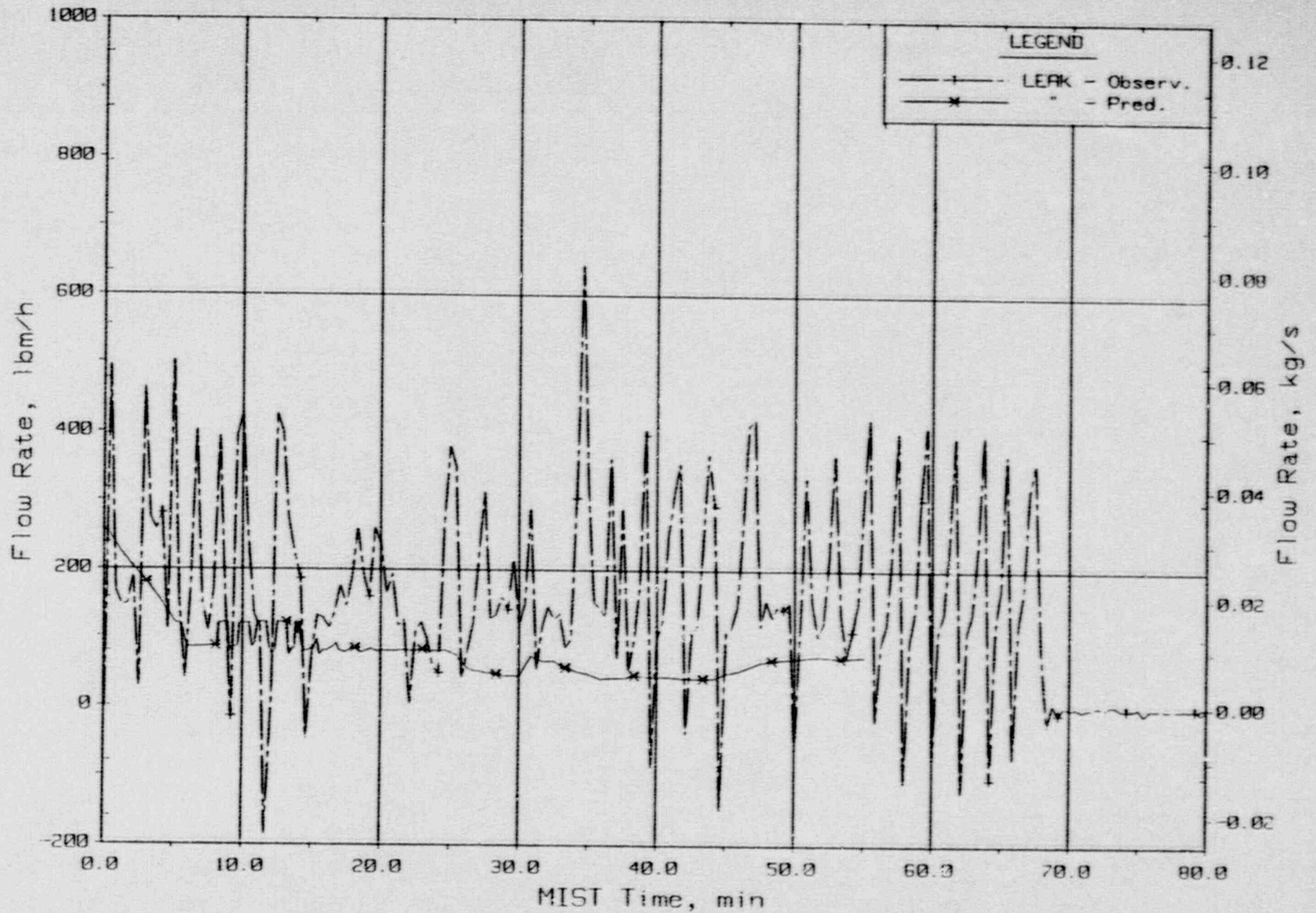


Figure 3.5.14. Primary System Boundary Flow Rates.

MIST TEST 3801AA POST TEST PREDICTION

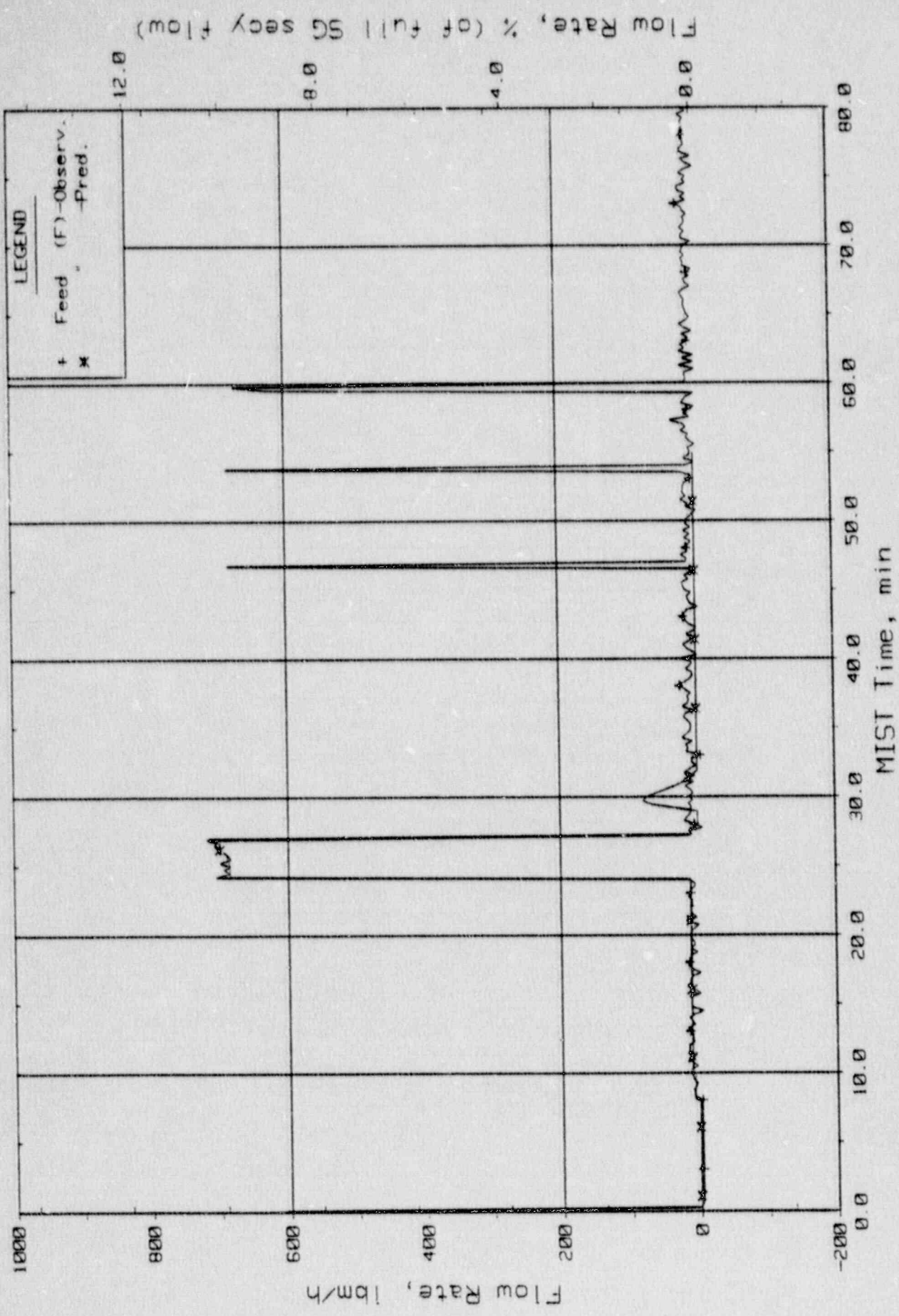


Figure 3.5.15. Steam Generator A Flow Rate (Ssfor20).

# MIST TEST 3801AA POST TEST PREDICTION

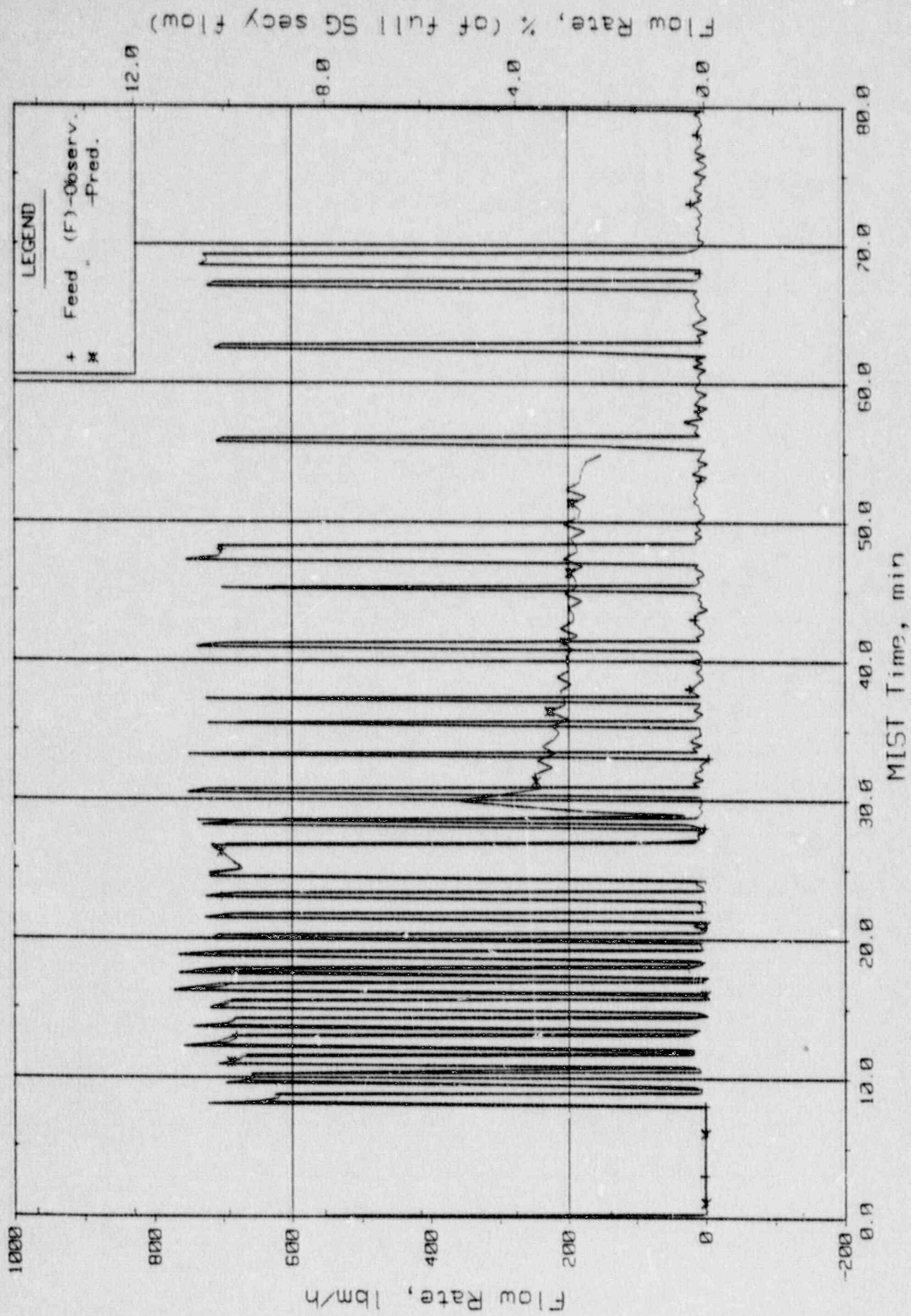


Figure 3.5.16. Steam Generator B Flow Rate (Ssfor21).

Csfor21

Wed Feb 24 09:07:50 1988

# MIST TEST 3801AA POST TEST PREDICTION

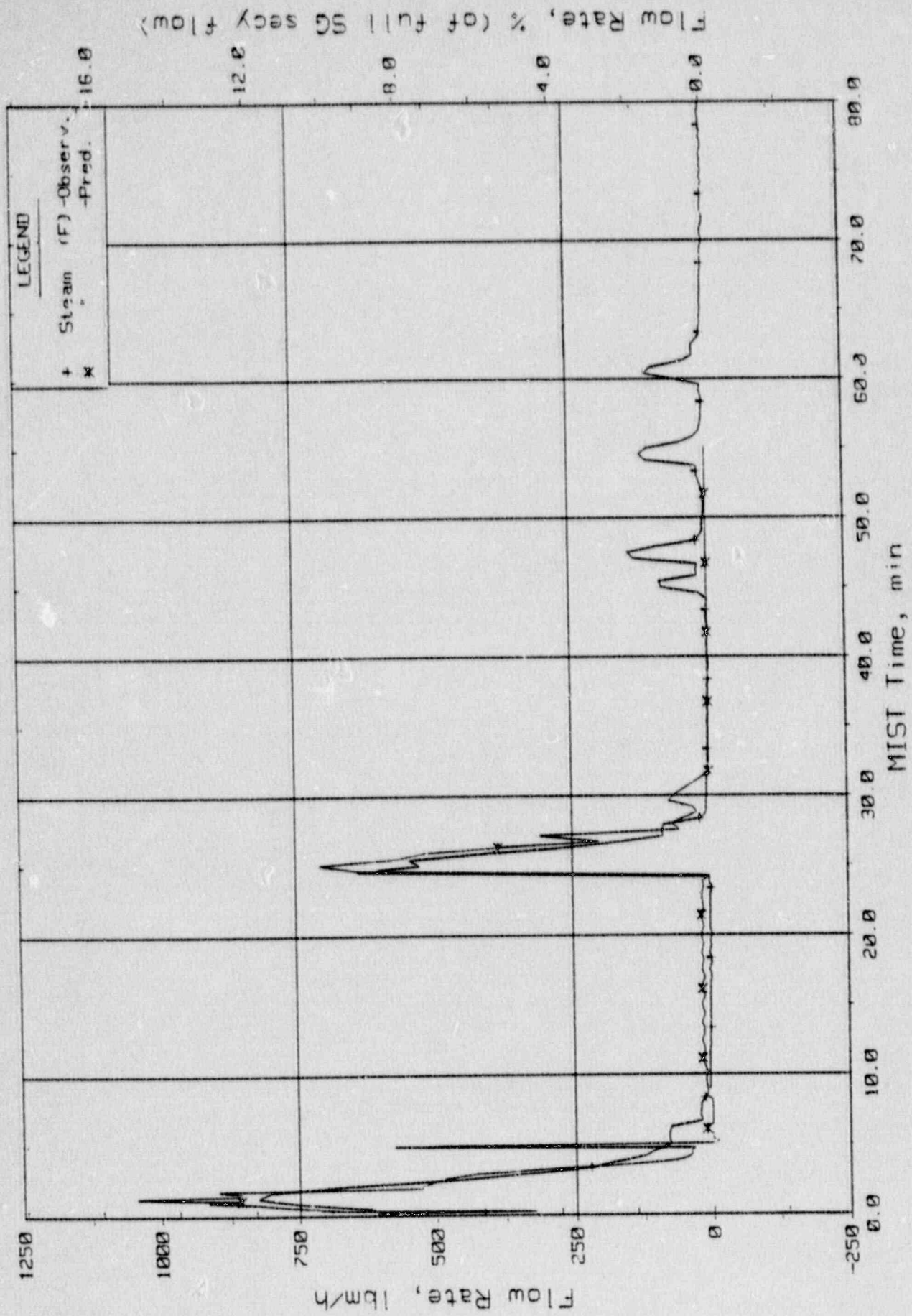


Figure 3.5.17. Steam Generator A Flow Rates (Csr020).

# MIS<sup>T</sup> TEST 3801AA POST TEST PREDICTION

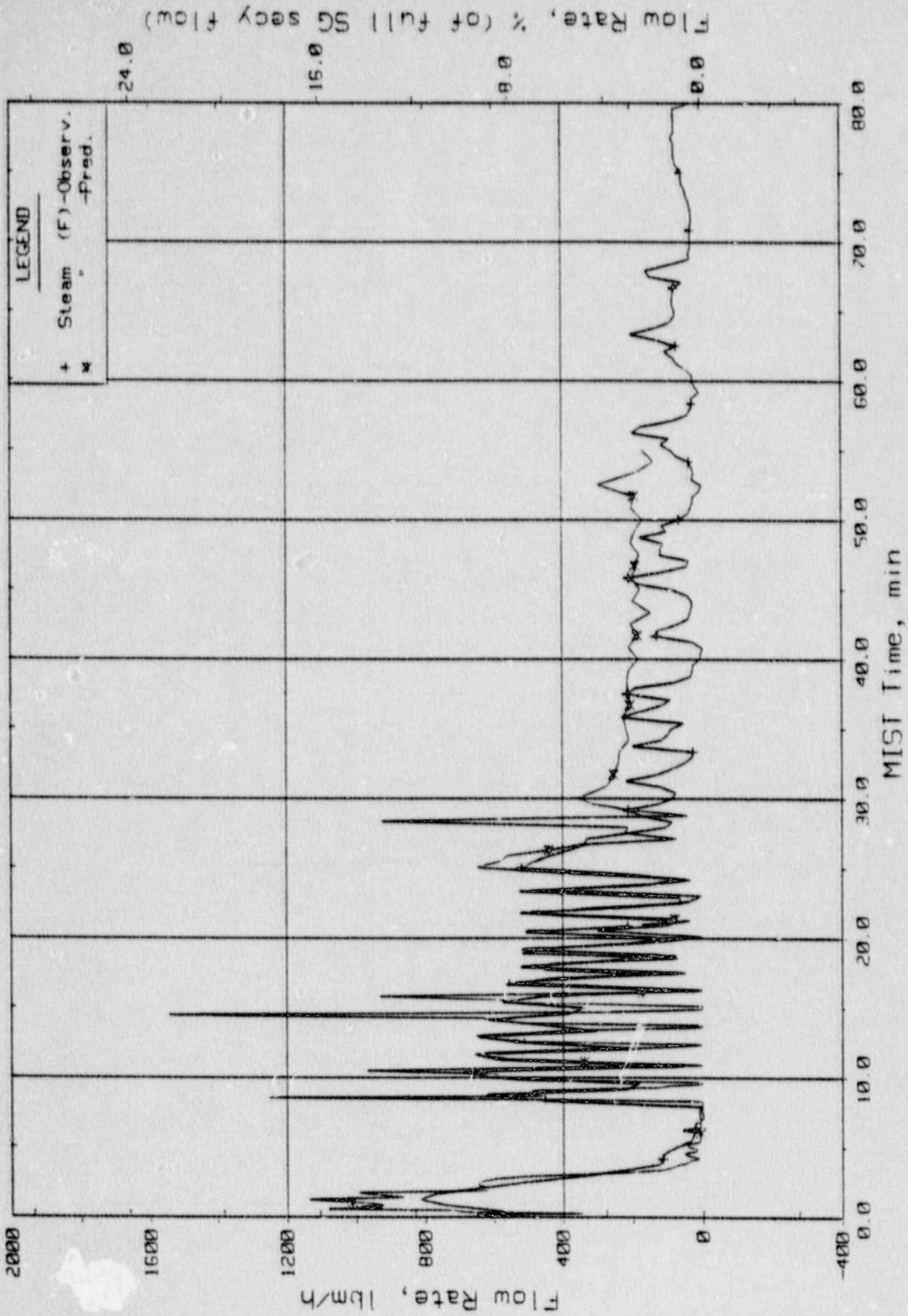


Figure 3.5.18. Steam Generator B Flow Rates (Sssor21).

MIST TEST 3801AA POST TEST PREDICTION

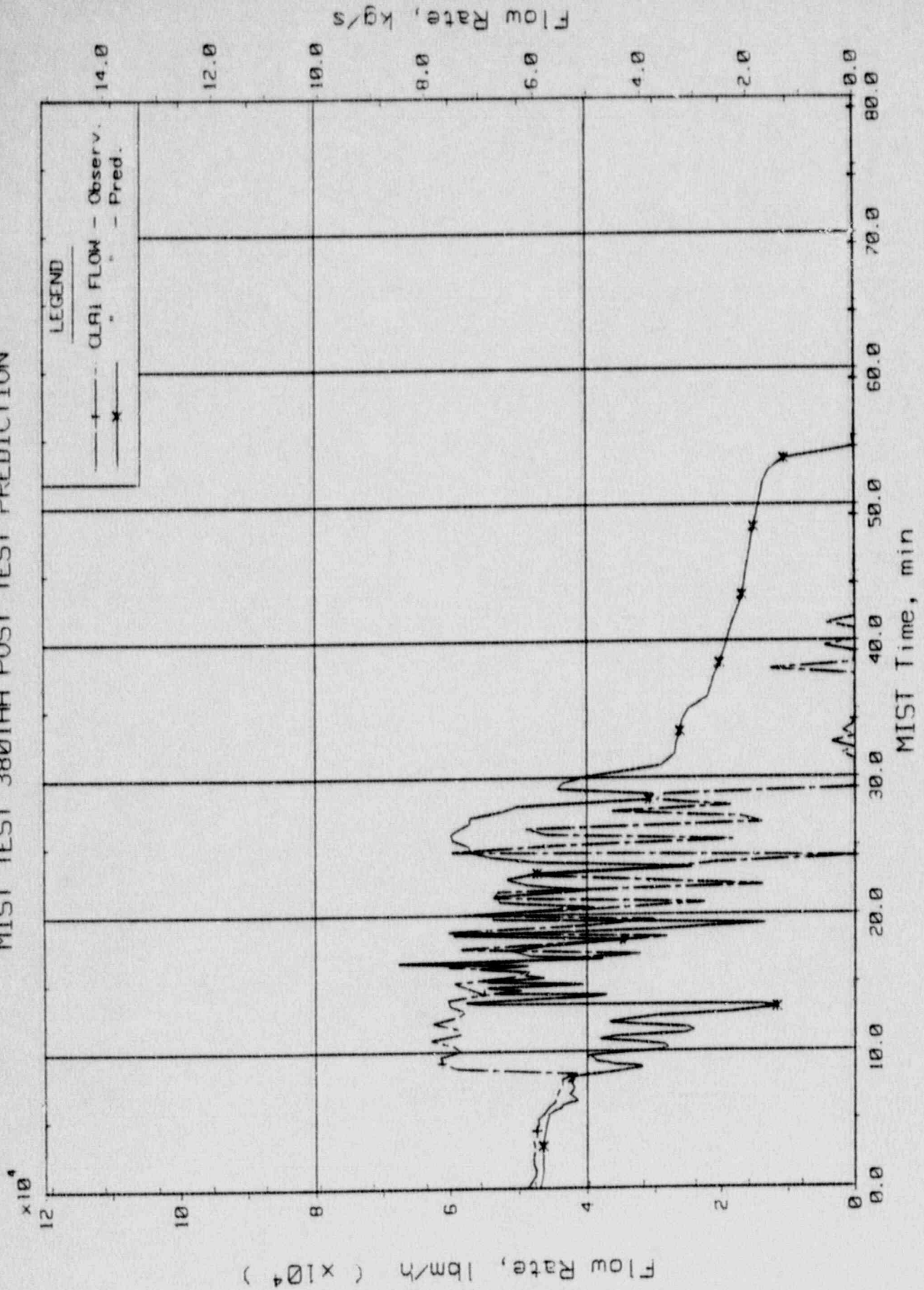


Figure 3.5.19. Cold Leg AI Flow

MIST TEST 3801RA POST TEST PREDICTION

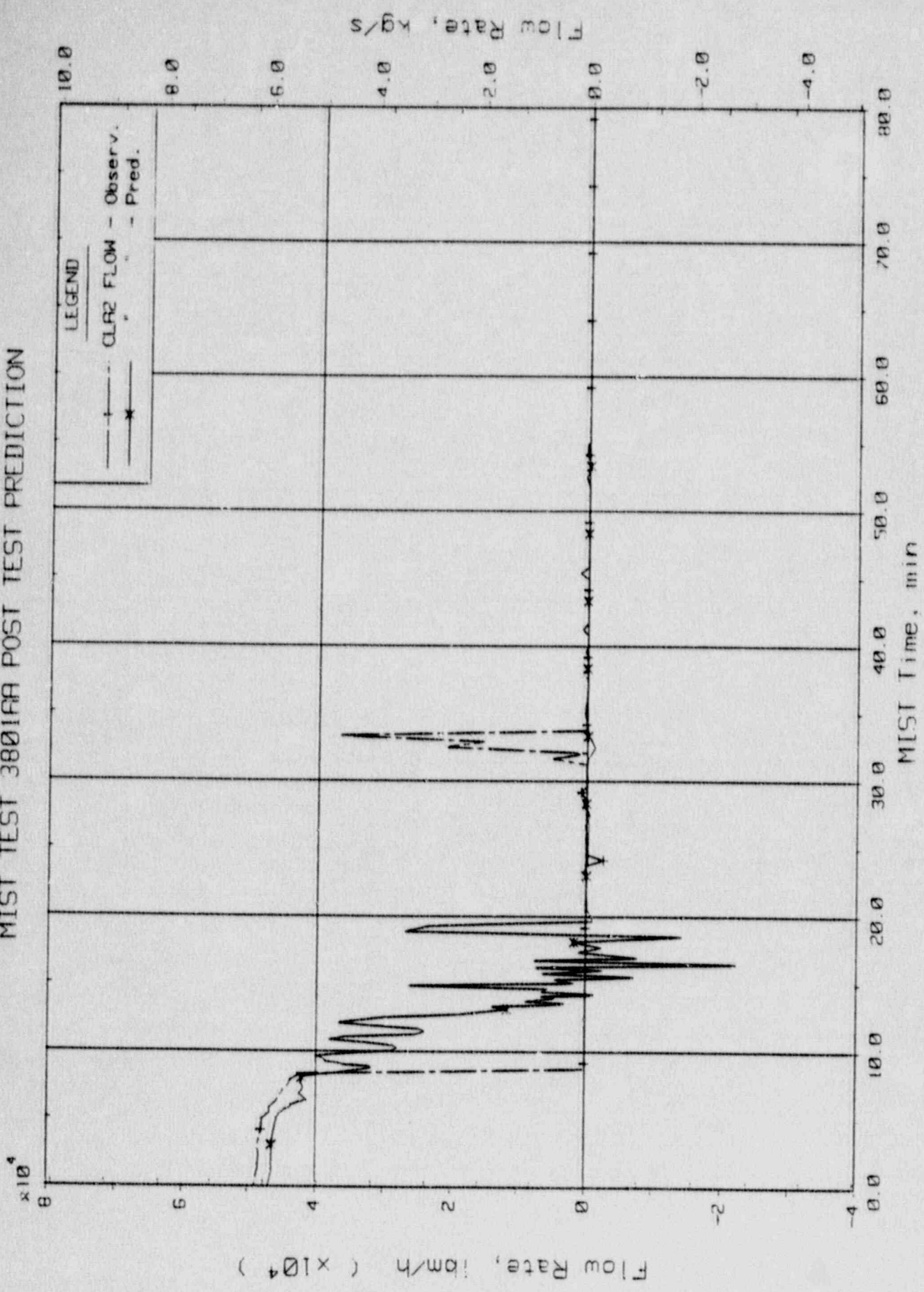


Figure 3.5.20. Cold Leg R2 Flow



MIST TEST 3801AA POST TEST PREDICTION

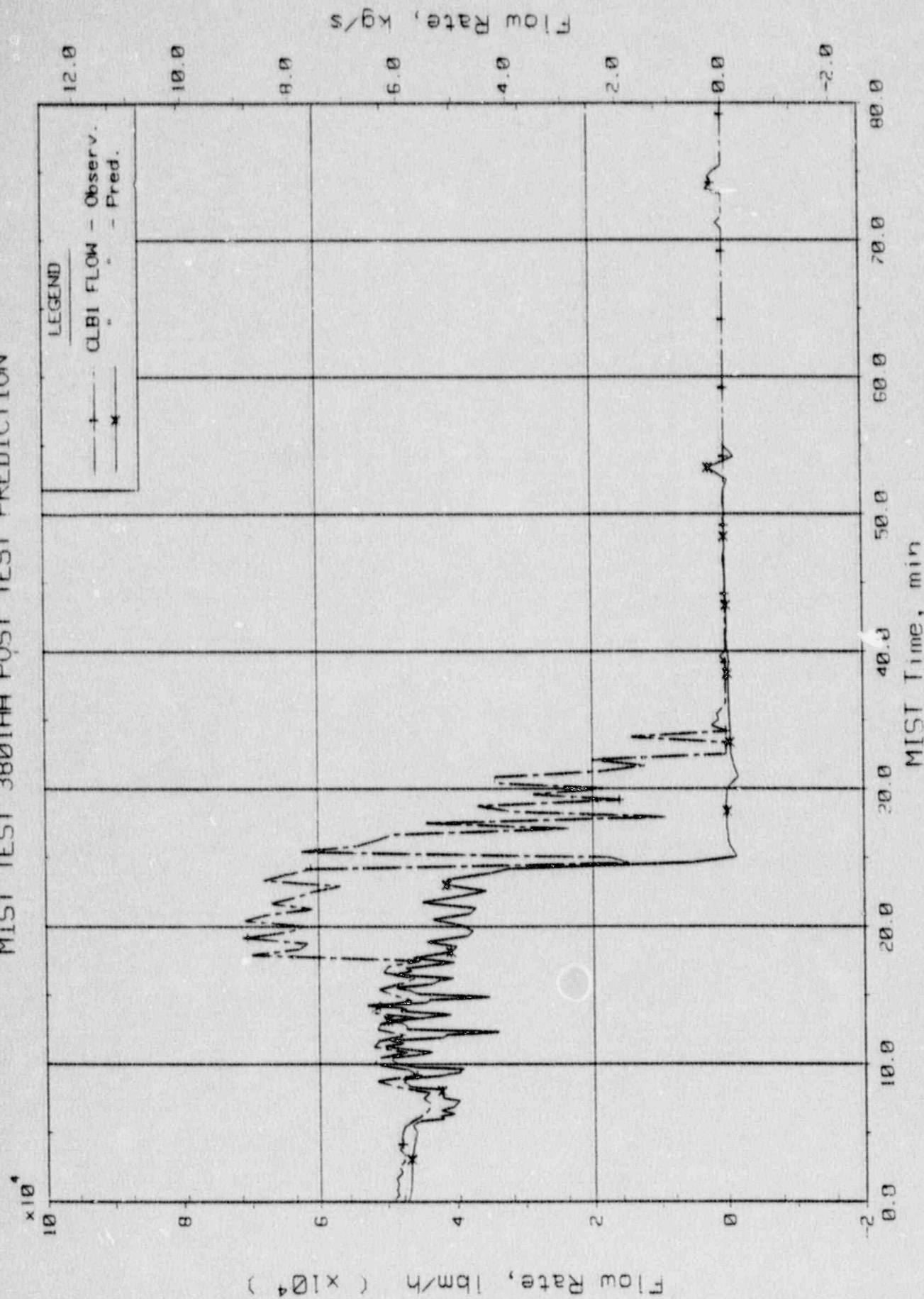


Figure 3.5.21. Cold Leg BI Flow

MIST TEST 3801AA POST TEST PREDICTION

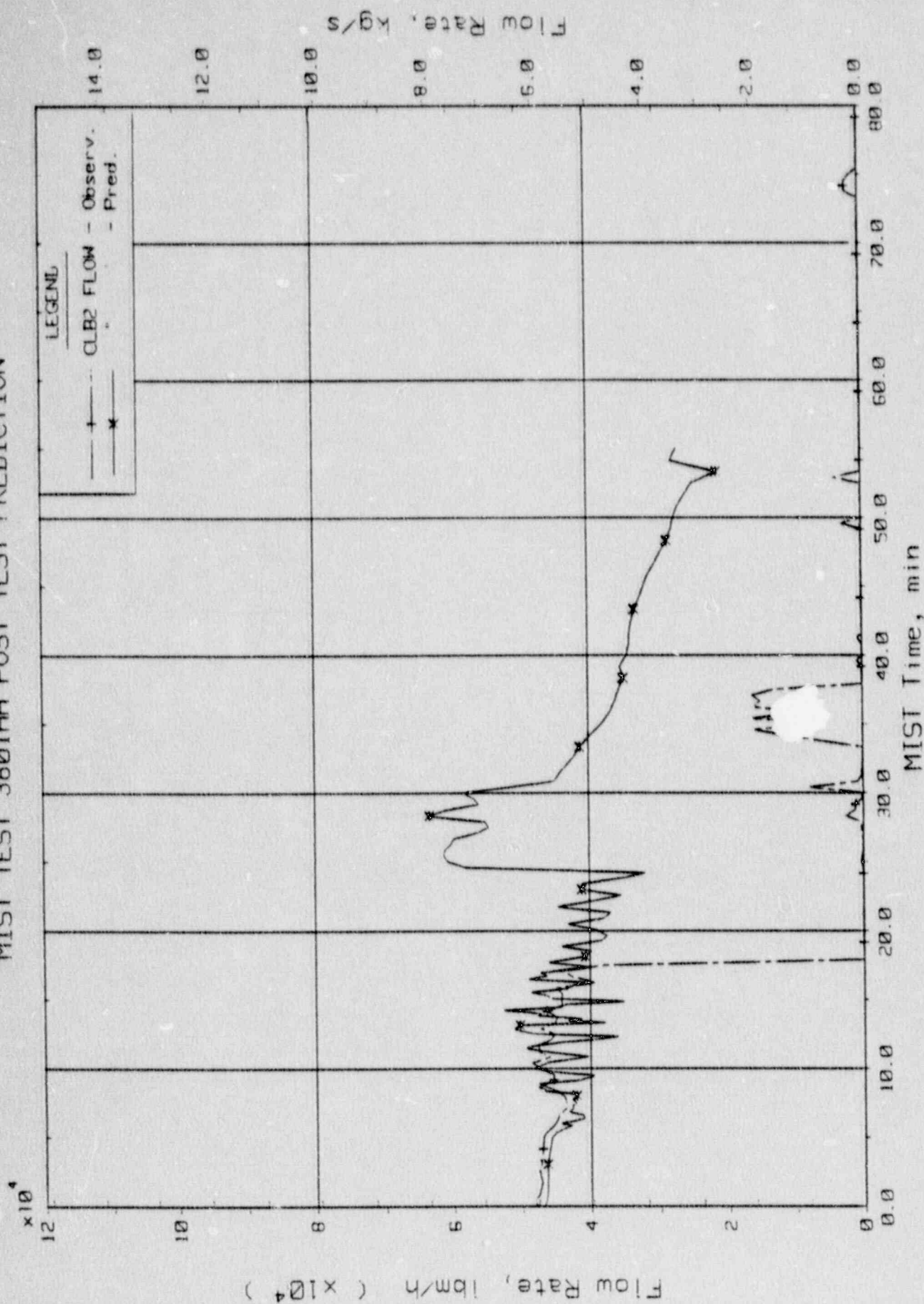


Figure 3.5.22. Cold Leg B2 Flow

Clb:04

MIST TEST 3801AA POST TEST PREDICTION

3-185

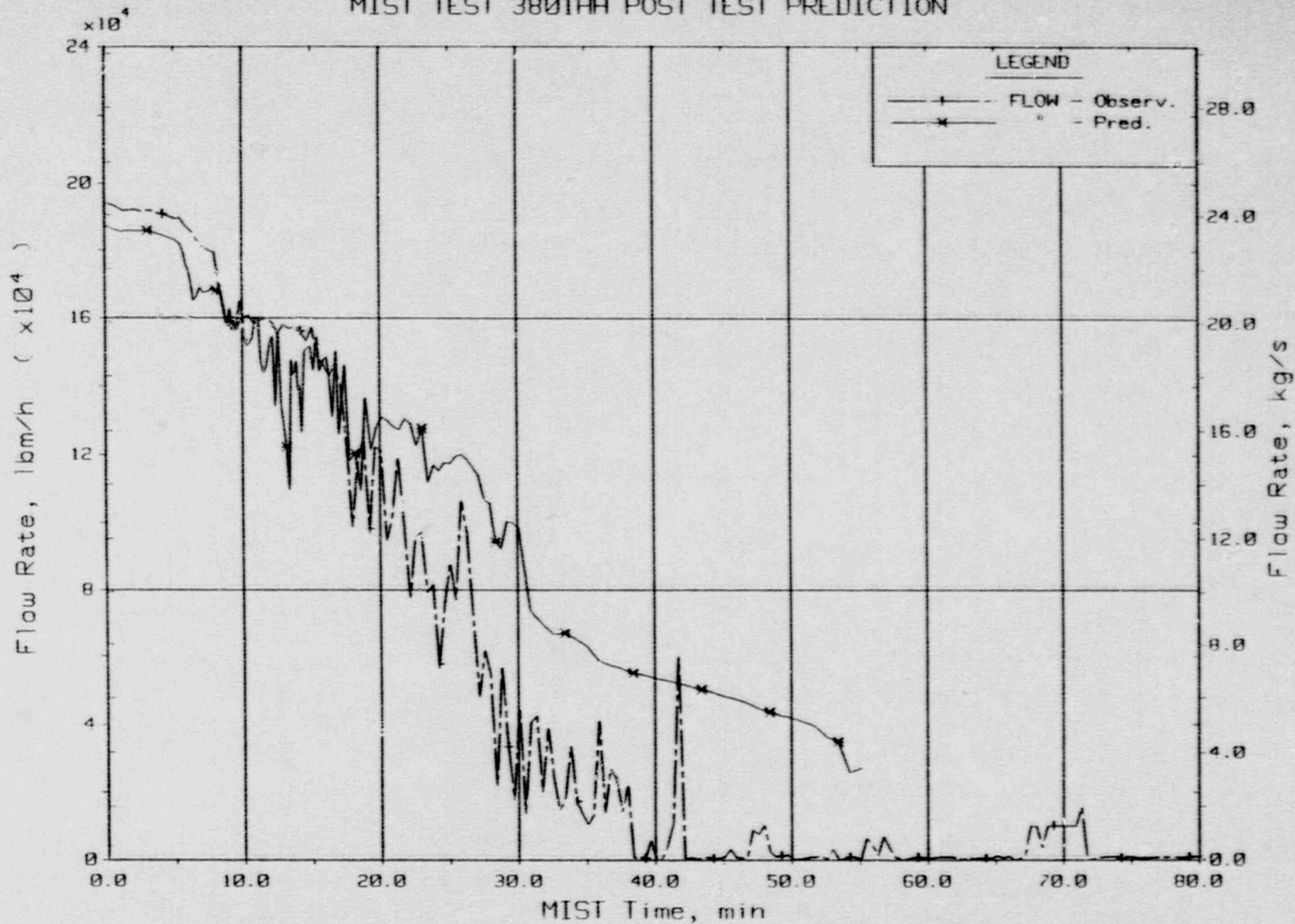


Figure 3.5.23. Primary System Venturi Flow Rates.

MIST TEST 3801AA POST TEST PREDICTION

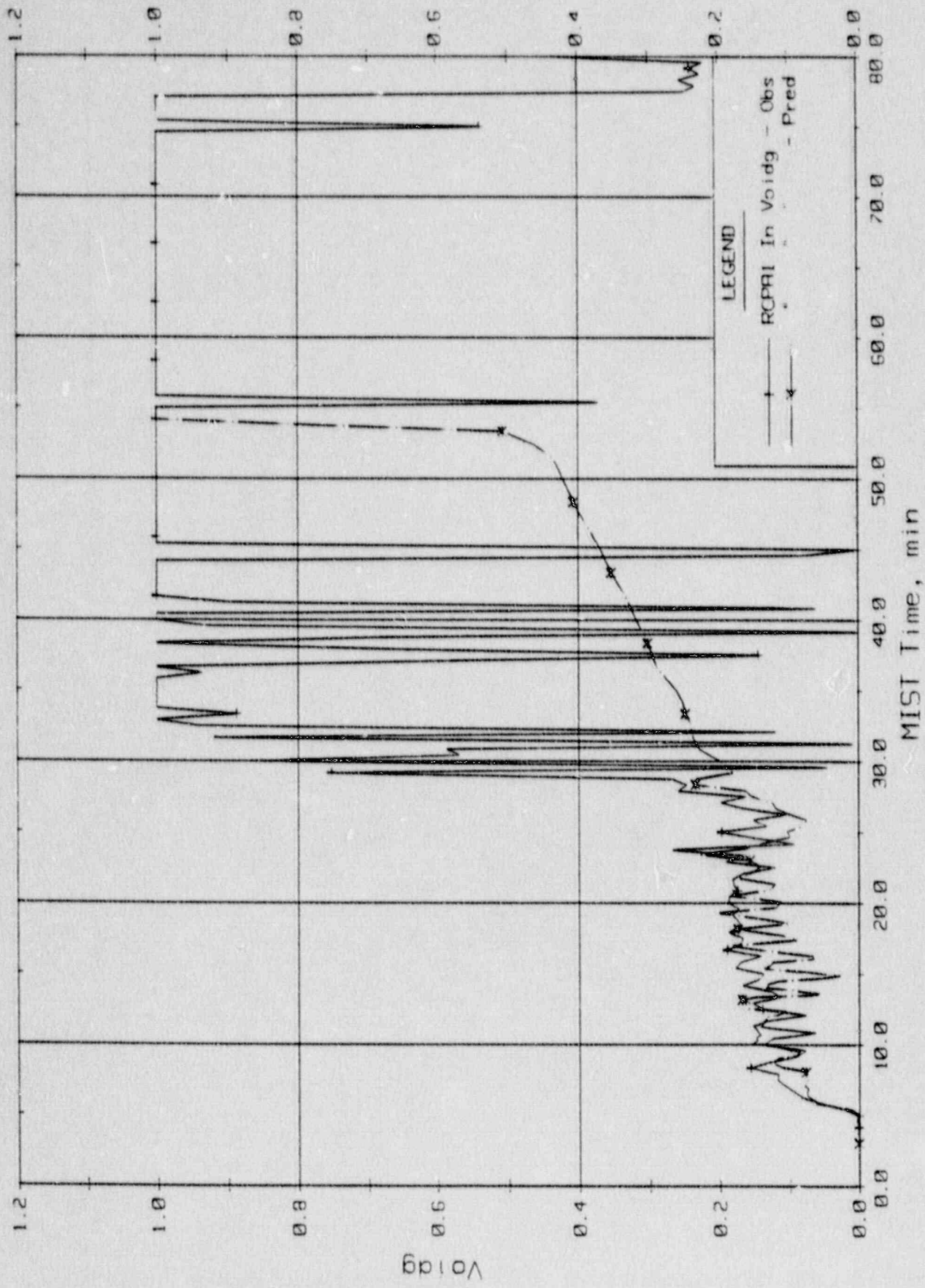


Figure 3.5.24. Void Fraction

MIST TEST 3801AA POST TEST PREDICTION

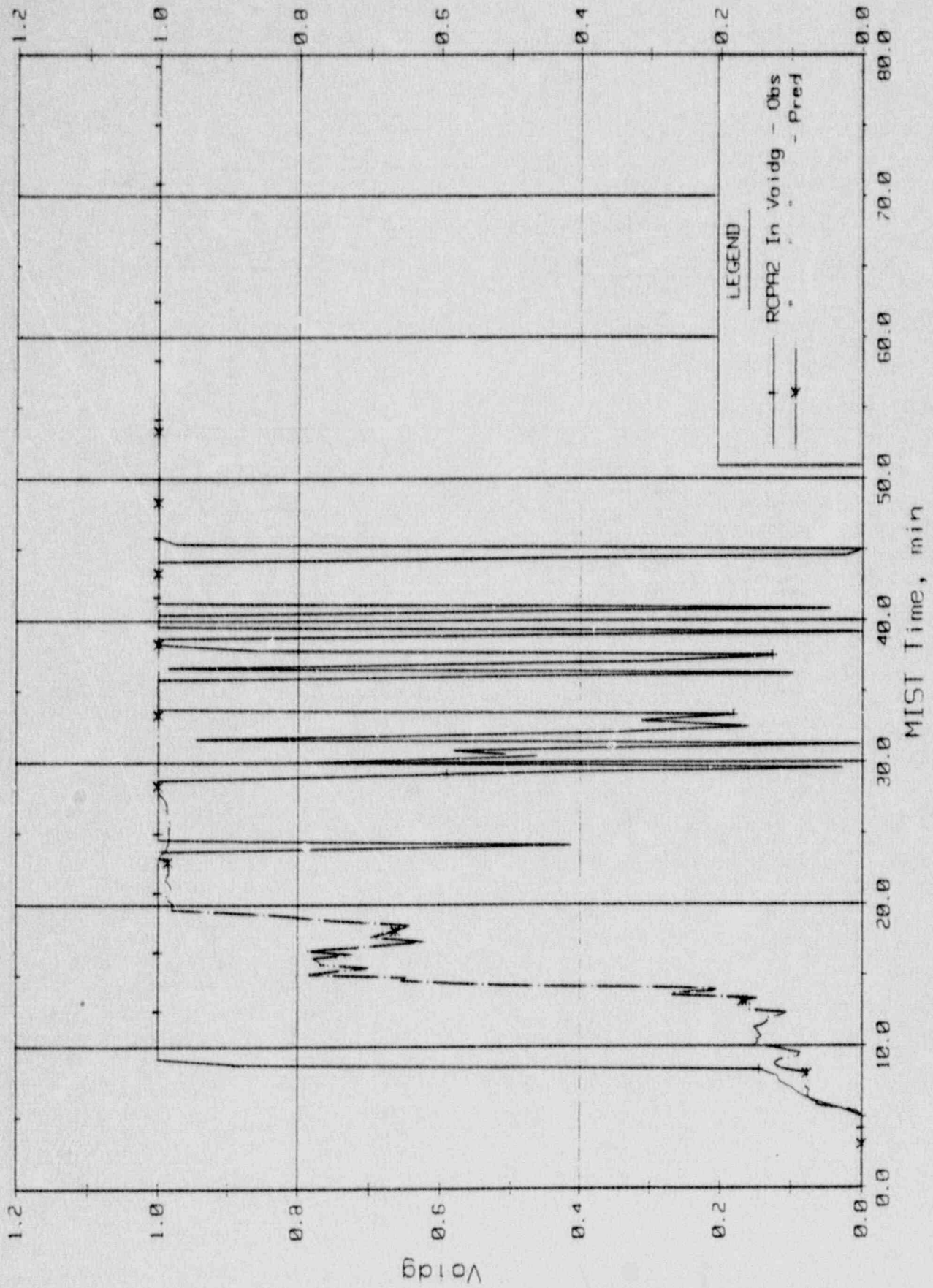


Figure 3.5.25. Void Fraction

MIST TEST 3801AA POST TEST PREDICTION

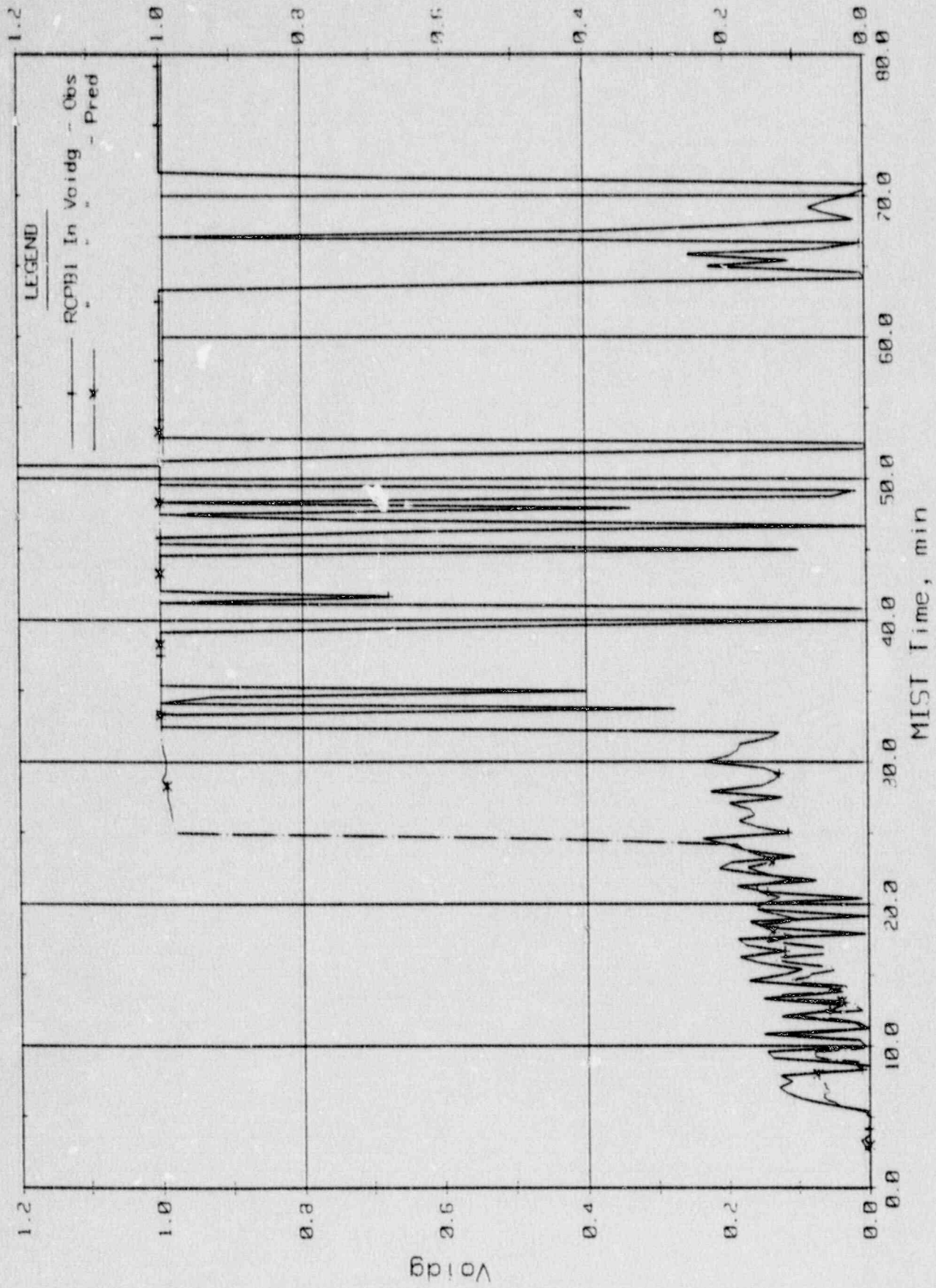


Figure 3.5.26. Void Fraction

MIST TEST 3801AA POST TEST PREDICTION

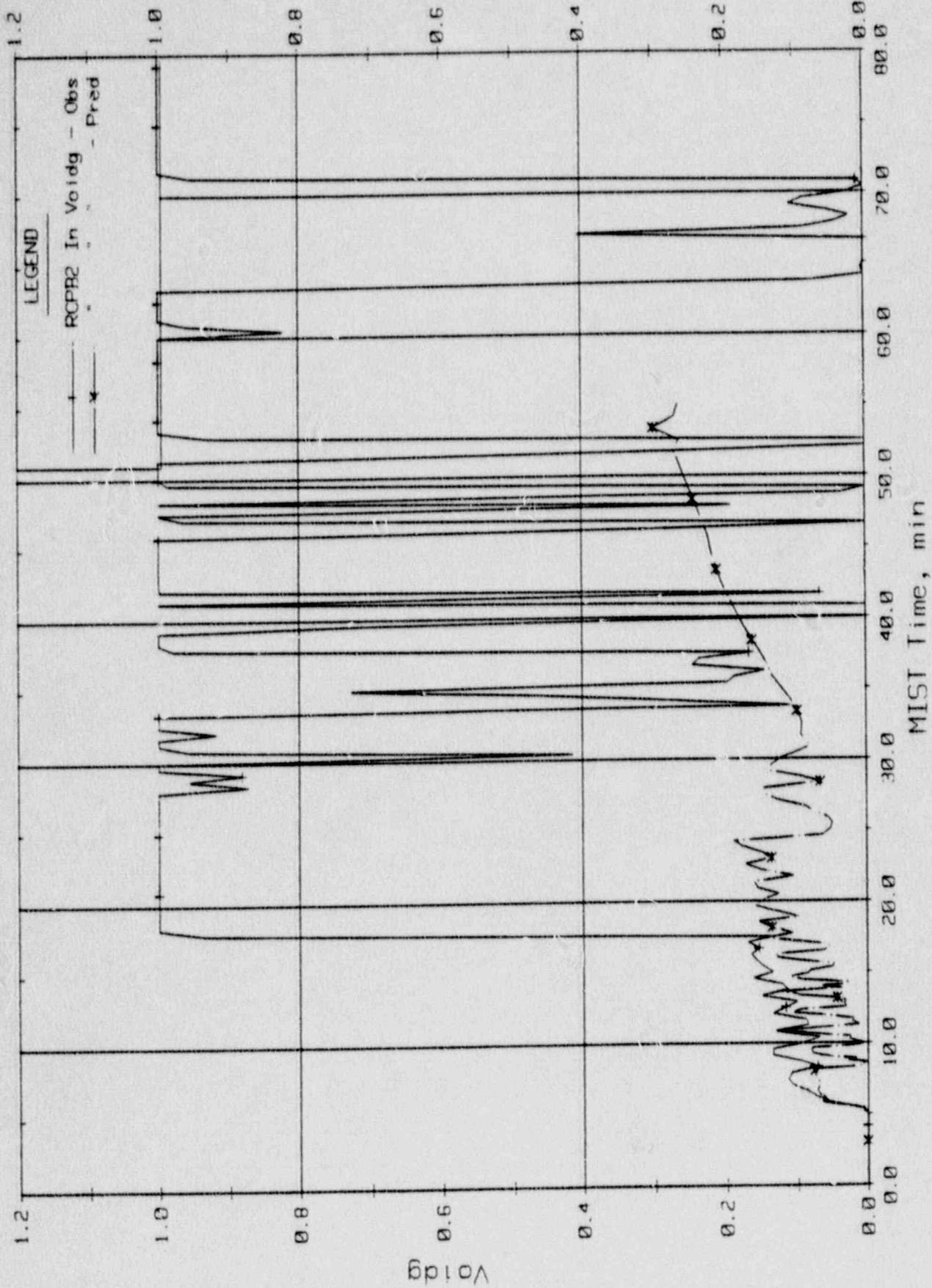


Figure 3.5.27. Void Fraction

# MIST TEST 3801AA POST TEST PREDICTION

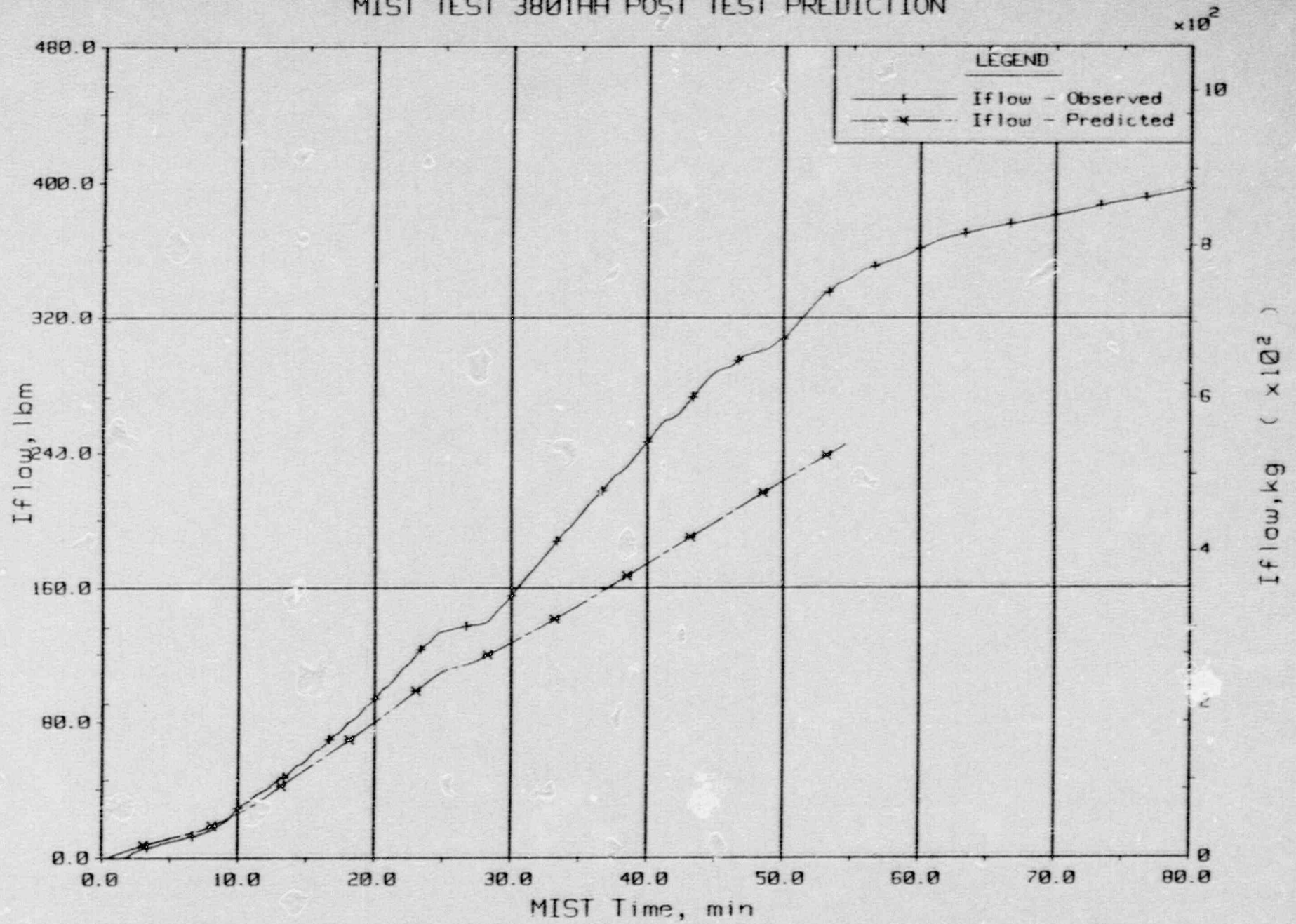


Figure 3.5.28. Integrated Porv Flow



MIST TEST 3801AA POST TEST PREDICTION

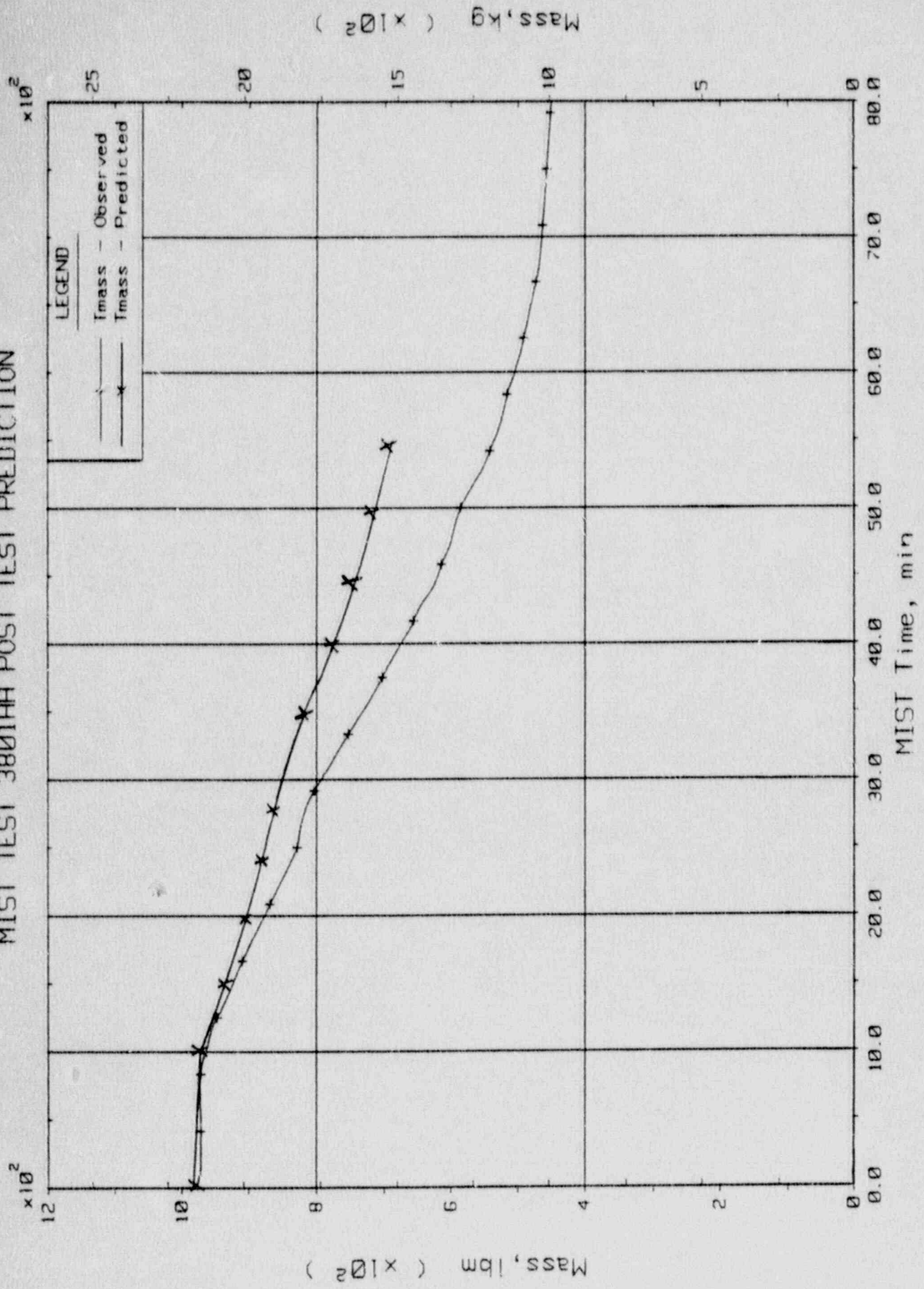


Figure 3.5.29. Total System Mass

# MIST TEST 3801AA POST TEST PREDICTION

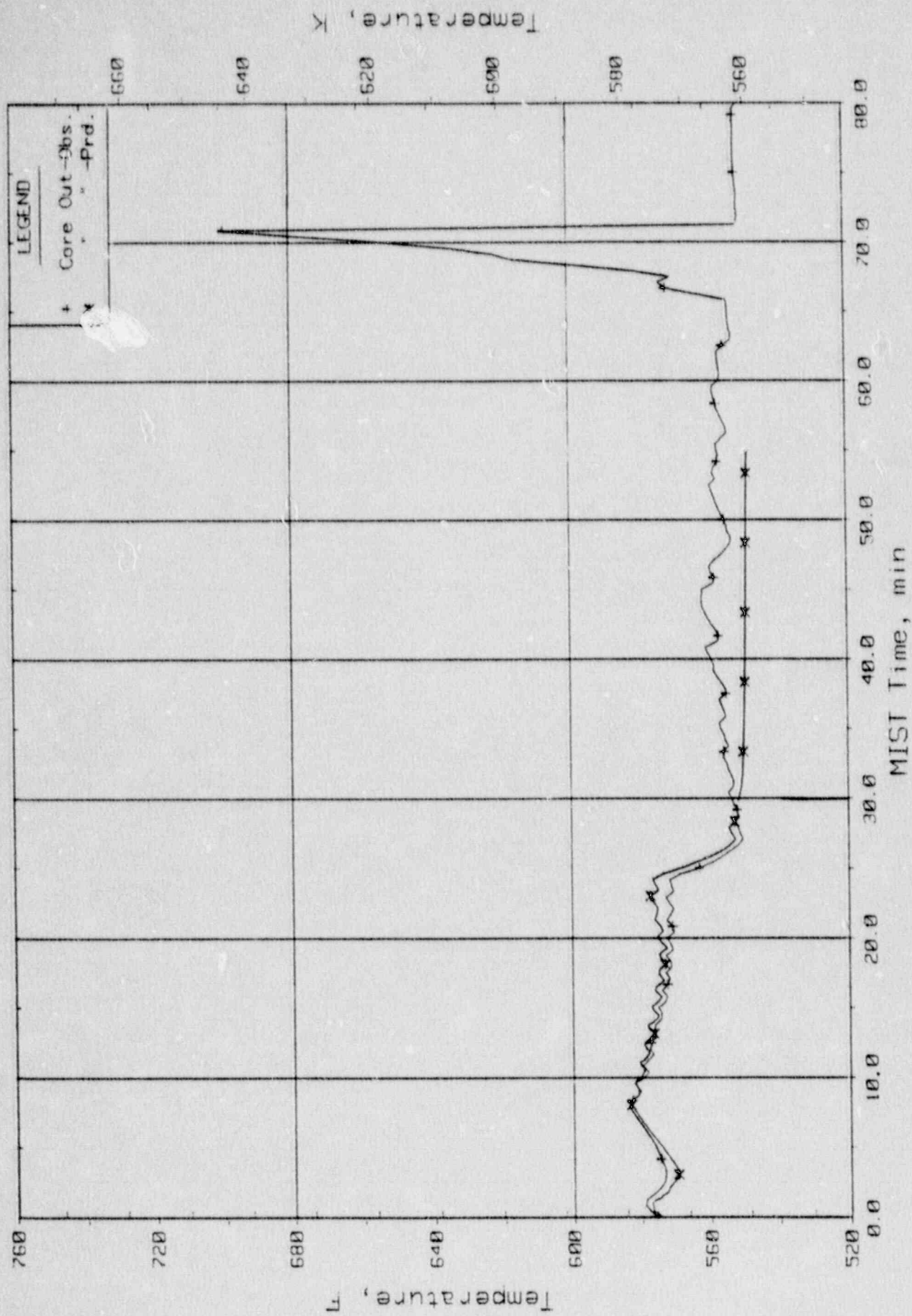


Figure 3.5.30. Core Exit Reactor Vessel Fluid Temperature (RVICH).

Top File: 3801AA-14-35-1000

Gr 10.11

MIST TEST 3801AA POST TEST PREDICTION

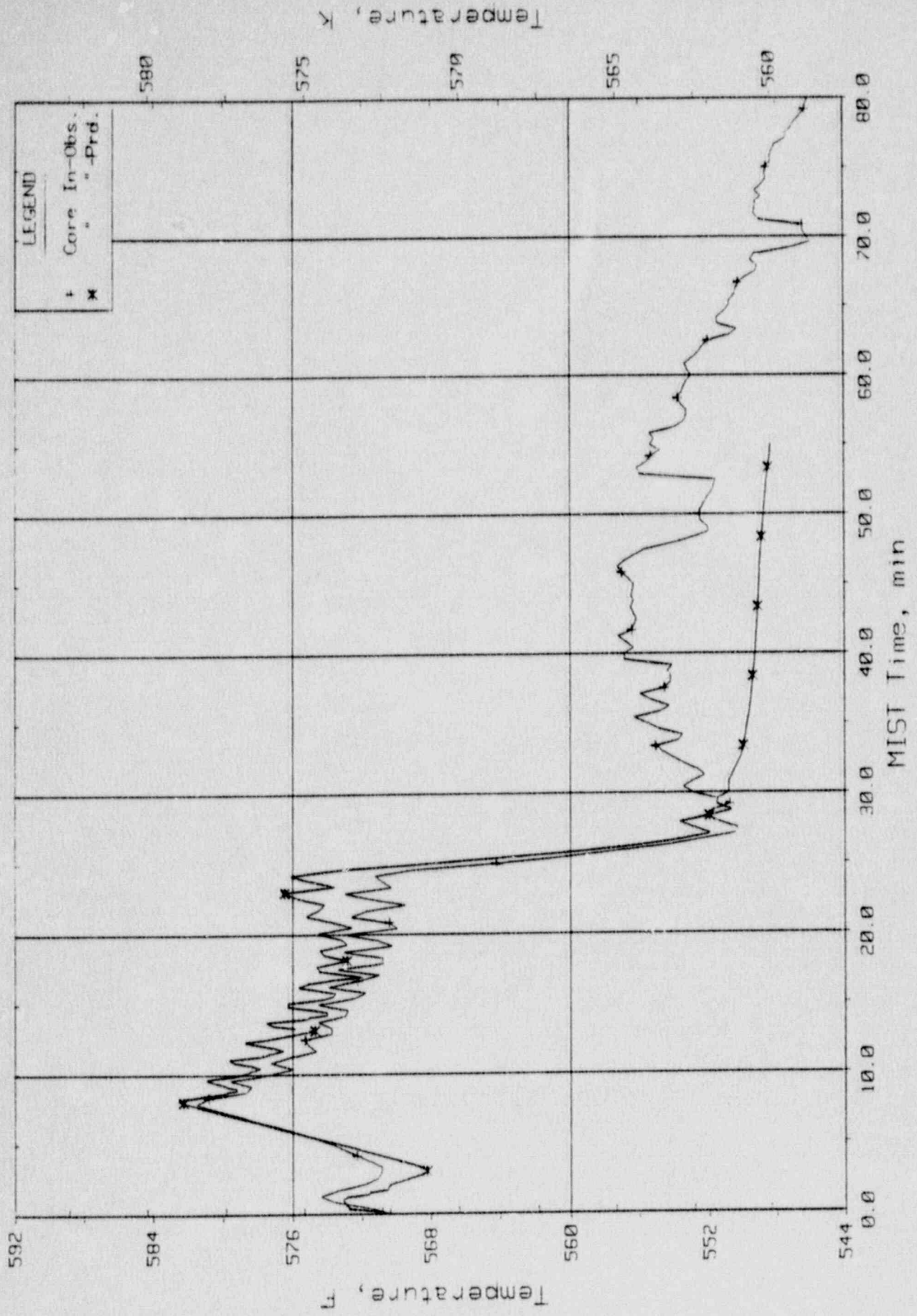


Figure 3.5.31. Core Inlet Reactor Vessel Fluid Temperature (MORT01).

# MIST TEST 3801AA POST TEST PREDICTION

3-192

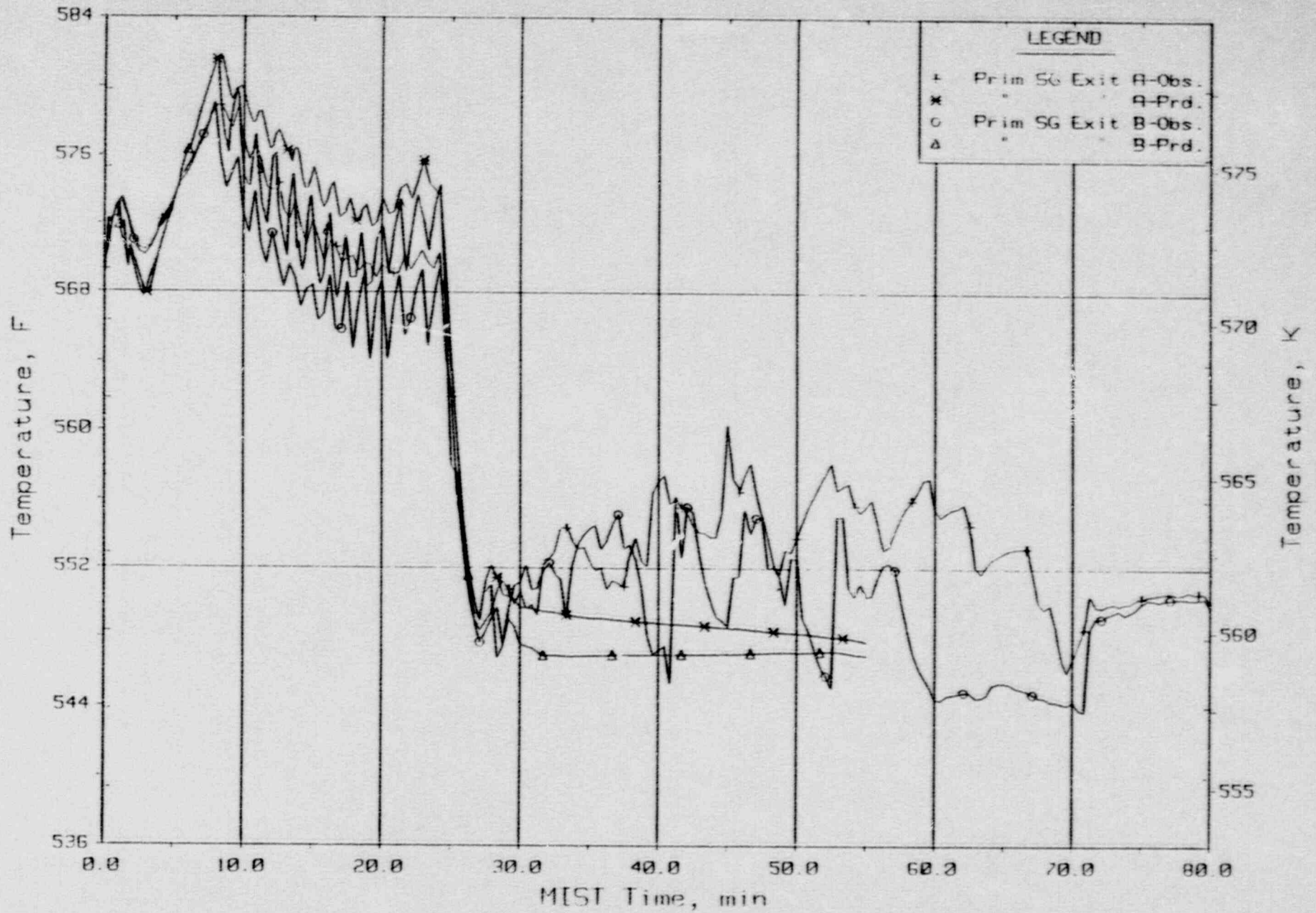


Figure 3.5.32. Loops A/B SG Exit Primary Fluid Temperatures (RTDs).

# MIST TEST 3801AA POST TEST PREDICTION

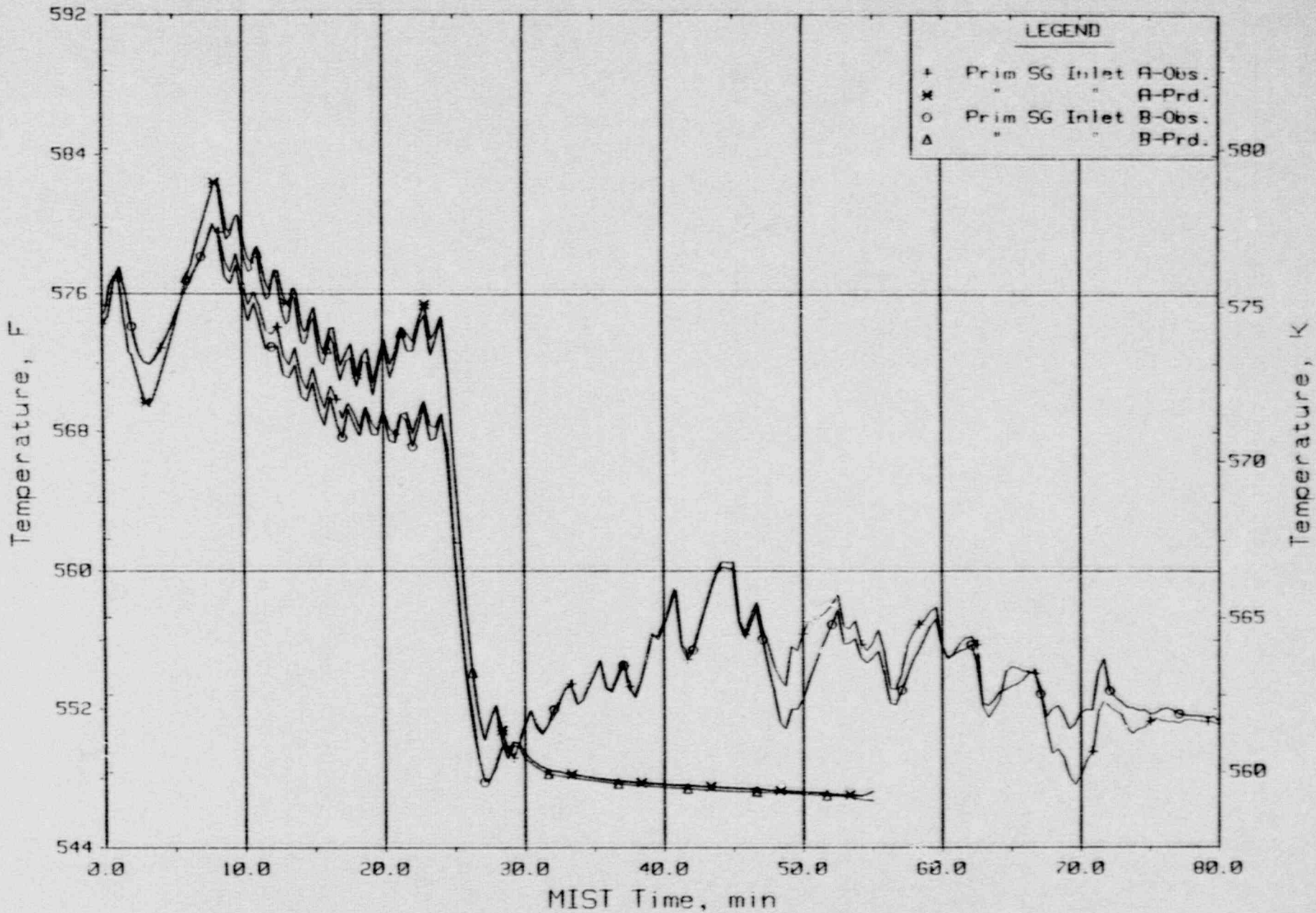


Figure 3.5.33. Loops A/B SG Primary Inlet Fluid Temperatures (RTDs).



#### 4. CONCLUSIONS

This report described a total of seven RELAP5/MOD2 MIST test predictions. Two pretest and five post-test predictions were performed using the B&W version of the RELAP5/MOD2 cycle 36.02 for the pretest or 36.04 for the post-test predictions. The code versions contained the B&W high AFW heat transfer model.

The comparison against test results was considered reasonable for all seven tests. Each test prediction included some calculated minor system trends which deviated somewhat from the observed facility behavior, however, these deviations would generally not impact the over-all conclusions which would be drawn. Divergence from most test results was generally in the form of timing phase shifts due to slightly different boundary conditions or controls between the prediction and the test. The most significant divergences from observed test behavior occurred during the noncondensable gas test (3502) and the core uncover test with pumps running (3801). The problems encountered during the NCG test concerned under-prediction of the interface condensation degradation between the two phases within a single control volume. The transport and wall condensation degradation of the NCG was reasonable. During the core uncover test, the complete two-phase degradation of the scaled reactor coolant pumps was predicted differently than what was observed for two of the four pumps. Inadequate characterization of the two-phase pump performance and the under-prediction of the initial leak flow rates were suspect for this prediction.

Another general area of disagreement which was observed in several of the tests concerned the closure of the RVVVs during the intermittent loop flow period. As the collapsed level decreased from the top of the downcomer region to the cold leg nozzle elevation the RVVVs in the facility would generally close for two to three minutes. In the prediction they remained open during that period due to over-prediction of the interface condensation

in the upper downcomer control volume. The MIST noding arrangement in this region caused this problem. A revised noding scheme in this region identical to full size B&W NSSS input decks is expected to improve the predicted behavior in this region.

Excellent or reasonable agreement in any integral system facility transient requires many interactions to be predicted correctly. During these transients nearly the entire code package is exercised. The results depend not only on the code formulation but on the input model configuration with correct boundary conditions and controls. Slight differences in any of these items may lead to minor divergences which can sometimes compound and result in more major system deviations. Benchmarking efforts such as these with the MIST facility provide the opportunity to evaluate both the code and the input modeling techniques. The quality and quantity of the data available from the facility enable adequate diagnosis and correction of any code or model shortcomings.

In summarizing the results from any benchmarking exercise it is much easier to describe the code deficiencies rather than the code strong points. Therefore, the transient phases or phenomena which were not correctly predicted are often emphasized over the periods where excellent agreement was observed. The intent of this benchmarking effort was obviously not to belittle the code. The overall goal was to quantify and improve the predictive powers of the code and input model for use in SBLOCA or similar transient applications. That is, to produce a package which can provide correct conclusions when used to analyze prototypical NSSS thermal-hydraulic behavior. The results of these seven MIST benchmarks indicated that the B&W version of RELAP5/MOD2 code and the base input modeling techniques are capable of providing for these needs.



## 5. REFERENCES

1. UPGD-TM-7, Rev. F, REDBL5 - An Advanced Computer Program for Light-Water Reactor LOCA and Non-LOCA Transient Analysis (B&W Version of RELAP5/MOD1), June, 1984.
2. UPGD-TM-44, Rev. H, RELAP5/MOD2 (B&W Version) - An Advanced Computer Program for Light-Water Reactor LOCA and Non-LOCA Transient Analysis, July, 1987.
3. J. A. Klingenfus, Multi-Loop Integral System Test Design Verification Report, November 15, 1984.
4. J. A. Klingenfus, RELAP5/MOD2 MIST Pre-test Predictions, March 10, 1986.
5. J. A. Klingenfus and J. C. Seals, BAW-1997, RELAP5/MOD2 MIST Post-Test Model Description, March, 1987.
6. J. A. Klingenfus, The Preliminary MIST Facility Input Model for the REDBL5 Code, August 1, 1984.
7. M. V. Parece and R. J. Schomaker, BAW-1903, RELAP5/MOD2 Benchmark of OTIS Feed and Bleed Test #220899, March 1986.
8. M. A. Rinckel and R. J. Schomaker, BAW-1902, RELAP5/MOD2 Benchmark of OTIS Leak Size Test #2202AA, January 1986.
9. G. E. Anderson, et. al., BAW-2002, MIST RELAP5/MOD2 Post-Test Benchmark of Test #320201 - 50 Sq. Cm. Pump Discharge Break, April 1987.
10. C. A. Schamp and J. A. Klingenfus, BAW-2033, RELAP5/MOD2 Post-Test Benchmark of MIST Test #3601AA - ATOG With Pumps Available, December 1988.
11. J. C. Seals and P. W. Ploch, BAW-2031, RELAP5/MOD2 MIST Post-Test Benchmark of Test #3404AA, February 1989.

12. M. K. Smith and M. V. Parece, BAW-2029, RELAP5/MOD2 MIST Post-Test Benchmark of Test #320604 - 10 cm<sup>2</sup> Pump Discharge Break, December 1988.
13. M. K. Smith and M. V. Parece, BAW-2030, RELAP5/MOD2 MIST Post-Test Benchmark of Test #3105AA, December 1988.
14. M. B. McGuirk and M. V. Parece, BAW-2032, RELAP5/MOD2 MIST Post-Test Benchmark of Test #350101, December 1988.
15. R. J. Schomaker (B&W) to B&W Owners Group Analysis Committee, "IST Test Selection Recommendation for Benchmarking," ESC-876, December 8, 1986.

**BIBLIOGRAPHIC DATA SHEET**

*(See instructions on the reverse.)*

1. REPORT NUMBER  
 (Assigned by NRC. Add Vol., Supp., Rev.,  
 and Addendum Numbers, if any.)

**NUREG/CR-5395, Vol. 10  
 EPRI/NP-6480  
 BAW-2078**

2. TITLE AND SUBTITLE

**Multiloop Integral System Test (MIST): Final Report  
 RELAP5/MOD2 MIST Analysis Comparisons**

3. DATE REPORT PUBLISHED

MONTH	YEAR
December	1989

4. FIN OR GRANT NUMBER

**B8909 & D1734**

5. AUTHOR(S)

**J. A. Klingenfus and M. V. Parece**

6. TYPE OF REPORT

**Technical**

7. PERIOD COVERED (Inclusive Dates)

**June 1986-March 1988**

8. PERFORMING ORGANIZATION - NAME AND ADDRESS (If NRC, provide Division, Office or Region, U.S. Nuclear Regulatory Commission, and mailing address. If contractor, provide name and mailing address.)

<b>Babcock &amp; Wilcox</b>	<b>Babcock &amp; Wilcox</b>
<b>Nuclear Power Division</b>	<b>Research &amp; Development Division</b>
<b>3315 Old Forest Road</b>	<b>Alliance Research Center</b>
<b>Lynchburg, VA 24506-0935</b>	<b>1562 Beeson Street</b>
	<b>Alliance, OH 44601</b>

9. SPONSORING ORGANIZATION - NAME AND ADDRESS (If NRC, type "Same as above"; if contractor, provide NRC Division, Office or Region, U.S. Nuclear Regulatory Commission, and mailing address.)

<b>Division of Systems Research</b>	<b>Electric Power Research Institute</b>	<b>Babcock &amp; Wilcox</b>
<b>Office of Nuclear Regulatory Research</b>	<b>P. O. Box 10412</b>	<b>Owners Group</b>
<b>U. S. Nuclear Regulatory Commission</b>	<b>Palo Alto, CA 94303</b>	<b>P. O. Box 10935</b>
<b>Washington, DC 20555</b>		<b>Lynchburg, VA 24506-0935</b>

10. SUPPLEMENTARY NOTES

11. ABSTRACT (200 words or less)

The Multiloop Integral System Test (MIST) is part of a multiphase program started in 1983 to address small-break loss-of-coolant accidents (SBLOCAs) specific to Babcock and Wilcox designed plants. MIST is sponsored by the U. S. Nuclear Regulatory Commission, the Babcock & Wilcox Owners Group, the Electric Power Research Institute, and Babcock and Wilcox. The unique features of the Babcock and Wilcox design, specifically the hot leg U-bends and steam generators, prevented the use of existing integral system data or existing integral facilities to address the thermal-hydraulic SBLOCA questions. MIST and two other supporting facilities were specifically designed and constructed for this program, and an existing facility--the Once Through Integral System (OTIS)--was also used. Data from MIST and the other facilities will be used to benchmark the adequacy of system codes, such as RELAP5 and TRAC, for predicting abnormal plant transients.

The MIST program is reported in 11 volumes. The program is summarized in Volume 1; Volumes 2 through 8 describes groups of tests by test type; Volume 9 presents inter-group comparisons; Volume 10 provides comparisons between the calculations of RELAP5/MOD2 and MIST observations, and Volume 11 presents the later Phase 4 tests. The comparisons of RELAP5/MOD2 against the MIST data and conclusions reached are the subject of this volume.

12. KEY WORDS/DESCRIPTORS (List words or phrases that will assist researchers in locating the report.)

**Multiloop Integral System Test (MIST), Babcock and Wilcox  
 Small break loss-of-coolant accident, transient testing, reactor safety  
 steam generator (once through), feed and bleed  
 steam generator tube rupture, station black out  
 Two-phase flow, SBLOCA without HPI injection, RELAP5/MOD2 calculations**

13. AVAILABILITY STATEMENT

**Unlimited**

14. SECURITY CLASSIFICATION

*(This Page)*

**Unclassified**

*(This Report)*

**Unclassified**

15. NUMBER OF PAGES

16. PRICE

UNITED STATES  
NUCLEAR REGULATORY COMMISSION  
WASHINGTON, D.C. 20555

OFFICIAL BUSINESS  
PENALTY FOR PRIVATE USE, \$300

SPECIAL FOURTH CLASS RATE  
POSTAGE & FEES PAID  
USNRC  
PERMIT No. G-67

120555139531 1 1AN1R2  
US NRC-DADM  
DIV FOIA & PUBLICATIONS SVCS  
TPS PDR-NUREG  
P-223  
WASHINGTON DC 20555